Small Break LOCA
Sensitivity Analyses for US-APWR

Non-Proprietary Version

May 2010

Revision History

Revision	Page	Description
0	All	Original issue
1	General	All cases were recalculated with latest version of M-RELAP5. Added cases with homogeneous break flow (section 5.3). Added DVI injection point noding sensitivity analysis (DCD RAI 15.6.5-61)
	2-2	Appendix-K requirements #4 and #29 are categorized to Category 1 (DCD RAIs 15.6.5-58 and 60)
	2-5	Sensitivity study for noding near ECC injection point is performed (DCD RAI 15.6.5-61)
	2-7	Modified to "Small break core recovery due to ECC water injection is modeled." (DCD RAIs 15.6.5-58 and 60)
	4-7	ACC water volume is replaced “2150 ft^3” with “2152 ft^3” (DCD RAI 15.6.5-63)
	4-10	Sensitivity study for noding near DVI injection point is performed (DCD RAI 15.6.5-61)
	4-12	The description of nodalization for sensitivity study near DVI injection point is added (DCD RAI 15.6.5-61)
	4-22	Figure 4.2-7 is added (DCD RAI 15.6.5-61)
	Section 5	All tables and figures are replaced Replaced “Core upper region uncovery” with “Fuel cladding starts heating up” and “Core upper region recovery” with “Fuel cladding rewets” in the tables (DCD RAI 15.6.5-66)
	5.1-8	Delete the sentence “This figure also shows that a slight core uncovery of about 4-ft occurs for the pressurizer steam phase break.” (DCD RAI 15.6.5-57)
	Section 5.4	Added the sections 5.4.3, some tables and some figures (DCD RAI 15.6.5-61)
	5.4-1	Replaced “perfectly in agreement” with “similar in terms of transient profile, magnitude and duration” (DCD RAI 15.6.5-78)
	5.4-4	Modified the last paragraph of section 5.4.1 part (2) (DCD RAI 15.6.5-69)

Mitsubishi Heavy Industries, Ltd.
16-5, Konan 2-chome, Minato-ku
Tokyo 108-8215 Japan

ABSTRACT

For the US-APWR small break loss of coolant accident (SBLOCA) analysis, MHI specifically selected RELAP5-3D and modified it as M-RELAP5 in order to meet the requirements in 10CFR Part 50 Appendix K ,"ECCS Evaluation Models". In support of the US-APWR Design Certification application, this Technical Report describes the sensitivity analyses on SBLOCA conducted using M-RELAP5. The report presents the results of the SBLOCA sensitivity analyses to show that M-RELAP5 meets the requirements of Appendix-K.

After the introductory chapter, in the second chapter, code version of M-RELAP5 and its compliance with Appendix-K requirements are discussed. In chapter three, plant modeling through system nodalization is elaborated. It covers the modeling of core and reactor vessel, steam generators, a broken loop, and intact loops. Analysis conditions and cases are presented in chapter four, covering main plant analytical condition, and the selection of sensitivity analysis cases and their conditions. In chapter five, the results of sensitivity analyses on break spectrum, break orientation, break location, plant nodalization, single failure assumption, offsite power availability and time step size are discussed in detail.

The results of the break spectrum sensitivity calculations specified the limiting break conditions including break location, break size, and break orientation for loop-seal PCT and boil-off PCT case. The sensitivity calculations also show the noding near break point and the noding of loop part are appropriate for SBLOCA of US-APWR. The time step size is sufficiently small for code solution convergence. The analyses results also show that assumptions of single failure and loss of offsite power are adequately selected.

It is confirmed by the sensitivity analyses that the ECCS of the US-APWR satisfies the required safety performance to mitigate a wide spectrum of postulated SBLOCAs.

Table of Contents

List of Tables

List of Figures

List of Acronyms

BOL	Beginning Of Life
CHF	Critical Heat Flux
DVI	Direct Vessel Injection
ECC	Emergency Core Cooling
ECCS	Emergency Core Cooling System
EFW	Emergency Feedwater
EFWS	Emergency Feedwater System
HHIS	High Head Injection System
LBLOCA	Large Break LOCA
LOCA	Loss Of Coolant Accident
LOOP	Loss Of Offsite Power
MFWS	Main Feedwater System
PCT	Peak Cladding Temperature
PIRT	Phenomena Identification and Ranking Table
PWR	Pressurized-Water Reactor
RCCA	Rod Cluster Control Assembly
RCP	Reactor Coolant Pump
RCS	Reactor Coolant system
RV	Reactor Vessel
RWSP	Refueling Water Storage Pit
SBLOCA	Small Break LOCA
SG	Steam Generator
SI	Safety Injection
SRP	Standard Review Plan

1.0 INTRODUCTION

For the US-APWR small break loss of coolant accident (SBLOCA) analysis, MHI specifically selected RELAP5-3D and modified it as M-RELAP5 in order to meet the requirements in 10CFR Part 50 Appendix K ,"ECCS Evaluation Models" (Ref.1-1). In M-RELAP5, some Appendix K requirements were achieved through the implementation of new models or the modification as described in Reference 1-2. M-RELAP5 capability to analyze the SBLOCA transient was confirmed by the validation analyses with integral effect tests and separate effect tests focused on the models related to the important phenomena in SBLOCA.

In support of the US-APWR Design Certification application, this Technical Report describes the sensitivity analyses on SBLOCA conducted using M-RELAP5. The necessary sensitivity study cases are selected based on the requirements of the Appendix-K and Standard Review Plan (SRP) 15.6.5 (Ref.1-3). The report presents the results of the SBLOCA sensitivity analyses to show that M-RELAP5 meets the requirements of Appendix-K and the SRP.

After the introductory chapter, in the second chapter, code version of M-RELAP5 and its compliance with Appendix-K requirements are discussed. In chapter three, plant modeling through system nodalization is elaborated. It covers the modeling of core and reactor vessel, steam generators, a broken loop, and intact loops. Analysis conditions and cases are presented in chapter four, covering main plant analytical condition, and the selection of sensitivity analysis cases and their conditions. In chapter five, the results of sensitivity analyses on break spectrum, break orientation, break location, plant nodalization, single failure assumption, off-site power availability and time step size are discussed in detail.

2.0 M-RELAP5 CODE AND COMPLIANCE WITH APPENDIX-K

2.1 M-RELAP5 Code

MHI uses M-RELAP5 for the US-APWR SBLOCA analysis, in order to satisfy the requirements in 10 CFR Part 50 Appendix K on the "ECCS Evaluation Models". M-RELAP5 is a modified version of RELAP5-3D originally developed by the INL (Ref. 2-1).

The capability of M-RELAP5 in simulating SBLOCA was demonstrated by the validation analyses with integral effect tests and separate effect tests focused on the models related to important phenomena identified in the Phenomena Identification and Ranking Table (PIRT). Some of the important phenomena are as follows: CHF/core dryout, uncovered core heat transfer, rewet, core mixture level, water hold up in SG primary side, SG primary and secondary heat transfer, water level in the SG outlet piping, loop seal formation and clearance, downcomer mixture level and downcomer void distribution. The results show that M-RELAP5 is capable to predict the high ranking key phenomena quite well. The modeling capabilities of M-RELAP5 were also examined and concluded to be applicable to the important phenomena specified in the PIRT with the constitutive equations. The sensitivity analyses on time step size for an integral test also demonstrate that M-RELAP5 is able to suppress numerical error to be sufficiently small.

It is concluded that M-RELAP5 is applicable to carry out the SBLOCA analysis of the US-APWR.

2.2 Compliance with Appendix-K Requirements

The required and acceptable features of the evaluation models (EM) and required documents are specified in Section I and II of Appendix K to Part 50 of Title 10 of the Code of Federal Regulations. Section I of Appendix K (Ref. 2-2) is divided into four subsections: A. Sources of Heat During LOCA; B. Swelling and Rupture of the Cladding and Fuel Rod Thermal Parameters; C. Blowdown Phenomena; and D. Post-Blowdown Phenomena; Heat Removal by the ECCS.

The evaluation models and analysis requirements stemming from these subsections are summarized in Table 2-1. The table shows each Appendix K requirement, the location of the requirement in the Appendix K, the acceptance criteria of the Appendix K requirement, and the approach for meeting the requirement. The Appendix K requirements are listed as 31 separate items in Table 2-1.

M-RELAP5 has a number of models that meet many of the Appendix K requirements. Other Appendix K requirements can be achieved by simply providing the appropriate input in the plant model. This includes the plant nodalization together with initial conditions, boundary conditions, and the code options. Some sensitivity calculations are necessary to be performed based on Appendix K requirements.

Appendix K requirements fall within three categories:

Category 1: models of M-RELAP5 addresses the requirements,

Category 2: appropriate inputs including noding addresses the requirements,

Category 3: sensitivity studies are needed

As noted in column 4 of Table 2-1, eleven requirements, 4, 7, 9, 12, 14, 19, 20, 21, 22, 27, and 29 belong to Category 1. Fifteen requirements, 1 through 6, 8, 10, 11, 17, 18, 23, 24, 26, and 28, belong to Category 2. Five requirements, 13, 16, 25, 30, and 31, belong to Category 3. Requirements 15, ECC water bypass is for the large break LOCA (LBLOCA) calculations and is not applicable to SBLOCA calculations.

Consequently, necessary sensitivity studies are as follows:

13. Break characteristics
16. Noding near break point
25. Single failure criterion

30. Solution convergence
31. Appropriate sensitivity studies

For Break characteristics, or, break spectrum sensitivity studies, in the SRP 15.6.5, requirements are defined more specifically as follows:

- smaller than integer diameter break sizes are necessary
- break location includes break orientation such as the bottom, side and top of the discharge leg

In addition, requirements of this SRP include the sensitivity study of the availability of offsite power.

In this report, plant noding is explained in Section 3, and basic analysis conditions are explained in Section 4.1. Finally, analysis condition of sensitivity studies are explained in Section 4.2 and calculation results are shown in Section 5.

Table 2-1(1/5) Appendix K Requirements and Compliance of M-RELAP5

Appendix K Requirement	Ref. (*1)	Acceptable Limits	Approach of M-RELAP5
1. Steady state power level	I. A	Power level shall be at least 1.02 times the licensed power level.	- Appropriate input is used as described in Section 4.1.
2. Maximum peaking factor	I. A	Maximum peaking factor shall be that allowed by the technical specification.	- Appropriate input is used as described in Section 4.1.
3. Power distribution shape	I. A	Power distribution shape and peaking factor combination giving highest PCT shall be considered.	- Appropriate input is used as described in Section 4.1.
4. Initial stored energy in fuel	I. A. 1	Steady state temperature distribution and stored energy in the fuel shall be calculated for the burn-up that yield highest PCT.	- Appropriate input is used as described in Section 4.1 - Gap conductance model consistent with fuel design code was installed. (*2)
5. Fission heat	I. A. 2	Fission heat shall be calculated using reactivity and reactor kinetics. Shutdown reactivity from temperature and voids shall be given their minimum plausible values.	- Appropriate input is used as described in Section 4.1.
6. Actinide decay heat	I. A. 3	The heat from actinide decay shall be calculated.	- Appropriate input is used as described in Section 4.1
7. Fission Product decay heat	I. A. 4	Fission product decay heat shall be 1.2 times the values for infinite operating time in the ANS standard 1971.	- ANS standard 1971 was installed. (*2)
8. Gamma energy redistribution	I. A. 4	The fraction of the gamma energy deposited in the fuel shall be justified by a suitable calculation.	- Appropriate input is used as described in Section 4.1
9. Metal water reaction rate	I. A. 5	Influence of the metal/water reaction shall be calculated using the Baker-Just equation. The reaction shall be assumed not to be steam limited. The inside of the cladding shall be assumed to react after the rupture.	- Baker-Just equation was installed. (*2)

(*1) 10 CFR Part 50, Appendix K, “ECCS Evaluation Models.”

(*2) New function of M-RELAP5

Table 2-1(2/5) Appendix K Requirements and Compliance of M-RELAP5

Appendix K Requirement	Ref.(*1)	Acceptable Limits	Approach of M-RELAP5
10. Reactor internal heat transfer	I. A. 6	Heat transfer from piping, vessel walls, and non-fuel internal hardware shall be taken into account.	- Appropriate input is used as described in Section 4.1.
11. SG heat transfer	I. A. 7	Heat transferred between primary and secondary systems through heat exchangers shall be taken into account.	- Appropriate input is used as described in Section 4.1.
12. Cladding swelling & rupture	I. B	Cladding swelling and rupture calculations shall be based on applicable data in such a way that the degree of swelling and incidence of rupture are not underestimated. The gap conductance shall be varied in accordance with changes in gap dimensions and any other applicable variables.	- Cladding swelling and rupture model for ZIRLO™ alloy was installed. (*2) - Gap conductance calculation for rupture node was installed. (*2)
13. Break characteristics	I. C. 1a	A spectrum of possible break shall be considered.	- **Sensitivity study is performed in Section 5.1 through 5.3.**
14. Discharge model	I. C. 1b	Two-phase discharge rate shall be calculated using the Moody model with at least three values of a discharge coefficient. Discharge coefficient will span 0.6 to 1.0 or even a lower value if a maximum PCT may be calculated at such values.	- The Moody model was installed. (*2)
15. ECC water bypass	I. C. 1c	ECC water shall be subtracted from the reactor vessel inventory during the bypass period. The end-of-bypass definition shall be justified by a suitable combination of analysis and experimental data.	- This requirement is for LBLOCA, and is not for SBLOCA.
16. Noding near break and ECC water injection points	I. C. 1d	Noding near break and ECC water injection point shall be chosen to permit a reliable analysis of the thermodynamic history in these regions.	- **Sensitivity study for noding near break point and near ECC injection point are performed in Section 5.4.** -

(*1) 10 CFR Part 50, Appendix K, "ECCS Evaluation Models."

(*2) New function of M-RELAP5

Table 2-1(3/5) Appendix K Requirements and Compliance of M-RELAP5

Appendix K Requirement	Ref.(*1)	Acceptable Limits	Approach of M-RELAP5
17. Frictional pressure drop	I. C. 2	The frictional losses shall be calculated using models that include Reynolds number dependency, and realistic two-phase friction multipliers that have been adequately verified.	- Appropriate input is used as described in Section 4.1.
18. Momentum equation	I. C. 3	Momentum equation shall include temporal change of momentum; momentum convection; area change of momentum flux; momentum change due to compressibility; pressure losses due to wall friction, and area change; and gravitational acceleration.	- Appropriate input is used as described in Section 4.1.
19. Critical heat flux	I. C. 4	Correlations developed from appropriate steady state and transient-state experimental data are acceptable. The computer programs shall contain suitable checks to assure that the physical parameters are within the range of parameters specified for use of the correlations.	- CHF correlation incorporated in RELAP5-3D satisfies this requirement. Additional validation was performed.
20. Return to nucleate boiling	I. C. 4e	After CHF is predicted during blowdown, the calculation shall not use nucleate boiling heat transfer correlations subsequently during the blowdown.	- The logic to prevent return to nucleate boiling during blowdown was installed. (*2)
21. Post-CHF heat transfer correlation	I. C. 5	Transition and film boiling correlation, compared to applicable steady-state and transient-state data, shall be shown to predict values of heat transfer coefficient equal to or less than the mean value of data throughout the range of parameters for which the correlations are to be used. The Dougall-Rohsenow correlation under conditions where nonconservative predictions of heat transfer result will no longer be acceptable.	- Post-CHF heat transfer correlation incorporated in RELAP5-3D satisfies this requirement. Additional validation was performed.

(*1) 10 CFR Part 50, Appendix K, “ECCS Evaluation Models.”

(*2) New function of M-RELAP5

Table 2-1(4/5) Appendix K Requirements and Compliance of M-RELAP5

Appendix K Requirement	Ref.(*1)	Acceptable Limits	Approach of M-RELAP5
22. Return to transition boiling	I. C. 5b	Transition boiling heat transfer shall not be used during the blowdown after the temperature difference between the clad and the saturated fluid first exceeds 300°F.	- The logic to prevent return to transition boiling during blowdown was installed. (*2)
23. Pump modeling	I. C. 6	The pump model for the two-phase region shall be verified by applicable two-phase pump performance data.	- Appropriate input is used as described in Section 4.1.
24. Core flow distribution	I. C. 7	The flow rate through the hot region of the core during blowdown shall be calculated as a function of time considering cross flow between regions and any flow blockage due to cladding swelling or rupture.	- Appropriate input is used as described in Section 4.1.
25. Single failure criterion	I. D. 1	The most damaging single failure of ECCS equipment shall be considered.	- **Sensitivity study is performed in Section 5.6.**
26. Containment pressure	I. D. 2	The containment pressure used during reflood shall not exceed a pressure calculated conservatively for this purpose.	- Appropriate input is used as described in Section 4.1.
27. Reflood rate	I. D. 3	The rate of reflooding of core shall be calculated by an acceptable model that takes into consideration the thermal and hydraulic characteristics of the core and of reactor systems.	- Small break core recovery due to ECC water injection or loop seal clearance is modeled.
28. ECC water/steam interaction	I. D. 4	The thermal-hydraulic interaction between steam and all emergency core cooling water shall be taken into account in calculating the core reflooding rate.	- Appropriate noding is used as described in Section 3
29. Refill/Reflood heat transfer	I. D. 6	For reflooding rates of 1 in/s or higher, heat transfer shall be used based on applicable experimental data. When For reflooding rates are 1 in/s, heat transfer calculation shall be based on the assumption that cooling is only by steam.	- Small break core recovery due to ECC water injection is modeled.

(*1) 10 CFR Part 50, Appendix K, "ECCS Evaluation Models."

(*2) New function of M-RELAP5

Table 2-1(5/5) Appendix K Requirements and Compliance of M-RELAP5

Appendix K Requirement	Ref.(*1)	Acceptable Limits	Approach of M-RELAP5
30. Solution convergence	II. 2	For each computer program, solution convergence shall be demonstrated by studies of system modeling or noding and calculational time steps.	**- Sensitivity study is performed in Section 5.5.**
31. Appropriate sensitivity studies	II. 3	Appropriate sensitivity studies shall be performed for each evaluation model, to evaluate the effect on the calculated results of variations in noding, phenomena assumed in the calculation to predominate, including pump operation or locking, and values of parameters over their applicable ranges. For items to which results are shown to be sensitive, the choices made shall be justified.	**- Sensitivity study is performed in Section 5.5.**

(*1) 10 CFR Part 50, Appendix K, “ECCS Evaluation Models.”

(*2) New function of M-RELAP5

3.0 PLANT MODELING

3.1 M-RELAP5 Plant Noding of US-APWR

This chapter describes the plant modeling using M-RELAP5 to simulate the US-APWR during an SBLOCA and focuses on the systems and components and how those systems are represented in the input model. The following subsystems of the US-APWR are modeled:

- Primary System (Reactor and Core, Reactor Coolant System, Emergency core cooling system)
- Secondary System (Main steam system, Main feedwater system (MFWS), Emergency feedwater system (EFWS))
- Containment Vessel

The primary system includes the reactor vessel, the steam generator (SG) primary side, the reactor coolant pumps, the pressurizer, the main coolant pipe and pressurizer surge line, the accumulators and direct vessel injection of safety injection (SI) pumps. The secondary system includes the SG secondary side main feedwater systems, main steam systems, emergency feedwater systems, and safety valves.

M-RELAP5 plant noding of the US-APWR is depicted in Figure 3-1. The definition of the symbols used in the nodalization diagram is as follows:

- **Component type** is expressed by the first alphabetic characters such as AN for annulus, P for pipe, B for branch, SV for single volume, SJ for single junction, ACC for accumulator, TV for time dependent volume, TJ for time dependent junction, MJ for multiple junction, and SP for separator.
- **Component number** is expressed by the three-digit number following the component type such as AN103 which means an annular component numbered 103. The same scheme is applied to single volumes and junctions such as SV170 and SJ203.
- **Component internal volume numbers** are expressed by the two-digit number enclosed in parentheses. For example, P116, pipe component numbered 116, has 20 internal volumes numbered from 01 to 20.

3.2 Reactor Vessel Modeling

The vessel nodalization of M-RELAP5 is shown in Figure 3-2. **[**

] During normal operation, the coolant enters from the cold legs into the downcomer, goes downward to the lower plenum and enters the bottom of the core with splitting small fraction into the neutron reflector channels. Then the coolant is heated in the core region before mixing in the upper plenum, and flows into the steam generator tubes through the hot legs.

The downcomer is annular region between the reactor vessel inner surface and outer surface of the core barrel from the bottom of the lower core support plate to the top of the upper core support plate flange. **[**

]

[

]

[

]

[

]

[

]

[

]

[

]

[

]

[

]

[

]

[

]

[

]

3.3 Reactor Coolant System Modeling

The reactor coolant system (RCS) provides the reactor cooling and energy transport functions. The RCS consists of the reactor vessel, the steam generators, the reactor coolant pumps, the pressurizer, the reactor coolant pipes, and valves. Figure 3-3 shows the nodalization of the broken loop, which is the loop with the pressurizer on it. Figure 3-4 shows the nodalization of the intact loop that 3 loops are lumped into. Following explanation of noding is for broken loop because nodalization of broken loop is same as that of intact loop except for the existence of the pressurizer and the break point.

3.3.1 Steam Generator

[

]

[

]

[

]

[

]

[ ]

[

]

3.3.2 Reactor Coolant Pump

[

]

3.3.3 Reactor Coolant Pipe

[

]

[

]

[

]

3.3.4 Pressurizer and Surge Line

[ ]

[

]

3.3.5 Emergency Core Cooling System

The emergency core cooling system (ECCS) injection nodalization is shown in Figure 3-5. ECCS includes the accumulator system and high-head injection system.

[

]

[

]

3.3.6 Break

The break is shown on Figure 3-3. [

]

Figure 3-1 Nodalization of Primary System for US-APWR SBLOCA Analysis

Figure 3-2 Nodalization Scheme of Reactor Vessel

Figure 3-3 Nodalization of the Broken Loop

Figure 3-4 Nodalization of the Intact Loop

Figure 3-5 Nodalization of the ECCS Injection

4.0 ANALYSIS CONDITIONS AND CASES

4.1 Main Plant Analysis Conditions for US-APWR

The major plant parameters used in the US-APWR small break LOCA licensing analysis are listed in Table 4.1-1. The initial and boundary conditions are conservatively established as follows to maximize the PCT in a manner consistent with the spirit of 10 CFR 50 Appendix K.

4.1.1 Plant Operating Conditions

・Pressurizer Pressure

Nominal value plus 30 psi, 2280psia, is assumed, considering measurement uncertainties.

・Primary Coolant Flow Rate

Thermal design flow corresponding to the 10 percent SG tube plugging, 112,000 gpm/loop, is assumed.

・RCS Average Temperature

Nominal value plus 4 ^{o}F, 587.8 ^{o}F, is assumed, considering measurement uncertainties.

4.1.2 Core and Fuel

・Core Power

The core power is assumed to be 102 percent of the rated power, 4540 MWt, taking account of calorimetric error.

・Hot Rod Peaking Factor F_Q

A conservative design value bounding the value for hot rod peaking factor, 2.6, is assumed as an analysis condition.

・Hot Channel Enthalpy Rise Factor $F_{\Delta H}$

A conservative design value bounding the value for hot channel enthalpy rise factor, 1.78, is assumed as analysis condition.

・Axial Power Shape

Top-Skew (double-hump) power shape is employed. It minimizes the core level swell while maximizing vapor superheating and fuel rod heat generation at uncovered elevation. Axial shape is conservatively biased to be consistent with F_Q and $F_{\Delta H}$ of the hot rod. Figure 4.1-1 shows the hot rod power shape used to conduct the SBLOCA analysis. **[**

]

· Initial Stored Energy in Fuel

The fuel rod burnup is assumed to be beginning of life (BOL). It provides the maximum (conservative) initial stored energy in the fuel. In addition, for the hot rod pellet temperature, the highest value considering uncertainties corresponding to the prediction model and fabrication is also assumed for conservatism.

· Fission Heat

Reactivity resulting from fuel temperature and void fraction changes in the core is given to maximize core power by assuming conservative coefficients for Doppler temperature and moderator density. **[**

]

Figure 4.1-2 shows the assumed moderator density coefficient. Control rod insertion is assumed to occur in the analysis. Single highest-reactivity-worth Rod Cluster Control Assemblies (RCCA) is conservatively assumed to fail to insert.

· Actinide Decay Heat

The code uses the ANSI/ANS 5.1-1979 standard for decay heat from actinide series, which is accepted in Section 9.2.5 Ultimate Heat Sink (Rev. 3) of NUREG-0800 (Ref. 4-2).

· Fission Product Decay Heat

The code uses 1.2 times the values for infinite operating time in the ANS Standard decay heat model of 1971 version.

· Gamma Energy Redistribution

The effect of gamma energy redistribution for hot rod is considered by multiplying local heat generation rate by a conservative value 0.974.

4.1.3 Reactor Vessel

・Core Flow Distribution

The total flow rate of the core is ninety-one percent of the RCS flow rate, the minimum flow rate of the core design flow. The core flow is divided into two regions, average core channel and hot core channel corresponding to one fuel assembly. The cross flow between the average and hot core flow channels is modeled by flow junctions connecting two volumes of at the same elevation as described in Section 3.

・Reactor Vessel Upper Head Temperature

Nominal temperature of the reactor vessel upper head is designed to be equal to the cold leg value, 554.6 ^{o}F. Nominal value plus 4 ^{o}F, which is measurement uncertainty of cold leg temperature, is assumed

4.1.4 Steam Generator

・Steam Generator Tube Plugging

10 percent SG tube plugging is assumed, which is overly estimated as a maximum tube plugging ratio in the next several core cycles.

・Steam Generator Heat Transfer

Main steam line is assumed to be isolated on turbine trip, while main feed water flow is assumed to be kept at the initial value until the main feedwater isolation valves close, to maximize the stored energy in the steam generators. Minimum emergency feed-water flow is assumed, and the main steam safety valves are assumed to open at their maximum set point value, to minimize the heat transfer from primary to secondary side. In addition, two EFWS trains are assumed to be lost. However, all the 4 steam generators are supplied with EFW flow by 2 EFW pumps through the tie-lines.

4.1.5 Pressurizer

・Pressurizer Water Level

The nominal value of the pressurizer level is assumed.

4.1.6 RCP

・Pump Characteristics

The pump head during the transient is calculated based on the fluid conditions using pump characteristics expressed with homologous curves. The pump coast-down is calculated using the angular momentum equation with the torque and the momentum of inertia as input for the calculations. As discussed in US-APWR Large Break LOCA Analysis Topical Report (Ref. 4-3), **[**

]

4.1.7 High Head Injection System (HHIS)

・Safety Injection Flow Characteristics

Uncertainty of the SI system is conservatively accounted for in the SI flow characteristics, which result in the minimum delivered SI line flow available to the RCS.

・Safety Injection Water Temperature

Higher bounding temperature throughout the LOCA transient is assumed. **[**

] This treatment gives conservative condition to calculate the PCT.

4.1.8 Accumulator

・Accumulator Water Temperature

Accumulator water temperature is assumed to be equal to the highest containment atmospheric temperature, 120^{o}F, allowed in the normal plant operation for conservatism. The temperature is also assumed to be constant throughout the transient.

・Accumulator Pressure

The lowest value allowed in the normal plant operation, 600 psia, is assumed.

・Accumulator Water Volume
The nominal value, 2150 ft^3, is assumed. This value is the initial water volume reduced by the ineffective water.

4.1.9 Signals

・Reactor Trip
Reactor trip signal due to the low pressurizer pressure, 1860 psia is generated during the US-APWR small break LOCA transient. The reactor trip signal initiates RCCAs insertion by gravity with a delay time of 1.8 seconds. In the analyses, the single highest-reactivity-worth RCCA is conservatively assumed to fail to insert.

・Turbine Trip
Turbine trip simultaneous with reactor trip is assumed. It is assumed that the main steam line is isolated with 1.8-second delay and the main feedwater is isolated with 8-second delay associated with the reactor trip, resulting in maximum SG stored energy.

・Safety Injection Initiation
Safety injection is initiated due to ECCS signal on low pressurizer pressure, which is generated when the setpoint of 1760 psia is reached. Uncertainty in the pressure setpoint is conservatively considered. Maximum delay time for safety injection initiation, 118 seconds, is assumed in consistency with loss of offsite power (LOOP) assumption.

4.1.10 Single Failure

The limiting single failure in the small break LOCA analysis is assumed, which is the loss of one entire train of ECCS, with one train out of service for maintenance. In this case, only two SI pumps are available.

4.1.11 Boundary Conditions

・Break Location and Type
A split break is postulated to occur at the cold leg piping of a loop.

・Break Size
The break size giving the highest PCT is determined based on the sensitivity analysis results

of this report.

· Containment Pressure

The containment pressure is assumed to be atmospheric throughout the transient. In SBLOCA, RCS pressure remains high, and thus break flow remains at critical flow conditions. Consequently the containment pressure does not affect the break flow behavior.

· Offsite Power

LOOP is assumed to occur simultaneously with the reactor trip, resulting in the delay of SI pumps and EFW pumps operations. In case of LOOP, RCPs automatically trip after 3 seconds time delay.

4.1.12 Others

· Reactor Internal Heat Transfer

Release of stored energy from the RCS component metal walls to the RCS fluids is considered, assuming that these metal walls are isolated from the containment atmosphere.

· Frictional Pressure Drop

Appropriate friction factor is used as described in Section 6.2.4 of US-APWR Small Break LOCA Analysis Topical Report (Ref. 4-4).

· Momentum Equation

Appropriate effects are included in the equation as described in Section 6.2.3 of US-APWR Small Break LOCA Analysis Topical Report (Ref. 4-4).

· ECC Water/Steam Interaction

Appropriate noding scheme is used as described in Section 3.

Table 4.1-1

US-APWR Major Plant Parameter Inputs Used in the

Appendix-K based Small Break LOCA Analysis

Parameters	Values
Core and Fuel Rod Condition	
Core Power	102% of rated power (4540 MWt)
Peaking factor	F_Q = 2.6
Hot channel enthalpy rise factor	$F_{\Delta H}$ = 1.78
Axial power shape	Top-Skew (double humps), as shown in Figure 4.1-1
Fuel rod burnup	Beginning of Life (BOL)
Fuel assembly type	17 X 17 ZIRLO^{TM} cladding
Plant Operating Condition	
Fraction of SG tube plugged	10% (maximum)
RCS average temperature	Nominal value + 4°F (587.8°F)
Pressurizer pressure	Nominal value + 30 psia (2280 psia)
Primary coolant flow	Thermal design flow (112,000 gpm/loop)
RV upper head temperature	Nominal (T_{cold})
Pressurizer level	Nominal
Accumulator temperature	Maximum (120°F)
Accumulator pressure	Minimum (600 psia)
Accumulator water volume	Nominal (2152 ft^3)
Accident Boundary Condition	
Break location	Cold leg
Break type	Split
Offsite power	Not available
Reactor trip signal	Low pressurizer pressure
Reactor trip signal delay time	1.8 seconds
RCP trip (at loss-of-offsite power)	3 seconds after reactor trip
ECCS actuation	Low pressurizer pressure
Safety injection delay	Maximum (118 seconds)
Number of available SI pumps	2 pumps for cold leg break 1 pump for DVI line break
Safety injection flow	Minimum
Safety injection water temperature	RWSP temperature rise is modeled

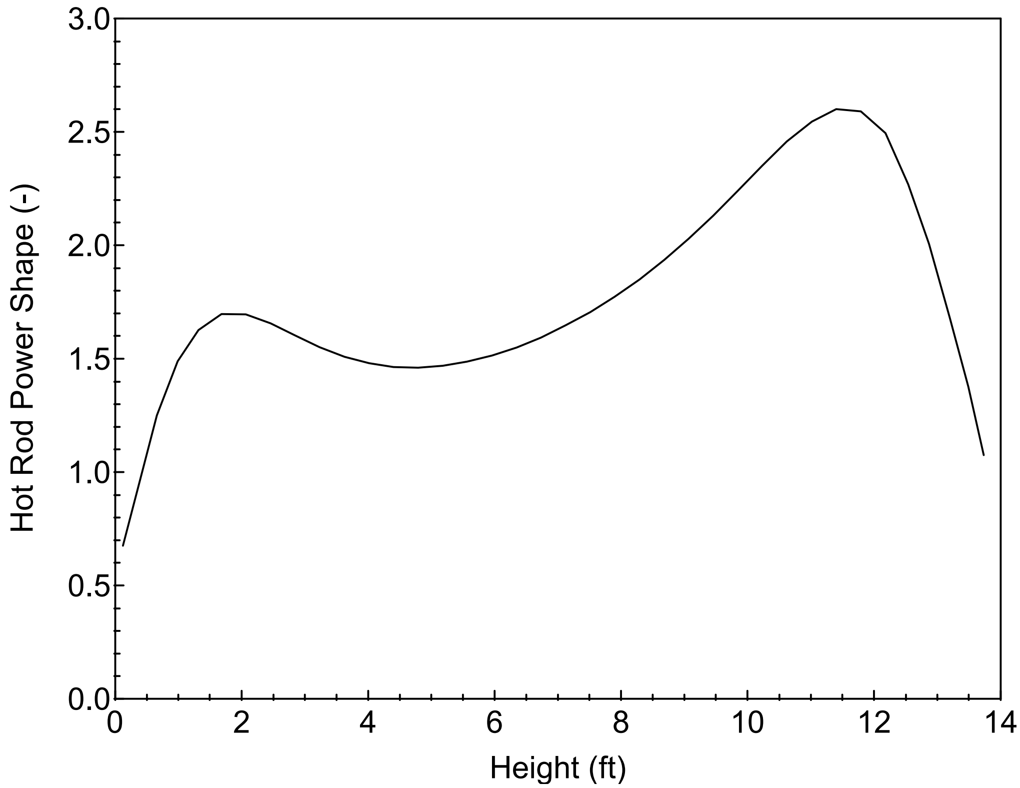

Figure 4.1-1 Hot Rod Power Shape Used for Small Break LOCA analysis

Figure 4.1-2 Moderator Density Reactivity Coefficient

4.2 Sensitivity Study Cases and Analysis Conditions

4.2.1 Sensitivity Study Cases

The following sensitivity study results are shown in this report according to the requirements of Appendix-K and SRP 15.6.5.

Sensitivity study cases	Requirement of Appendix-K
• Break spectrum including locations and orientations*	I.C.1a Break characteristics
• Noding near break point	I.C.1d Noding near break point
• Noding near the DVI injection point	I.C.1d Noding near ECC water injection point
• Time step size	II.2 Solution convergence
• Noding of SG U-tube and crossover leg	II.2 Solution convergence
• No Single failure assumption	II.3 Appropriate sensitivity studies
• Offsite power available case	II.3 Appropriate sensitivity studies

(NOTE) *: Requirement of SRP 15.6.5

4.2.2 Break spectrum analyses

Break spectrum analyses were performed in three steps. First, the sensitivity study for representative break locations (cold leg, hot leg, crossover leg, DVI line and pressurizer steam phase) were performed to confirm the limiting break location is cold leg. For the cold leg, hot leg, and crossover leg, 2-inch break and 1-ft^2 break were performed to cover the range of small break LOCA. For the DVI break and pressurizer steam phase break, pipe break at largest diameter were assumed.

Second, break spectrum analyses for the cold leg break with integer inch diameter were performed to obtain the break size spectrum for loop-seal PCT and boil-off PCT. Break size from 1-inch through 13-inch and 1-ft^2 (13.5-inch) break were calculated.

Then, additional break spectrum analyses with 0.5-inch intervals in break diameter were performed to determine the final limiting break size for loop-seal PCT and boil-off PCT. In these sensitivity calculations, the effects of break orientations (bottom, top, side, and homogeneous) were also considered.

The noding of the cold leg break case is explained in Section 3. Figures 4.2-1 through 4.2-4 show the noding for the hot leg break, crossover leg break, DVI break, and pressurizer steam phase break, respectively.

[

]

For the break orientation sensitivity calculations, bottom break, top break and side break were considered using break orientation related option associated with horizontal stratified flow model of M-RELAP5.

4.2.3 Noding sensitivity study

Figure 4.2-5 shows the nodalization for noding sensitivity study near the break point. [

] Two cases of 7.5-inch break (top break) and 1 ft^2 break (top break) were calculated.

Figure 4.2-6 shows the nodalization for the sensitivity study for SG U-tube and crossover leg noding. [

]

[ ] 7.5-inch break at the top of the pipe was calculated for the effect for Loop-seal PCT.

Figure 4.2-7 shows the nodalization for the sensitivity study near the injection point of DVI. **[**

] Two cases of 7.5-inch break (top break) and 1 ft^2 break (top break) were calculated.

4.2.4 Time step size sensitivity study

Time step size sensitivity calculations were performed for the following cases:

- 7.5-inch top break (limiting case for Loop-seal-PCT)
- 1-ft^2 top break (limiting case for Boil-off -PCT)
- DVI line break, 3.4-inch break

For 7.5-inch break and 1-ft^2 break, the maximum time step size is **[ ]** for the base case and **[ ]** for the sensitivity study case. For DVI break, the maximum time step size is **[ ]** for the base case and **[ ]** for the sensitivity study case.

4.2.5 Additional sensitivity study

No single failure of SI pump case and offsite power available case were performed as additional sensitivity study cases.

For no single failure of SI pump case, only one train out of service was assumed like the base case so that 3 SI pumps and 3 EFW pumps were assumed to be available. Two cases of 7.5-inch top break and 1-ft^2 top break were calculated.

For offsite power available case, reduction of the time delay for the actuation of SI pumps and EFW pumps was assumed as follows:

	Base case (LOOP)	Offsite power available case
Time delay of SI pumps (sec)	118	18
Time delay of EFW pumps (sec)	133	60

For the sensitivity case, RCP trip was assumed to occur 15 seconds after the ECCS actuation signal, while 3-second delay time after LOOP is assumed for the base case. Two cases of 7.5-inch top break and 1-ft^2 top break were calculated.

4.2.6 Summary of sensitivity study cases

Table 4.2-1 shows the summary of the break spectrum sensitivity study cases and Table 4.2-2 shows the summary of the other sensitivity study cases performed in this report.

Table 4.2-1 Summary of Break Spectrum Sensitivity Study Cases

Break Location	Break Size or Break Area	Break Orientation
Cold leg	1-inch	bottom
	2-inch	bottom
	3-inch	bottom
	4-inch	bottom
	5-inch	bottom
	6 inch	bottom, top, side
	6.5-inch	bottom, top, side
	7-inch	bottom, top, side
	7.5-inch	bottom, top, side
	8-inch	bottom, top, side
	9-inch	bottom
	10-inch	bottom
	11-inch	bottom
	12-inch	bottom, top, side
	13-inch	bottom, top, side
	1-ft^2 (=13.5-inch)	bottom, top, side
Hot leg	2-inch	bottom
	1-ft^2 (=13.5-inch)	bottom
Crossover leg	2-inch	bottom
	1-ft^2 (=13.5-inch)	bottom
DVI injection line	3.4-inch	N/A
Pressurizer steam phase	about 6.7-inch	N/A

Table 4.2-2 Summary of Sensitivity Study Cases

Sensitivity Study Cases	Conditions of Base case	Conditions of Sensitivity Study cases	Break conditions
Noding near break point	Base noding	Finer noding of broken cold leg	- 7.5-inch top break - 1-ft^2 top break
Noding of SG U-tube and crossover leg	Base noding	Finer noding of SG U-tube and crossover leg	- 7.5-inch top break
Time step size	Base maximum time step	Half maximum time step	- 7.5-inch top break - 1-ft^2 top break - DVI break
No single failure case	Single failure of SI pump with one train out of service case	No single failure of SI pump, with one train out of service case	- 7.5-inch top break - 1-ft^2 top break
Offsite power available case	Loss of offsite power	Offsite power available	- 7.5-inch top break - 1-ft^2 top break

Figure 4.2-1 Nodalization for Hot Leg Break

Figure 4.2-2 Nodalization for Crossover Leg Break

Figure 4.2-3 Nodalization for DVI Break

Figure 4.2-4 Nodalization for Pressurizer Steam Phase Break

Figure 4.2-5 Nodalization for Noding Sensitivity Study near Break Point

Figure 4.2-6 Nodalization for Sensitivity Study for SG U-tube and Crossover Leg noding

Figure 4.2-7 Nodalization for Sensitivity Study near the injection point of DVI

5.0 ANALYSIS RESULTS

5.1 Break Location Sensitivity Study

At first, the sensitivity analyses for representative break locations (cold-leg, hot-leg, crossover-leg, DVI line and pressurizer steam phase) were performed to confirm that the limiting break location is at the cold-leg. Bottom orientation breaks with sizes of 2-inch and 1-ft^2 are assumed for the cold-leg, hot-leg, and crossover-leg break cases calculation to cover the range of SBLOCAs. Afterwards, the sensitivity analyses for DVI-line break and pressurizer steam-phase breaks were carried out, assuming the largest diameter.

5.1.1 Break location sensitivity for cold-leg, hot-leg and crossover-leg

(1) Results of 2-inch cold-leg bottom orientation break

Table 5.1.1.a-1 shows the sequence of events and Table 5.1.1.a-2 shows the main results. Figure 5.1.1.a-1 shows the pressure transient in the reactor coolant system (RCS) represented by the pressure response of the pressurizer. Immediately after the break the RCS depressurizes, causing the coolant from the pressurizer to flow into the loop. This results in the decrease in pressurizer level. A reactor trip signal is generated when the low pressurizer pressure setpoint of 1860 psia is reached.

Figure 5.1.1.a-2 shows normalized core power for 2-inch cold-leg bottom orientation SBLOCA. The reactor trips at 81 seconds due to the low pressurizer pressure setpoint of 1860 psia. Then, the control rod insertion starts at 83 seconds. Accordingly, the core power decreases as shown in the figure. The insertion of control rod itself is assumed concurrent with turbine trip and main steam isolation. The increase of void fraction in the core also causes the core power to decrease.

The liquid and vapor discharges from the break are shown in Figure 5.1.1.a-3. Early in the transient, the break discharge flow rate is not high enough to overcome the upward flow through the core that is maintained by the coasting RCPs. The figure shows that the discharge is mostly in liquid phase throughout the transient. After 1200 seconds, vapor phase begins to form and discharge from the break as a two-phase mixture.

The ECCS actuation signal is generated when the low pressurizer pressure setpoint of 1760 psia is reached. Figure 5.1.1.a-4 shows that for the 2-inch SBLOCA case, the High Head

Injection System (HHIS) alone provides the core cooling function, through the injection of borated water into the reactor core by the safety injection (SI) pumps. It implies that accumulators injection is not required for this case.

As a result of the break, the coolant inventory of RCS is gradually lost. Figure 5.1.1.a-5 shows that the RCS inventory gradually depletes as the coolant discharges from the break. The SI pumps supplies borated-water into the reactor core to prevent further reduction in inventory. Then the RCS mass inventory of about 300,000 lbm is maintained.

Figure 5.1.1.a-6 shows the collapsed liquid level in the downcomer. For more than 10 minutes after the break, the collapsed level stays at its normal operating level. Then, an abrupt reduction of collapsed level occurs in the downcomer. However, further reduction is prevented by the direct injection of borated-water into the reactor by the SI pumps.

Figure 5.1.1.a-7 depicts that the transient characteristic of collapsed levels in the average core channel, hot assembly channel, as well as in the upper plenum are quite similar, as these parameters fluctuate in the same phase (direction). This figure also shows that there occurs a slight reduction in the collapsed level. The slow pressure transient and immediate SI pumps actuation prevent further core reduction.

Figure 5.1.1.a-8 shows the PCT at all elevations for the hot rod. No heatup occurs after the break.

The hot assembly exit vapor and liquid mass flow rates are shown in Figure 5.1.1.a-9. Mass flow rates of both phases rapidly reduce after the RCP trips due to the loss-of-offsite power (LOOP) assumption. This figure demonstrates that after the blowdown phase ends, two-phase natural circulation is established in the RCS loops with the decay heat being removed by condensation and convection heat transfers to the steam generator secondary side.

(2) Results of 1-ft^2 cold-leg bottom orientation break

Table 5.1.1.a-3 shows the sequence of events and Table 5.1.1.a-4 shows the main result. Figure 5.1.1.a-10 shows the RCS (Pressurizer) pressure transient for 1-ft^2 cold-leg SBLOCA case. Compared to the 2-inch small break case, depressurization rate for the 1-ft^2 case is much higher. The rapid depressurization rate causes quicker reactor trip due to the low pressurizer pressure setpoint of 1860 psia.

The faster pressure reduction causes early reactor trip signal initiation due to the low RCS pressure setpoint. Rapid increase of void fraction in the core causes the core power to decrease before the insertion of control rods. Figure 5.1.1.a-11 shows the normalized core power transient for 1-ft^2 SBLOCA case. The control rod insertion starts at 8.7 seconds. Turbine trip and main steam isolation are assumed concurrent with the control rod insertion. Higher void fraction in the core due to the rapid pressure reduction also helps in reducing the core power.

The liquid and vapor discharges out of the break are shown in Figure 5.1.1.a-12. Early in the transient, the effect of the break discharge flow rate is not strong enough to overcome the upward flow through the core that is maintained by the coasting RCPs. The figure shows that the discharge is mostly liquid phase until about 20 seconds after the break occurs. Later on, vapor phase begins to form and discharge from the break.

Figure 5.1.1.a-13 shows the operational sequence of the safety injection systems of the US-APWR in mitigating a SBLOCA. The pressure transient (depressurization) for the 1-ft^2 small break is considered fast. The quick pressure reduction reaches ECCS signal on the low pressurizer pressure setpoint of 1760 psia and initiates the accumulators to inject the borated water into the RCS through the cold legs. The accumulators operate in large flow rate mode. In parallel, the SI pumps supply the borated water from the refueling water storage pit (RWSP) into the core.

As a result of the larger size break, the coolant inventory of RCS is rapidly lost. Figure 5.1.1.a-14 shows that the RCS inventory depletes quickly as the coolant discharges from the break. The actuation of accumulators and SI pumps prevent further reduction in inventory, so the RCS mass inventory is maintained above 200,000 lbm.

Figure 5.1.1.a-15 shows the collapsed liquid level in the downcomer. Within 100 seconds after the break, the collapsed level quickly decreases. The lost of RCS mass inventory through the break reduces the collapsed level in the downcomer. Further reduction is prevented by the injection of ECC water into the reactor by the SI pumps and accumulator injection.

Figure 5.1.1.a-16 depicts that the transient characteristic of collapsed levels in the average core channel, hot assembly channel, as well as in the upper plenum are quite similar, as these parameters fluctuate in the same phase. This figure also implies that a remarkable core uncovery occurs for the 1-ft^2 SBLOCA. The accumulators injection and ECC water injection by

the SI pumps prevent further core uncovery.

Figure 5.1.1.a-17 shows the PCT at all elevations for the hot rod. The PCT of 1029°F occurs at 153 seconds. This figure demonstrates that the PCT is substantially lower than 2200°F. The cladding temperature then quickly reduces before settling at around 350°F and gradually decreases corresponding to the RCS pressure.

The hot assembly exit vapor and liquid mass flow rates are shown in Figure 5.1.1.a-18. Mass flow rates of both phases rapidly reduce after the RCP trips due to the reactor trip.

(3) Results of 2-inch hot-leg bottom orientation break

Table 5.1.1.b-1 shows the sequence of events and Table 5.1.1.b-2 summarizes the main results. Figure 5.1.1.b-1 through 5.1.1.b-9 present the principal parameters of interest for the 2-inch SBLOCA at the hot-leg. The following transient parameters are presented:

5.1.1.b-1 RCS or pressurizer pressure transient
5.1.1.b-2 Normalized core power
5.1.1.b-3 Liquid and vapor discharges through the break
5.1.1.b-4 Accumulator and safety injection mass flow rates
5.1.1.b-5 RCS mass inventory
5.1.1.b-6 Collapsed level in the downcomer
5.1.1.b-7 Collapsed level in the core and upper plenum.
5.1.1.b-8 PCT at all elevations for hot rod in hot assembly
5.1.1.b-9 Hot assembly exit vapor and liquid mass flow rates

It is concluded that there exists large upward flow through the core, inducing a higher collapsed level. Hence, similar with the 2-inch cold leg break, no heatup occurs after the break in this case.

(4) Results of 1-ft^2 hot-leg bottom orientation break

Table 5.1.1.b-3 shows the sequence of events and Table 5.1.1.b-4 tabulates the main results. Figure 5.1.1.b-10 through 5.1.1.b-18 present the principal parameters of interest for the 1-ft^2 SBLOCA at the hot-leg. The following transient parameters are presented:

5.1.1.b-10 RCS or pressurizer pressure transient
5.1.1.b-11 Normalized core power
5.1.1.b-12 Liquid and vapor discharges through the break
5.1.1.b-13 Accumulator and safety injection mass flow rates

5.1.1.b-14 RCS mass inventory
5.1.1.b-15 Collapsed level in the downcomer
5.1.1.b-16 Collapsed level in the core and upper plenum.
5.1.1.b-17 PCT at all elevations for hot rod in hot assembly
5.1.1.b-18 Hot assembly exit vapor and liquid mass flow rates

This case also generates a higher collapsed level in the core induced by the high upward flow through the core. Then, core heatup is prevented.

(5) Results of 2-inch crossover-leg bottom orientation break

Table 5.1.1.c-1 shows the sequence of events and Table 5.1.1.c-2 shows the main results. Figure 5.1.1.c-1 through 5.1.1.c-9 present the principal parameters of interest for the 2-inch SBLOCA at the crossover-leg. The following transient parameters are presented:

5.1.1.c-1 RCS or pressurizer pressure transient
5.1.1.c-2 Normalized core power
5.1.1.c-3 Liquid and vapor discharges through the break
5.1.1.c-4 Accumulator and safety injection mass flow rates
5.1.1.c-5 RCS mass inventory
5.1.1.c-6 Collapsed level in the downcomer
5.1.1.c-7 Collapsed level in the core and upper plenum.
5.1.1.c-8 PCT at all elevations for hot rod in hot assembly
5.1.1.c-9 Hot assembly exit vapor and liquid mass flow rates

The same as the cold-leg and hot-leg cases, no heatup occurs for the 2-inch cross-over legs.

(6) Results of 1-ft^2 crossover-leg bottom orientation break

Table 5.1.1.c-3 shows the sequence of events and Table 5.1.1.c-4 shows the main results. Figure 5.1.1.c-10 through 5.1.1.c-18 present the principal parameters of interest for the 1-ft^2 SBLOCA at the crossover-leg. The following transient parameters are presented:

5.1.1.c-10 RCS or pressurizer pressure transient
5.1.1.c-11 Normalized core power
5.1.1.c-12 Liquid and vapor discharges through the break
5.1.1.c-13 Accumulator and safety injection mass flow rates
5.1.1.c-14 RCS mass inventory
5.1.1.c-15 Collapsed level in the downcomer
5.1.1.c-16 Collapsed level in the core and upper plenum.

5.1.1.c-17 PCT at all elevations for hot rod in hot assembly

5.1.1.c-18 Hot assembly exit vapor and liquid mass flow rates

These results are about in between the cold-leg and hot-leg cases. Several heatup occurs, however they do not increase higher than the cladding temperature at the initiation of the break. Sufficiently large upward flow through the core exists that results in a higher core collapsed level. The accumulator injections and SI pumps also contribute to preventing any PCT occurrence.

(7) Summary of results for cold-leg, hot-leg and crossover-leg breaks

The results show that cold-leg is the limiting break location, because heatup does not occur after the hot-leg and crossover-leg breaks.

5.1.2 Results of DVI line break

Table 5.1.2-1 shows the sequence of events and Table 5.1.2-2 shows the main results. Figure 5.1.2-1 shows the immediate depressurization of the RCS after the break, causing the coolant to flow out from the pressurizer into the loop resulting in a decrease in the pressurizer level. At 25.8 seconds, the low pressurizer pressure setpoint of 1860 psia is reached then the reactor trip signal is generated.

Figure 5.1.2-2 shows the normalized core power transient after the reactor trip, which is caused by the low RCS pressure following the DVI-line SBLOCA. Control rod insertion starts at 27.6 seconds. Turbine trip and main steam isolation are assumed to occur concurrent with the control rod insertion.

Figure 5.1.2-3 presents the liquid and vapor discharges through the break. In the first 700 seconds, mostly liquid-phase flows out the break then it diminishes. Subsequently, only vapor-phase discharges from the break that characterizes the DVI-line SBLOCA case.

Figure 5.1.2-4 explains that only the high pressure safety injection pumps are required to supply borated water into the reactor core. This particular DVI-line small break does not demand any accumulator injection.

Figure 5.1.2-5 shows that a substantial loss of RCS mass inventory occurs following the DVI-line small break. The loss is then compensated by the injected borated water by the SI pumps, as the discharge mainly consists of steam-phase.

Figure 5.1.2-6 presents the collapsed level transient in the downcomer following a DVI-line SBLOCA. After about 300 seconds following the break, the collapsed level decreases step wise. The collapsed level goes up again after the HHIS is actuated.

Figure 5.1.2-7 illustrates the collapsed level transient in the core and upper plenum following a DVI-line SBLOCA. The collapsed level comes down about 4-ft below the core top. The behavior of collapsed levels in the upper plenum and in the core is related to each other, except that they fluctuate in different phase (direction).

Figure 5.1.2-8 shows maximum cladding temperature for the hot rod in the hot assembly, which shows that core heat does not happen.

5.1.3 Results of the Steam Phase Pressurizer break

Table 5.1.3-1 shows the sequence of events and Table 5.1.3-2 shows the main results. Figure 5.1.3-1 shows that following a steam-phase break of the pressurizer, the RCS depressurizes rapidly to the low pressurizer pressure setpoint of 1860 psia, actuating a reactor trip signal. Further decrease in RCS pressure actuates the safety injection system at 1760 psia.

Figure 5.1.3-2 shows the normalized core power transient following the pressurizer steam-phase SBLOCA.

Figure 5.1.3-3 presents the plot of liquid and vapor discharges through the break for the steam-phase small break on the pressurizer. The transient is characterized by a high flow rate liquid phase discharge that steeply diminishes within 300 seconds. The liquid-phase discharge flow rate then increases before almost settling at relatively lower flow rate. The dotted lines indicate that vapor-phase presents in the mixture from the beginning of the break. This parameter transient corresponds to the RCS mass inventory described later. There is a time frame (i.e. between 300 and 600 seconds) where the vapor-phase is dominant in the discharge flow.

Figure 5.1.3-4 demonstrates that the SI system comes to function at 7.1 seconds when the low pressurizer pressure setpoint of 1760 psia is reached. The SI pumps supply borated water makeup into the core at 125 seconds. Further reduction in the RCS pressure actuates the accumulator injection that initially works at large flow rate mode. Accumulator injection flow oscillation characterizes the steam phase SBLOCA on the pressurizer.

As a result of the break, the coolant inventory of RCS is gradually lost. Figure 5.1.3-5 shows that the RCS inventory steadily lessens as the coolant discharges. However, the actuation of SI pumps supply borated-water into the reactor core to prevent further reduction and maintain the RCS mass inventory at about 300,000 lbm.

Figure 5.1.3-6 displays the plot of collapsed level transient in the downcomer following a pressurizer steam phase small break.

Figure 5.1.3-7 clarifies that the transient characteristic of collapsed levels in the average core channel, hot assembly channel, as well as in the upper plenum are quite similar, as these parameters fluctuate almost in the same phase and magnitude.

Figure 5.1.3-8 demonstrates that there is no core heatup as a result of this transient.

The hot assembly exit vapor and liquid mass flow rates are shown in Figure 5.1.3-9. Mass flow rates of both phases reduce after the RCP trips following the reactor trip. This figure proves that after the blowdown phase ends, two-phase natural circulation takes place in the RCS loops with to remove the decay heat by condensation and convection heat transfers.

Figure 5.1.3-10 shows the pressurizer collapsed level, which is one of the parameters of interest for this SBLOCA case. Initially, the collapsed level sharply increases indicating the break occurs in the steam-phase region. It then decreases as the RCS pressure decreases and pressurizer inventory also losses. The collapsed level recovers due to the SIS and accumulators injection into the RCS loops.

5.1.4 Summary of results of break locations sensitivity analysis

The results of the sensitivity study for representative break locations (cold-leg, hot-leg, crossover-leg, DVI line and pressurizer steam phase) confirm that the limiting break location is cold-leg. In the following sections, the results of break spectrum analyses for cold-leg break are discussed.

Table 5.1.1.a-1 Sequence of Events for 2-inch Break (Bottom) (Break Location Sensitivity Study for Cold-leg Break)

Event	Time (sec)
Break occurs; blowdown initiation	0.0
Reactor trip (loss-of-offsite power is assumed)	81
Control rod insertion starts	82
Main steam isolation	82
RCP trip	84
Main feedwater isolation	89
ECCS actuation signal	103
Main steam safety valve open	116
Emergency Power Source initiates	206
High Head Injection System begins	236
Emergency feedwater flow begins	236
Accumulator injection begins	not actuated
Fuel cladding starts heating up	not occur
Peak Cladding Temperature occurs	lower than the initial temperature
Fuel cladding rewets	N/A

Table 5.1.1.a-2 Core Performance Results for 2-inch Break (Bottom) (Break Location Sensitivity Study for Cold-leg Break)

	Values
Peak Cladding Temperature (°F)	lower than the initial temperature
Maximum local cladding oxidation (%)	0.2
Maximum core wide cladding oxidation (%)	less than 0.2

Table 5.1.1.a-3 Sequence of Events for 1-ft^2 Break (Bottom)
(Break Location Sensitivity Study for Cold-leg Break)

Event	Time (sec)
Break occurs; blowdown initiation	0.0
Reactor trip (loss-of-offsite power is assumed)	6.9
ECCS actuation signal	8.3
Control rod insertion starts	8.7
Main steam isolation	8.7
RCP trip	9.9
Main feedwater isolation	14.9
Main steam safety valve open	not actuated
Accumulator injection begins	90
Fuel cladding starts heating up	97
Emergency Power Source initiates	111
High Head Injection System begins	126
Emergency feedwater flow begins	141
Peak Cladding Temperature occurs	153
Fuel cladding rewets	172

Table 5.1.1.a-4 Core Performance Results for 1-ft^2 Break (Bottom)
(Break Location Sensitivity Study for Cold-leg Break)

	Values
Peak Cladding Temperature (°F)	1029
Maximum local cladding oxidation (%)	0.2
Maximum core wide cladding oxidation (%)	less than 0.2

Table 5.1.1.b-1 Sequence of Events for 2-inch Break (Bottom)
(Break Location Sensitivity Study for Hot-leg Break)

Event	Time (sec)
Break occurs; blowdown initiation	0.0
Reactor trip (loss-of-offsite power is assumed)	124
Control rod insertion starts	126
Main steam isolation	126
RCP trip	127
Main feedwater isolation	132
Main steam safety valve open	161
ECCS actuation signal	162
Emergency Power Source initiates	265
High Head Injection System begins	308
Emergency feedwater flow begins	295
Accumulator injection begins	not actuated
Fuel cladding starts heating up	not occur
Peak Cladding Temperature occurs	lower than the initial temperature
Fuel cladding rewets	N/A

Table 5.1.1.b-2 Core Performance Results for 2-inch Break (Bottom)
(Break Location Sensitivity Study for Hot-leg Break)

	Values
Peak Cladding Temperature (°F)	lower than the initial temperature
Maximum local cladding oxidation (%)	0.2
Maximum core wide cladding oxidation (%)	less than 0.2

Table 5.1.1.b-3 Sequence of Events for 1-ft^2 Break (Bottom)
(Break Location Sensitivity Study for Hot-leg Break)

Event	Time (sec)
Break occurs; blowdown initiation	0.0
Reactor trip (loss-of-offsite power is assumed)	6.9
ECCS actuation signal	8.5
Control rod insertion starts	8.7
Main steam isolation	8.7
RCP trip	9.9
Main feedwater isolation	14.9
Main steam safety valve open	not actuated
Accumulator injection begins	96
Emergency Power Source initiates	112
High Head Injection System begins	127
Emergency feedwater flow begins	142
Fuel cladding starts heating up	Not Occur
Peak Cladding Temperature occurs	lower than the initial temperature
Fuel cladding rewets	N/A

Table 5.1.1.b-4 Core Performance Results for 1-ft^2 Break (Bottom)
(Break Location Sensitivity Study for Hot-leg Break)

	Values
Peak Cladding Temperature (°F)	lower than the initial temperature
Maximum local cladding oxidation (%)	0.2
Maximum core wide cladding oxidation (%)	less than 0.2

Table 5.1.1.c-1 Sequence of Events for 2-inch Break (Bottom)
(Break Location Sensitivity Study for Crossover-leg Break)

Event	Time (sec)
Break occurs; blowdown initiation	0.0
Reactor trip (loss-of-offsite power is assumed)	84
Control rod insertion starts	86
Main steam isolation	86
RCP trip	87
Main feedwater isolation	92
ECCS actuation signal	108
Main steam safety valve open	117
Emergency Power Source initiates	211
High Head Injection System begins	238
Emergency feedwater flow begins	241
Accumulator injection begins	not actuated
Fuel cladding starts heating up	not occur
Peak Cladding Temperature occurs	lower than the initial temperature
Fuel cladding rewets	N/A

Table 5.1.1.c-2 Core Performance Results for 2-inch Break (Bottom)
(Break Location Sensitivity Study for Crossover-leg Break)

	Values
Peak Cladding Temperature (°F)	lower than the initial temperature
Maximum local cladding oxidation (%)	0.2
Maximum core wide cladding oxidation (%)	less than 0.2

Table 5.1.1.c-3 Sequence of Events for 1-ft^2 Break (Bottom)
(Break Location Sensitivity Study for Crossover-leg Break)

Event	Time (sec)
Break occurs; blowdown initiation	0.0
Reactor trip (loss-of-offsite power is assumed)	6.8
ECCS actuation signal	8.2
Control rod insertion starts	8.6
Main steam isolation	8.6
RCP trip	9.8
Main feedwater isolation	14.8
Main steam safety valve open	not actuated
Fuel cladding starts heating up	56
Accumulator injection begins	97
Emergency Power Source initiates	111
High Head Injection System begins	126
Emergency feedwater flow begins	141
Peak Cladding Temperature occurs	lower than the initial temperature
Fuel cladding rewets	166

Table 5.1.1.c-4 Core Performance Results for 1-ft^2 Break (Bottom)
(Break Location Sensitivity Study for Crossover-leg Break)

	Values
Peak Cladding Temperature (°F)	lower than the initial temperature
Maximum local cladding oxidation (%)	0.2
Maximum core wide cladding oxidation (%)	less than 0.2

Table 5.1.2-1 Sequence of Events for DVI-line Break (Break Location Sensitivity Study)

Event	Time (sec)
Break occurs; blowdown initiation	0.0
Reactor trip (loss-of-offsite power is assumed)	25.8
Control rod insertion starts	27.6
Main steam isolation	27.6
RCP trip	28.8
Main feedwater isolation	33.8
ECCS actuation signal	35.4
Main steam safety valve open	57
Emergency Power Source initiates	138
High Head Injection System begins	153
Emergency feedwater flow begins	168
Accumulator injection begins	not actuated
Fuel cladding starts heating up	not occur
Peak Cladding Temperature occurs	lower than the initial temperature
Fuel cladding rewets	N/A

Table 5.1.2-2 Core Performance Results for DVI-line Break (Break Location Sensitivity Study)

	Values
Peak Cladding Temperature (°F)	lower than the initial temperature
Maximum local cladding oxidation (%)	0.2
Maximum core wide cladding oxidation (%)	less than 0.2

Table 5.1.3-1 Sequence of Events for Pressurizer Steam Phase Break (Break Location Sensitivity Study)

Event	Time (sec)
Break occurs; blowdown initiation	0.0
Reactor trip (loss-of-offsite power is assumed)	5.3
Control rod insertion starts	7.1
Main steam isolation	7.1
ECCS actuation signal	7.1
RCP trip	8.3
Main feedwater isolation	13.3
Main steam safety valve open	83
Emergency Power Source initiates	110
High Head Injection System begins	125
Emergency feedwater flow begins	140
Accumulator injection begins	491
Fuel cladding starts heating up	not occur
Peak Cladding Temperature occurs	lower than the initial temperature
Fuel cladding rewets	N/A

Table 5.1.3-2 Core Performance Results for Pressurizer Steam Phase Break (Break Location Sensitivity Study)

	Values
Peak Cladding Temperature (°F)	lower than the initial temperature
Maximum local cladding oxidation (%)	0.2
Maximum core wide cladding oxidation (%)	less than 0.2

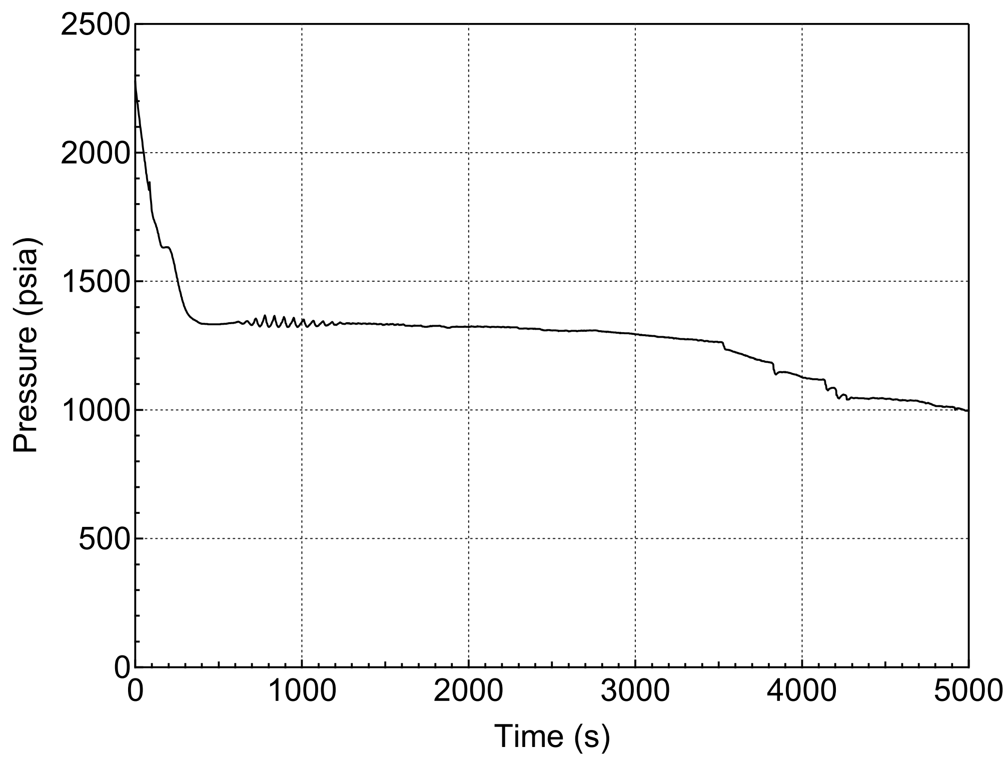

Figure 5.1.1.a-1 RCS (Pressurizer) Pressure Transient for 2-inch Break (Bottom) (Break Location Sensitivity Study for Cold-leg Break)

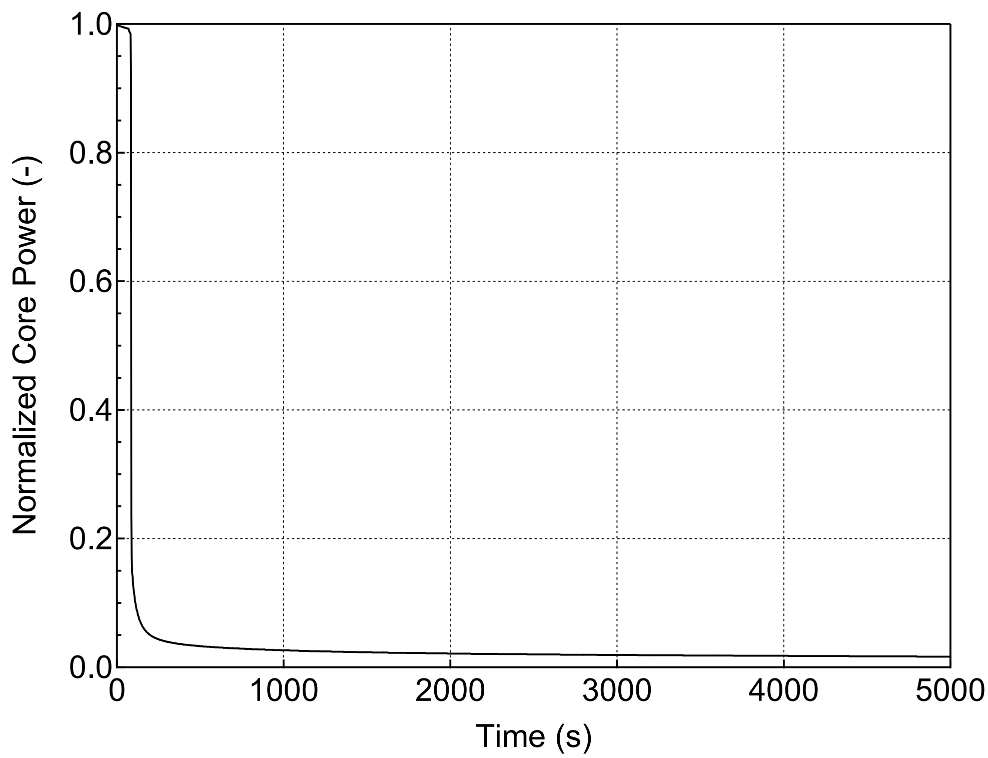

Figure 5.1.1.a-2 Normalized Core Power for 2-inch Break (Bottom)
(Break Location Sensitivity Study for Cold-leg Break)

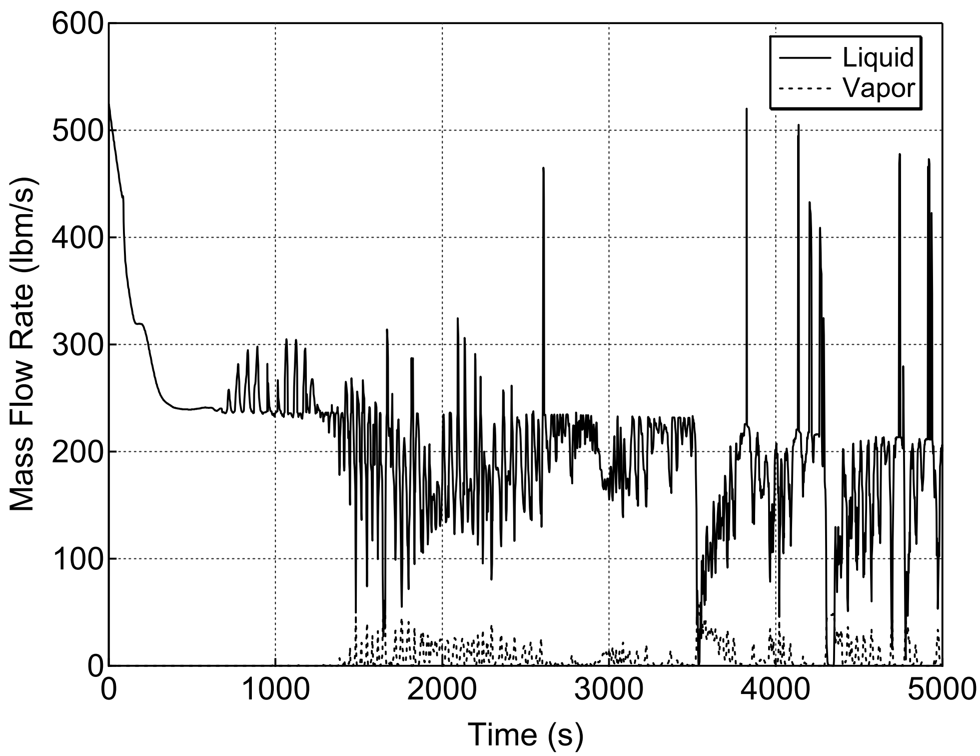

Figure 5.1.1.a-3 Liquid and Vapor Discharges through the Break for 2-inch Break (Bottom) (Break Location Sensitivity Study for Cold-leg Break)

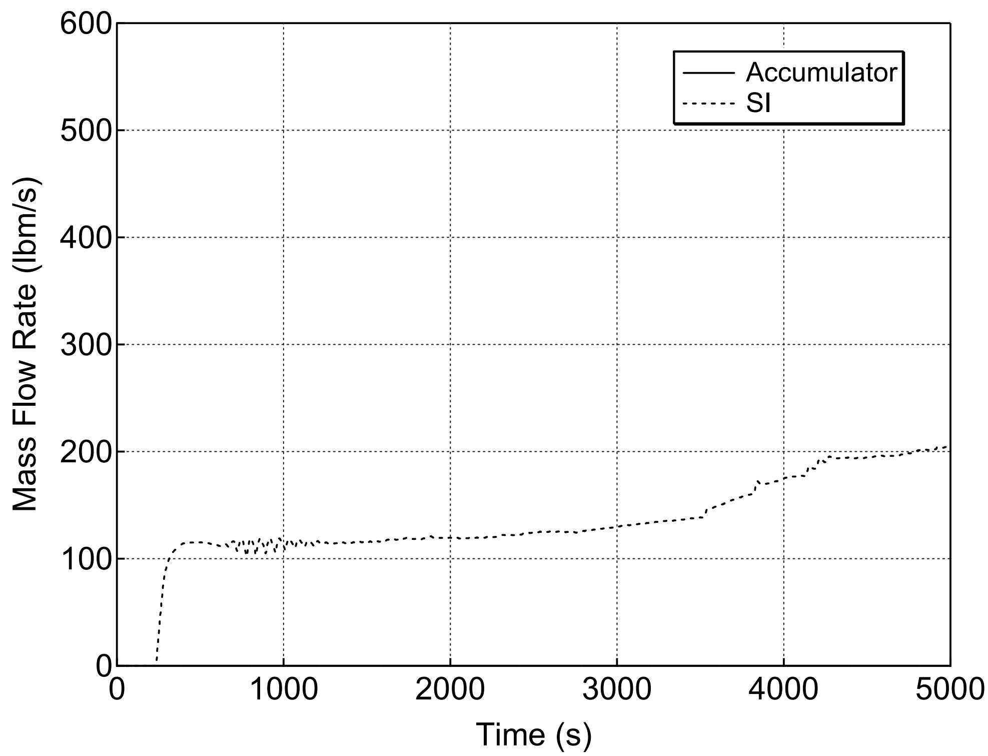

Figure 5.1.1.a-4 Accumulator and Safety Injection Mass Flowrates for 2-inch Break (Bottom) (Break Location Sensitivity Study for Cold-leg Break)

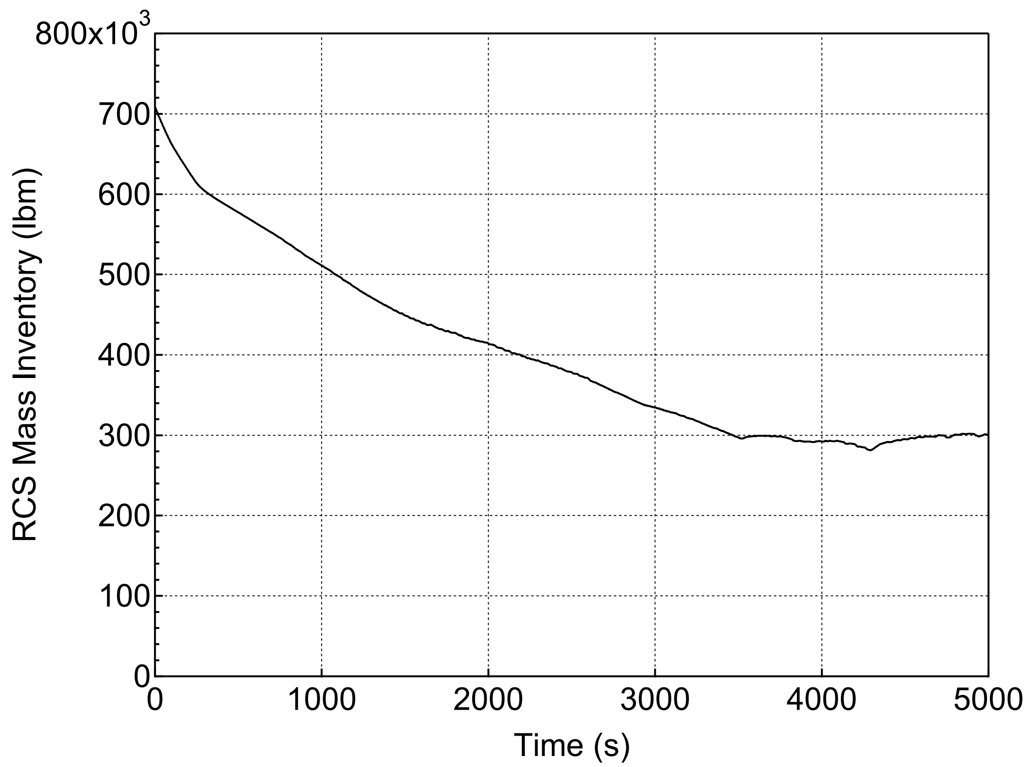

Figure 5.1.1.a-5 RCS Mass Inventory for 2-inch Break (Bottom)
(Break Location Sensitivity Study for Cold-leg Break)

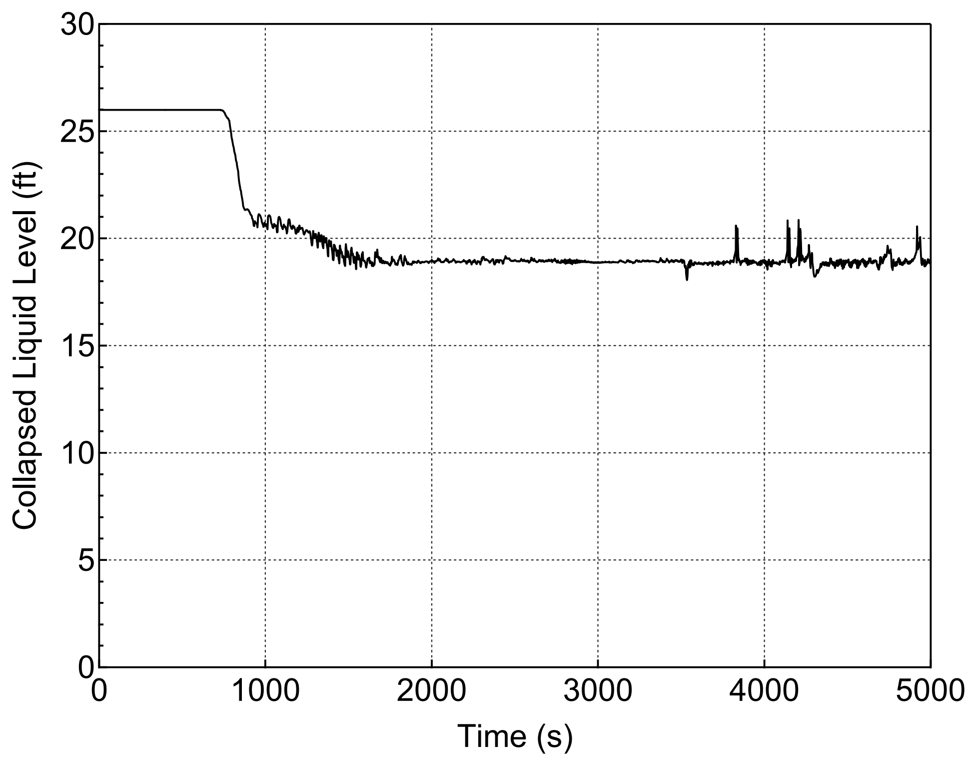

Figure 5.1.1.a-6 Downcomer Collapsed Level for 2-inch Break (Bottom)
(Break Location Sensitivity Study for Cold-leg Break)

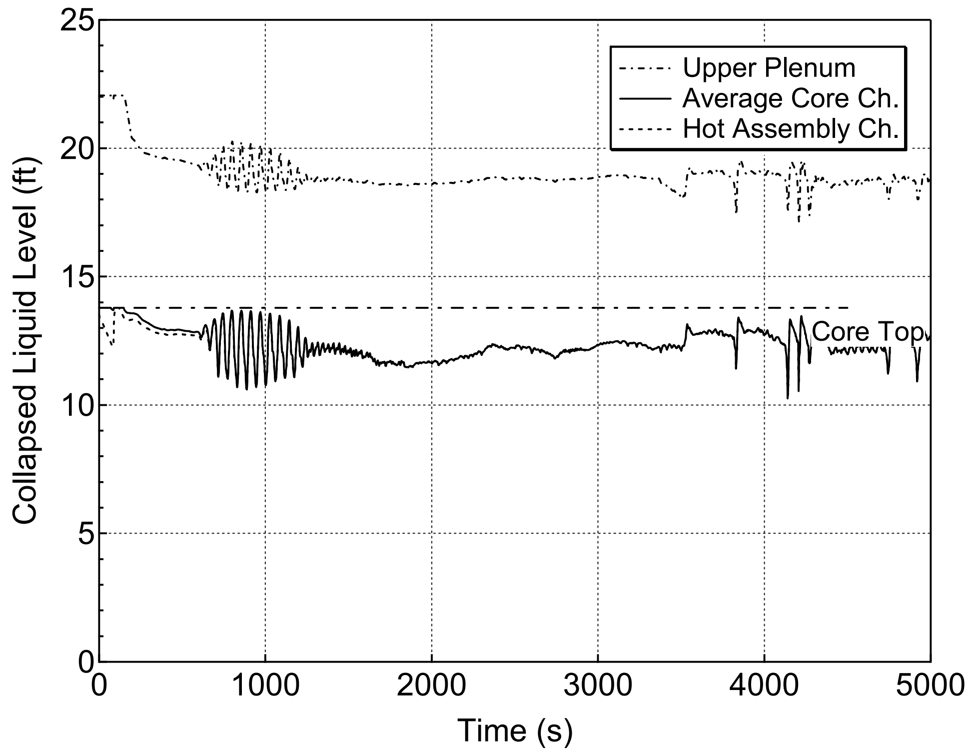

Figure 5.1.1.a-7 Core and Upper Plenum Collapsed Levels for 2-inch Break (Bottom) (Break Location Sensitivity Study for Cold-leg Break)

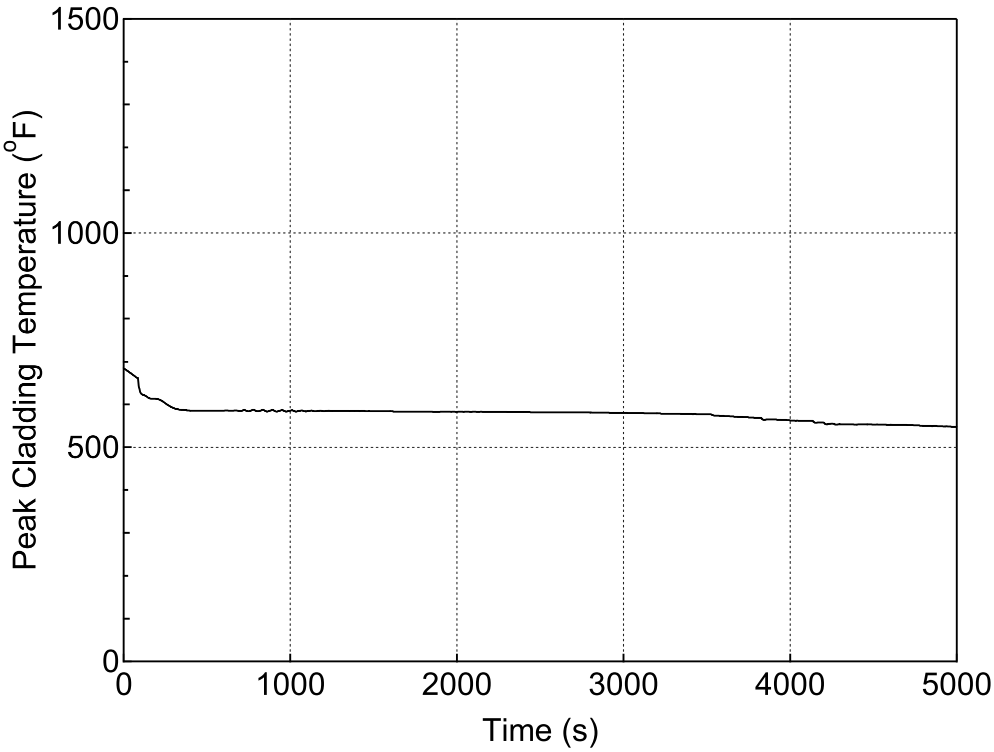

Figure 5.1.1.a-8 PCT at All Elevations for Hot Rod in Hot Assembly for 2-inch Break (Bottom) (Break Location Sensitivity Study for Cold-leg Break)

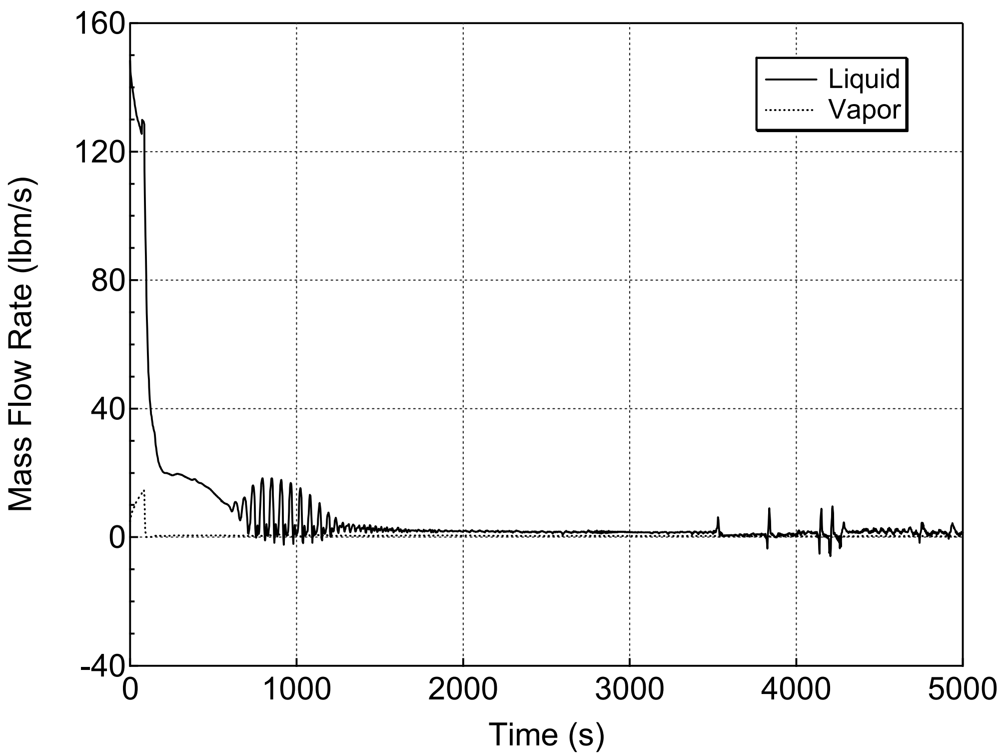

Figure 5.1.1.a-9 Hot Assembly Exit Vapor and Liquid Mass Flowrates for 2-inch Break (Bottom) (Break Location Sensitivity Study for Cold-leg Break)

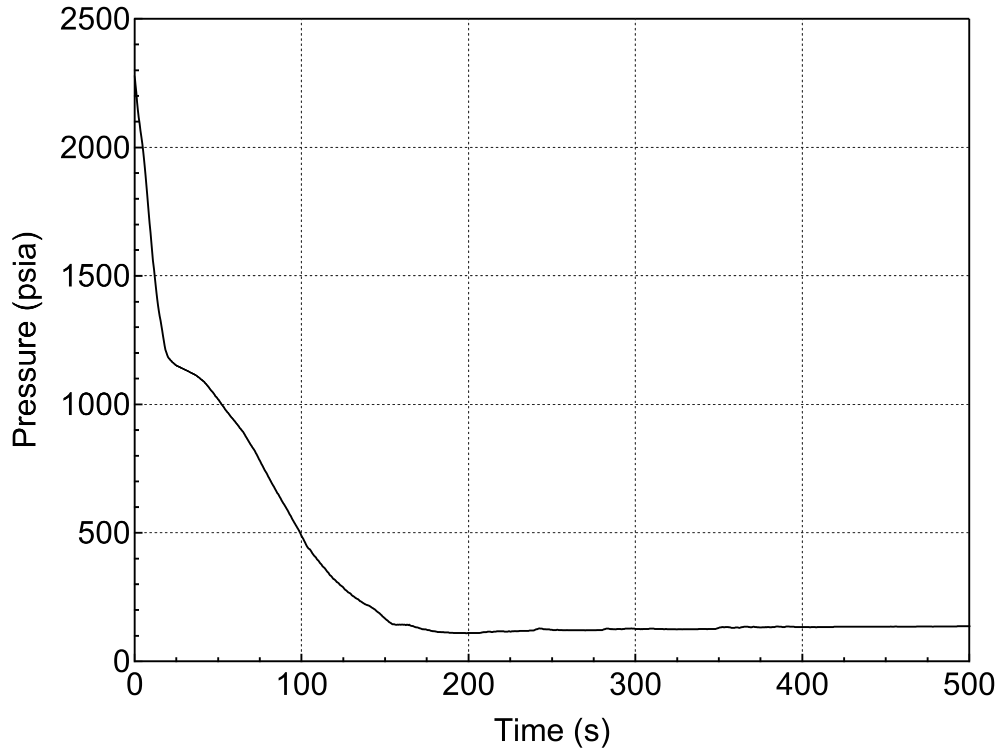

Figure 5.1.1.a-10 RCS (Pressurizer) Pressure Transient for 1-ft^2 Break (Bottom) (Break Location Sensitivity Study for Cold-leg Break)

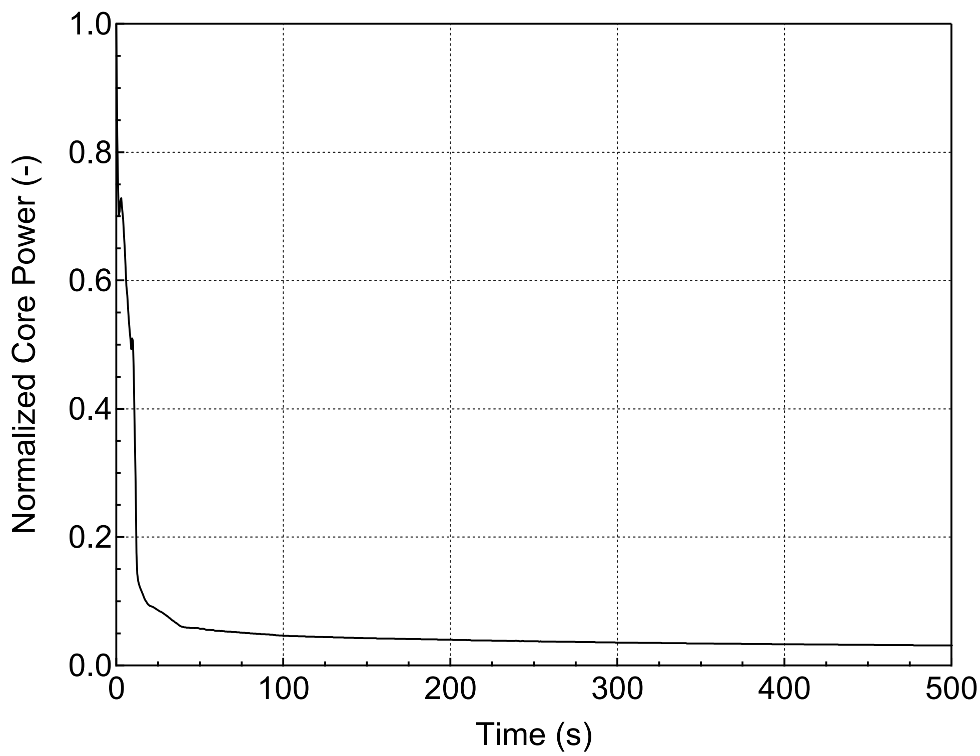

Figure 5.1.1.a-11 Normalized Core Power for 1-ft^2 Break (Bottom)
(Break Location Sensitivity Study for Cold-leg Break)

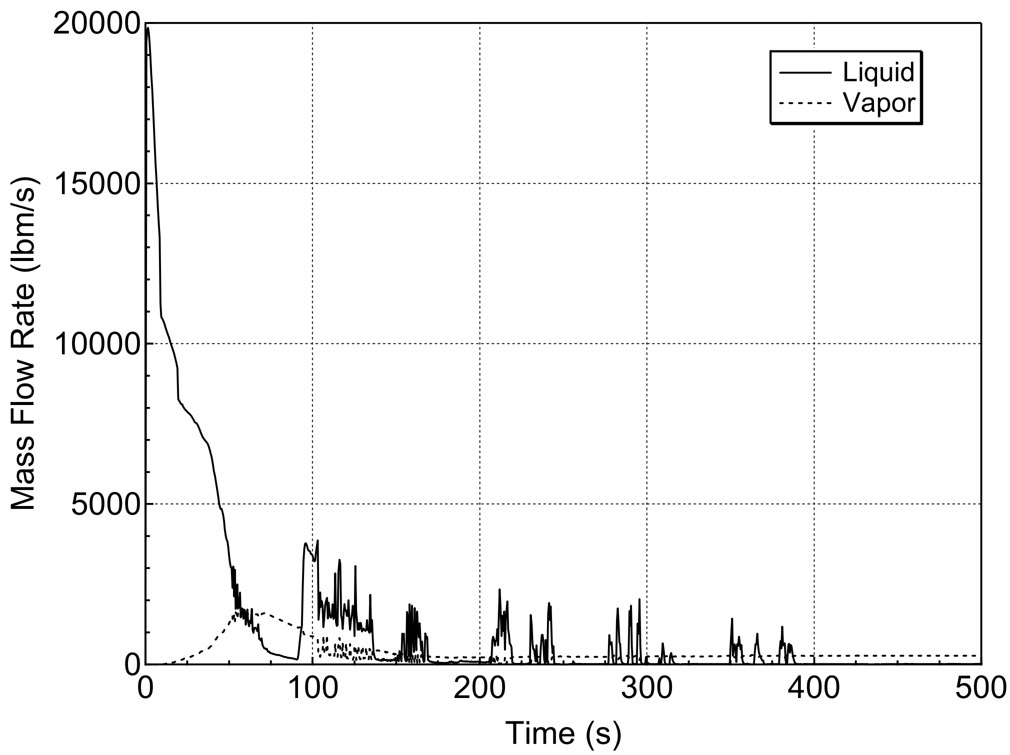

Figure 5.1.1.a-12 Liquid and Vapor Discharges through the Break for 1-ft^2 Break (Bottom) (Break Location Sensitivity Study for Cold-leg Break)

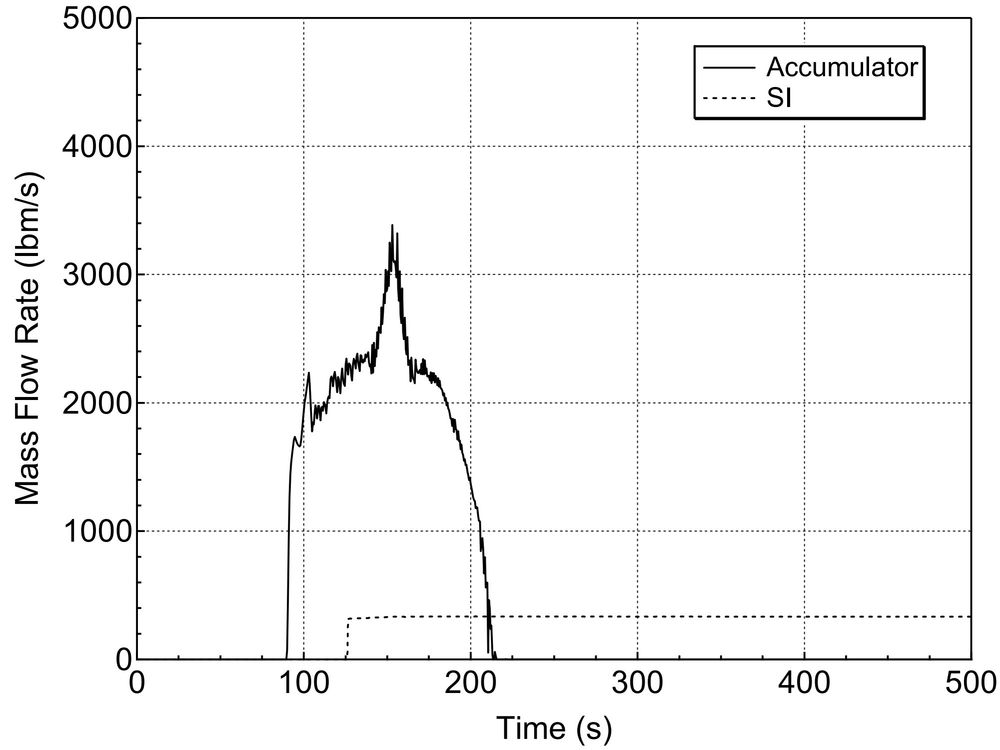

Figure 5.1.1.a-13 Accumulator and Safety Injection Mass Flowrates for 1-ft^2 Break (Bottom)
(Break Location Sensitivity Study for Cold-leg Break)

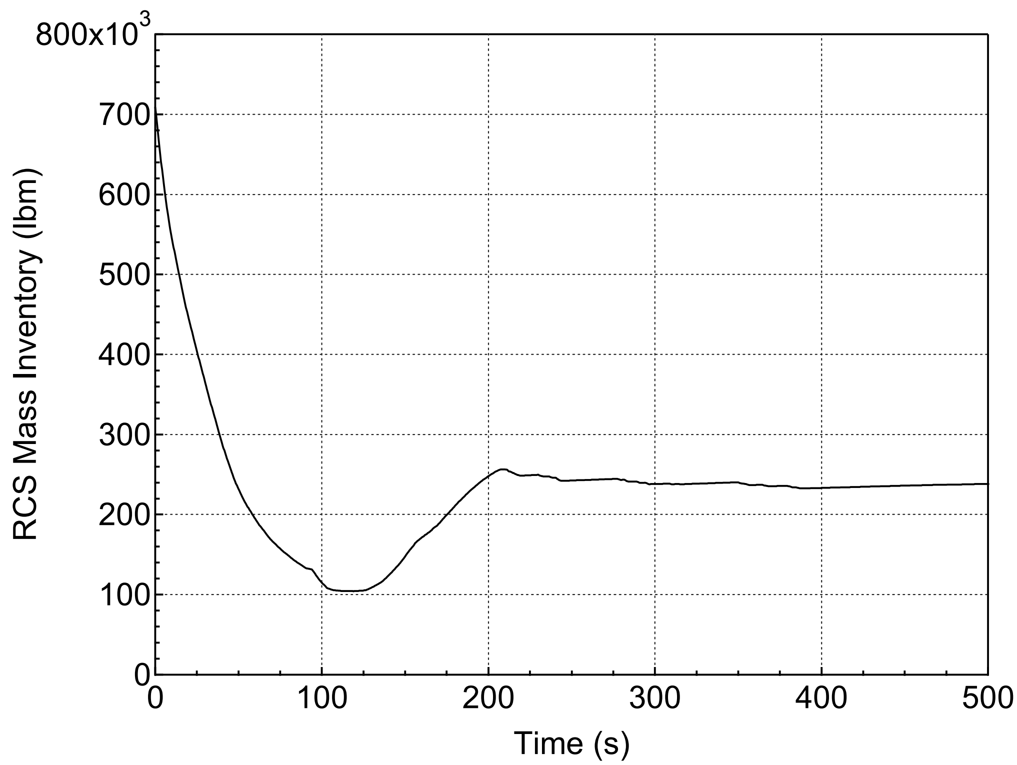

Figure 5.1.1.a-14 RCS Mass Inventory for 1-ft^2 Break (Bottom)
(Break Location Sensitivity Study for Cold-leg Break)

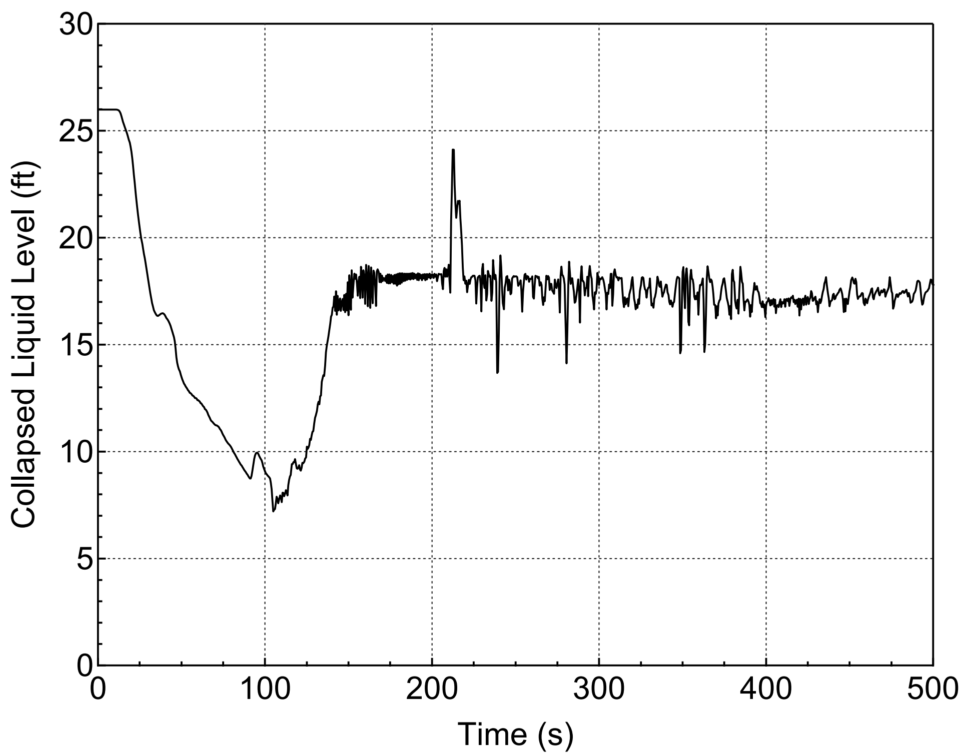

Figure 5.1.1.a-15 Downcomer Collapsed Level for 1-ft^2 Break (Bottom) (Break Location Sensitivity Study for Cold-leg Break)

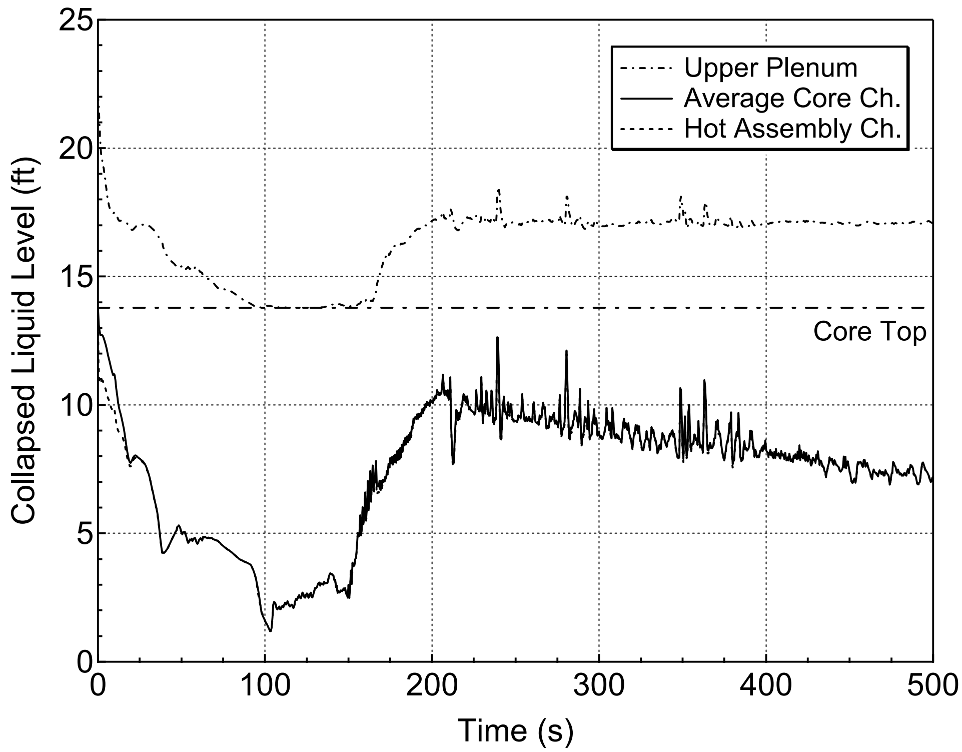

Figure 5.1.1.a-16 Core and Upper Plenum Collapsed Levels for 1-ft^2 Break (Bottom) (Break Location Sensitivity Study for Cold-leg Break)

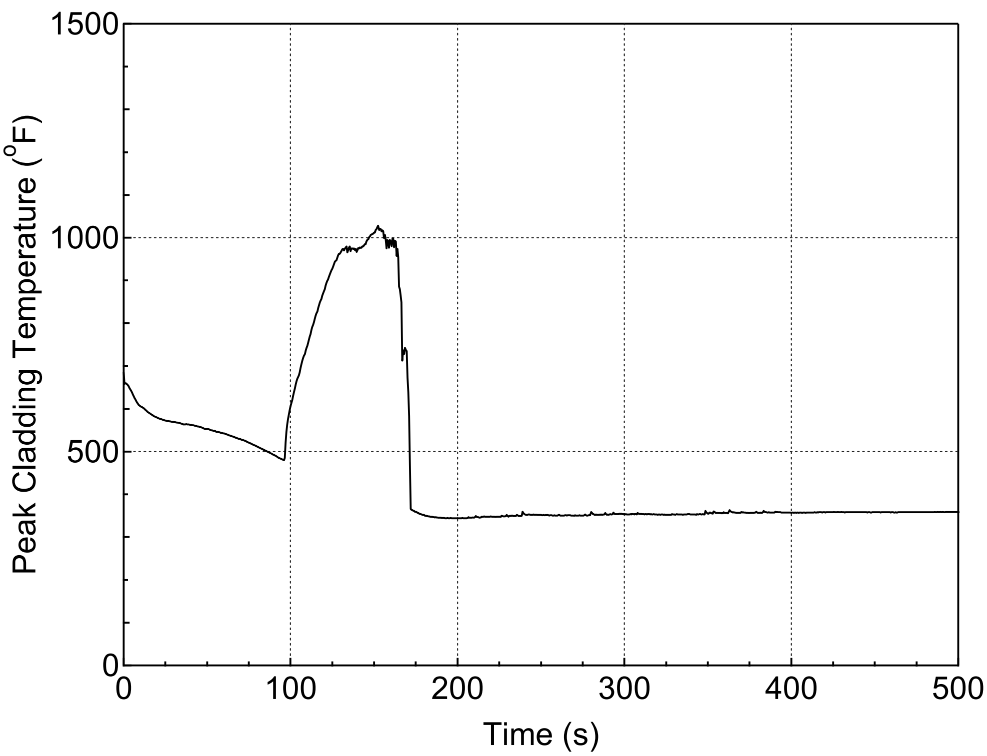

Figure 5.1.1.a-17 PCT at All Elevations for Hot Rod in Hot Assembly for 1-ft^2 Break (Bottom)
(Break Location Sensitivity Study for Cold-leg Break)

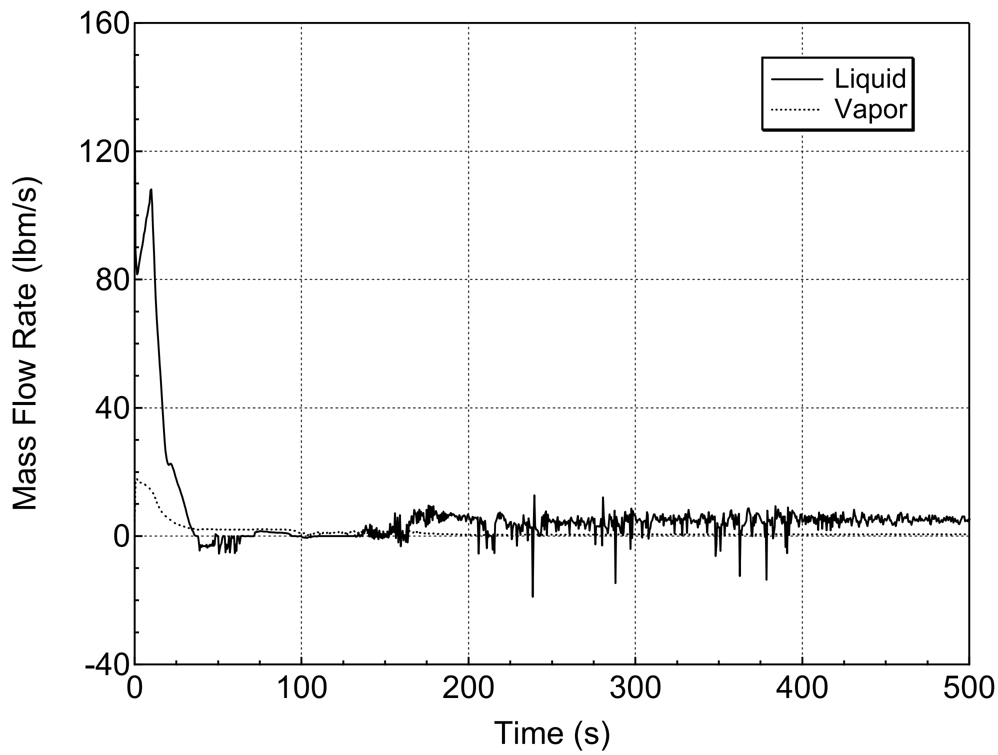

Figure 5.1.1.a-18 Hot Assembly Exit Vapor and Liquid Mass Flowrates for 1-ft^2 Break (Bottom)
(Break Location Sensitivity Study for Cold-leg Break)

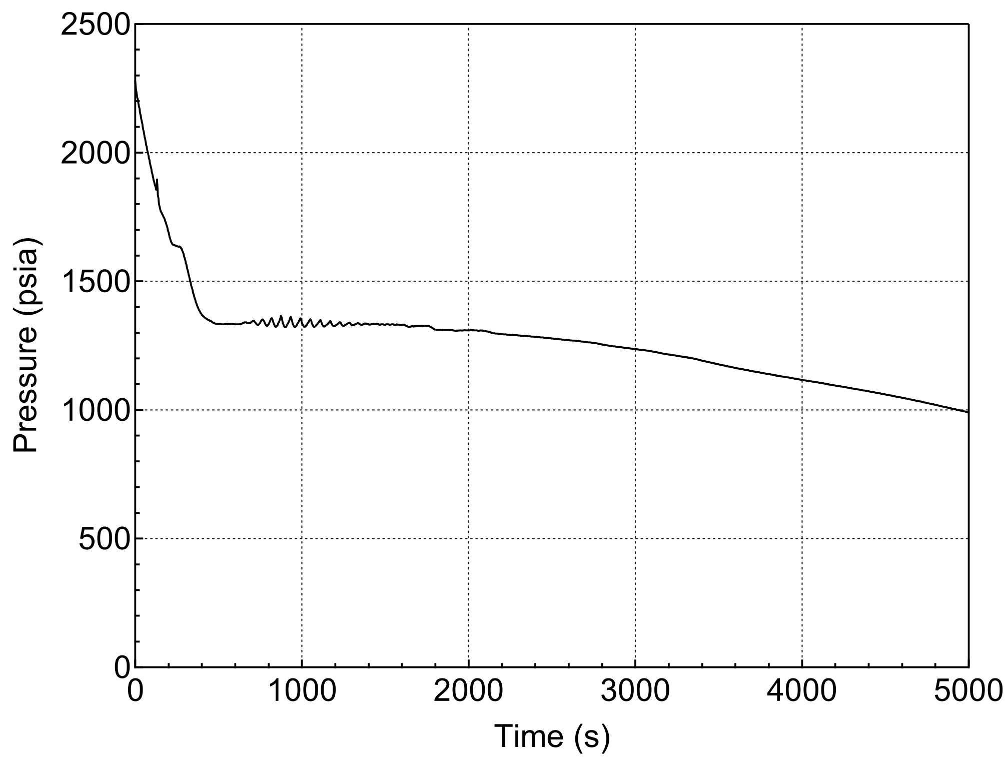

Figure 5.1.1.b-1 RCS (Pressurizer) Pressure Transient for 2-inch Break (Bottom) (Break Location Sensitivity Study for Hot-leg Break)

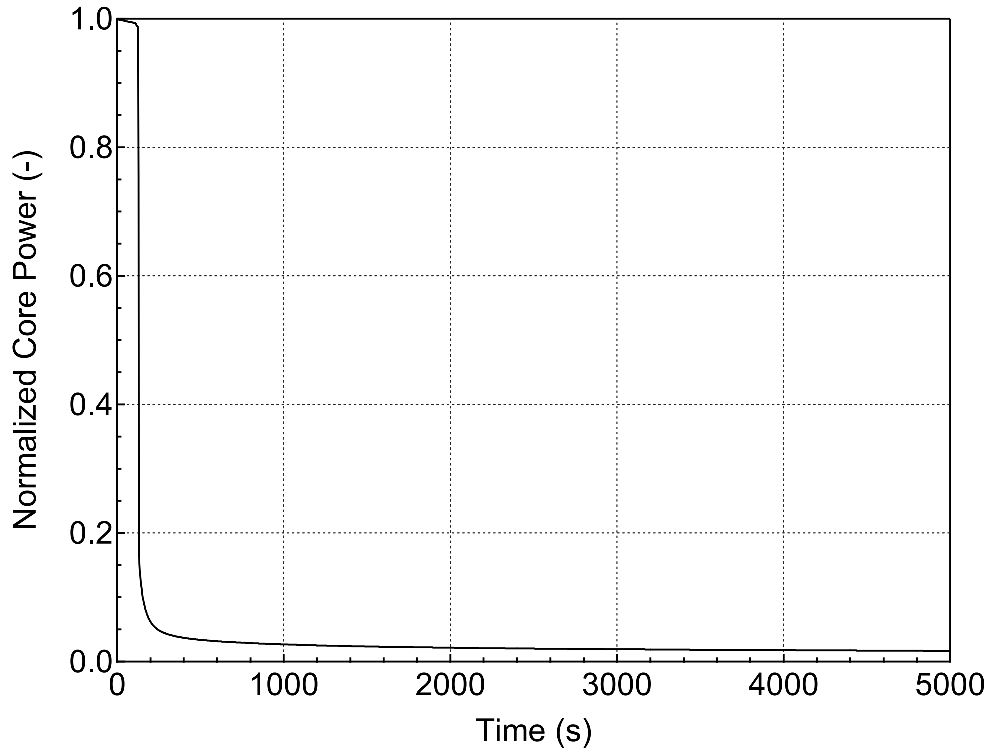

Figure 5.1.1.b-2 Normalized Core Power for 2-inch Break (Bottom)
(Break Location Sensitivity Study for Hot-leg Break)

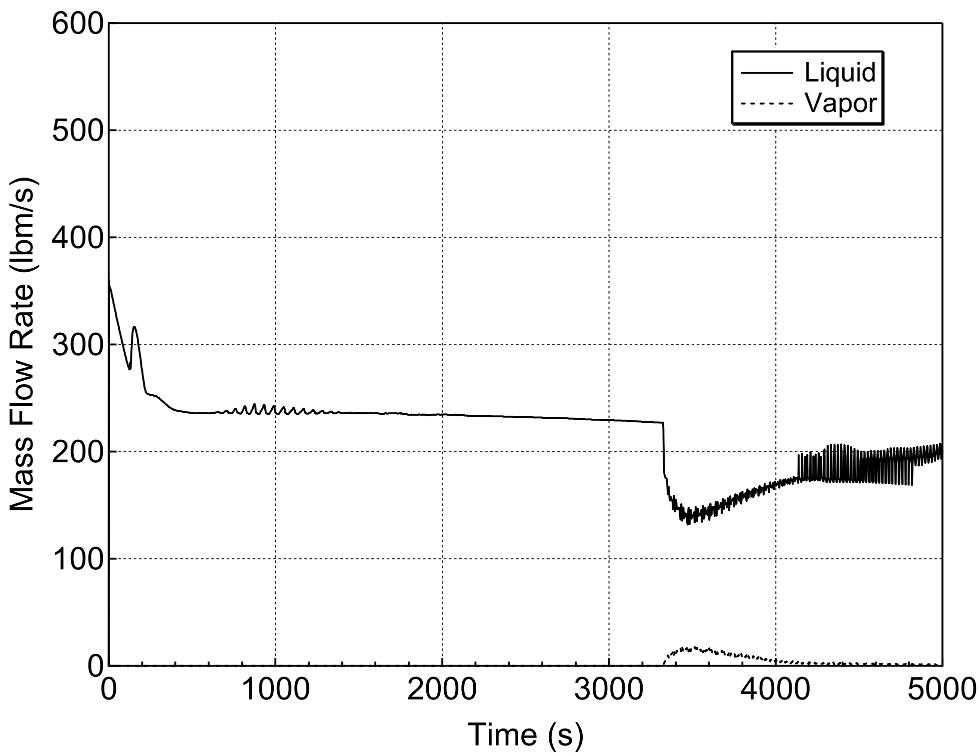

Figure 5.1.1.b-3 Liquid and Vapor Discharges through the Break for 2-inch Break (Bottom) (Break Location Sensitivity Study for Hot-leg Break)

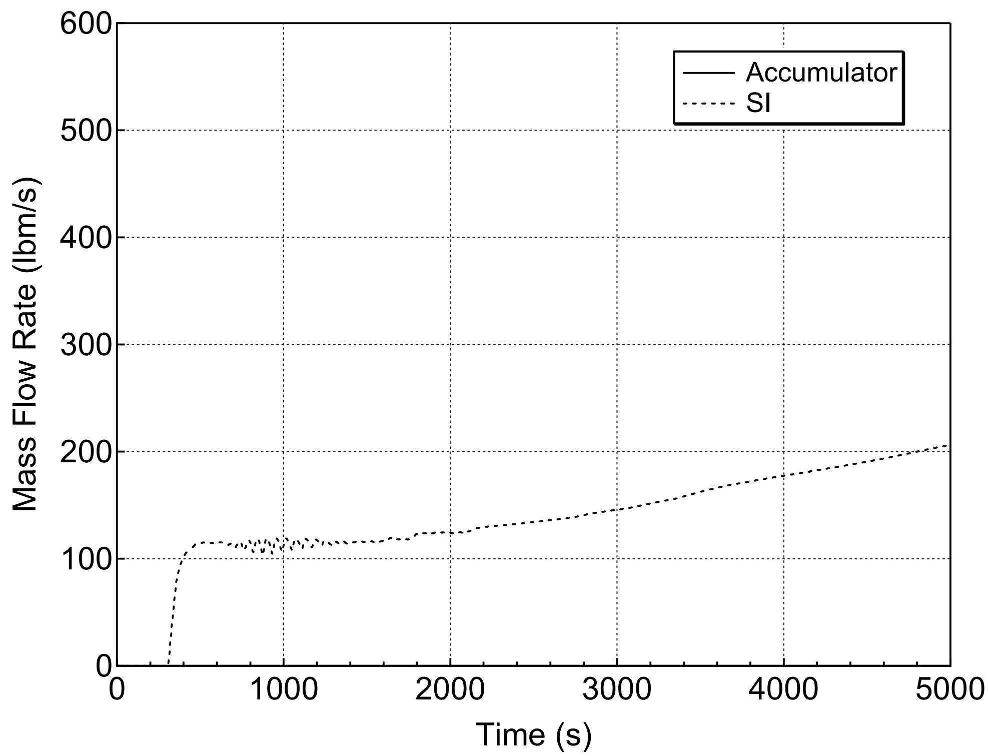

Figure 5.1.1.b-4 Accumulator and Safety Injection Mass Flowrates for 2-inch Break (Bottom) (Break Location Sensitivity Study for Hot-leg Break)

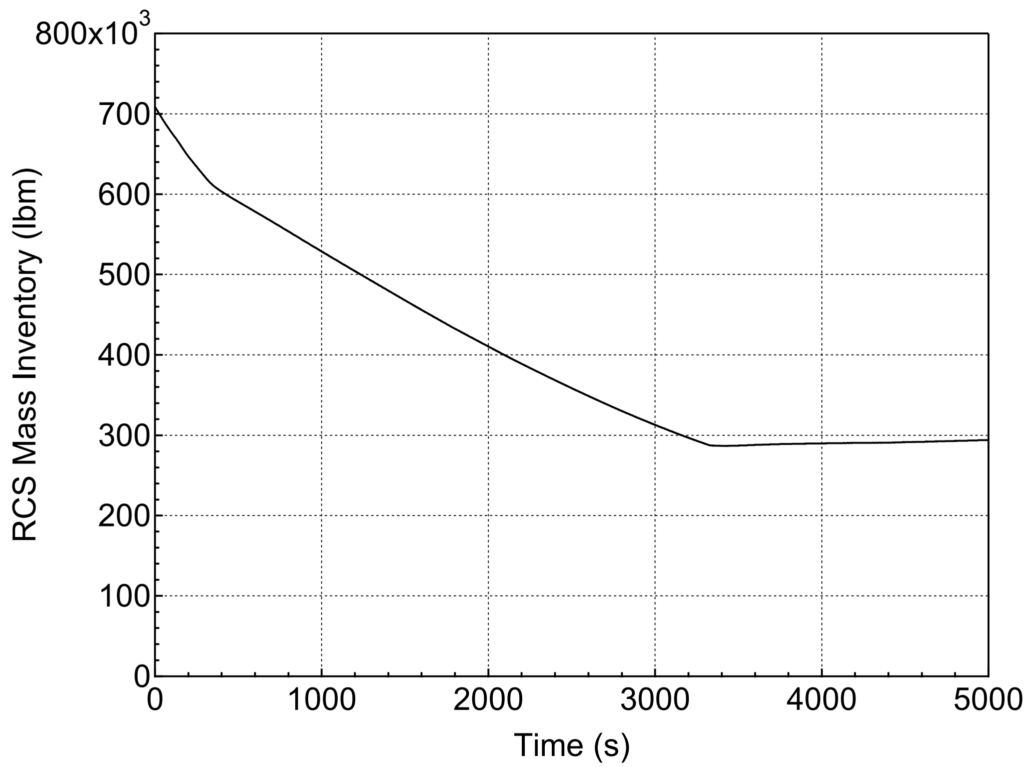

Figure 5.1.1.b-5 RCS Mass Inventory for 2-inch Break (Bottom)
(Break Location Sensitivity Study for Hot-leg Break)

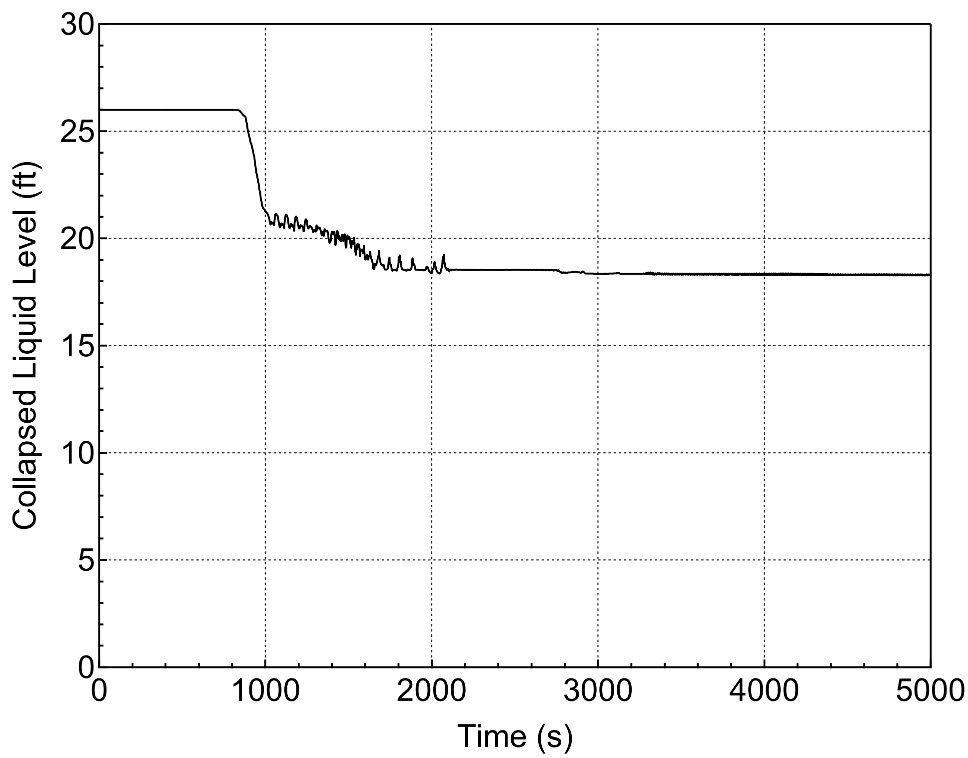

Figure 5.1.1.b-6 Downcomer Collapsed Level for 2-inch Break (Bottom)
(Break Location Sensitivity Study for Hot-leg Break)

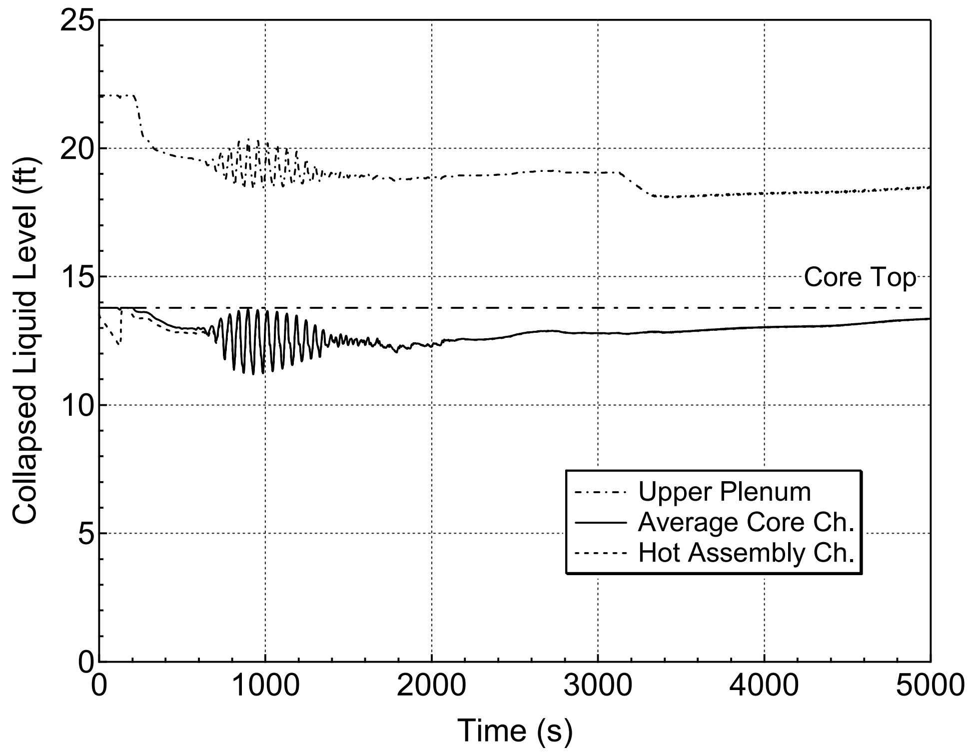

Figure 5.1.1.b-7 Core and Upper Plenum Collapsed Levels for 2-inch Break (Bottom) (Break Location Sensitivity Study for Hot-leg Break)

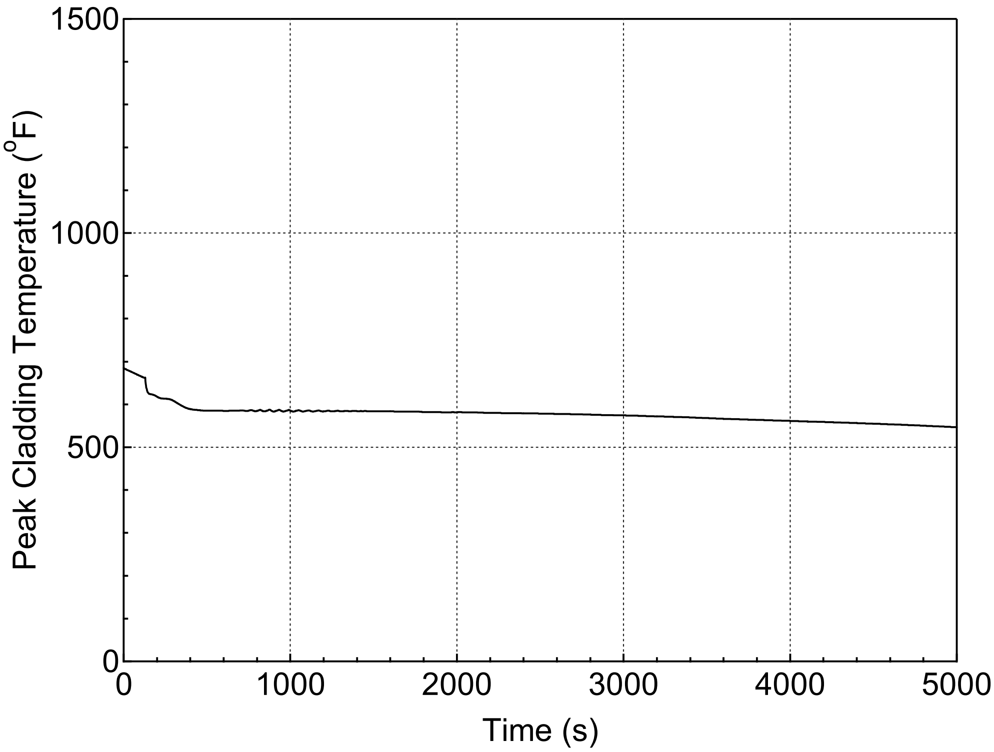

Figure 5.1.1.b-8 PCT at All Elevations for Hot Rod in Hot Assembly for 2-inch Break (Bottom) (Break Location Sensitivity Study for Hot-leg Break)

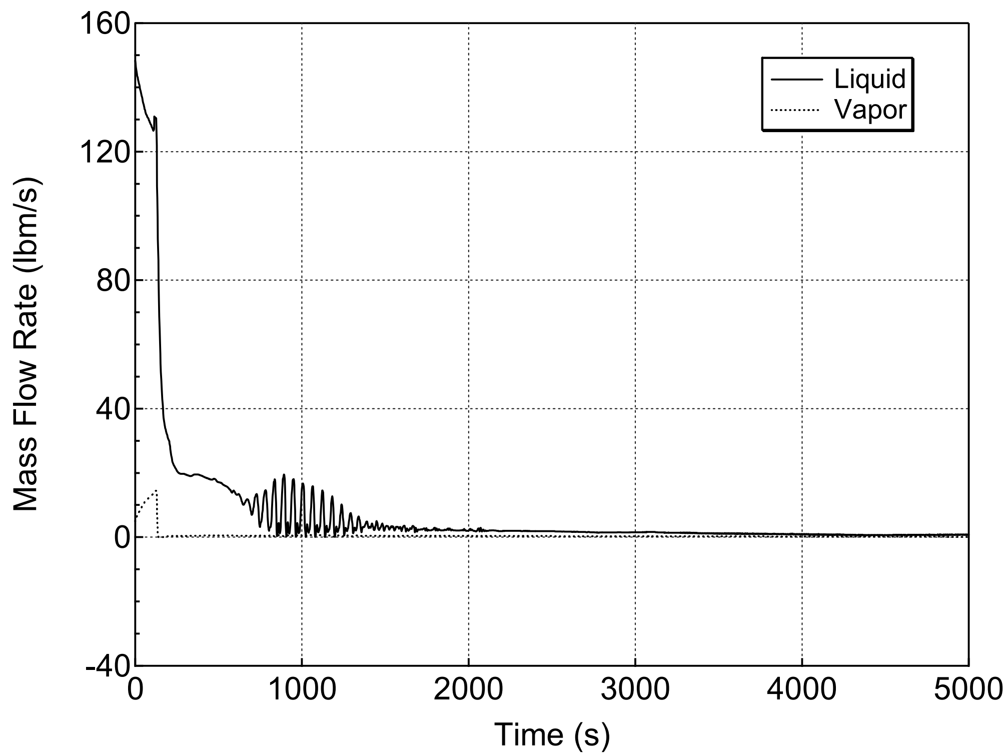

Figure 5.1.1.b-9 Hot Assembly Exit Vapor and Liquid Mass Flowrates for 2-inch Break (Bottom) (Break Location Sensitivity Study for Hot-leg Break)

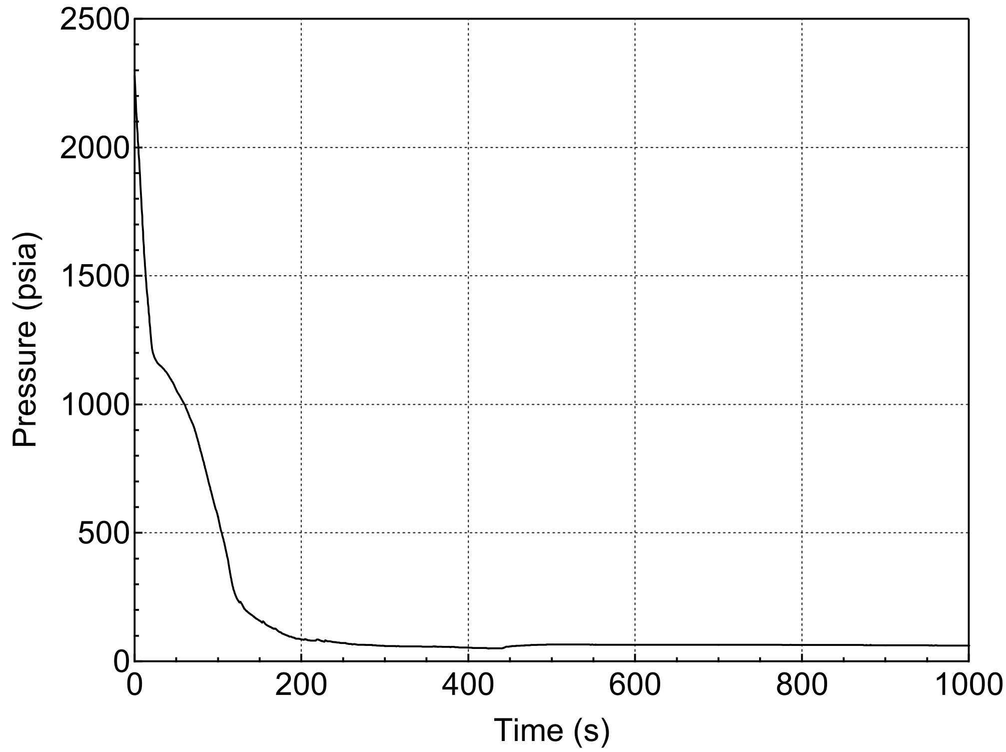

Figure 5.1.1.b-10 RCS (Pressurizer) Pressure Transient for 1-ft^2 Break (Bottom) (Break Location Sensitivity Study for Hot-leg Break)

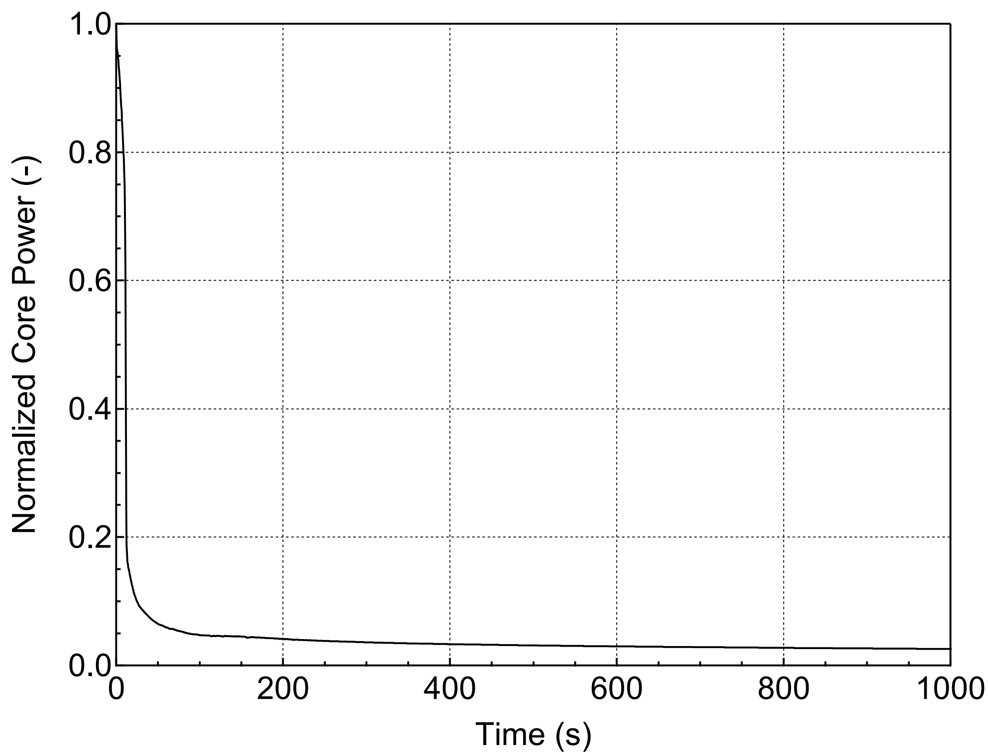

Figure 5.1.1.b-11 Normalized Core Power for 1-ft^2 Break (Bottom)
(Break Location Sensitivity Study for Hot-leg Break)

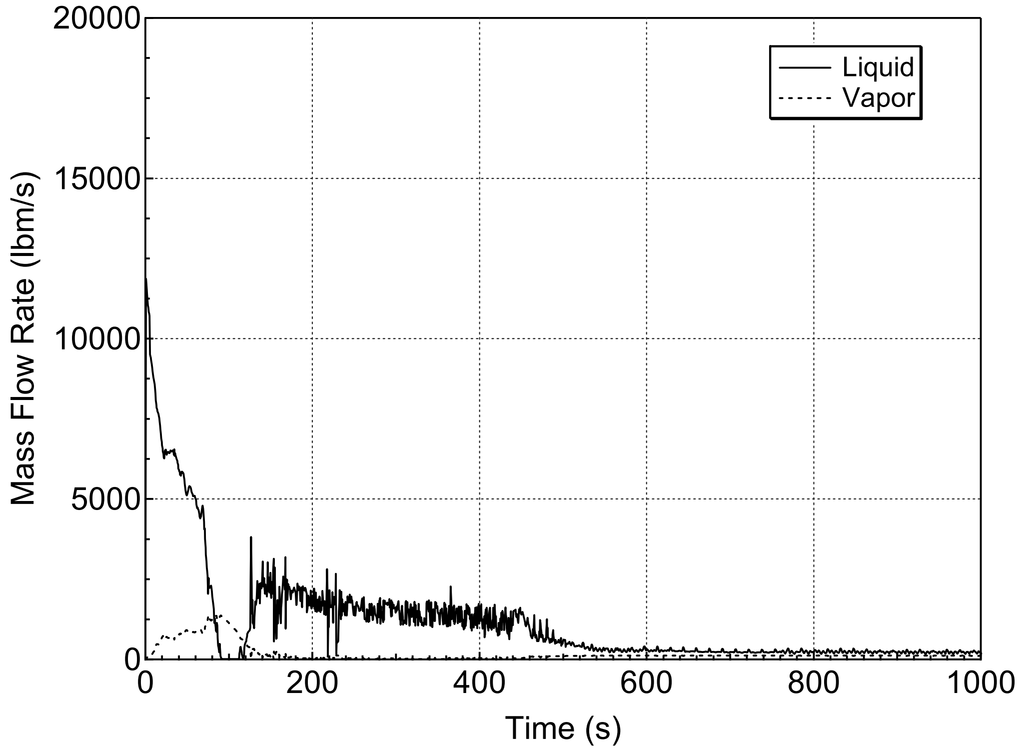

Figure 5.1.1.b-12 Liquid and Vapor Discharges through the Break for 1-ft^2 Break (Bottom) (Break Location Sensitivity Study for Hot-leg Break)

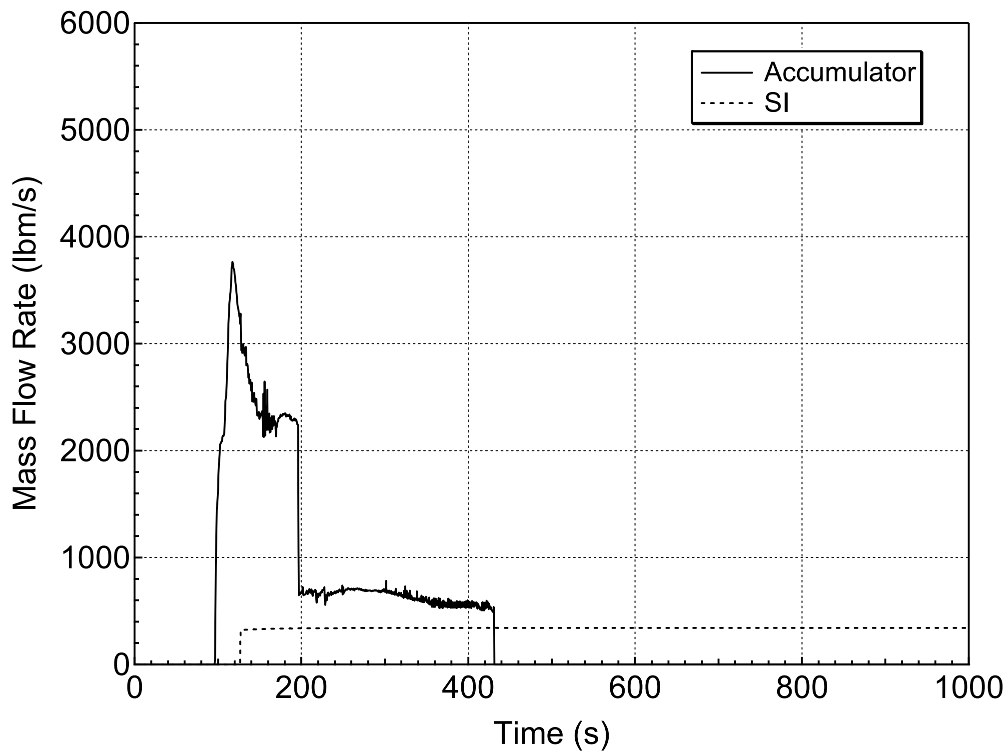

Figure 5.1.1.b-13 Accumulator and Safety Injection Mass Flowrates for 1-ft^2 Break (Bottom)
(Break Location Sensitivity Study for Hot-leg Break)

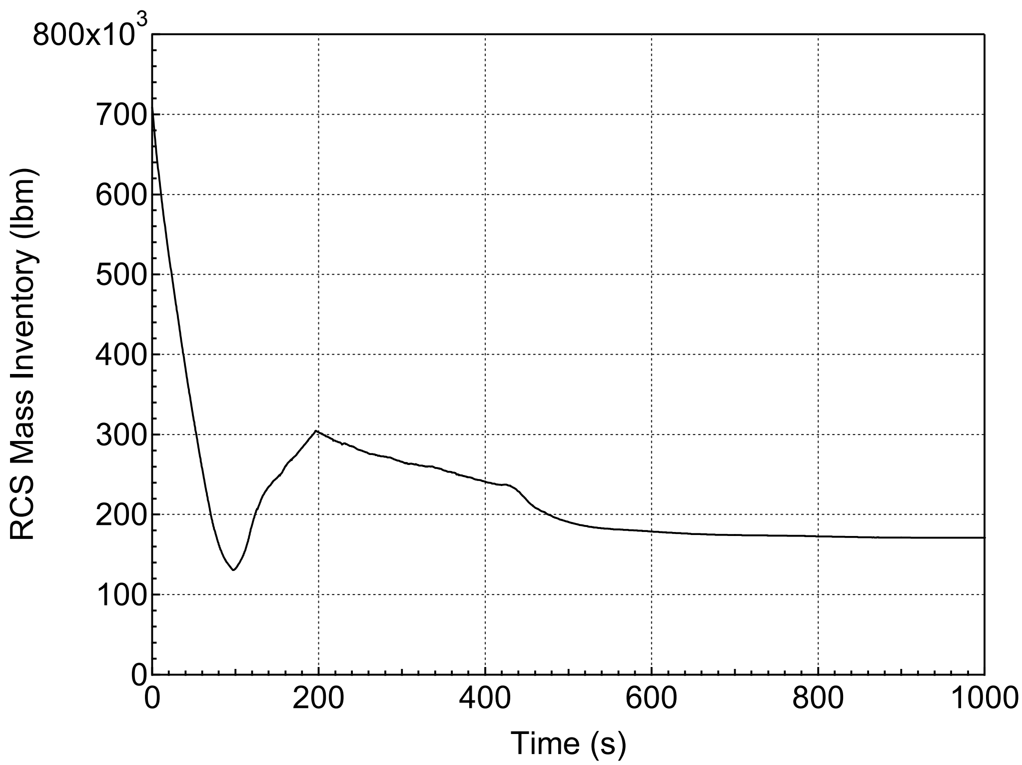

Figure 5.1.1.b-14 RCS Mass Inventory for 1-ft^2 Break (Bottom)
(Break Location Sensitivity Study for Hot-leg Break)

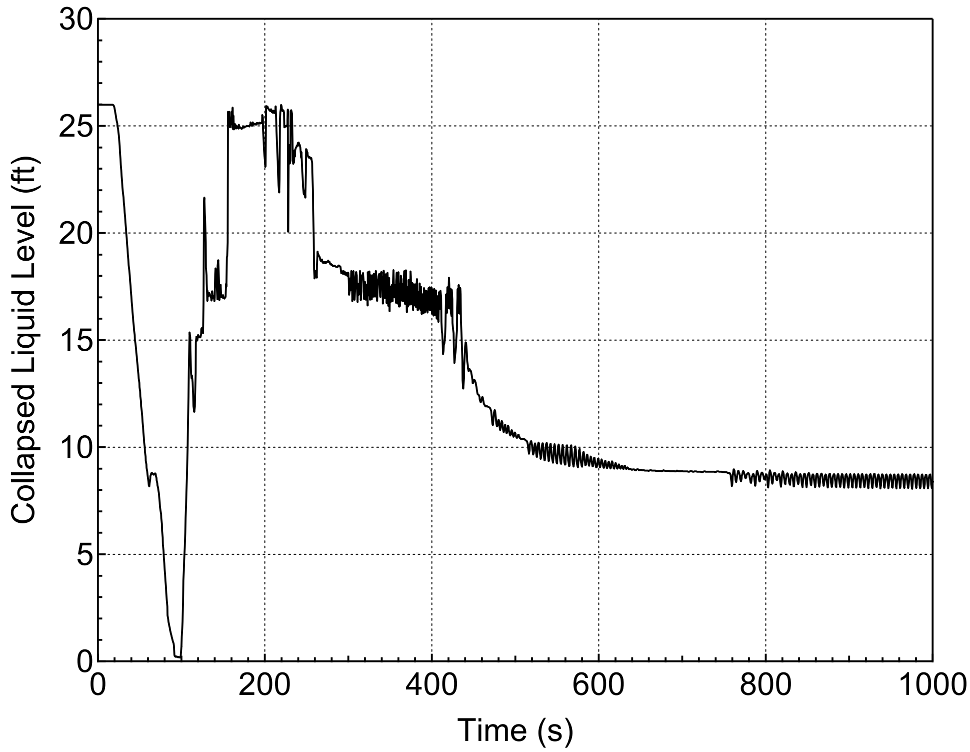

Figure 5.1.1.b-15 Downcomer Collapsed Level for 1-ft^2 Break (Bottom) (Break Location Sensitivity Study for Hot-leg Break)

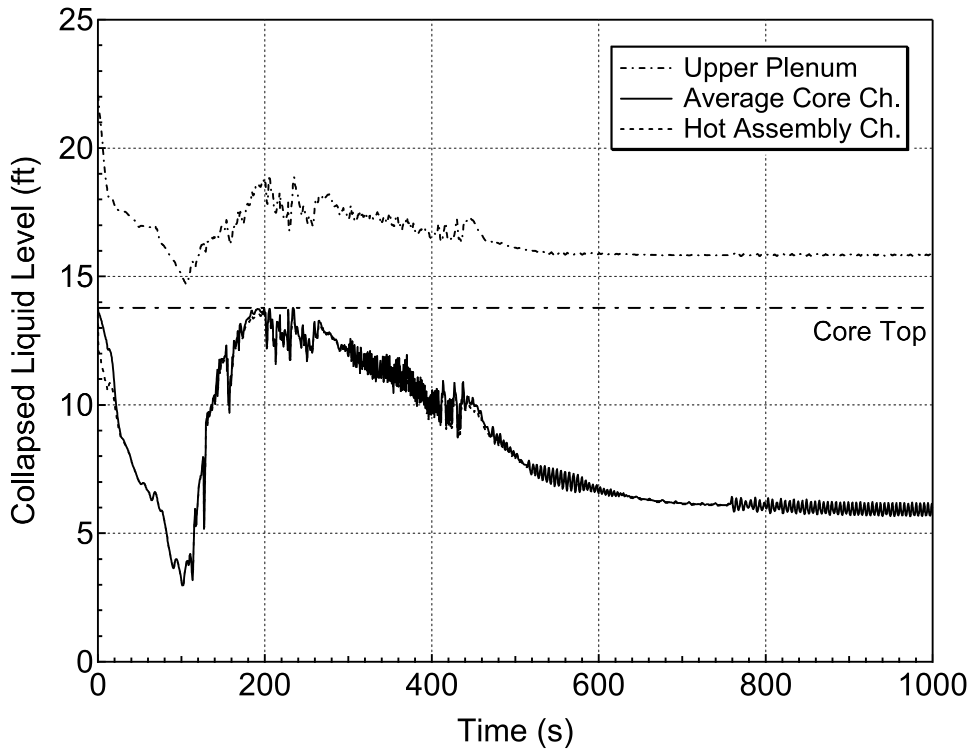

Figure 5.1.1.b-16 Core and Upper Plenum Collapsed Levels for 1-ft² Break (Bottom) (Break Location Sensitivity Study for Hot-leg Break)

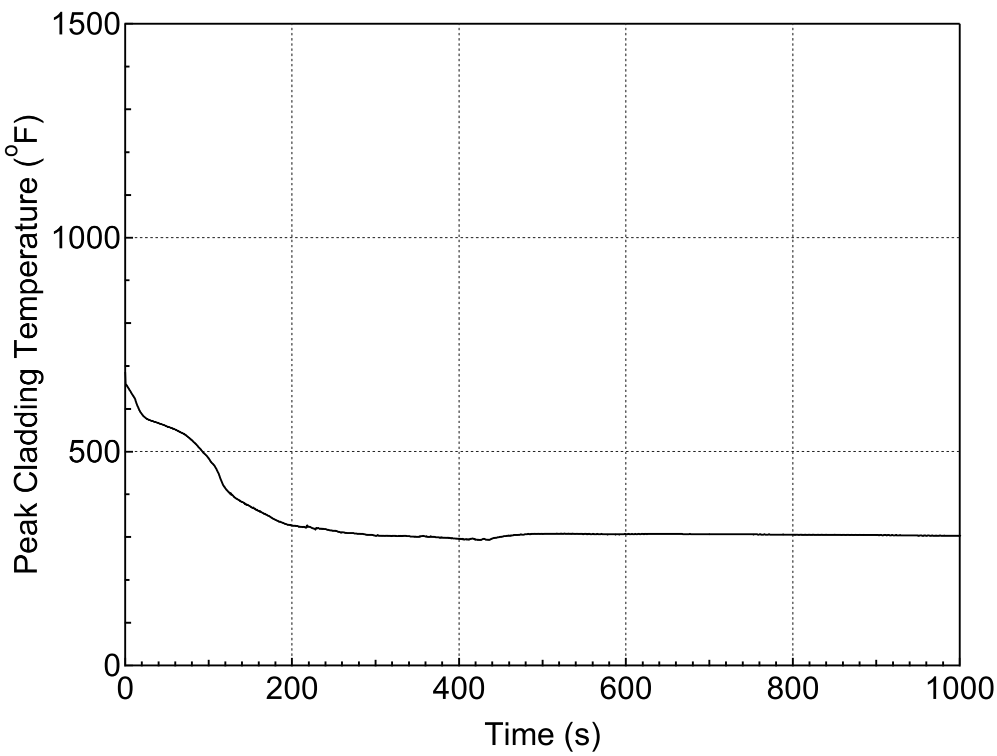

Figure 5.1.1.b-17 PCT at All Elevations for Hot Rod in Hot Assembly for 1-ft^2 Break (Bottom)
(Break Location Sensitivity Study for Hot-leg Break)

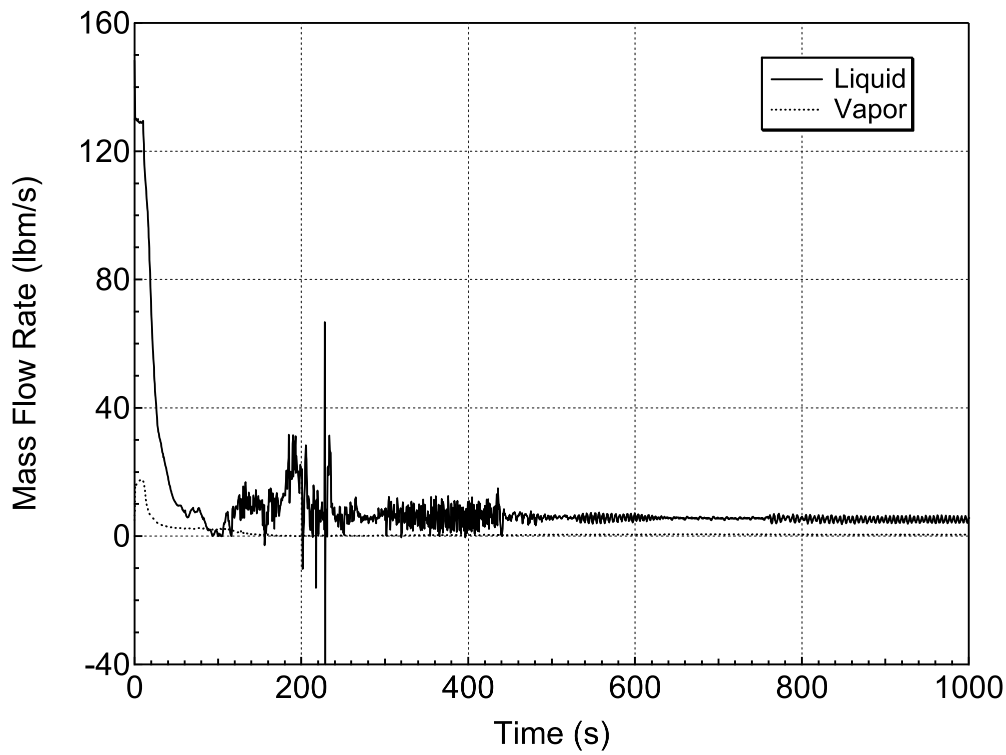

Figure 5.1.1.b-18 Hot Assembly Exit Vapor and Liquid Mass Flowrates for 1-ft^2 Break (Bottom)
(Break Location Sensitivity Study for Hot-leg Break)

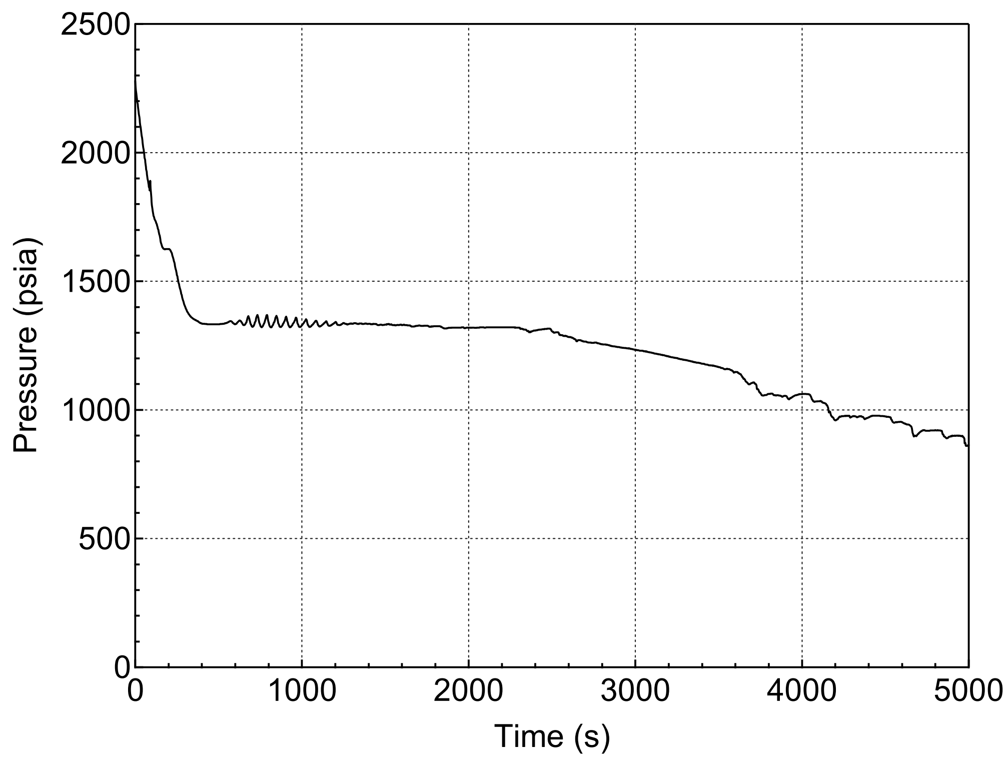

Figure 5.1.1.c-1 RCS (Pressurizer) Pressure Transient for 2-inch Break (Bottom) (Break Location Sensitivity Study for Crossover-leg Break)

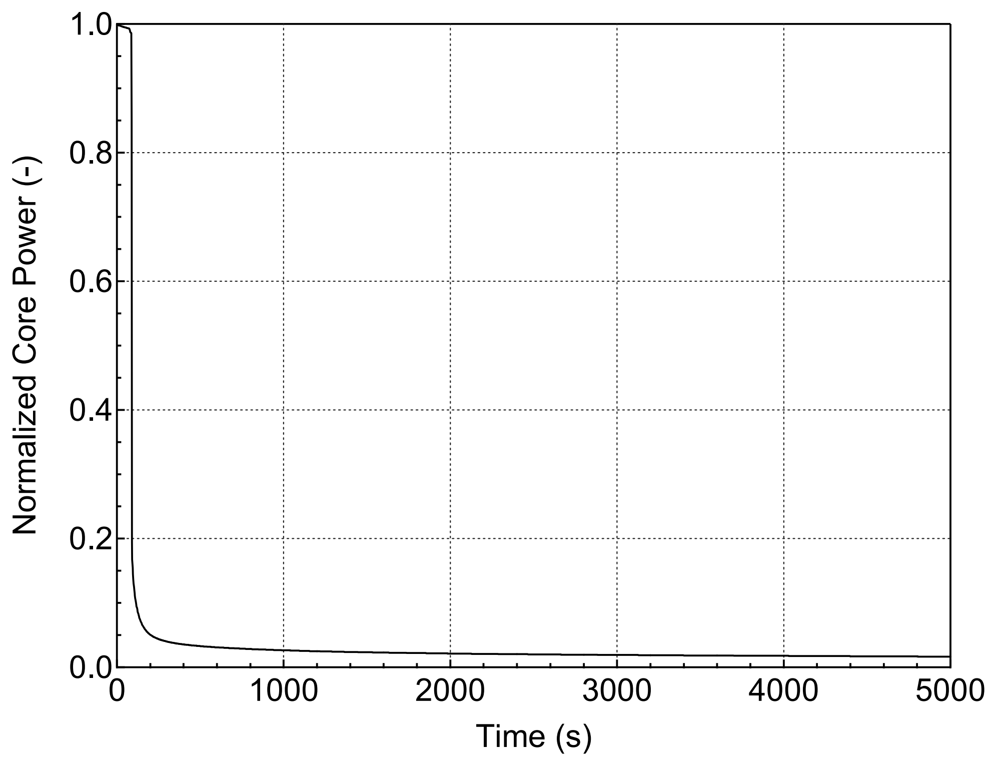

Figure 5.1.1.c-2 Normalized Core Power for 2-inch Break (Bottom)
(Break Location Sensitivity Study for Crossover-leg Break)

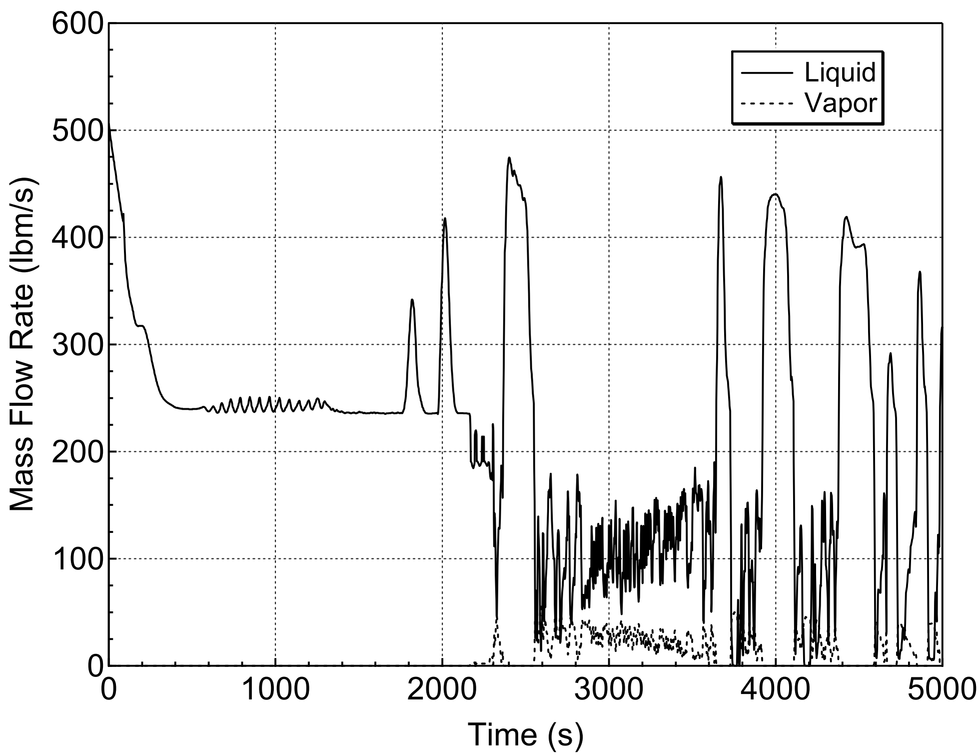

Figure 5.1.1.c-3 Liquid and Vapor Discharges through the Break for 2-inch Break (Bottom) (Break Location Sensitivity Study for Crossover-leg Break)

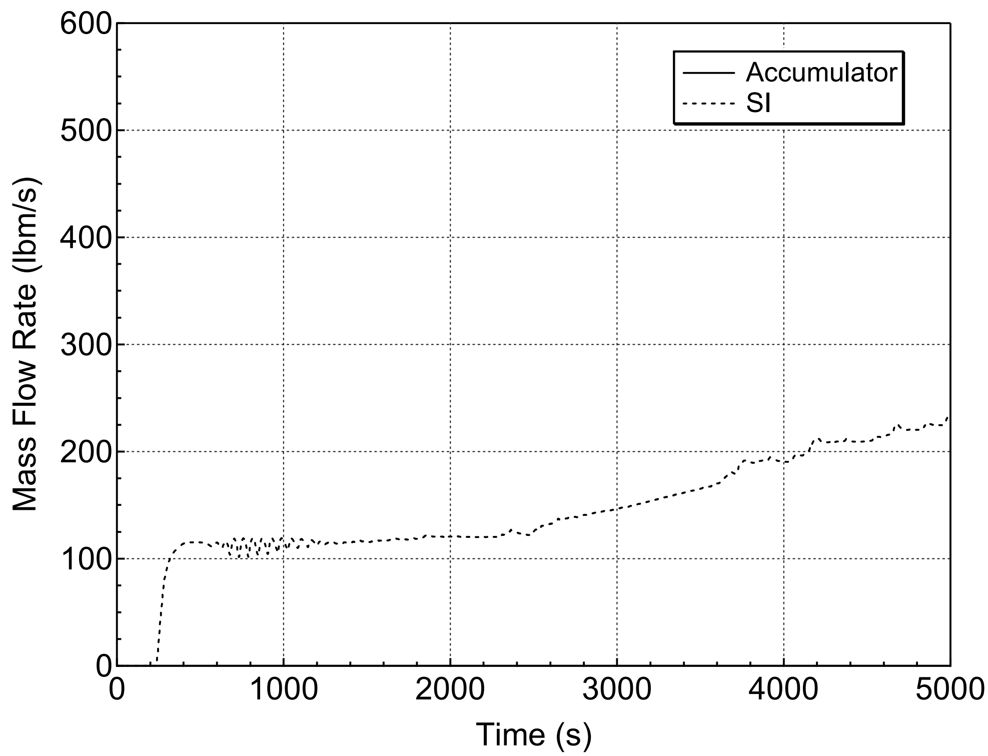

Figure 5.1.1.c-4 Accumulator and Safety Injection Mass Flowrates for 2-inch Break (Bottom) (Break Location Sensitivity Study for Crossover-leg Break)

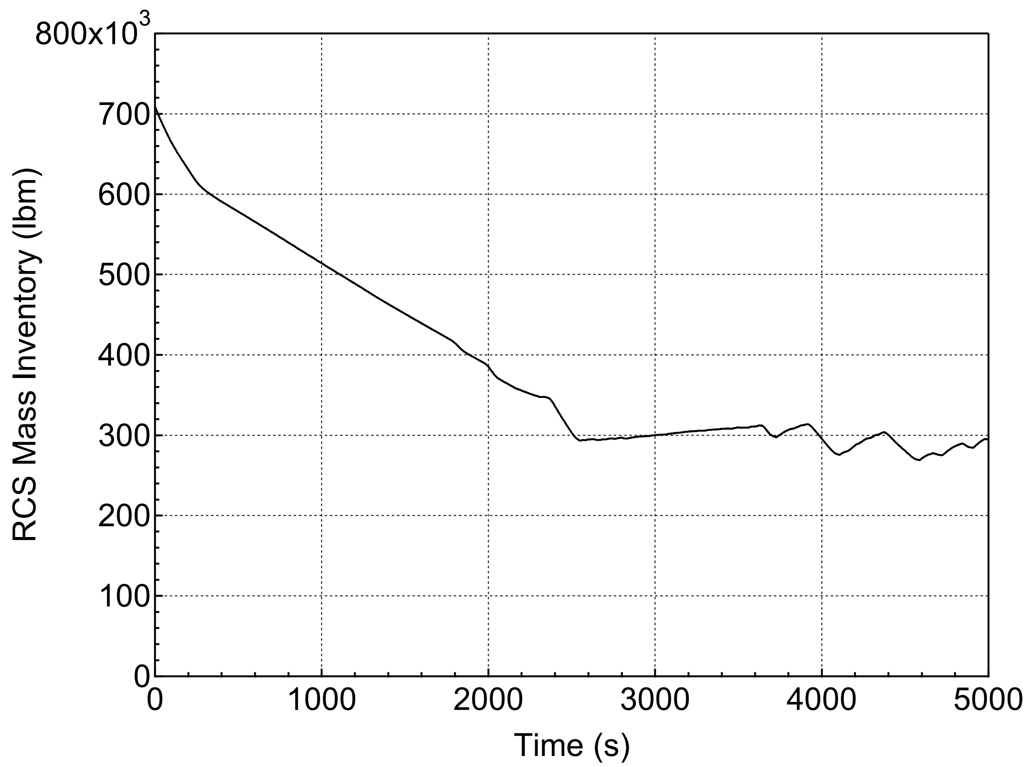

Figure 5.1.1.c-5 RCS Mass Inventory for 2-inch Break (Bottom)
(Break Location Sensitivity Study for Crossover-leg Break)

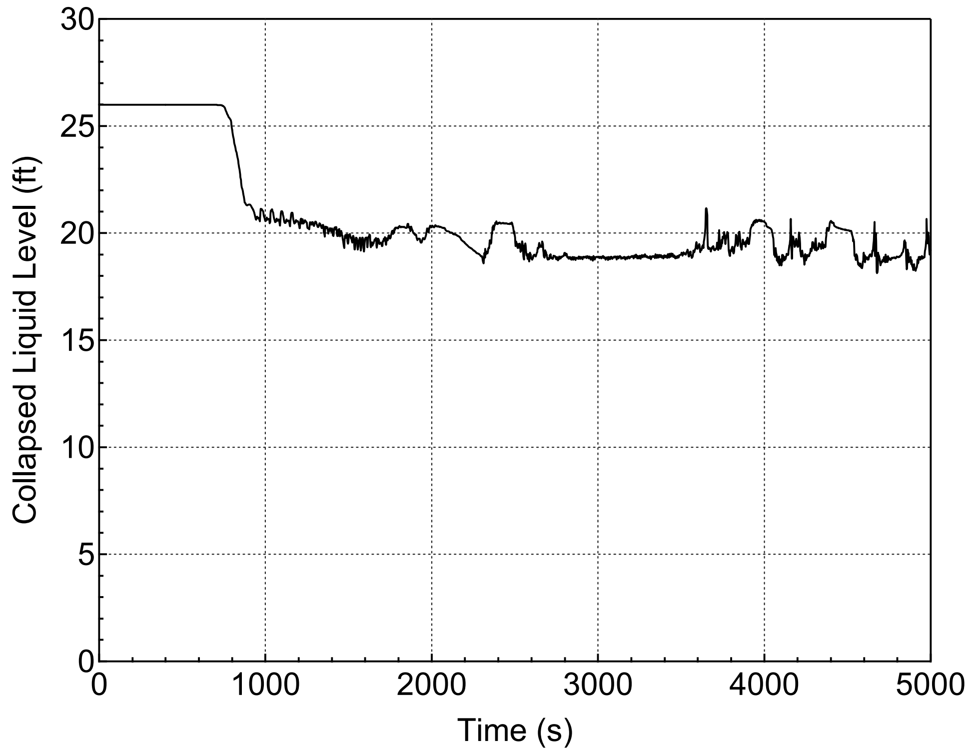

Figure 5.1.1.c-6 Downcomer Collapsed Level for 2-inch Break (Bottom)
(Break Location Sensitivity Study for Crossover-leg Break)

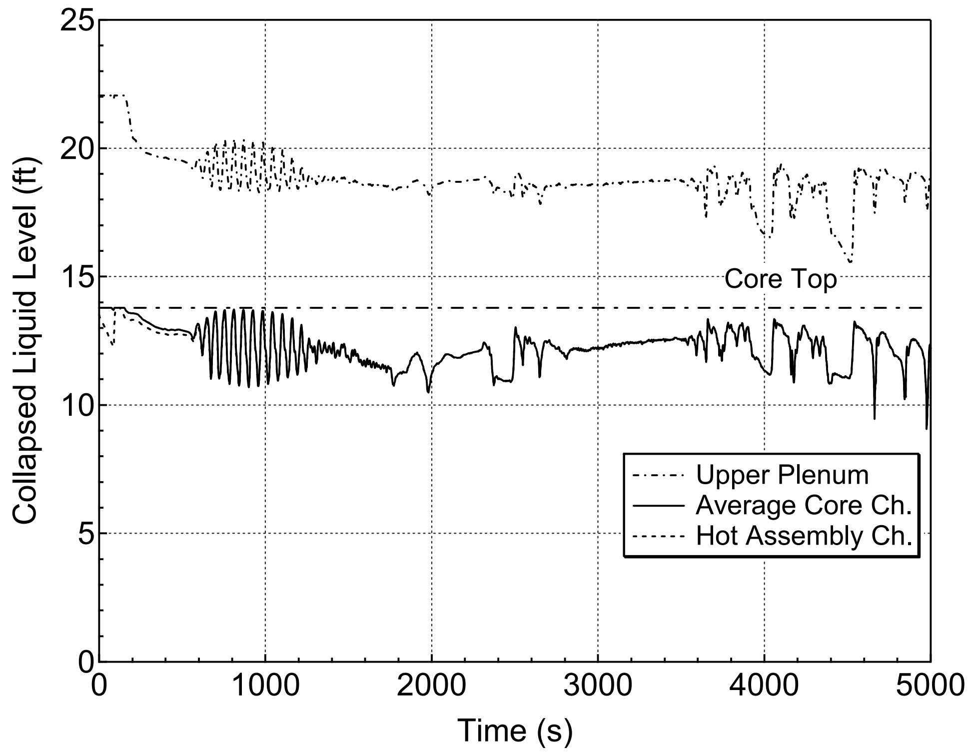

Figure 5.1.1.c-7 Core and Upper Plenum Collapsed Levels for 2-inch Break (Bottom) (Break Location Sensitivity Study for Crossover-leg Break)

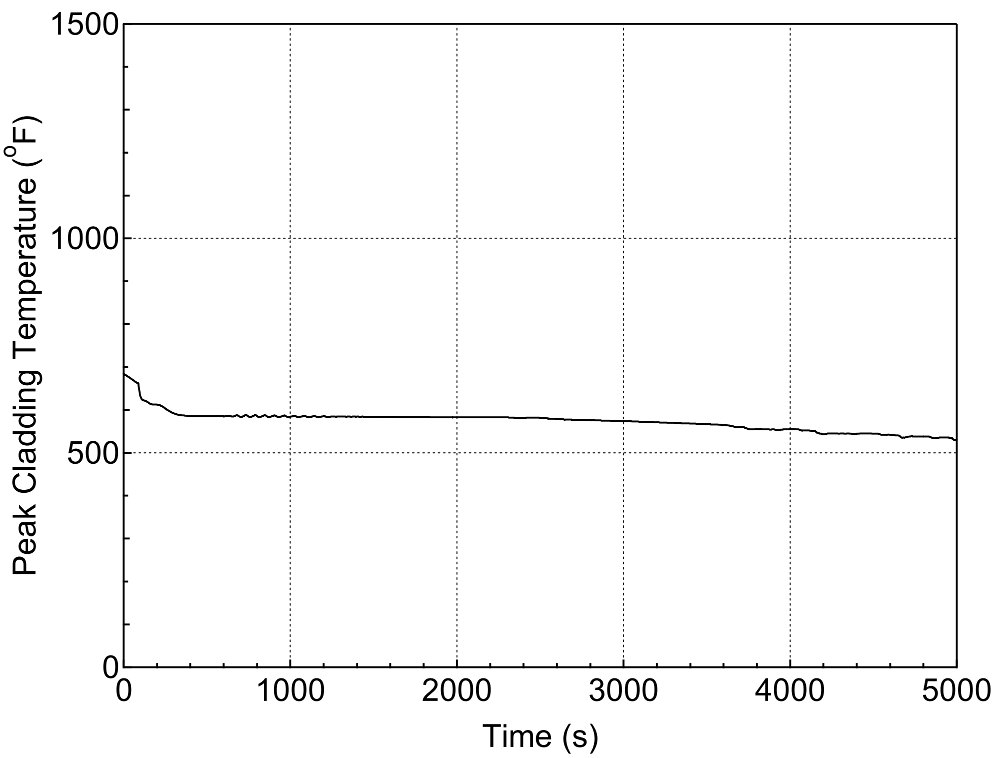

Figure 5.1.1.c-8 PCT at All Elevations for Hot Rod in Hot Assembly for 2-inch Break (Bottom) (Break Location Sensitivity Study for Crossover-leg Break)

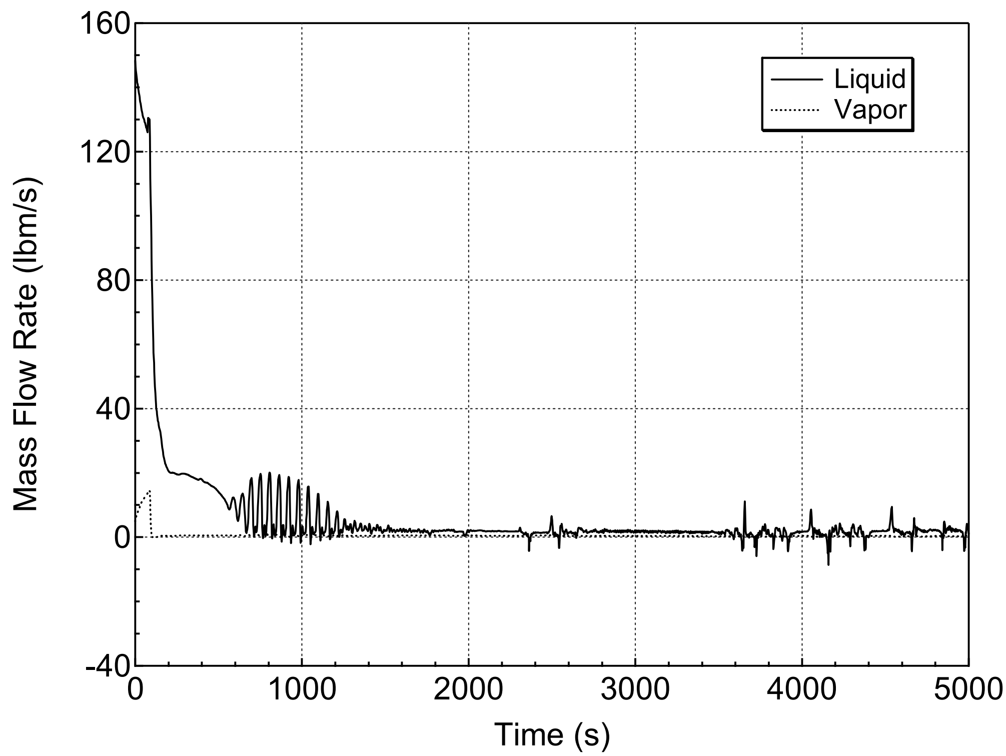

Figure 5.1.1.c-9 Hot Assembly Exit Vapor and Liquid Mass Flowrates for 2-inch Break (Bottom) (Break Location Sensitivity Study for Crossover-leg Break)

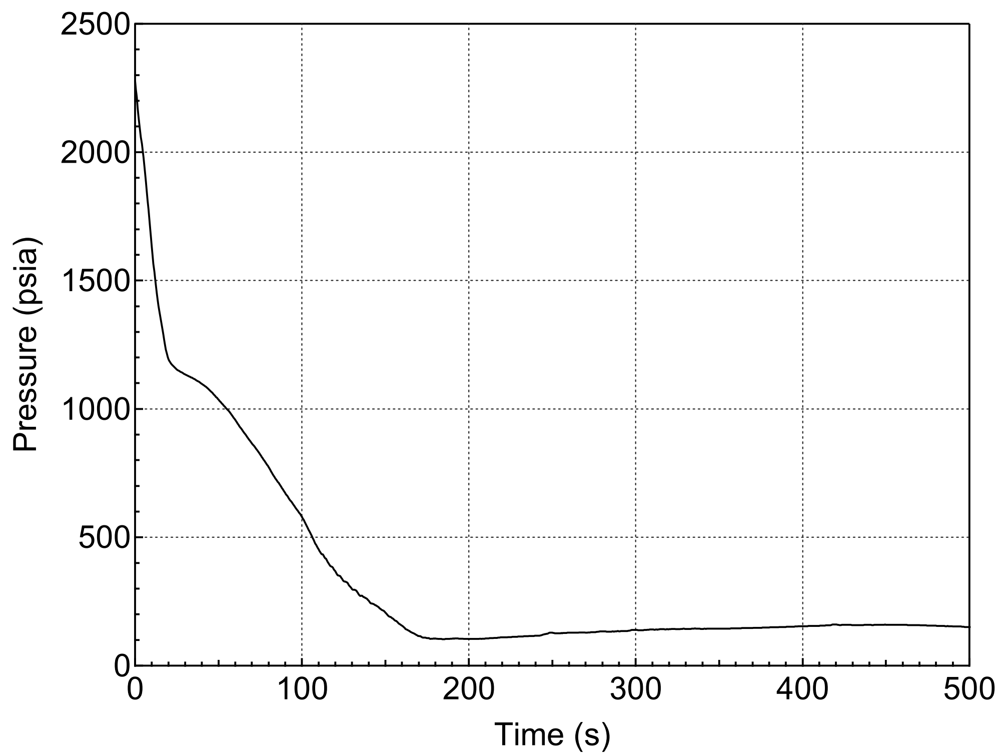

Figure 5.1.1.c-10 RCS (Pressurizer) Pressure Transient for 1-ft^2 Break (Bottom)
(Break Location Sensitivity Study for Crossover-leg Break)

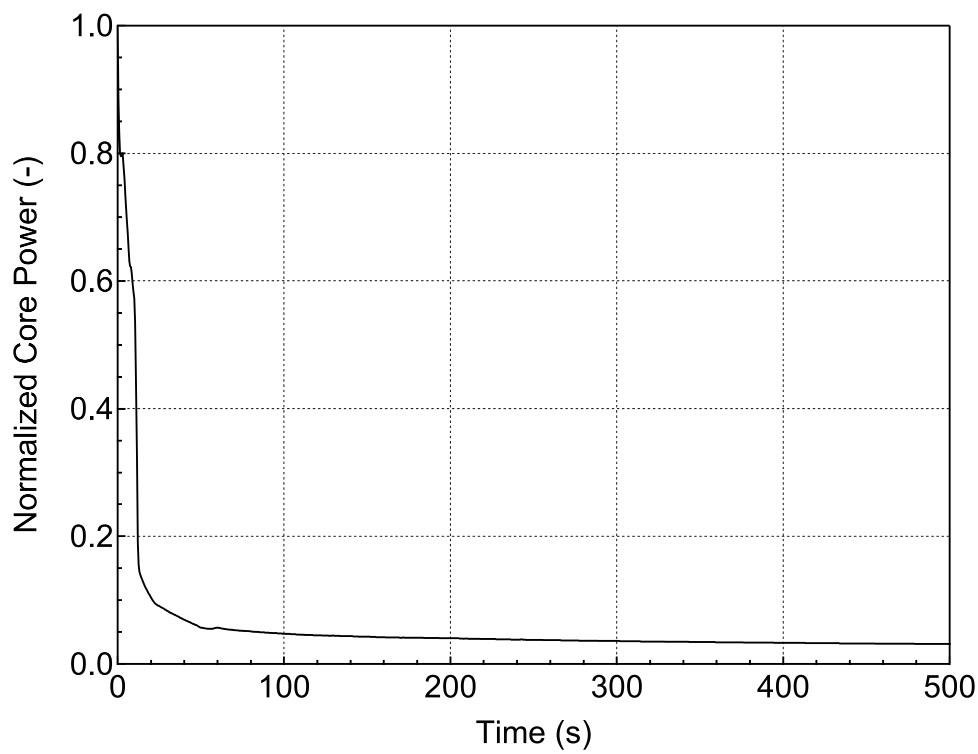

Figure 5.1.1.c-11 Normalized Core Power for 1-ft^2 Break (Bottom)
(Break Location Sensitivity Study for Crossover-leg Break)

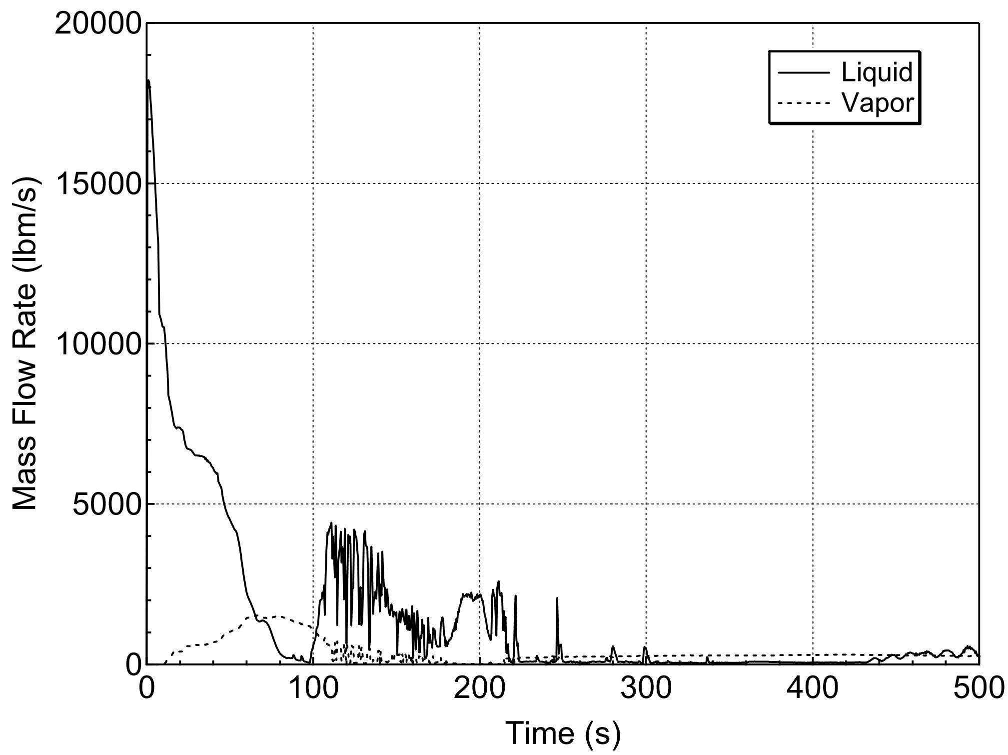

Figure 5.1.1.c-12 Liquid and Vapor Discharges through the Break for 1-ft^2 Break (Bottom) (Break Location Sensitivity Study for Crossover-leg Break)

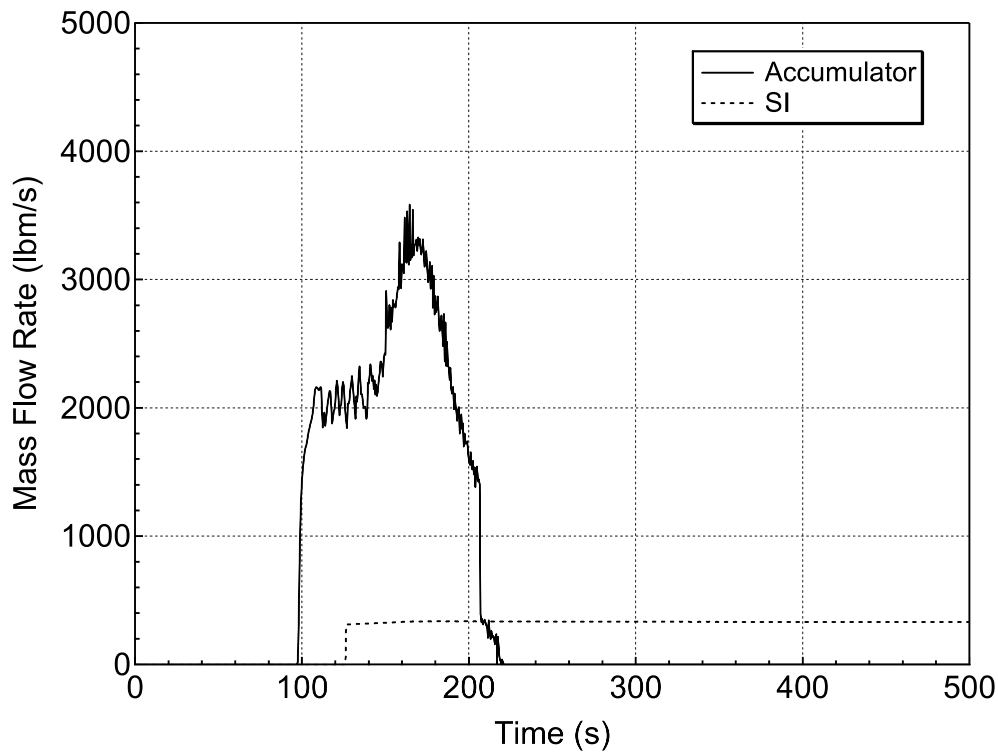

Figure 5.1.1.c-13 Accumulator and Safety Injection Mass Flowrates for 1-ft^2 Break (Bottom)
(Break Location Sensitivity Study for Crossover-leg Break)

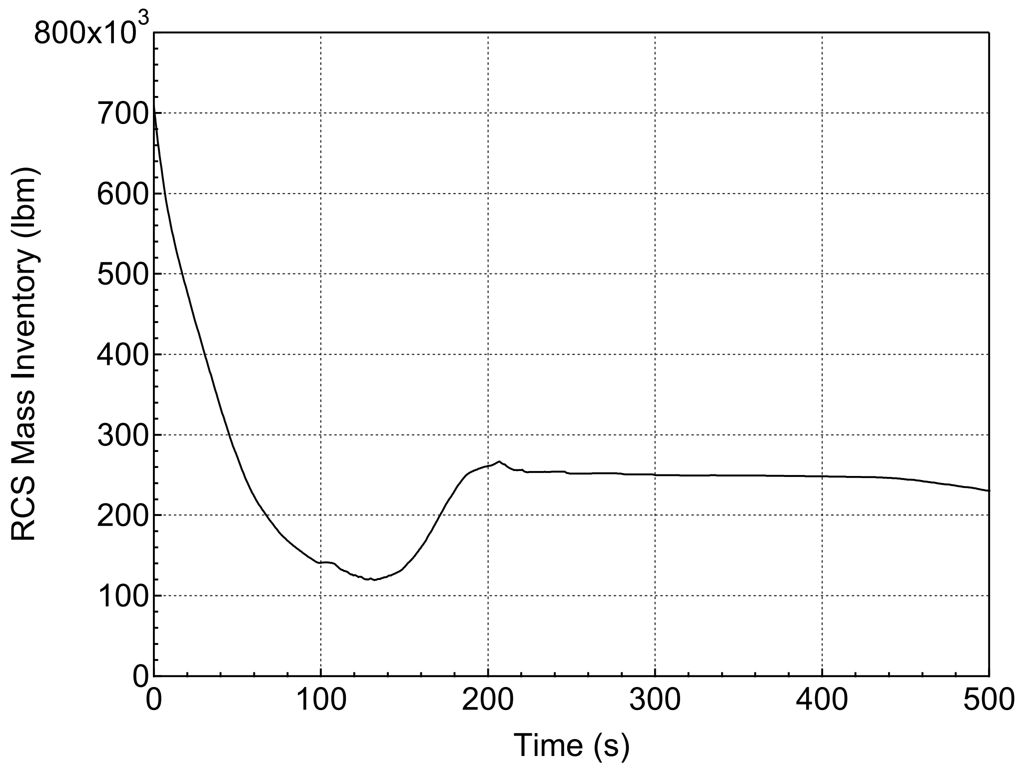

Figure 5.1.1.c-14 RCS Mass Inventory for 1-ft^2 Break (Bottom)
(Break Location Sensitivity Study for Crossover-leg Break)

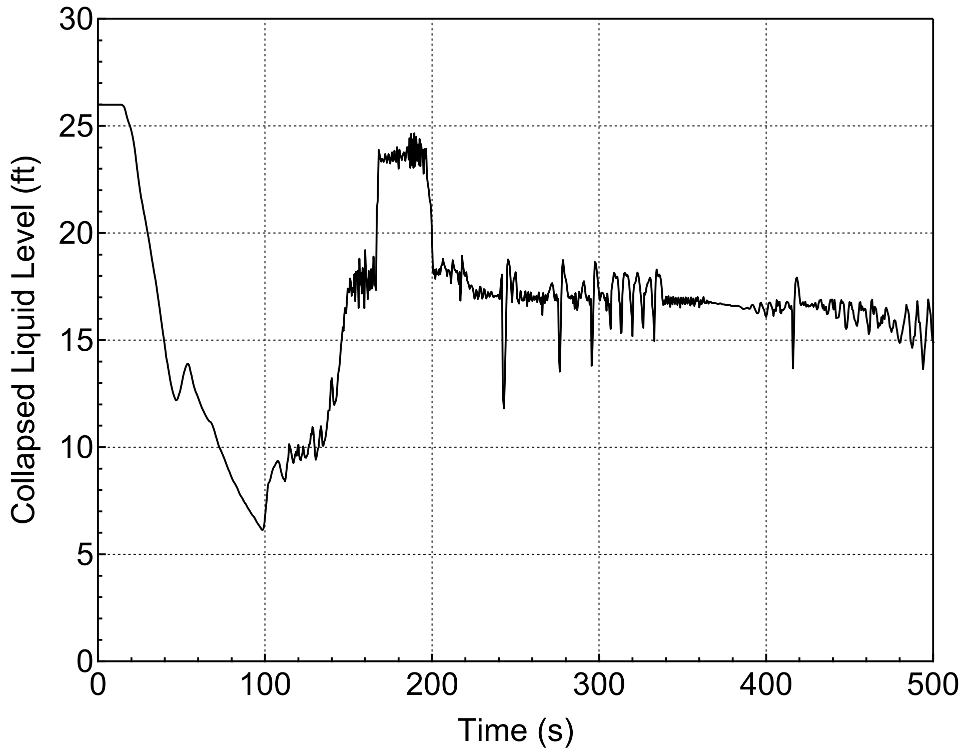

Figure 5.1.1.c-15 Downcomer Collapsed Level for 1-ft² Break (Bottom)
(Break Location Sensitivity Study for Crossover-leg Break)

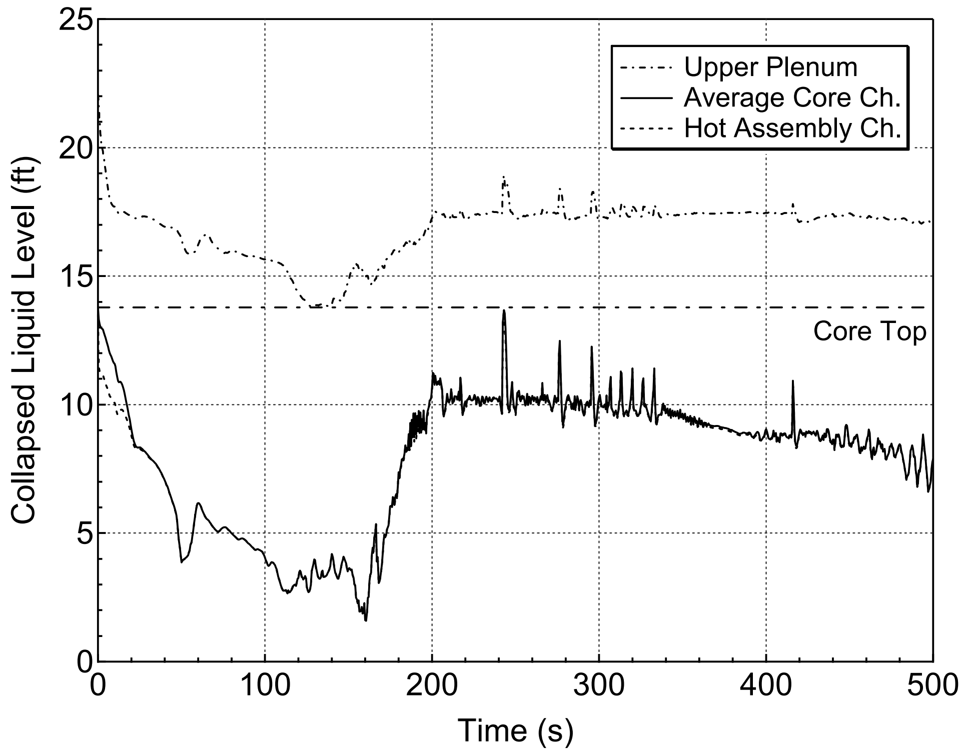

Figure 5.1.1.c-16 Core and Upper Plenum Collapsed Levels for 1-ft^2 Break (Bottom) (Break Location Sensitivity Study for Crossover-leg Break)

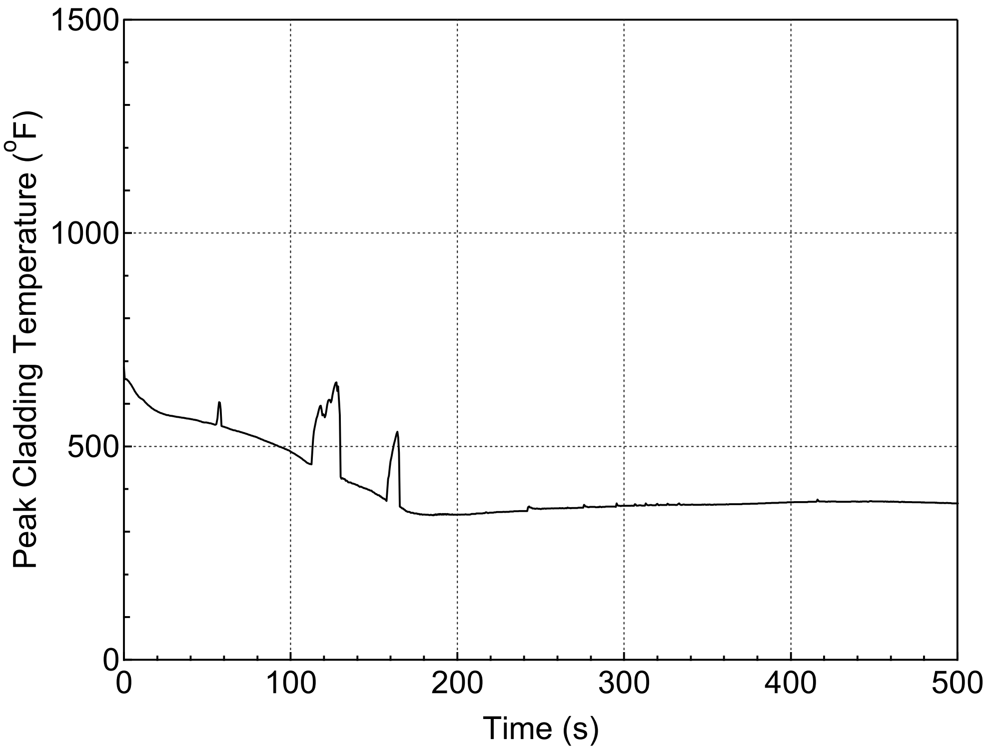

Figure 5.1.1.c-17 PCT at All Elevations for Hot Rod in Hot Assembly for 1-ft^2 Break (Bottom)
(Break Location Sensitivity Study for Crossover-leg Break)

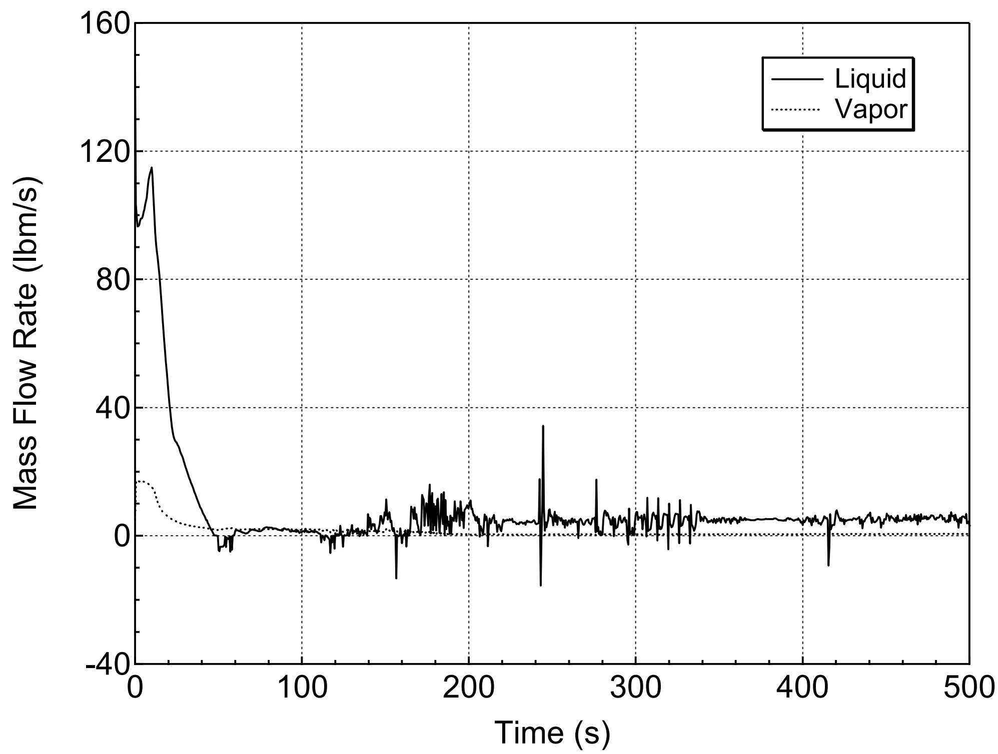

Figure 5.1.1.c-18 Hot Assembly Exit Vapor and Liquid Mass Flowrates for 1-ft^2 Break (Bottom)

(Break Location Sensitivity Study for Crossover-leg Break)

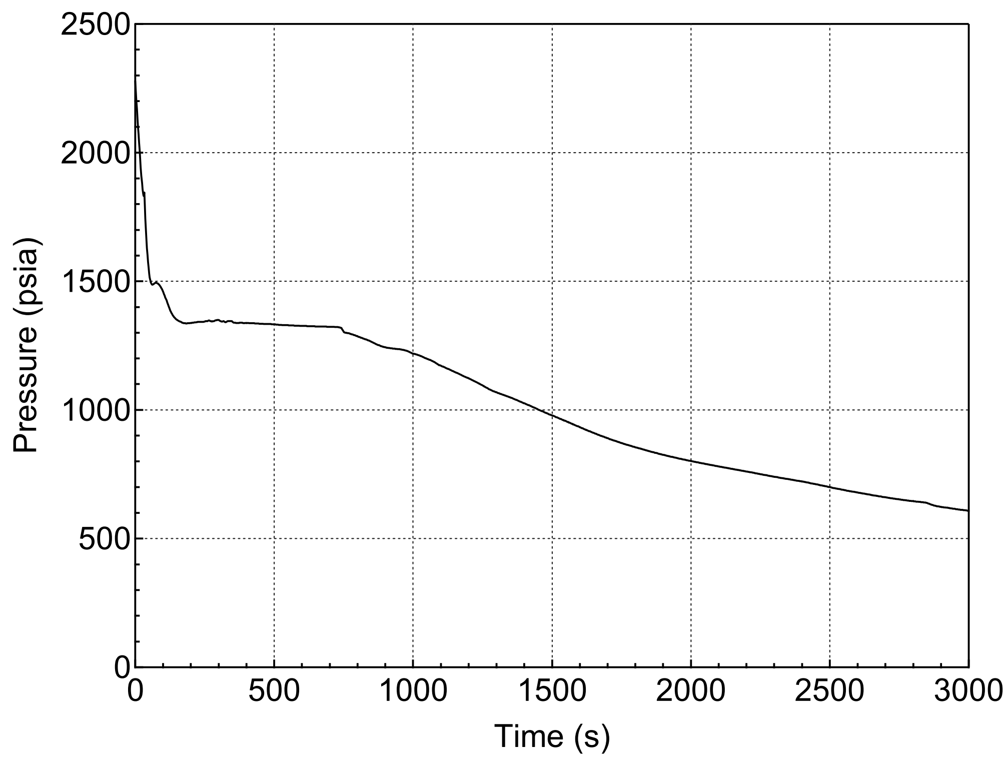

Figure 5.1.2-1 RCS (Pressurizer) Pressure Transient for DVI-line Break (Break Location Sensitivity Study)

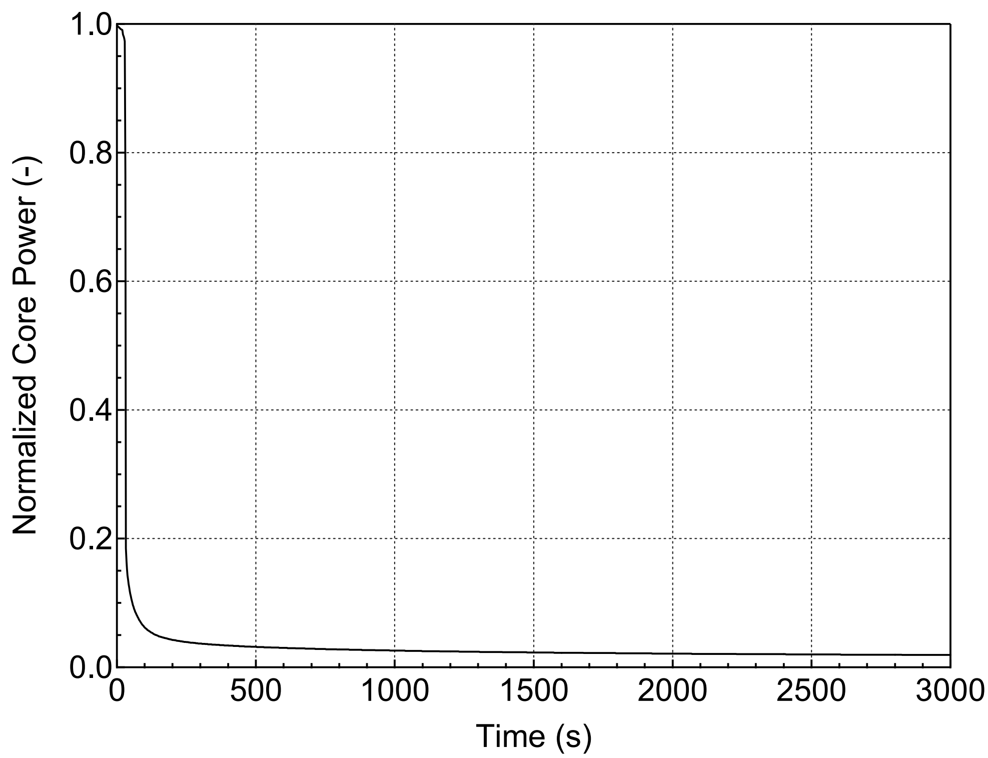

Figure 5.1.2-2 Normalized Core Power for DVI-line Break
(Break Location Sensitivity Study)

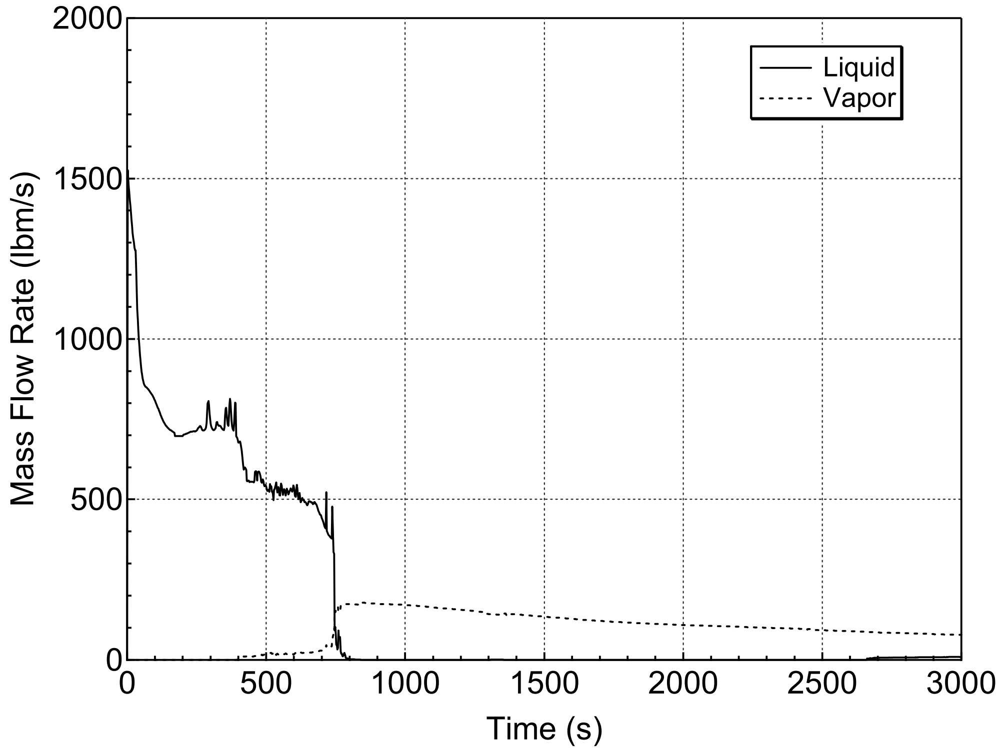

Figure 5.1.2-3 Liquid and Vapor Discharges through the Break for DVI-line Break (Break Location Sensitivity Study)

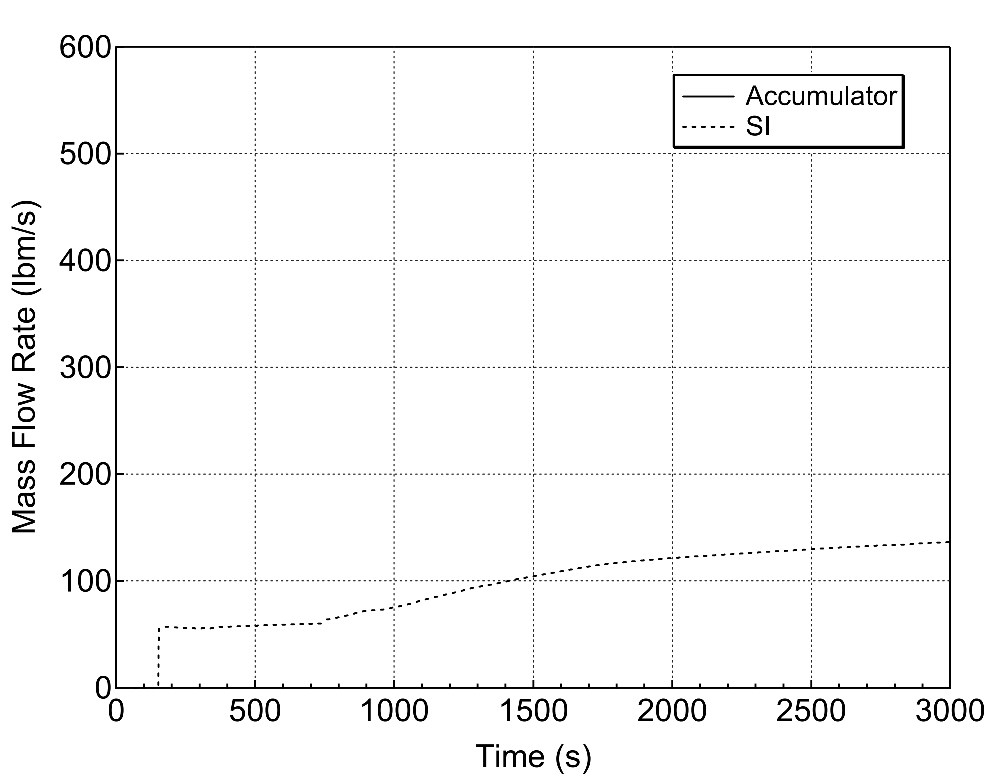

Figure 5.1.2-4 Accumulator and Safety Injection Mass Flowrates for DVI-line Break (Break Location Sensitivity Study)

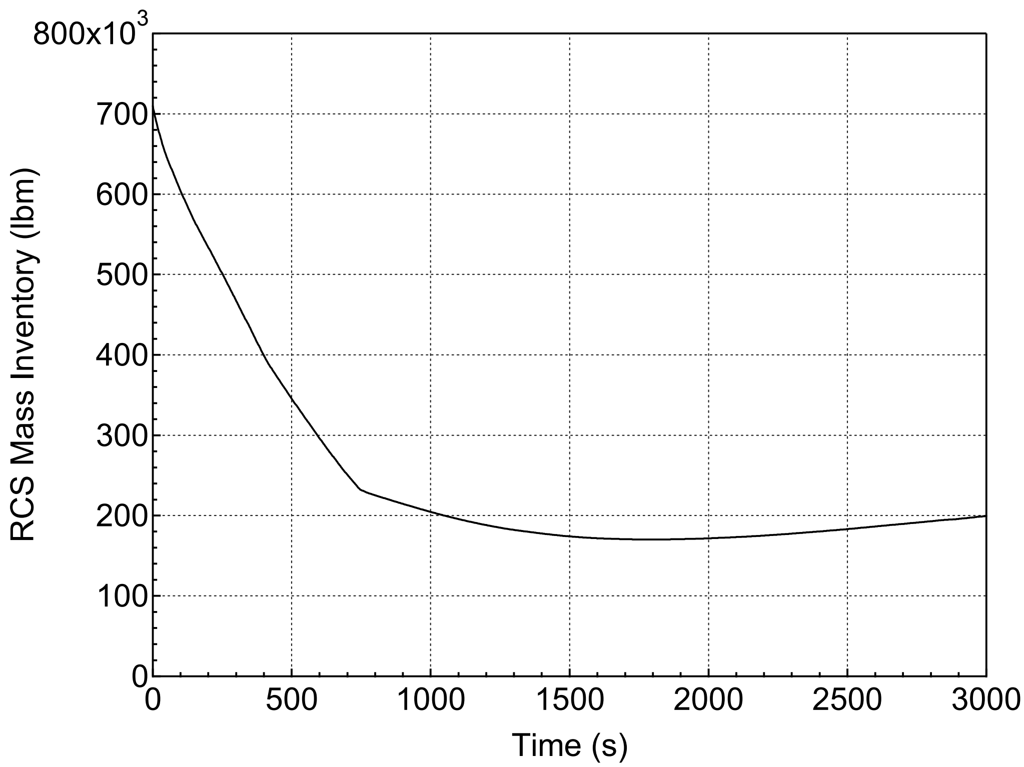

Figure 5.1.2-5 RCS Mass Inventory for DVI-line Break (Break Location Sensitivity Study)

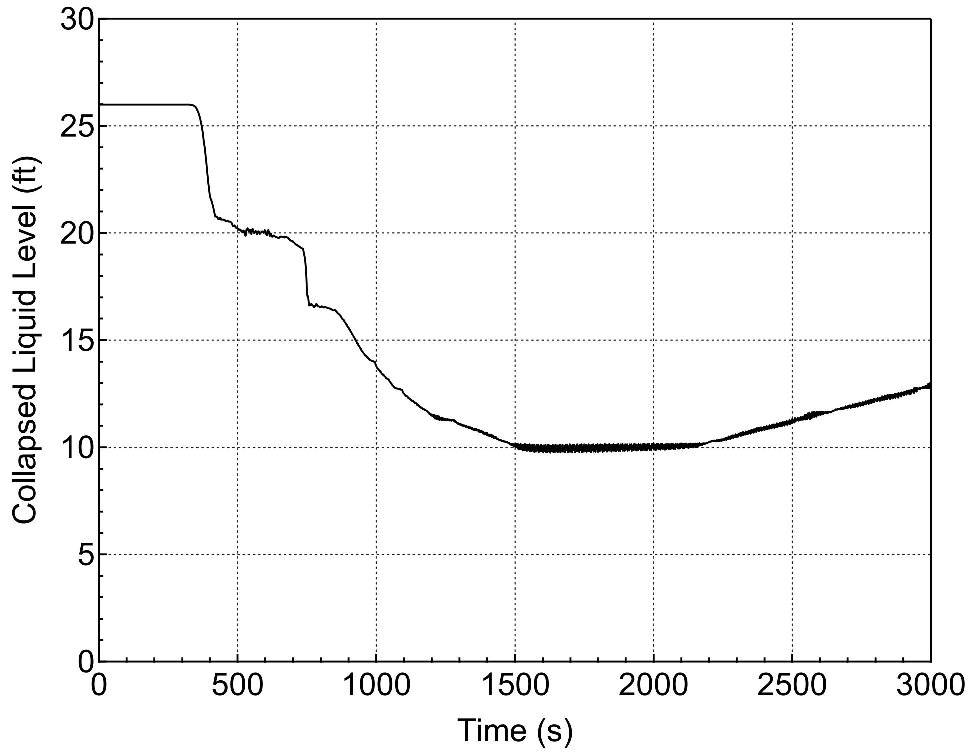

Figure 5.1.2-6 Downcomer Collapsed Level for DVI-line Break (Break Location Sensitivity Study)

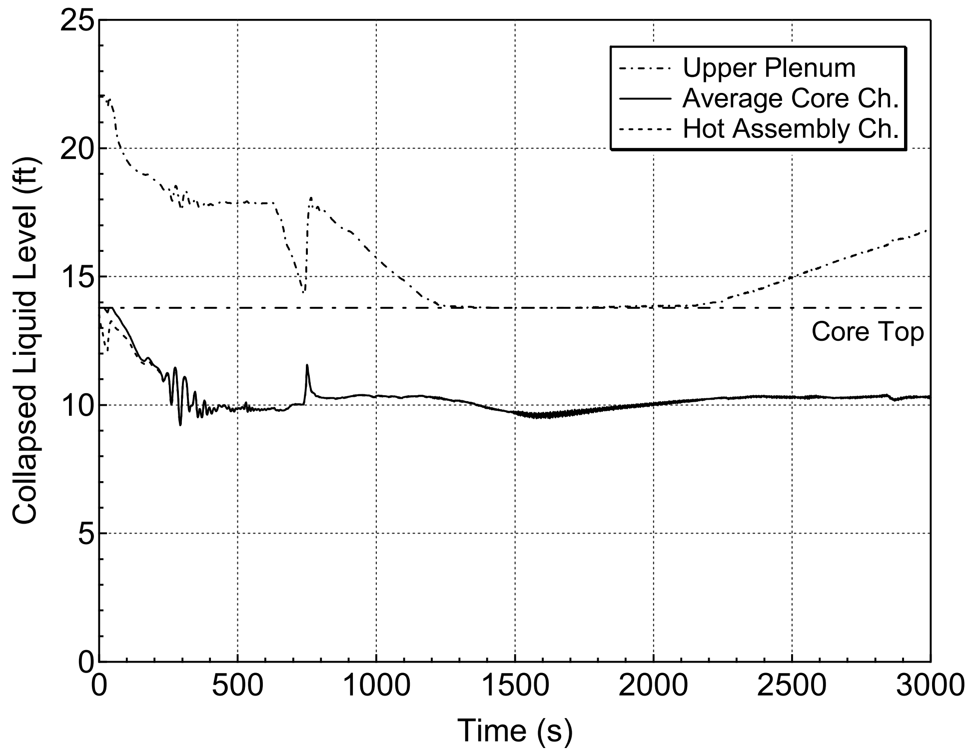

Figure 5.1.2-7 Core and Upper Plenum Collapsed Levels for DVI-line Break (Break Location Sensitivity Study)

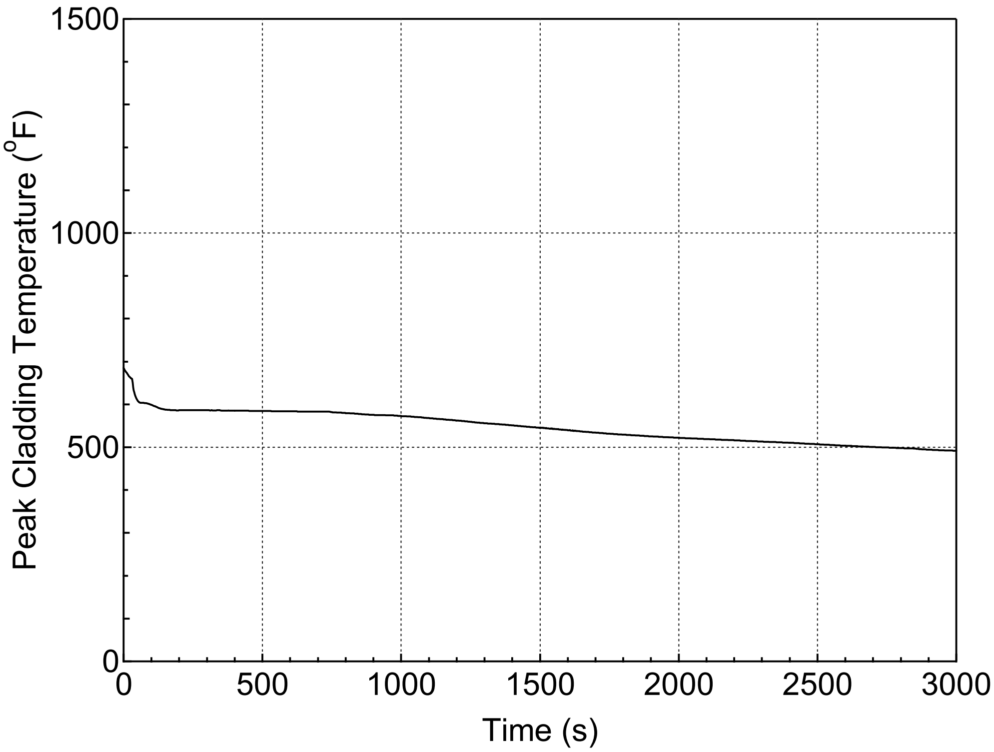

Figure 5.1.2-8 PCT at All Elevations for Hot Rod in Hot Assembly for DVI-line Break (Break Location Sensitivity Study)

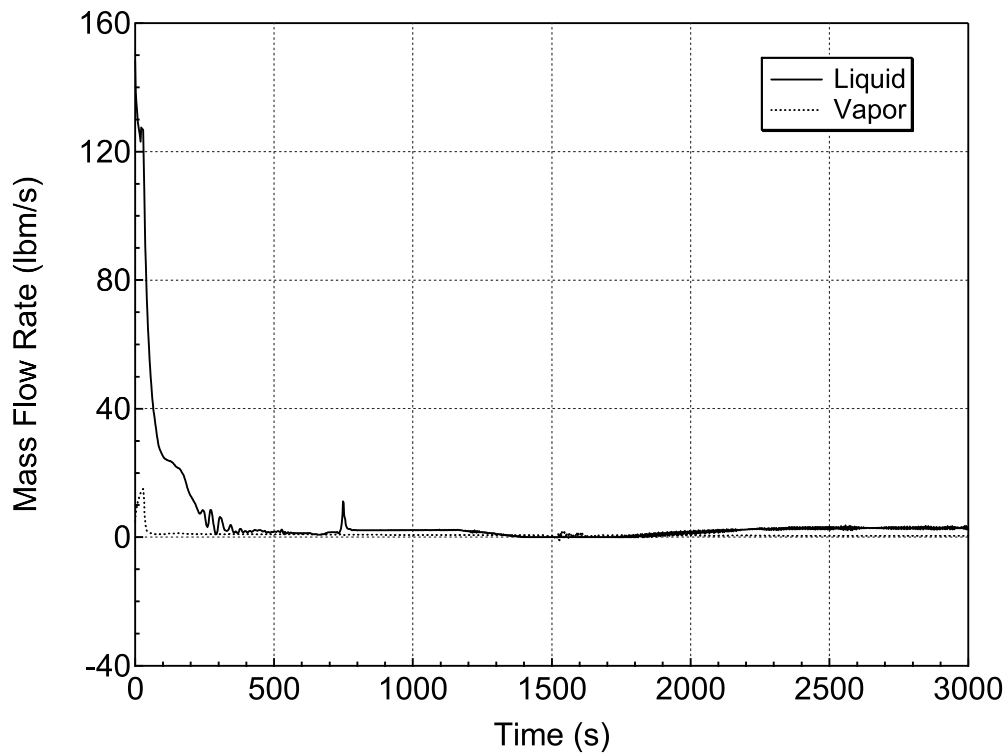

Figure 5.1.2-9 Hot Assembly Exit Vapor and Liquid Mass Flowrates for DVI-line Break (Break Location Sensitivity Study)

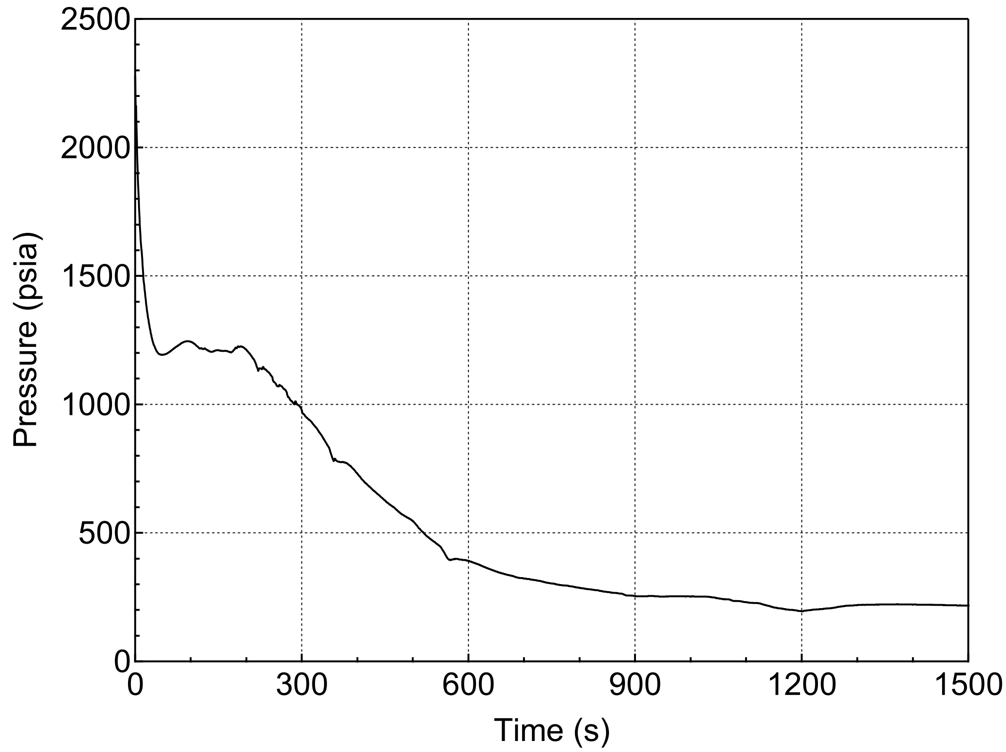

Figure 5.1.3-1 RCS (Pressurizer) Pressure Transient for Pressurizer Steam Phase Break (Break Location Sensitivity Study)

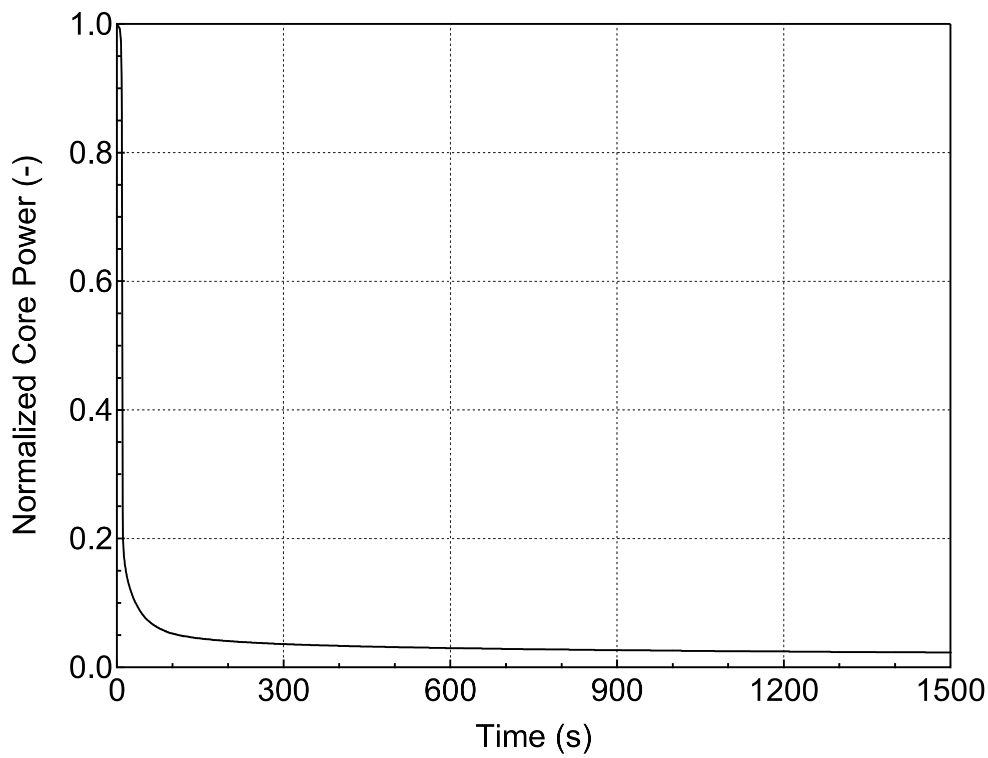

Figure 5.1.3-2 Normalized Core Power for Pressurizer Steam Phase Break (Break Location Sensitivity Study)

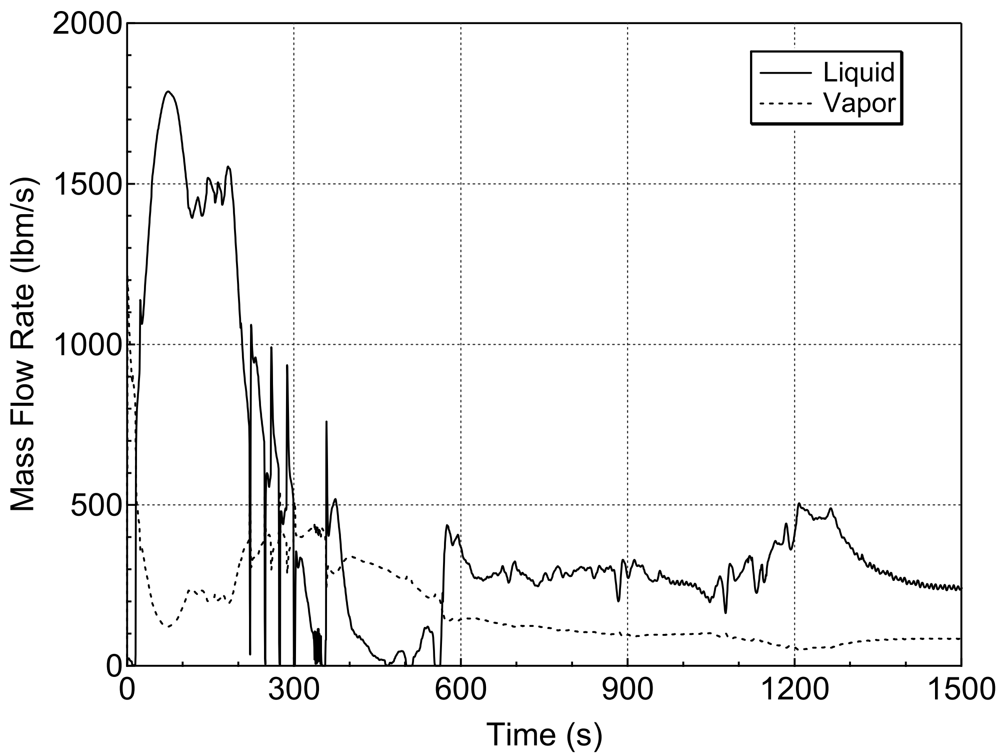

Figure 5.1.3-3 Liquid and Vapor Discharges through the Break for Pressurizer Steam Phase Break (Break Location Sensitivity Study)

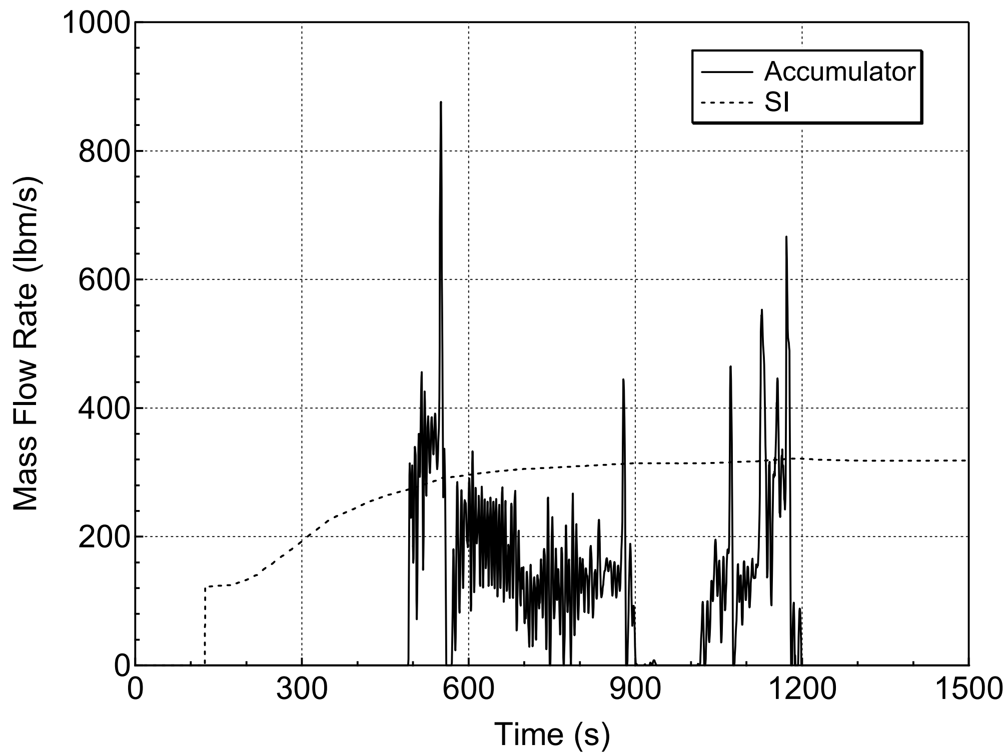

Figure 5.1.3-4 Accumulator and Safety Injection Mass Flowrates for Pressurizer Steam Phase Break (Break Location Sensitivity Study)

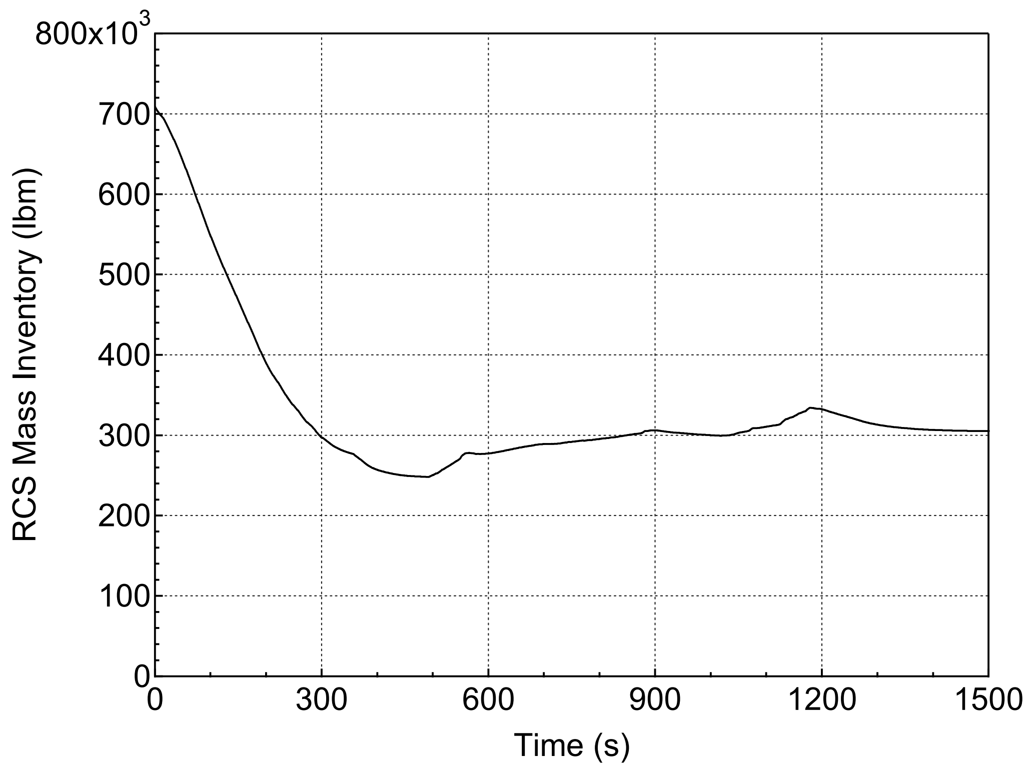

Figure 5.1.3-5 RCS Mass Inventory for Pressurizer Steam Phase Break (Break Location Sensitivity Study)

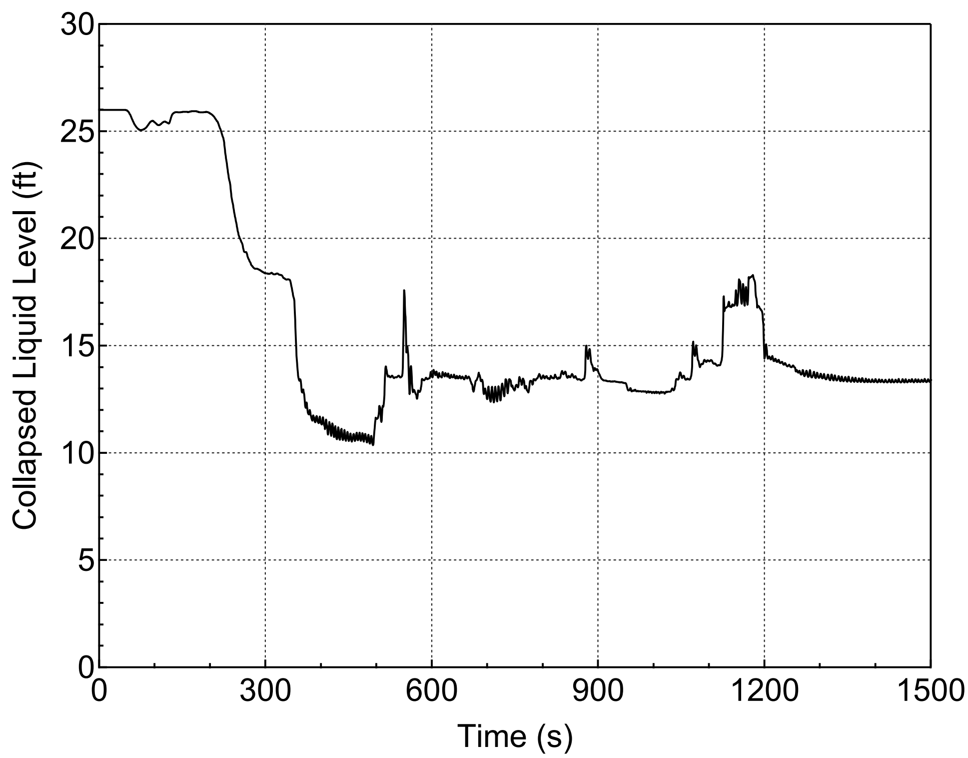

Figure 5.1.3-6 Downcomer Collapsed Level for Pressurizer Steam Phase Break (Break Location Sensitivity Study)

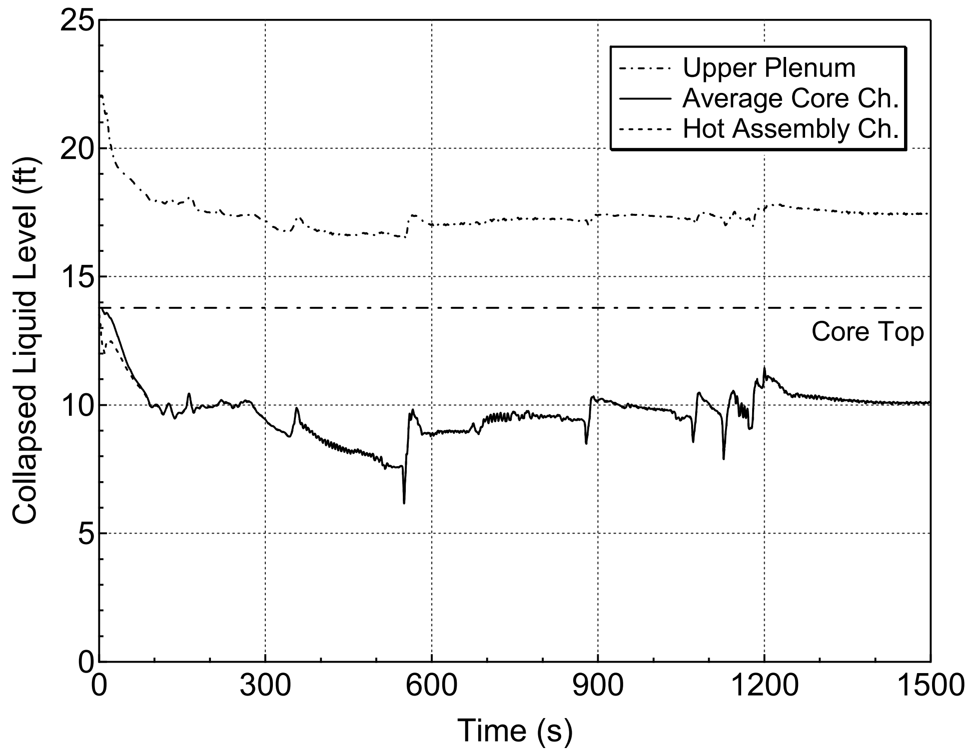

Figure 5.1.3-7 Core and Upper Plenum Collapsed Levels for Pressurizer Steam Phase Break (Break Location Sensitivity Study)

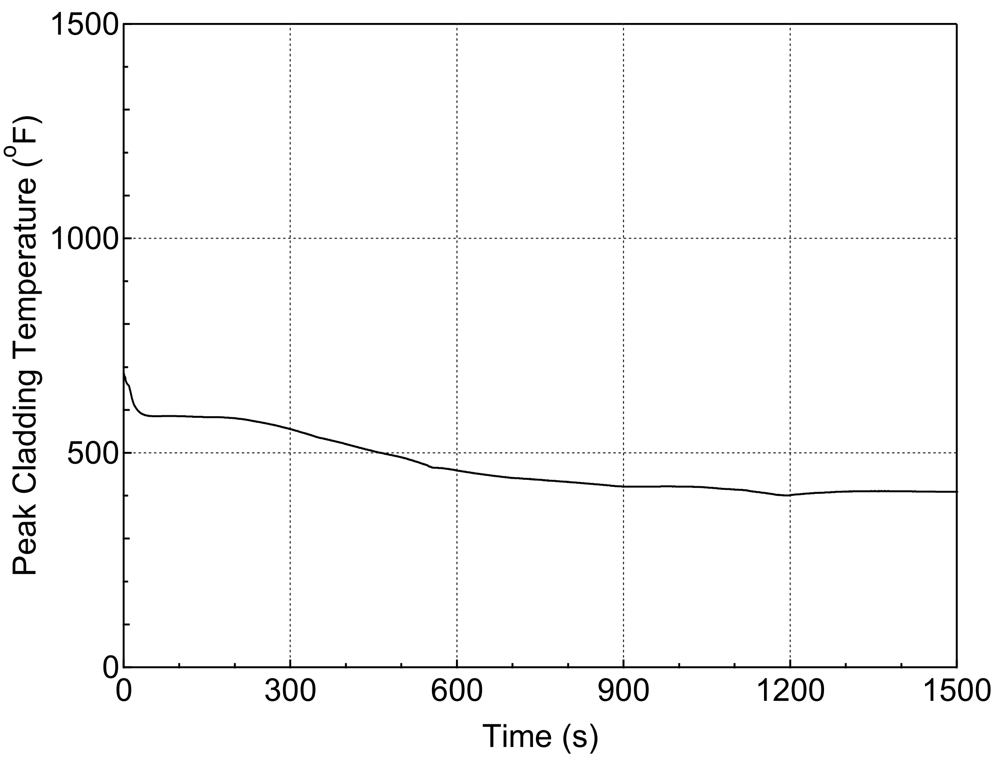

Figure 5.1.3-8 PCT at All Elevations for Hot Rod in Hot Assembly for Pressurizer Steam Phase Break (Break Location Sensitivity Study)

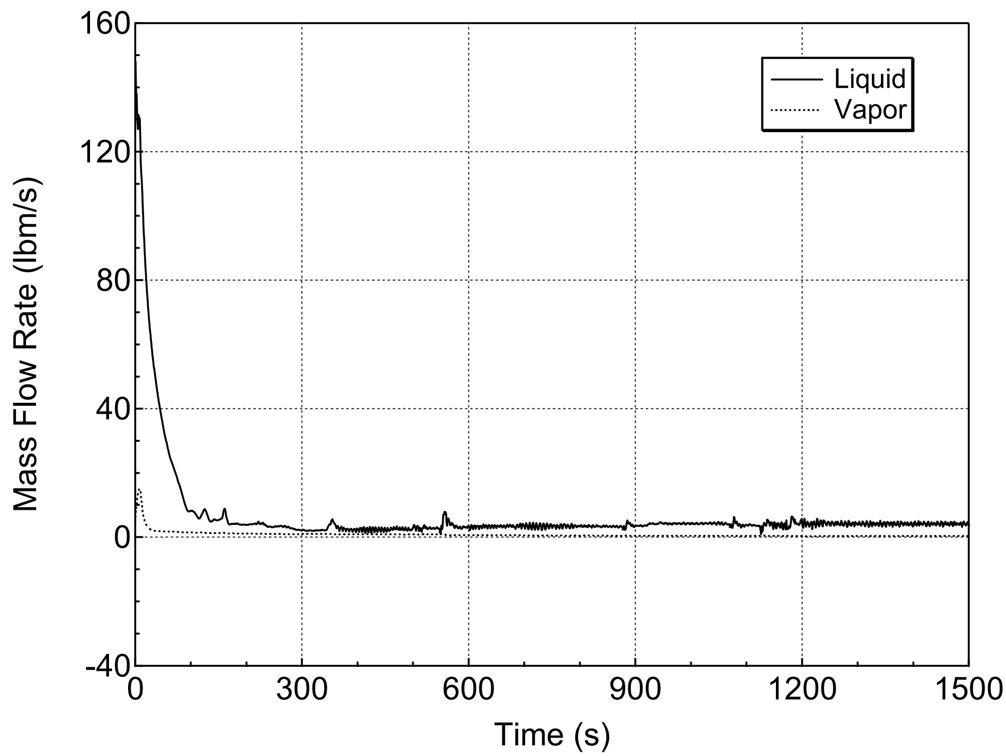

Figure 5.1.3-9 Hot Assembly Exit Vapor and Liquid Mass Flowrates for Pressurizer Steam Phase Break (Break Location Sensitivity Study)

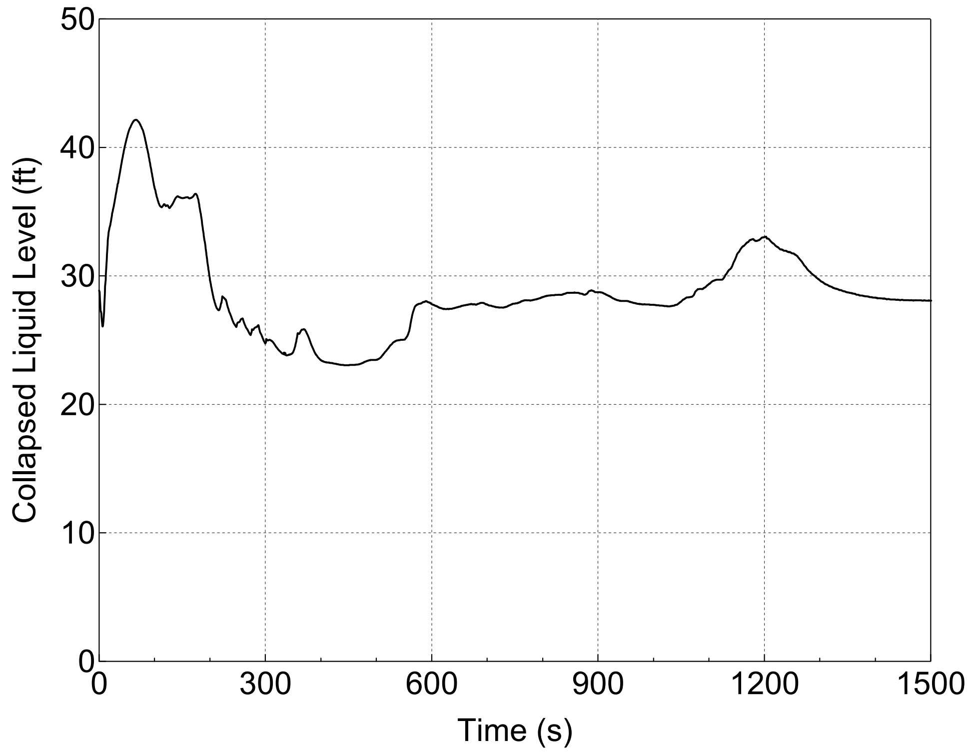

Figure 5.1.3-10 Pressurizer Collapsed Level for Pressurizer Steam Phase Break (Break Location Sensitivity Study)

5.2 Spectrum Analysis for Cold Leg Break

In the preceding section 5.1, it is confirmed that the limiting break location for the US-APWR is at the cold-leg. In this section, break spectrum analyses for cold leg break with integer inch diameter were performed to obtain the break size spectrum for loop-seal PCT and boil-off PCT. Break sizes ranging from 1-inch through 13-inch and 1ft^2 (13.5 inch) break were calculated. Bottom breaks were assumed for all calculations. The spectrum has sufficient resolution to locate the limiting conditions. The analyses were carried out until the top of the core recovered with a two-phase mixture and the cladding temperatures were reduced to temperatures near the saturation temperature.

Table 5.2-1 shows the PCT of all cases. The highest loop-seal PCT is resulted from the 7-inch break and the highest boil-off PCT is resulted from the 1-ft^2 break.

From the results, it is concluded that for most of the break sizes and orientations, the cladding temperatures are lower than the initial cladding temperature at the start of the break. It implies that the calculation either does not result in PCT or even though the heatups occur in some cases, they do not increase higher than the initial temperature at the break initiation. Only cases with break sizes of 6-inch, 7-inch, 8inch, 12-inch, 13-inch and 1-ft^2 resulted in higher PCTs than the initial temperature at the break initiation. It is confirmed that the SI-pumps and accumulators perform well and have the capability to mitigate all the spectrum of cold-leg breaks.

Table 5.2-1 Spectrum of Peak Cladding Temperatures for Cold-leg Break

Break size and orientation	Peak Cladding Temperature
1-inch at cold leg (bottom)	lower than the initial temperature
2-inch at cold leg (bottom)	lower than the initial temperature
3-inch at cold leg (bottom)	lower than the initial temperature
4-inch at cold leg (bottom)	lower than the initial temperature
5-inch at cold leg (bottom)	lower than the initial temperature
6-inch at cold leg (bottom)	719 (^oF)
7-inch at cold leg (bottom)	759 (^oF)
8-inch at cold leg (bottom)	696 (^oF)
9-inch at cold leg (bottom)	lower than the initial temperature
10-inch at cold leg (bottom)	lower than the initial temperature
11-inch at cold leg (bottom)	lower than the initial temperature
12-inch at cold leg (bottom)	741 (^oF)
13-inch at cold leg (bottom)	971 (^oF)
1-ft^2 at cold leg (bottom)	1029 (^oF)

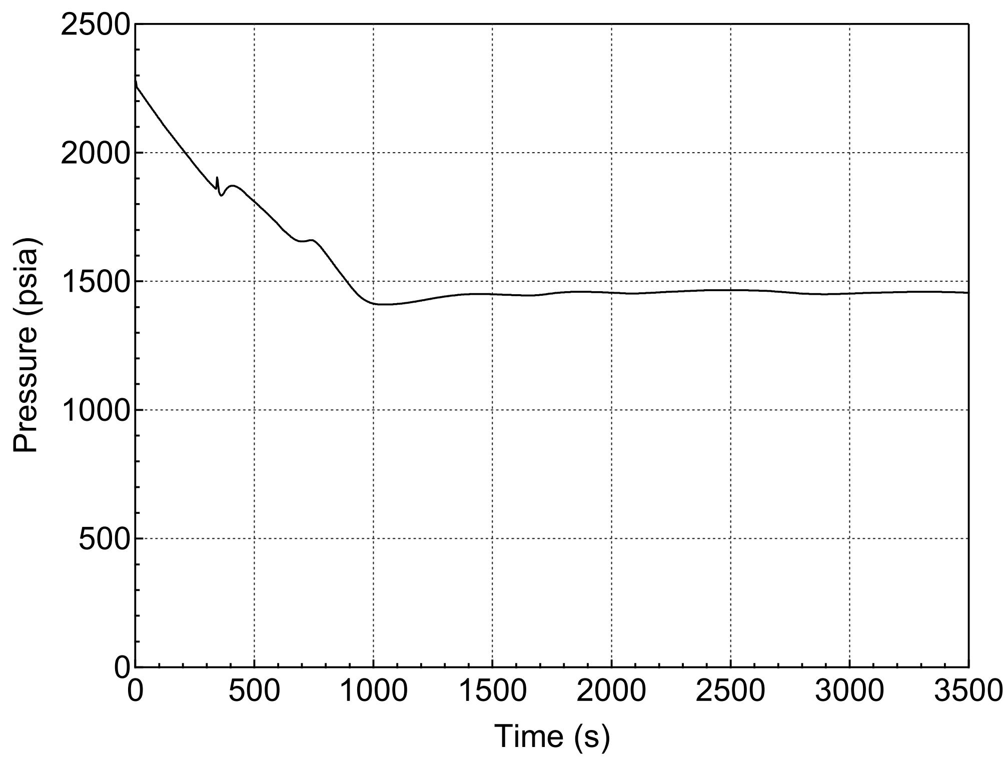

Figure 5.2.a-1 RCS (Pressurizer) Pressure Transient for 1-inch Break (Bottom) (Spectrum Analysis)

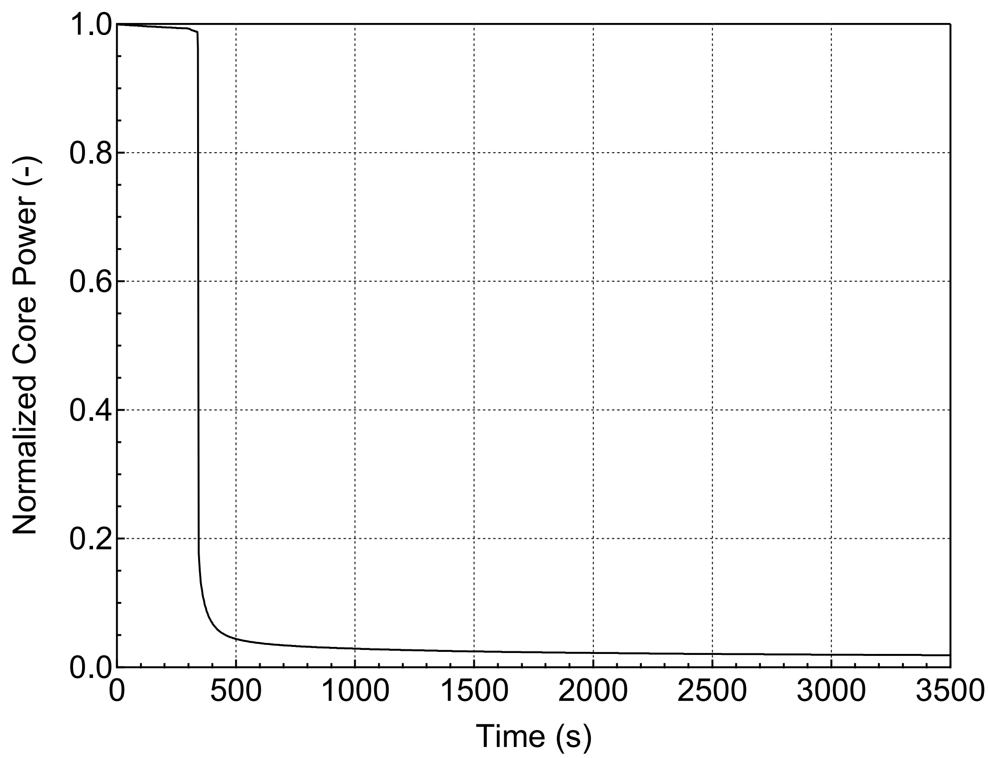

Figure 5.2.a-2 Normalized Core Power for 1-inch Break (Bottom) (Spectrum Analysis)

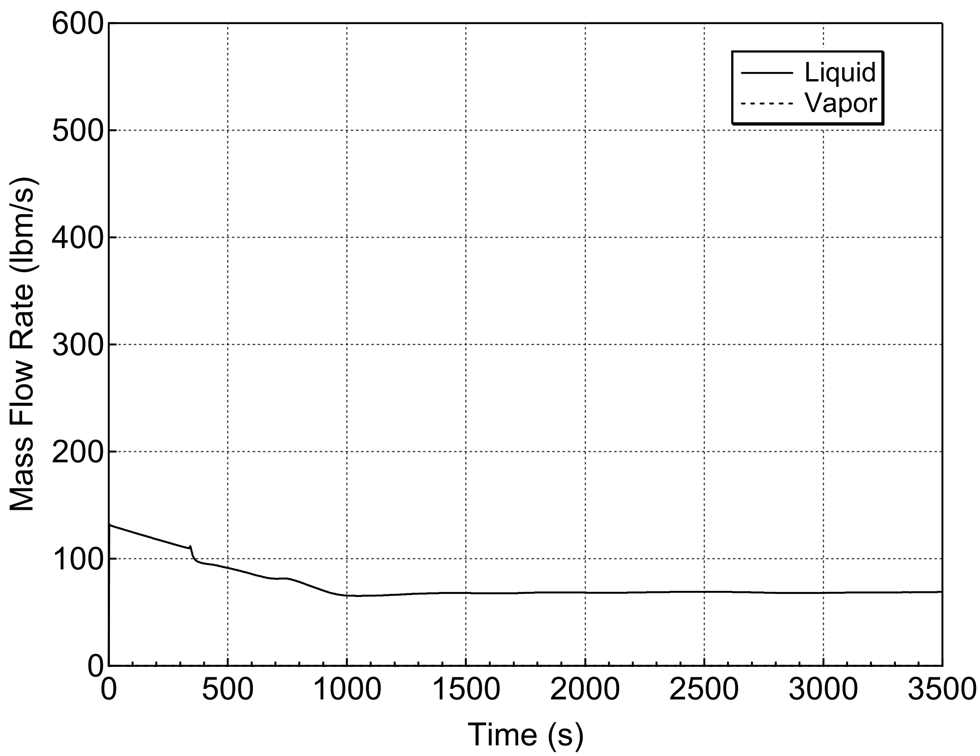

Figure 5.2.a-3 Liquid and Vapor Discharges through the Break for 1-inch Break (Bottom) (Spectrum Analysis)

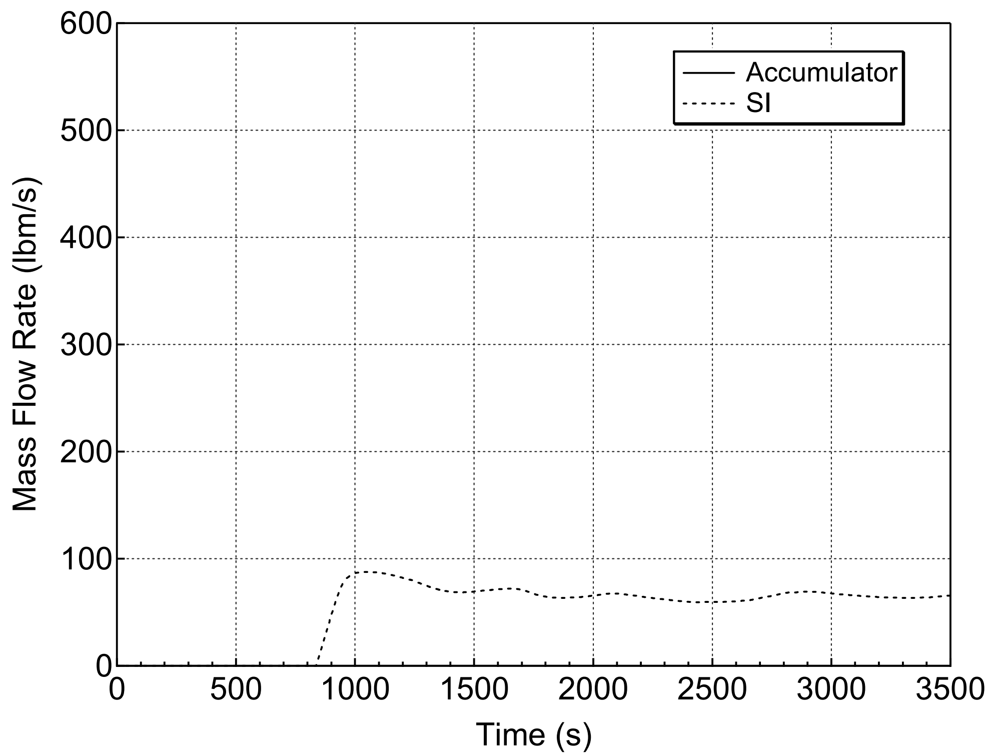

Figure 5.2.a-4 Accumulator and Safety Injection Mass Flowrates for 1-inch Break (Bottom) (Spectrum Analysis)

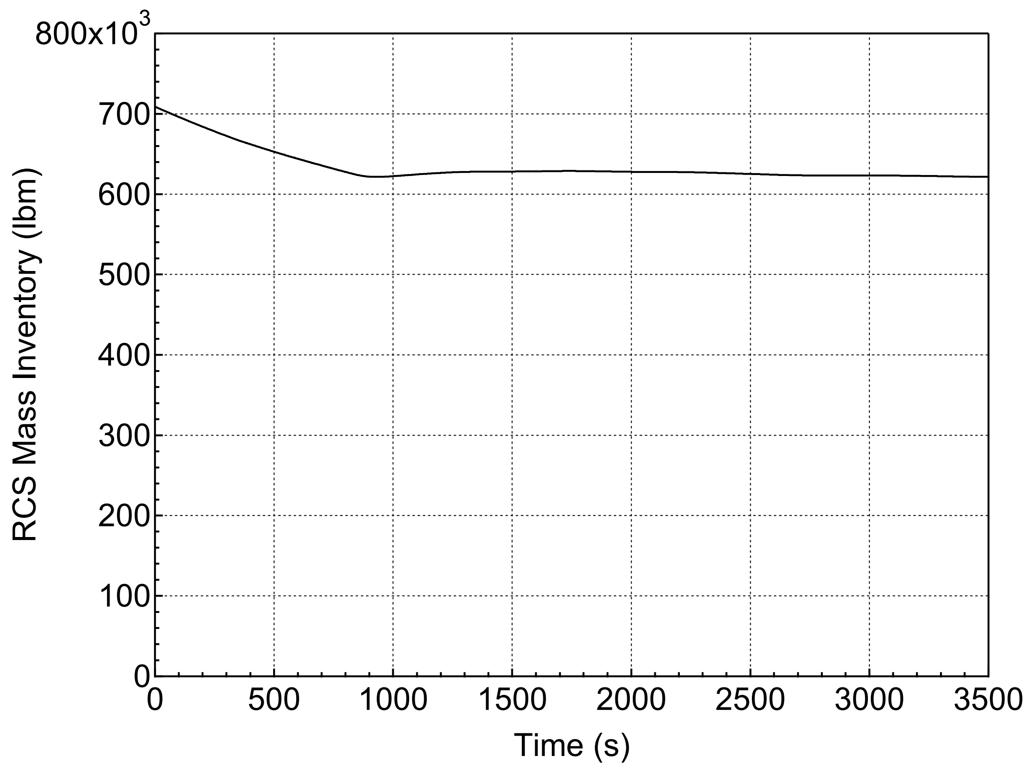

Figure 5.2.a-5 RCS Mass Inventory for 1-inch Break (Bottom) (Spectrum Analysis)

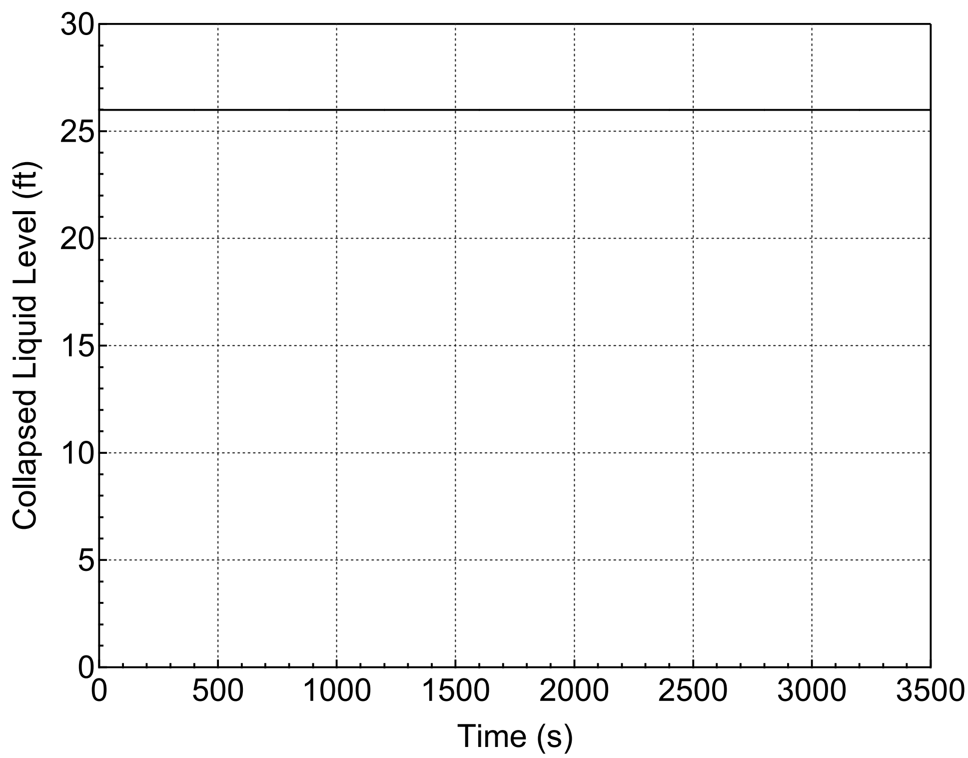

Figure 5.2.a-6 Downcomer Collapsed Level for 1-inch Break (Bottom) (Spectrum Analysis)

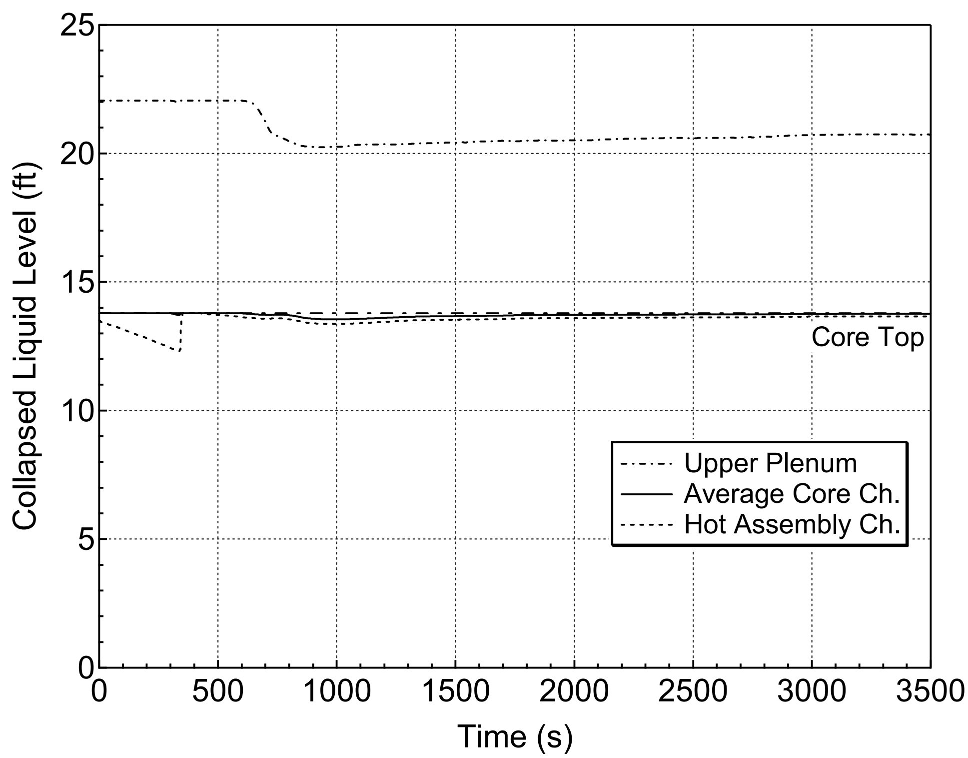

Figure 5.2.a-7 Core and Upper Plenum Collapsed Levels for 1-inch Break (Bottom) (Spectrum Analysis)

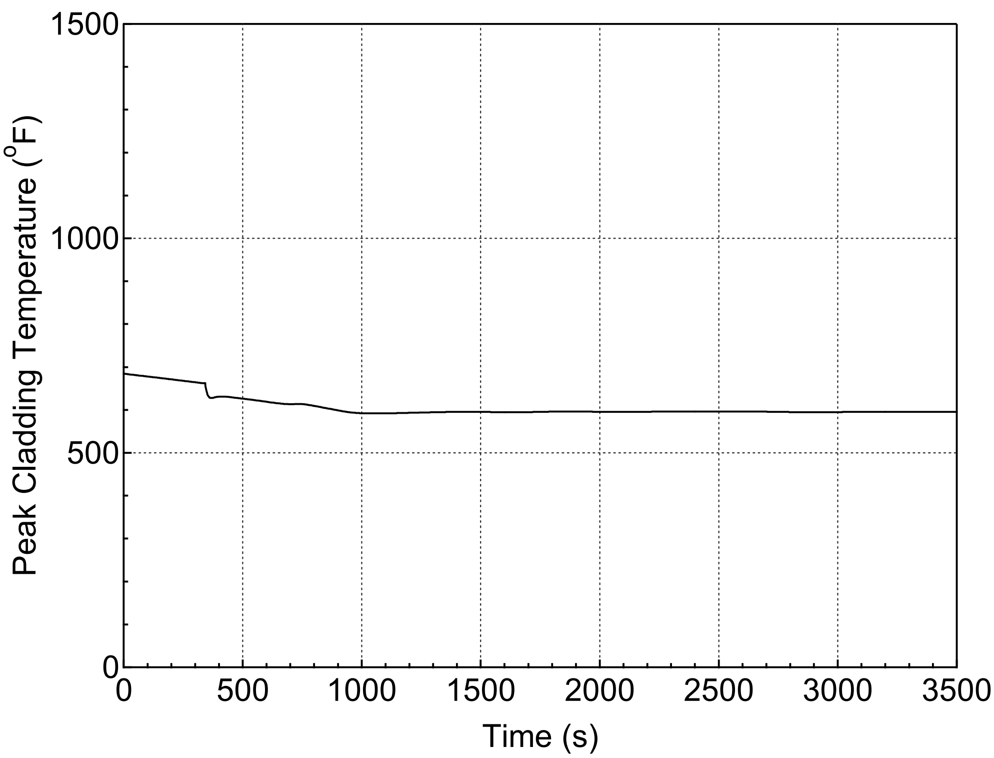

Figure 5.2.a-8 PCT at All Elevations for Hot Rod in Hot Assembly for 1-inch Break (Bottom) (Spectrum Analysis)

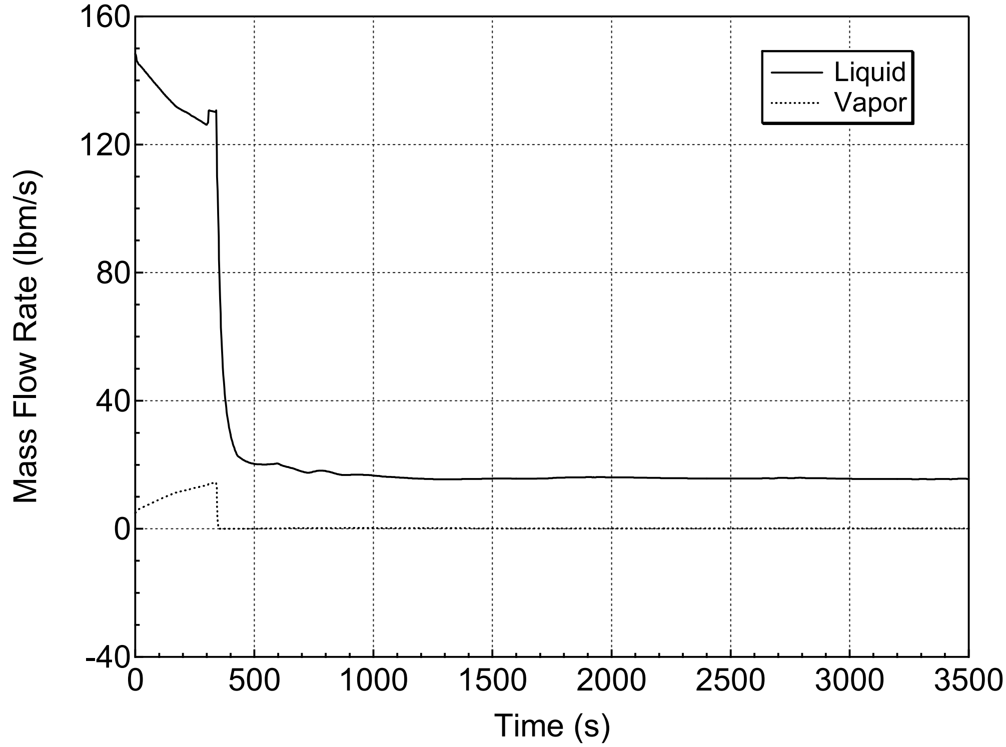

Figure 5.2.a-9 Hot Assembly Exit Vapor and Liquid Mass Flowrates for 1-inch Break (Bottom) (Spectrum Analysis)

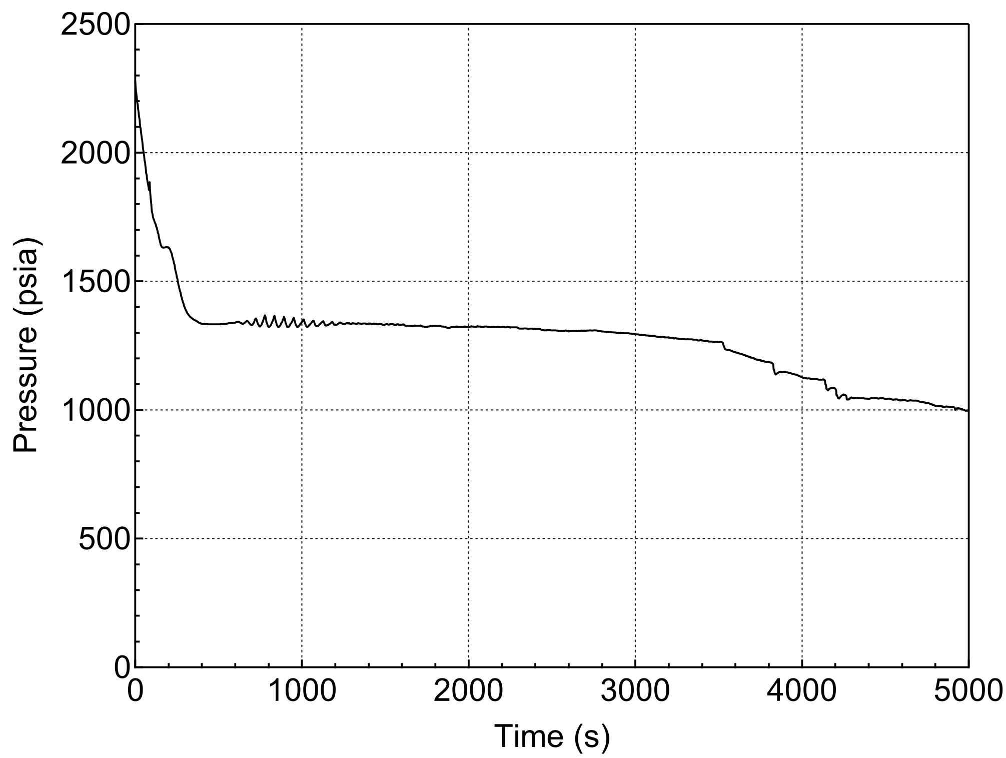

Figure 5.2.b-1 RCS (Pressurizer) Pressure Transient for 2-inch Break (Bottom) (Spectrum Analysis)

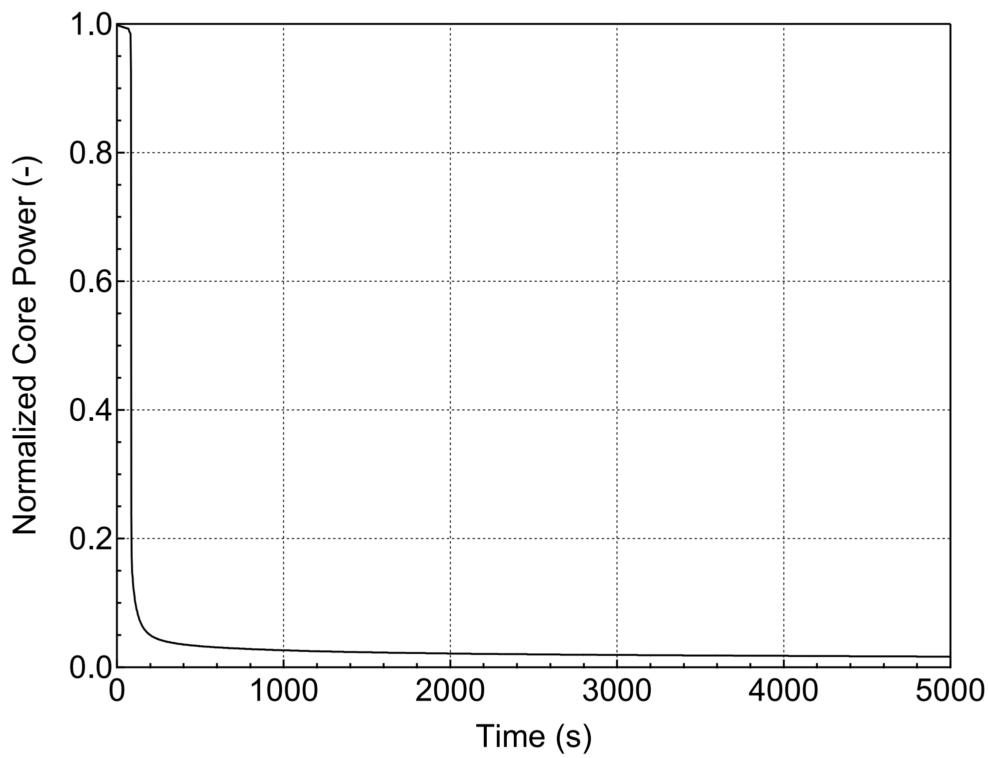

Figure 5.2.b-2 Normalized Core Power for 2-inch Break (Bottom) (Spectrum Analysis)

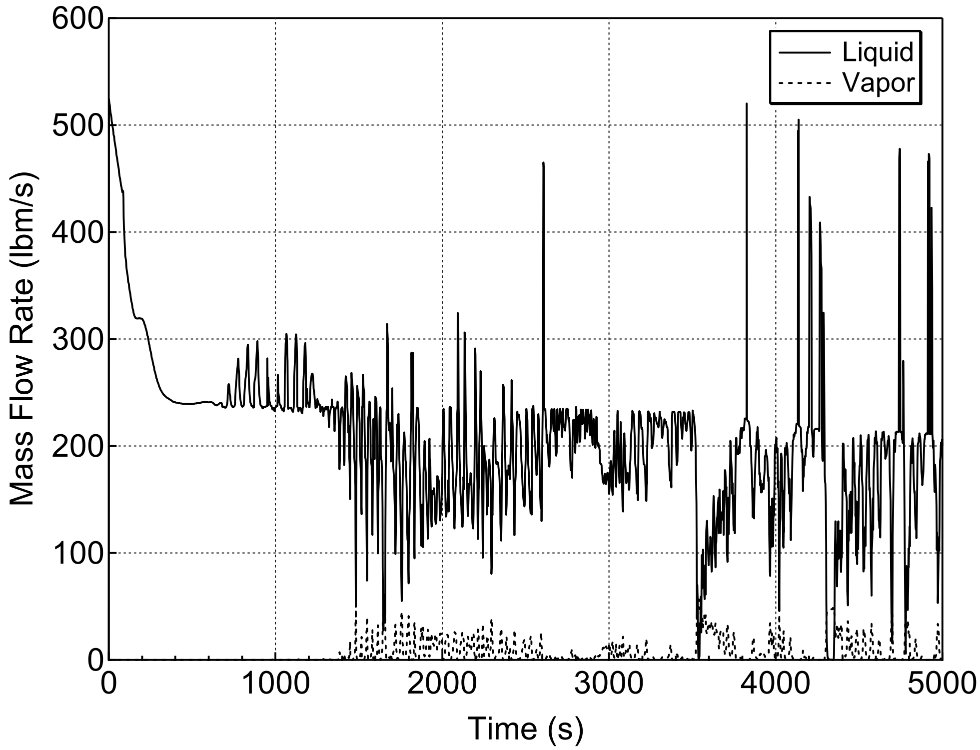

Figure 5.2.b-3 Liquid and Vapor Discharges through the Break for 2-inch Break (Bottom) (Spectrum Analysis)

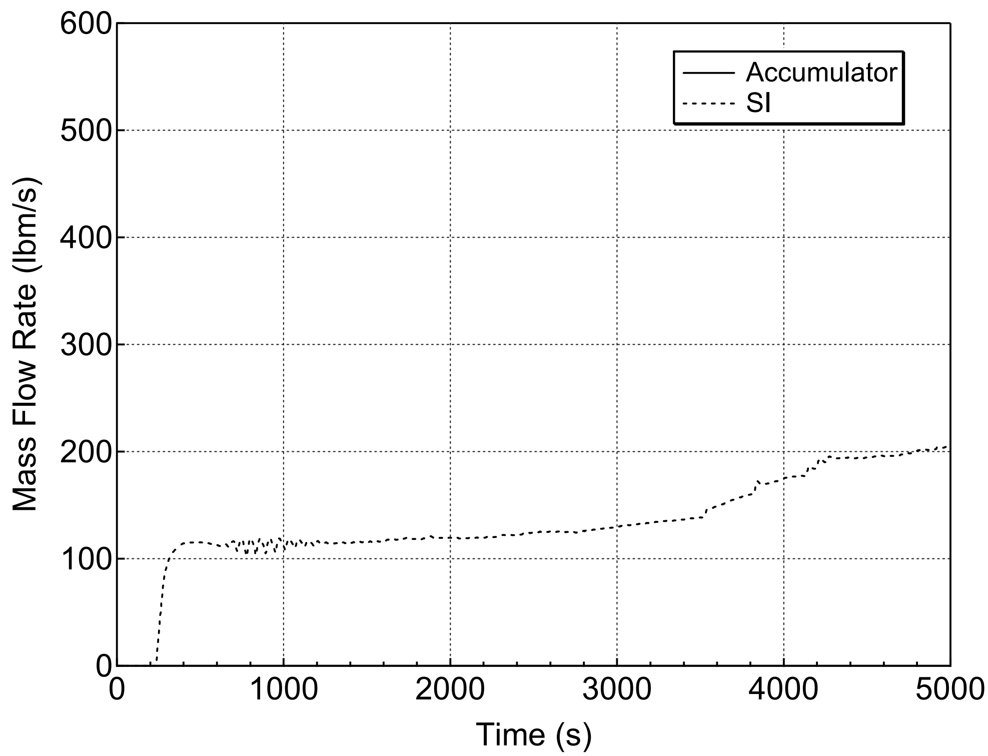

Figure 5.2.b-4 Accumulator and Safety Injection Mass Flowrates for 2-inch Break (Bottom) (Spectrum Analysis)

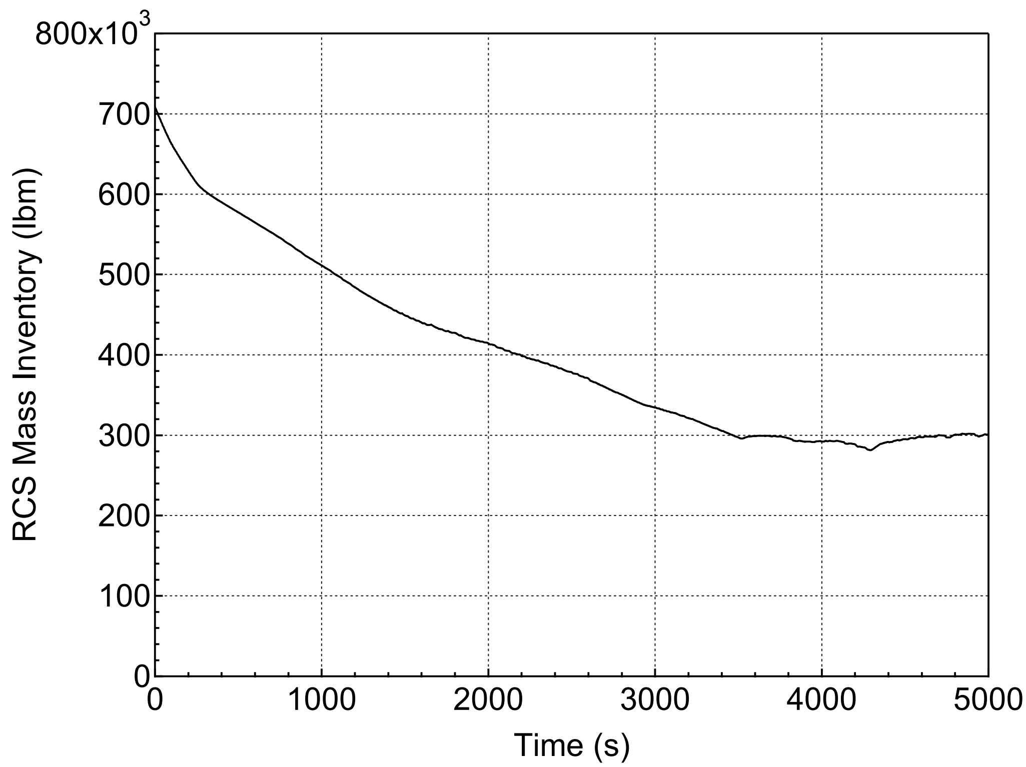

Figure 5.2.b-5 RCS Mass Inventory for 2-inch Break (Bottom) (Spectrum Analysis)

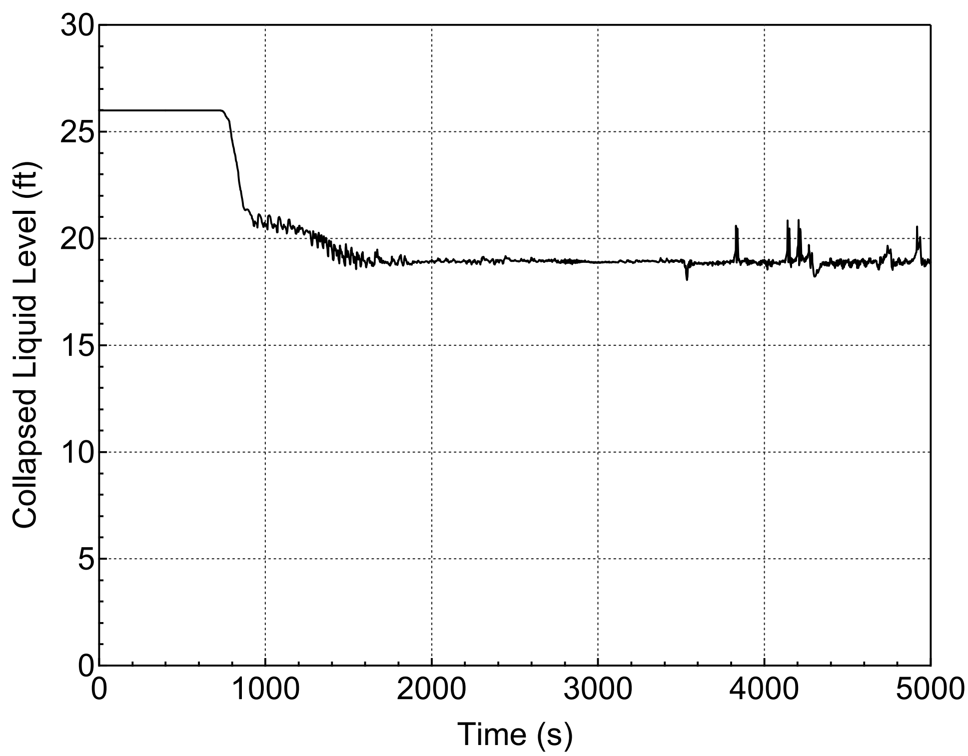

Figure 5.2.b-6 Downcomer Collapsed Level for 2-inch Break (Bottom) (Spectrum Analysis)

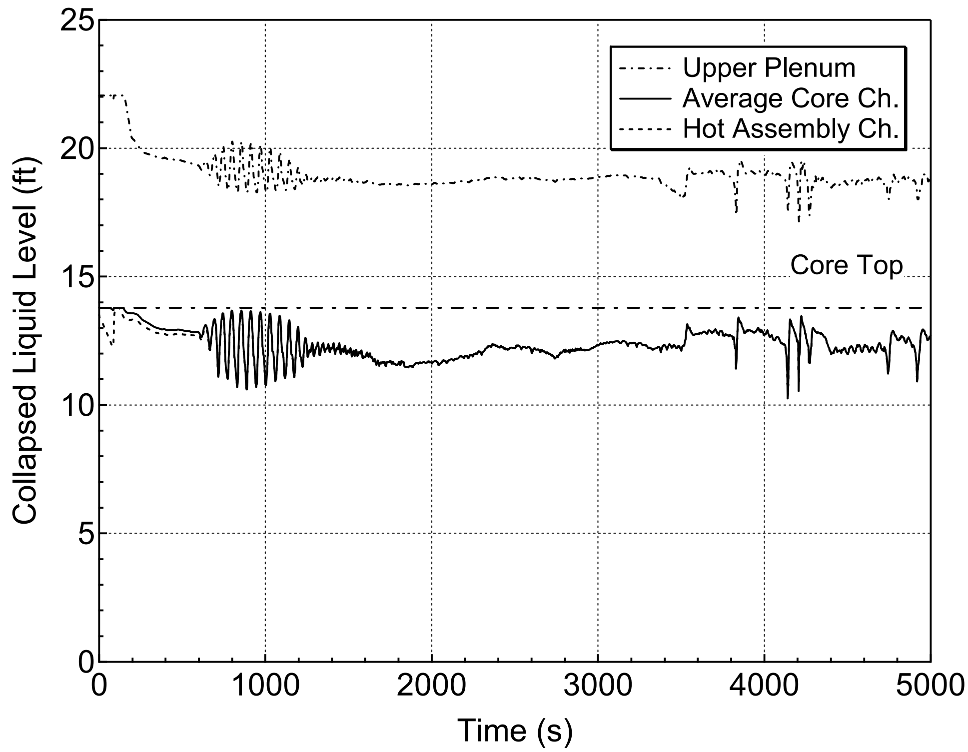

Figure 5.2.b-7 Core and Upper Plenum Collapsed Levels for 2-inch Break (Bottom) (Spectrum Analysis)

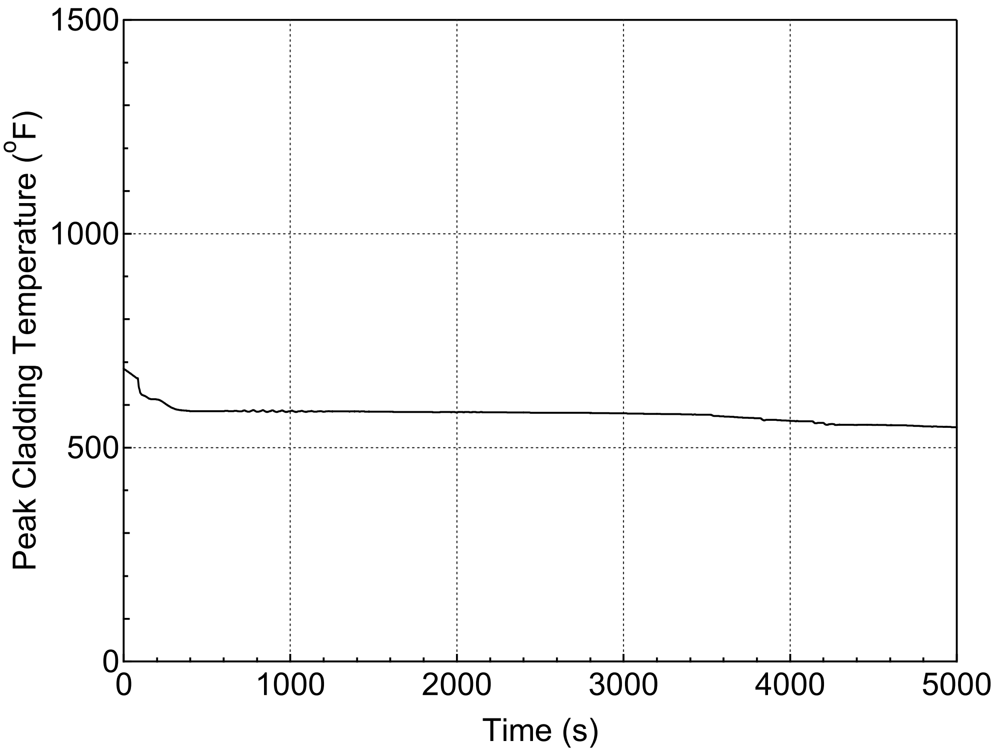

Figure 5.2.b-8 PCT at All Elevations for Hot Rod in Hot Assembly for 2-inch Break (Bottom) (Spectrum Analysis)

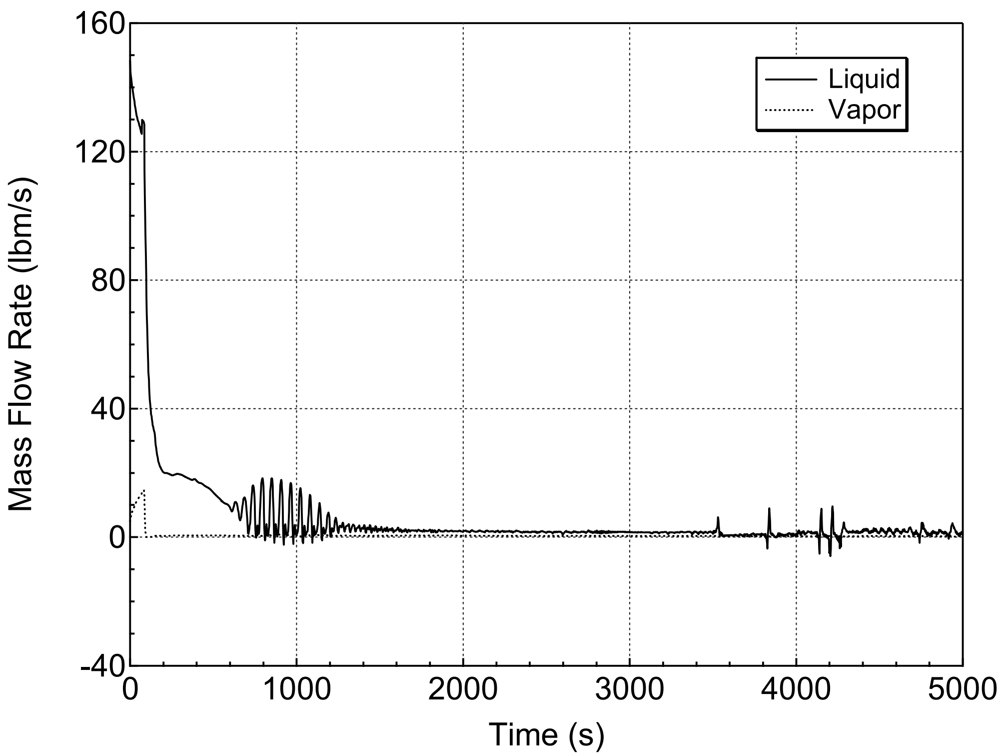

Figure 5.2.b-9 Hot Assembly Exit Vapor and Liquid Mass Flowrates for 2-inch Break (Bottom) (Spectrum Analysis)

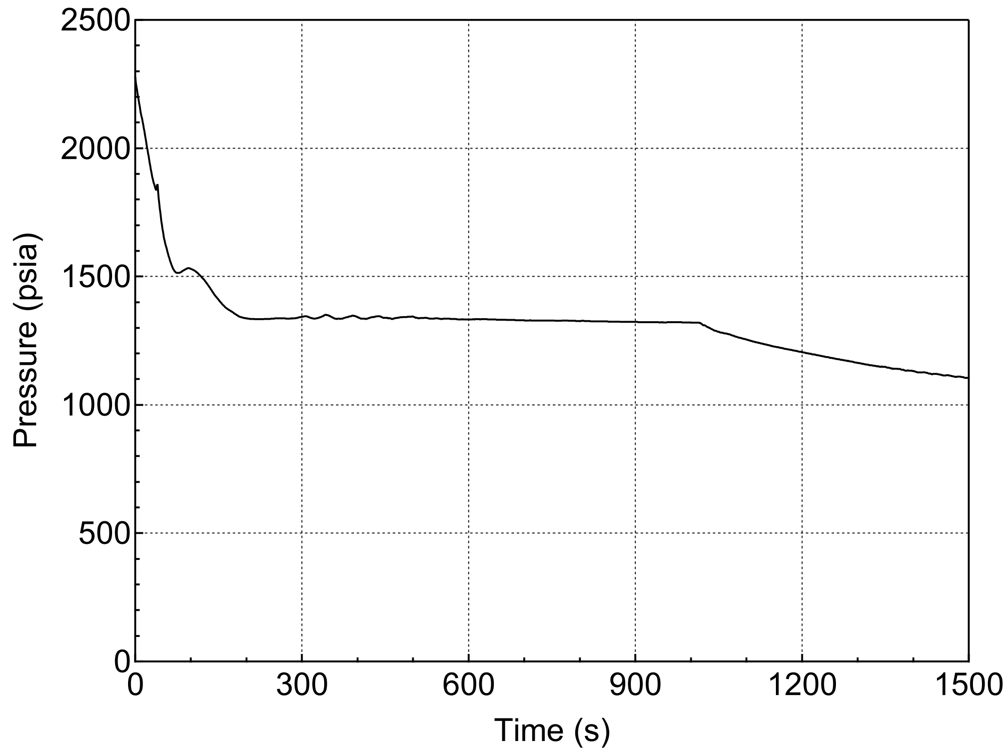

Figure 5.2.c-1 RCS (Pressurizer) Pressure Transient for 3-inch Break (Bottom) (Spectrum Analysis)

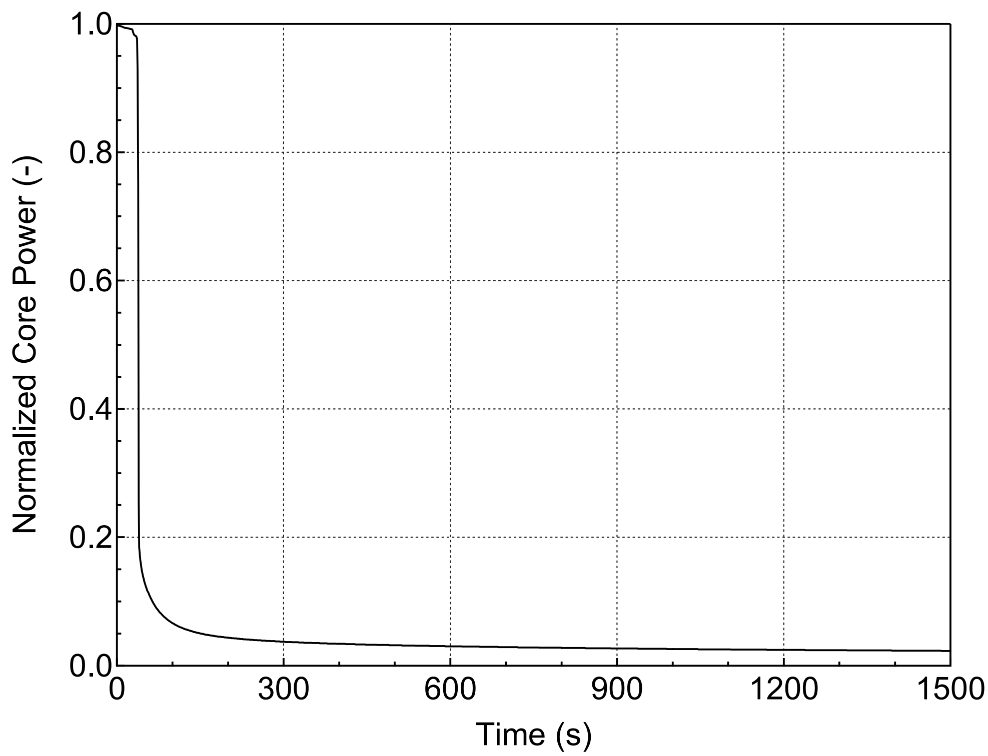

Figure 5.2.c-2 Normalized Core Power for 3-inch Break (Bottom) (Spectrum Analysis)

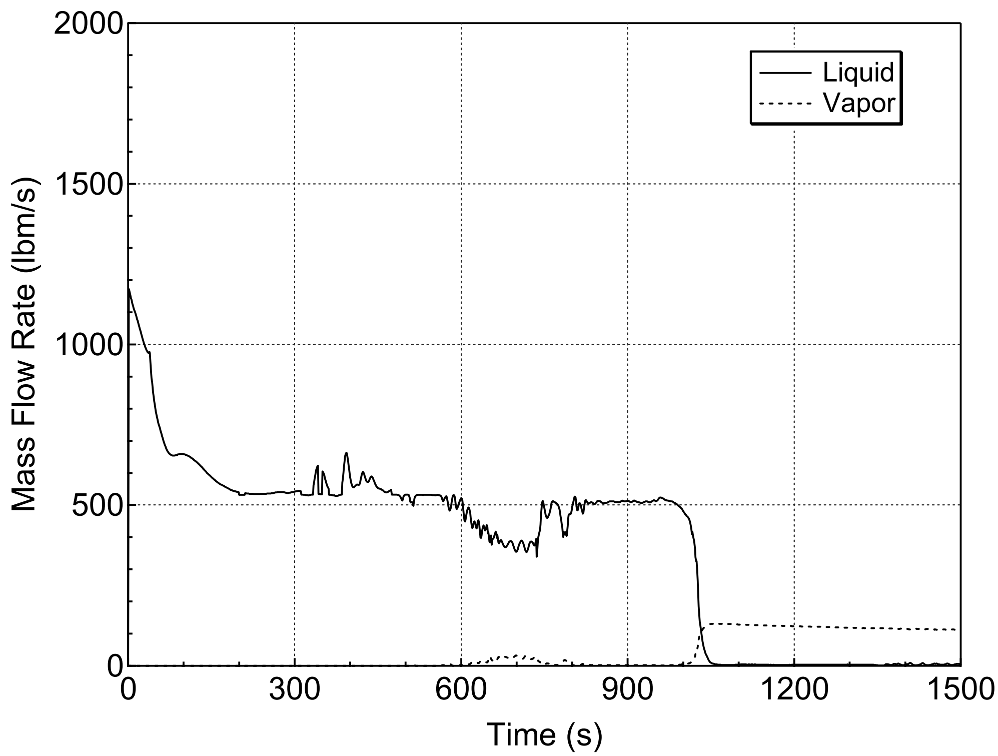

Figure 5.2.c-3 Liquid and Vapor Discharges through the Break for 3-inch Break (Bottom) (Spectrum Analysis)

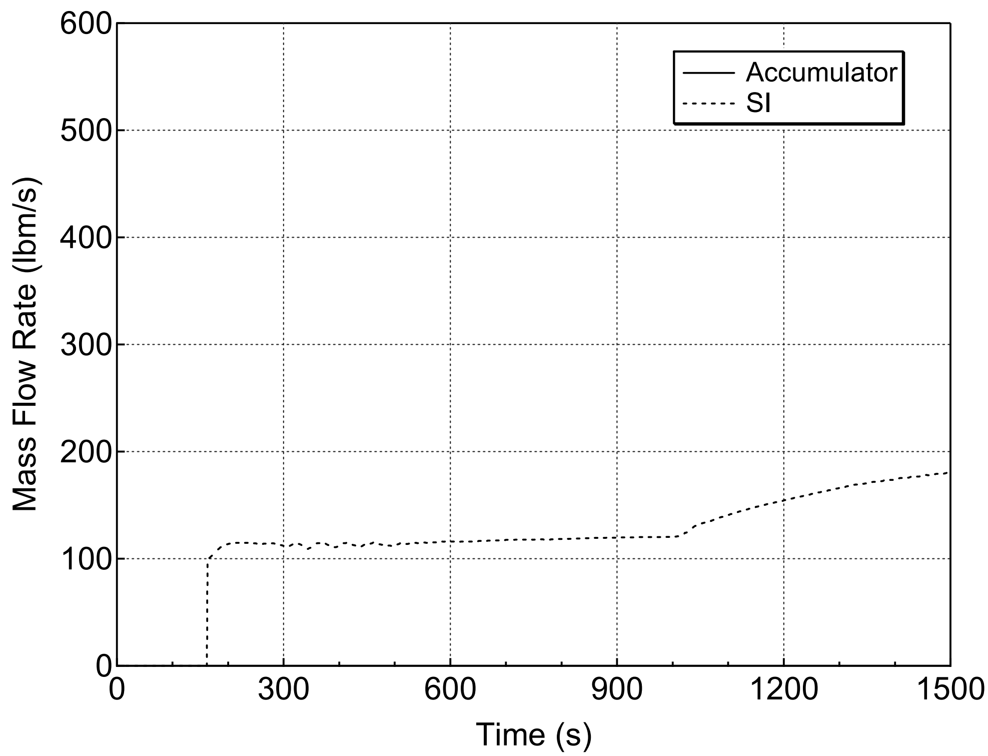

Figure 5.2.c-4 Accumulator and Safety Injection Mass Flowrates for 3-inch Break (Bottom) (Spectrum Analysis)

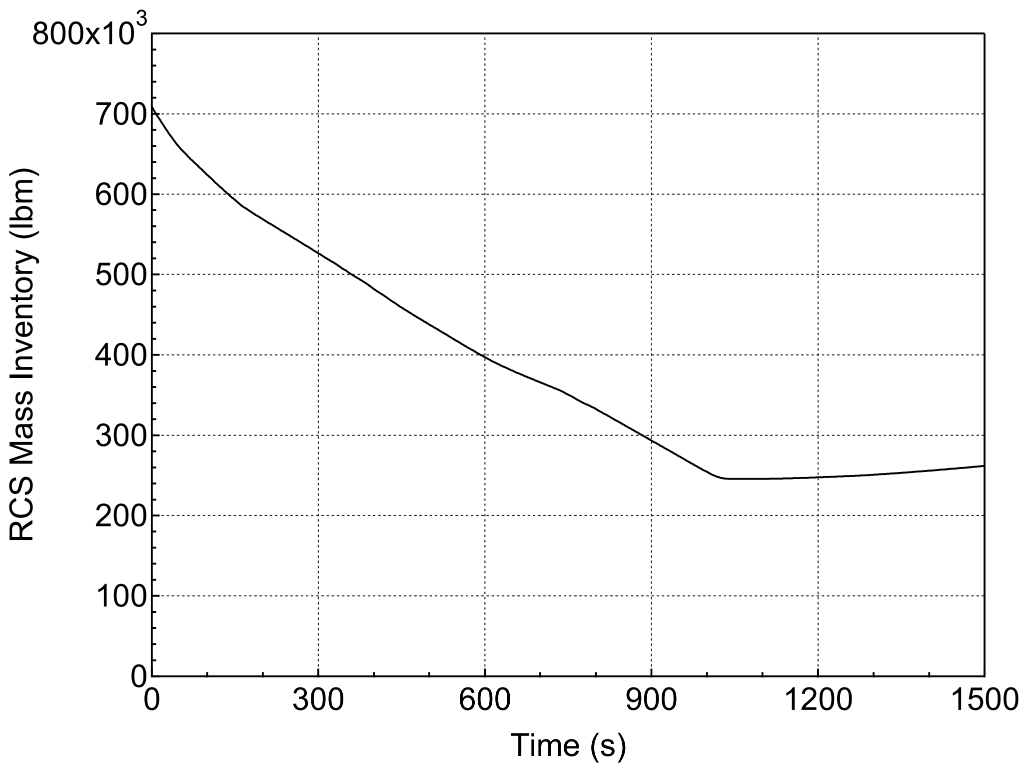

Figure 5.2.c-5 RCS Mass Inventory for 3-inch Break (Bottom) (Spectrum Analysis)

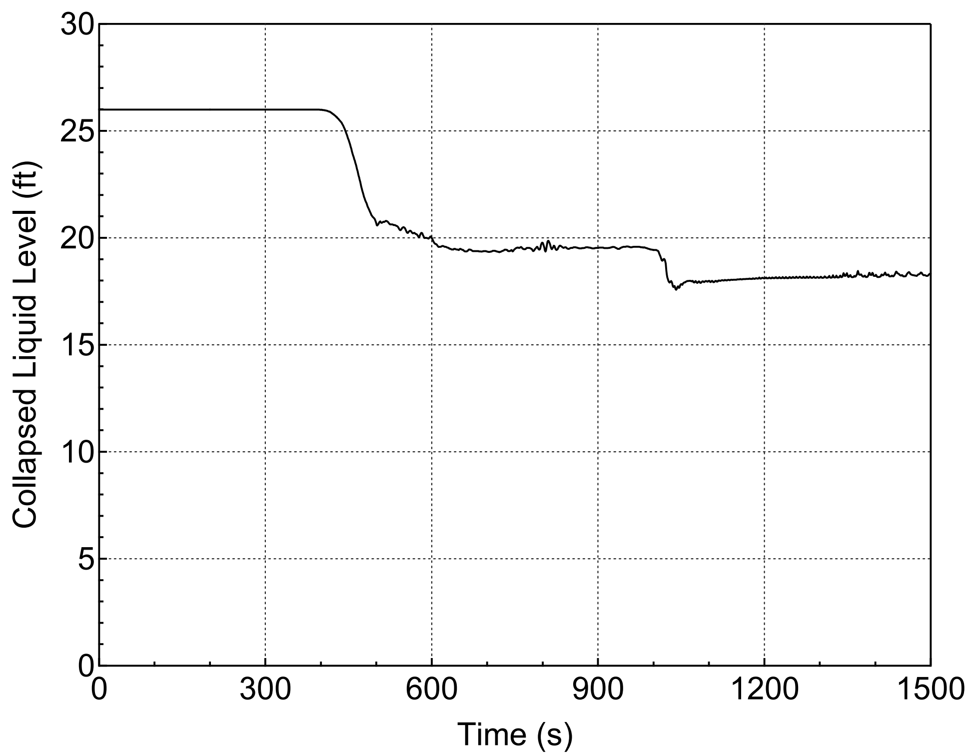

Figure 5.2.c-6 Downcomer Collapsed Level for 3-inch Break (Bottom) (Spectrum Analysis)

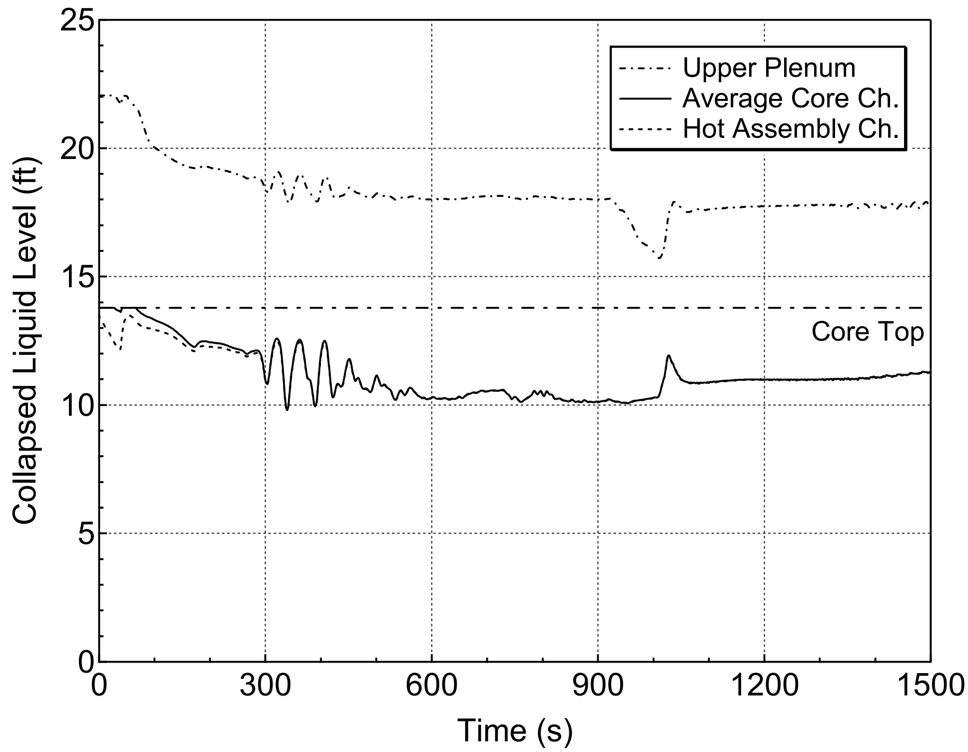

Figure 5.2.c-7 Core and Upper Plenum Collapsed Levels for 3-inch Break (Bottom) (Spectrum Analysis)

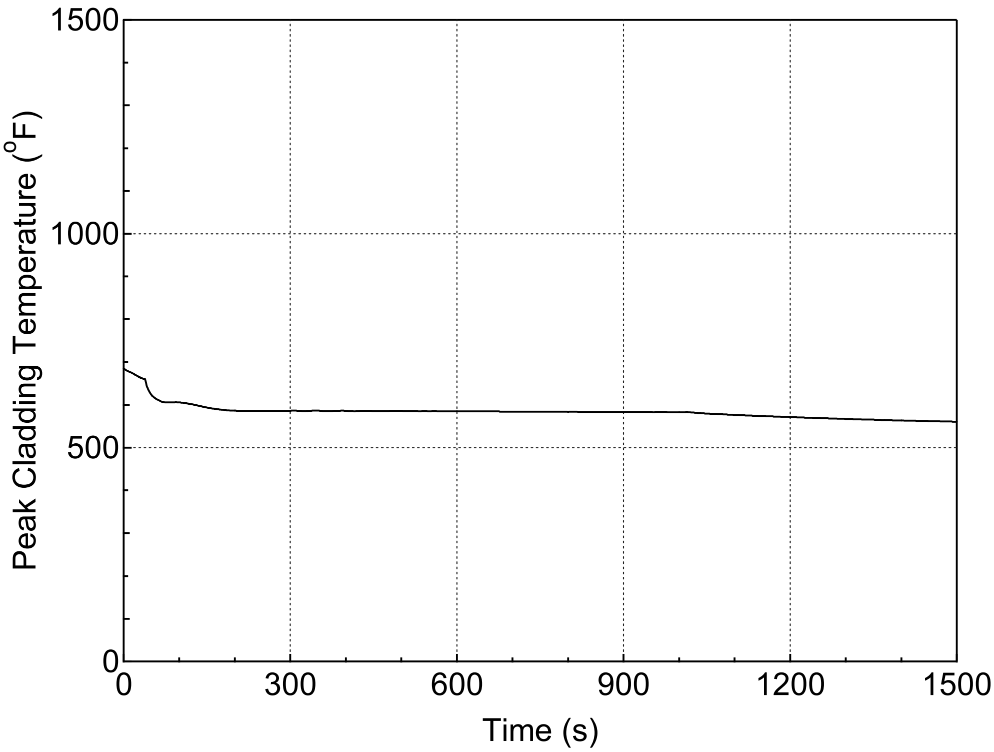

Figure 5.2.c-8 PCT at All Elevations for Hot Rod in Hot Assembly for 3-inch Break (Bottom) (Spectrum Analysis)

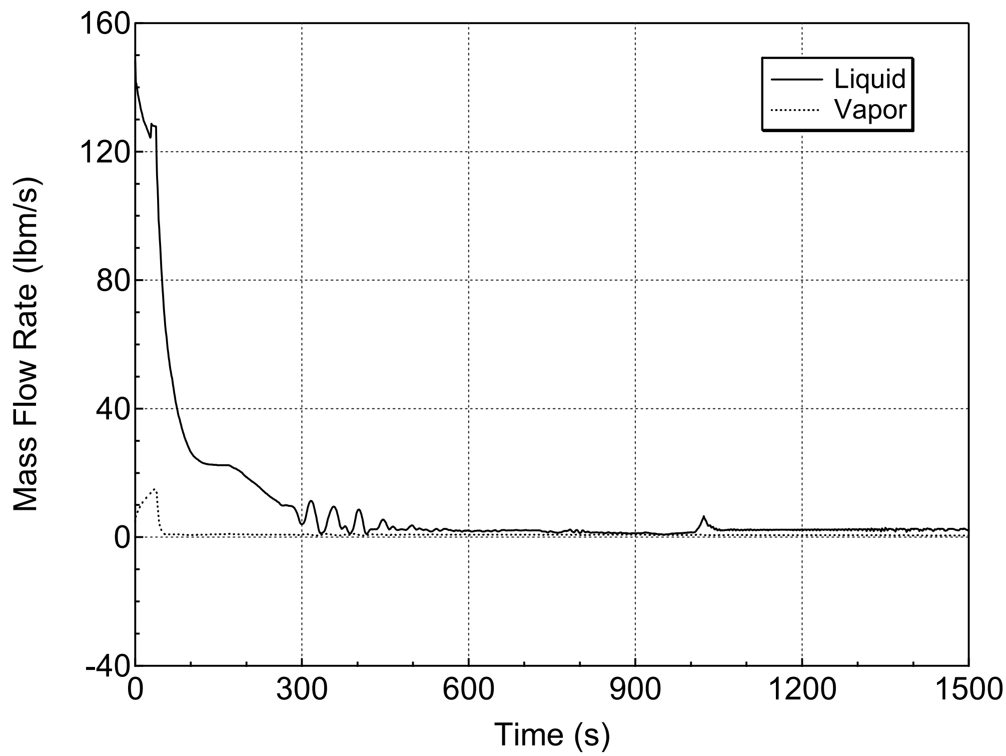

Figure 5.2.c-9 Hot Assembly Exit Vapor and Liquid Mass Flowrates for 3-inch Break (Bottom) (Spectrum Analysis)

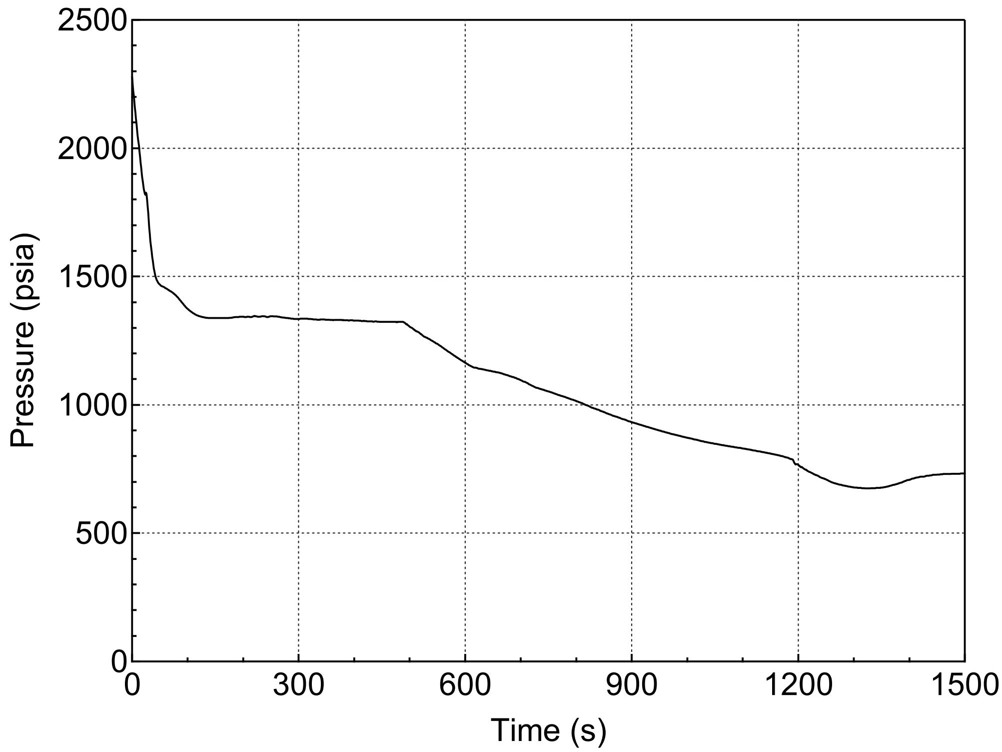

Figure 5.2.d-1 RCS (Pressurizer) Pressure Transient for 4-inch Break (Bottom) (Spectrum Analysis)

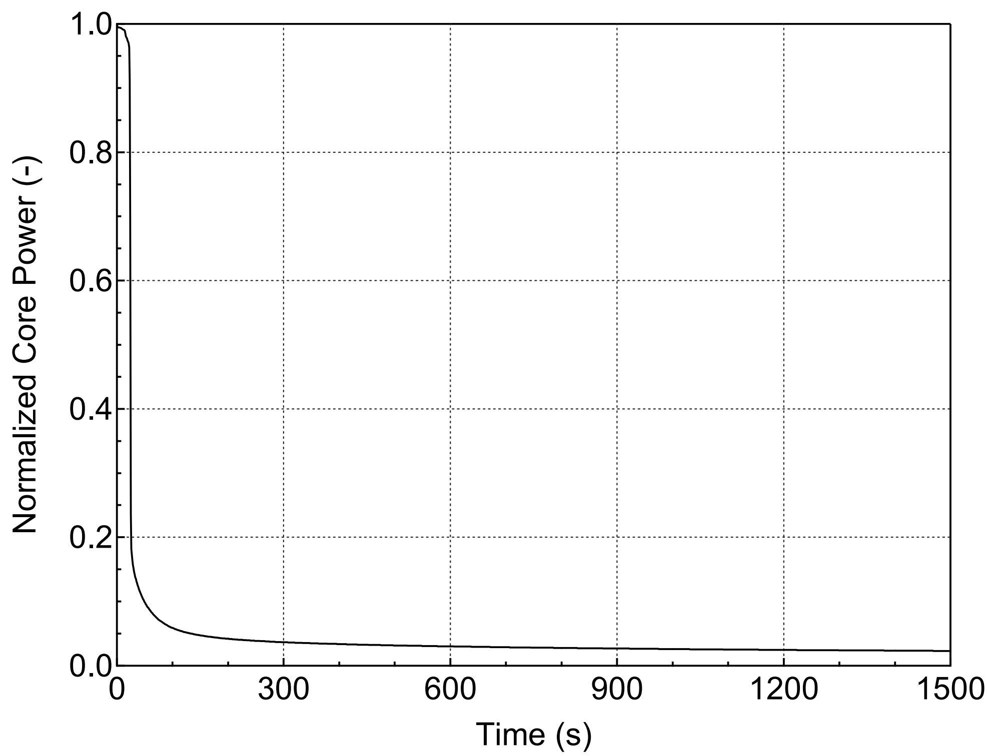

Figure 5.2.d-2 Normalized Core Power for 4-inch Break (Bottom) (Spectrum Analysis)

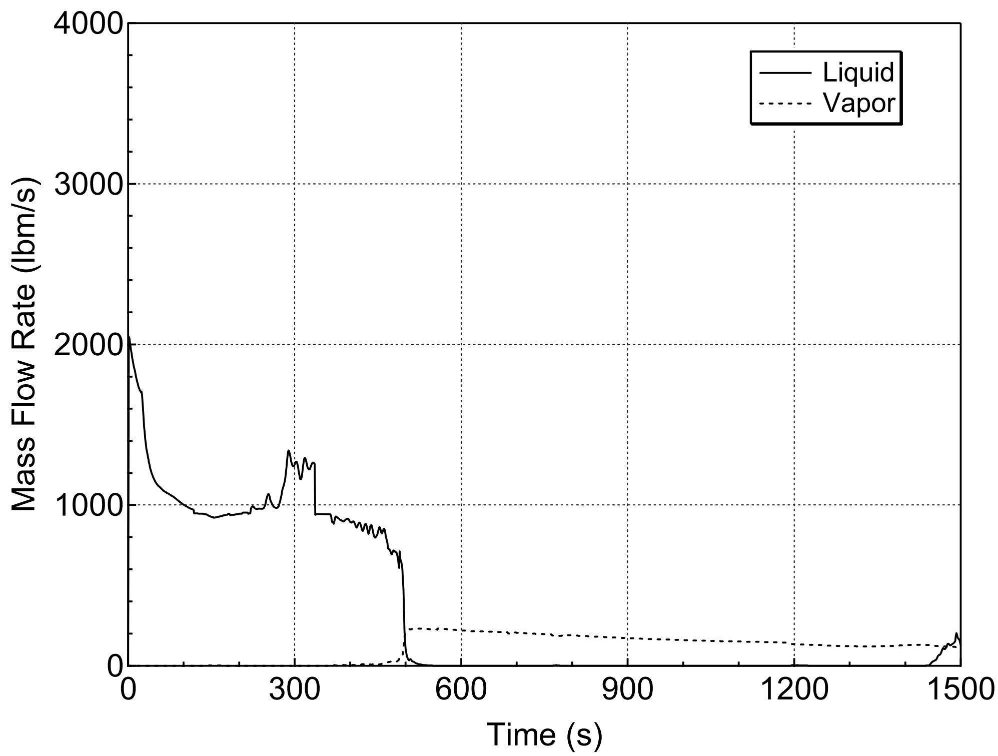

Figure 5.2.d-3 Liquid and Vapor Discharges through the Break for 4-inch Break (Bottom) (Spectrum Analysis)

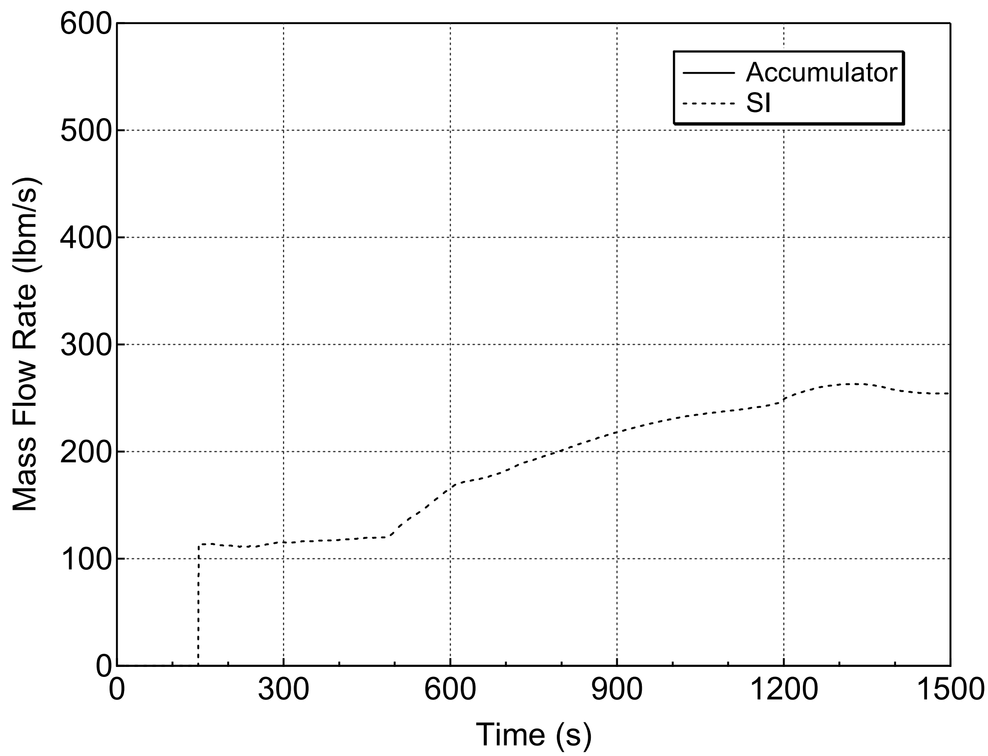

Figure 5.2.d-4 Accumulator and Safety Injection Mass Flowrates for 4-inch Break (Bottom) (Spectrum Analysis)

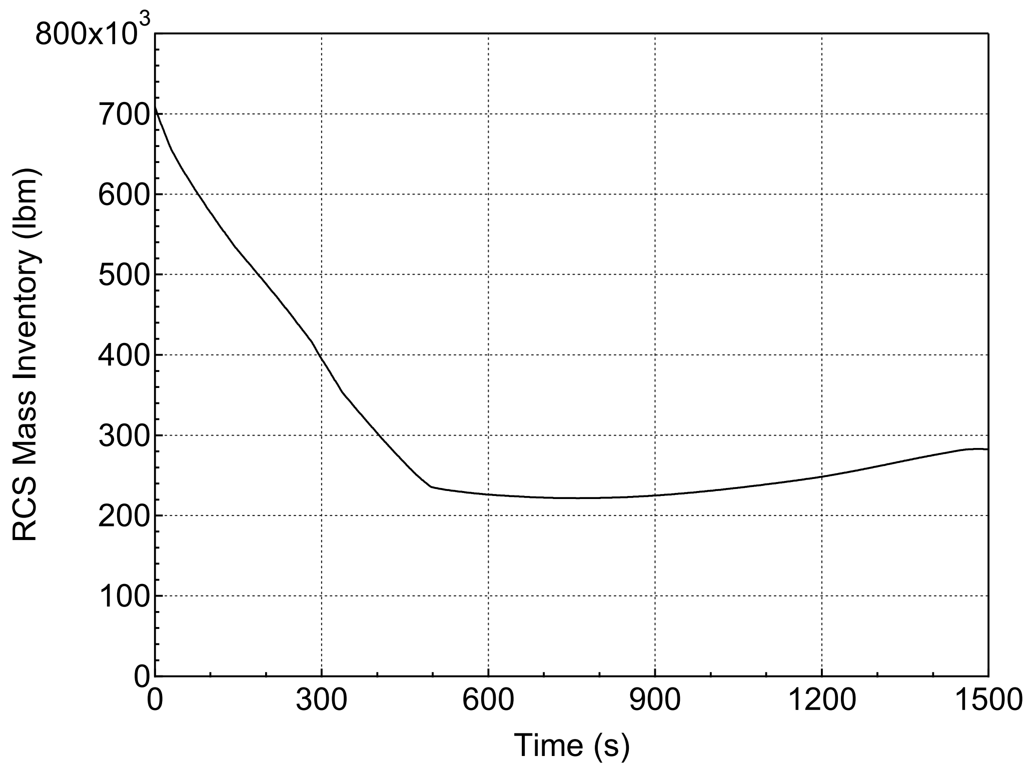

Figure 5.2.d-5 RCS Mass Inventory for 4-inch Break (Bottom) (Spectrum Analysis)

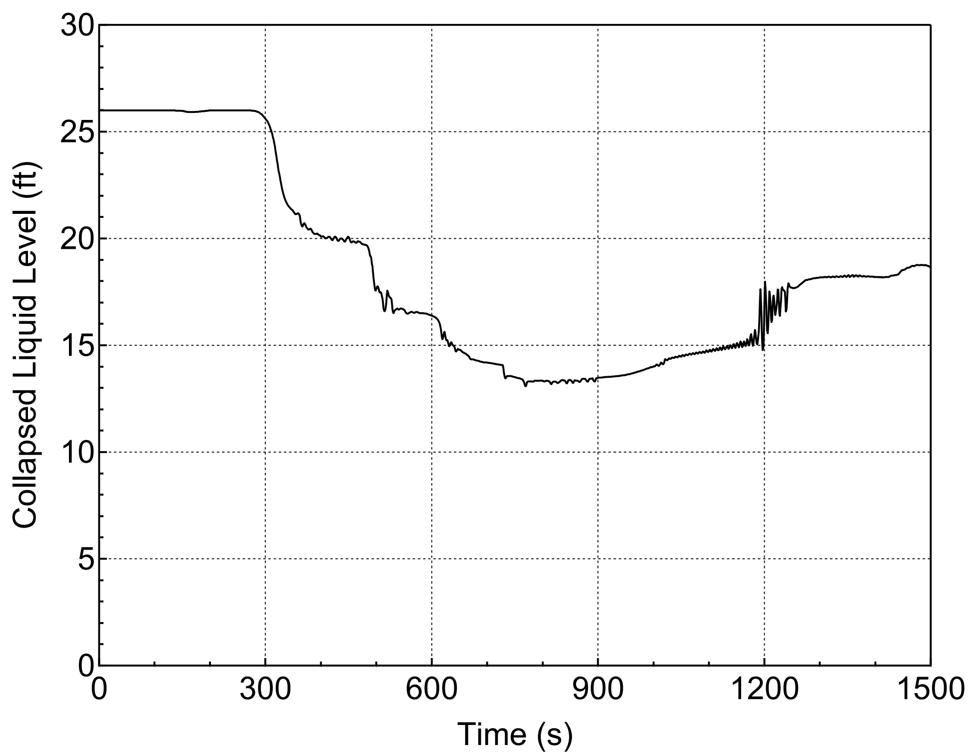

Figure 5.2.d-6 Downcomer Collapsed Level for 4-inch Break (Bottom) (Spectrum Analysis)

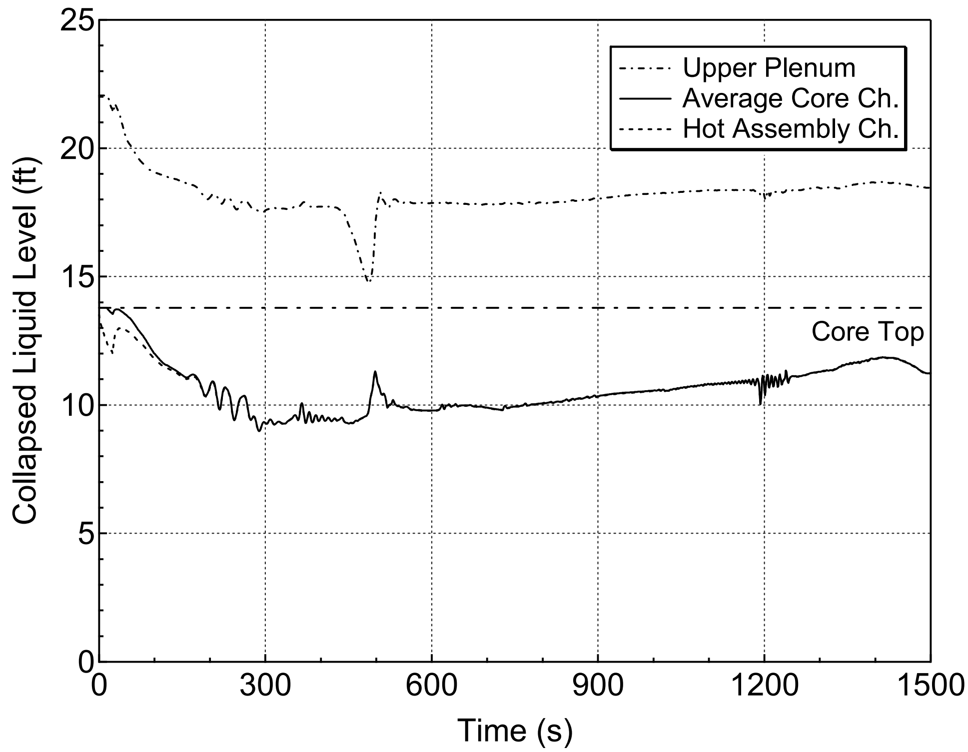

Figure 5.2.d-7 Core and Upper Plenum Collapsed Levels for 4-inch Break (Bottom) (Spectrum Analysis)

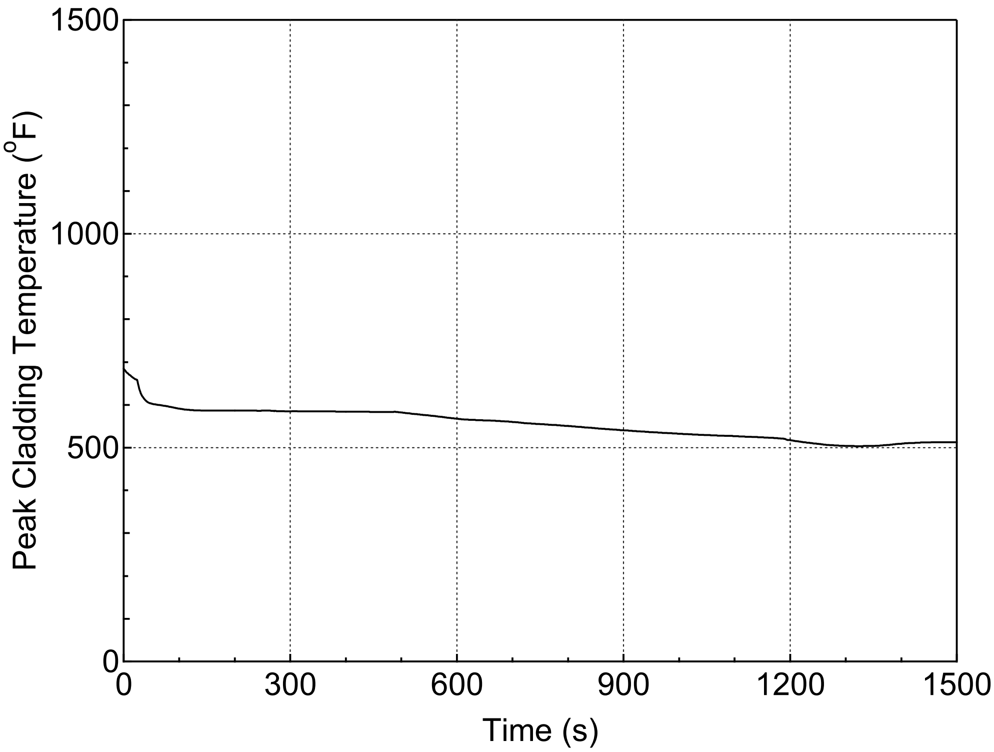

Figure 5.2.d-8 PCT at All Elevations for Hot Rod in Hot Assembly for 4-inch Break (Bottom) (Spectrum Analysis)

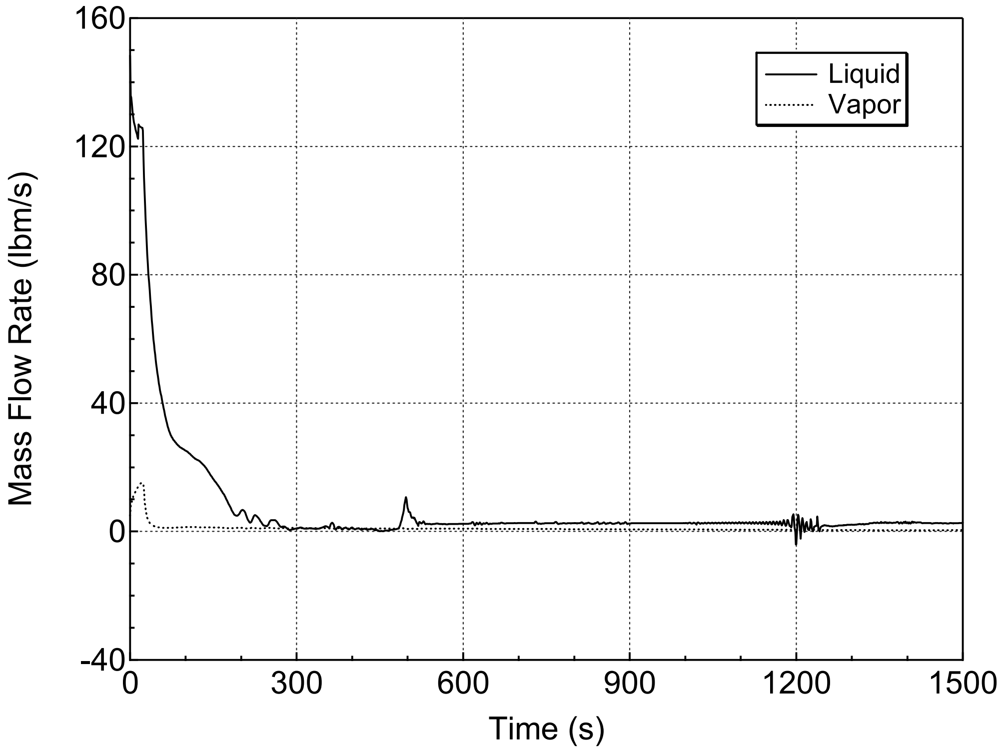

Figure 5.2.d-9 Hot Assembly Exit Vapor and Liquid Mass Flowrates for 4-inch Break (Bottom) (Spectrum Analysis)

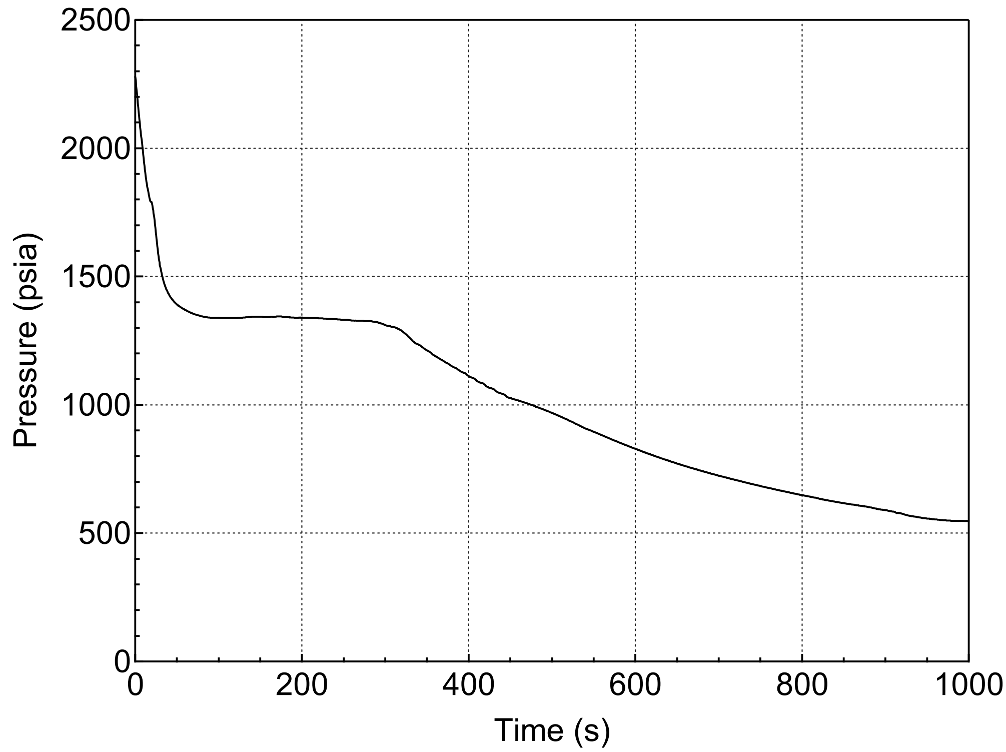

Figure 5.2.e-1 RCS (Pressurizer) Pressure Transient for 5-inch Break (Bottom) (Spectrum Analysis)

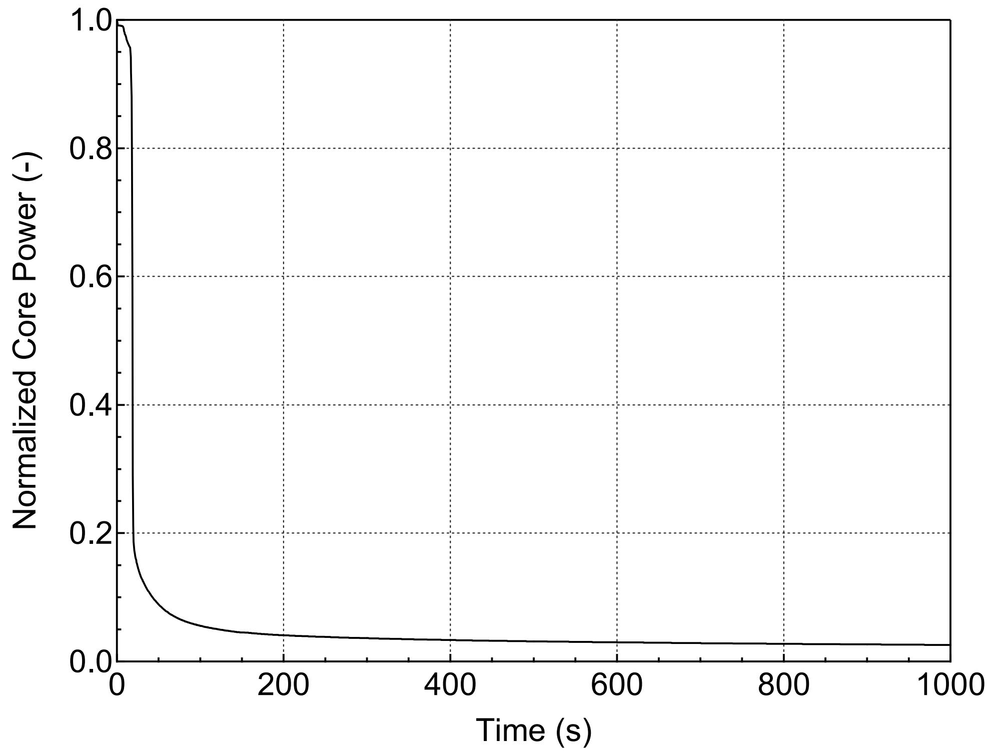

Figure 5.2.e-2 Normalized Core Power for 5-inch Break (Bottom) (Spectrum Analysis)

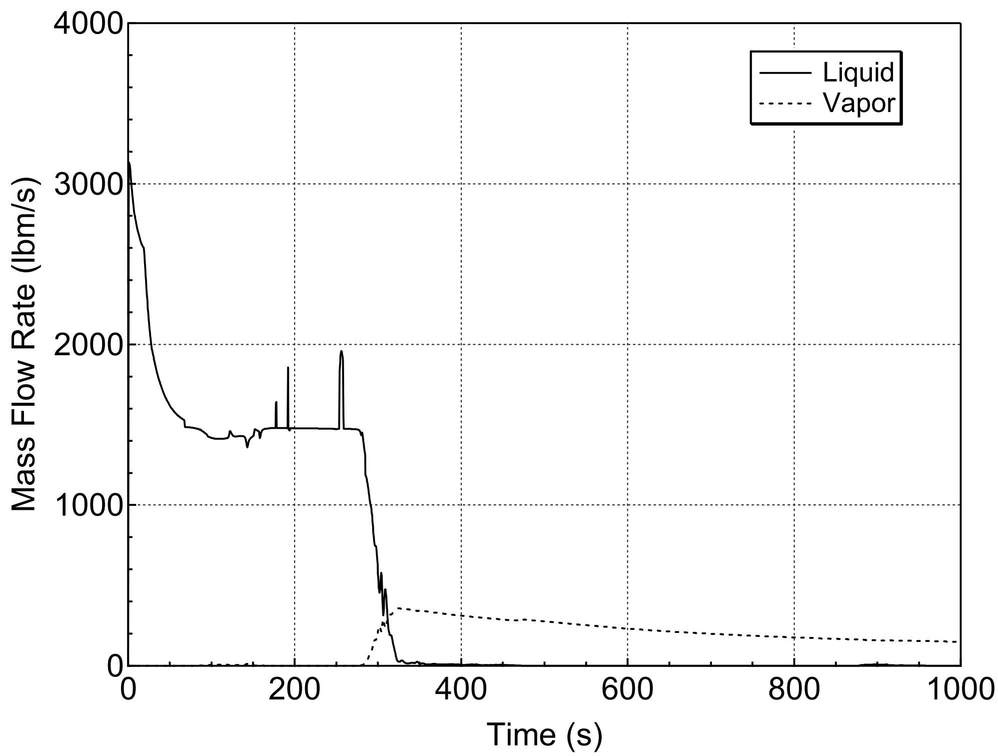

Figure 5.2.e-3 Liquid and Vapor Discharges through the Break for 5-inch Break (Bottom) (Spectrum Analysis)

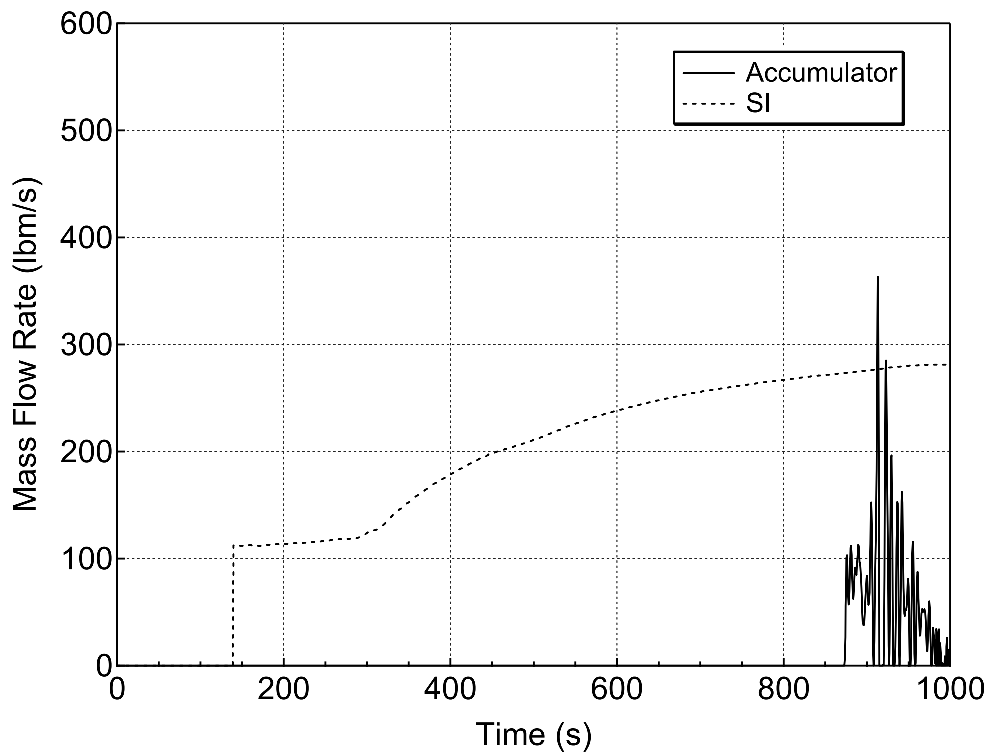

Figure 5.2.e-4 Accumulator and Safety Injection Mass Flowrates for 5-inch Break (Bottom) (Spectrum Analysis)

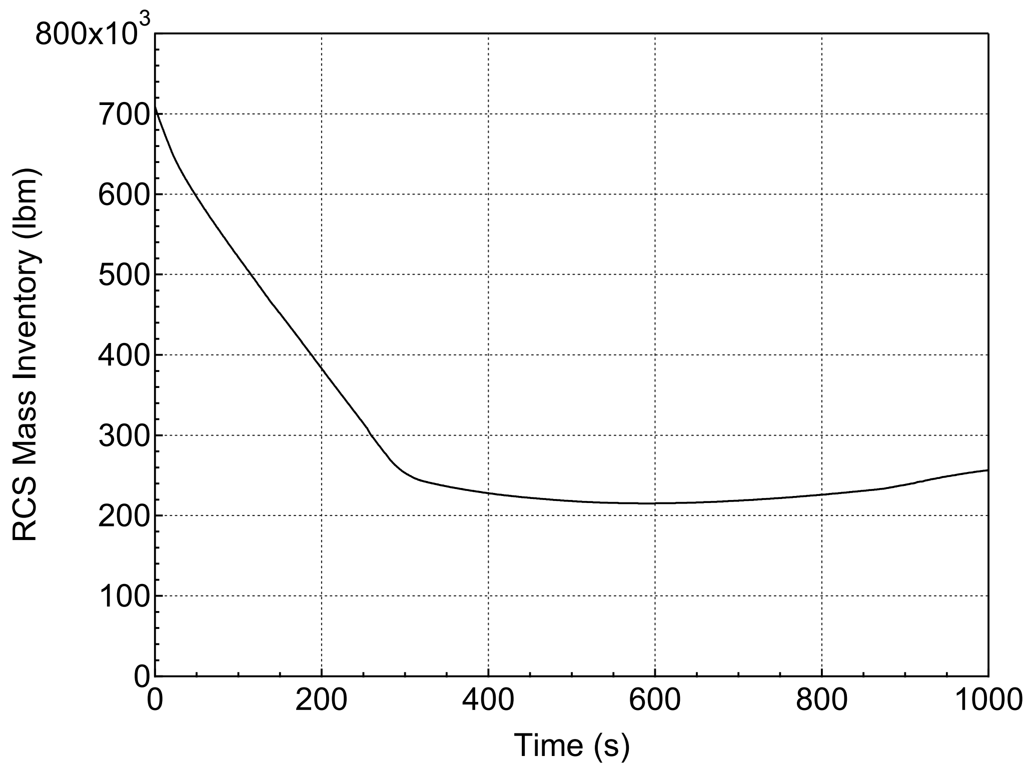

Figure 5.2.e-5 RCS Mass Inventory for 5-inch Break (Bottom) (Spectrum Analysis)

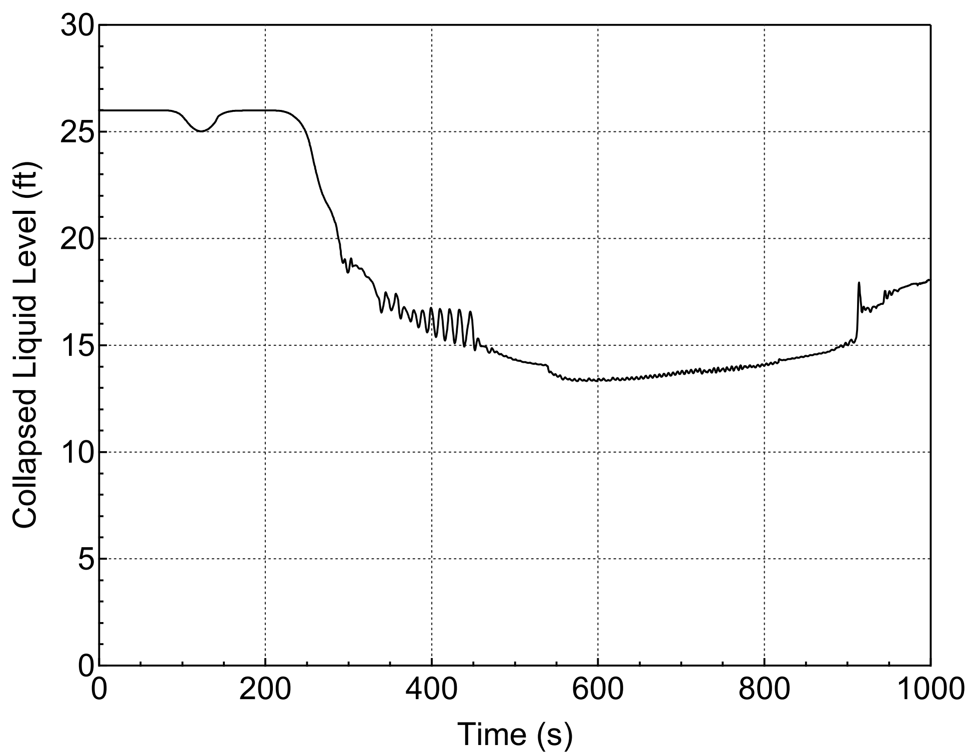

Figure 5.2.e-6 Downcomer Collapsed Level for 5-inch Break (Bottom) (Spectrum Analysis)

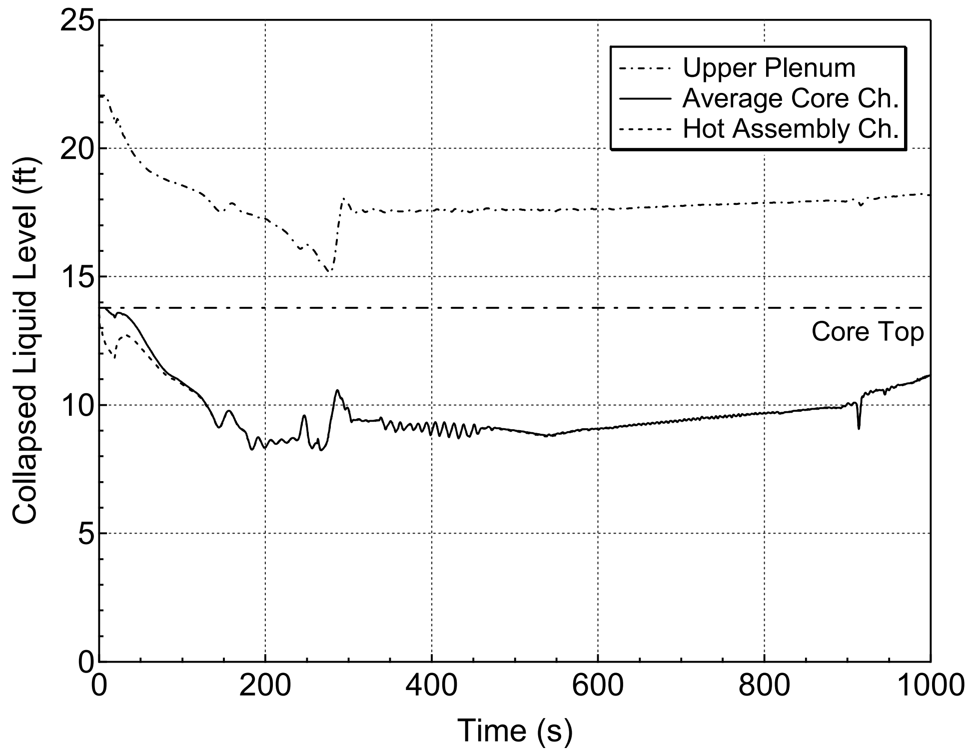

Figure 5.2.e-7 Core and Upper Plenum Collapsed Levels for 5-inch Break (Bottom) (Spectrum Analysis)

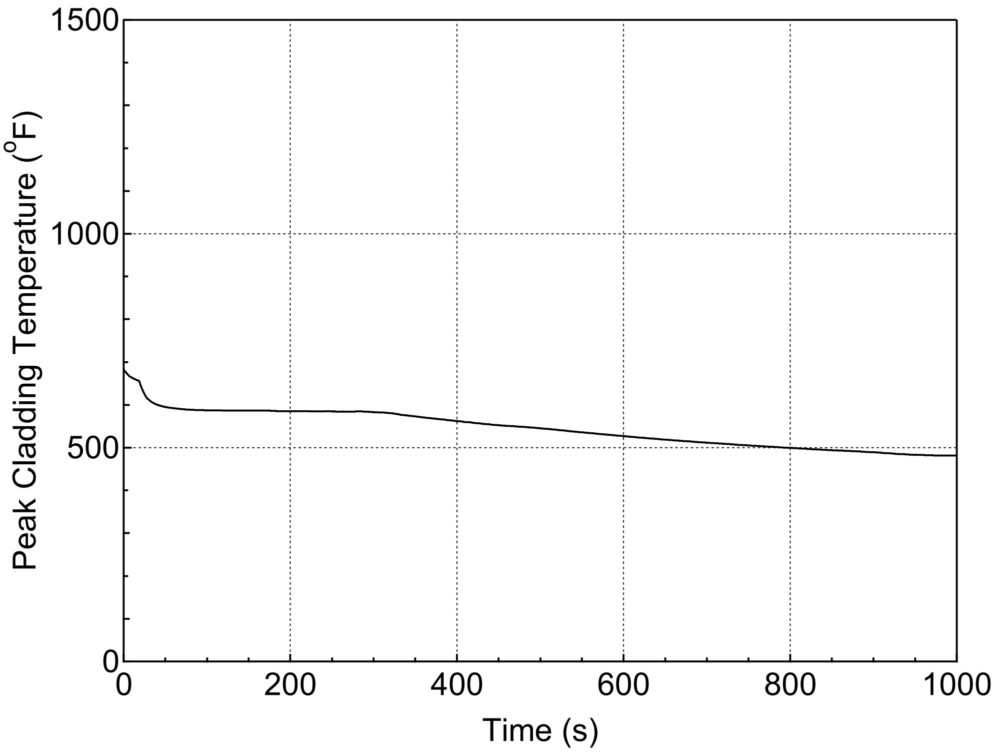

Figure 5.2.e-8 PCT at All Elevations for Hot Rod in Hot Assembly for 5-inch Break (Bottom) (Spectrum Analysis)

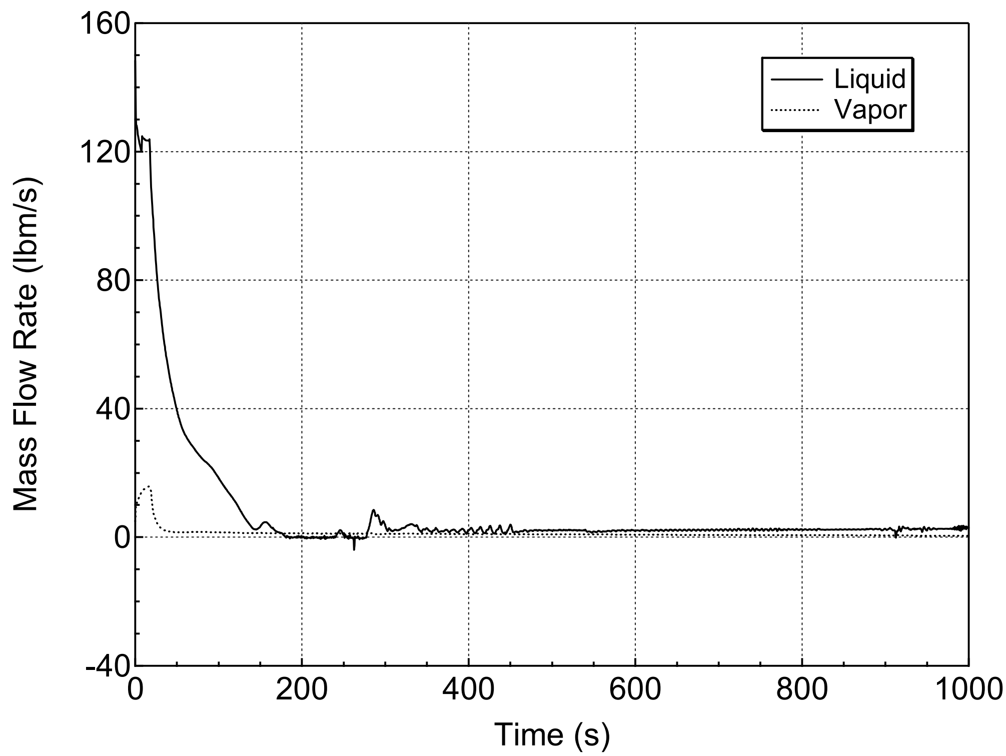

Figure 5.2.e-9 Hot Assembly Exit Vapor and Liquid Mass Flowrates for 5-inch Break (Bottom) (Spectrum Analysis)

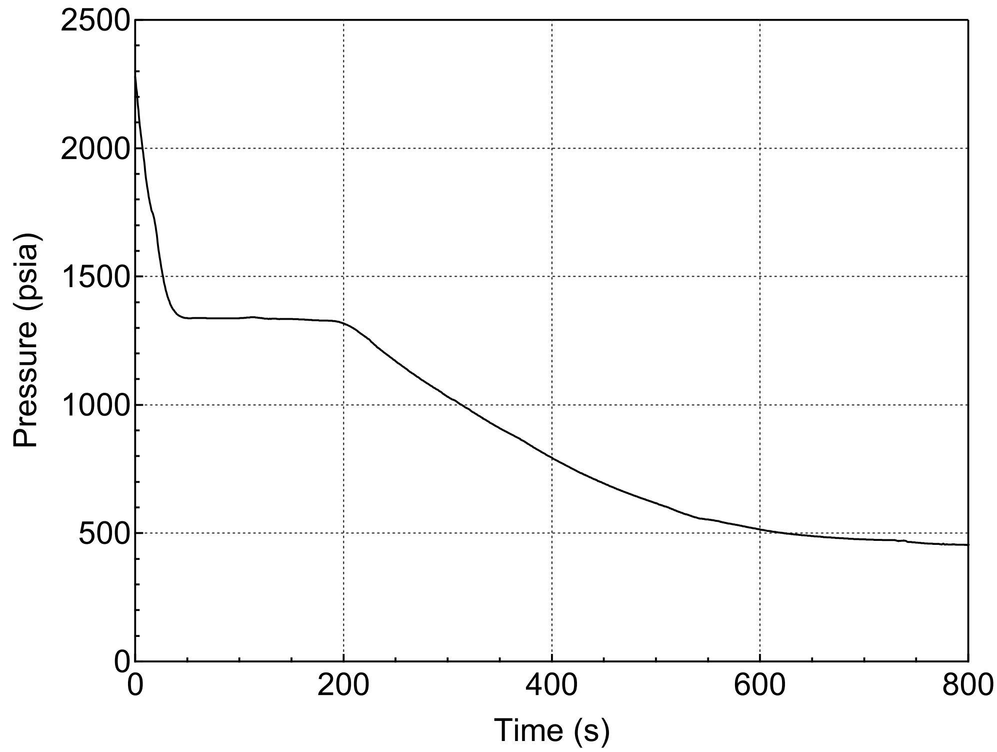

Figure 5.2.f-1 RCS (Pressurizer) Pressure Transient for 6-inch Break (Bottom) (Spectrum Analysis)

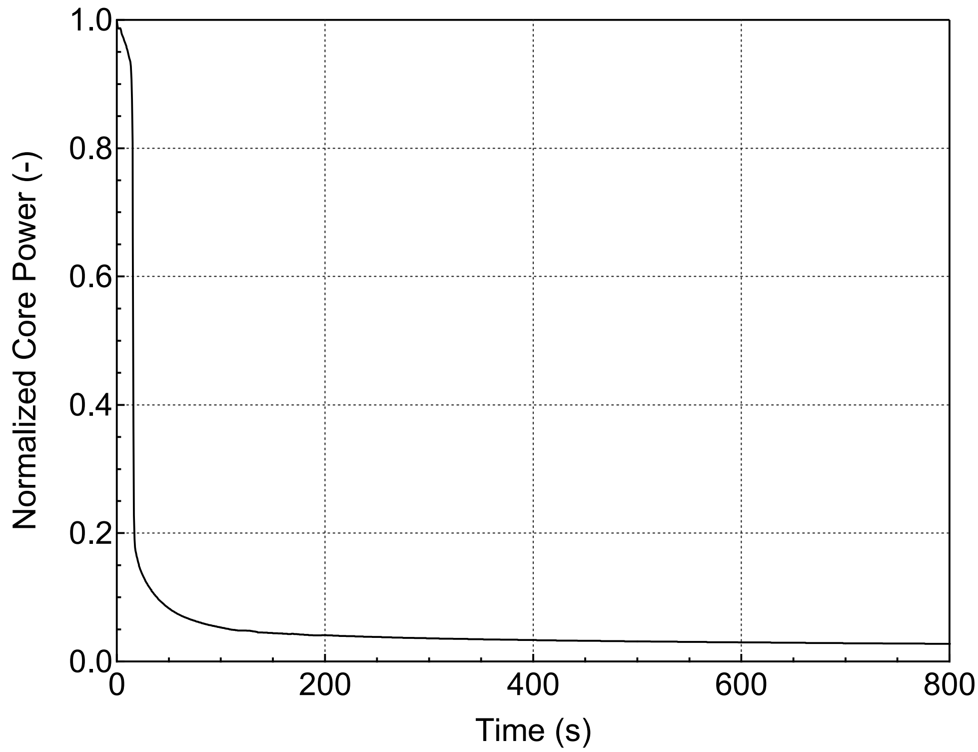

Figure 5.2.f-2 Normalized Core Power for 6-inch Break (Bottom) (Spectrum Analysis)

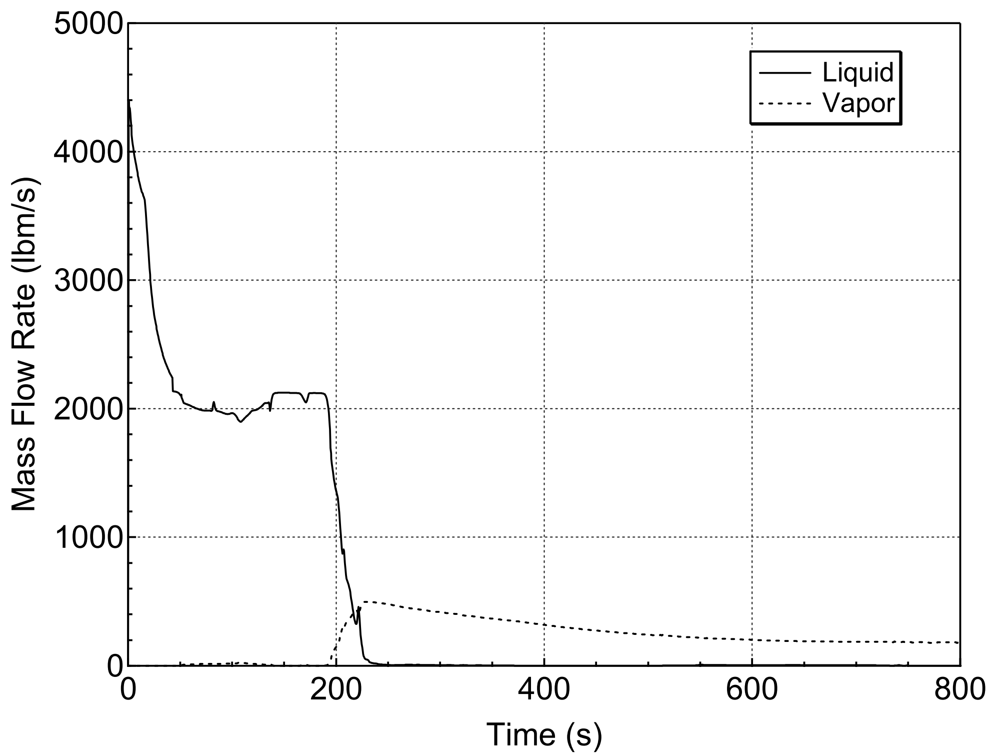

Figure 5.2.f-3 Liquid and Vapor Discharges through the Break for 6-inch Break (Bottom) (Spectrum Analysis)

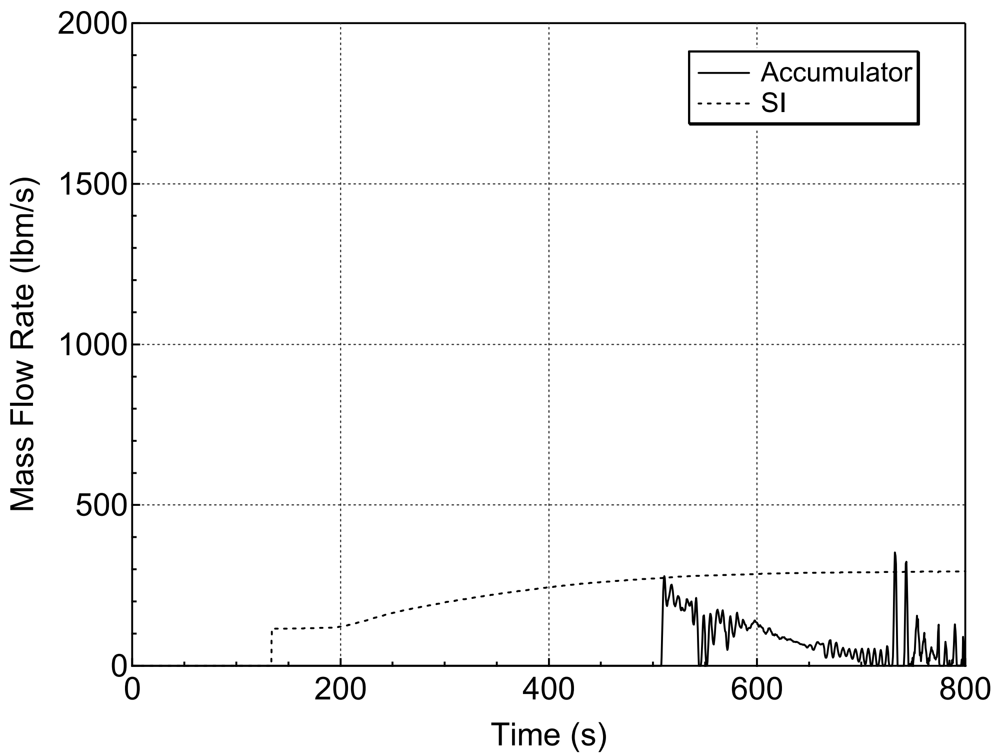

Figure 5.2.f-4 Accumulator and Safety Injection Mass Flowrates for 6-inch Break (Bottom) (Spectrum Analysis)

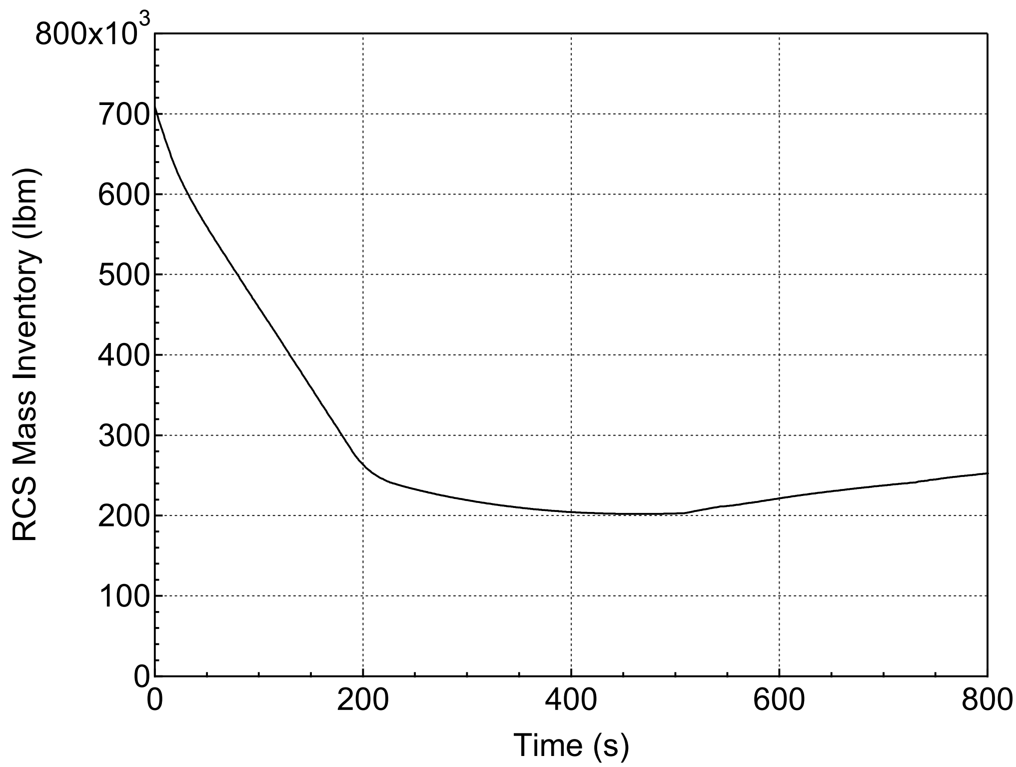

Figure 5.2.f-5 RCS Mass Inventory for 6-inch Break (Bottom) (Spectrum Analysis)

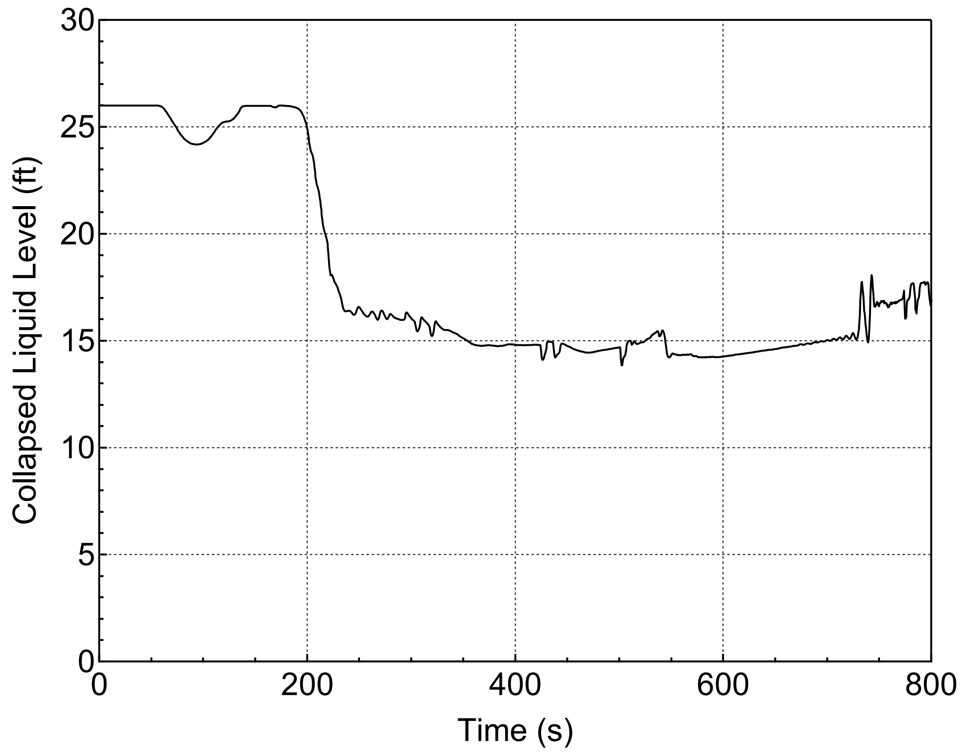

Figure 5.2.f-6 Downcomer Collapsed Level for 6-inch Break (Bottom) (Spectrum Analysis)

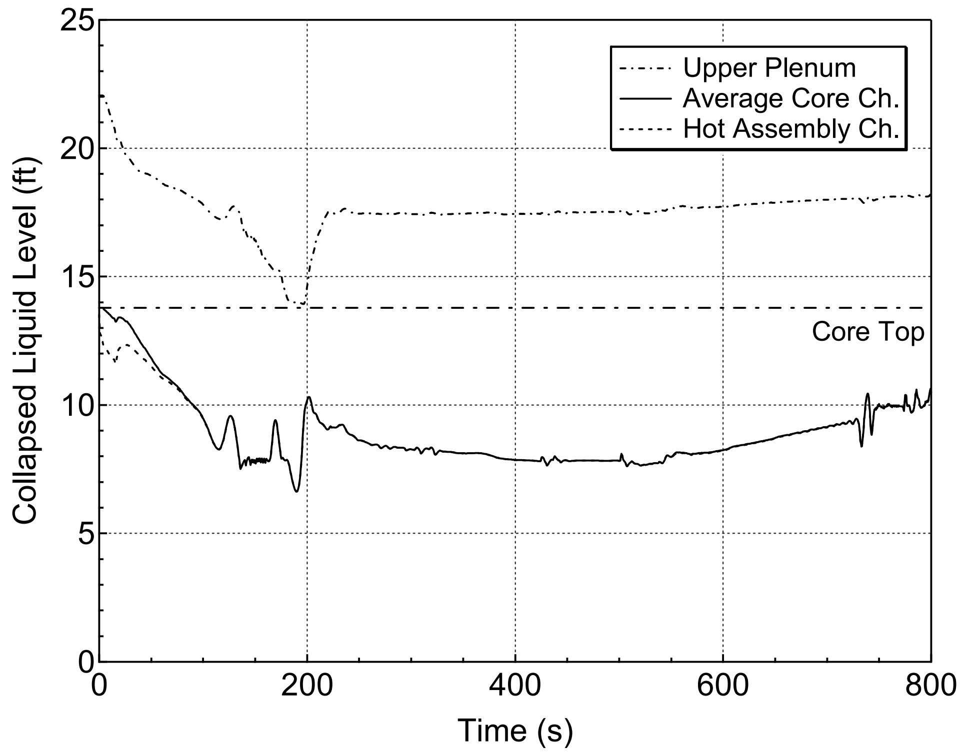

Figure 5.2.f-7 Core and Upper Plenum Collapsed Levels for 6-inch Break (Bottom) (Spectrum Analysis)

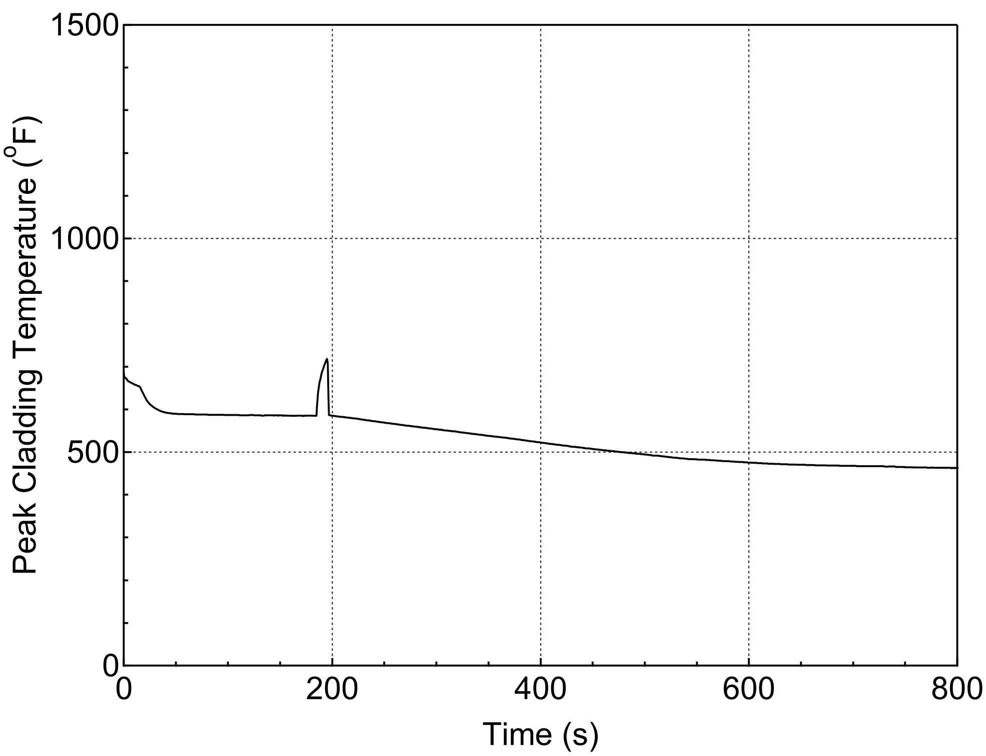

Figure 5.2.f-8 PCT at All Elevations for Hot Rod in Hot Assembly for 6-inch Break (Bottom) (Spectrum Analysis)

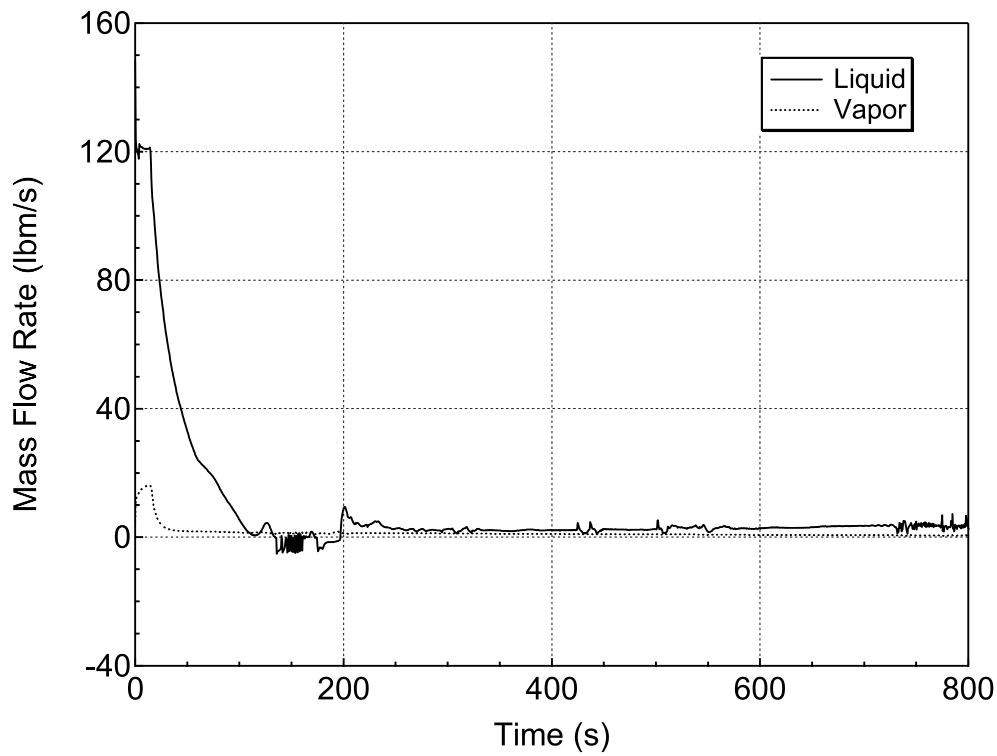

Figure 5.2.f-9 Hot Assembly Exit Vapor and Liquid Mass Flowrates for 6-inch Break (Bottom) (Spectrum Analysis)

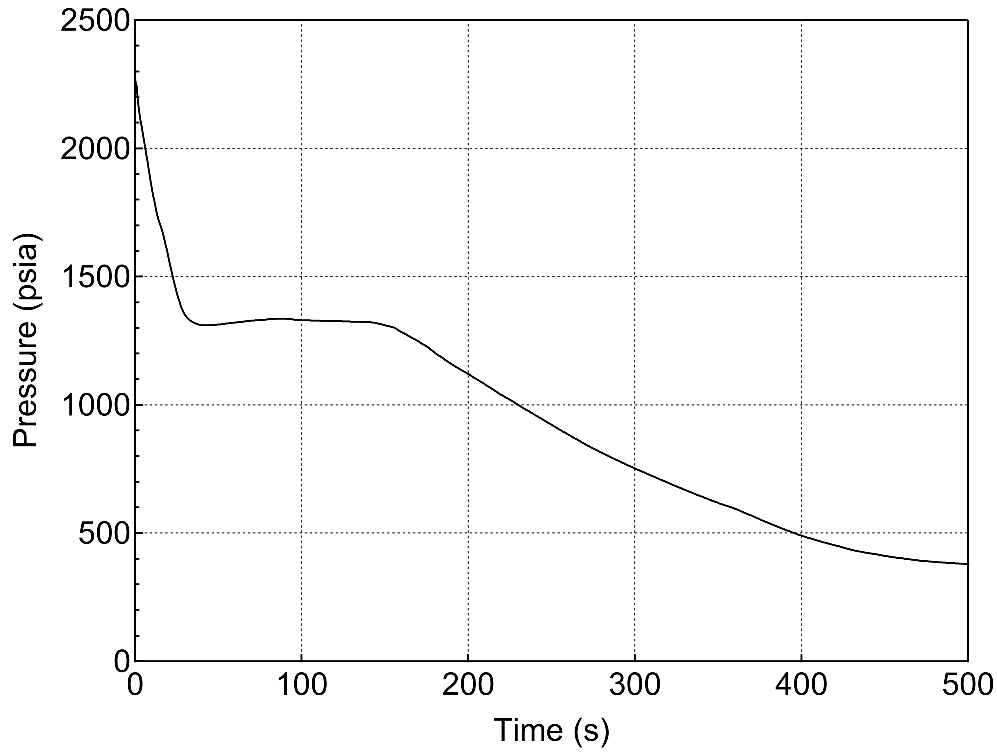

Figure 5.2.g-1 RCS (Pressurizer) Pressure Transient for 7-inch Break (Bottom) (Spectrum Analysis)

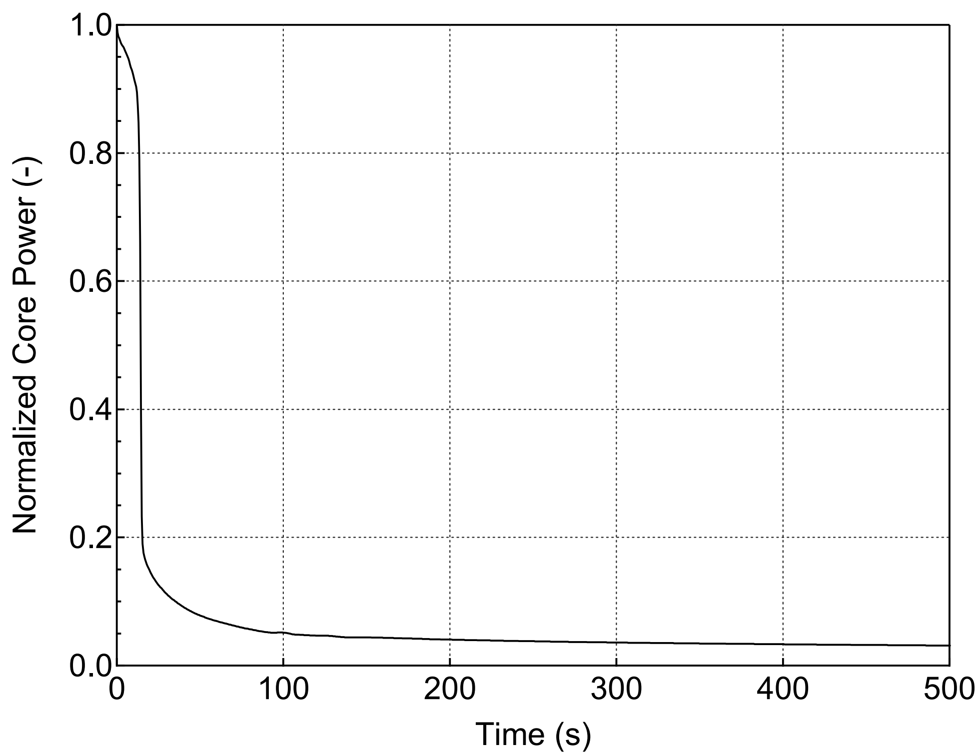

Figure 5.2.g-2 Normalized Core Power for 7-inch Break (Bottom) (Spectrum Analysis)

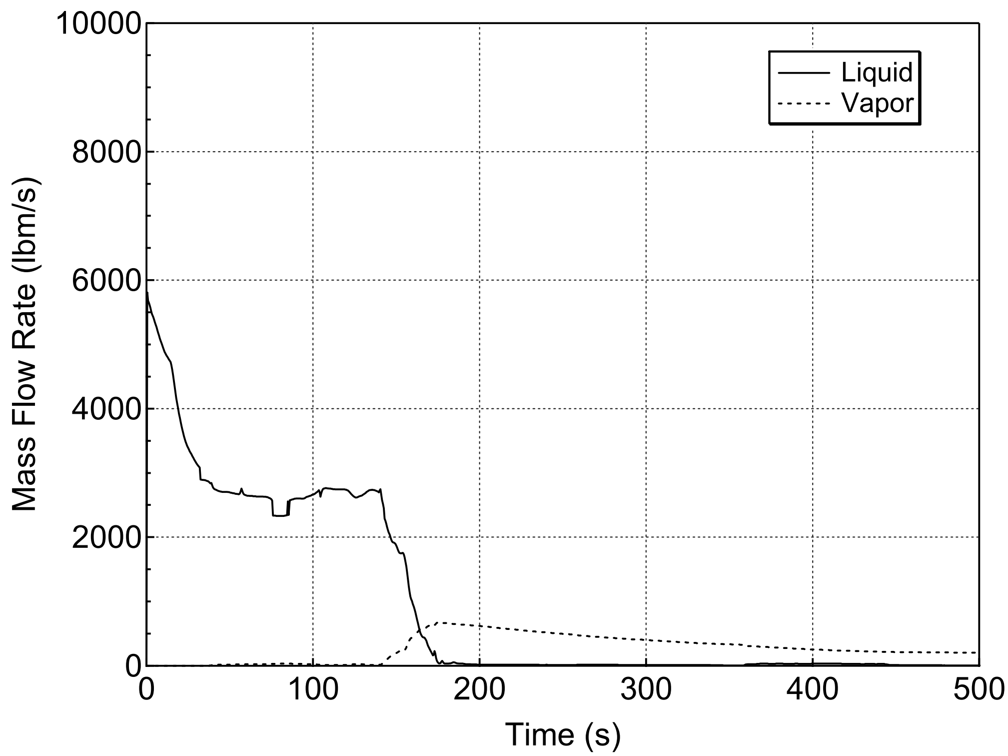

Figure 5.2.g-3 Liquid and Vapor Discharges through the Break for 7-inch Break (Bottom) (Spectrum Analysis)

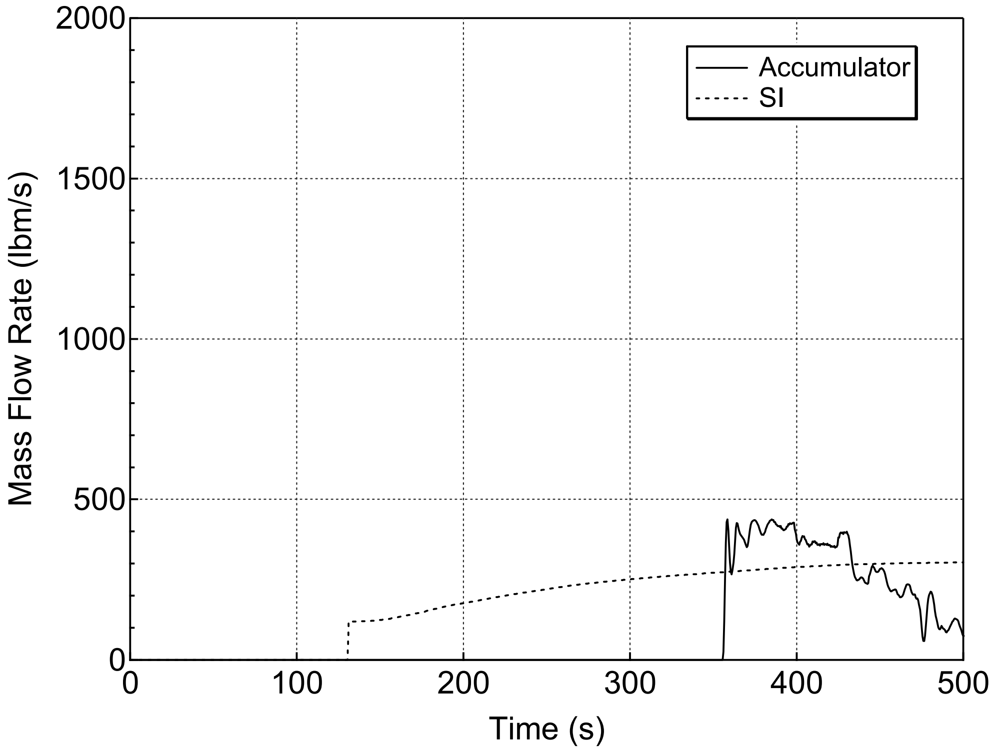

Figure 5.2.g-4 Accumulator and Safety Injection Mass Flowrates for 7-inch Break (Bottom) (Spectrum Analysis)

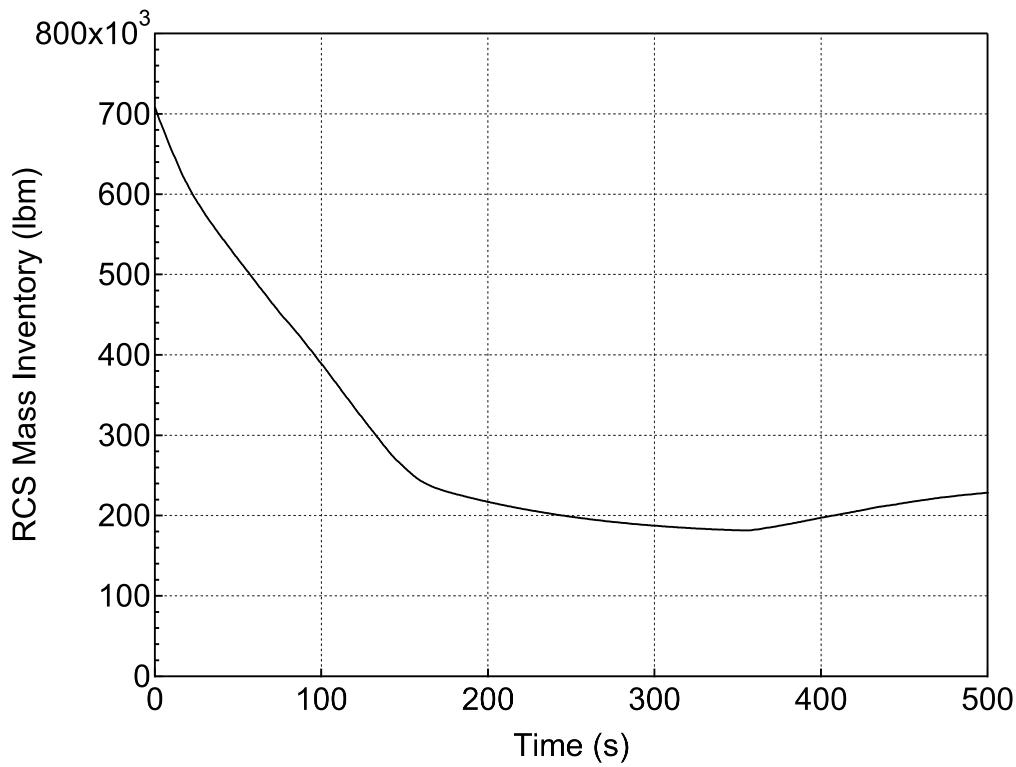

Figure 5.2.g-5 RCS Mass Inventory for 7-inch Break (Bottom) (Spectrum Analysis)

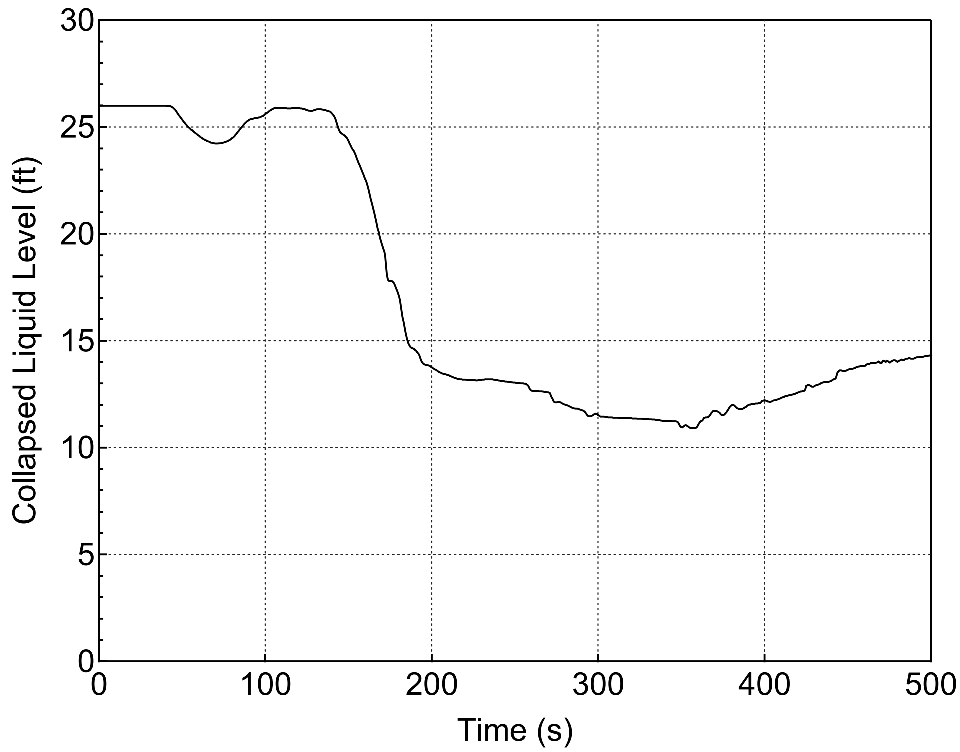

Figure 5.2.g-6 Downcomer Collapsed Level for 7-inch Break (Bottom) (Spectrum Analysis)

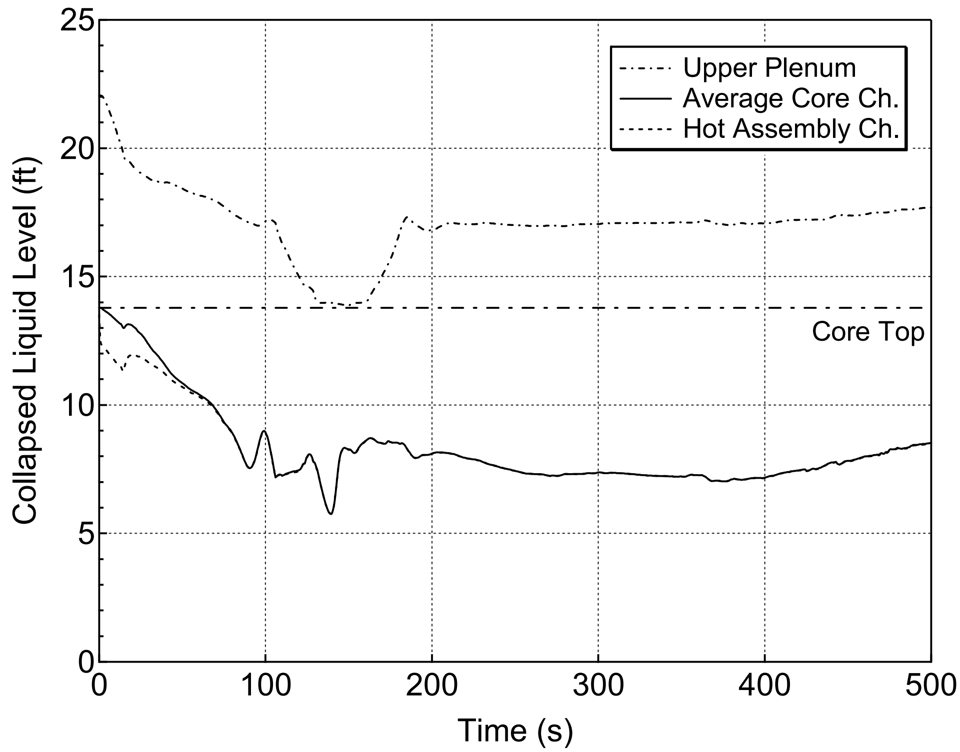

Figure 5.2.g-7 Core and Upper Plenum Collapsed Levels for 7-inch Break (Bottom) (Spectrum Analysis)

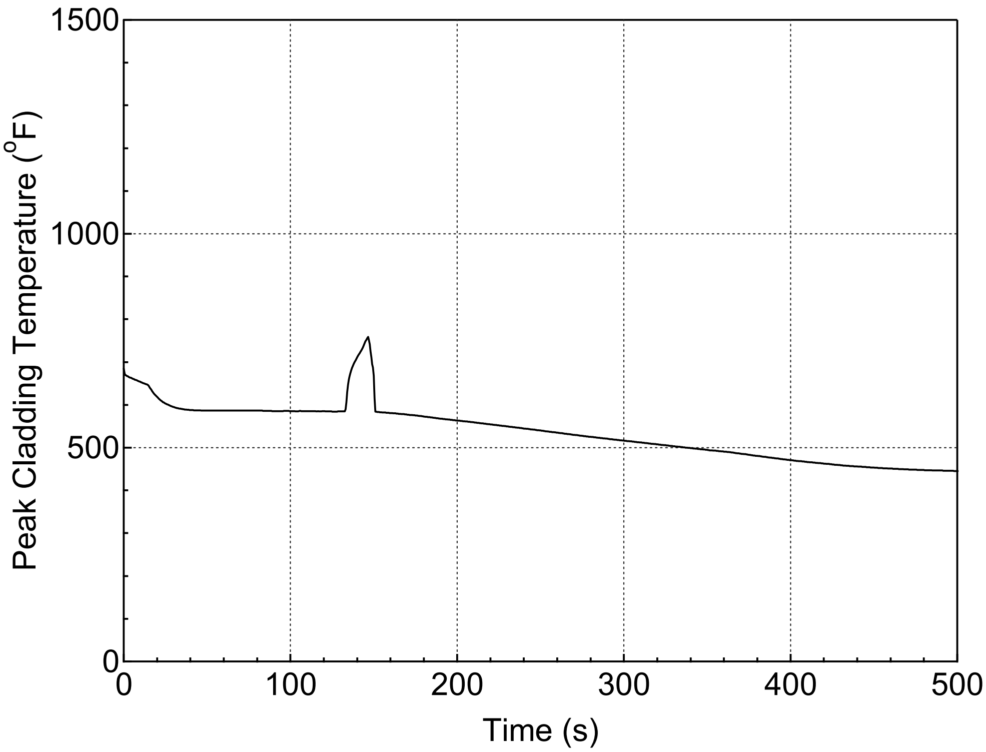

Figure 5.2.g-8 PCT at All Elevations for Hot Rod in Hot Assembly for 7-inch Break (Bottom) (Spectrum Analysis)

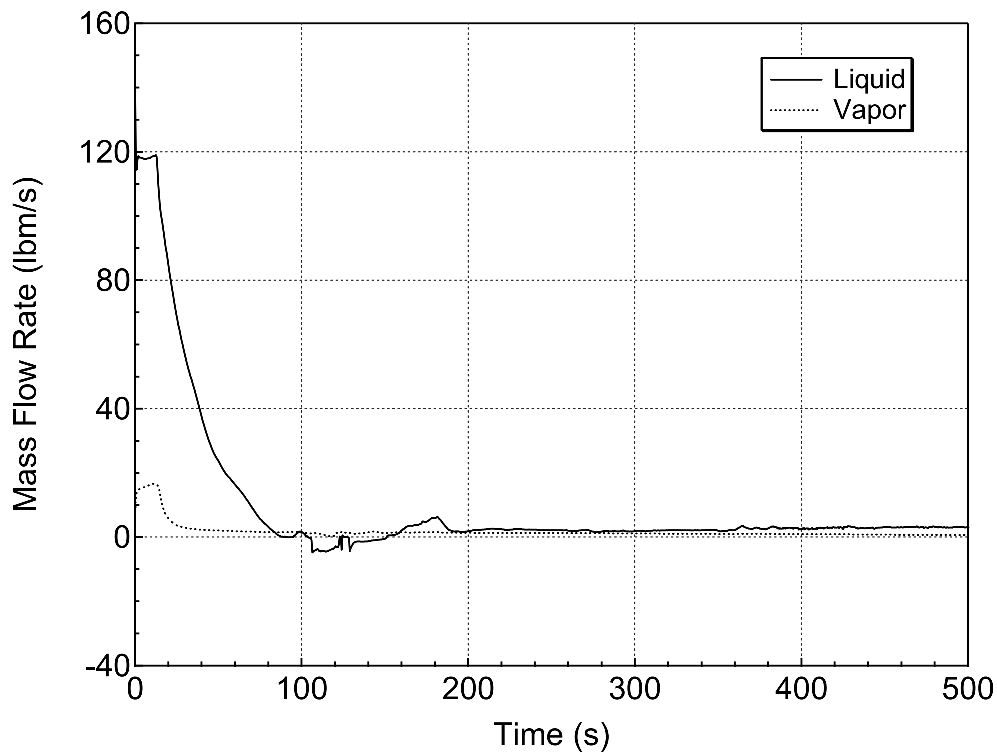

Figure 5.2.g-9 Hot Assembly Exit Vapor and Liquid Mass Flowrates for 7-inch Break (Bottom) (Spectrum Analysis)

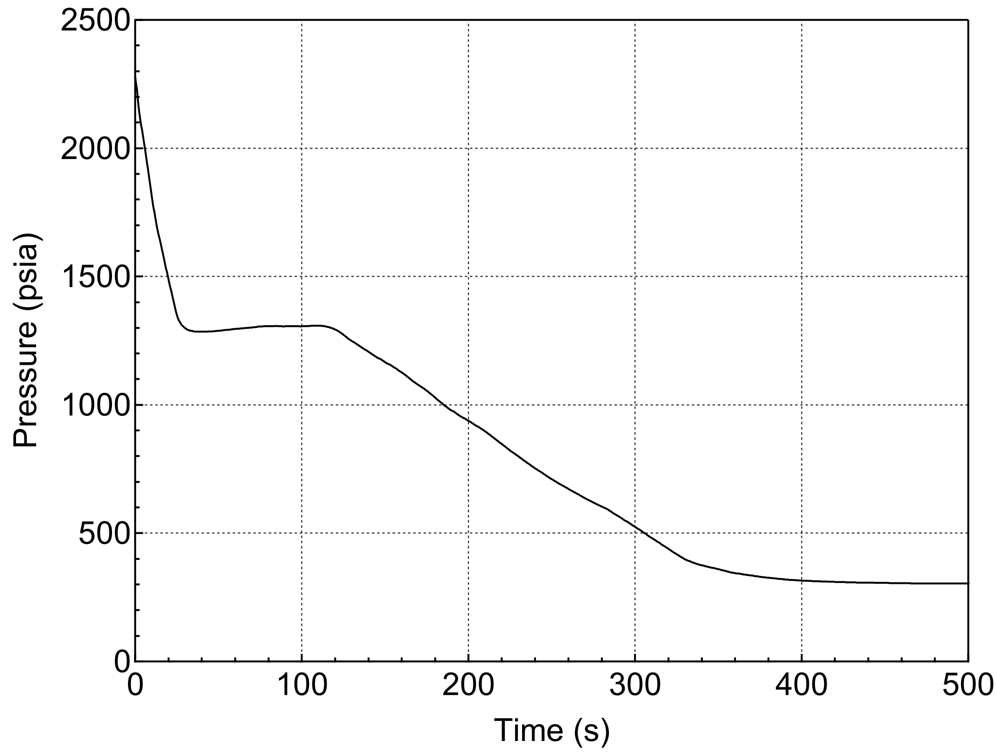

Figure 5.2.h-1 RCS (Pressurizer) Pressure Transient for 8-inch Break (Bottom) (Spectrum Analysis)

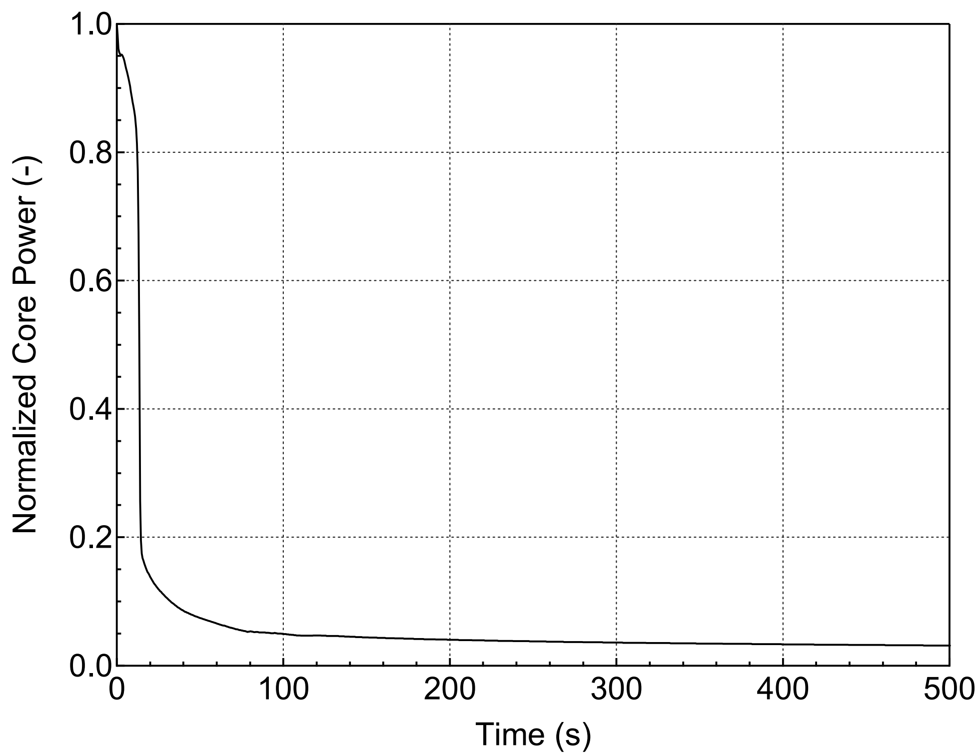

Figure 5.2.h-2 Normalized Core Power for 8-inch Break (Bottom) (Spectrum Analysis)

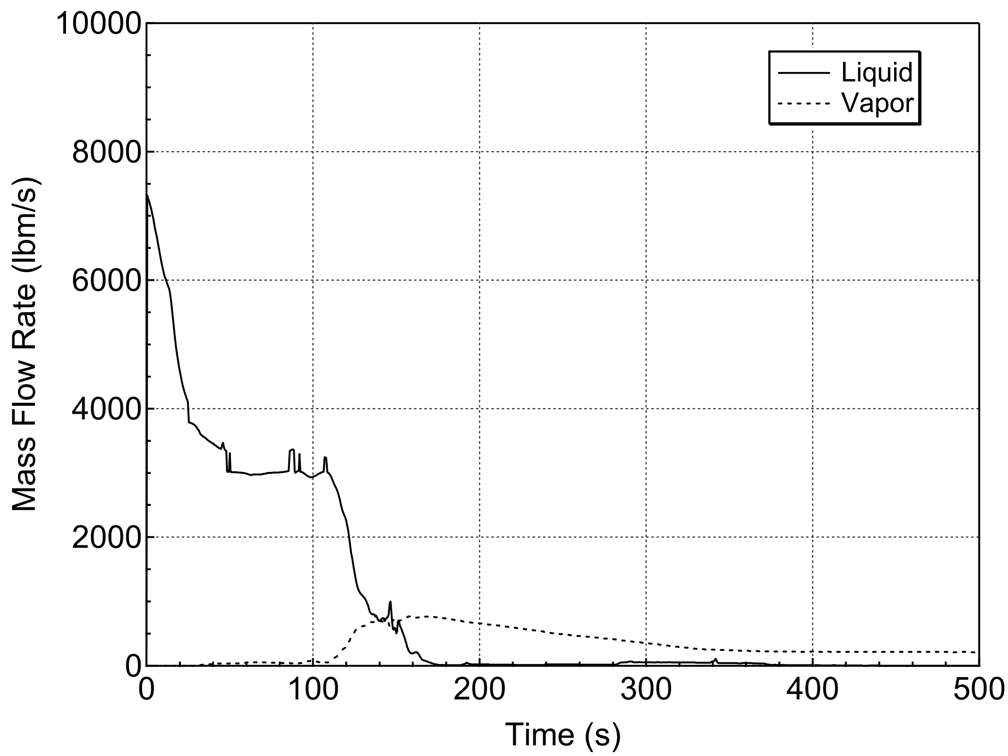

Figure 5.2.h-3 Liquid and Vapor Discharges through the Break for 8-inch Break (Bottom) (Spectrum Analysis)

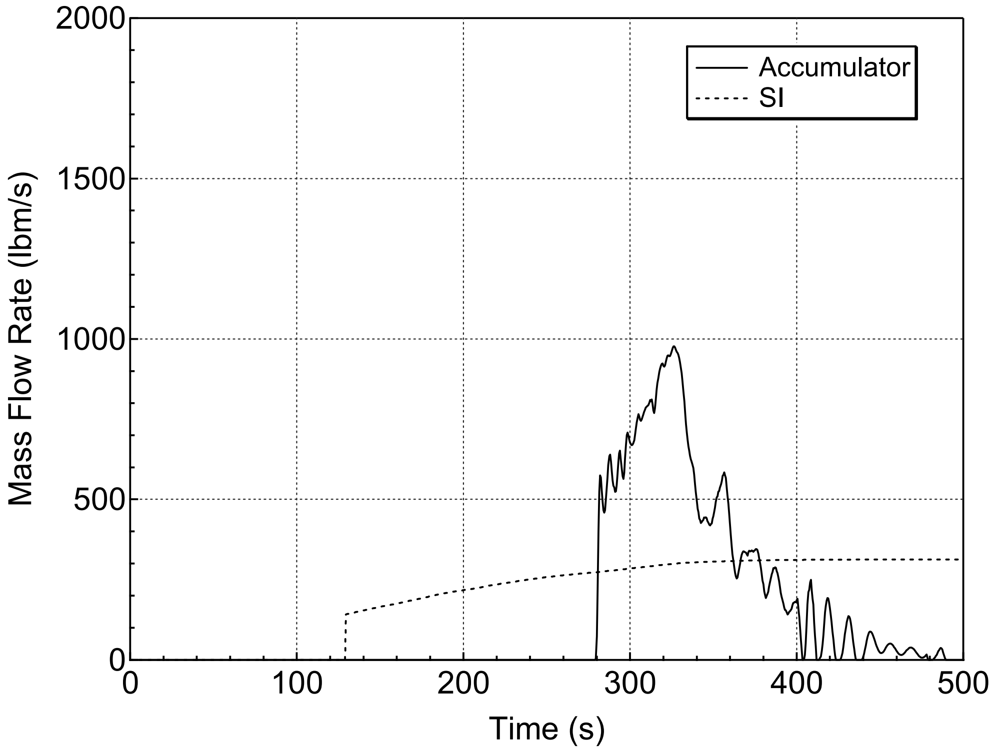

Figure 5.2.h-4 Accumulator and Safety Injection Mass Flowrates for 8-inch Break (Bottom) (Spectrum Analysis)

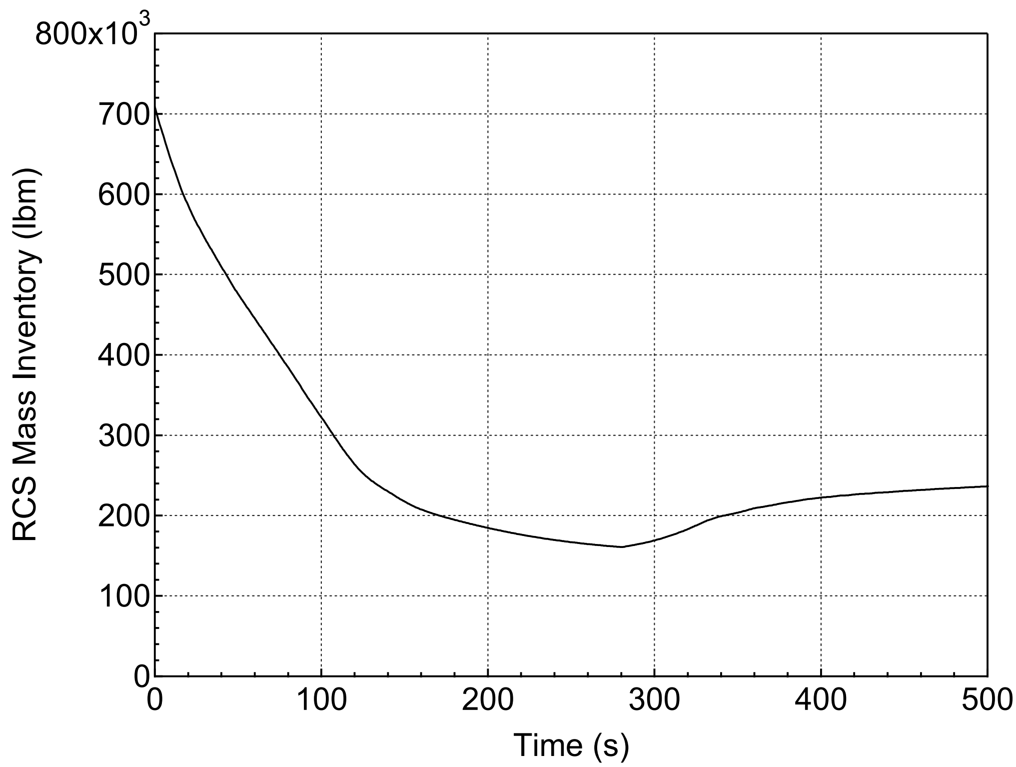

Figure 5.2.h-5 RCS Mass Inventory for 8-inch Break (Bottom) (Spectrum Analysis)

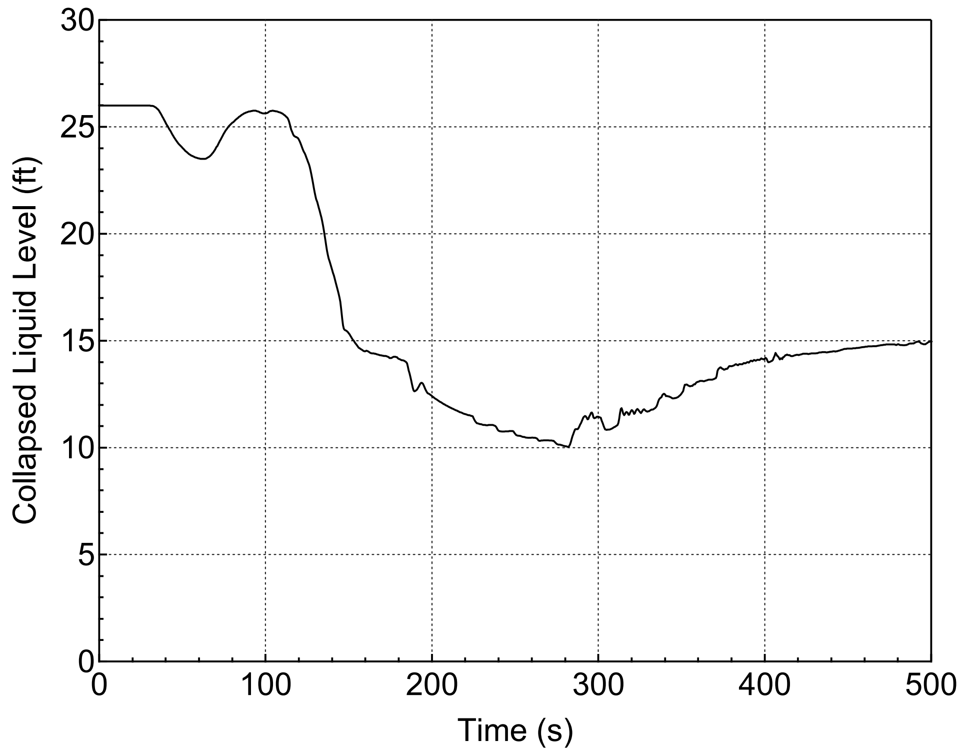

Figure 5.2.h-6 Downcomer Collapsed Level for 8-inch Break (Bottom) (Spectrum Analysis)

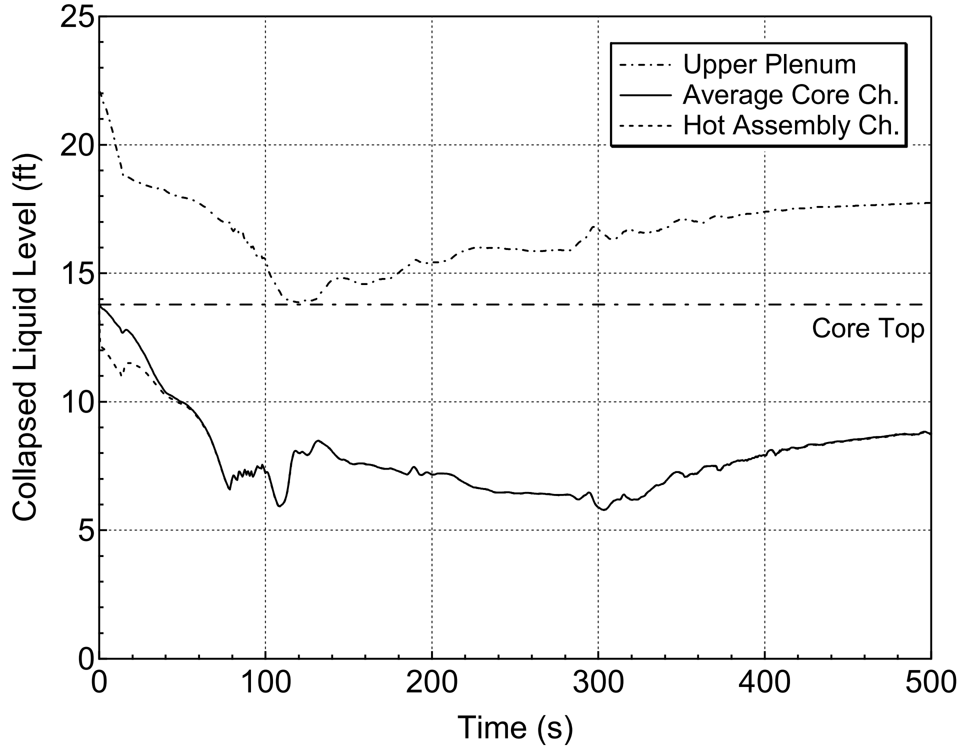

Figure 5.2.h-7 Core and Upper Plenum Collapsed Levels for 8-inch Break (Bottom) (Spectrum Analysis)

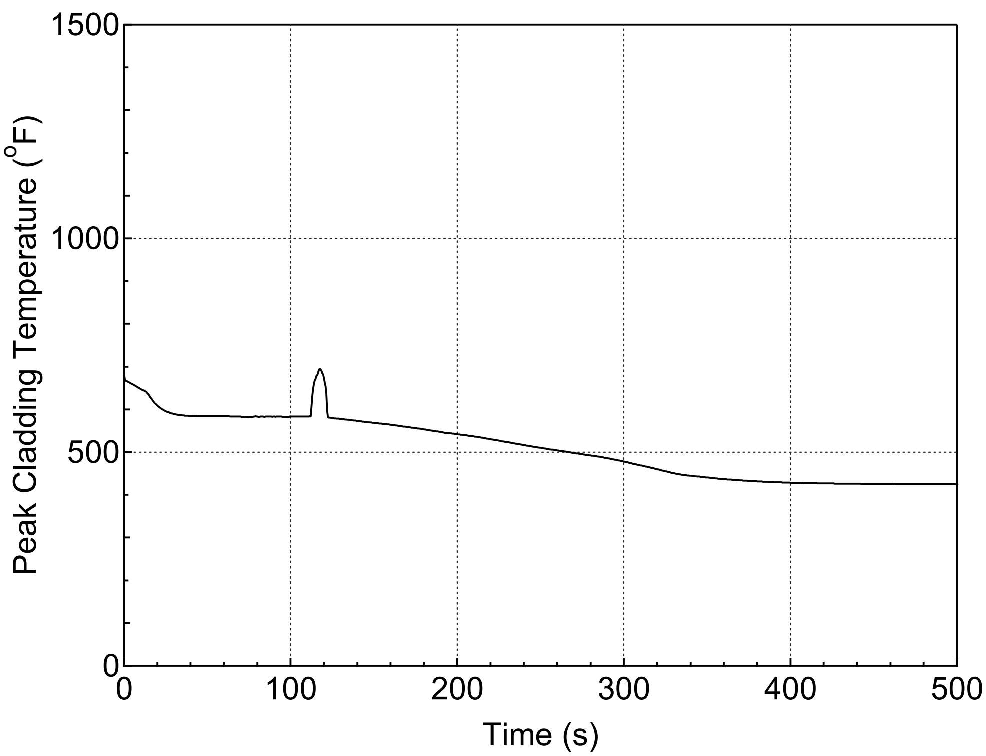

Figure 5.2.h-8 PCT at All Elevations for Hot Rod in Hot Assembly for 8-inch Break (Bottom) (Spectrum Analysis)

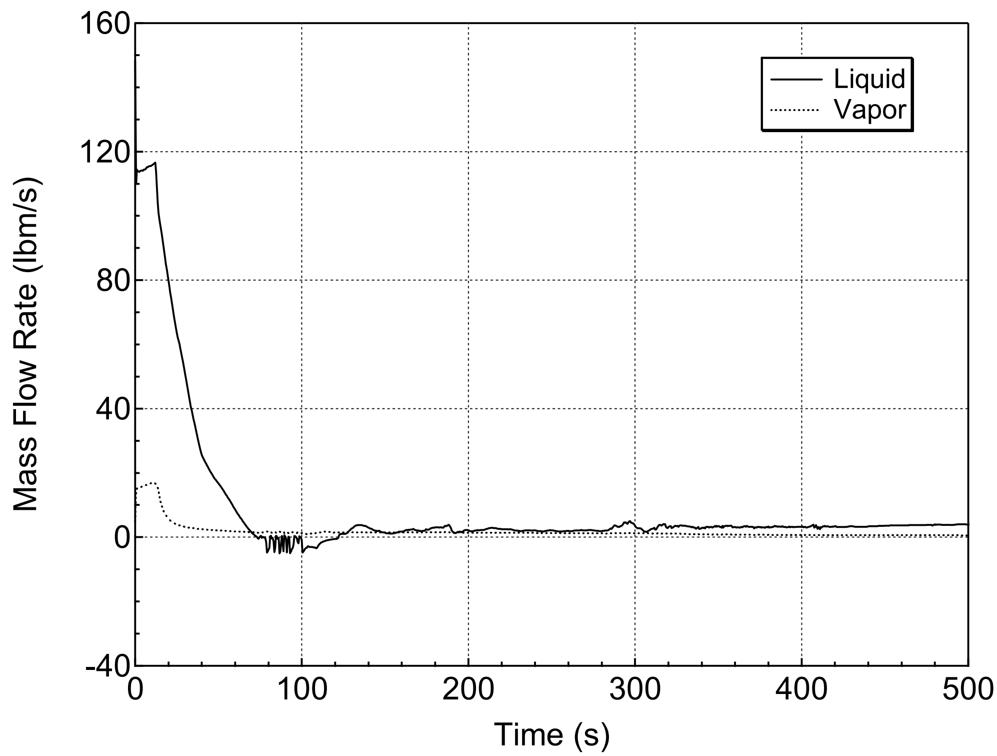

Figure 5.2.h-9 Hot Assembly Exit Vapor and Liquid Mass Flowrates for 8-inch Break (Bottom) (Spectrum Analysis)

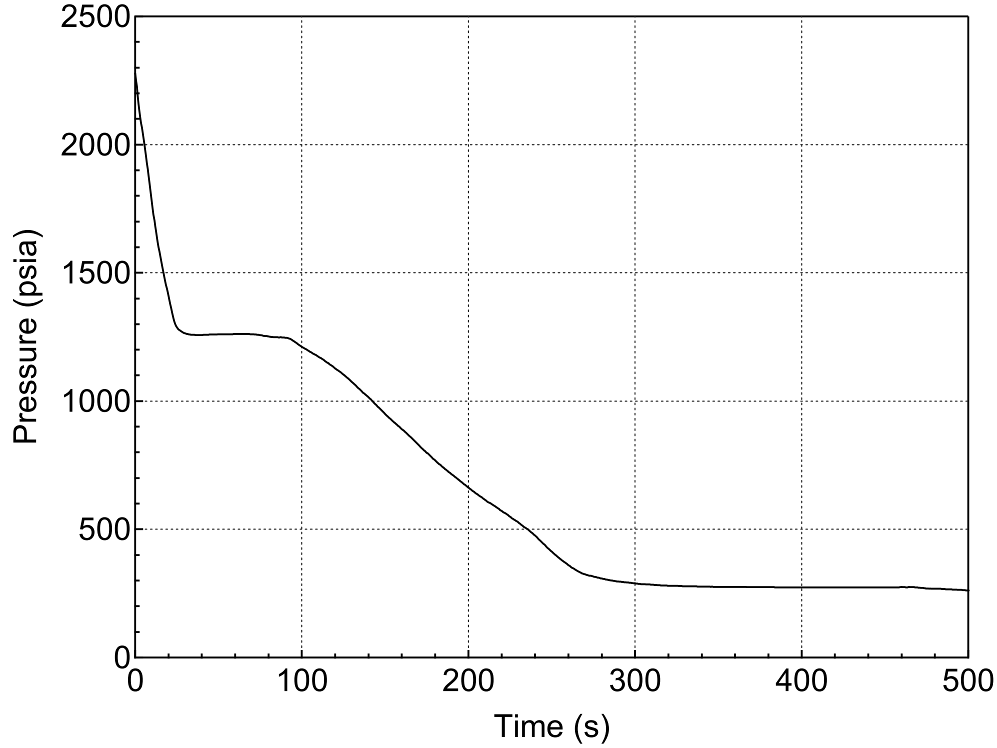

Figure 5.2.i-1 RCS (Pressurizer) Pressure Transient for 9-inch Break (Bottom) (Spectrum Analysis)

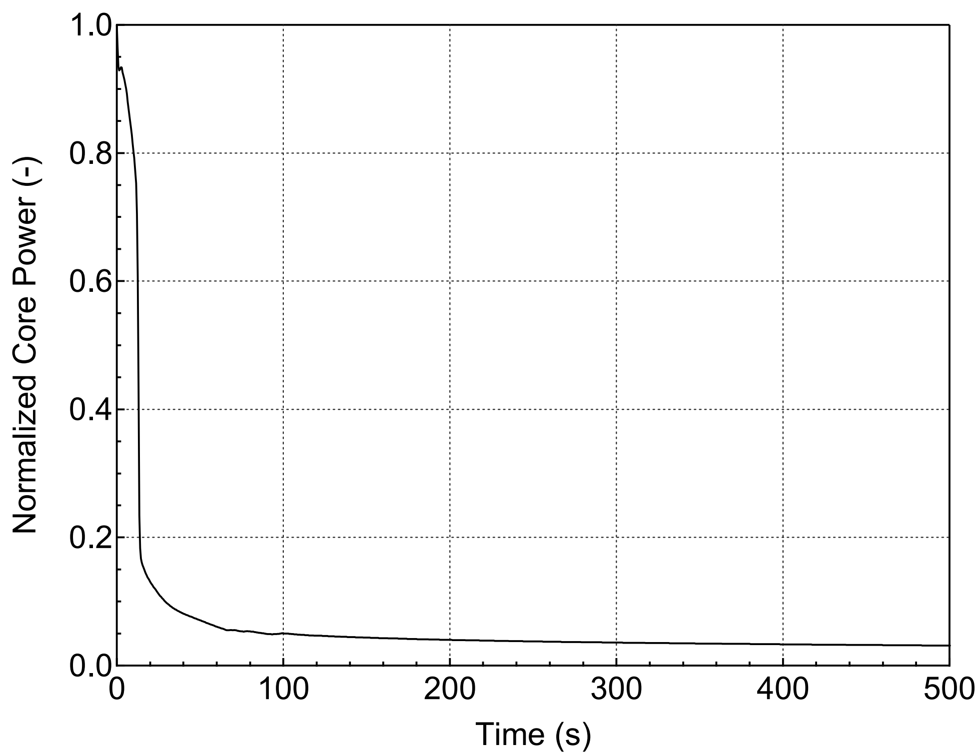

Figure 5.2.i-2 Normalized Core Power for 9-inch Break (Bottom) (Spectrum Analysis)

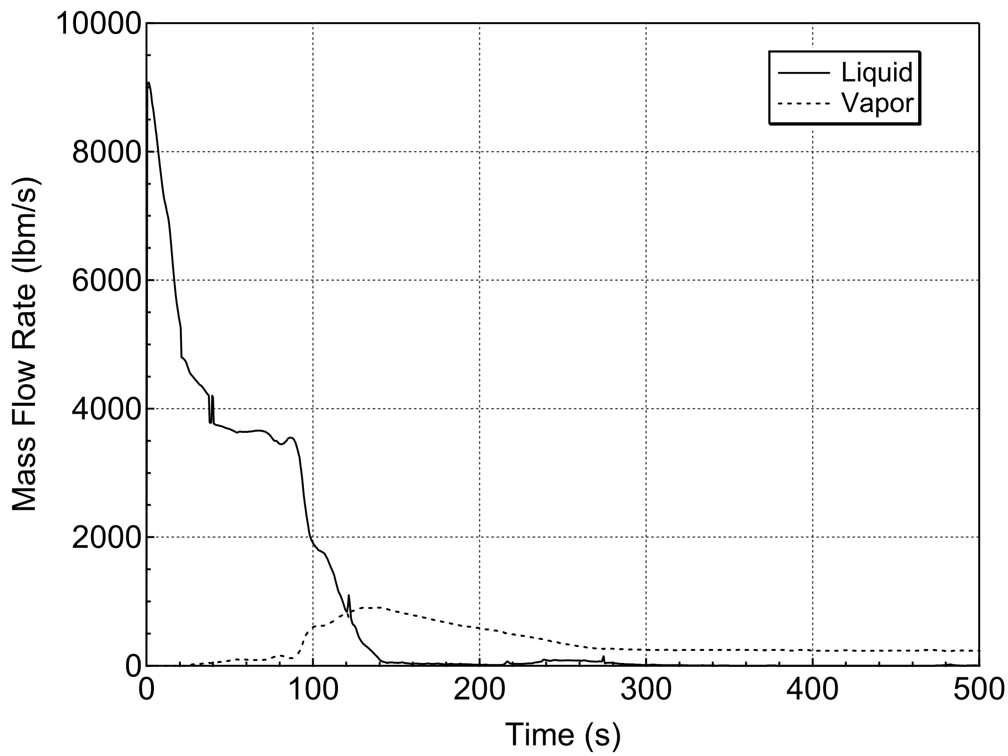

Figure 5.2.i-3 Liquid and Vapor Discharges through the Break for 9-inch Break (Bottom) (Spectrum Analysis)

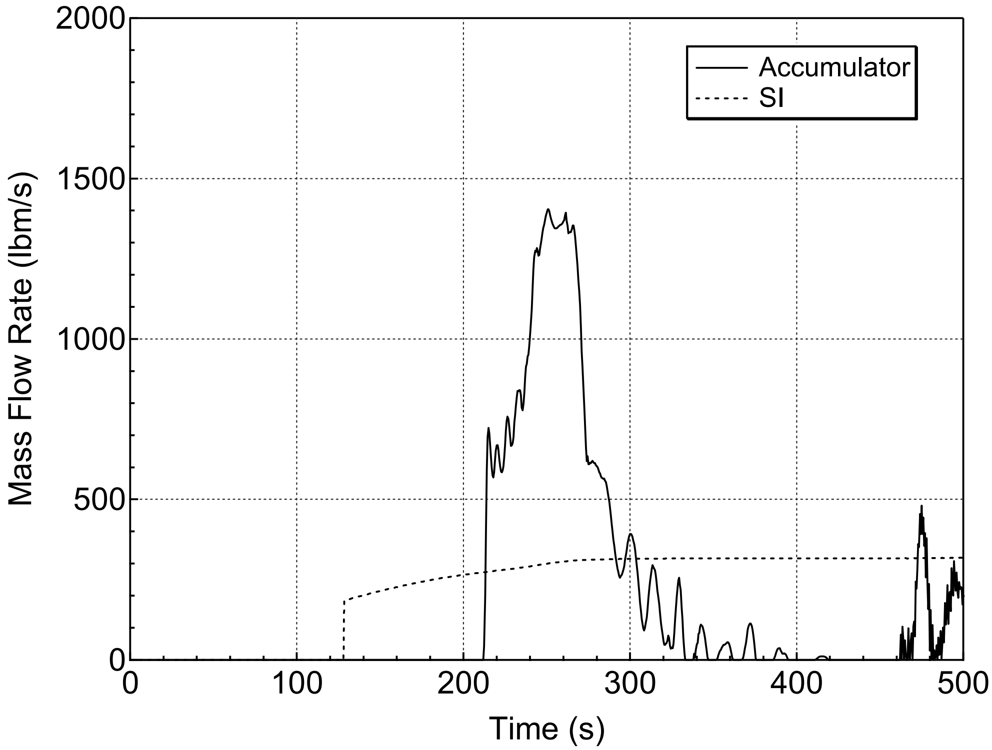

Figure 5.2.i-4 Accumulator and Safety Injection Mass Flowrates for 9-inch Break (Bottom) (Spectrum Analysis)

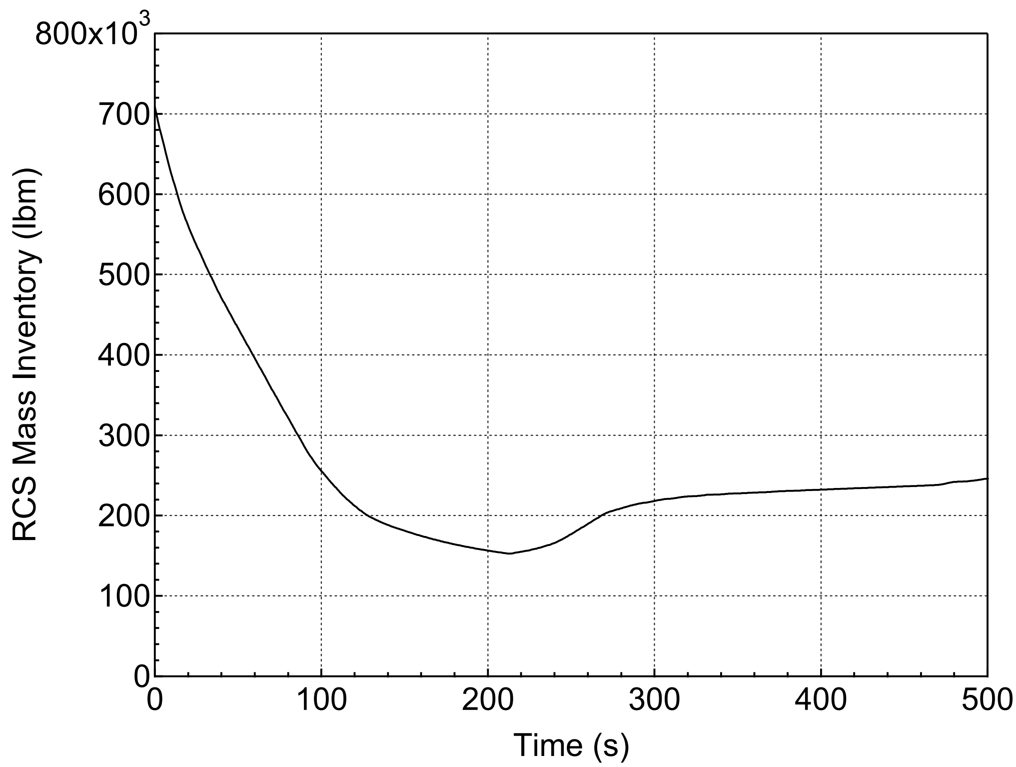

Figure 5.2.i-5 RCS Mass Inventory for 9-inch Break (Bottom) (Spectrum Analysis)

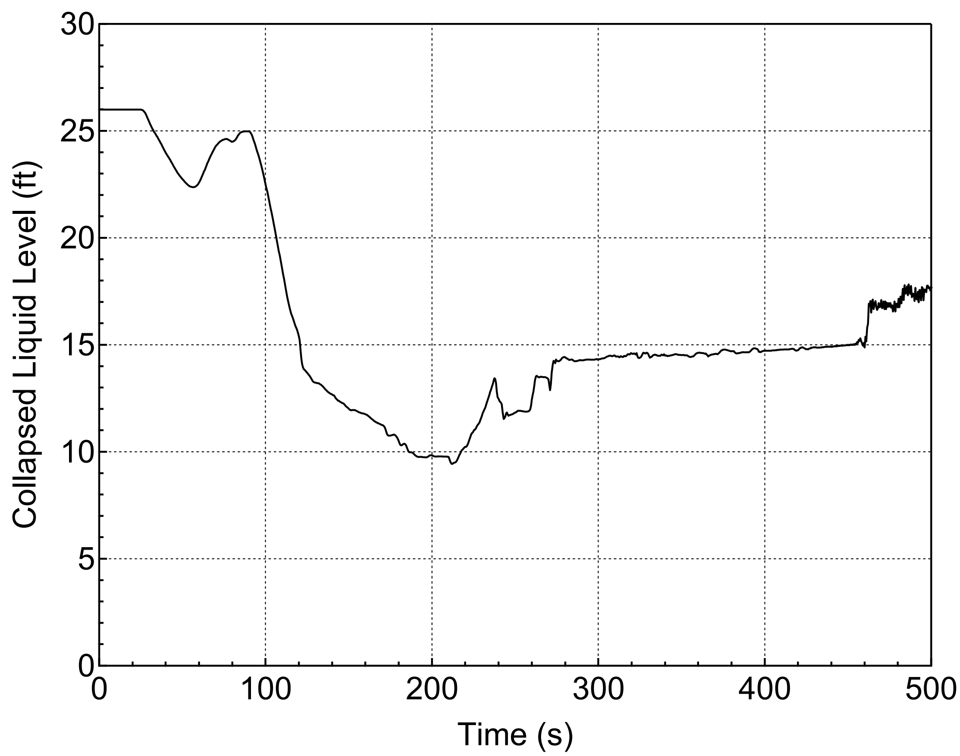

Figure 5.2.i-6 Downcomer Collapsed Level for 9-inch Break (Bottom) (Spectrum Analysis)

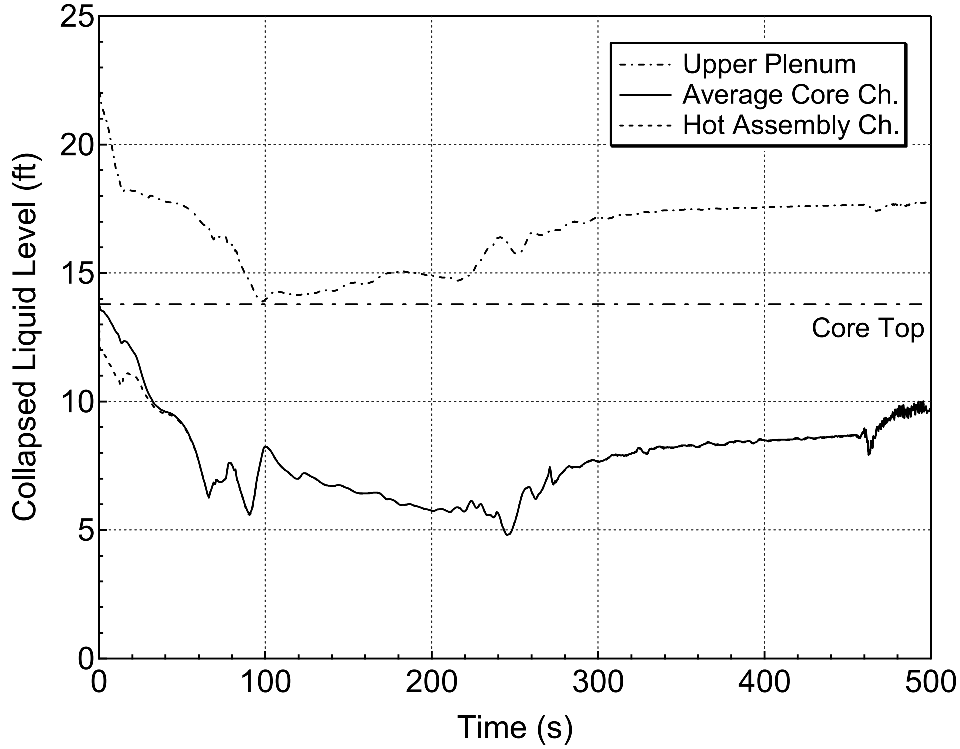

Figure 5.2.i-7 Core and Upper Plenum Collapsed Levels for 9-inch Break (Bottom) (Spectrum Analysis)

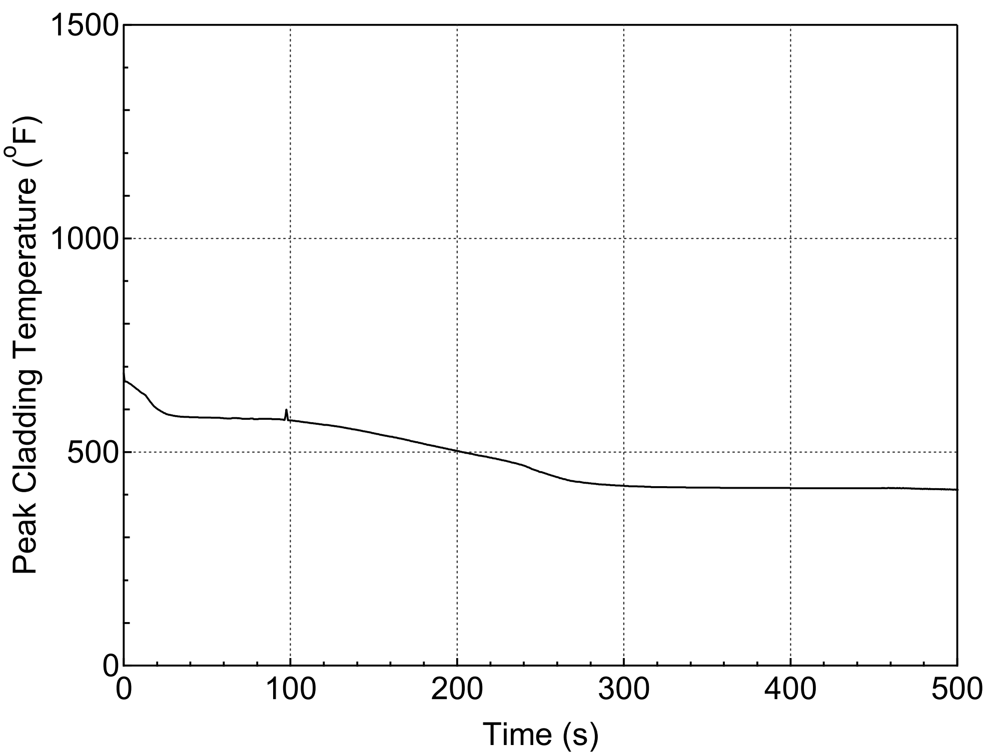

Figure 5.2.i-8 PCT at All Elevations for Hot Rod in Hot Assembly for 9-inch Break (Bottom) (Spectrum Analysis)

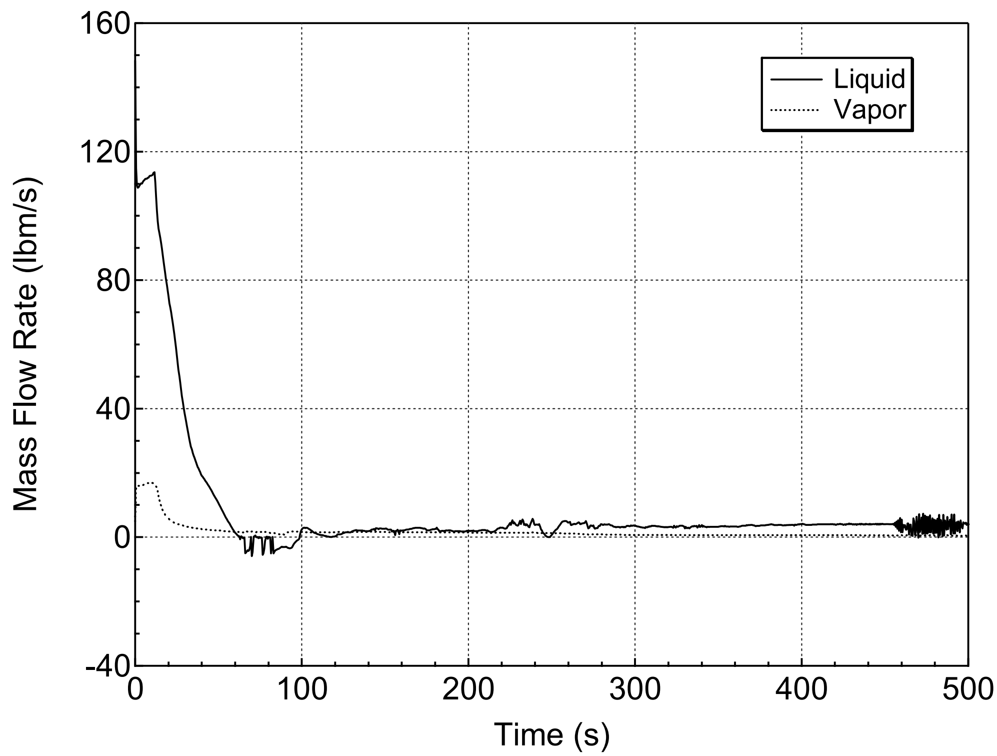

Figure 5.2.i-9 Hot Assembly Exit Vapor and Liquid Mass Flowrates for 9-inch Break (Bottom) (Spectrum Analysis)

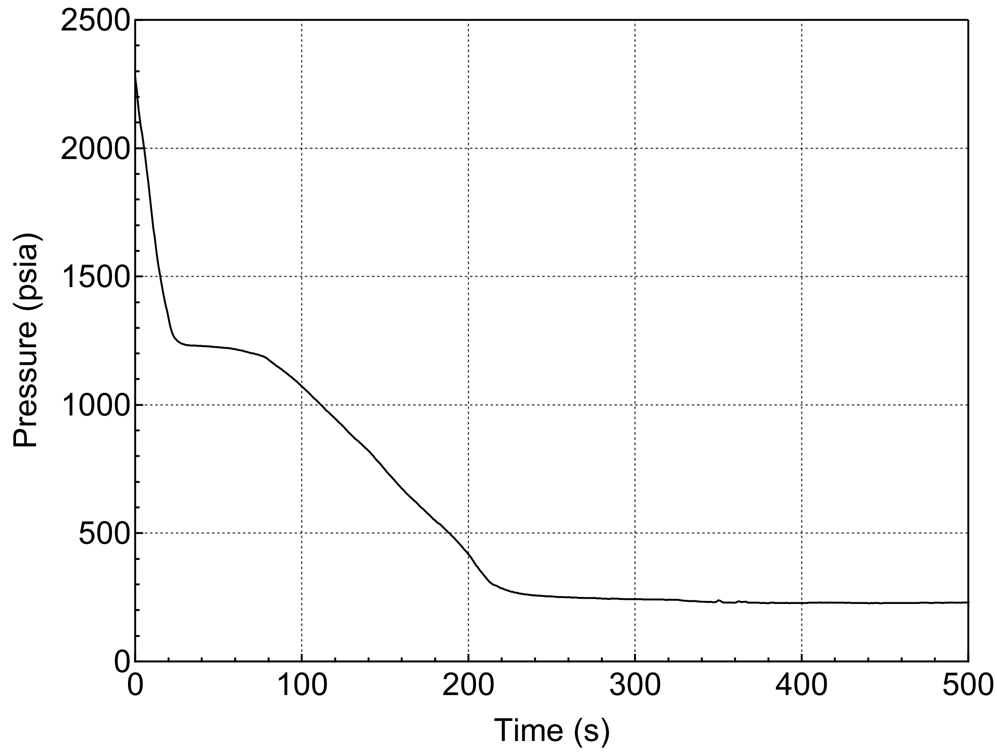

Figure 5.2.j-1 RCS (Pressurizer) Pressure Transient for 10-inch Break (Bottom) (Spectrum Analysis)

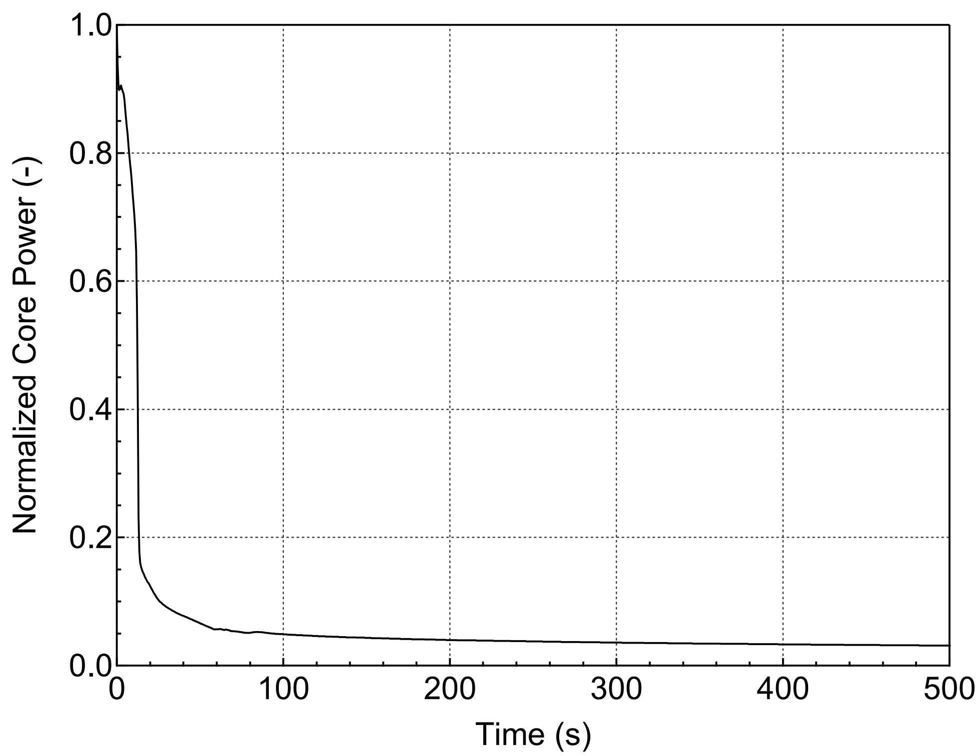

Figure 5.2.j-2 Normalized Core Power for 10-inch Break (Bottom) (Spectrum Analysis)

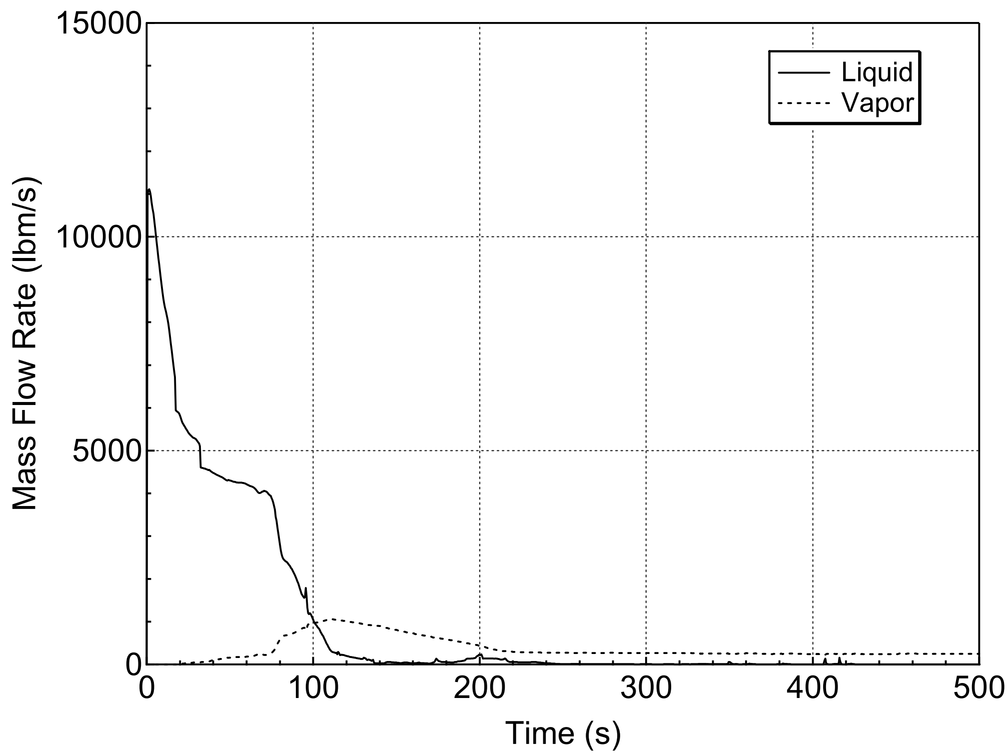

Figure 5.2.j-3 Liquid and Vapor Discharges through the Break for 10-inch Break (Bottom) (Spectrum Analysis)

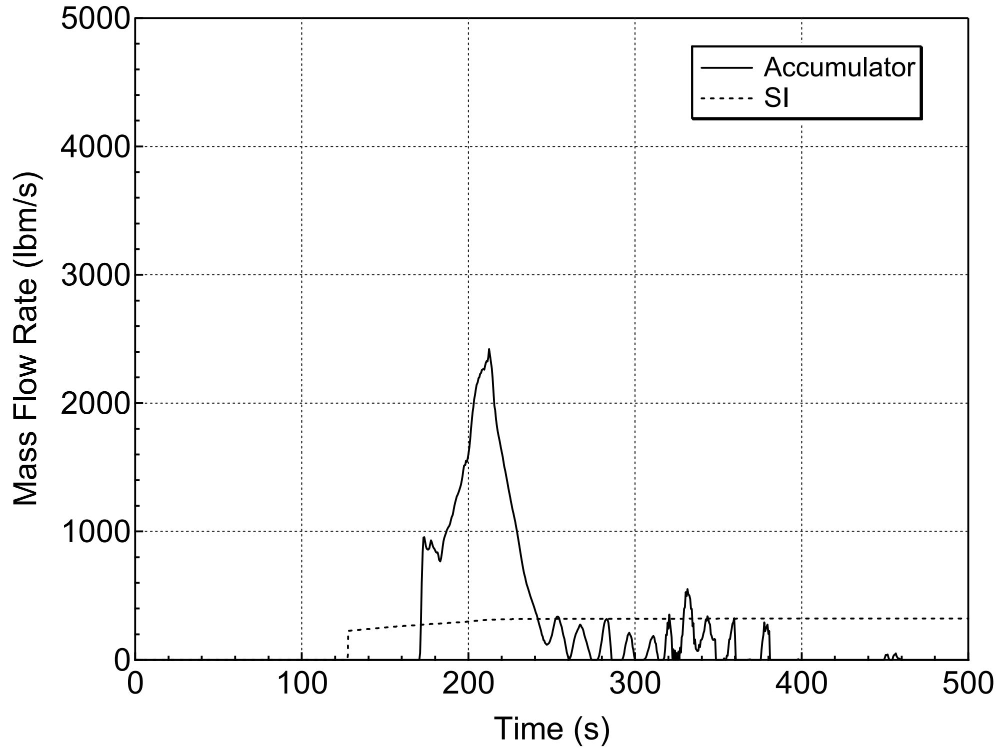

Figure 5.2.j-4 Accumulator and Safety Injection Mass Flowrates for 10-inch Break (Bottom) (Spectrum Analysis)

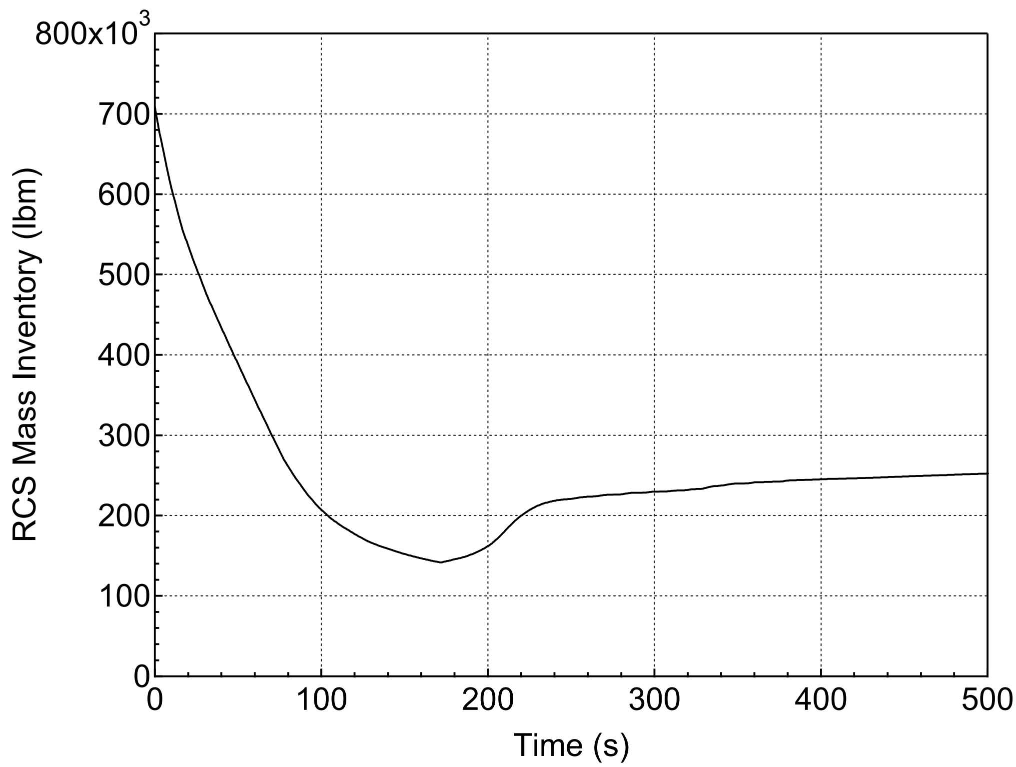

Figure 5.2.j-5 RCS Mass Inventory for 10-inch Break (Bottom) (Spectrum Analysis)

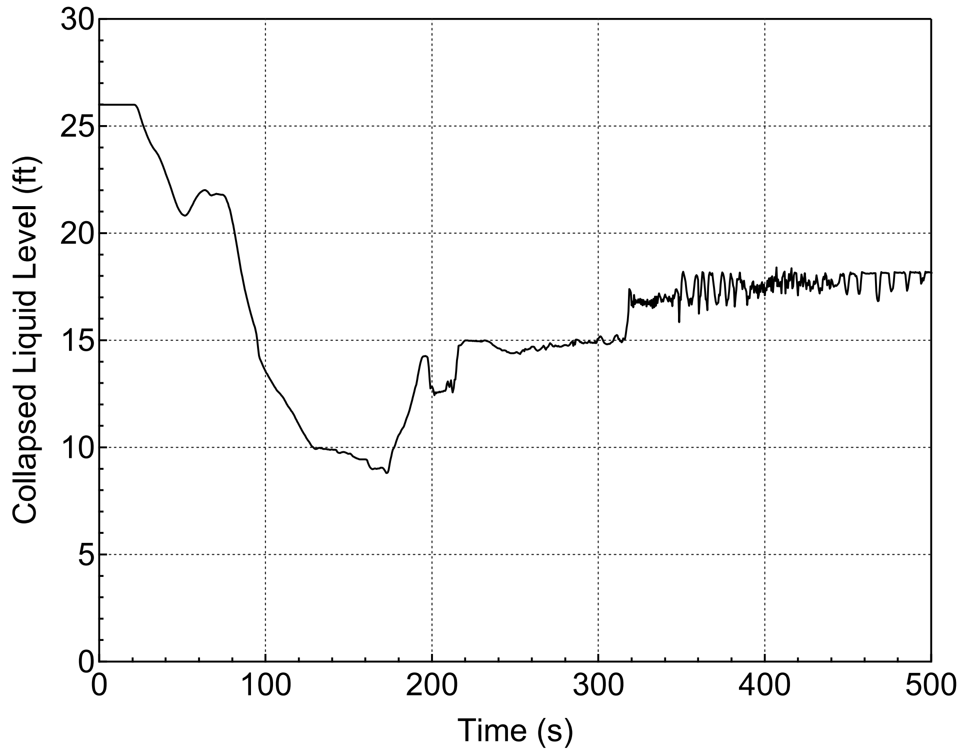

Figure 5.2.j-6 Downcomer Collapsed Level for 10-inch Break (Bottom) (Spectrum Analysis)

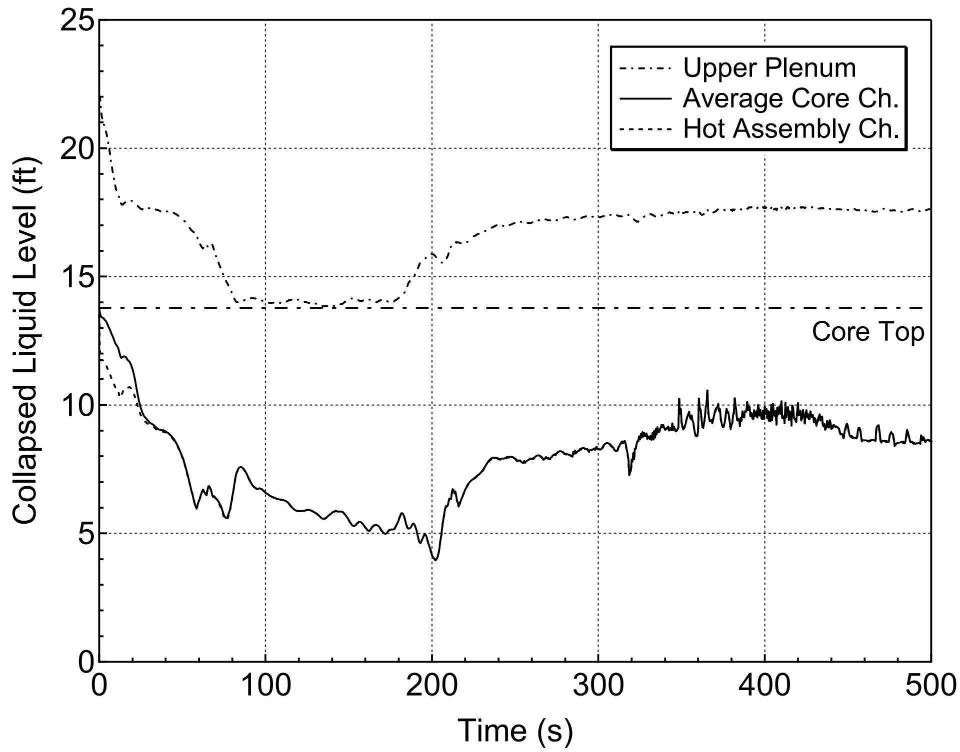

Figure 5.2.j-7 Core and Upper Plenum Collapsed Levels for 10-inch Break (Bottom) (Spectrum Analysis)

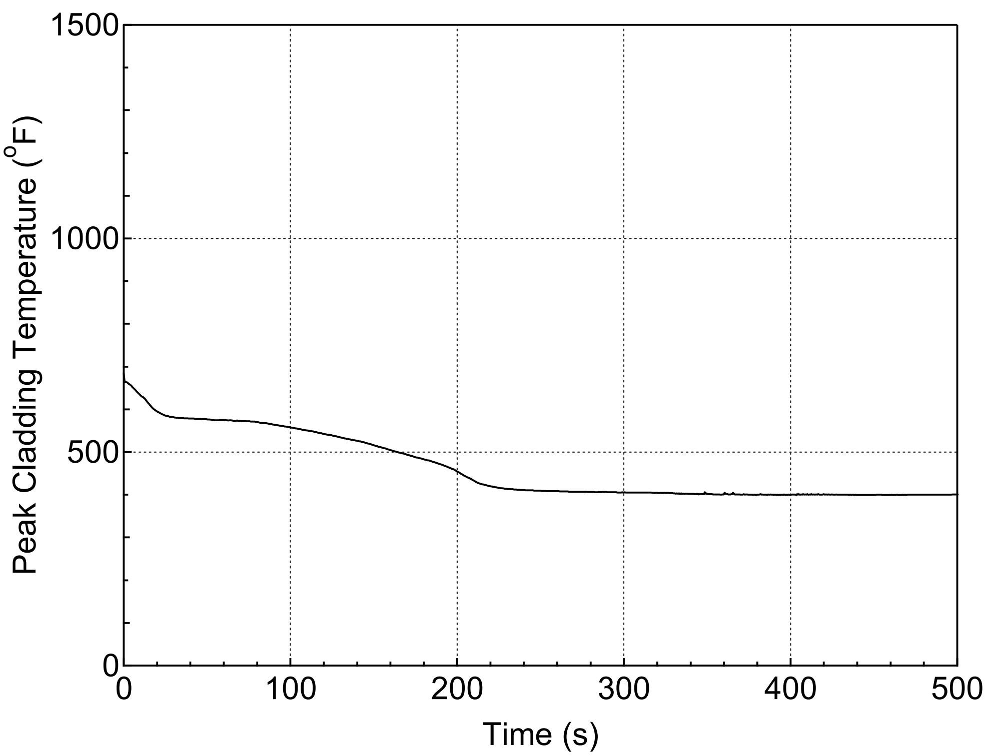

Figure 5.2.j-8 PCT at All Elevations for Hot Rod in Hot Assembly for 10-inch Break (Bottom) (Spectrum Analysis)

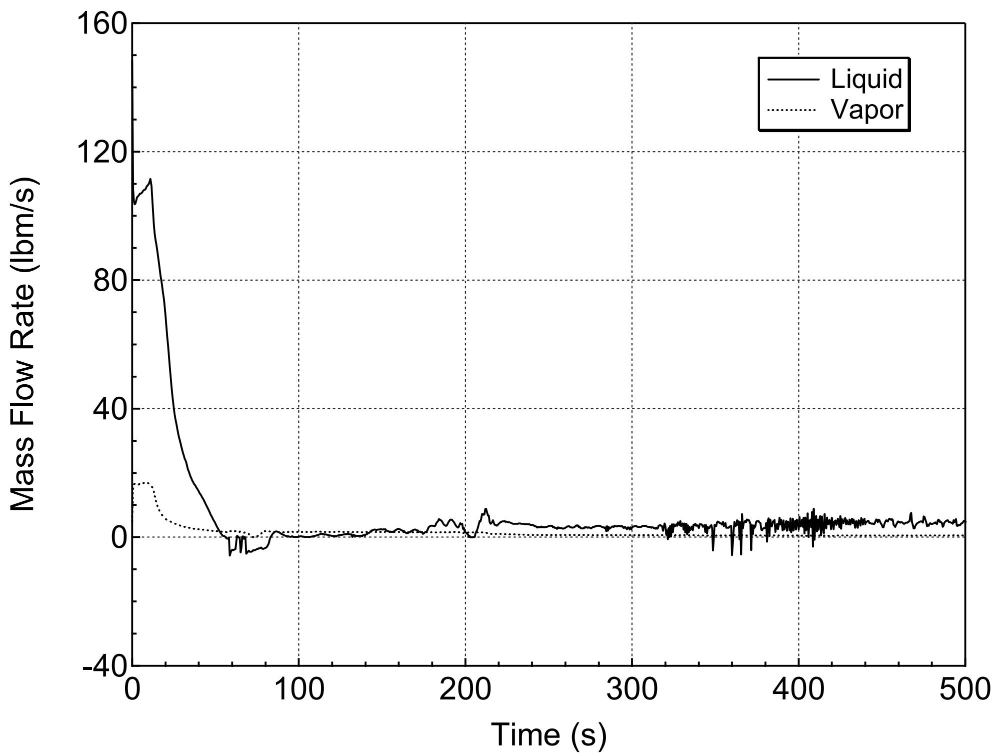

Figure 5.2.j-9 Hot Assembly Exit Vapor and Liquid Mass Flowrates for 10-inch Break (Bottom) (Spectrum Analysis)

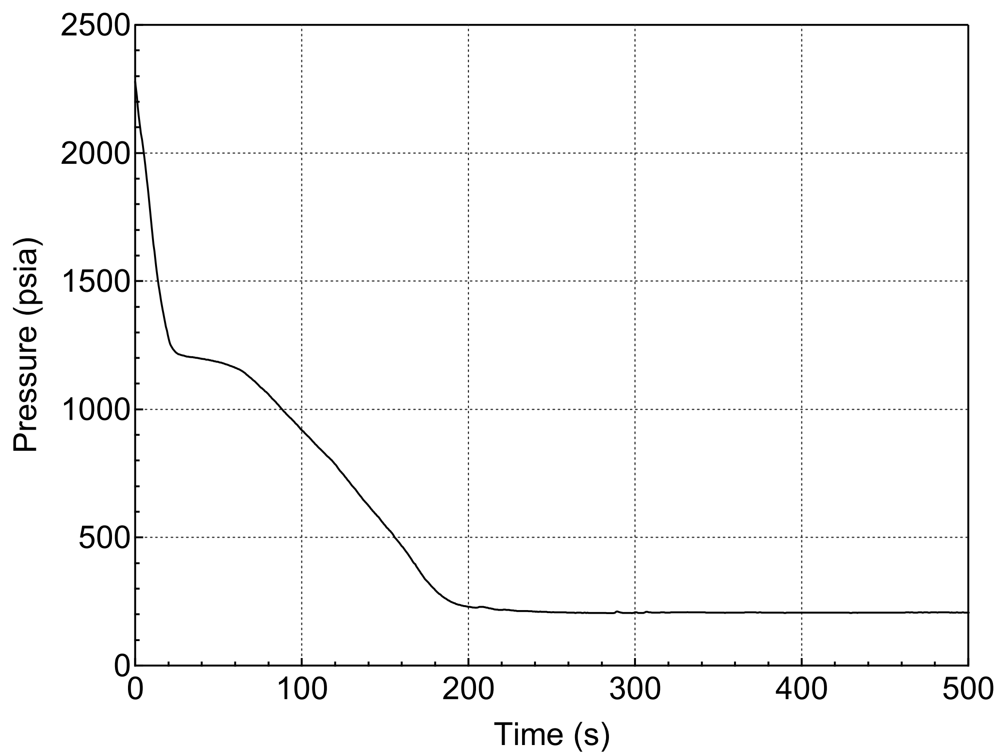

Figure 5.2.k-1 RCS (Pressurizer) Pressure Transient for 11-inch Break (Bottom) (Spectrum Analysis)

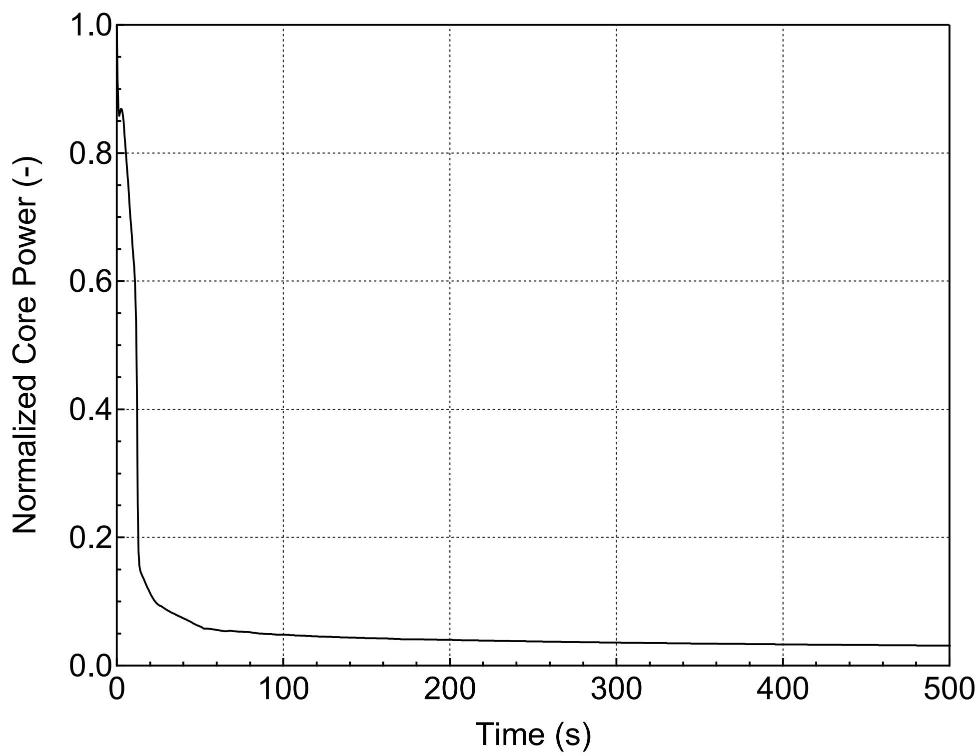

Figure 5.2.k-2 Normalized Core Power for 11-inch Break (Bottom) (Spectrum Analysis)

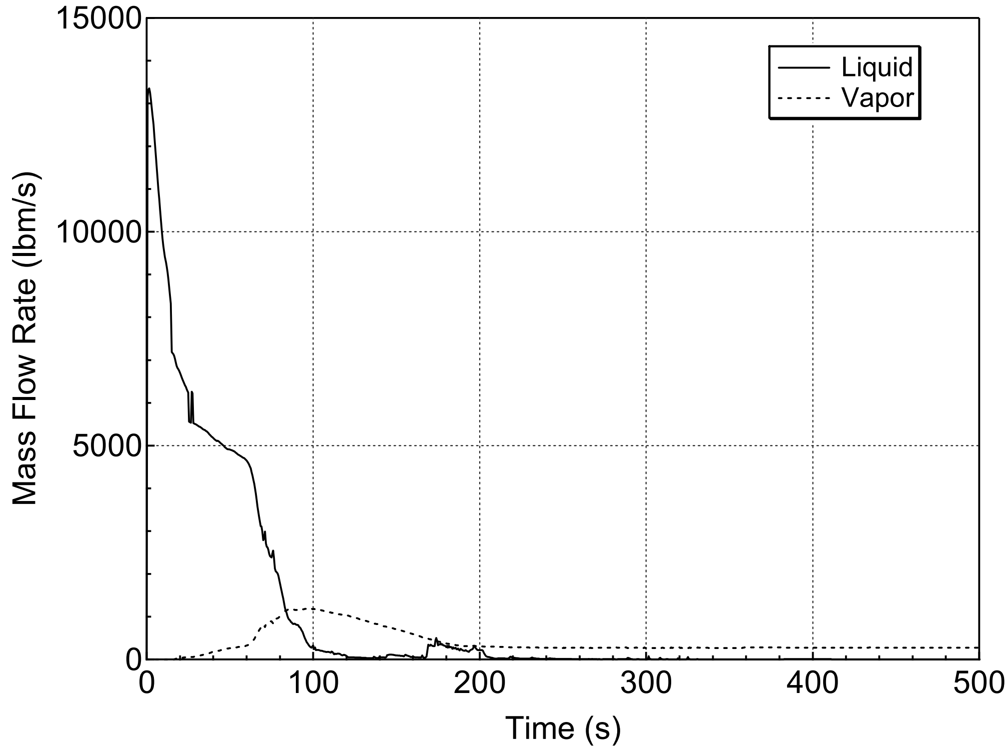

Figure 5.2.k-3 Liquid and Vapor Discharges through the Break for 11-inch Break (Bottom) (Spectrum Analysis)

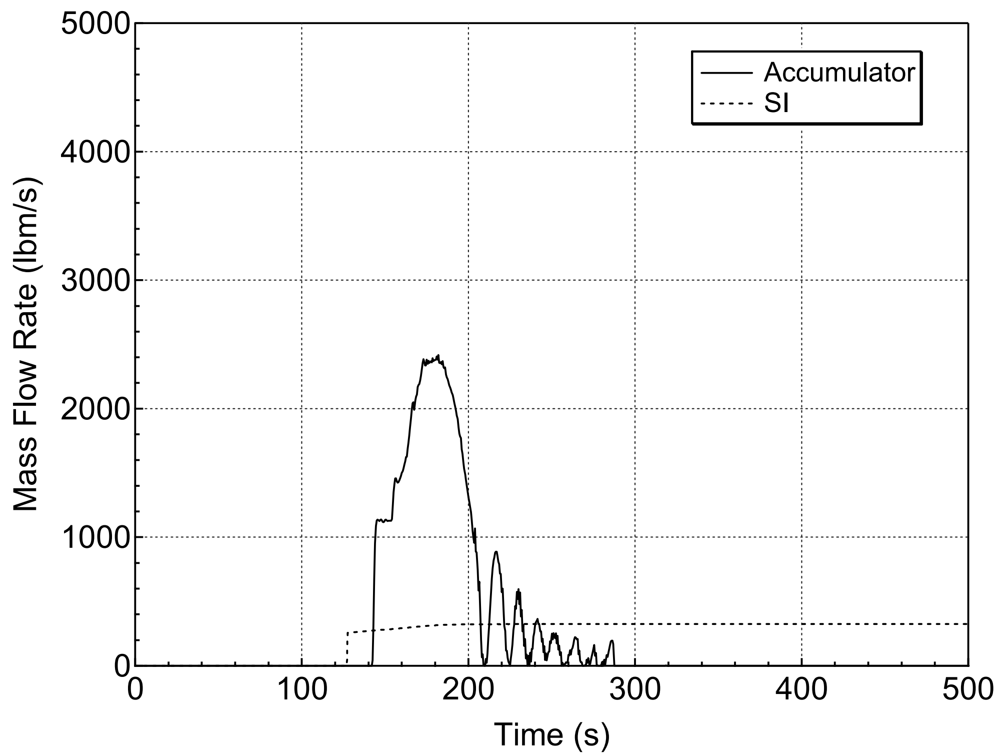

Figure 5.2.k-4 Accumulator and Safety Injection Mass Flowrates for 11-inch Break (Bottom) (Spectrum Analysis)

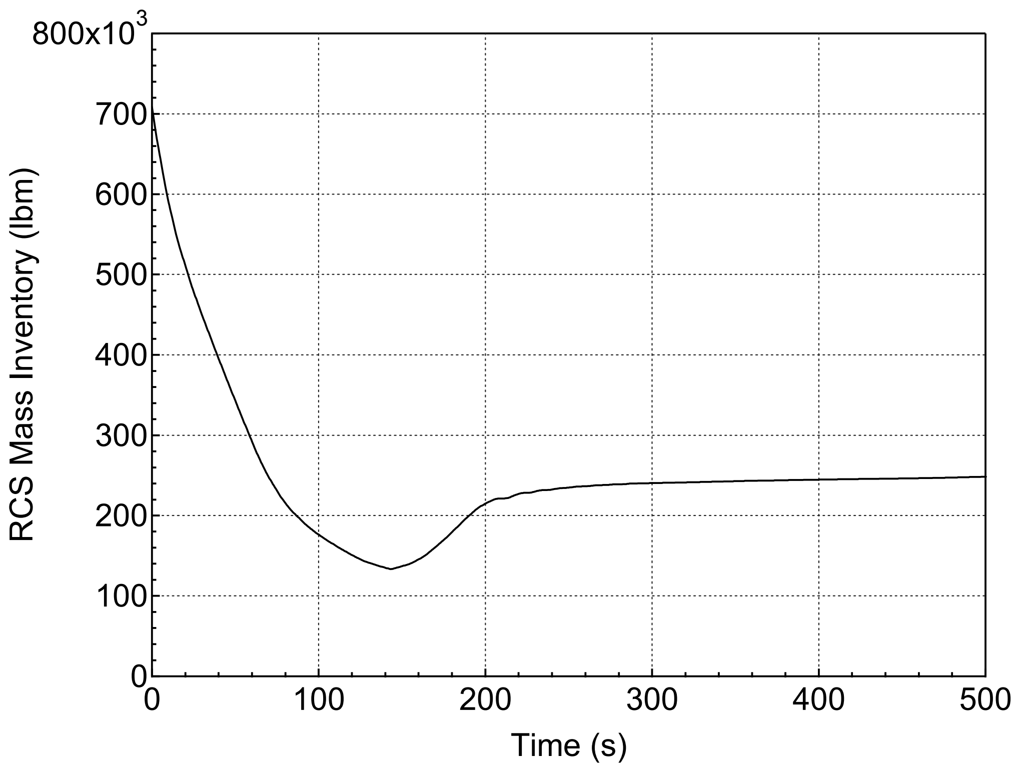

Figure 5.2.k-5 RCS Mass Inventory for 11-inch Break (Bottom) (Spectrum Analysis)

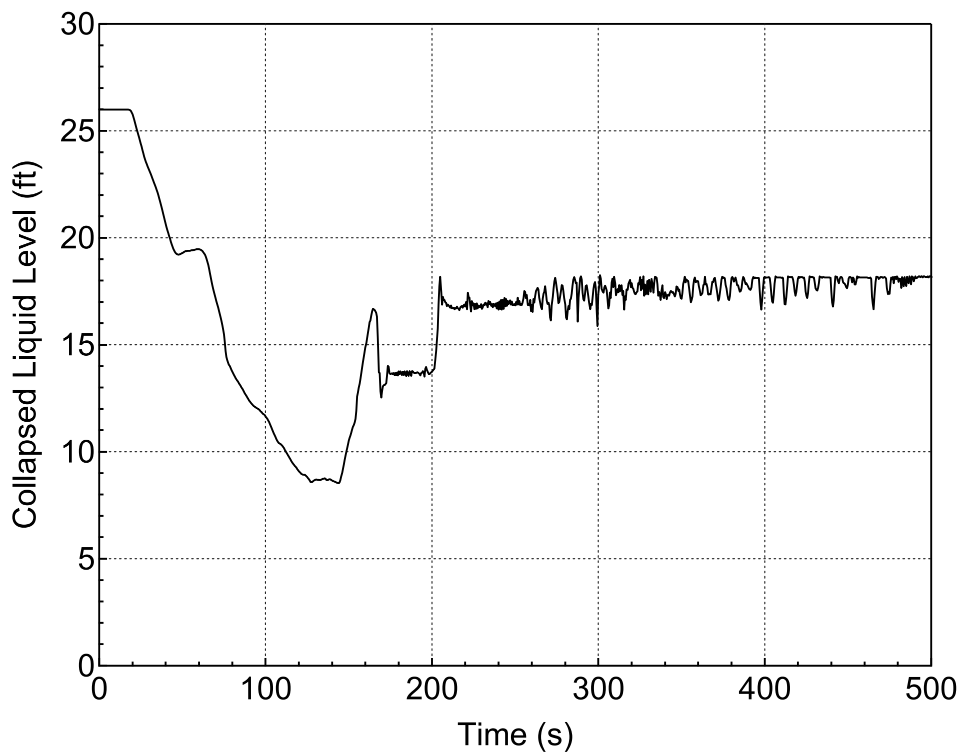

Figure 5.2.k-6 Downcomer Collapsed Level for 11-inch Break (Bottom) (Spectrum Analysis)

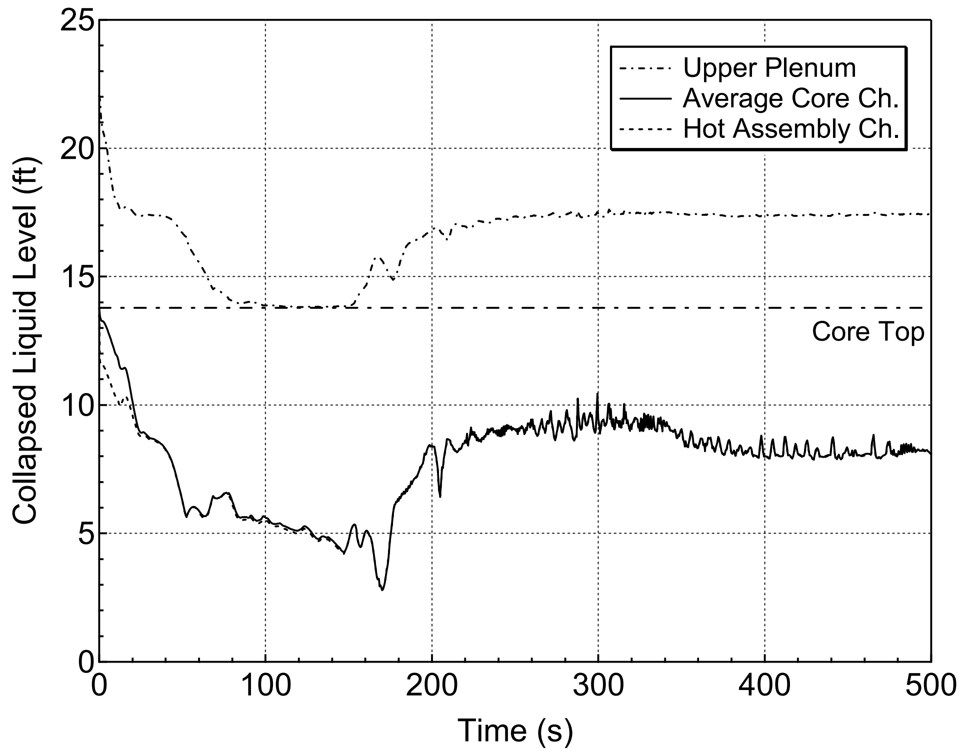

Figure 5.2.k-7 Core and Upper Plenum Collapsed Levels for 11-inch Break (Bottom) (Spectrum Analysis)

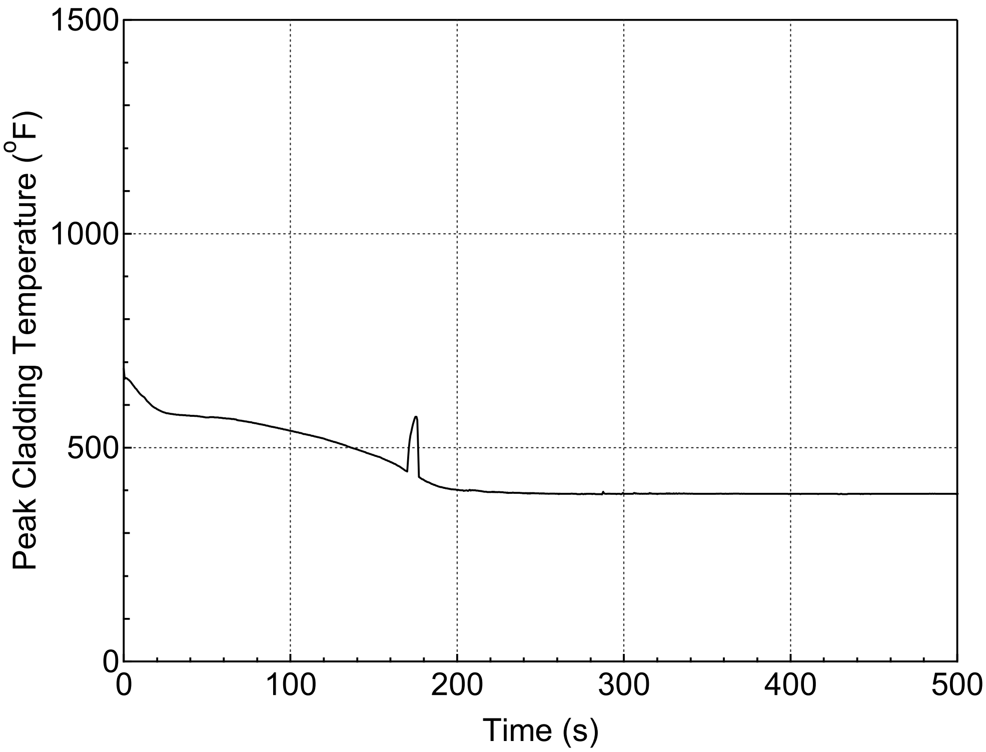

Figure 5.2.k-8 PCT at All Elevations for Hot Rod in Hot Assembly for 11-inch Break (Bottom) (Spectrum Analysis)

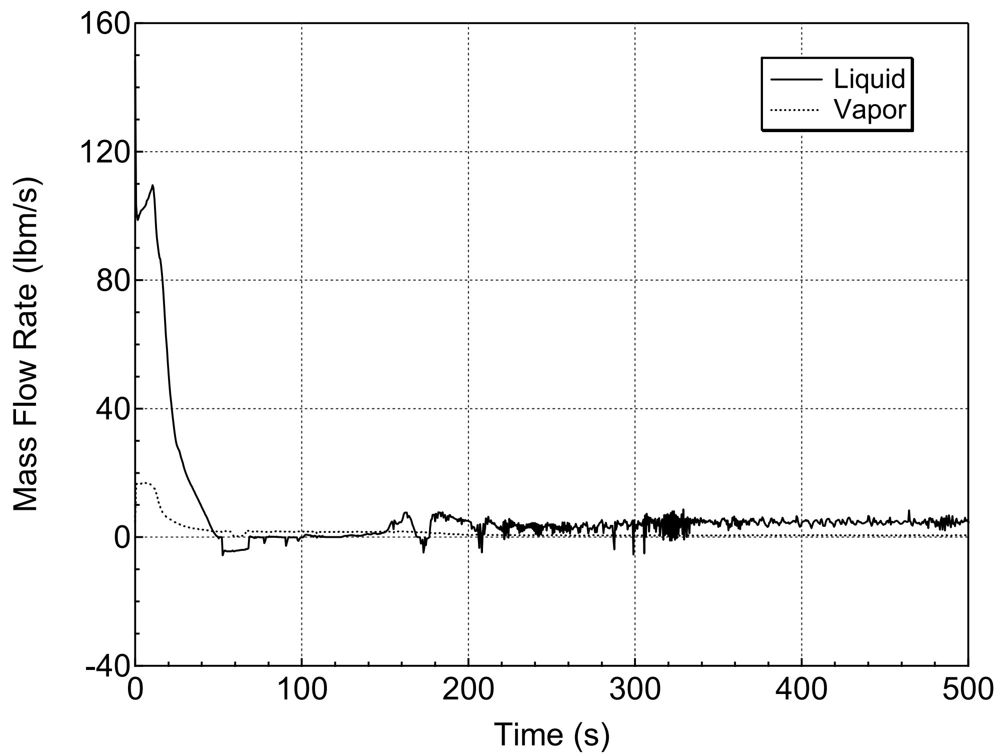

Figure 5.2.k-9 Hot Assembly Exit Vapor and Liquid Mass Flowrates for 11-inch Break (Bottom) (Spectrum Analysis)

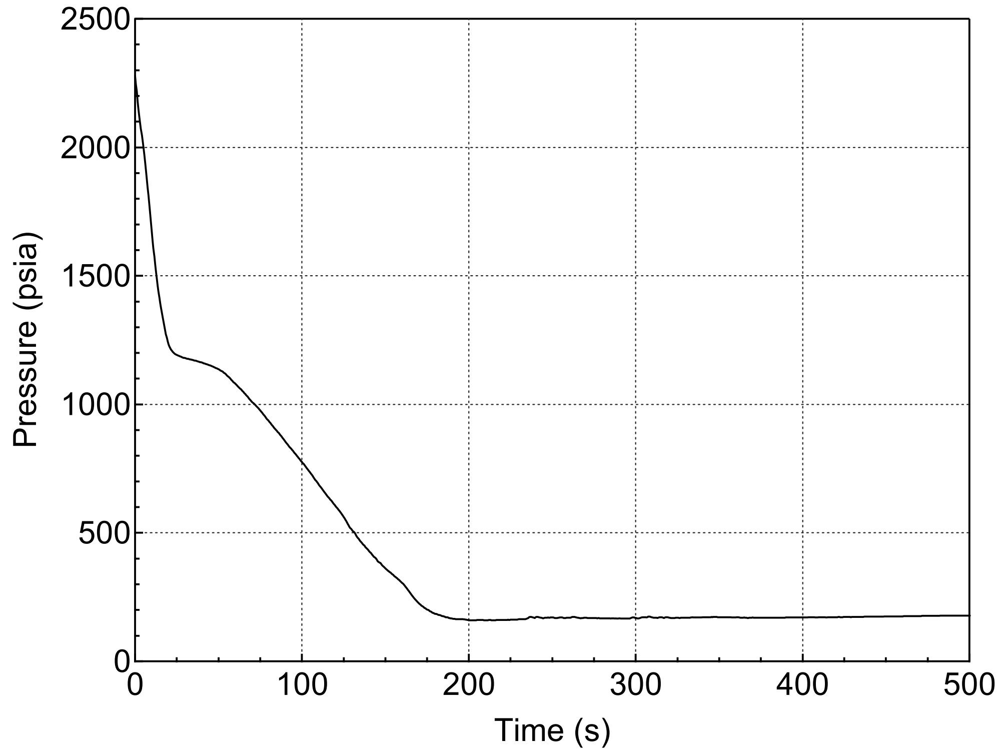

Figure 5.2.I-1 RCS (Pressurizer) Pressure Transient for 12-inch Break (Bottom) (Spectrum Analysis)

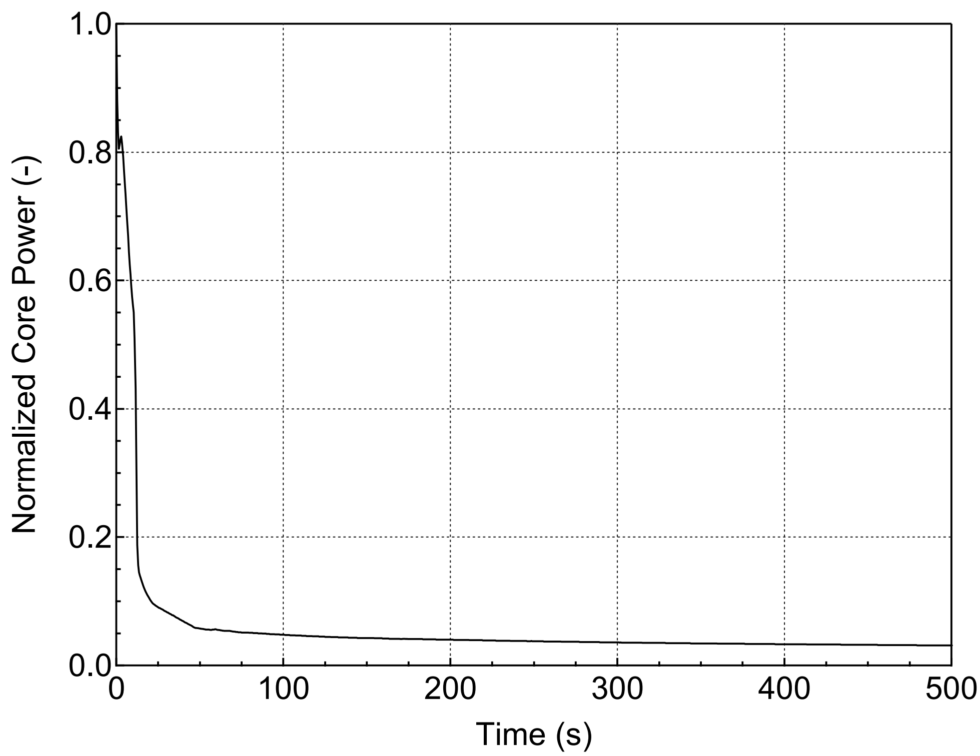

Figure 5.2.I-2 Normalized Core Power for 12-inch Break (Bottom) (Spectrum Analysis)

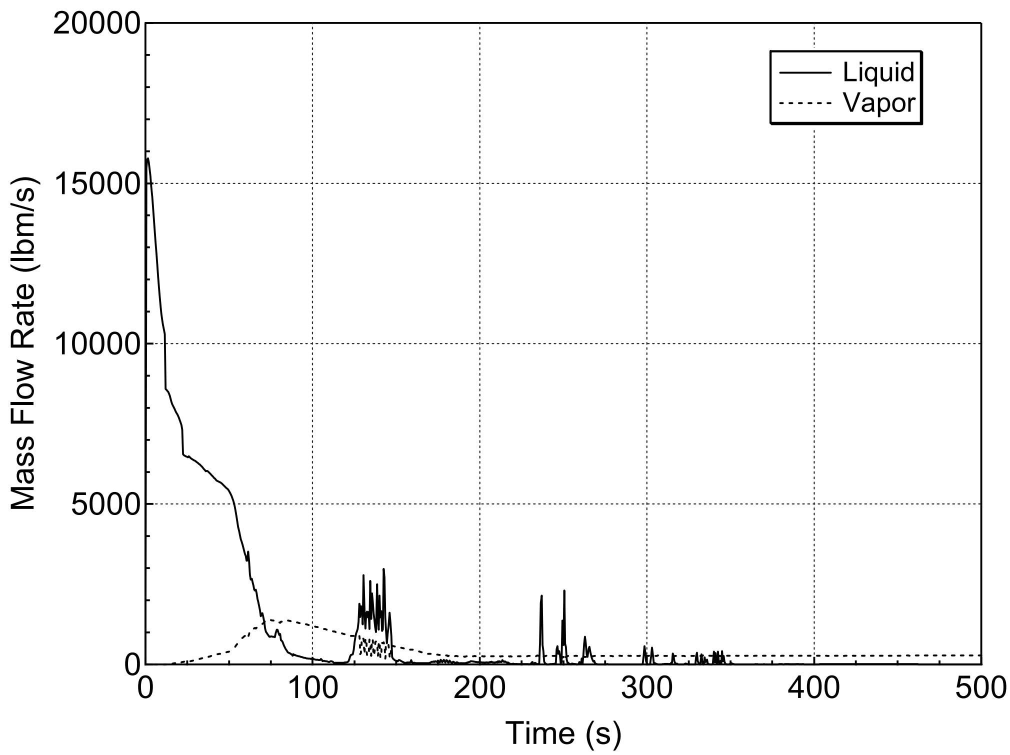

Figure 5.2.I-3 Liquid and Vapor Discharges through the Break for 12-inch Break (Bottom) (Spectrum Analysis)

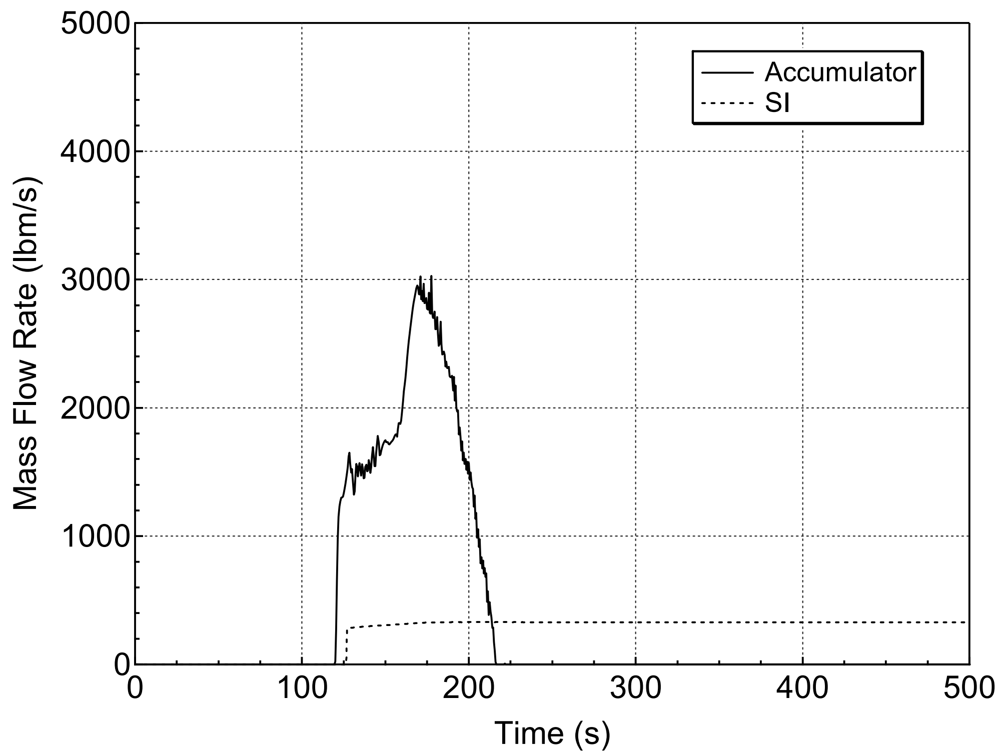

Figure 5.2.I-4 Accumulator and Safety Injection Mass Flowrates for 12-inch Break (Bottom) (Spectrum Analysis)

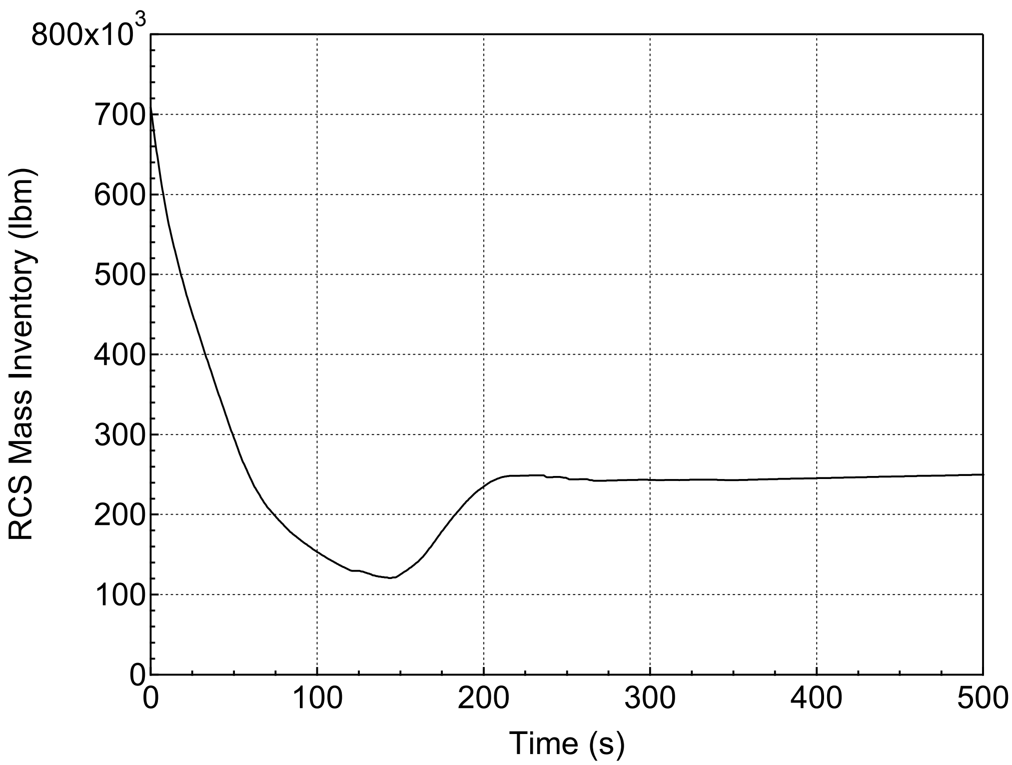

Figure 5.2.I-5 RCS Mass Inventory for 12-inch Break (Bottom) (Spectrum Analysis)

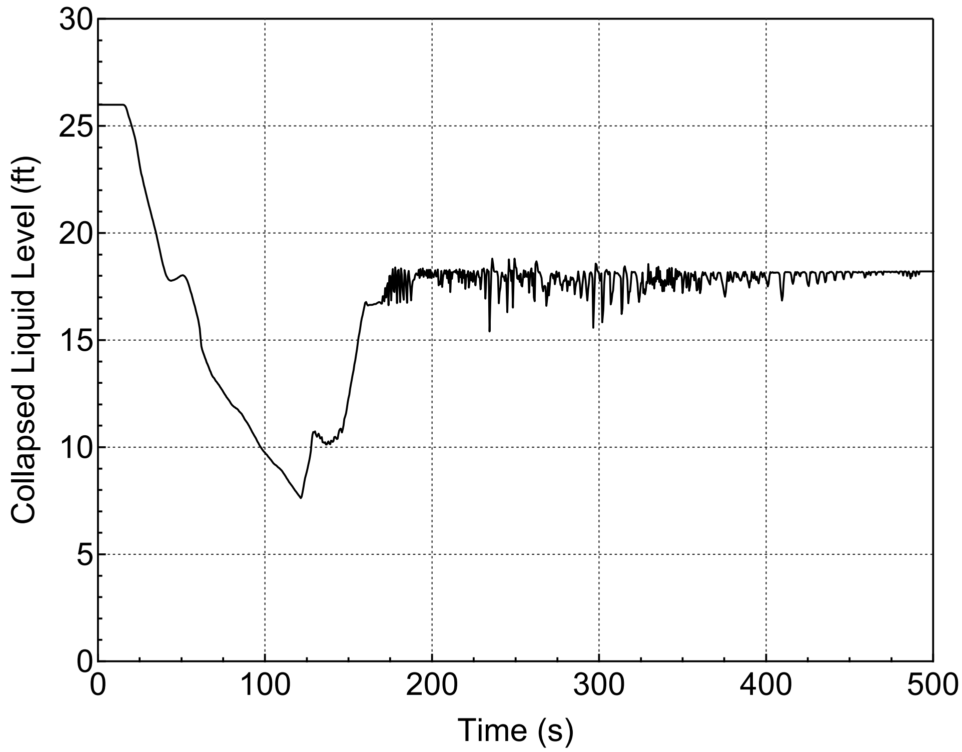

Figure 5.2.I-6 Downcomer Collapsed Level for 12-inch Break (Bottom) (Spectrum Analysis)

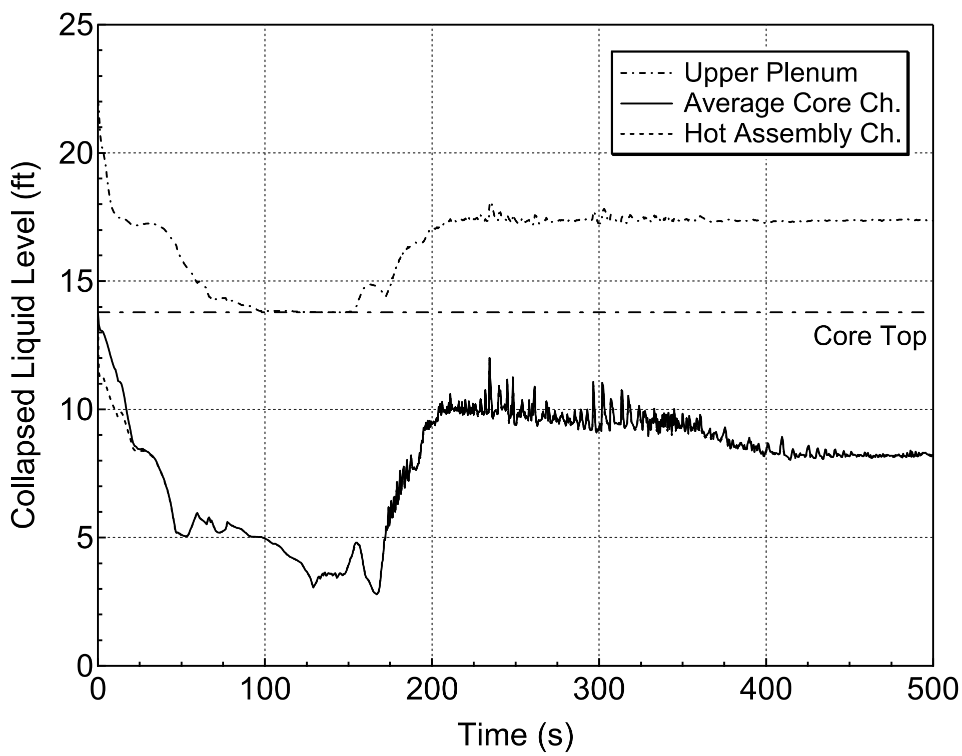

Figure 5.2.I-7 Core and Upper Plenum Collapsed Levels for 12-inch Break (Bottom) (Spectrum Analysis)

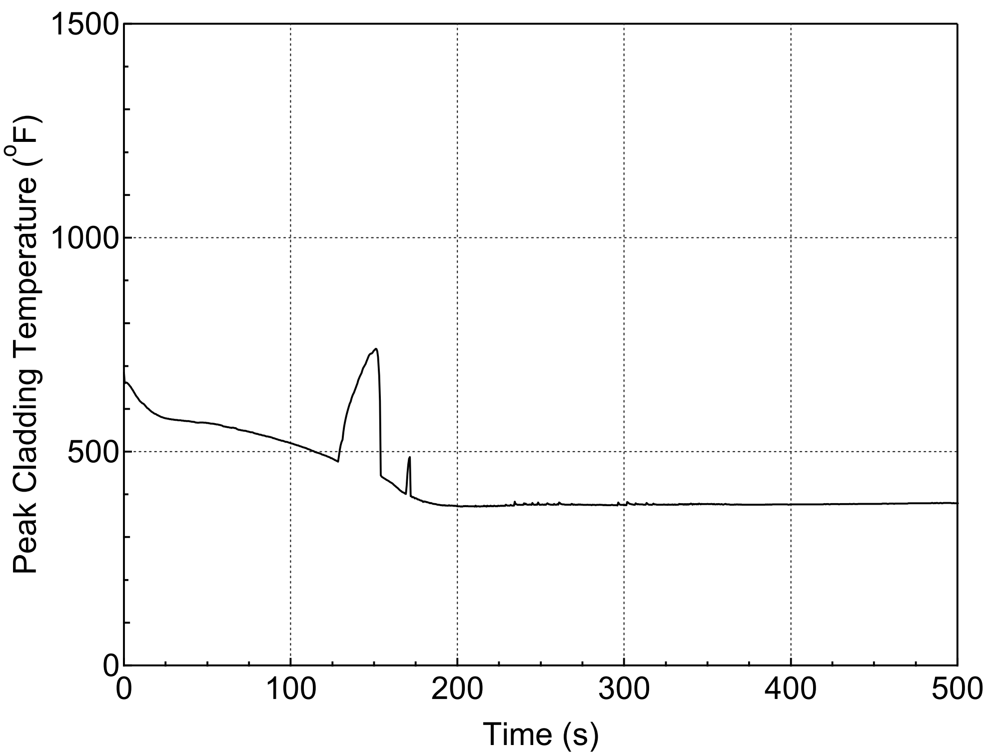

Figure 5.2.I-8 PCT at All Elevations for Hot Rod in Hot Assembly for 12-inch Break (Bottom) (Spectrum Analysis)

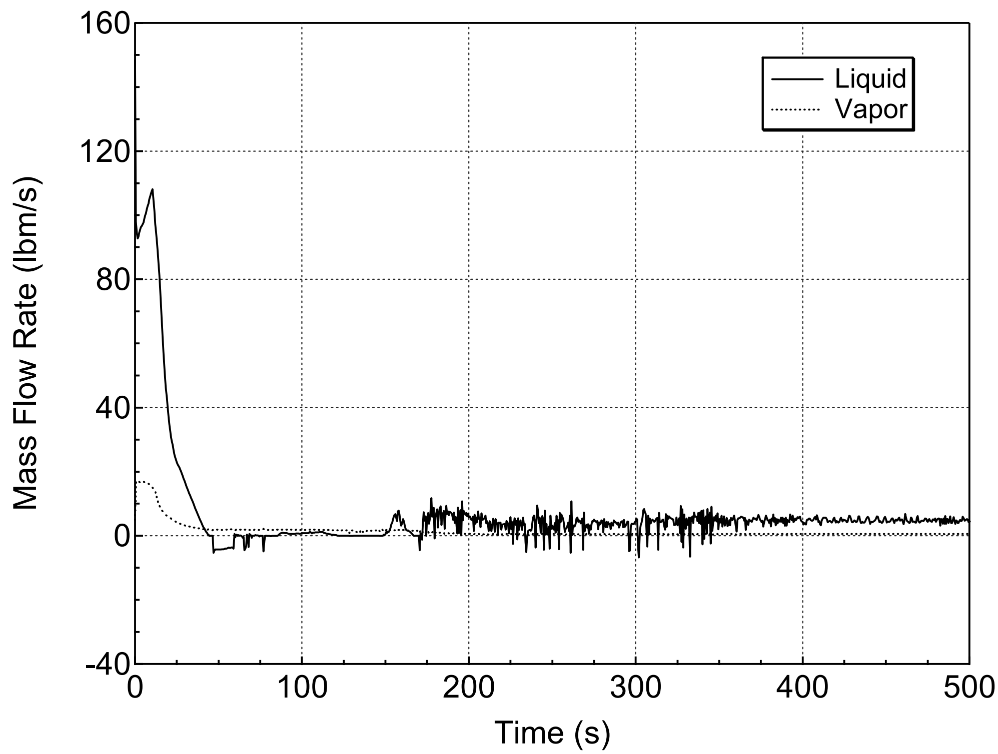

Figure 5.2.I-9 Hot Assembly Exit Vapor and Liquid Mass Flowrates for 12-inch Break (Bottom) (Spectrum Analysis)

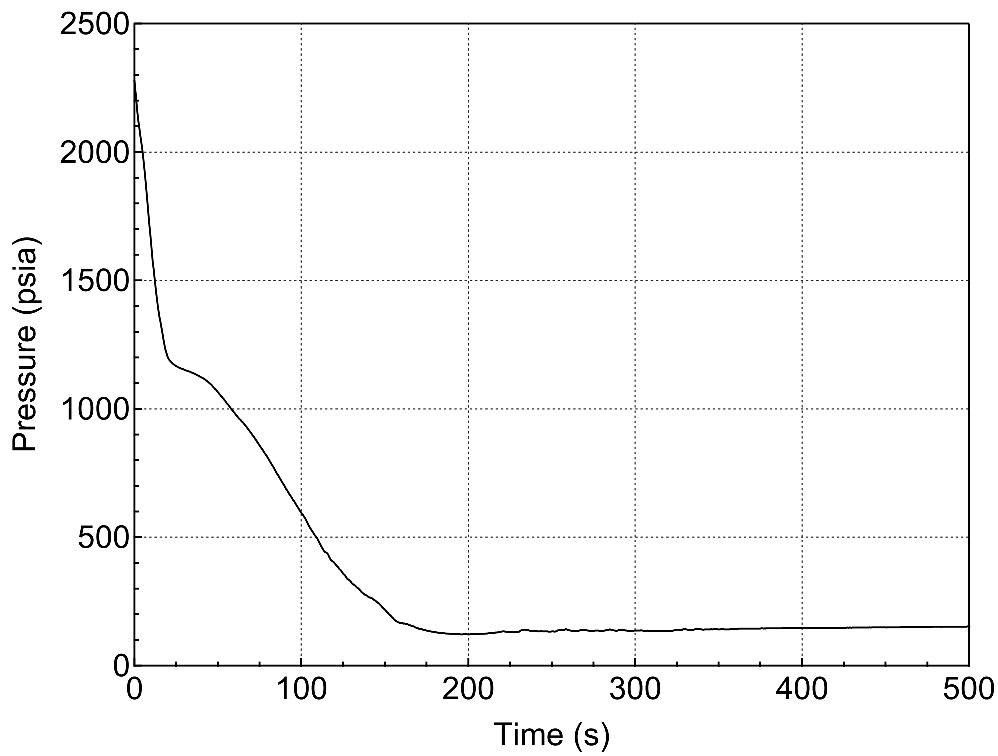

Figure 5.2.m-1 RCS (Pressurizer) Pressure Transient for 13-inch Break (Bottom) (Spectrum Analysis)

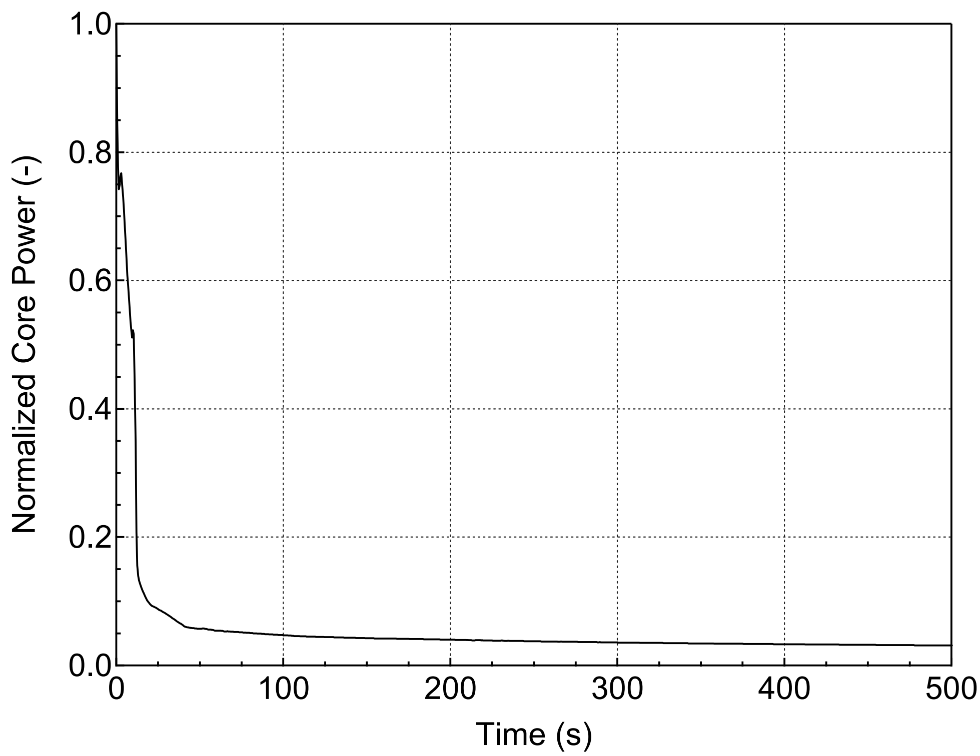

Figure 5.2.m-2 Normalized Core Power for 13-inch Break (Bottom) (Spectrum Analysis)

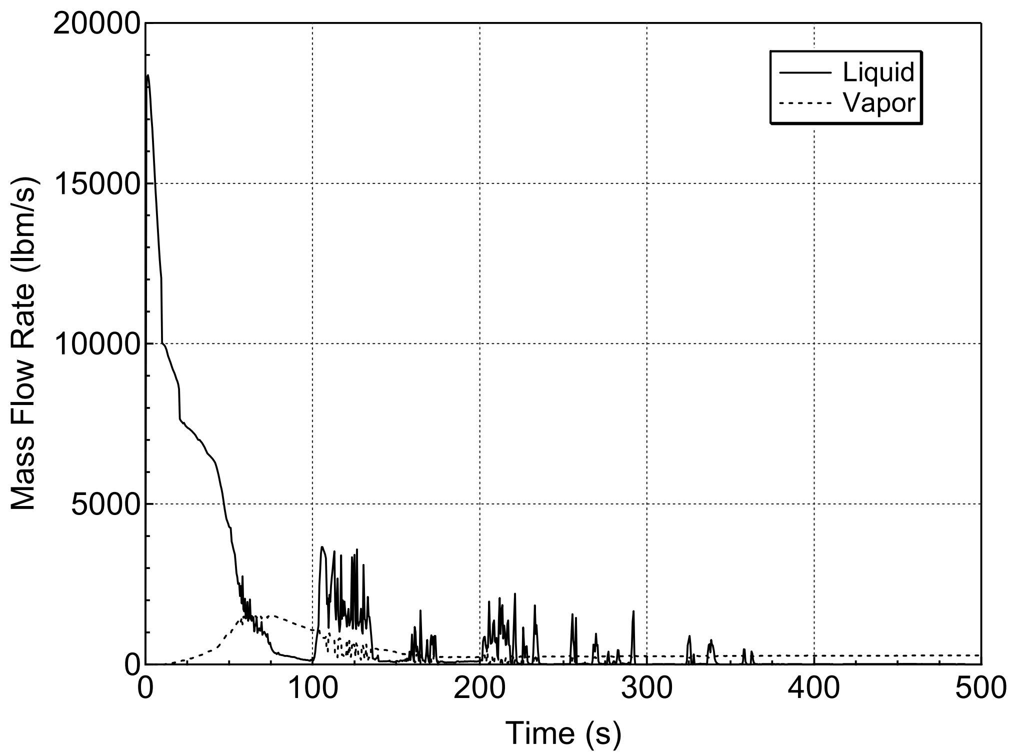

Figure 5.2.m-3 Liquid and Vapor Discharges through the Break for 13-inch Break (Bottom) (Spectrum Analysis)

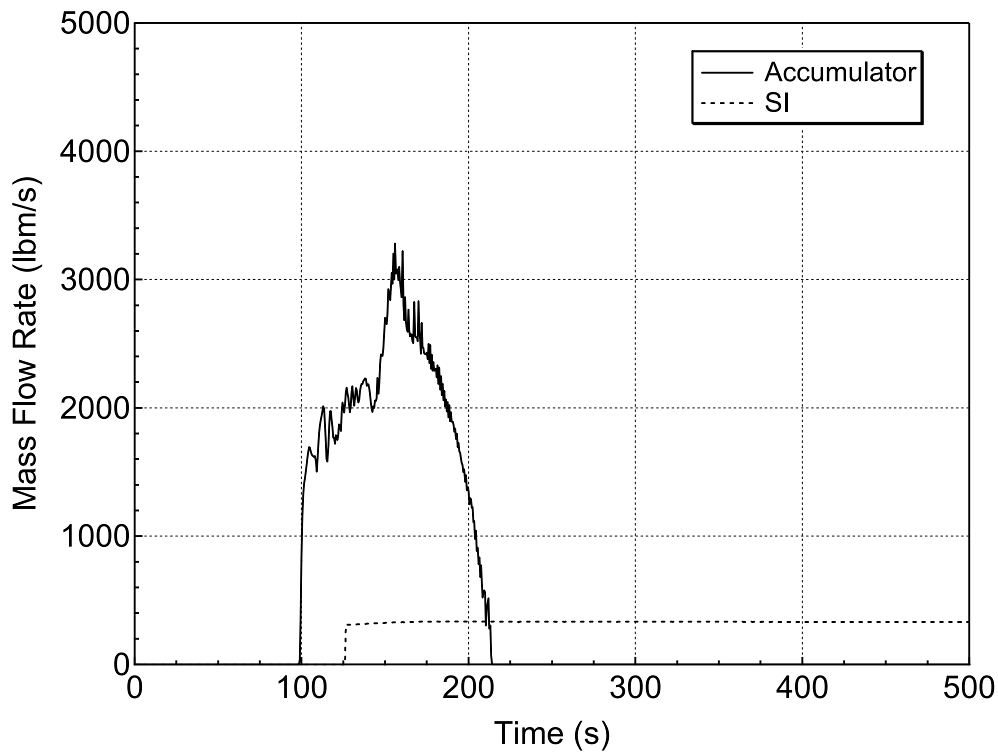

Figure 5.2.m-4 Accumulator and Safety Injection Mass Flowrates for 13-inch Break (Bottom) (Spectrum Analysis)

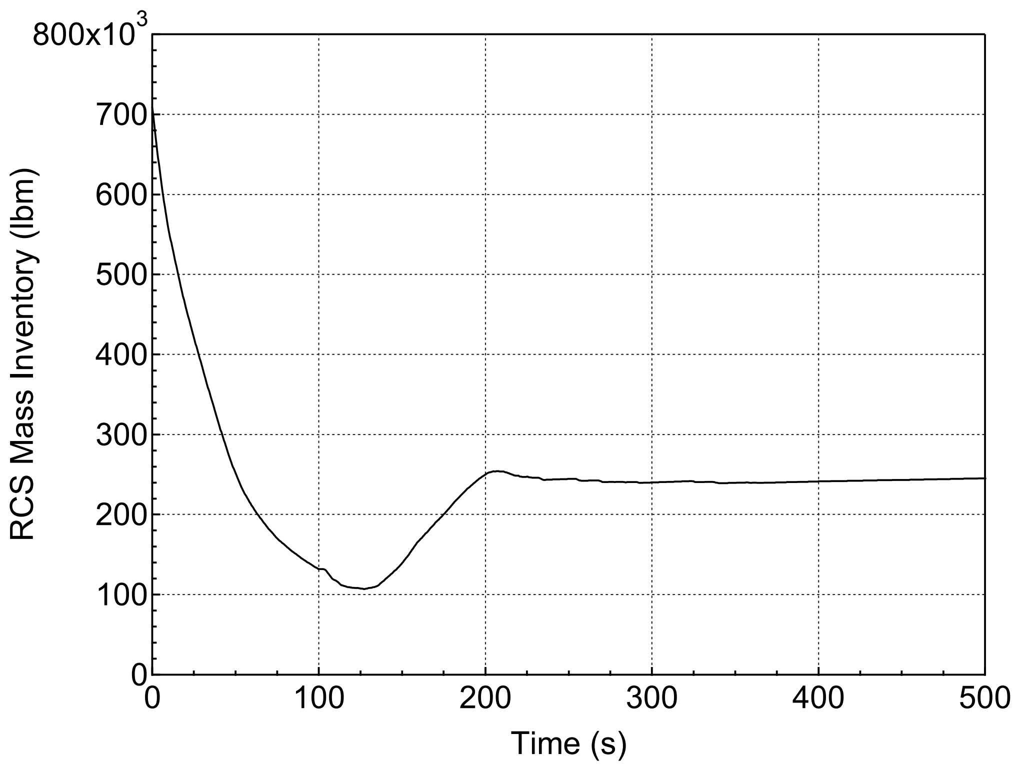

Figure 5.2.m-5 RCS Mass Inventory for 13-inch Break (Bottom) (Spectrum Analysis)

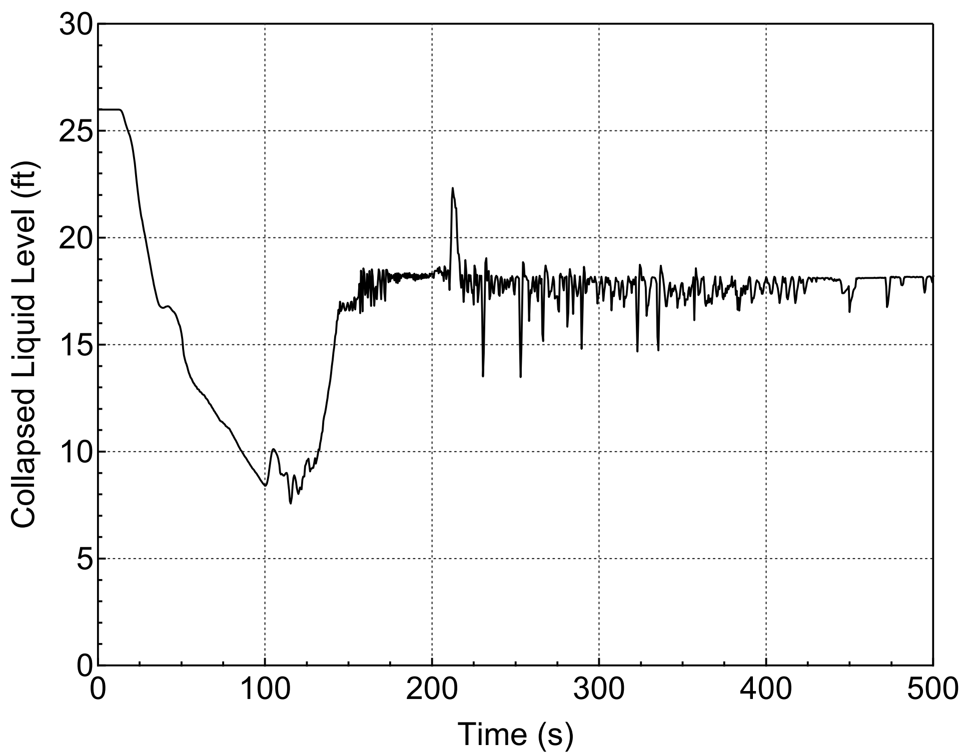

Figure 5.2.m-6 Downcomer Collapsed Level for 13-inch Break (Bottom) (Spectrum Analysis)

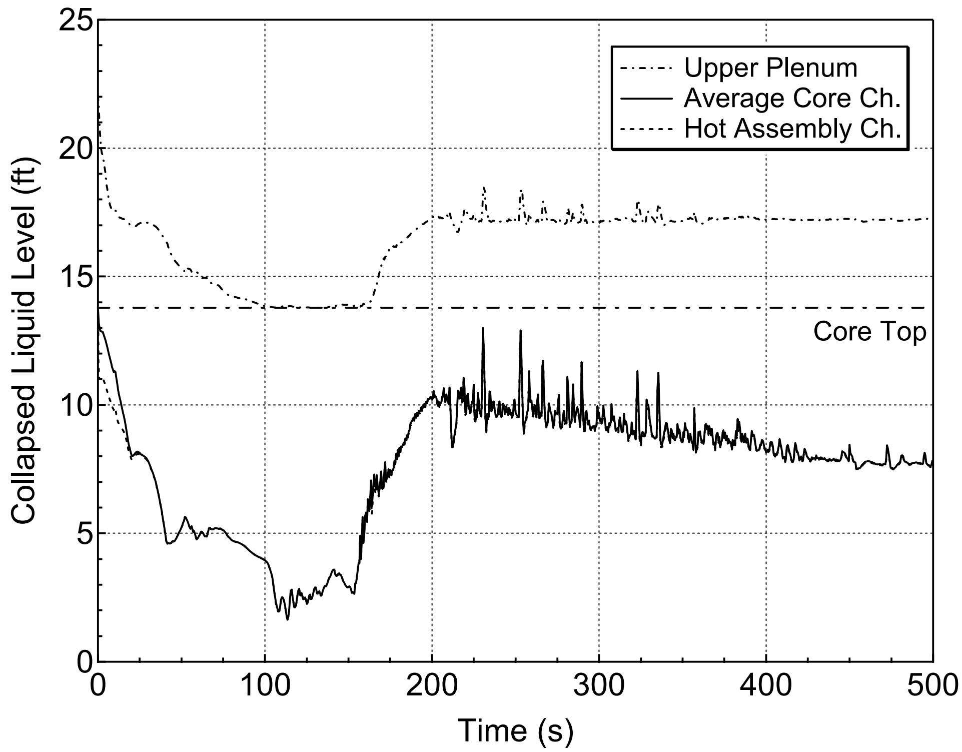

Figure 5.2.m-7 Core and Upper Plenum Collapsed Levels for 13-inch Break (Bottom) (Spectrum Analysis)

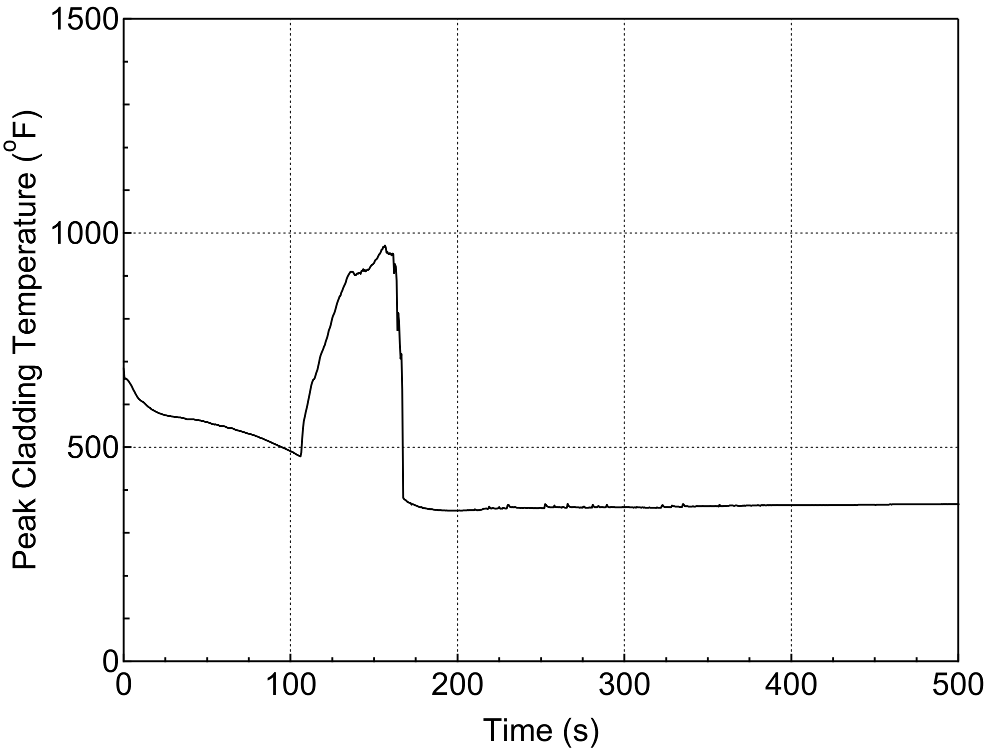

Figure 5.2.m-8 PCT at All Elevations for Hot Rod in Hot Assembly for 13-inch Break (Bottom) (Spectrum Analysis)

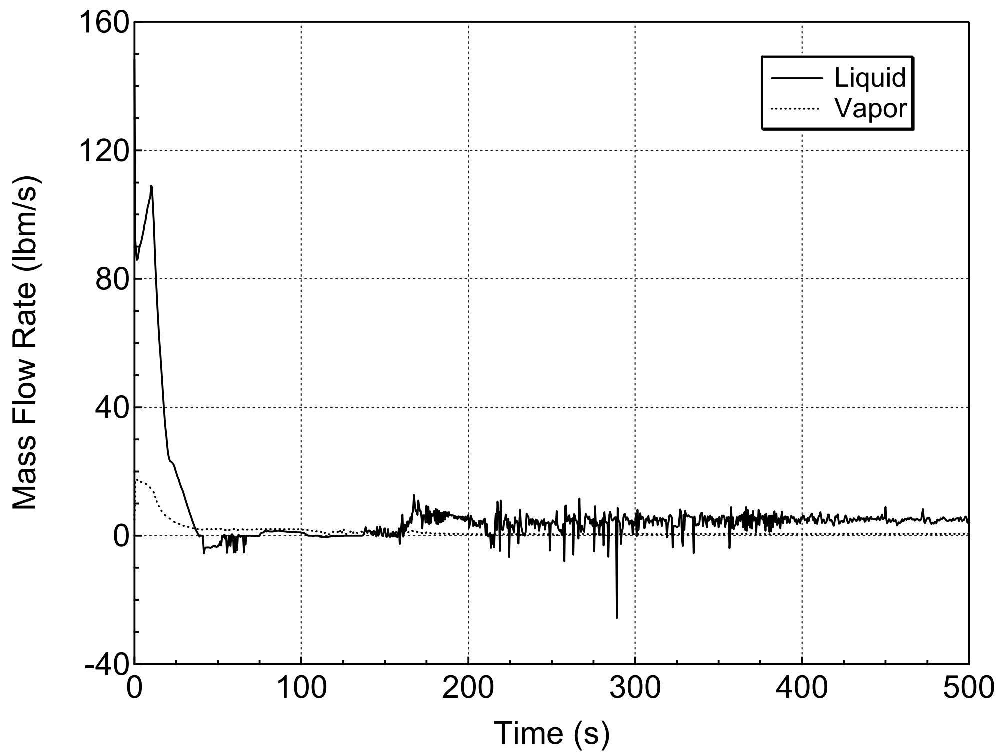

Figure 5.2.m-9 Hot Assembly Exit Vapor and Liquid Mass Flowrates for 13-inch Break (Bottom) (Spectrum Analysis)

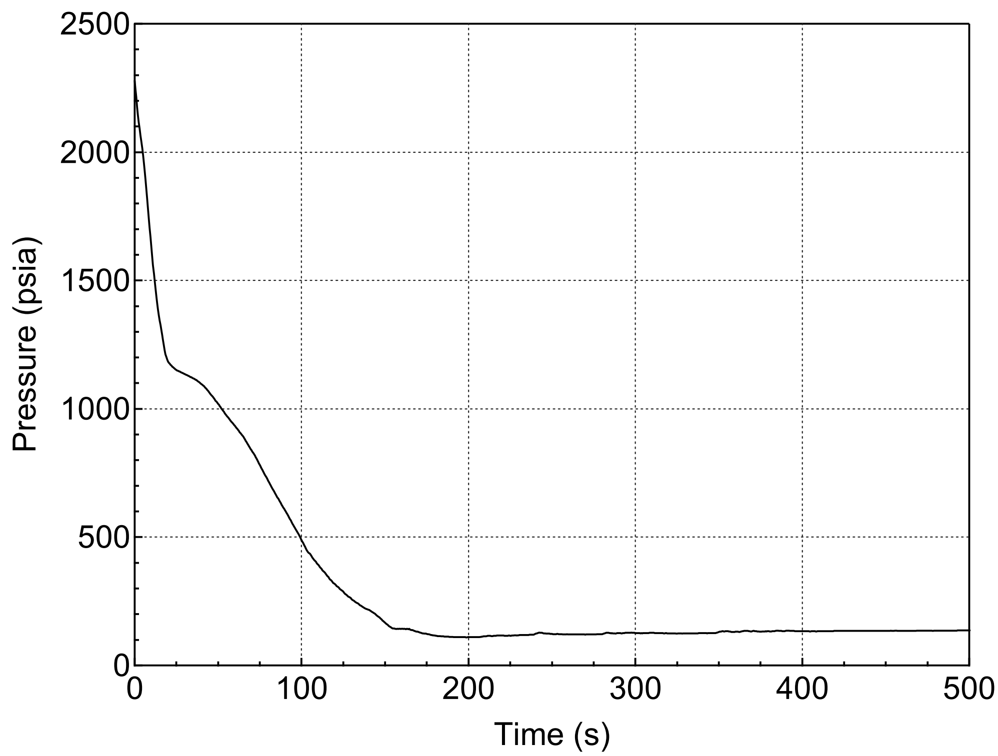

Figure 5.2.n-1 RCS (Pressurizer) Pressure Transient for 1-ft^2 Break (Bottom) (Spectrum Analysis)

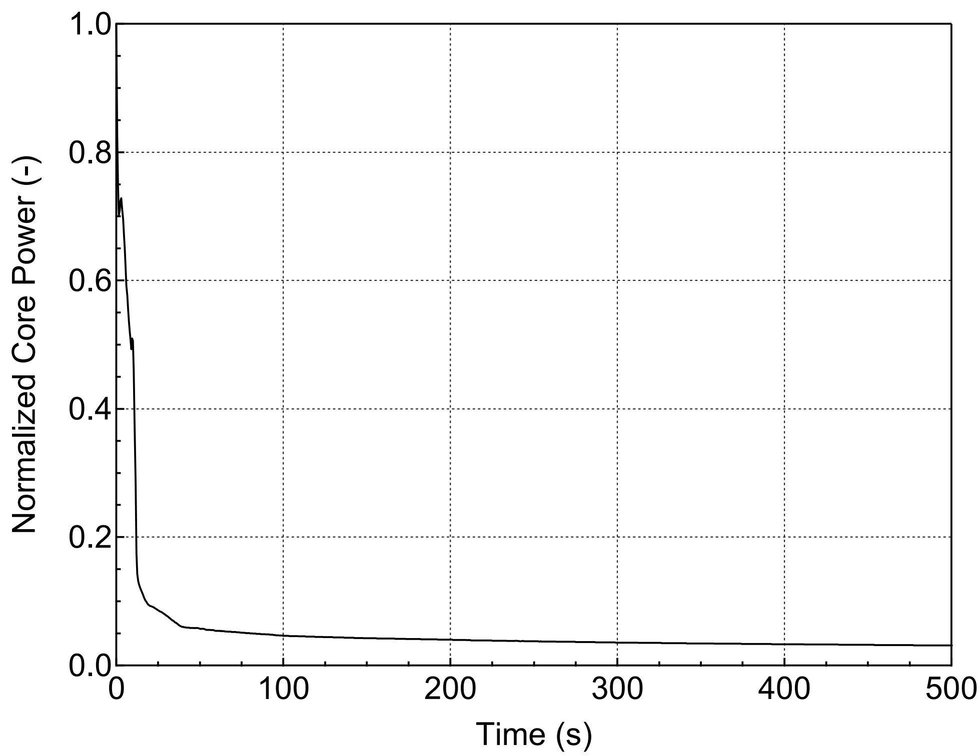

Figure 5.2.n-2 Normalized Core Power for 1-ft^2 Break (Bottom) (Spectrum Analysis)

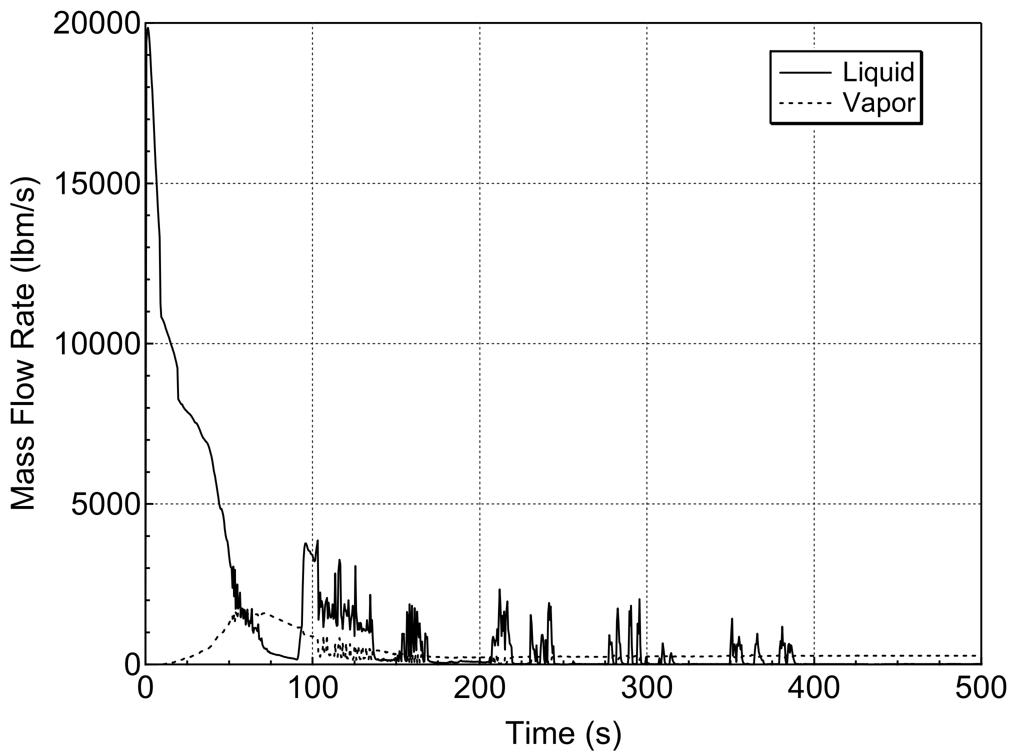

Figure 5.2.n-3 Liquid and Vapor Discharges through the Break for 1-ft^2 Break (Bottom) (Spectrum Analysis)

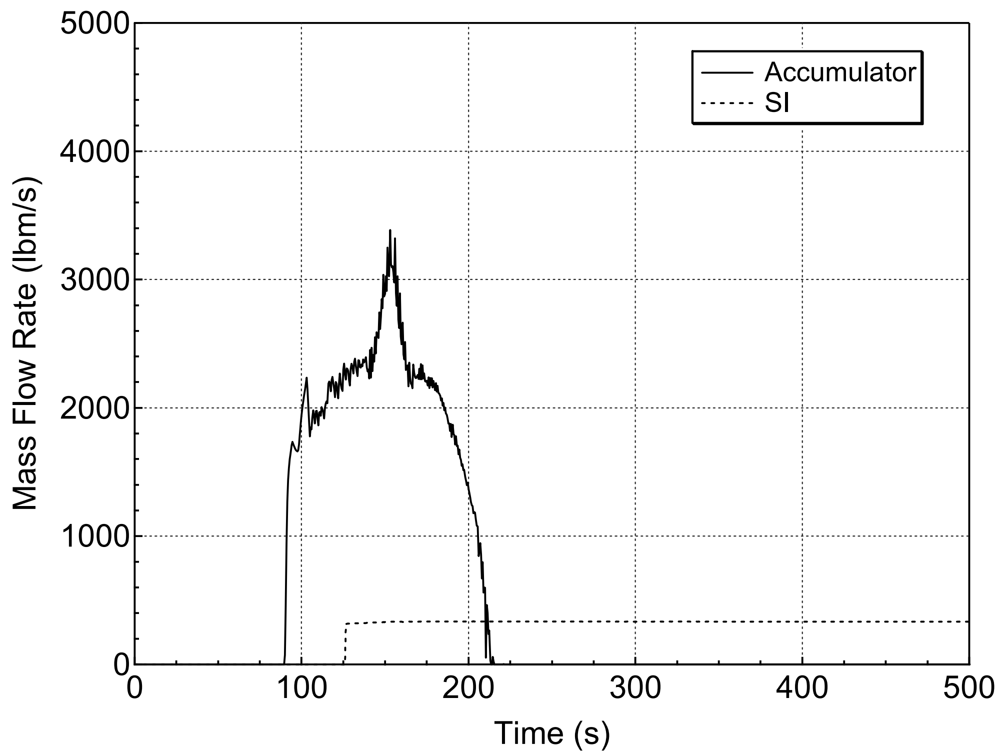

Figure 5.2.n-4 Accumulator and Safety Injection Mass Flowrates for 1-ft^2 Break (Bottom) (Spectrum Analysis)

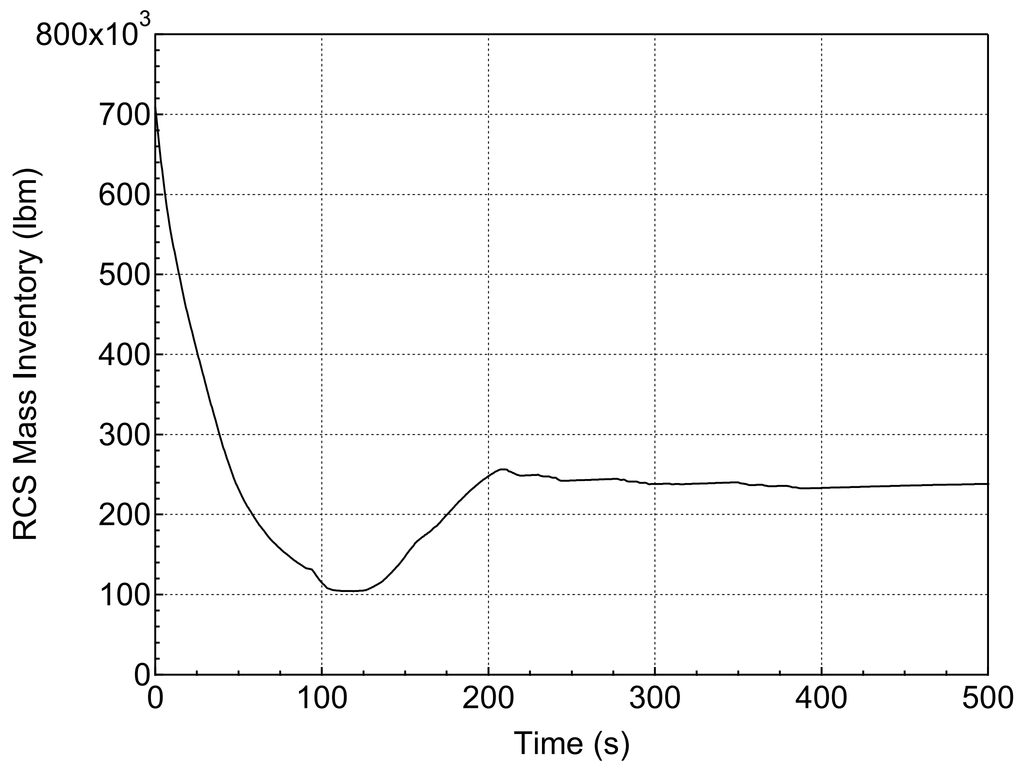

Figure 5.2.n-5 RCS Mass Inventory for 1-ft^2 Break (Bottom) (Spectrum Analysis)

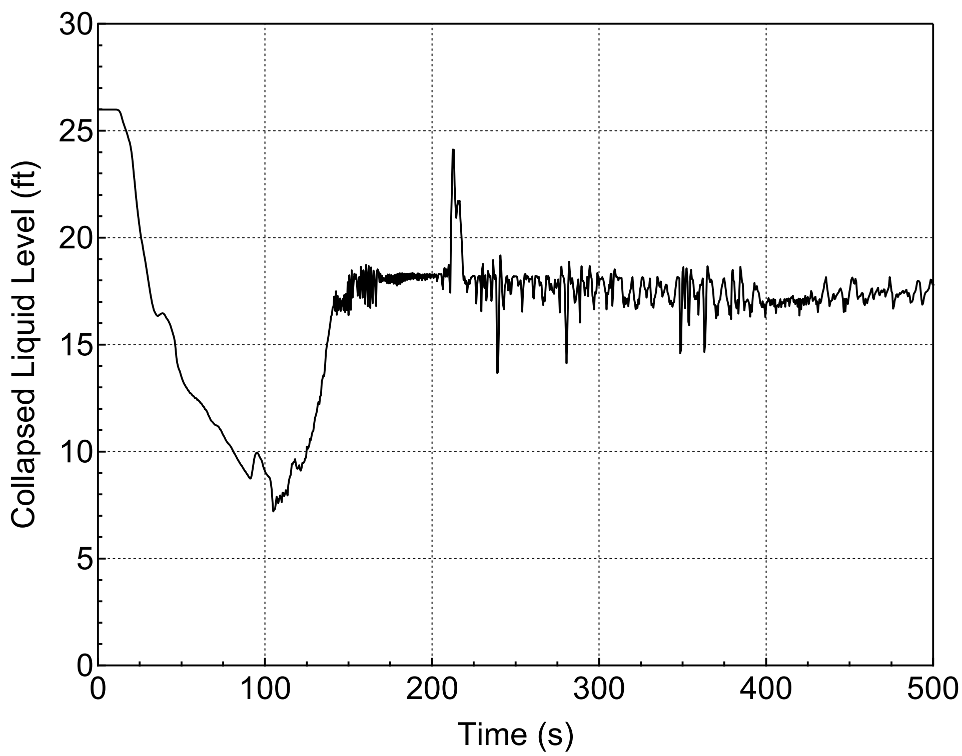

Figure 5.2.n-6 Downcomer Collapsed Level for 1-ft^2 Break (Bottom) (Spectrum Analysis)

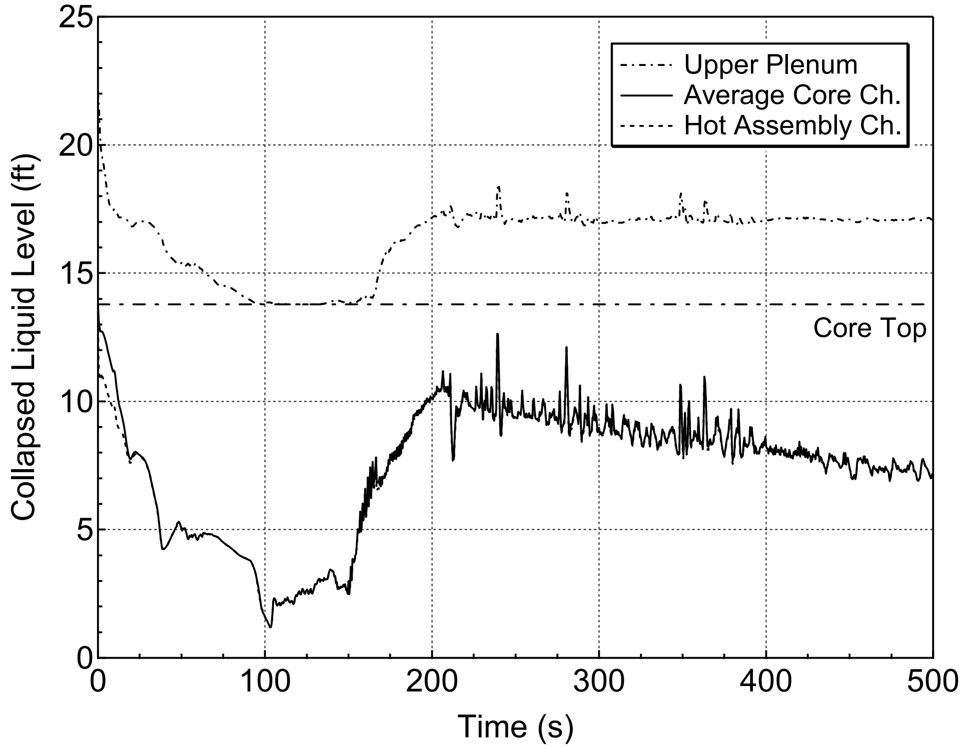

Figure 5.2.n-7 Core and Upper Plenum Collapsed Levels for 1-ft^2 Break (Bottom) (Spectrum Analysis)

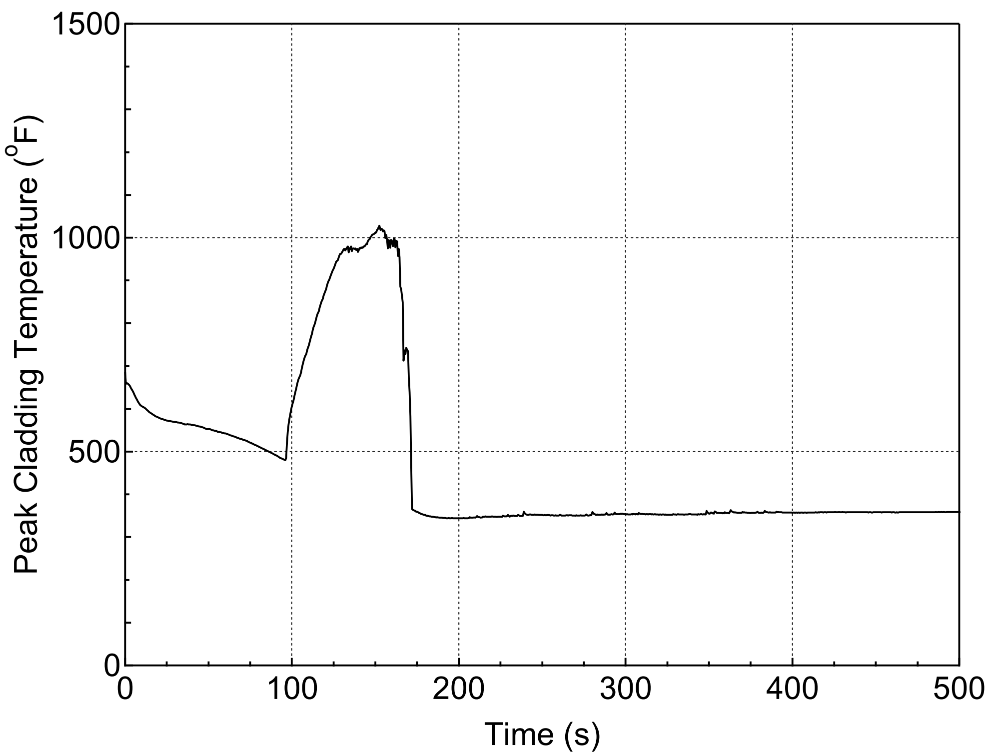

Figure 5.2.n-8 PCT at All Elevations for Hot Rod in Hot Assembly for 1-ft^2 Break (Bottom) (Spectrum Analysis)

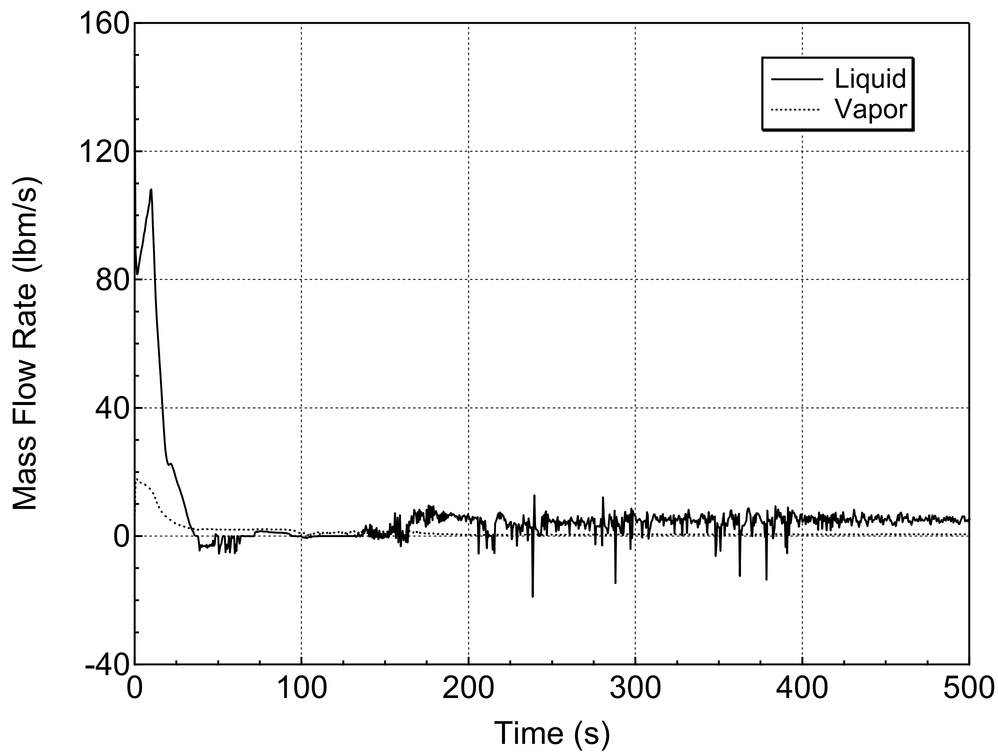

Figure 5.2.n-9 Hot Assembly Exit Vapor and Liquid Mass Flowrates for 1-ft² Break (Bottom) (Spectrum Analysis)

5.3 Break Orientation Sensitivity Study

Additional break spectrum analyses with 0.5 inch increment were performed to determine the final limiting break size for loop-seal PCT and boil-off PCT. In these sensitivity calculations, the effects of break orientations (bottom, top, side, and homogeneous) were also considered.

5.3.1 Loop-seal-PCT

Five break size cases (6 inch, 6.5 inch, 7 inch, 7.5 inch, and 8 inch break) were calculated with break orientations of bottom, top, and side breaks, and homogeneous break flow. Figure 5.3.1.a-1 through 5.3.1.e-18 show the main plots and Table 5.3.1-1 summarizes the PCT results for all cases. The highest PCT is 775°F for 7.5 inch break of top break. Table 5.3.1-2 shows the sequence of events and Table 5.3.1-3 shows the main results for this case and the results of this case is explained below in detail.

Figure 5.3.1.d-10 shows the RCS (Pressurizer) pressure transient for the 7.5-inch cold leg top orientation break. As a result of the break, the coolant of RCS is rapidly lost. The RCS pressure initially decreases rapidly from 2280 psia to about 1300 psia, keeps steady at this pressure for about 60 seconds, then gradually decreases at a constant slope to about 500 psia. The coolant from the pressurizer flows into the loops, hence the pressurizer level decreases. When the low pressurizer pressure setpoint of 1860 psia is reached, a reactor trip signal is generated.

Figure 5.3.1.d-11 displays the normalized core power transient following the break. The reactor trips at 9.3 seconds due to the low pressurizer pressure setpoint of 1860 psia. Then, the control rod insertion starts at 11 seconds resulting in the decrease of the core power.

Figure 5.3.1.d-12 presents the liquid and vapor discharges through the break. In the first 120 seconds, the discharge flow is single-phase liquid that gradually diminishing. Thereafter, the flow in the cold leg is stratified with vapor phase on top through the rest of the transient, which almost ceases liquid to flow out because the break is on the top orientation.

Figure 5.3.1.d-13 illustrates the accumulator and safety injection system mass flow rates. The ECCS actuation signal is initiated when the low pressurizer pressure setpoint of 1760 psia is attained at 12 seconds. After a 118 seconds time delay in the case of LOOP, the SI pumps supply borated-water from the RWSP into the core. The SI pumps mass flow rate gradually

increases as the RCS pressure gradually decreases. At 315 seconds, the accumulators inject borated water at a large flow rate.

As a result of the break, the coolant inventory of the RCS is gradually lost. Figure 5.3.1.d-14 shows that the RCS inventory steadily reduces as the coolant discharges from the break. The actuation of SI pumps and accumulators injection prevent further reduction in inventory, then the RCS mass inventory of about 250,000 lbm is regained. Mass inventory is regained after the accumulator injection at 315 seconds.

Figure 5.3.1.d-15 shows the collapsed liquid level in the downcomer. In the first 120 seconds after the break, the collapsed level stays at its normal operation level. During the process of loop seal formation and clearance, a sudden reduction of collapsed level is observable within 20 seconds. The reduction of RCS mass inventory eventually reduces the collapsed level in the downcomer. Further reduction is prevented by the HHIS through DVI lines, and accumulators injection into the cold legs. Downcomer collapsed level gradually regains after 300 seconds.

Figure 5.3.1.d-16 depicts that the transient characteristic of collapsed levels in the average core channel, hot assembly channel, as well as in the upper plenum are quite similar, as these parameters fluctuates in the same vertical direction. This figure shows that for the 7.5-inch cold leg top orientation break, a 7-ft reduction of collapsed level occurs at 300 seconds. Borated water injection from the accumulators prevents further decrease in the core collapsed level.

Figure 5.3.1.d-17 shows the PCT at all elevations for the hot rod. The PCT of 775°F occurs at 136 seconds. This figure demonstrates that the PCT is substantially lower than 2200°F. After the occurrence of loop seal PCT, the cladding temperature immediately reduces to about 600°F and gradually decreases until the end of transient. The SI pumps are capable to prevent any heatup after the loop seal PCT. The accumulators perform well to keep the high water level in the core.

The hot assembly exit vapor and liquid mass flow rates are shown in Figure 5.3.1.d-18. Mass flow rates of both phases rapidly reduce after the RCP trips due to the LOOP assumption. During the loop seal clearance period, a liquid flow reversal occurs at 90 seconds and lasts for 20 seconds.

It is concluded that this case is characterized by the occurrence of the highest limiting PCT.

The SI pumps prevent any heatup after the loop seal PCT and the accumulator injection keeps the high water level in the core.

Table 5.3.1-1 Spectrum of Peak Cladding Temperature for Loop-seal-PCT Cases

Break Orientation / Break Size & Location	Bottom	Top	Side	Homogeneous
6-inch at cold leg	719 (°F)	717 (°F)	lower than the initial temperature	720 (°F)
6.5-inch at cold leg	718 (°F)	lower than the initial temperature	lower than the initial temperature	lower than the initial temperature
7-inch at cold leg	759 (°F)	760 (°F)	759 (°F)	755 (°F)
7.5-inch at cold leg	758 (°F)	775 (°F)	768 (°F)	763 (°F)
8-inch at cold leg	696 (°F)	lower than the initial temperature	688 (°F)	691 (°F)

Table 5.3.1-2 Sequence of Events for 7.5-inch Break (Top) (Break Orientation Sensitivity Study)

Event	Time (sec)
Break occurs; blowdown initiation	0.0
Reactor trip (loss-of-offsite power is assumed)	9.3
Control rod insertion starts	11.1
Main steam isolation	11.1
ECCS actuation signal	11.9
RCP trip	12.3
Main feedwater isolation	17.3
Main steam safety valve open	81
Emergency Power Source initiates	115
Fuel cladding starts heating up	122
High Head Injection System begins	130
Peak Cladding Temperature occurs	136
Fuel cladding rewets	143
Emergency feedwater flow begins	145
Accumulator injection begins	315

Table 5.3.1-3 Core Performance Results for 7.5-inch Break (Top) (Break Orientation Sensitivity Study)

	Values
Peak Cladding Temperature (°F)	775
Maximum local cladding oxidation (%)	0.2
Maximum core wide cladding oxidation (%)	less than 0.2

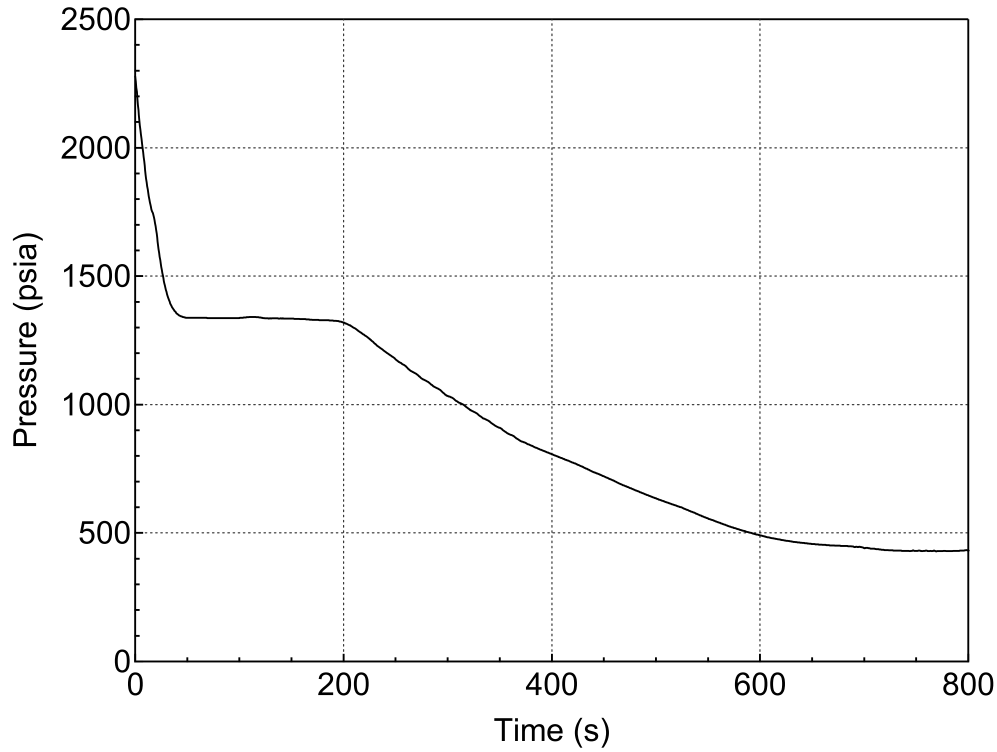

Figure 5.3.1.a-1 RCS (Pressurizer) Pressure Transient for 6-inch Break (Top) (Break Orientation Sensitivity Study)

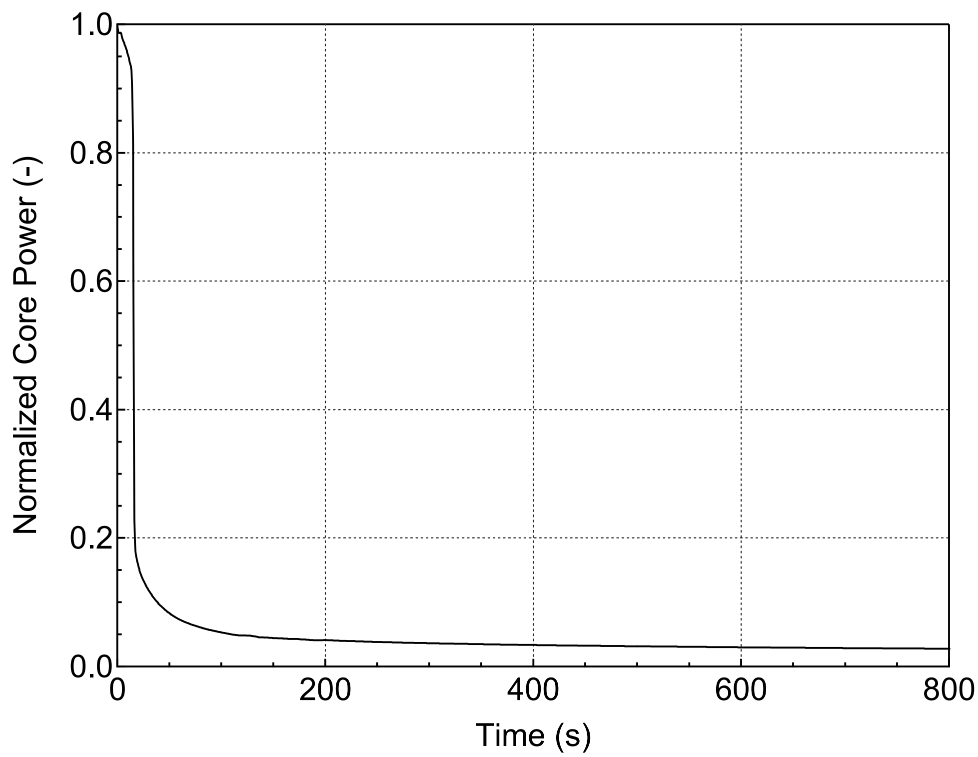

Figure 5.3.1.a-2 Normalized Core Power for 6-inch Break (Top) (Break Orientation Sensitivity Study)

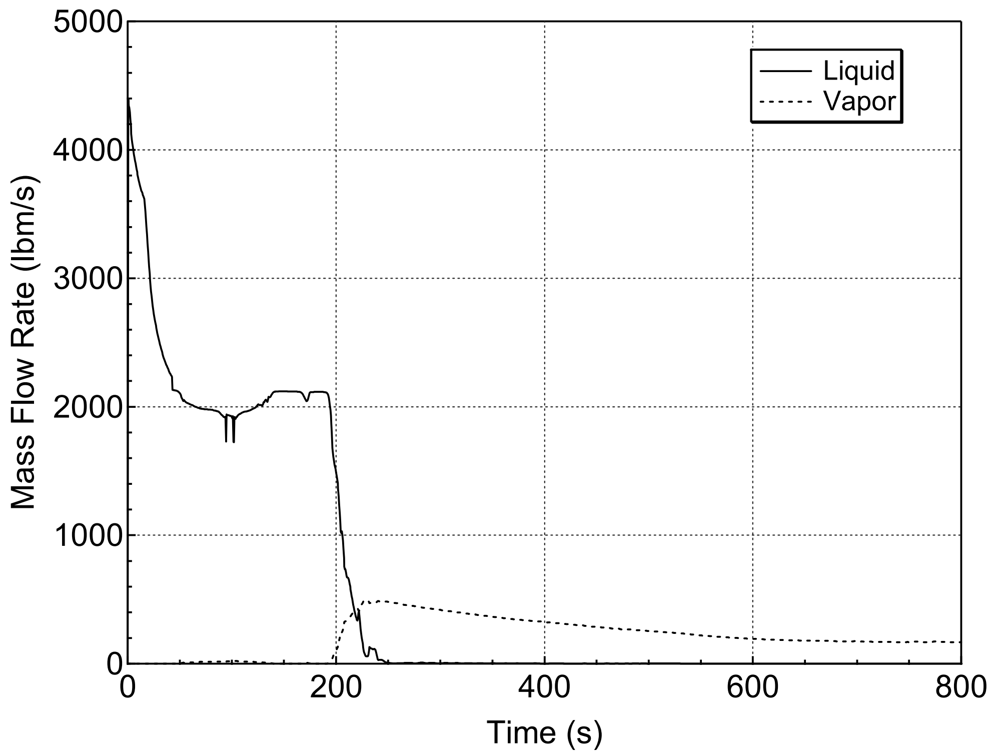

Figure 5.3.1.a-3 Liquid and Vapor Discharges through the Break for 6-inch Break (Top) (Break Orientation Sensitivity Study)

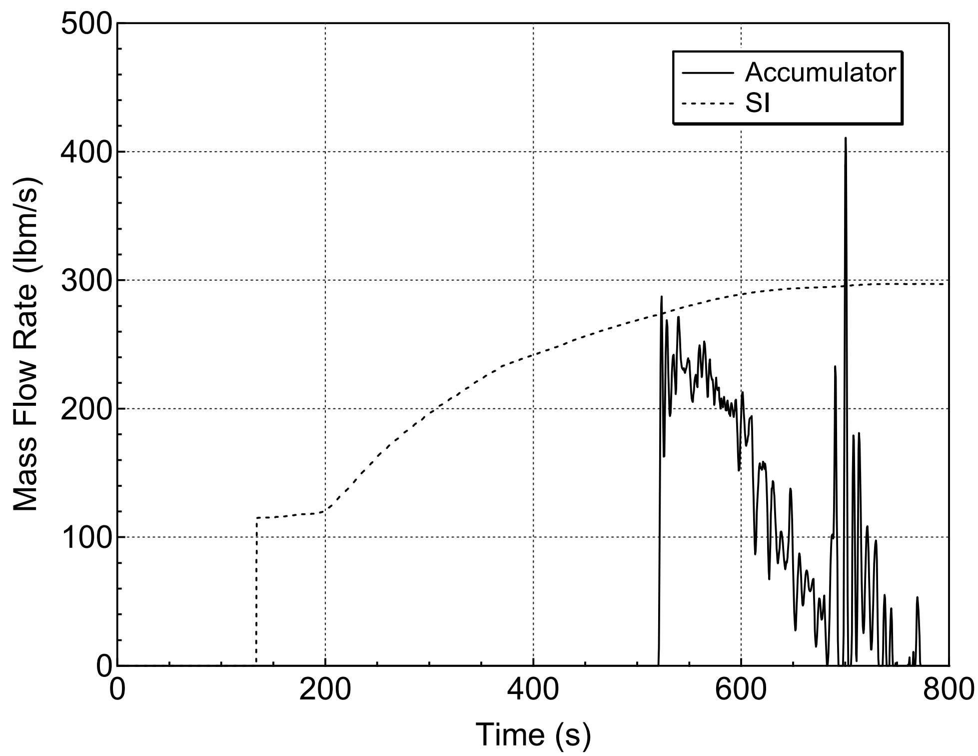

Figure 5.3.1.a-4 Accumulator and Safety Injection Mass Flowrates for 6-inch Break (Top) (Break Orientation Sensitivity Study)

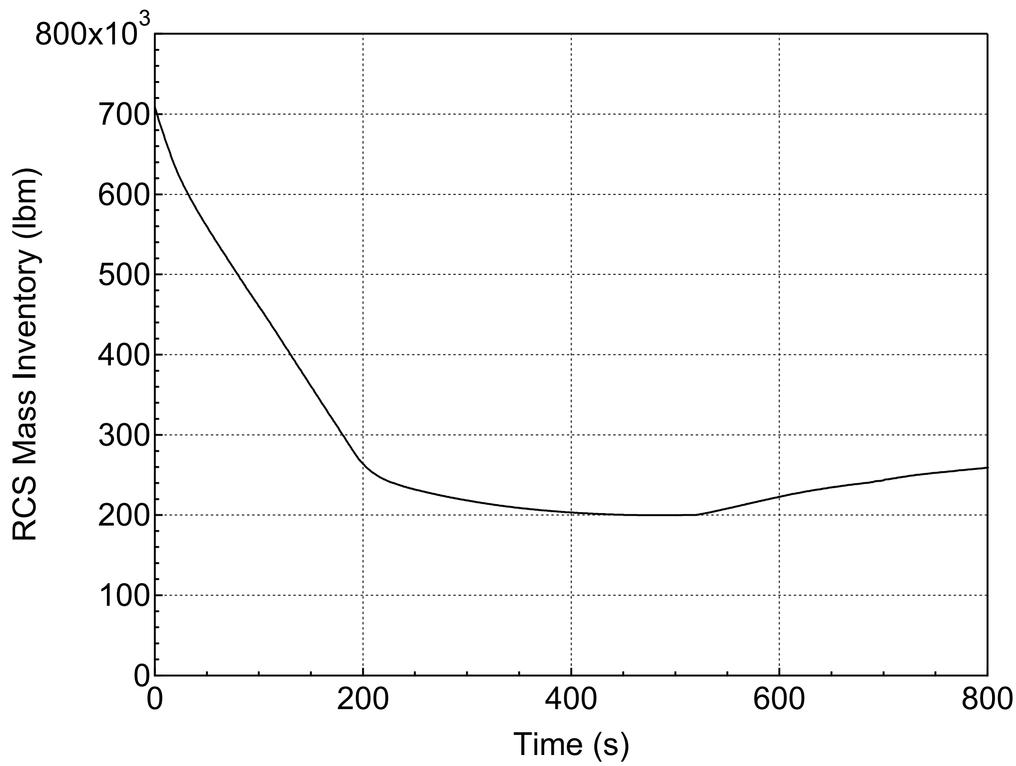

Figure 5.3.1.a-5 RCS Mass Inventory for 6-inch Break (Top)
(Break Orientation Sensitivity Study)

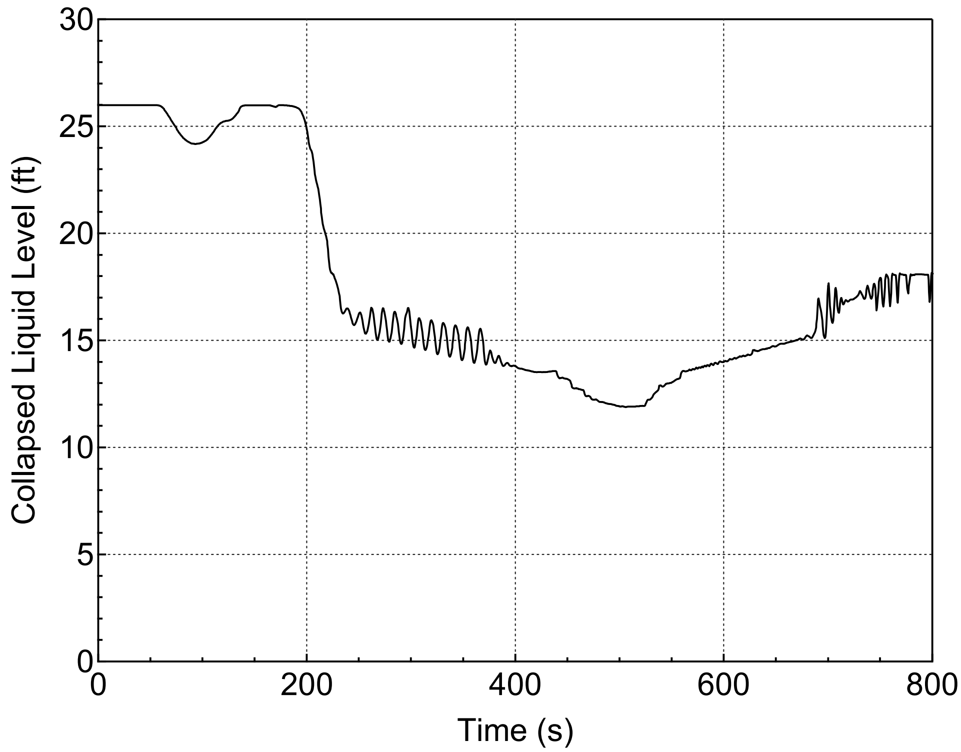

Figure 5.3.1.a-6 Downcomer Collapsed Level for 6-inch Break (Top) (Break Orientation Sensitivity Study)

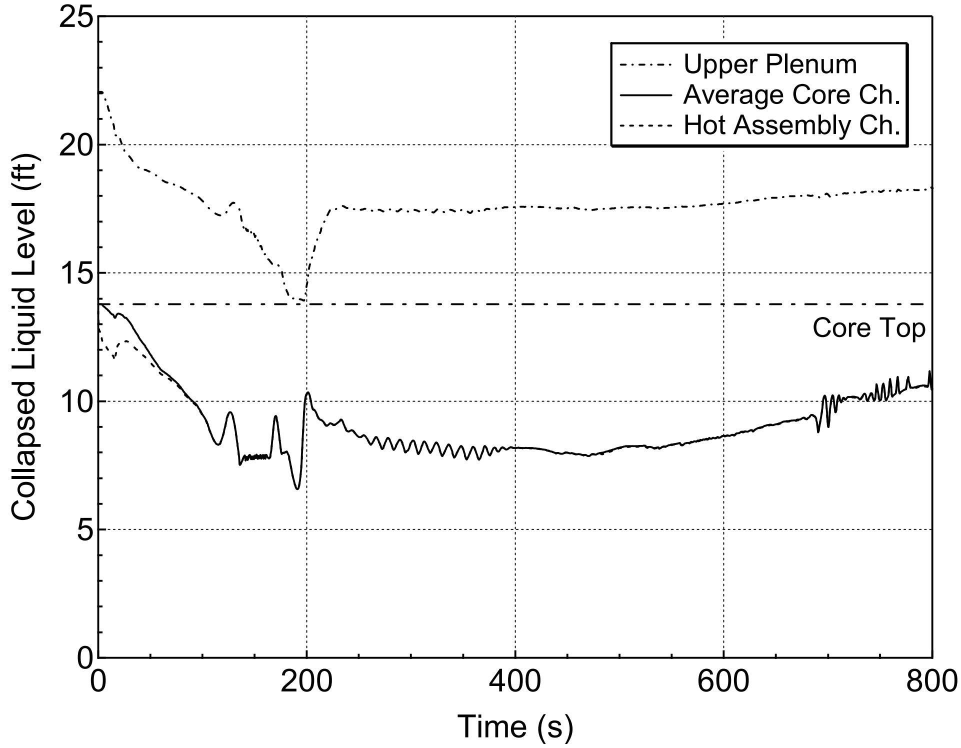

Figure 5.3.1.a-7 Core and Upper Plenum Collapsed Levels for 6-inch Break (Top) (Break Orientation Sensitivity Study)

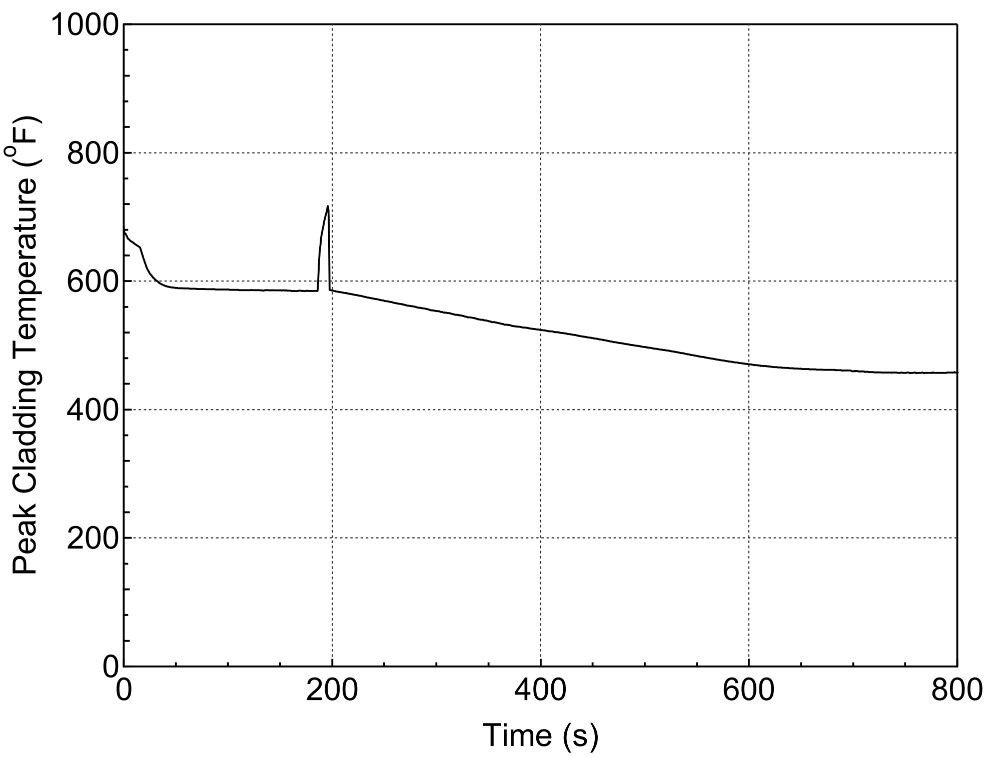

Figure 5.3.1.a-8 PCT at All Elevations for Hot Rod in Hot Assembly for 6-inch Break (Top) (Break Orientation Sensitivity Study)

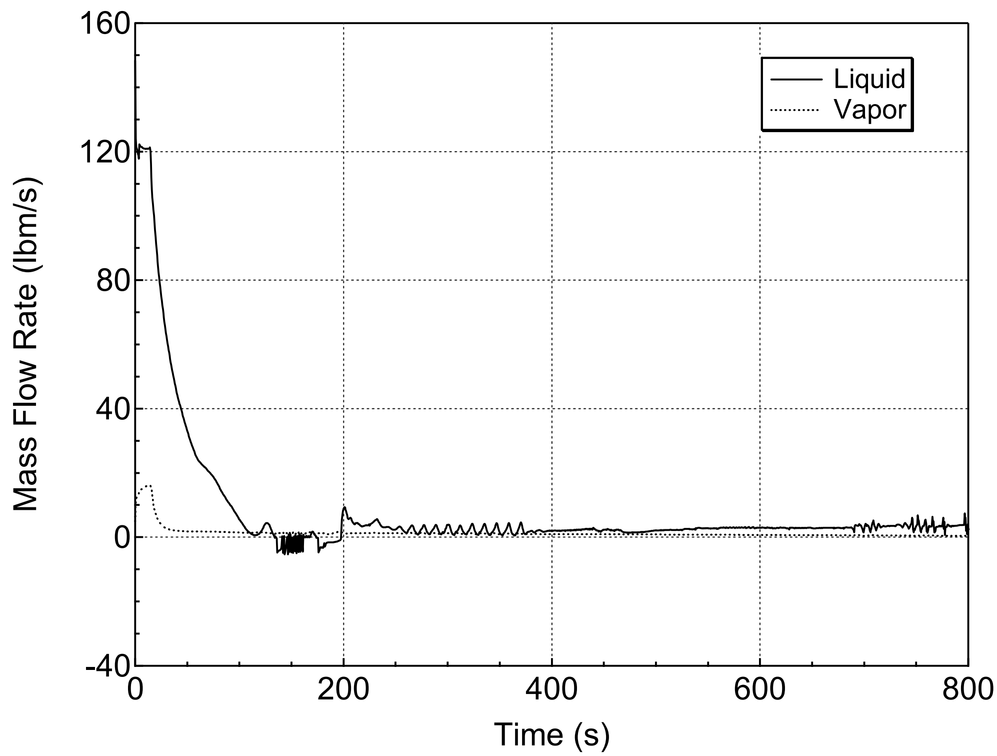

Figure 5.3.1.a-9 Hot Assembly Exit Vapor and Liquid Mass Flowrates for 6-inch Break (Top) (Break Orientation Sensitivity Study)

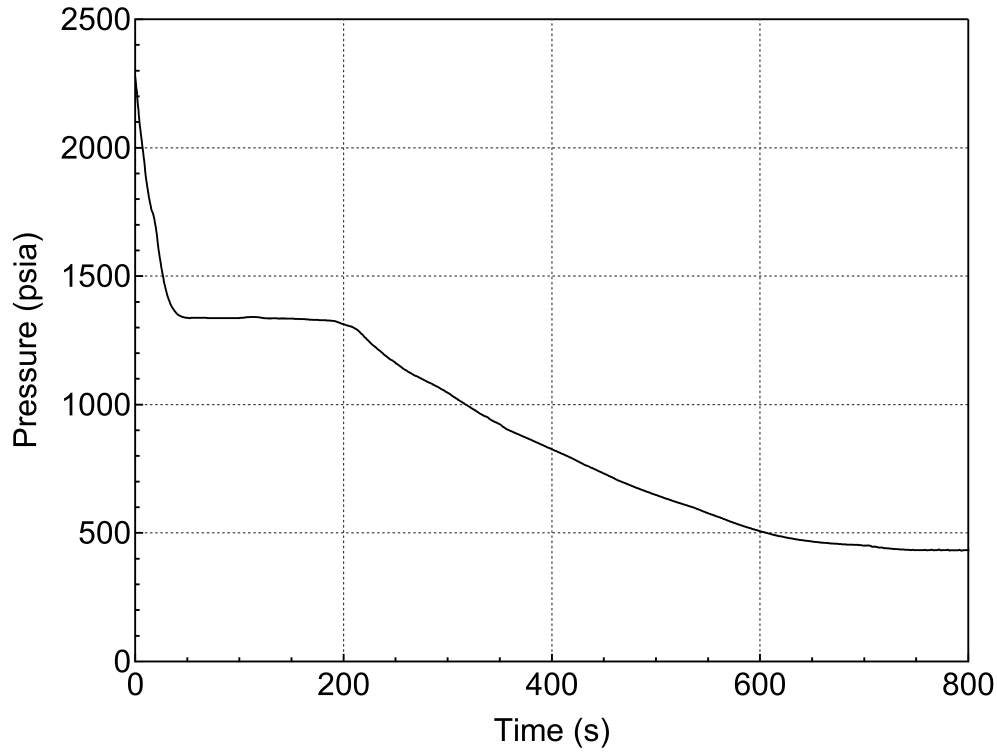

Figure 5.3.1.a-10 RCS (Pressurizer) Pressure Transient for 6-inch Break (Side) (Break Orientation Sensitivity Study)

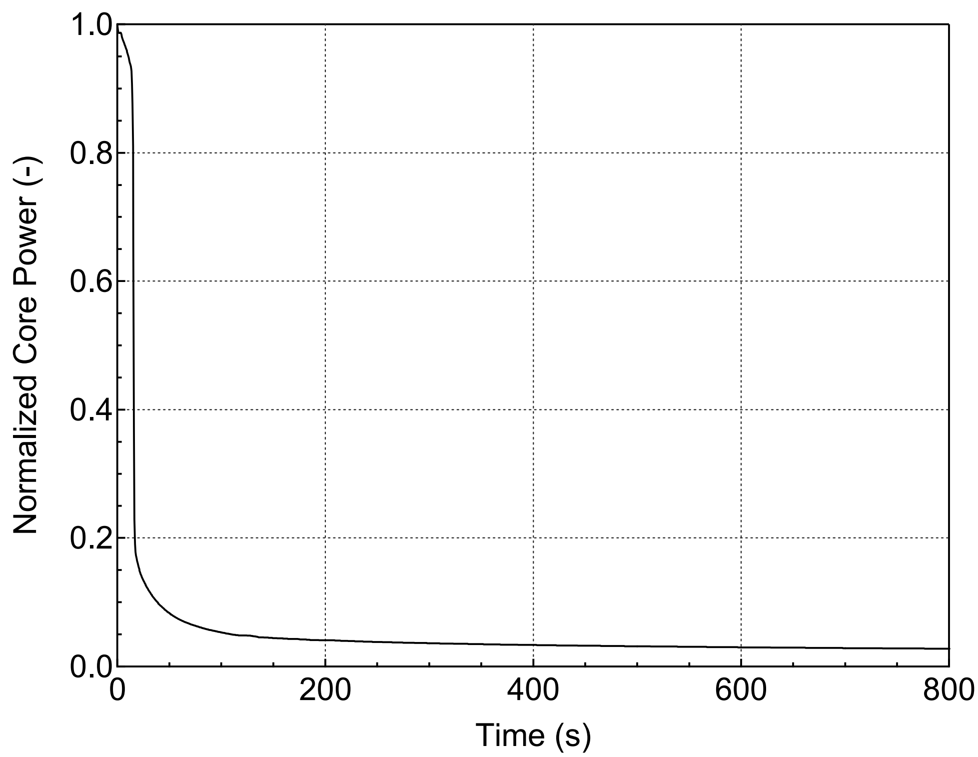

Figure 5.3.1.a-11 Normalized Core Power for 6-inch Break (Side)
(Break Orientation Sensitivity Study)

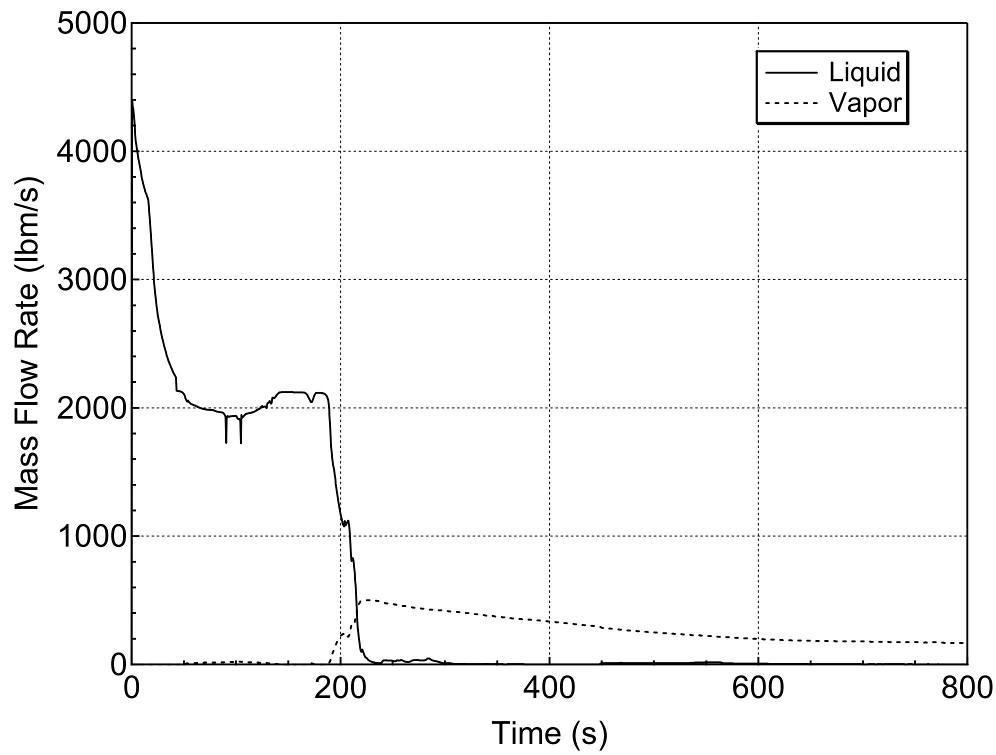

Figure 5.3.1.a-12 Liquid and Vapor Discharges through the Break for 6-inch Break (Side) (Break Orientation Sensitivity Study)

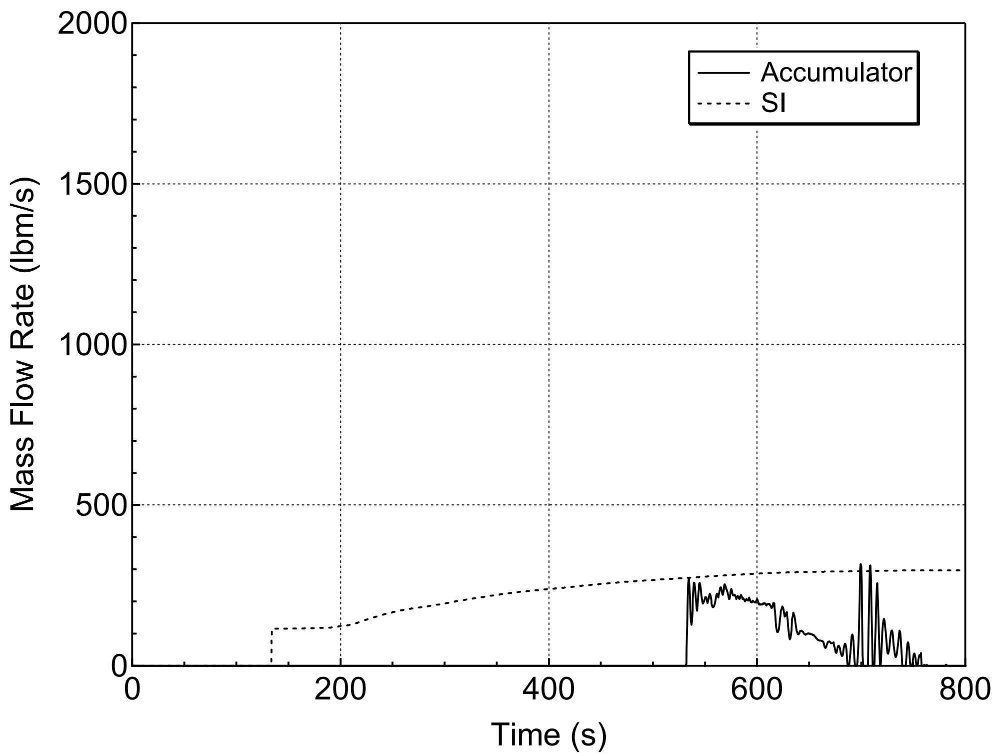

Figure 5.3.1.a-13 Accumulator and Safety Injection Mass Flowrates for 6-inch Break (Side) (Break Orientation Sensitivity Study)

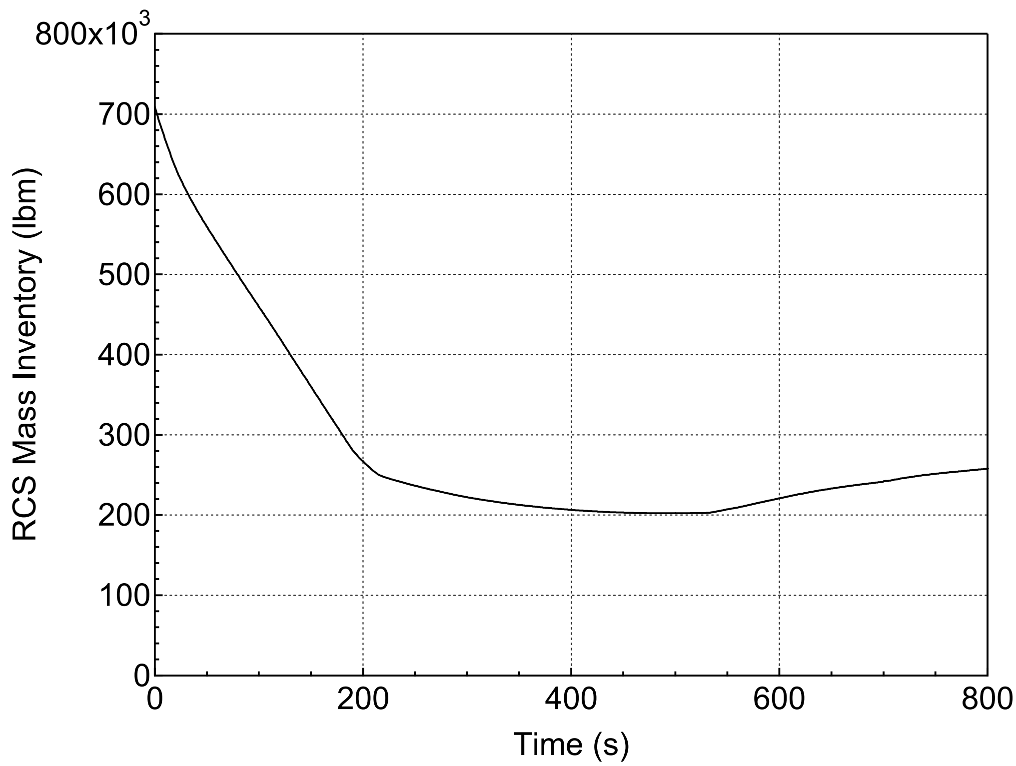

Figure 5.3.1.a-14 RCS Mass Inventory for 6-inch Break (Side)
(Break Orientation Sensitivity Study)

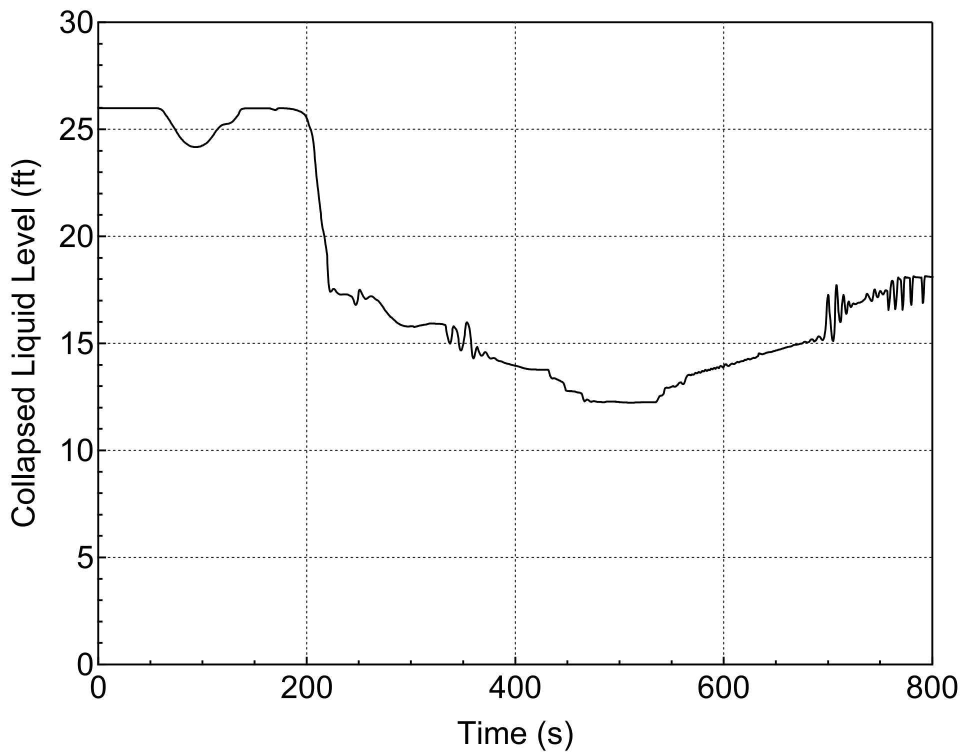

Figure 5.3.1.a-15 Downcomer Collapsed Level for 6-inch Break (Side) (Break Orientation Sensitivity Study)

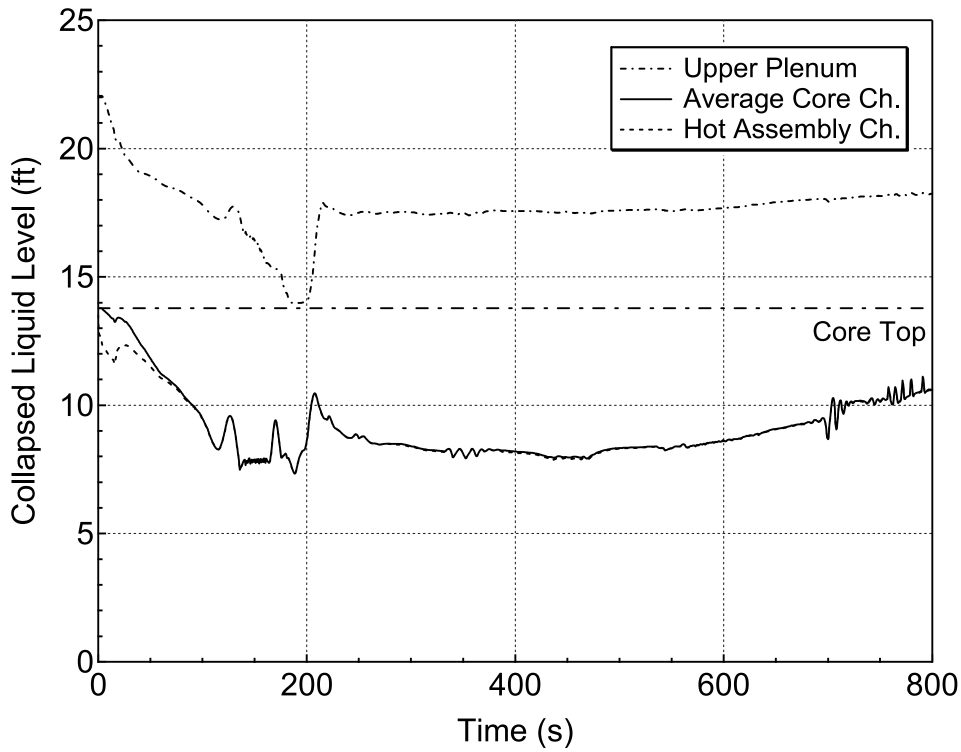

Figure 5.3.1.a-16 Core and Upper Plenum Collapsed Levels for 6-inch Break (Side) (Break Orientation Sensitivity Study)

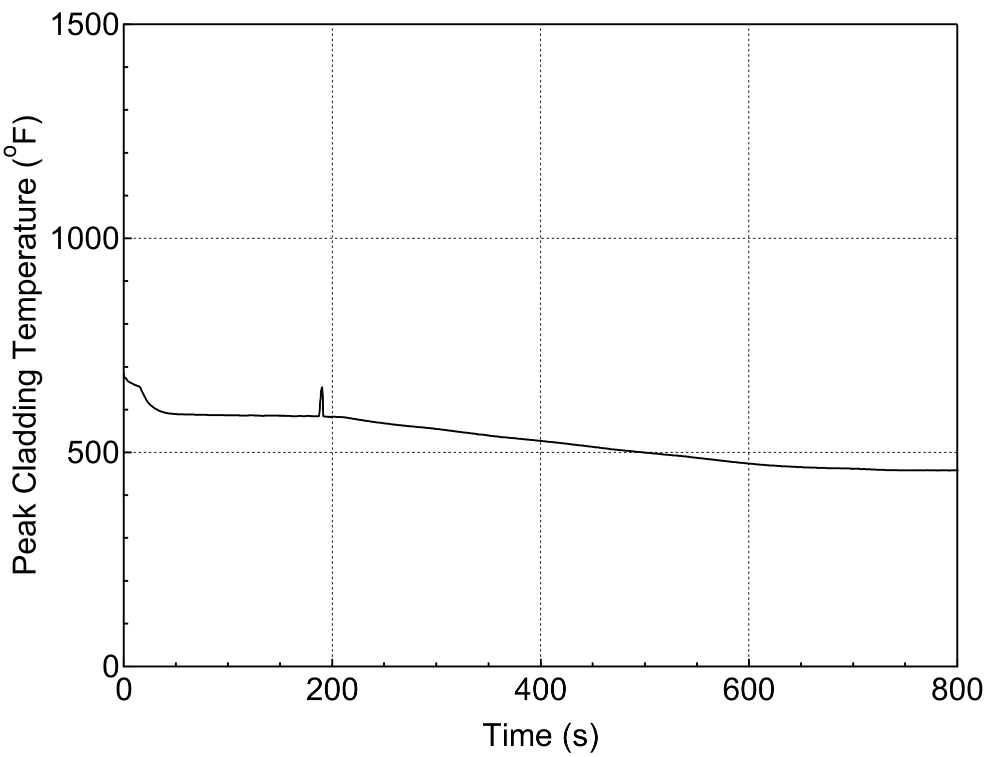

Figure 5.3.1.a-17 PCT at All Elevations for Hot Rod in Hot Assembly for 6-inch Break (Side) (Break Orientation Sensitivity Study)

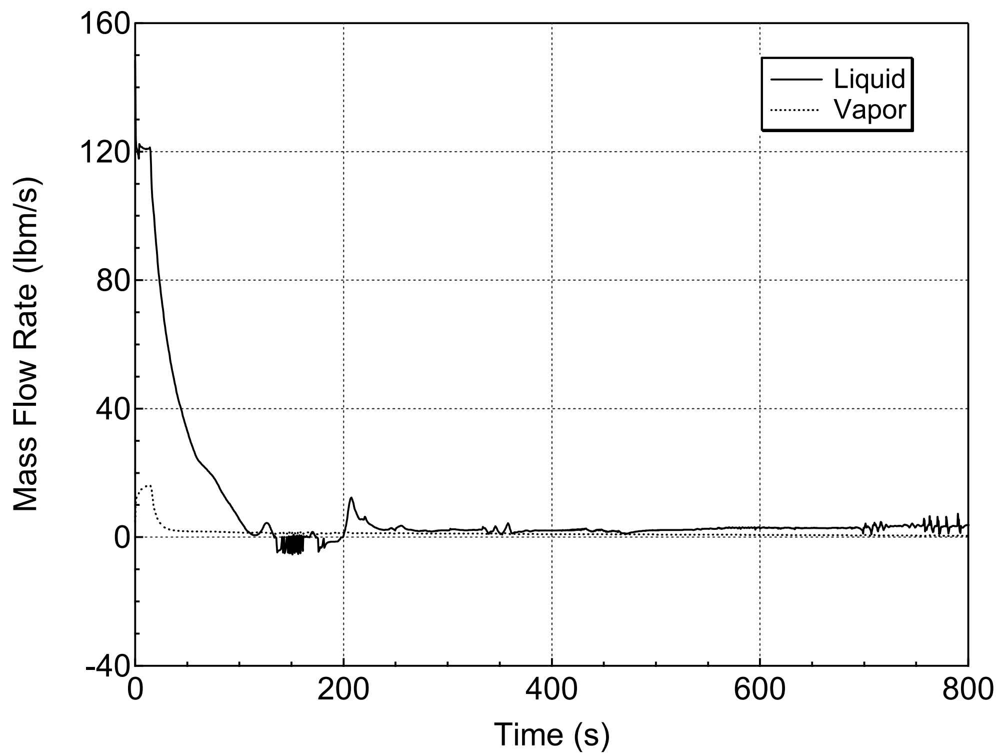

Figure 5.3.1.a-18 Hot Assembly Exit Vapor and Liquid Mass Flowrates for 6-inch Break (Side) (Break Orientation Sensitivity Study)

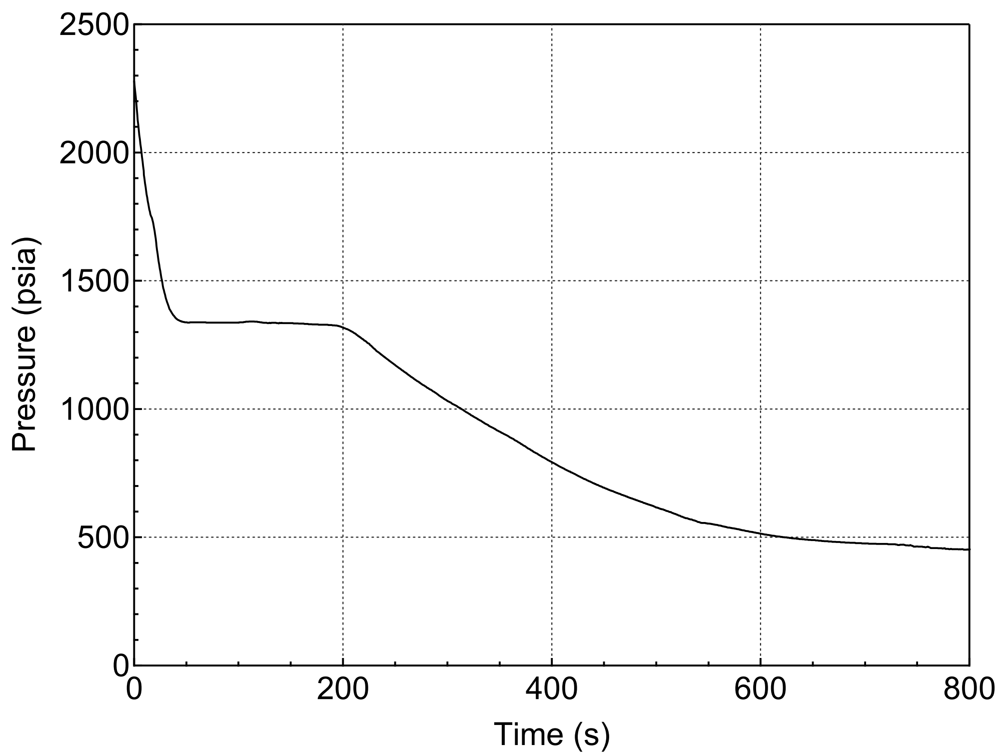

Figure 5.3.1.a-19 RCS (Pressurizer) Pressure Transient for 6-inch Break (Homogeneous) (Break Orientation Sensitivity Study)

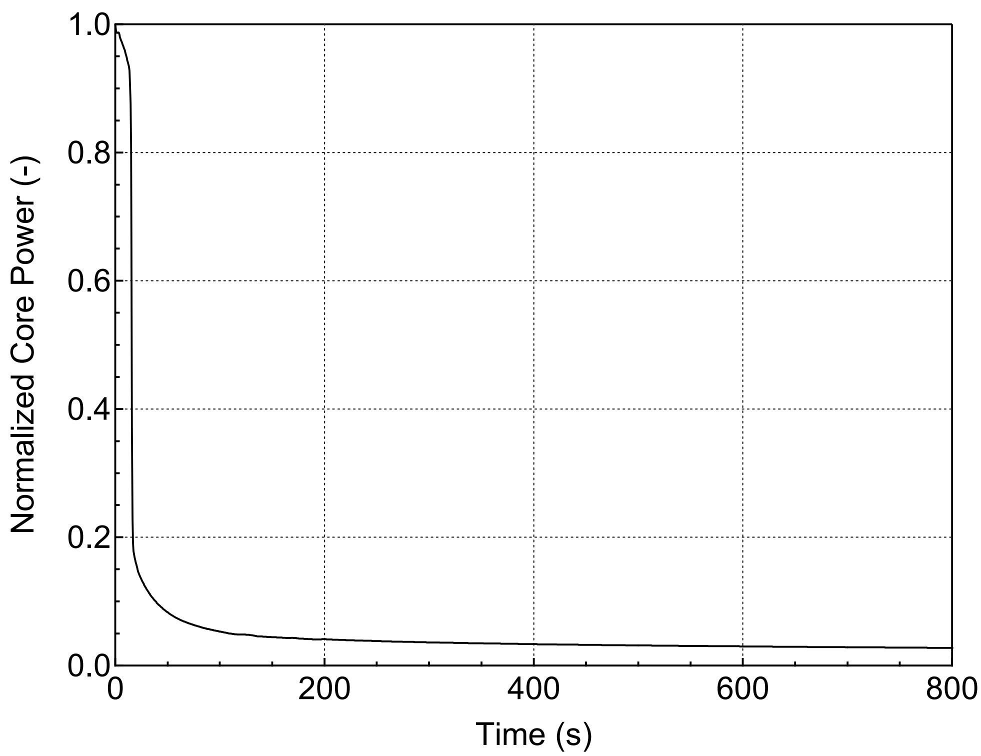

Figure 5.3.1.a-20 Normalized Core Power for 6-inch Break (Homogeneous) (Break Orientation Sensitivity Study)

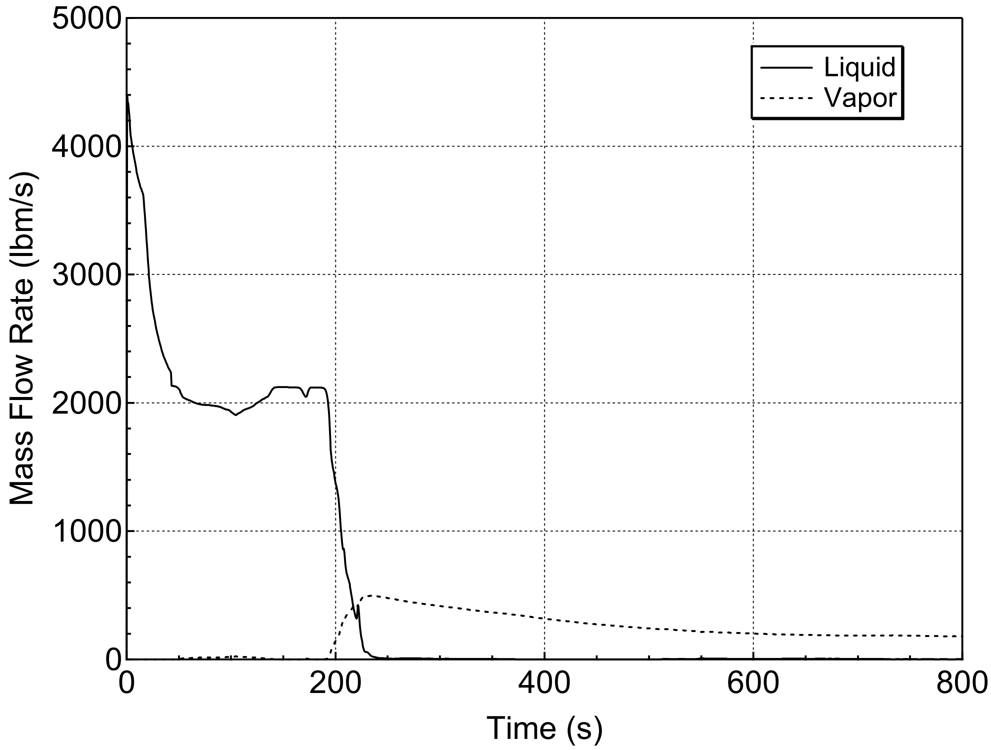

Figure 5.3.1.a-21 Liquid and Vapor Discharges through the Break for 6-inch Break (Homogeneous) (Break Orientation Sensitivity Study)

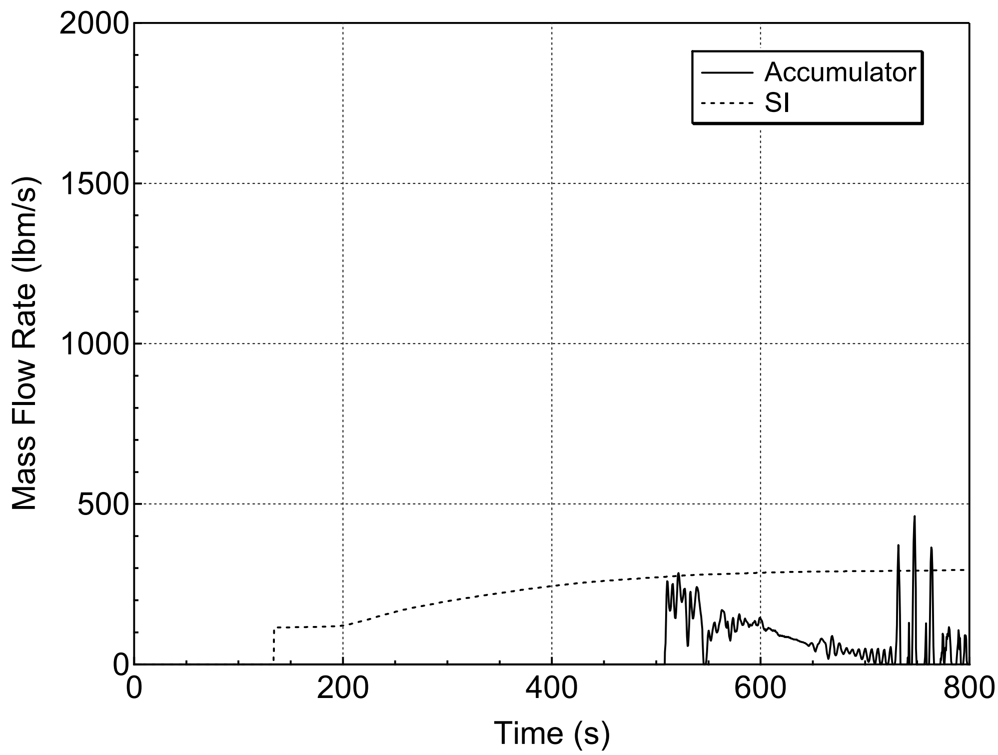

Figure 5.3.1.a-22 Accumulator and Safety Injection Mass Flowrates for 6-inch Break (Homogeneous) (Break Orientation Sensitivity Study)

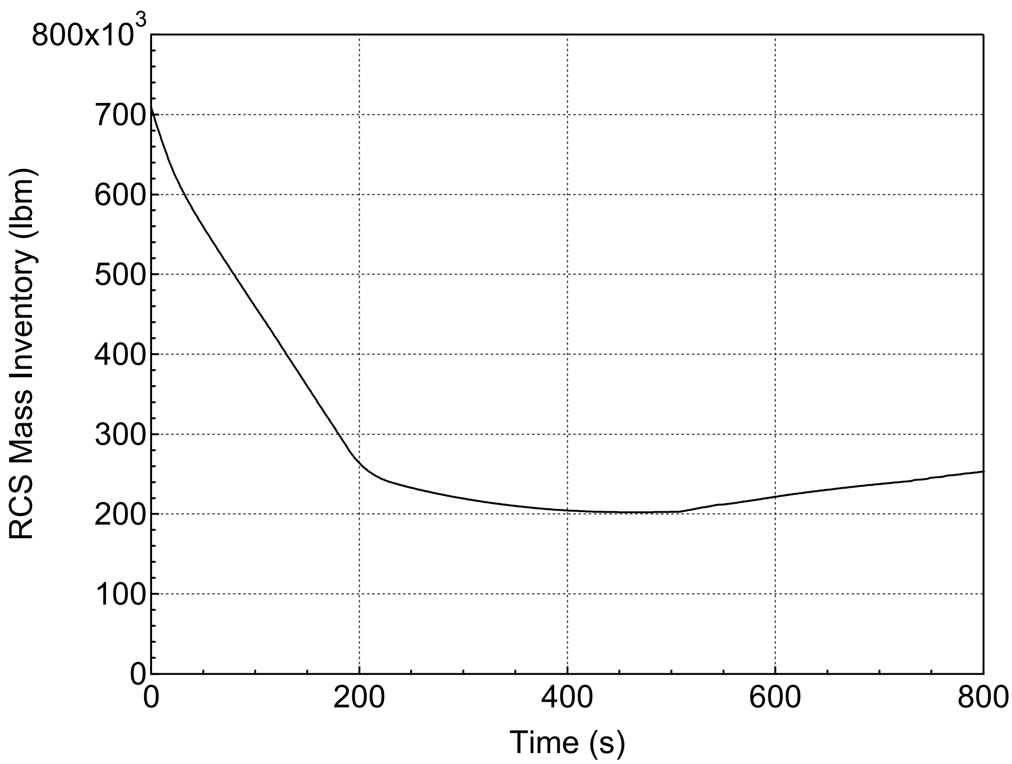

Figure 5.3.1.a-23 RCS Mass Inventory for 6-inch Break (Homogeneous) (Break Orientation Sensitivity Study)

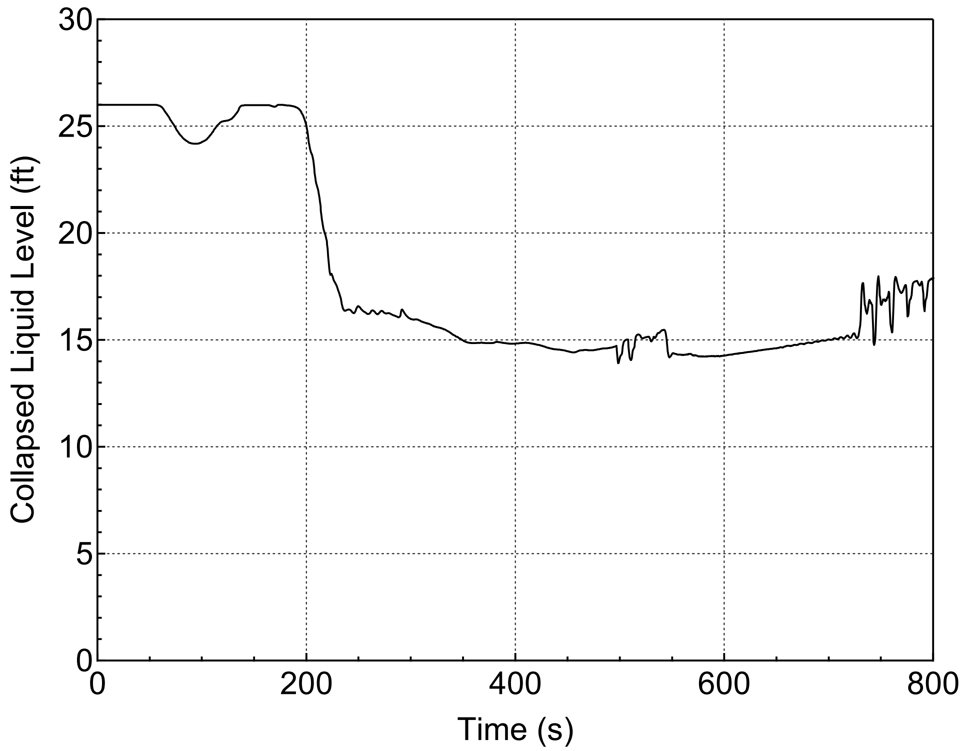

Figure 5.3.1.a-24 Downcomer Collapsed Level for 6-inch Break (Homogeneous) (Break Orientation Sensitivity Study)

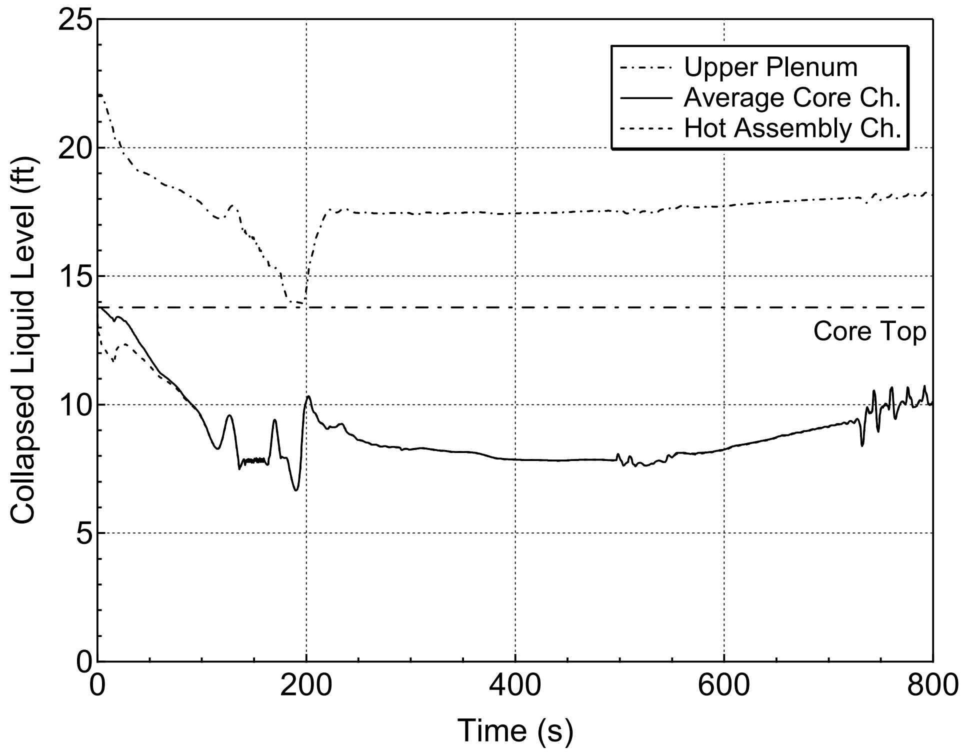

Figure 5.3.1.a-25 Core and Upper Plenum Collapsed Levels for 6-inch Break (Homogeneous) (Break Orientation Sensitivity Study)

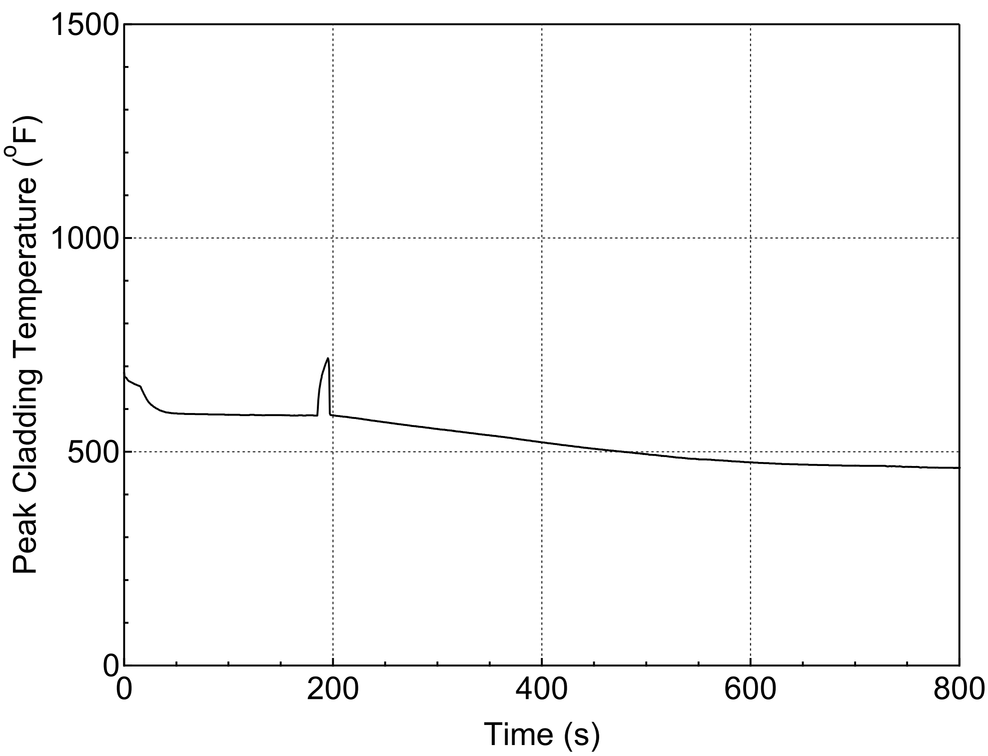

Figure 5.3.1.a-26 PCT at All Elevations for Hot Rod in Hot Assembly for 6-inch Break (Homogeneous) (Break Orientation Sensitivity Study)

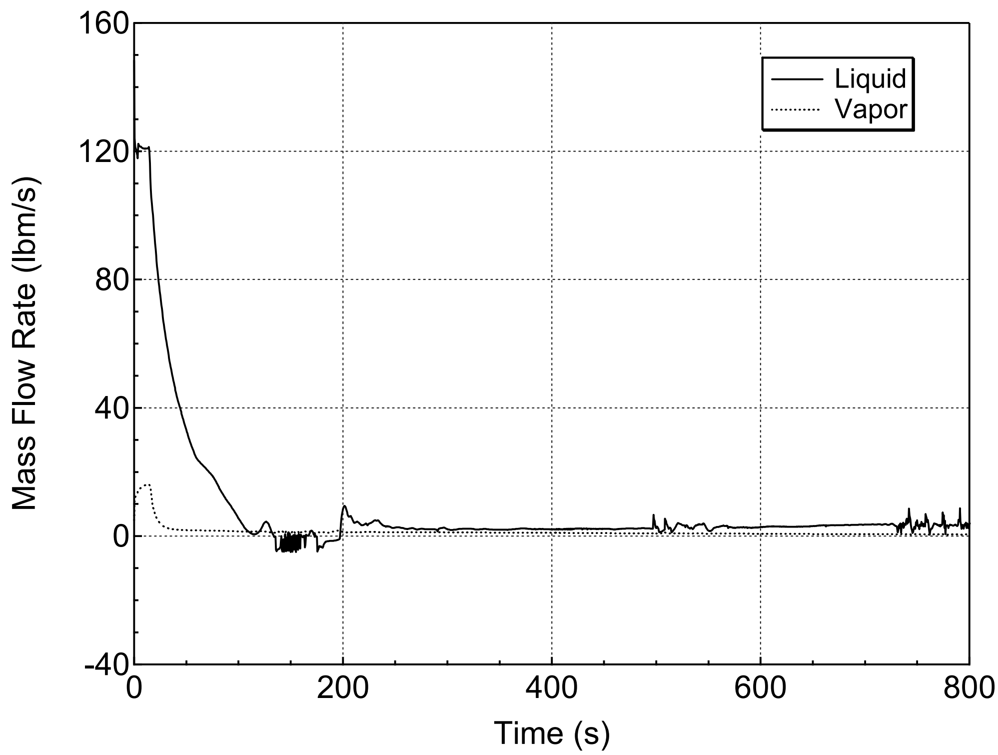

Figure 5.3.1.a-27 Hot Assembly Exit Vapor and Liquid Mass Flowrates for 6-inch Break (Homogeneous) (Break Orientation Sensitivity Study)

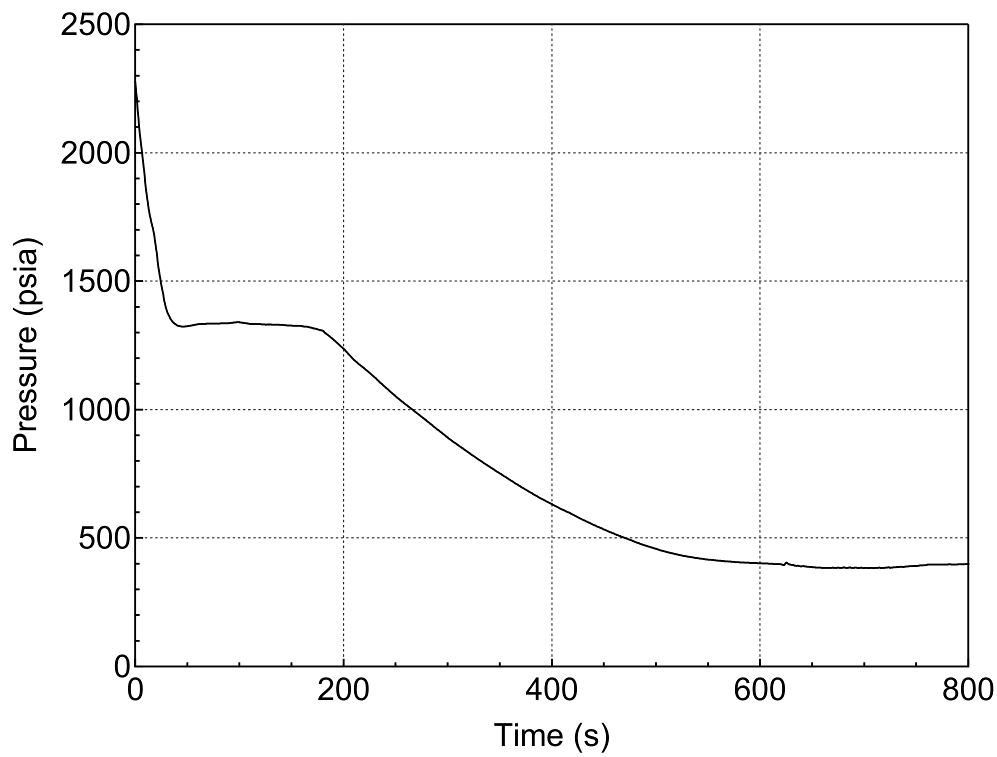

Figure 5.3.1.b-1 RCS (Pressurizer) Pressure Transient for 6.5-inch Break (Bottom) (Break Orientation Sensitivity Study)

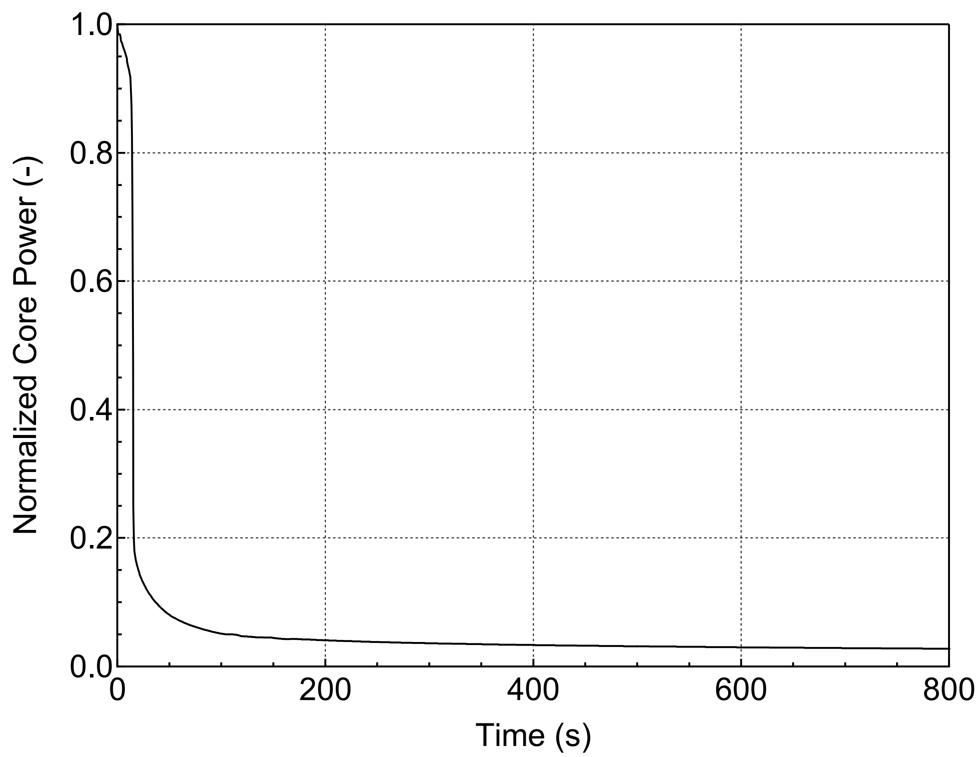

Figure 5.3.1.b-2 Normalized Core Power for 6.5-inch Break (Bottom) (Break Orientation Sensitivity Study)

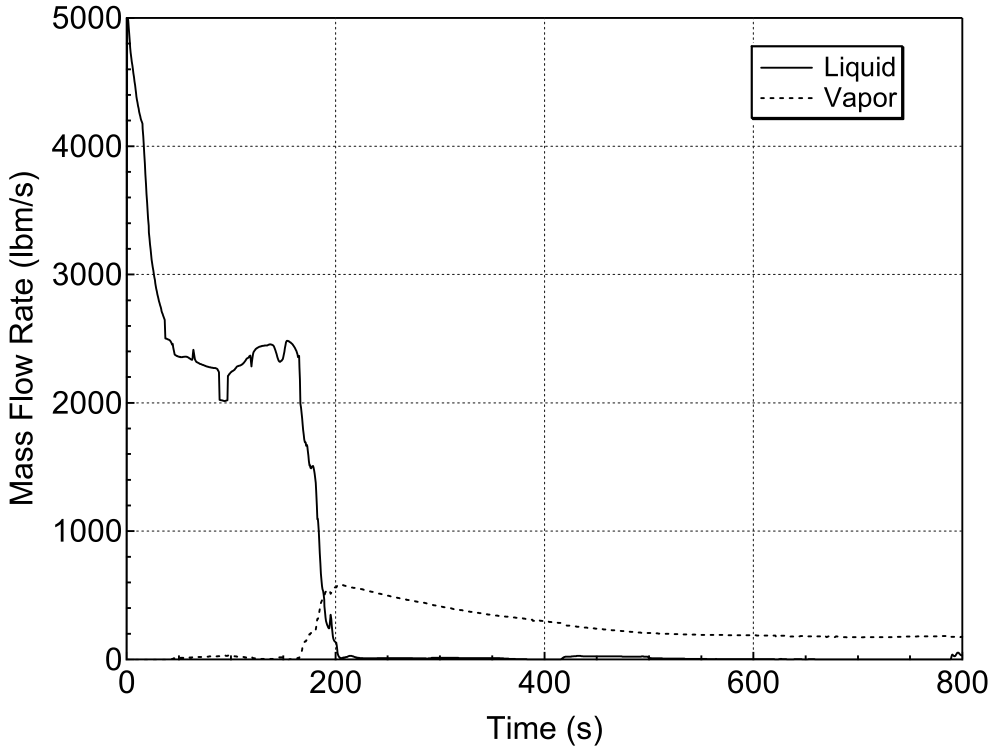

Figure 5.3.1.b-3 Liquid and Vapor Discharges through the Break for 6.5-inch Break (Bottom) (Break Orientation Sensitivity Study)

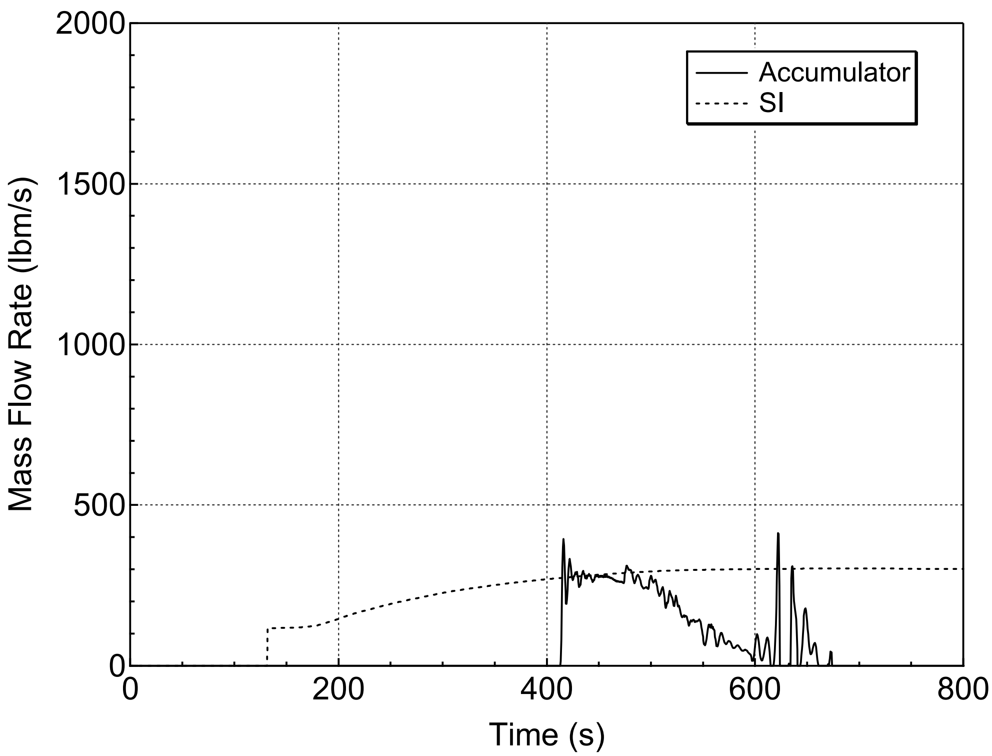

Figure 5.3.1.b-4 Accumulator and Safety Injection Mass Flowrates for 6.5-inch Break (Bottom) (Break Orientation Sensitivity Study)

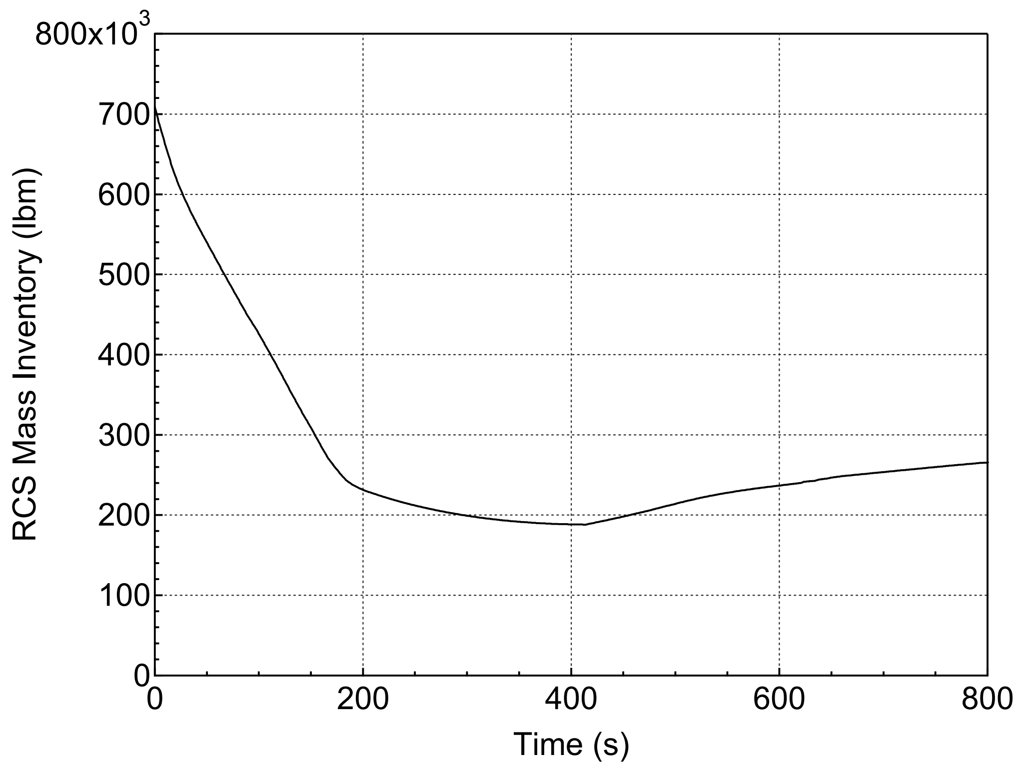

Figure 5.3.1.b-5 RCS Mass Inventory for 6.5-inch Break (Bottom) (Break Orientation Sensitivity Study)

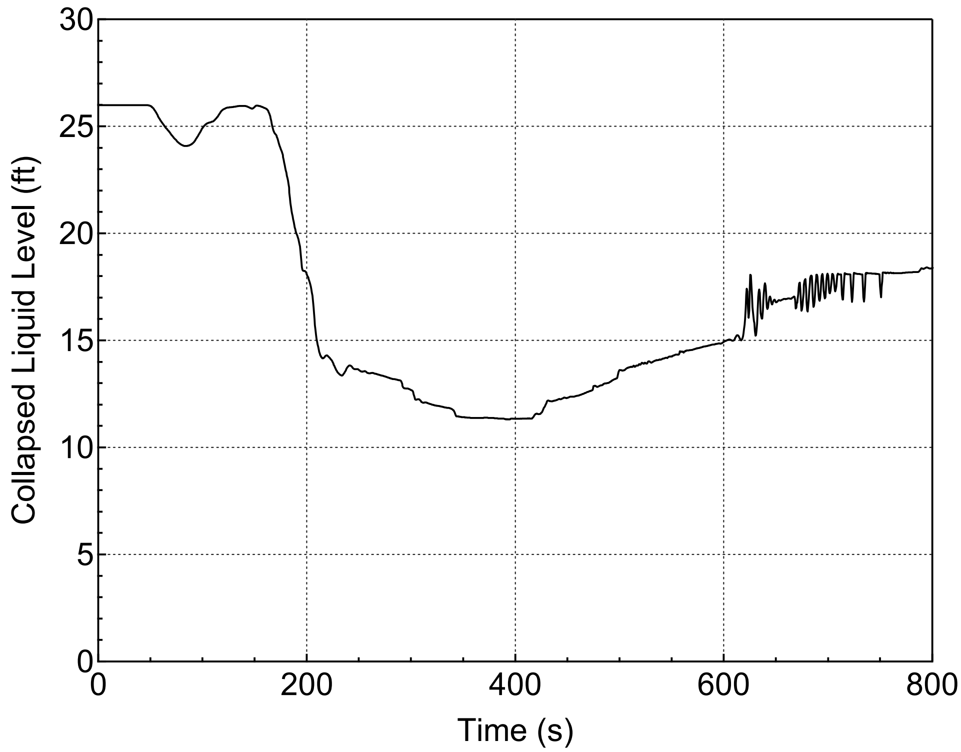

Figure 5.3.1.b-6 Downcomer Collapsed Level for 6.5-inch Break (Bottom) (Break Orientation Sensitivity Study)

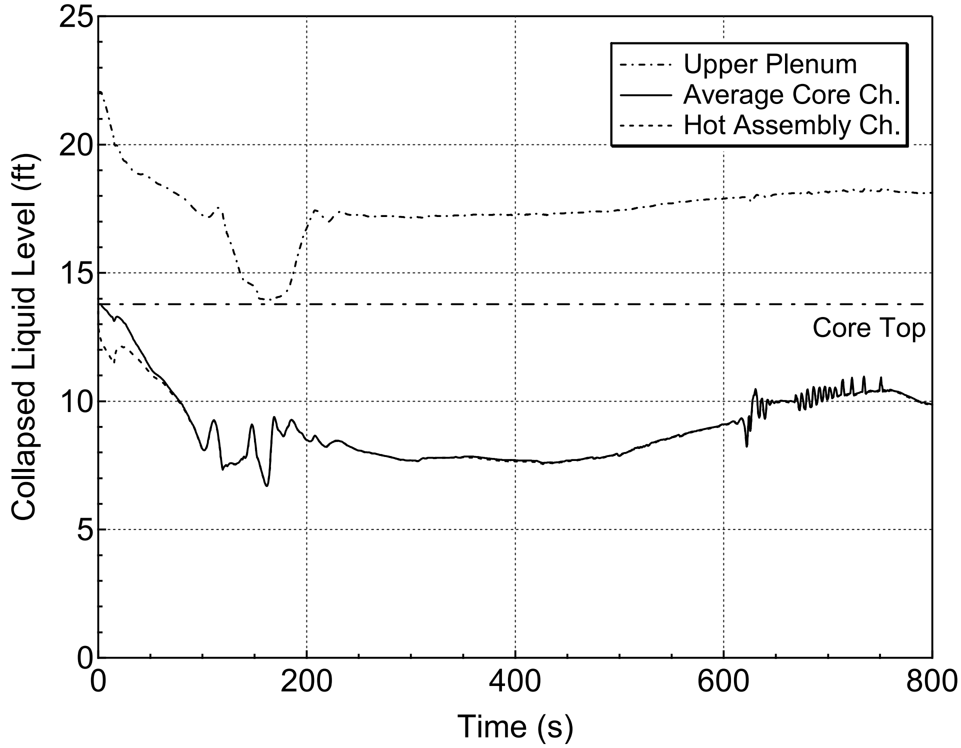

Figure 5.3.1.b-7 Core and Upper Plenum Collapsed Levels for 6.5-inch Break (Bottom) (Break Orientation Sensitivity Study)

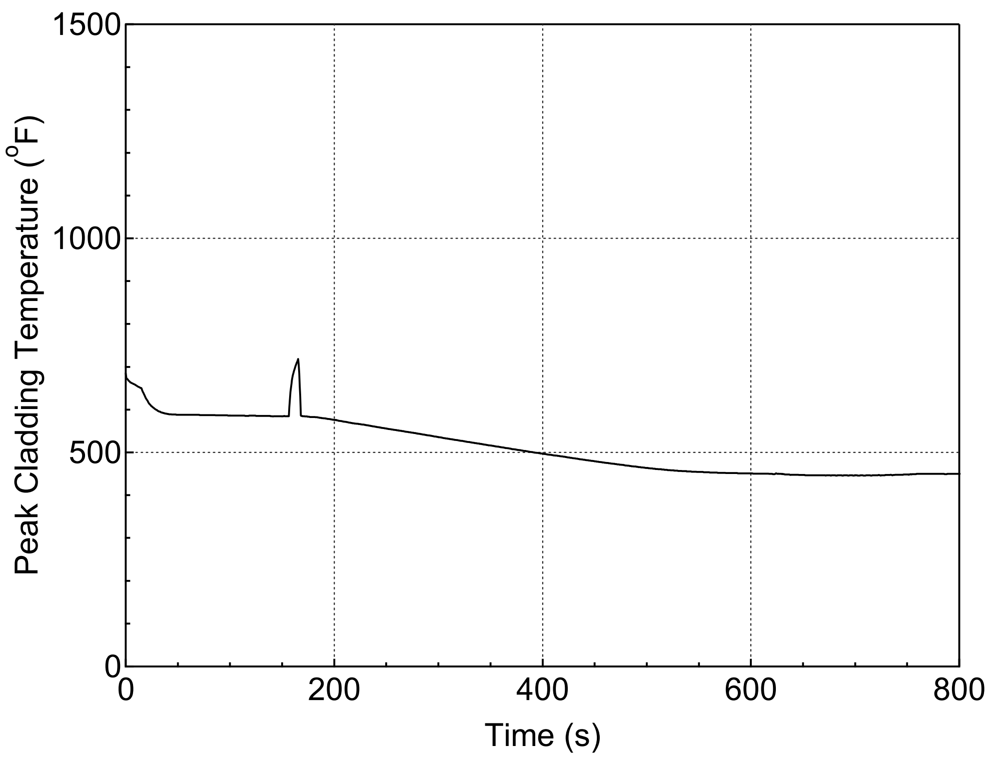

Figure 5.3.1.b-8 PCT at All Elevations for Hot Rod in Hot Assembly for 6.5-inch Break (Bottom) (Break Orientation Sensitivity Study)

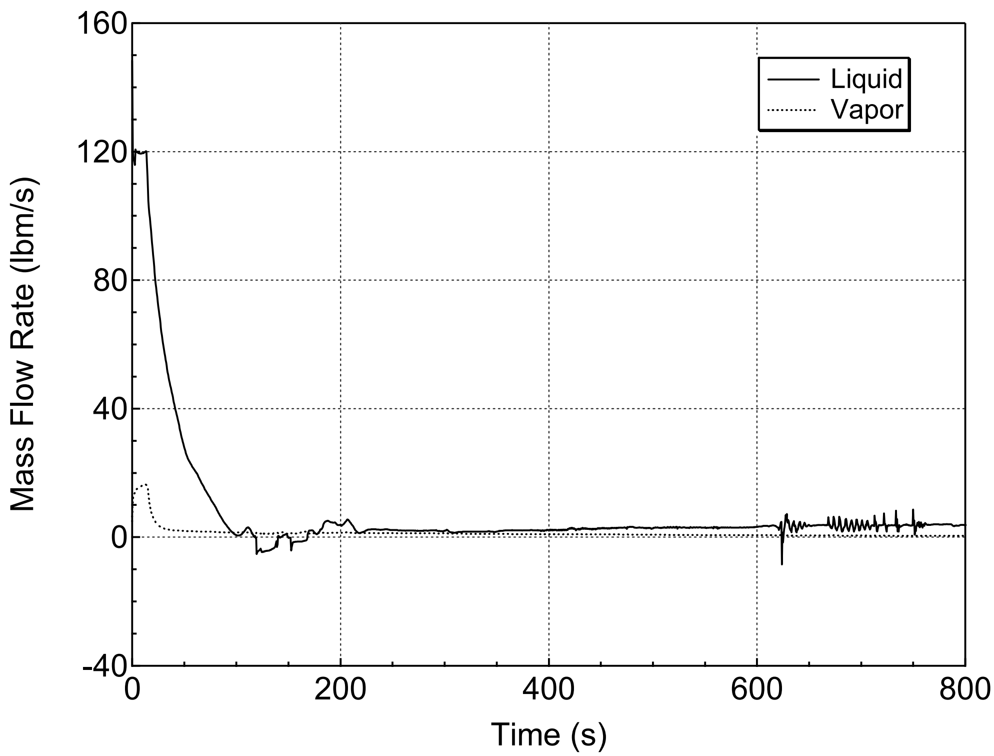

Figure 5.3.1.b-9 Hot Assembly Exit Vapor and Liquid Mass Flowrates for 6.5-inch Break (Bottom) (Break Orientation Sensitivity Study)

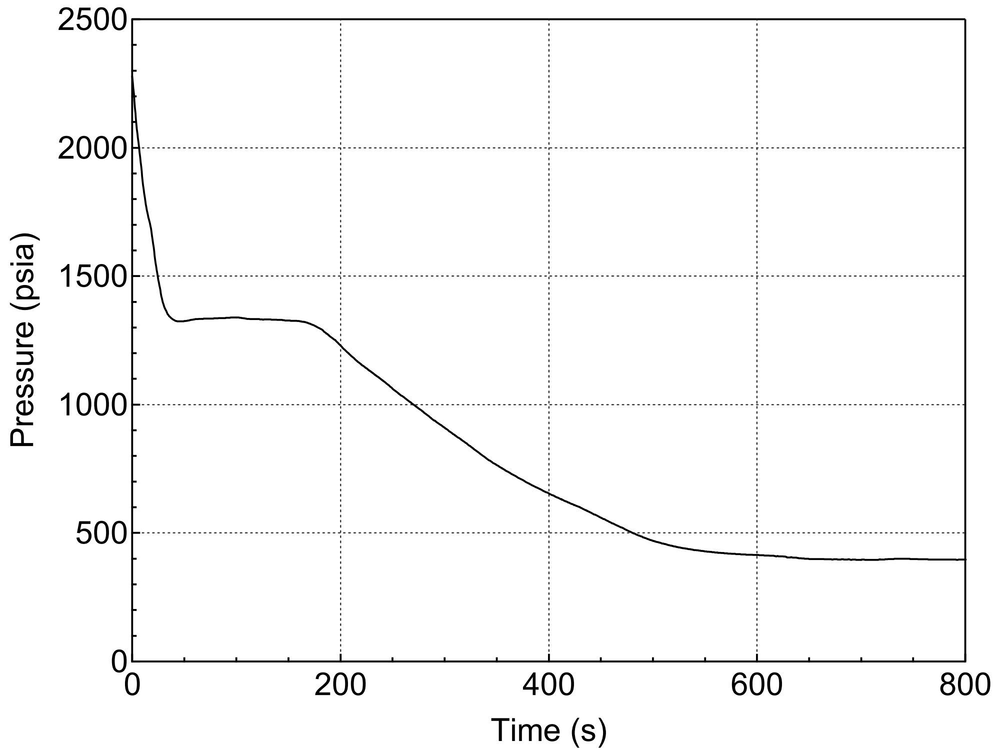

Figure 5.3.1.b-10 RCS (Pressurizer) Pressure Transient for 6.5-inch Break (Top) (Break Orientation Sensitivity Study)

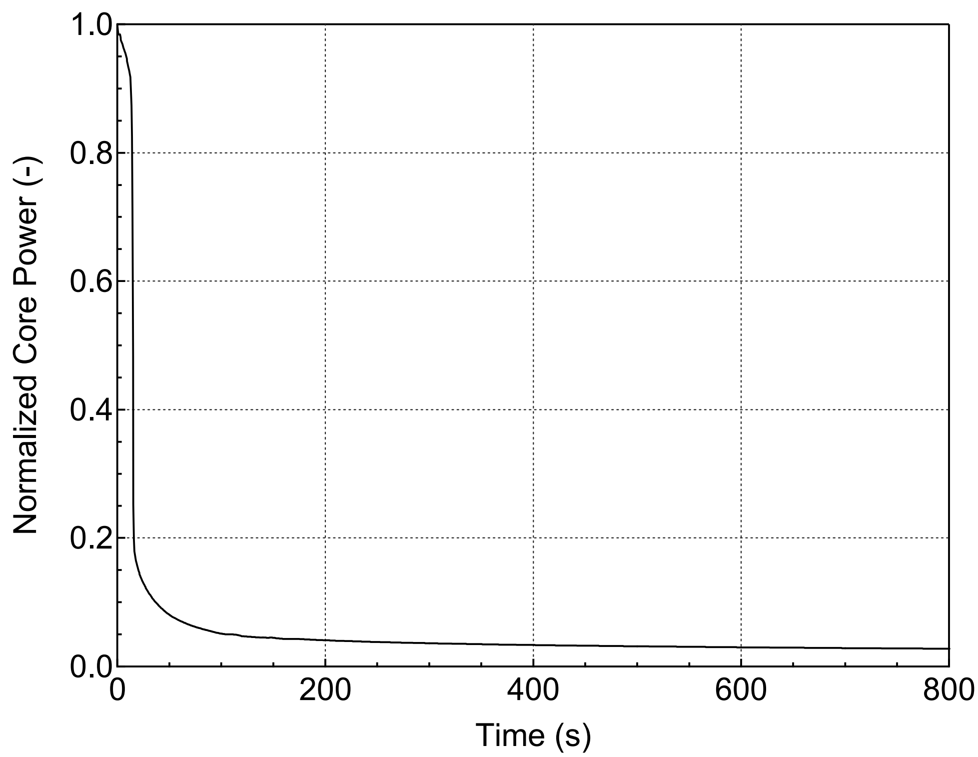

Figure 5.3.1.b-11 Normalized Core Power for 6.5-inch Break (Top)
(Break Orientation Sensitivity Study)

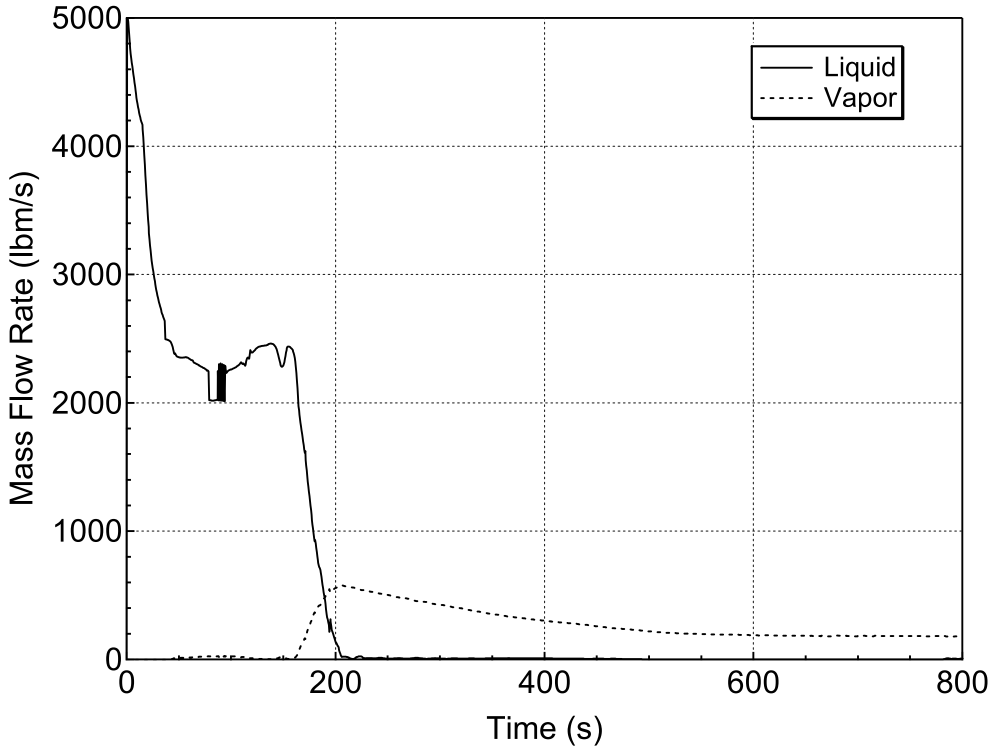

Figure 5.3.1.b-12 Liquid and Vapor Discharges through the Break for 6.5-inch Break (Top) (Break Orientation Sensitivity Study)

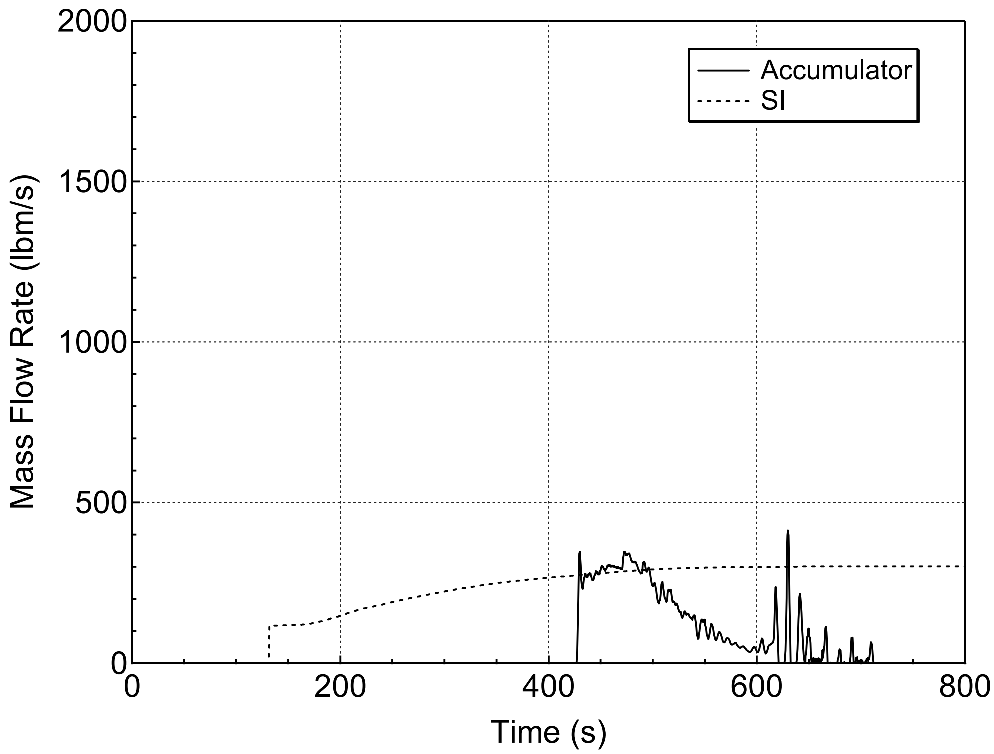

Figure 5.3.1.b-13 Accumulator and Safety Injection Mass Flowrates for 6.5-inch Break (Top) (Break Orientation Sensitivity Study)

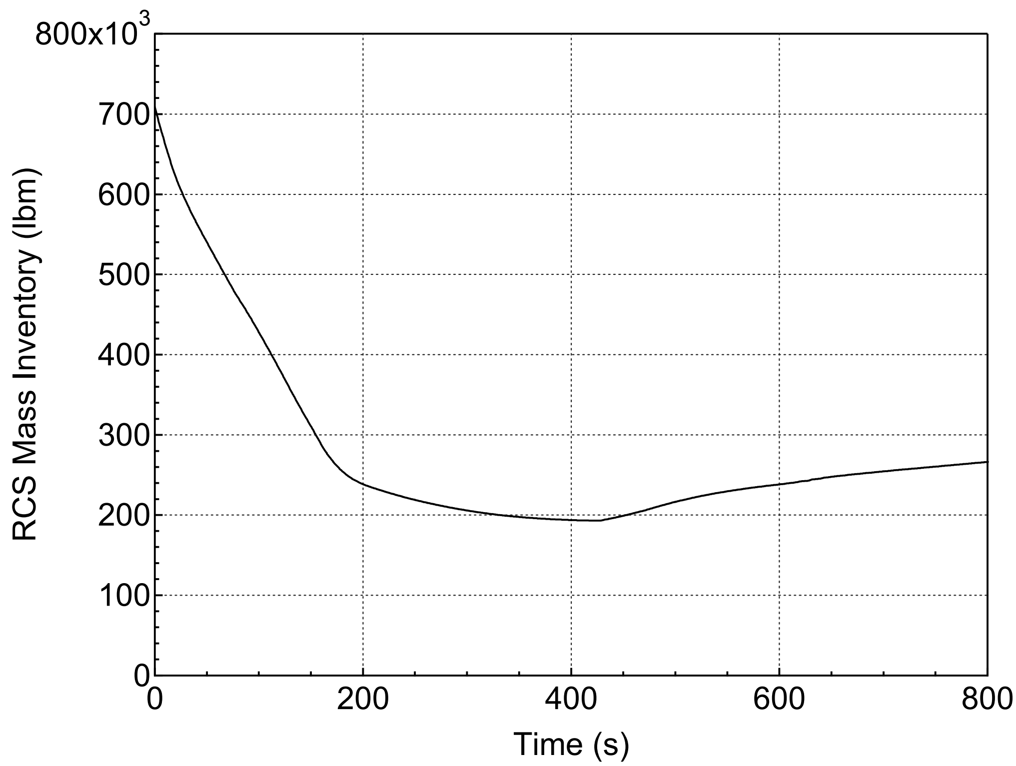

Figure 5.3.1.b-14 RCS Mass Inventory for 6.5-inch Break (Top) (Break Orientation Sensitivity Study)

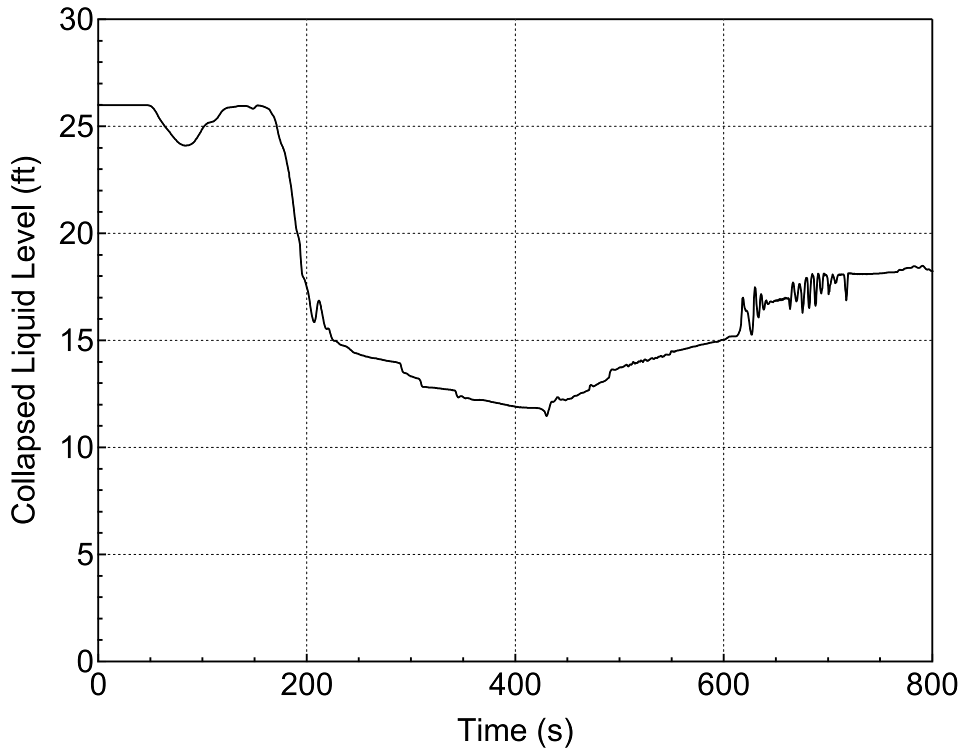

Figure 5.3.1.b-15 Downcomer Collapsed Level for 6.5-inch Break (Top) (Break Orientation Sensitivity Study)

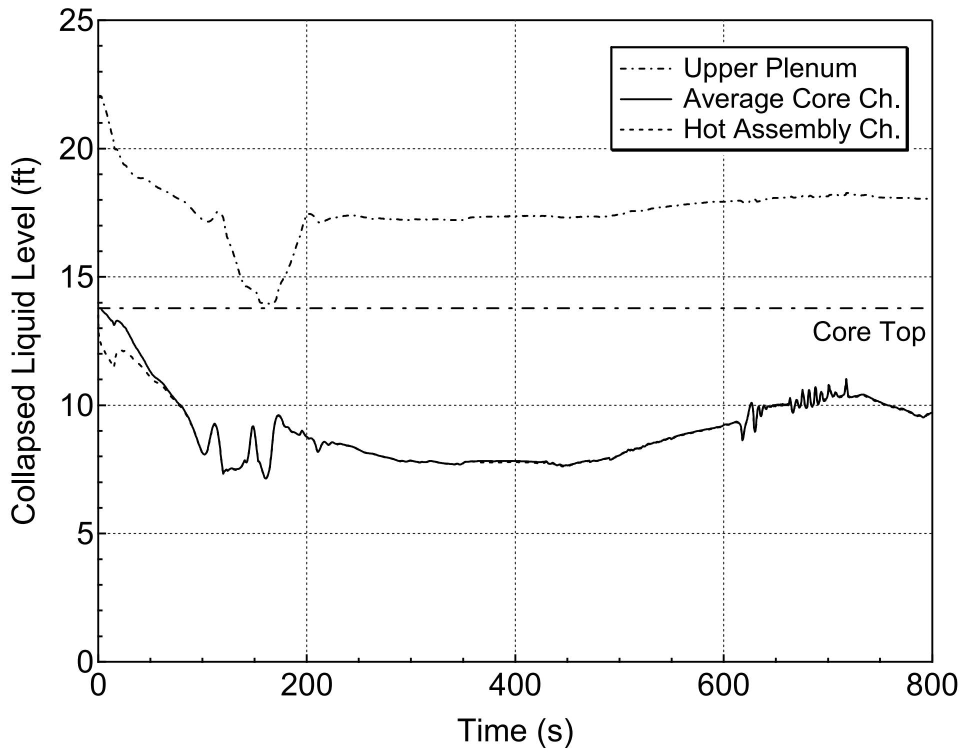

Figure 5.3.1.b-16 Core and Upper Plenum Collapsed Levels for 6.5-inch Break (Top) (Break Orientation Sensitivity Study)

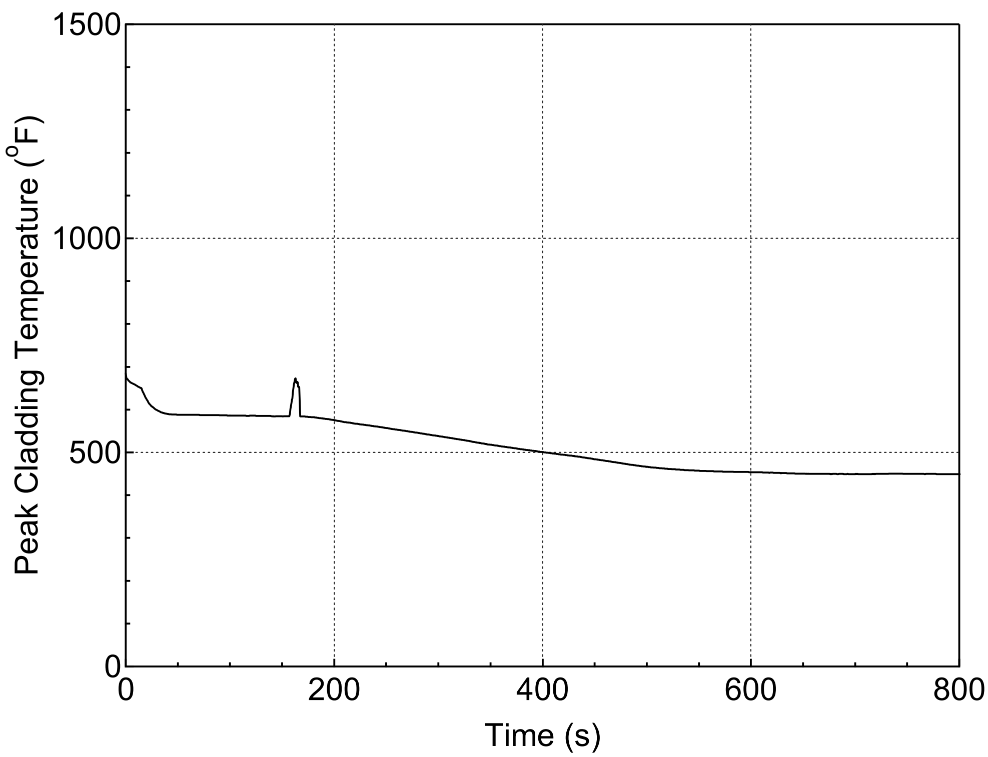

Figure 5.3.1.b-17 PCT at All Elevations for Hot Rod in Hot Assembly for 6.5-inch Break (Top) (Break Orientation Sensitivity Study)

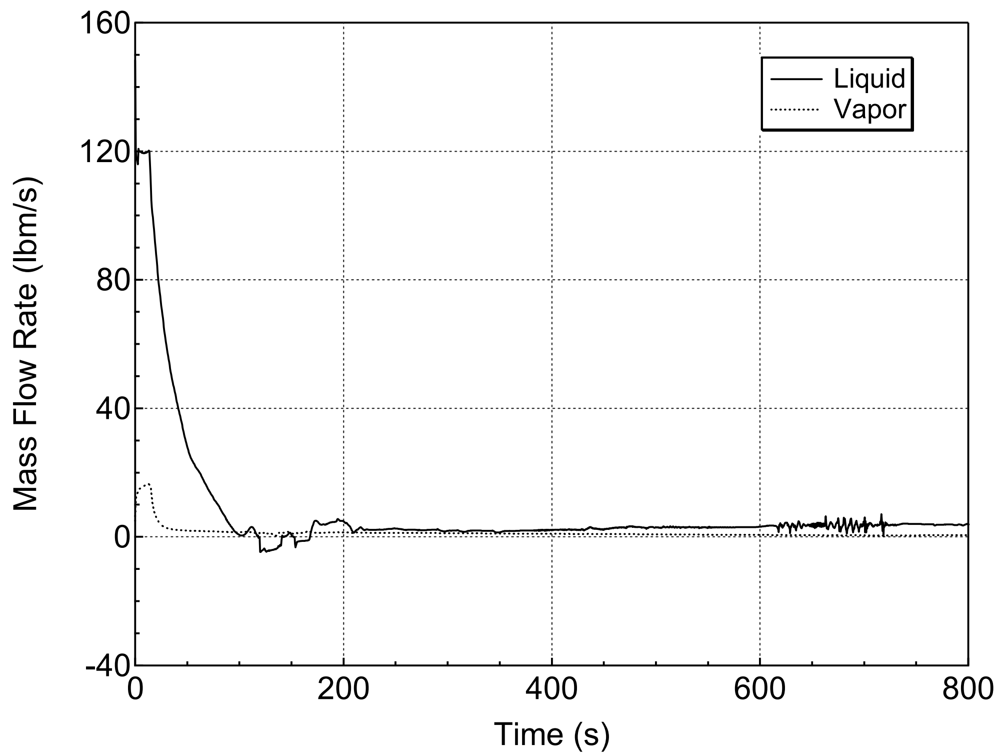

Figure 5.3.1.b-18 Hot Assembly Exit Vapor and Liquid Mass Flowrates for 6.5-inch Break (Top) (Break Orientation Sensitivity Study)

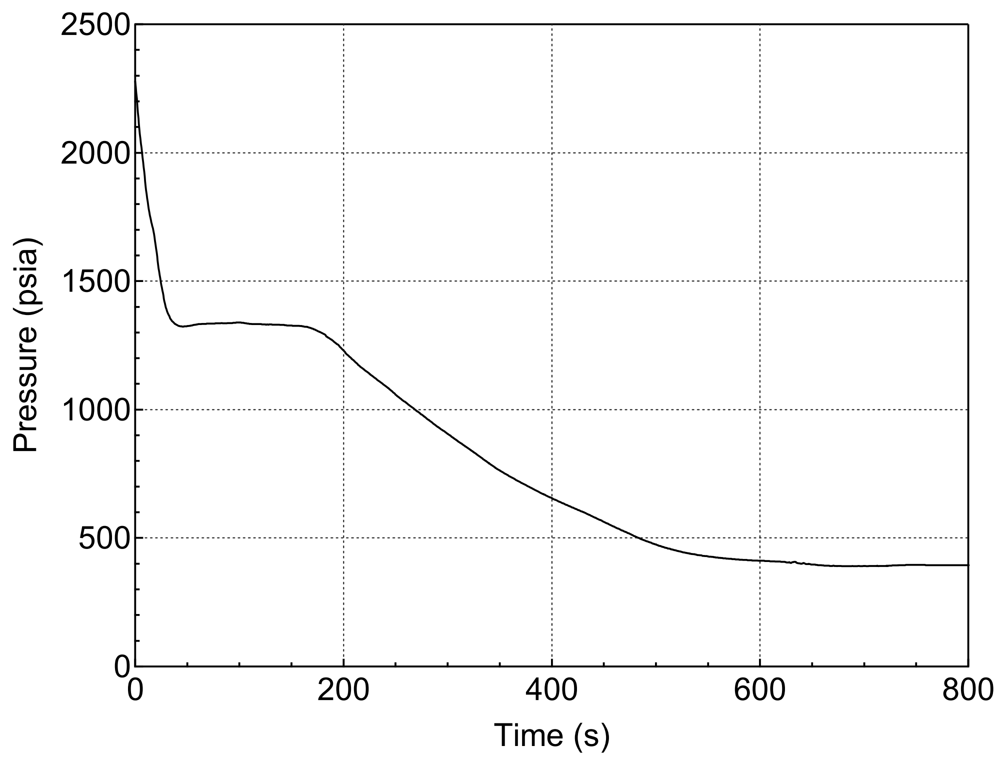

Figure 5.3.1.b-19 RCS (Pressurizer) Pressure Transient for 6.5-inch Break (Side) (Break Orientation Sensitivity Study)

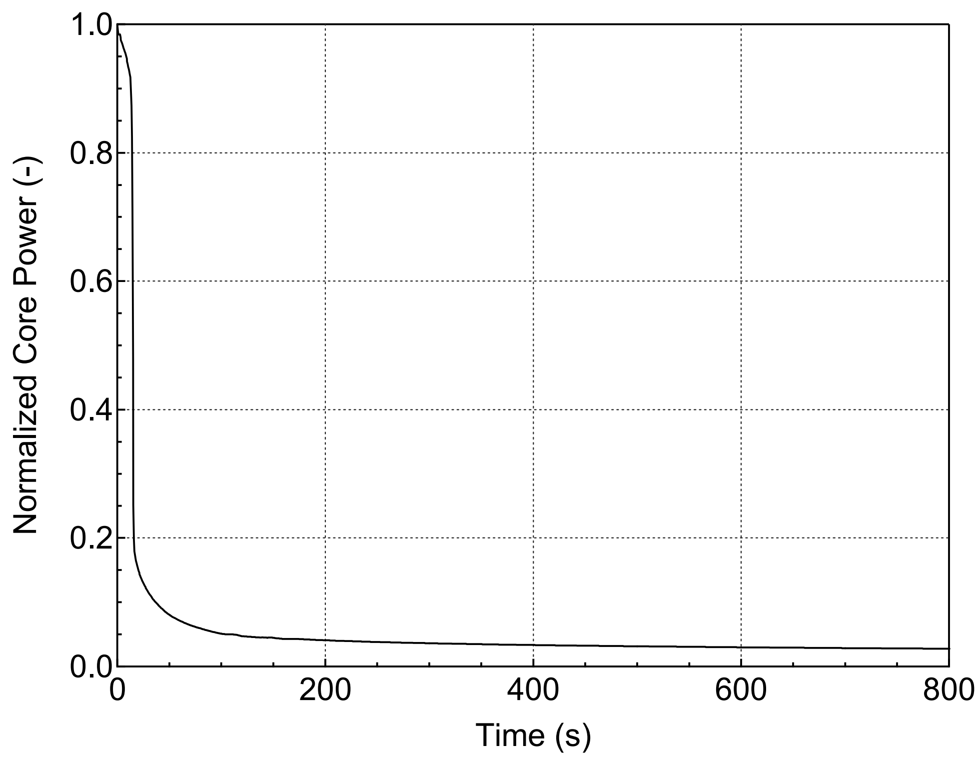

Figure 5.3.1.b-20 Normalized Core Power for 6.5-inch Break (Side)
(Break Orientation Sensitivity Study)

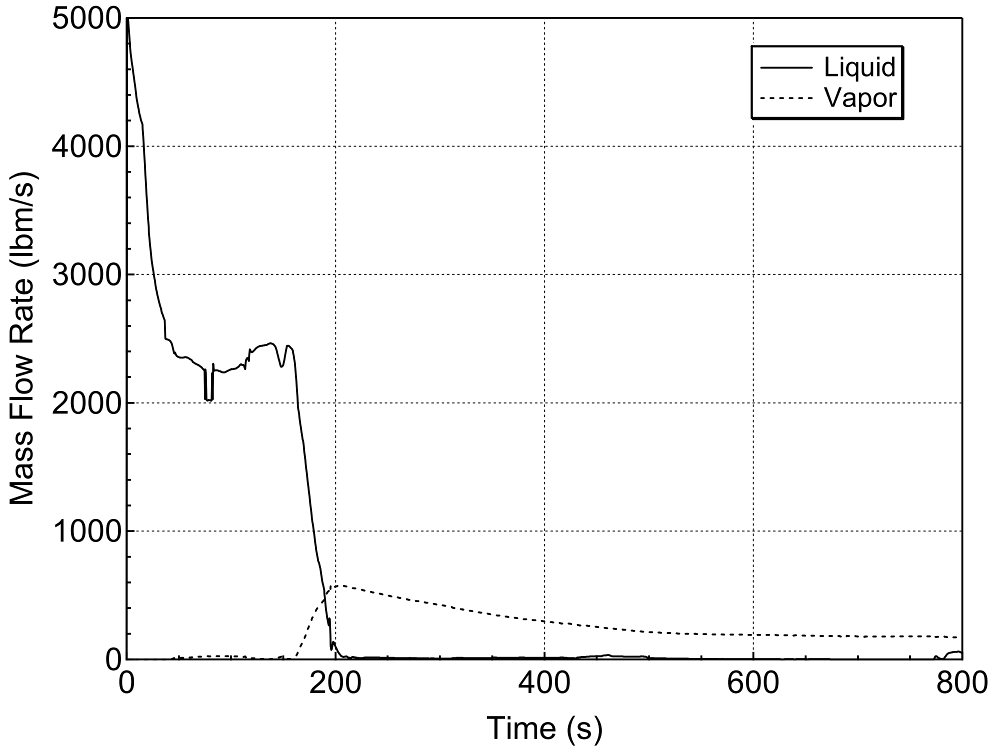

Figure 5.3.1.b-21 Liquid and Vapor Discharges through the Break for 6.5-inch Break (Side) (Break Orientation Sensitivity Study)

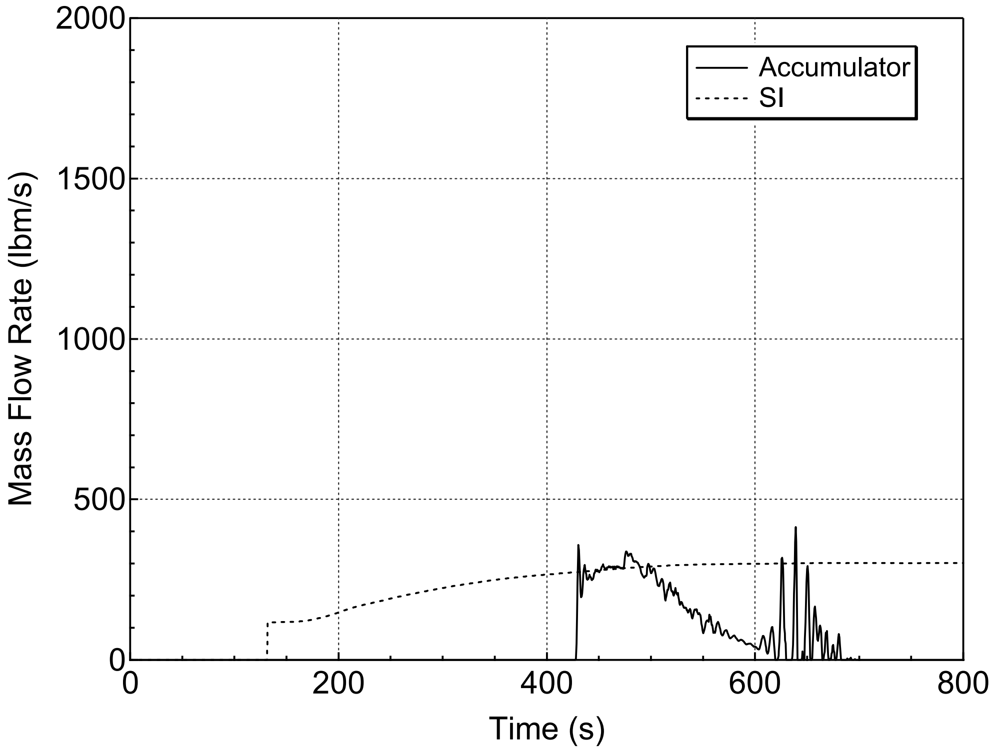

Figure 5.3.1.b-22 Accumulator and Safety Injection Mass Flowrates for 6.5-inch Break (Side) (Break Orientation Sensitivity Study)

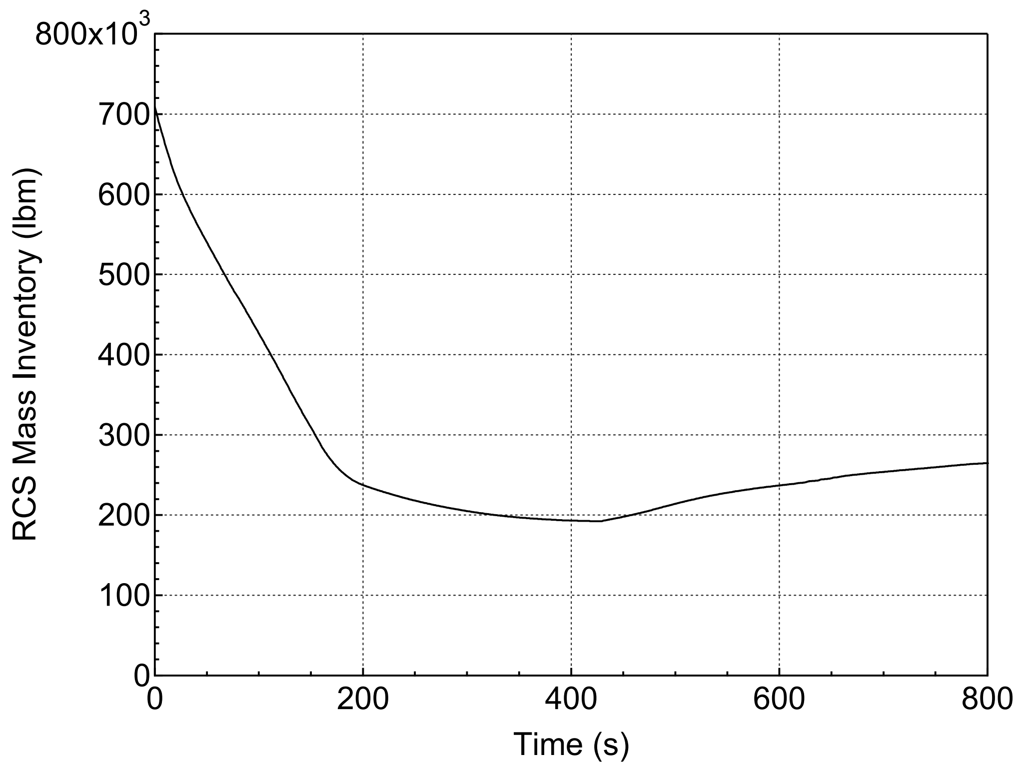

Figure 5.3.1.b-23 RCS Mass Inventory for 6.5-inch Break (Side) (Break Orientation Sensitivity Study)

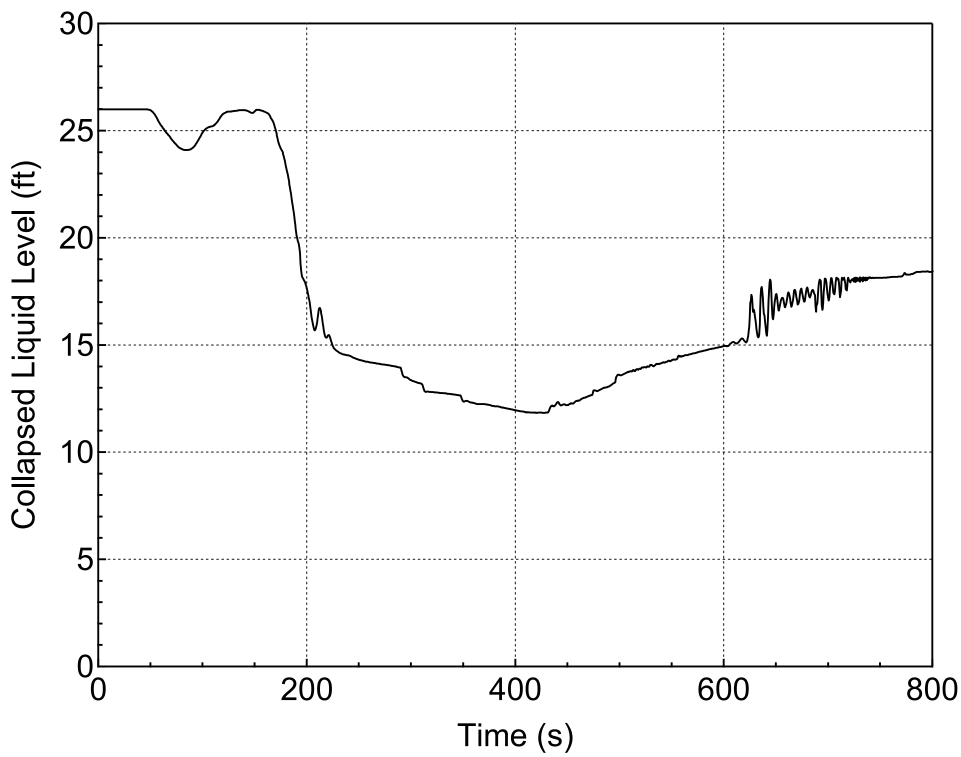

Figure 5.3.1.b-24 Downcomer Collapsed Level for 6.5-inch Break (Side) (Break Orientation Sensitivity Study)

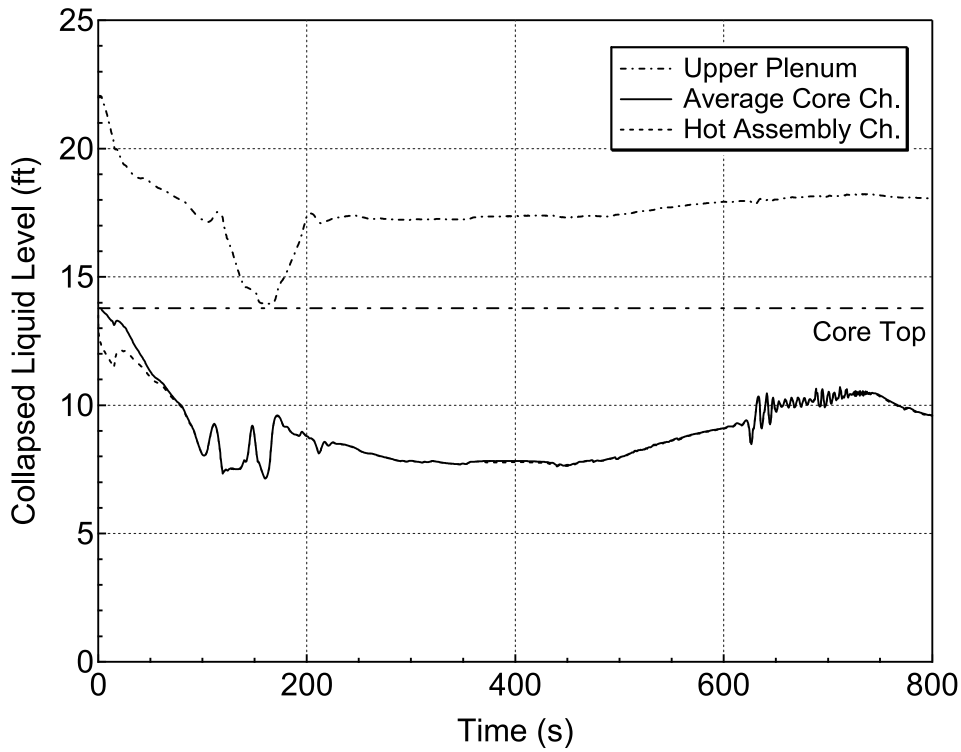

Figure 5.3.1.b-25 Core and Upper Plenum Collapsed Levels for 6.5-inch Break (Side) (Break Orientation Sensitivity Study)

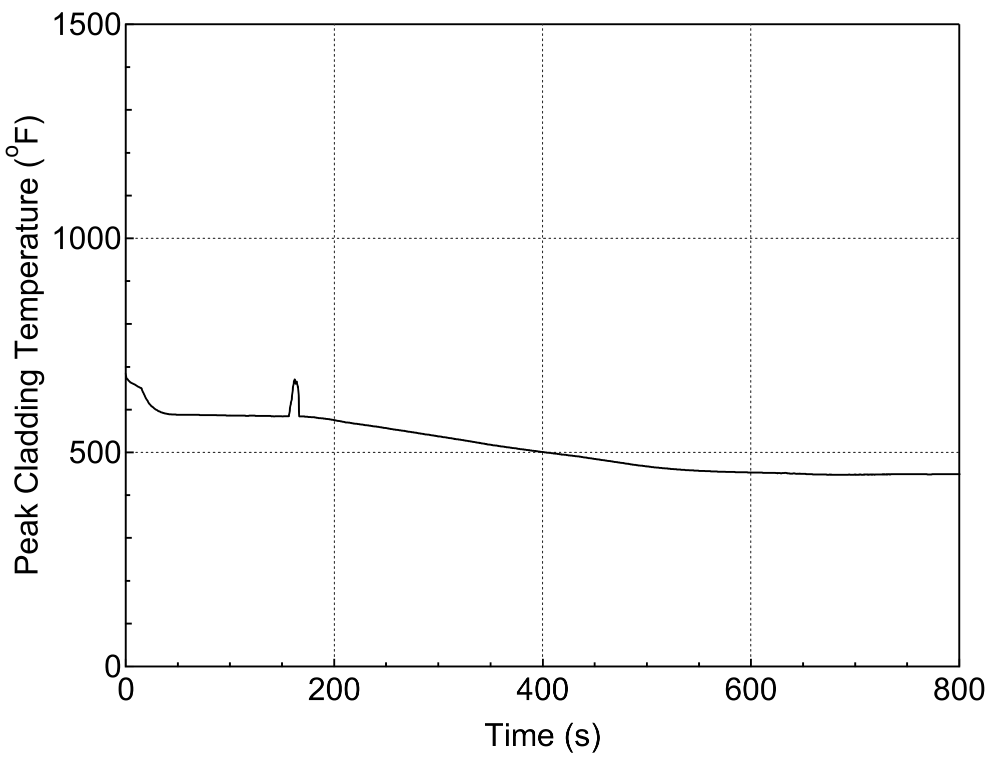

Figure 5.3.1.b-26 PCT at All Elevations for Hot Rod in Hot Assembly for 6.5-inch Break (Side) (Break Orientation Sensitivity Study)

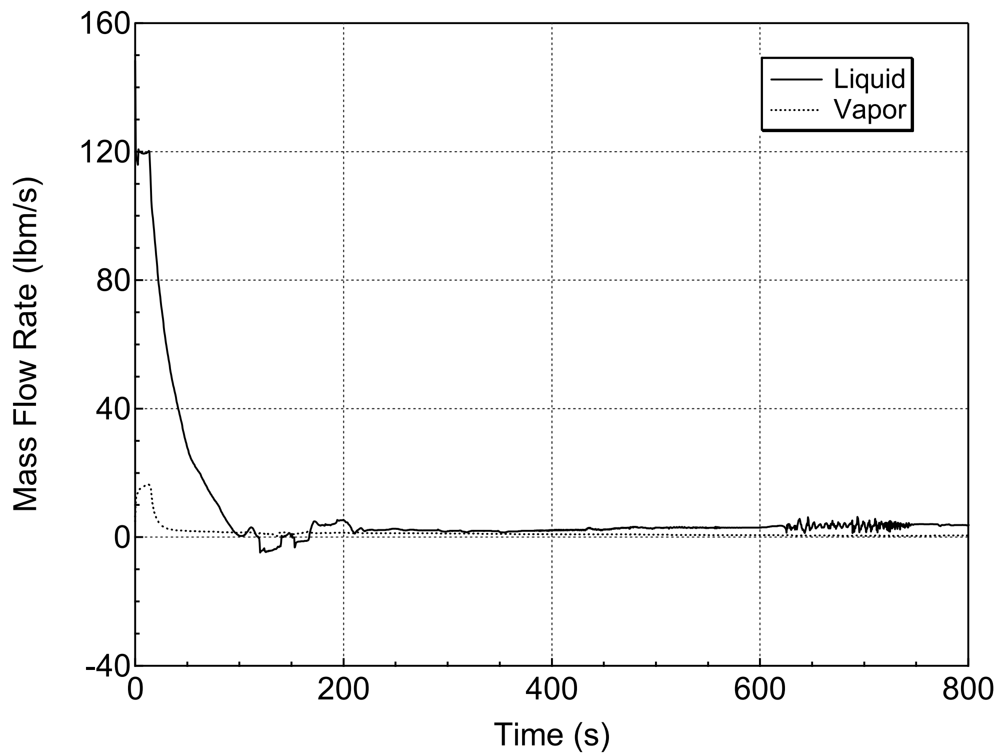

Figure 5.3.1.b-27 Hot Assembly Exit Vapor and Liquid Mass Flowrates for 6.5-inch Break (Side) (Break Orientation Sensitivity Study)

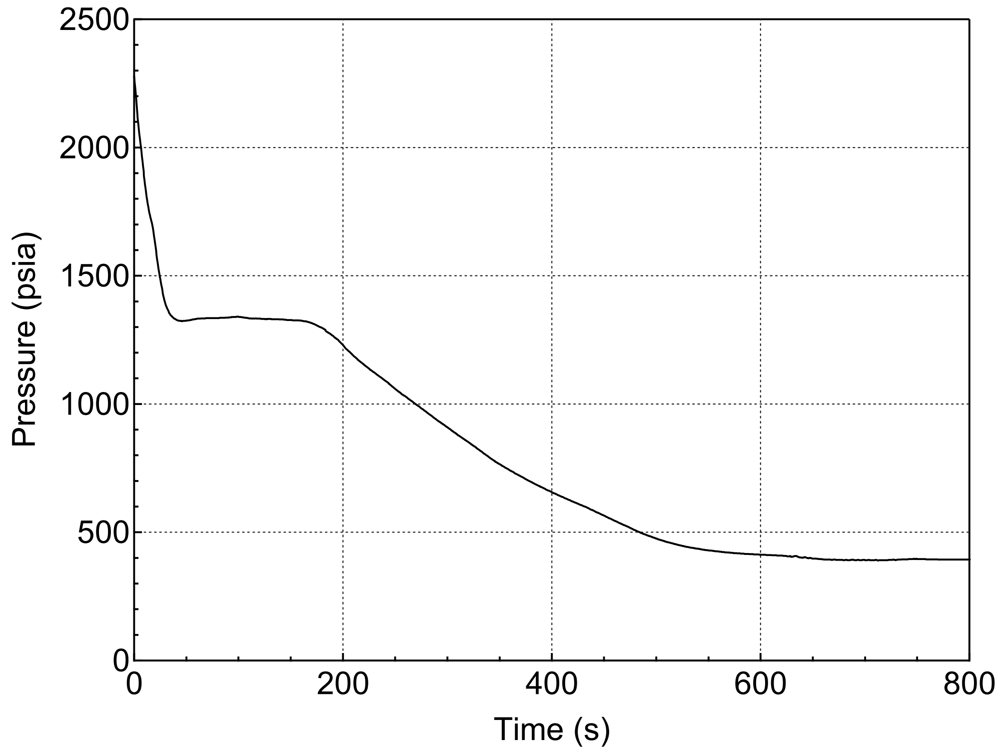

Figure 5.3.1.b-28 RCS (Pressurizer) Pressure Transient for 6.5-inch Break (Homogeneous) (Break Orientation Sensitivity Study)

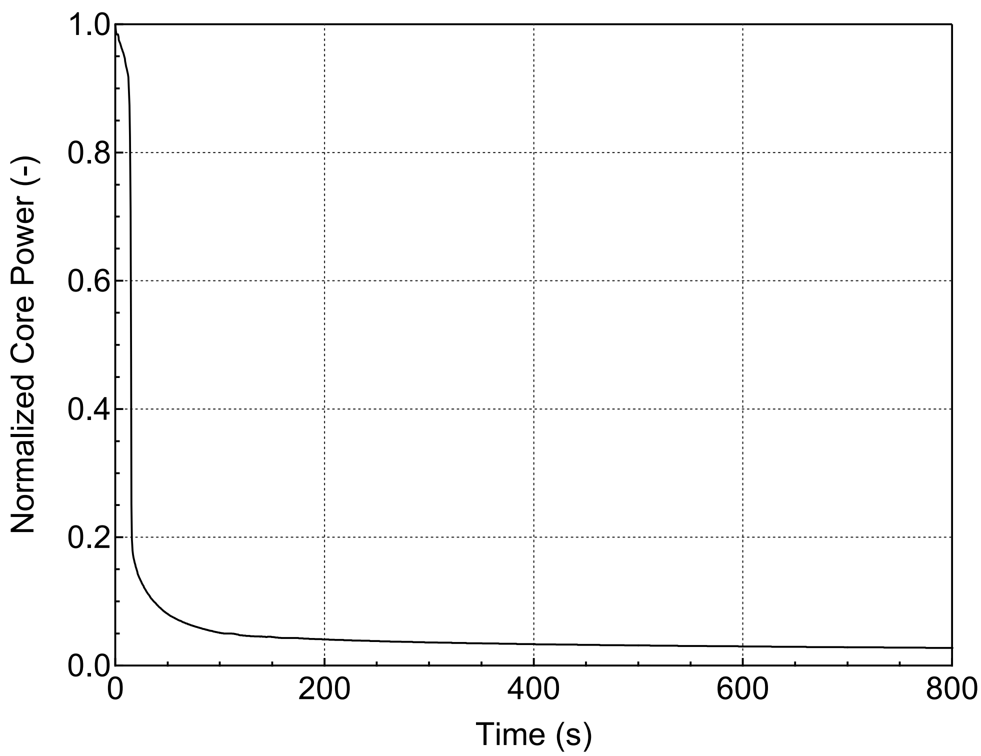

Figure 5.3.1.b-29 Normalized Core Power for 6.5-inch Break (Homogeneous) (Break Orientation Sensitivity Study)

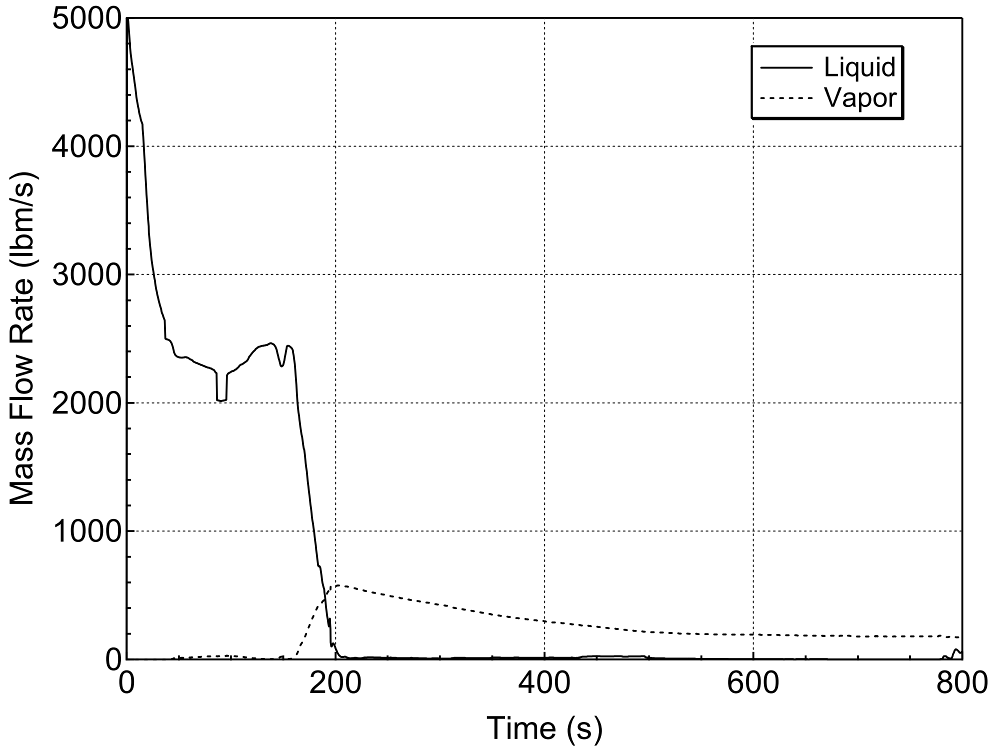

Figure 5.3.1.b-30 Liquid and Vapor Discharges through the Break for 6.5-inch Break (Homogeneous) (Break Orientation Sensitivity Study)

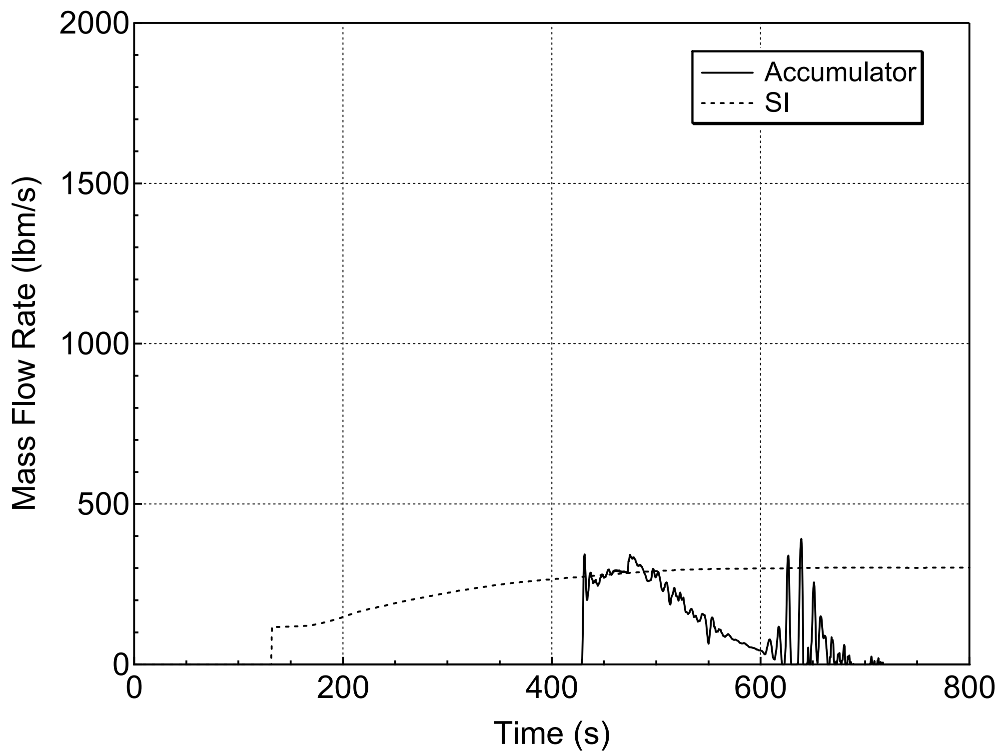

Figure 5.3.1.b-31 Accumulator and Safety Injection Mass Flowrates for 6.5-inch Break (Homogeneous) (Break Orientation Sensitivity Study)

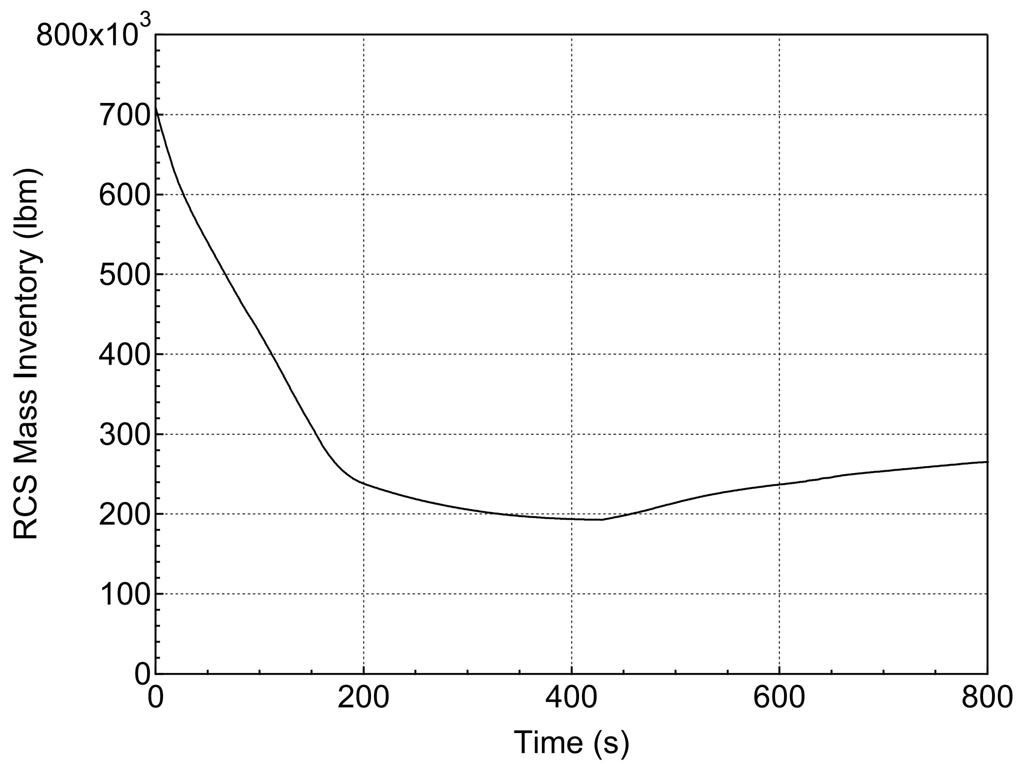

Figure 5.3.1.b-32 RCS Mass Inventory for 6.5-inch Break (Homogeneous) (Break Orientation Sensitivity Study)

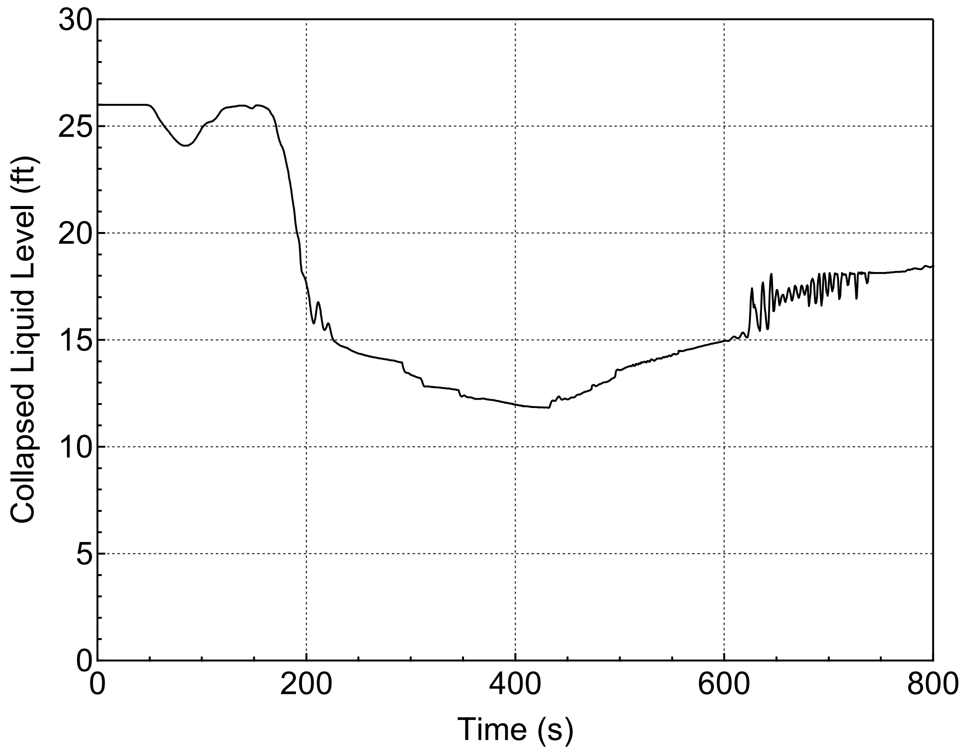

Figure 5.3.1.b-33 Downcomer Collapsed Level for 6.5-inch Break (Homogeneous) (Break Orientation Sensitivity Study)

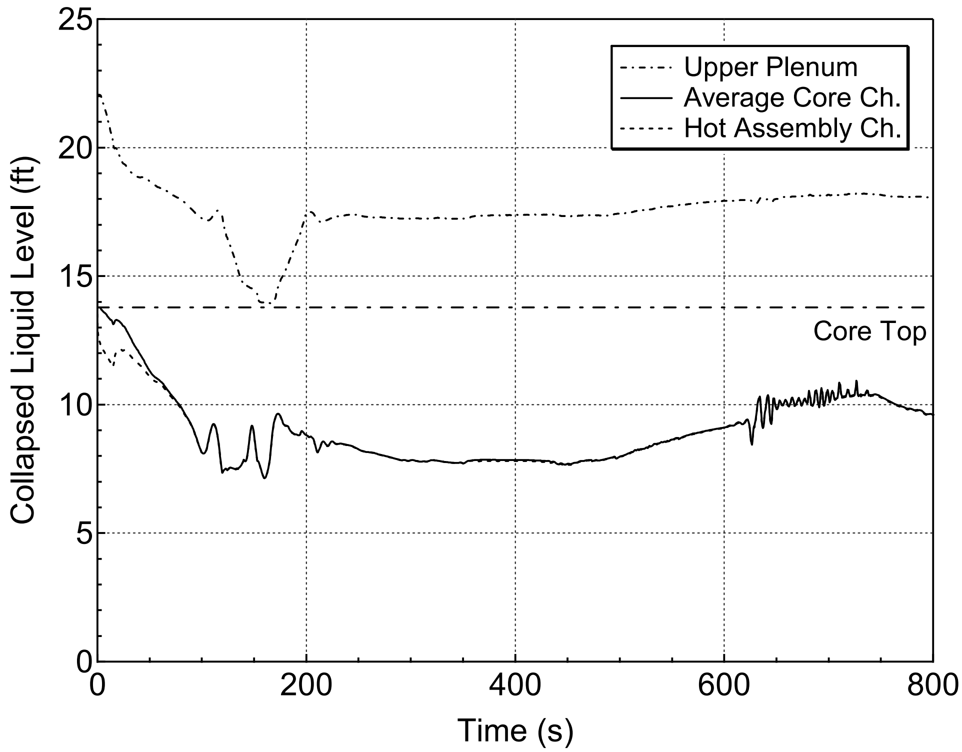

Figure 5.3.1.b-34 Core and Upper Plenum Collapsed Levels for 6.5-inch Break (Homogeneous) (Break Orientation Sensitivity Study)

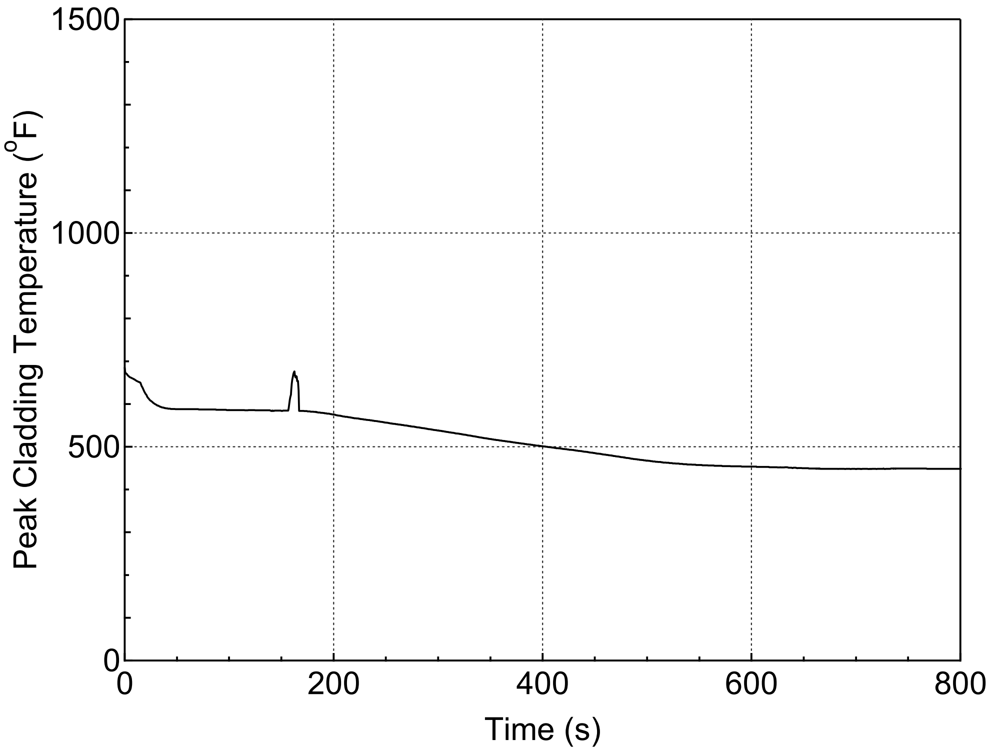

Figure 5.3.1.b-35 PCT at All Elevations for Hot Rod in Hot Assembly for 6.5-inch Break (Homogeneous) (Break Orientation Sensitivity Study)

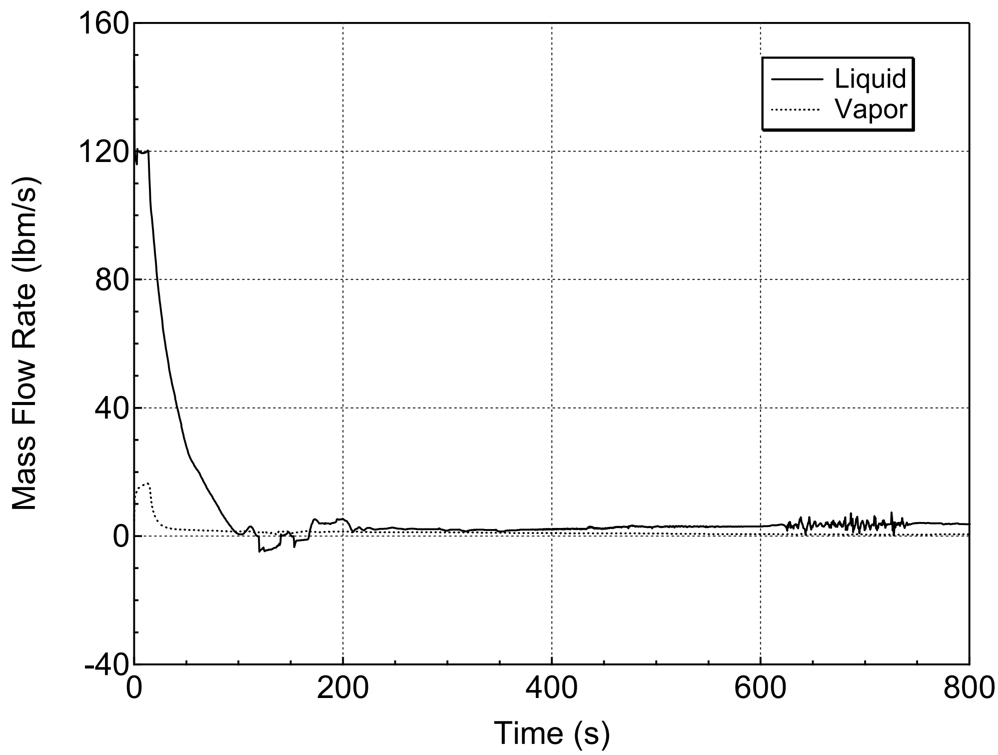

Figure 5.3.1.b-36 Hot Assembly Exit Vapor and Liquid Mass Flowrates for 6.5-inch Break (Homogeneous) (Break Orientation Sensitivity Study)

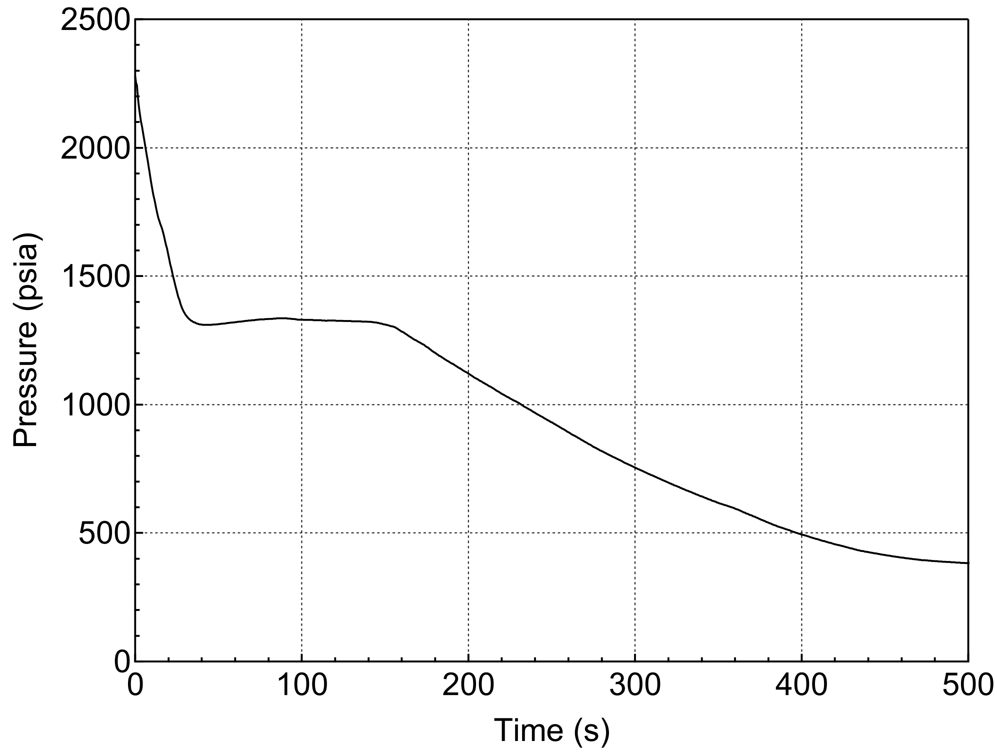

Figure 5.3.1.c-1 RCS (Pressurizer) Pressure Transient for 7-inch Break (Top) (Break Orientation Sensitivity Study)

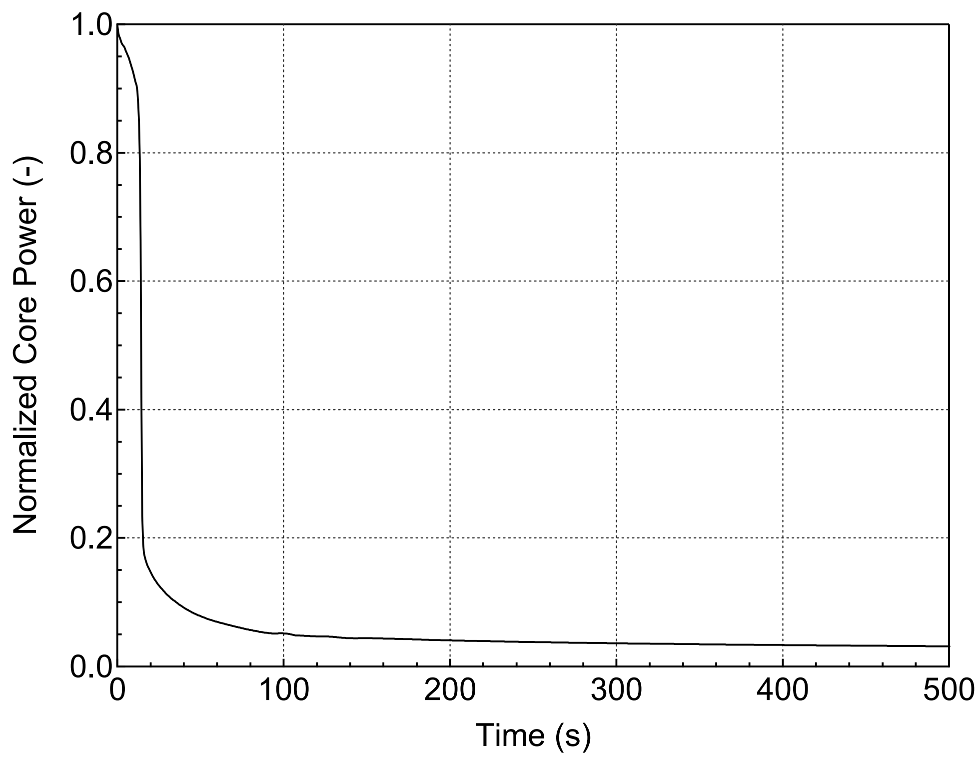

Figure 5.3.1.c-2 Normalized Core Power for 7-inch Break (Top) (Break Orientation Sensitivity Study)

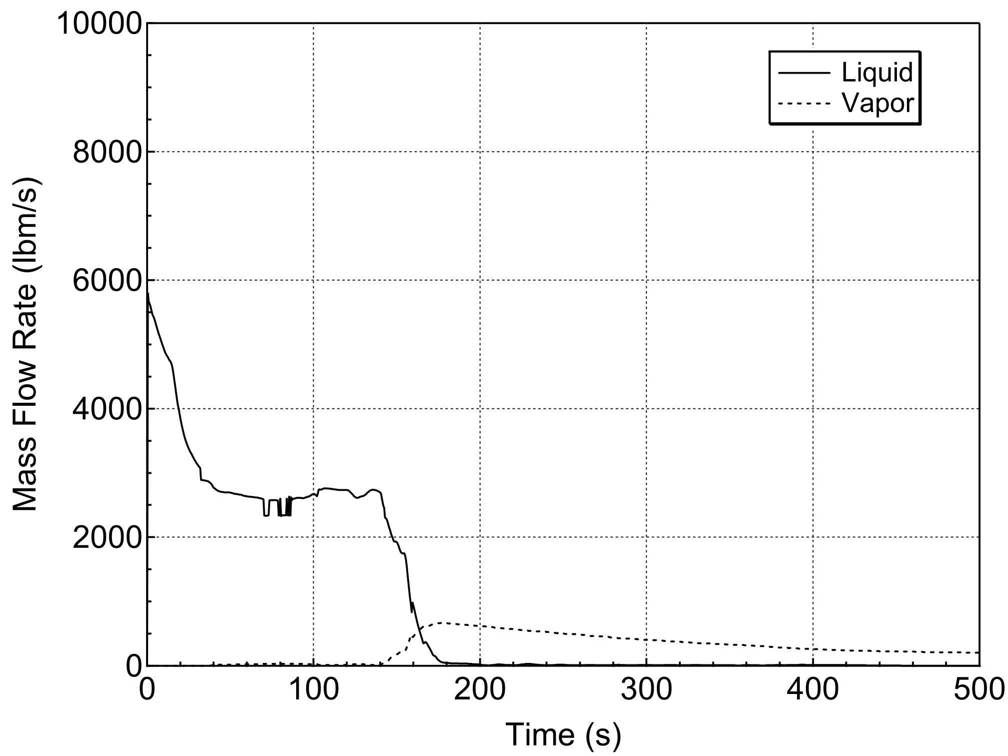

Figure 5.3.1.c-3 Liquid and Vapor Discharges through the Break for 7-inch Break (Top) (Break Orientation Sensitivity Study)

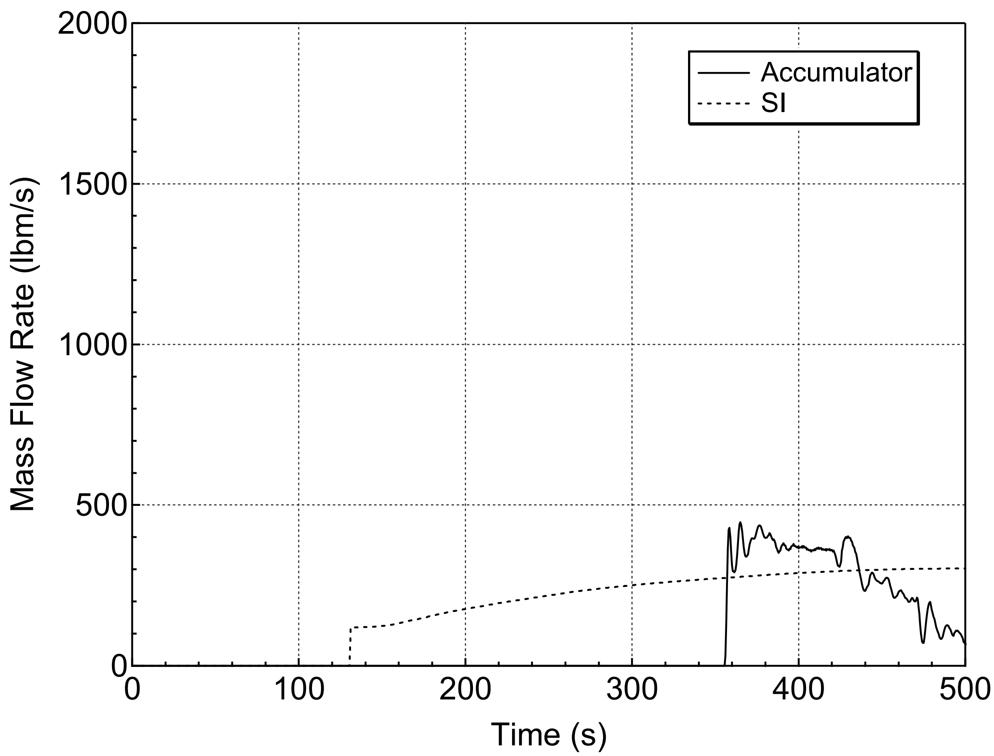

Figure 5.3.1.c-4 Accumulator and Safety Injection Mass Flowrates for 7-inch Break (Top) (Break Orientation Sensitivity Study)

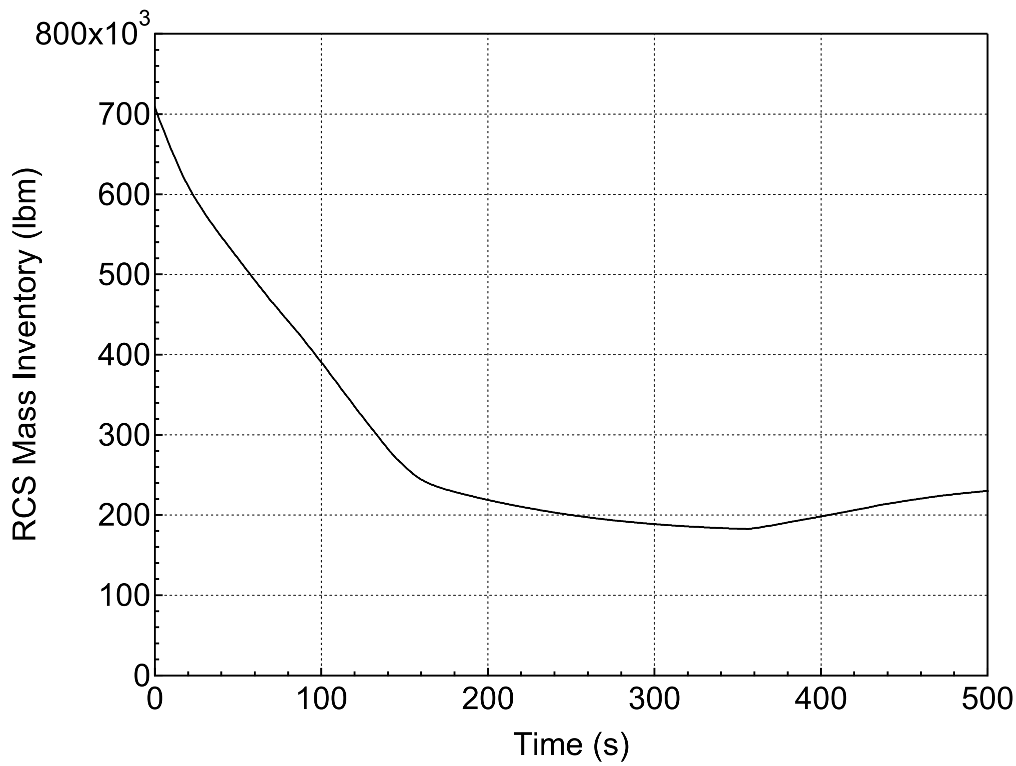

Figure 5.3.1.c-5 RCS Mass Inventory for 7-inch Break (Top)
(Break Orientation Sensitivity Study)

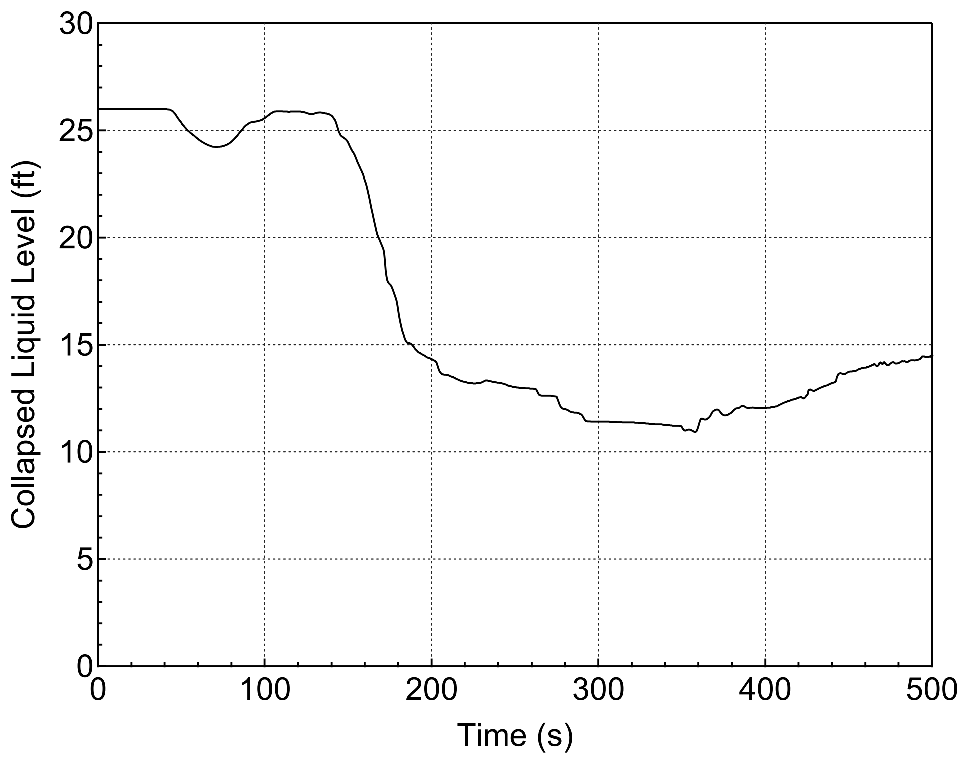

Figure 5.3.1.c-6 Downcomer Collapsed Level for 7-inch Break (Top) (Break Orientation Sensitivity Study)

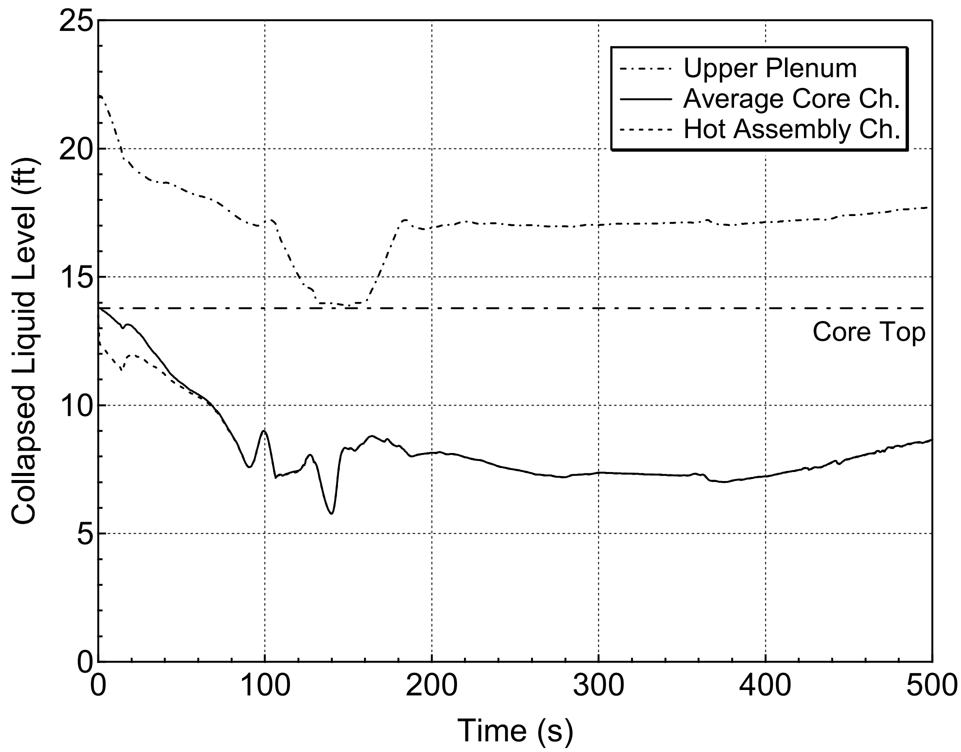

Figure 5.3.1.c-7 Core and Upper Plenum Collapsed Levels for 7-inch Break (Top) (Break Orientation Sensitivity Study)

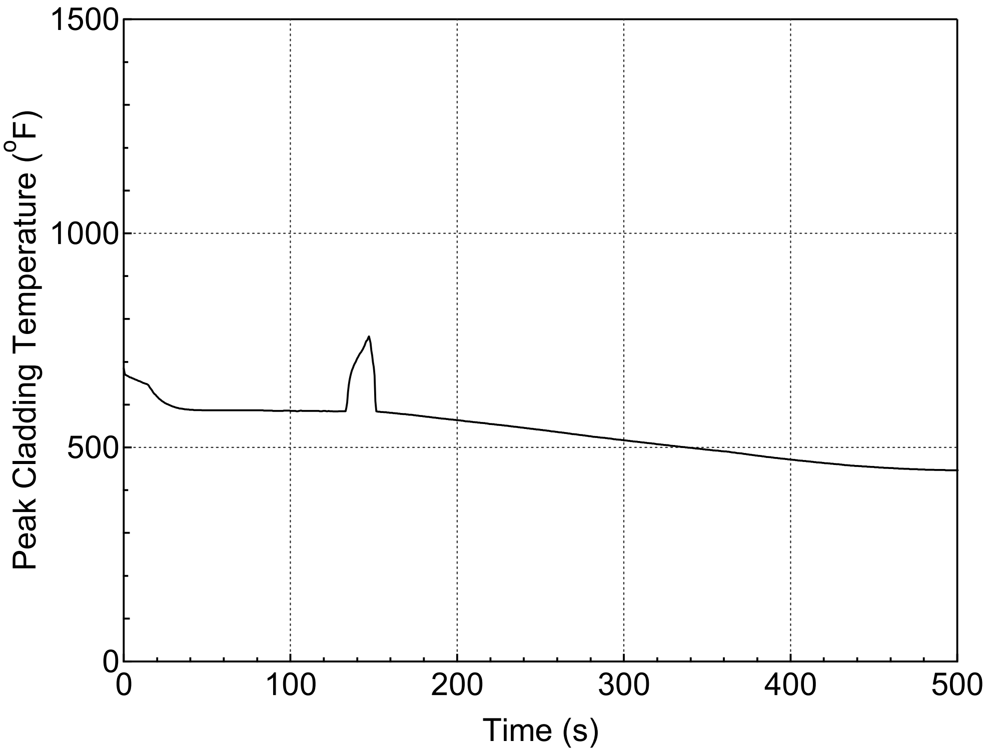

Figure 5.3.1.c-8 PCT at All Elevations for Hot Rod in Hot Assembly for 7-inch Break (Top) (Break Orientation Sensitivity Study)

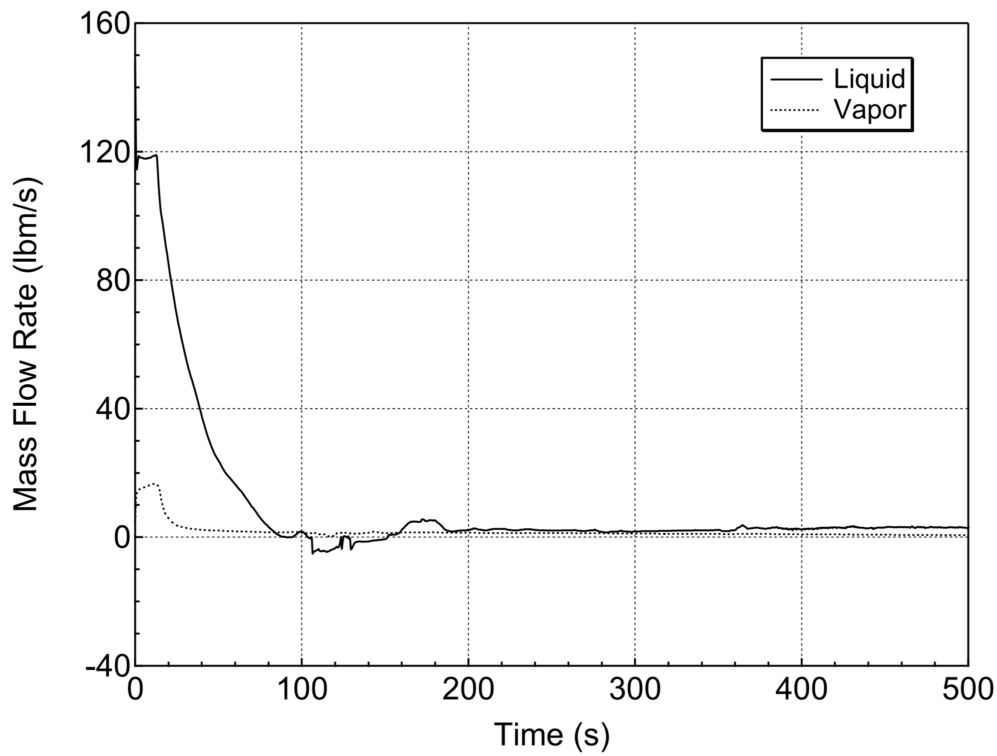

Figure 5.3.1.c-9 Hot Assembly Exit Vapor and Liquid Mass Flowrates for 7-inch Break (Top) (Break Orientation Sensitivity Study)

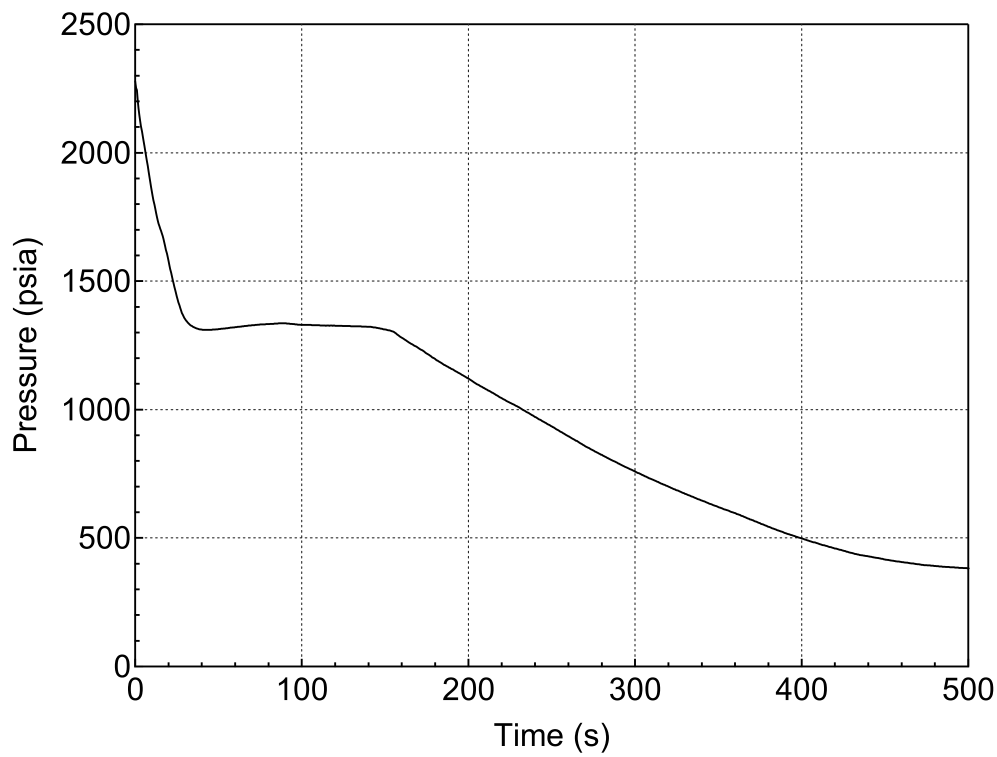

Figure 5.3.1.c-10 RCS (Pressurizer) Pressure Transient for 7-inch Break (Side) (Break Orientation Sensitivity Study)

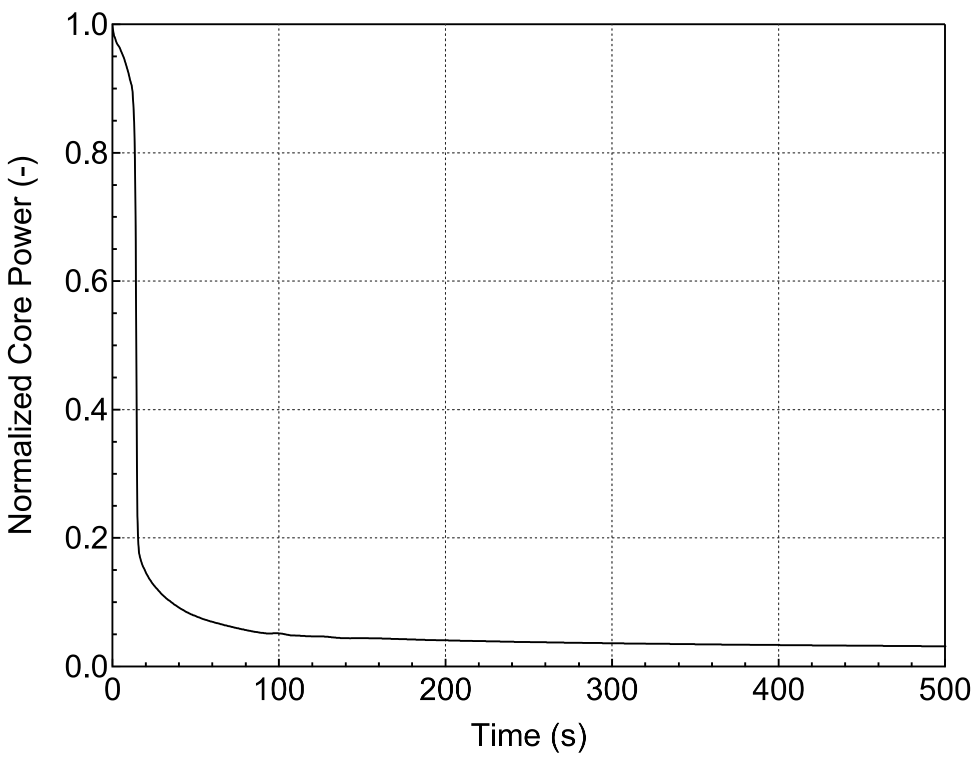

Figure 5.3.1.c-11 Normalized Core Power for 7-inch Break (Side) (Break Orientation Sensitivity Study)

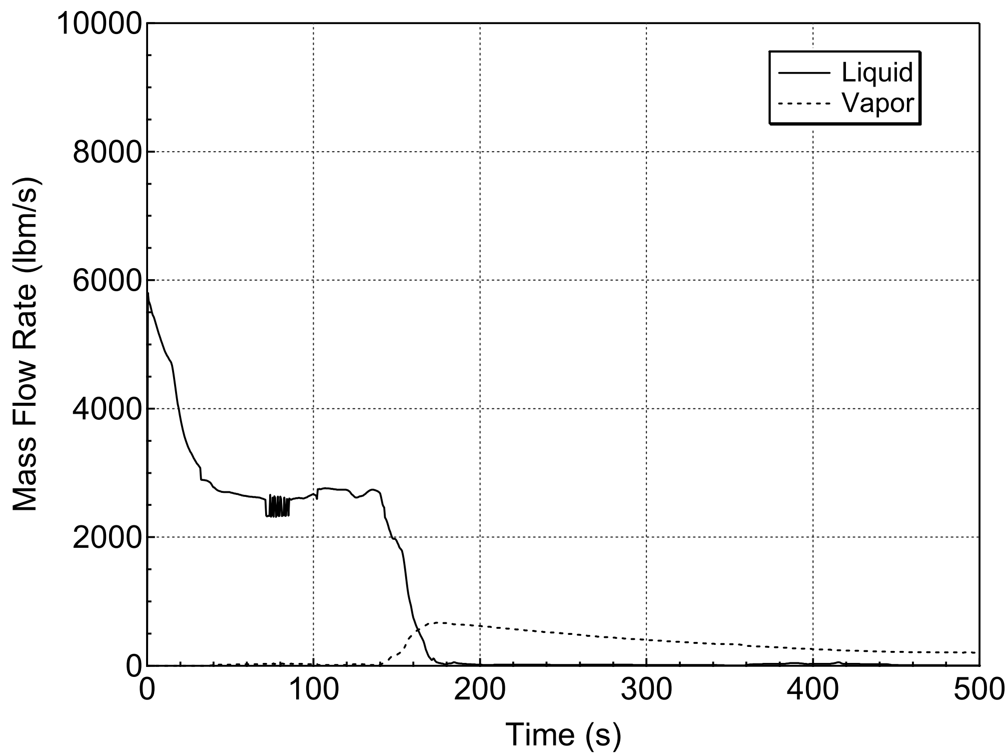

Figure 5.3.1.c-12 Liquid and Vapor Discharges through the Break for 7-inch Break (Side) (Break Orientation Sensitivity Study)

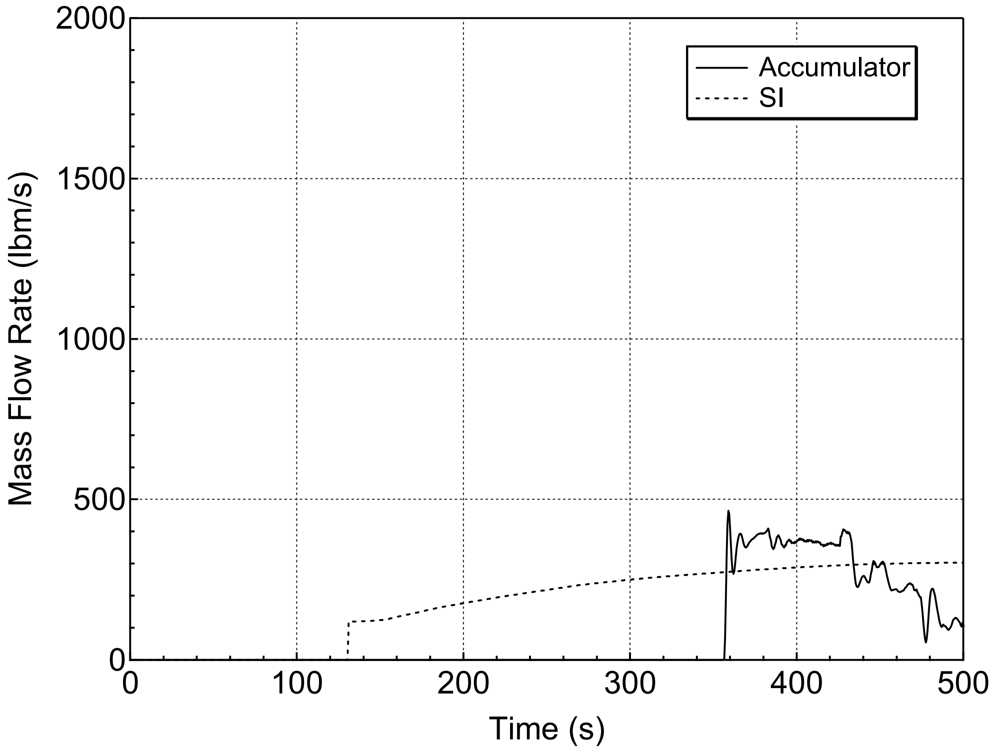

Figure 5.3.1.c-13 Accumulator and Safety Injection Mass Flowrates for 7-inch Break (Side) (Break Orientation Sensitivity Study)

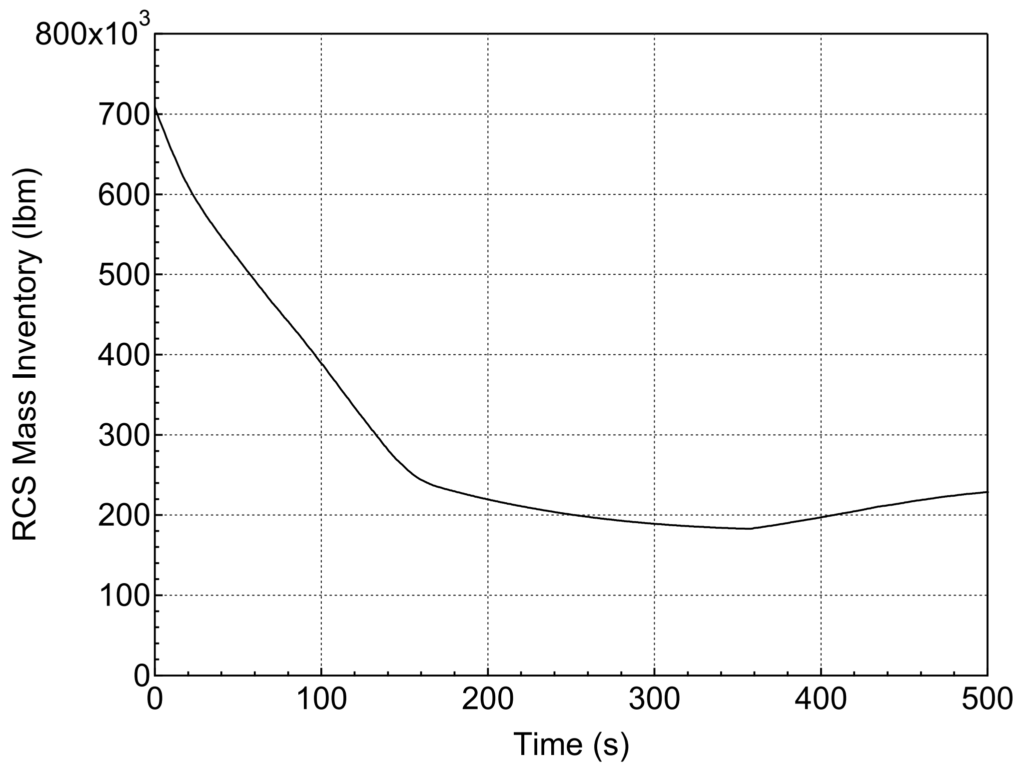

Figure 5.3.1.c-14 RCS Mass Inventory for 7-inch Break (Side)
(Break Orientation Sensitivity Study)

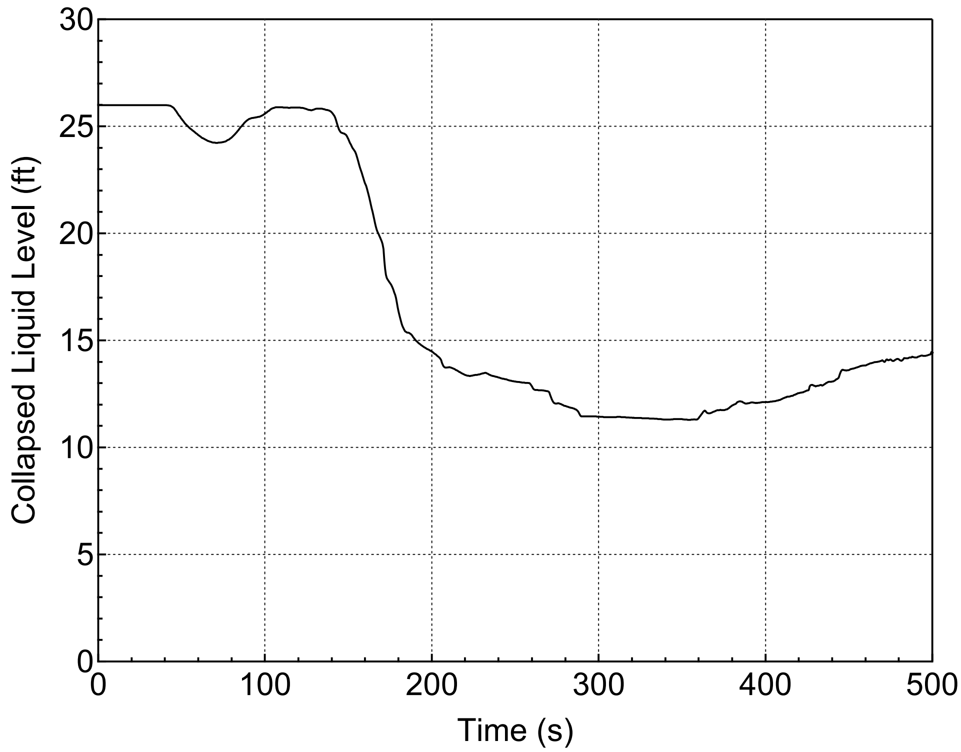

Figure 5.3.1.c-15 Downcomer Collapsed Level for 7-inch Break (Side) (Break Orientation Sensitivity Study)

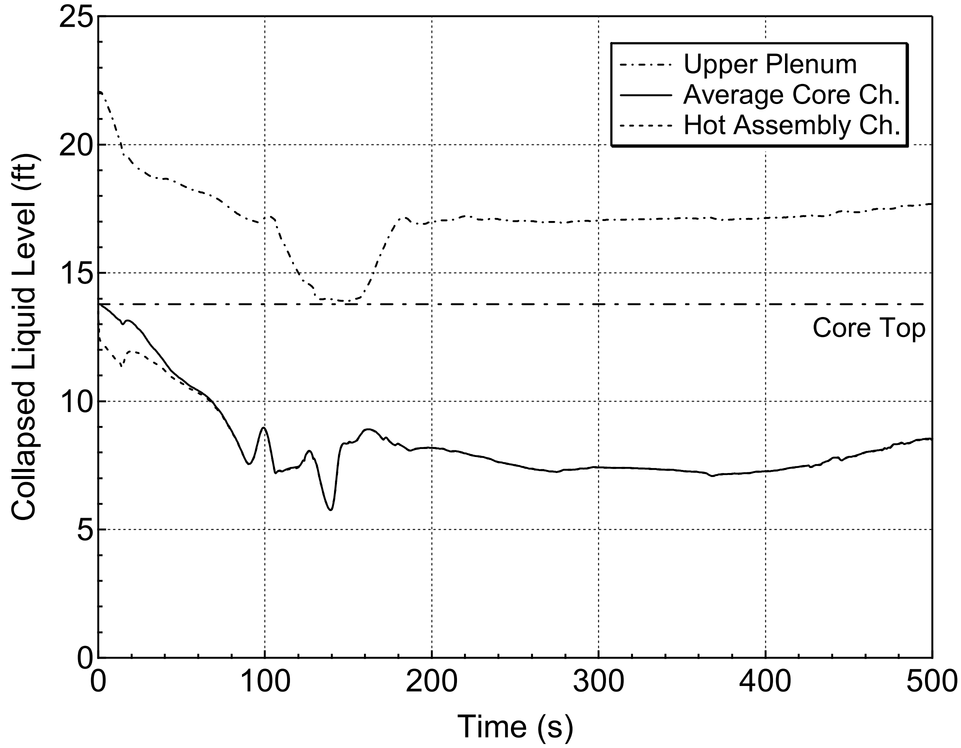

Figure 5.3.1.c-16 Core and Upper Plenum Collapsed Levels for 7-inch Break (Side) (Break Orientation Sensitivity Study)

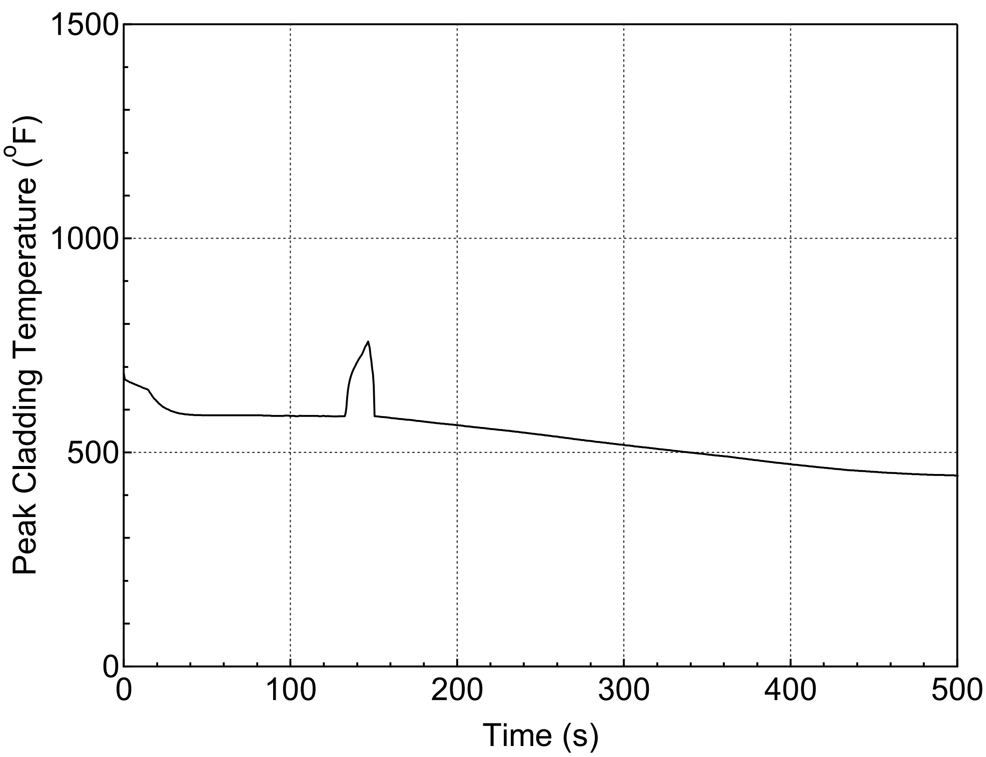

Figure 5.3.1.c-17 PCT at All Elevations for Hot Rod in Hot Assembly for 7-inch Break (Side) (Break Orientation Sensitivity Study)

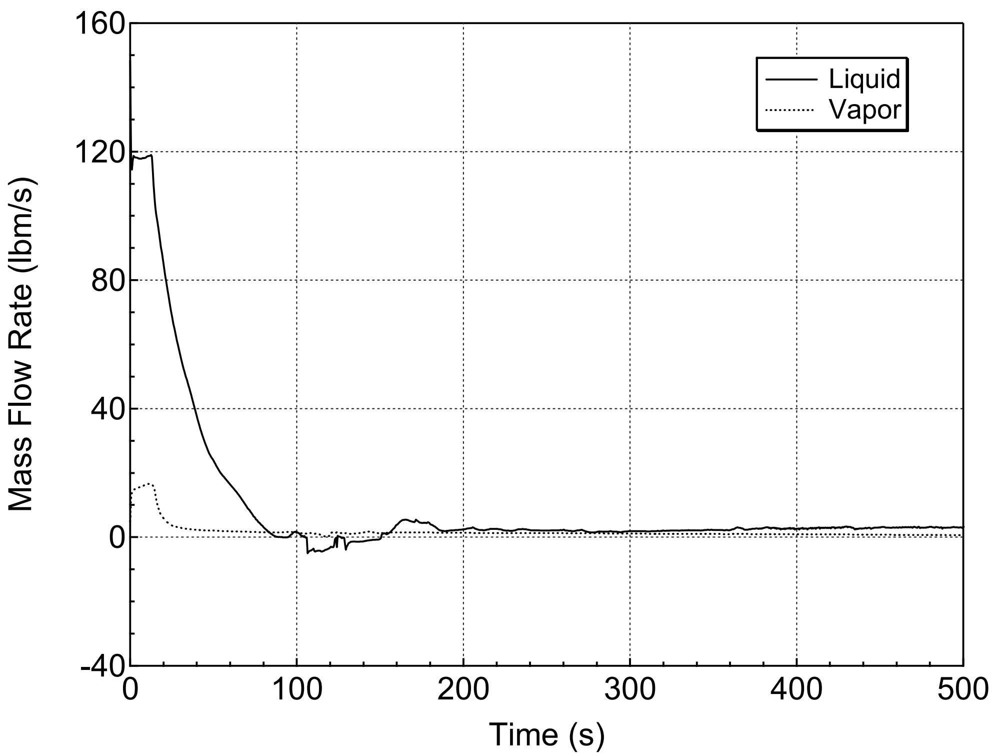

Figure 5.3.1.c-18 Hot Assembly Exit Vapor and Liquid Mass Flowrates for 7-inch Break (Side) (Break Orientation Sensitivity Study)

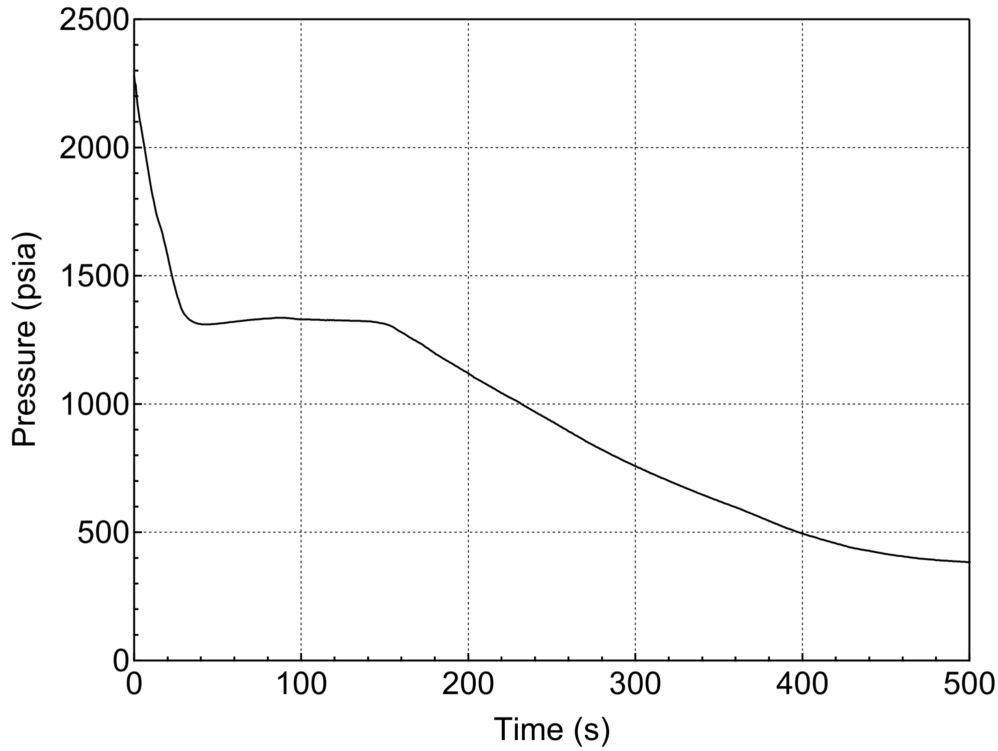

Figure 5.3.1.c-19 RCS (Pressurizer) Pressure Transient for 7-inch Break (Homogeneous) (Break Orientation Sensitivity Study)

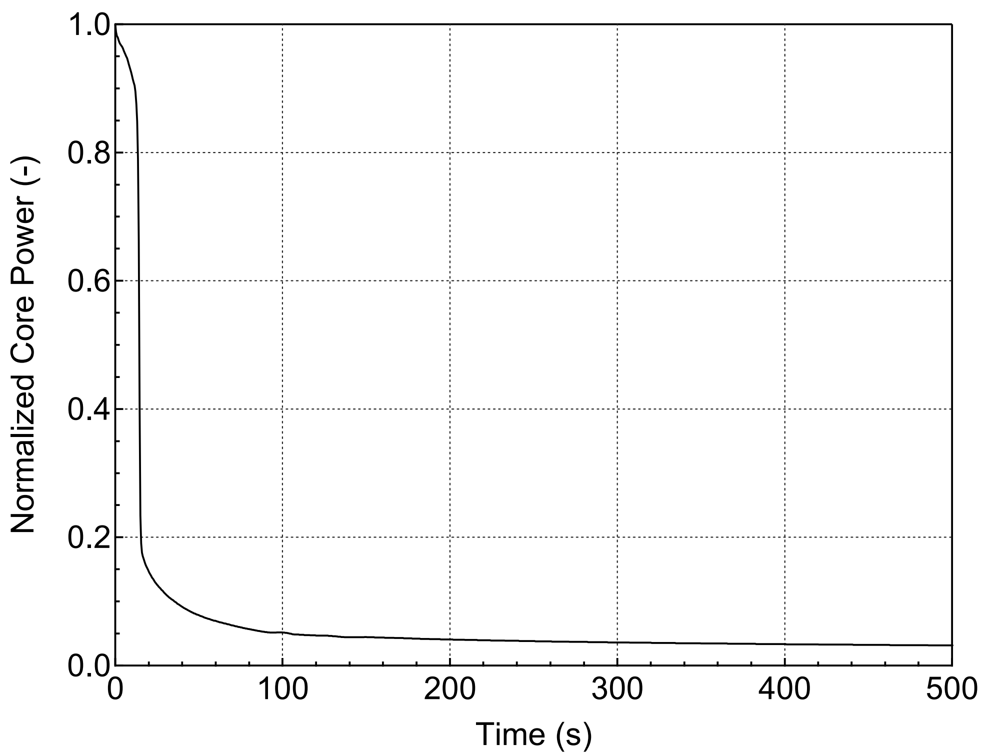

Figure 5.3.1.c-20 Normalized Core Power for 7-inch Break (Homogeneous) (Break Orientation Sensitivity Study)

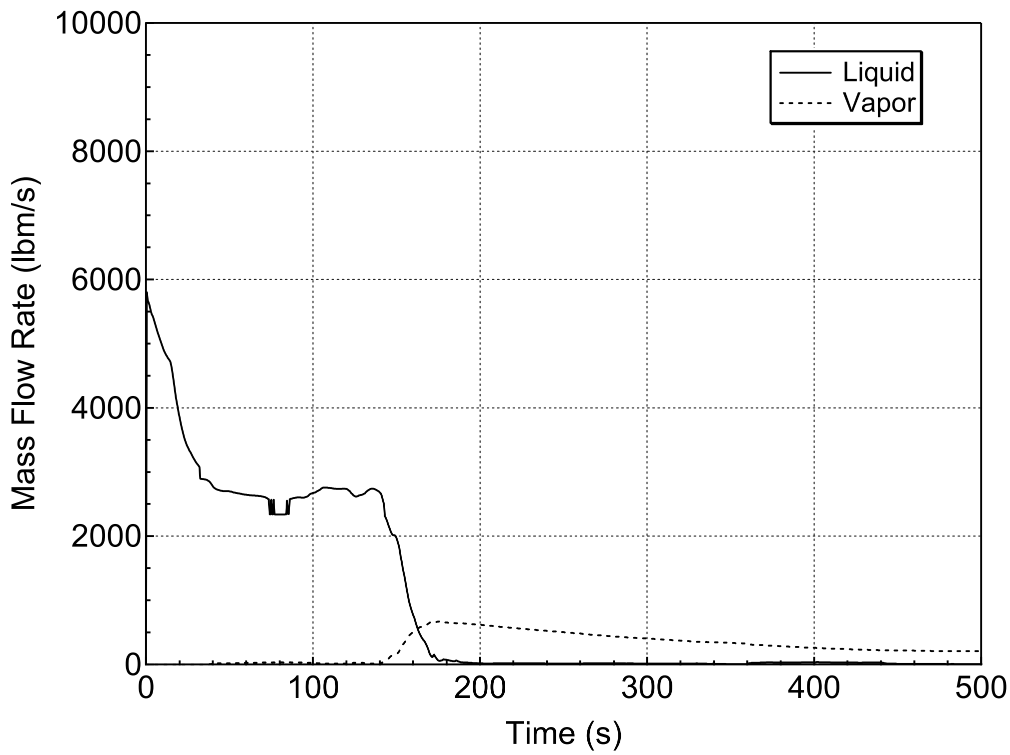

Figure 5.3.1.c-21 Liquid and Vapor Discharges through the Break for 7-inch Break (Homogeneous) (Break Orientation Sensitivity Study)

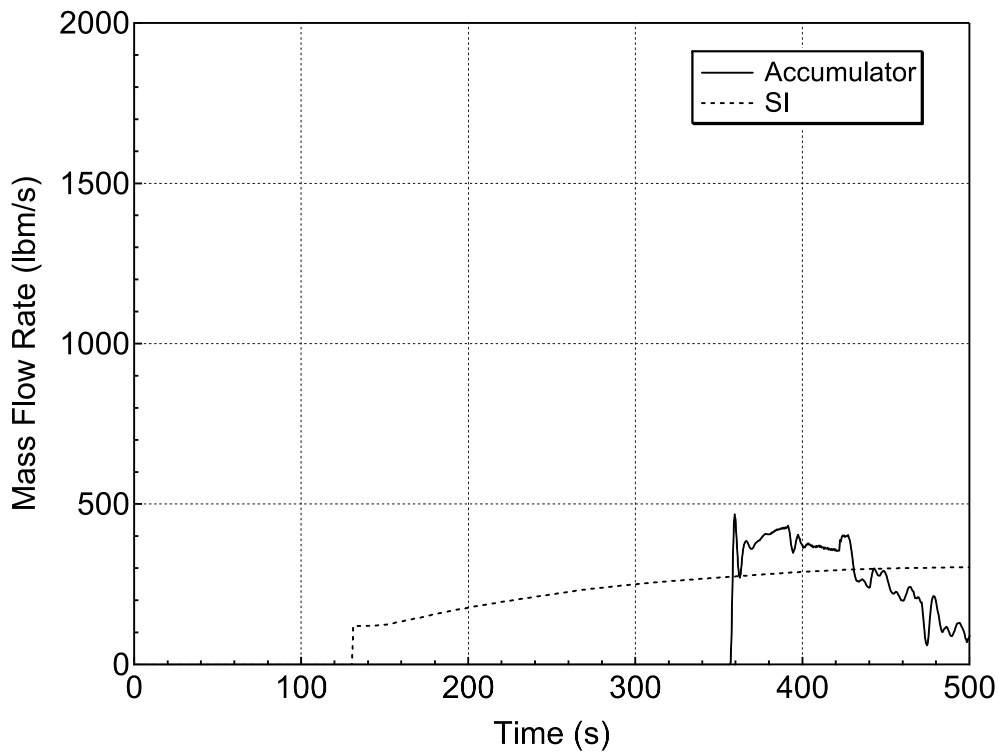

Figure 5.3.1.c-22 Accumulator and Safety Injection Mass Flowrates for 7-inch Break (Homogeneous) (Break Orientation Sensitivity Study)

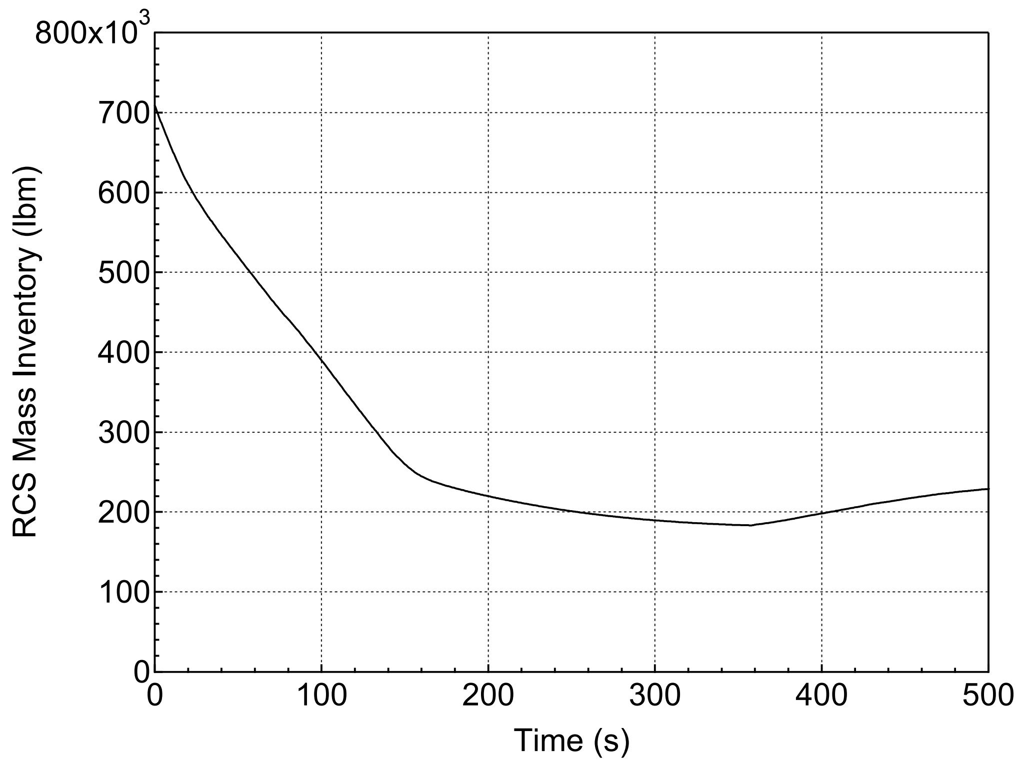

Figure 5.3.1.c-23 RCS Mass Inventory for 7-inch Break (Homogeneous) (Break Orientation Sensitivity Study)

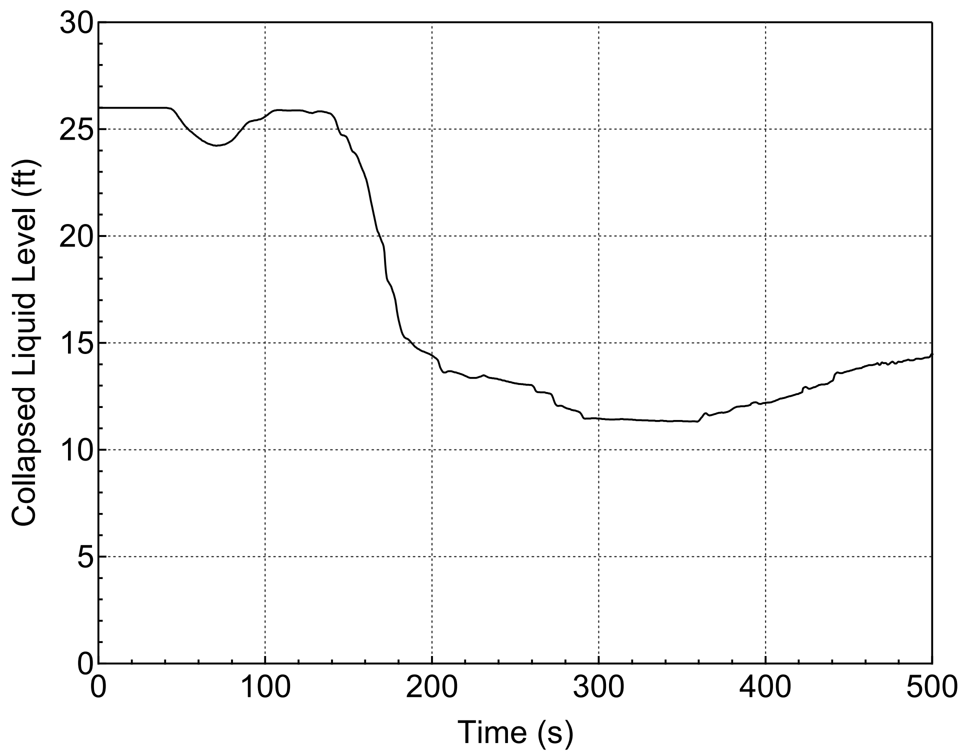

Figure 5.3.1.c-24 Downcomer Collapsed Level for 7-inch Break (Homogeneous) (Break Orientation Sensitivity Study)

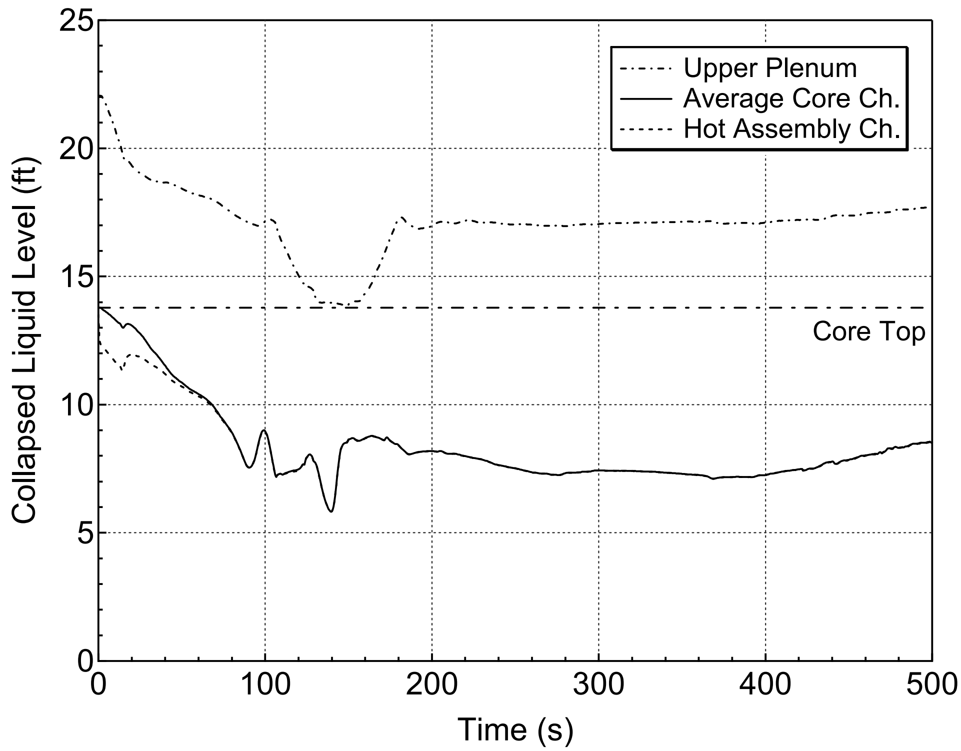

Figure 5.3.1.c-25 Core and Upper Plenum Collapsed Levels for 7-inch Break (Homogeneous) (Break Orientation Sensitivity Study)

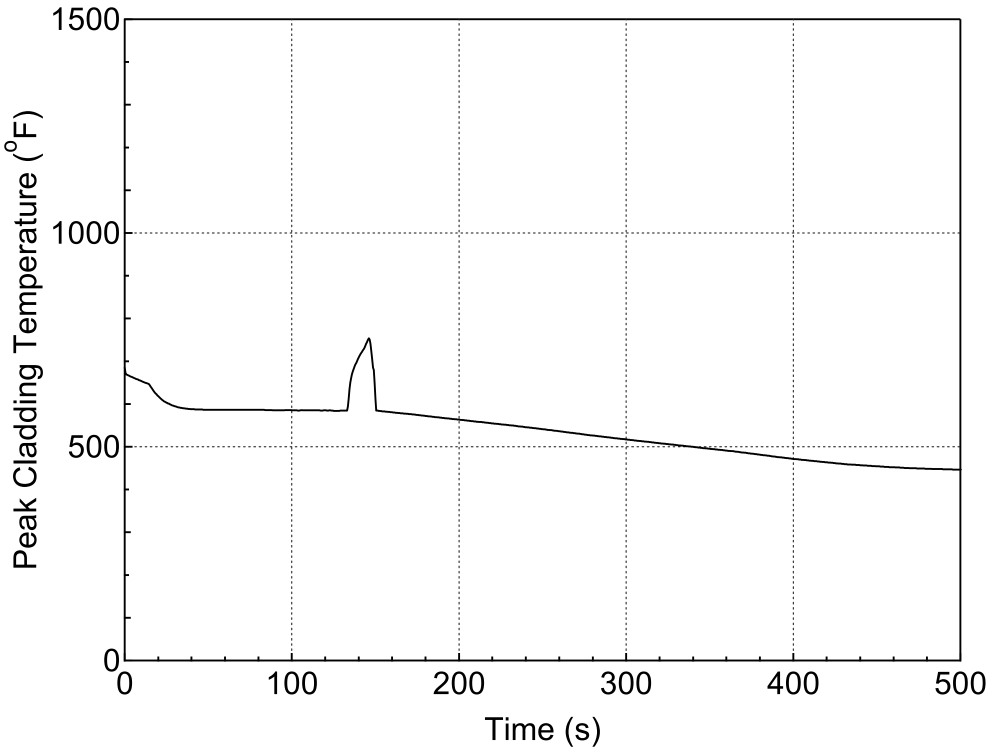

Figure 5.3.1.c-26 PCT at All Elevations for Hot Rod in Hot Assembly for 7-inch Break (Homogeneous) (Break Orientation Sensitivity Study)

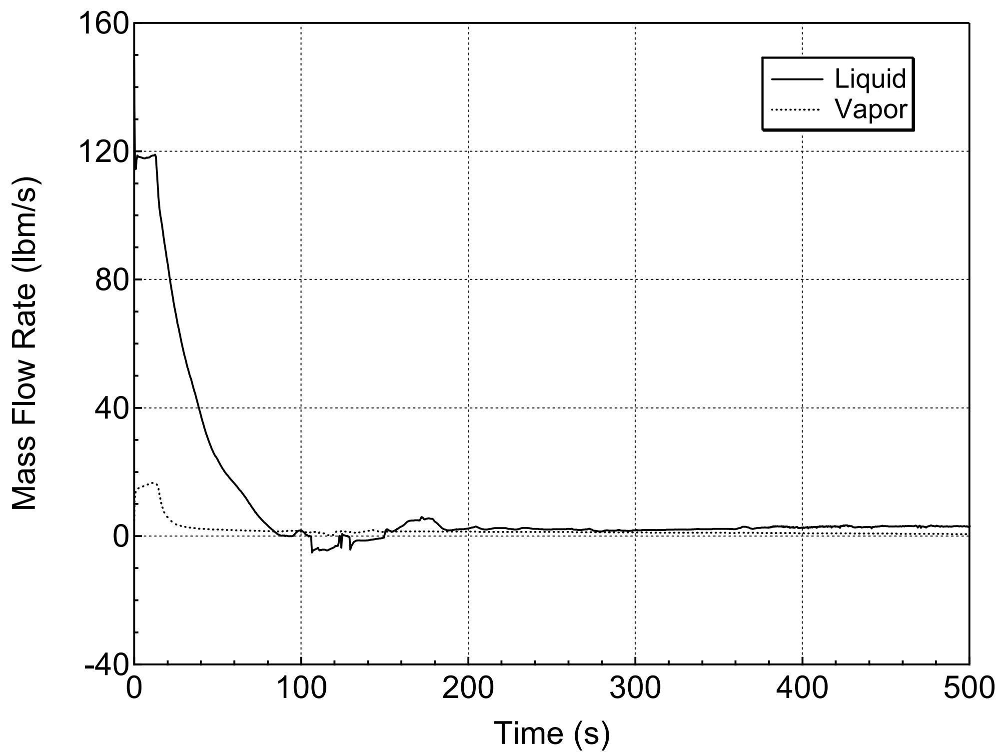

Figure 5.3.1.c-27 Hot Assembly Exit Vapor and Liquid Mass Flowrates for 7-inch Break (Homogeneous) (Break Orientation Sensitivity Study)

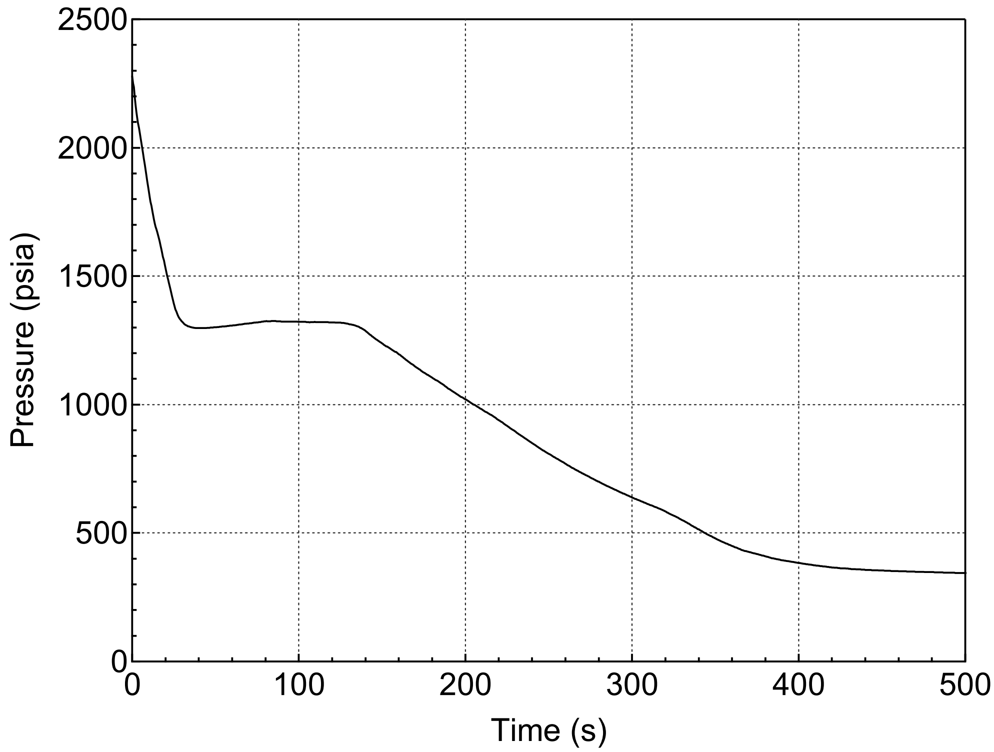

Figure 5.3.1.d-1 RCS (Pressurizer) Pressure Transient for 7.5-inch Break (Bottom) (Break Orientation Sensitivity Study)

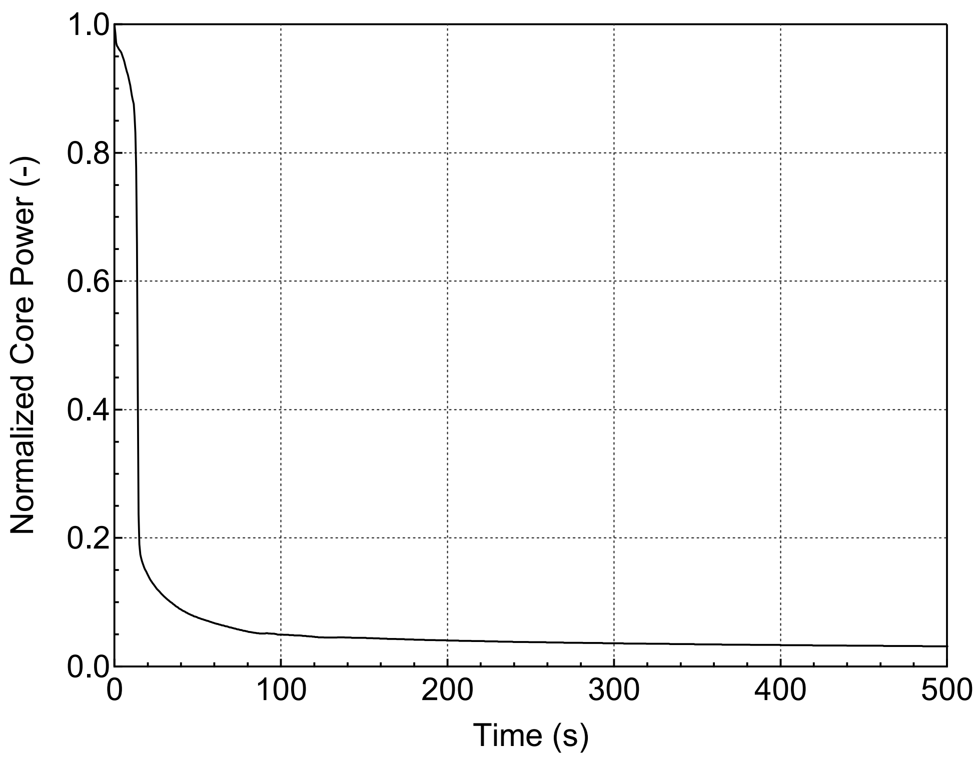

Figure 5.3.1.d-2 Normalized Core Power for 7.5-inch Break (Bottom) (Break Orientation Sensitivity Study)

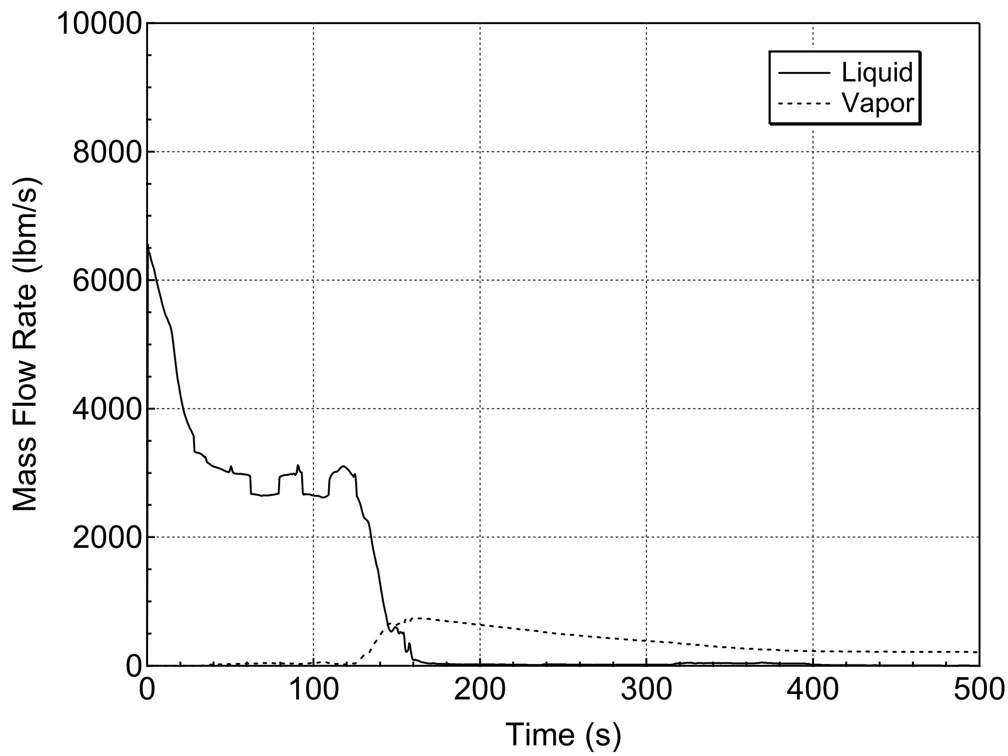

Figure 5.3.1.d-3 Liquid and Vapor Discharges through the Break for 7.5-inch Break (Bottom) (Break Orientation Sensitivity Study)

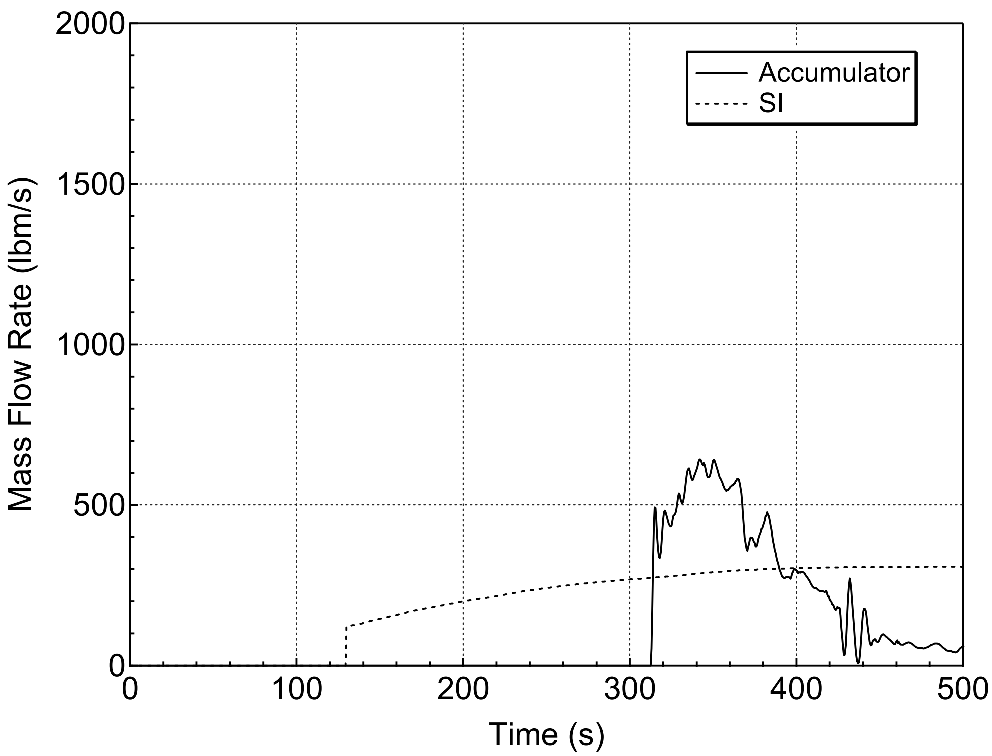

Figure 5.3.1.d-4 Accumulator and Safety Injection Mass Flowrates for 7.5-inch Break (Bottom) (Break Orientation Sensitivity Study)

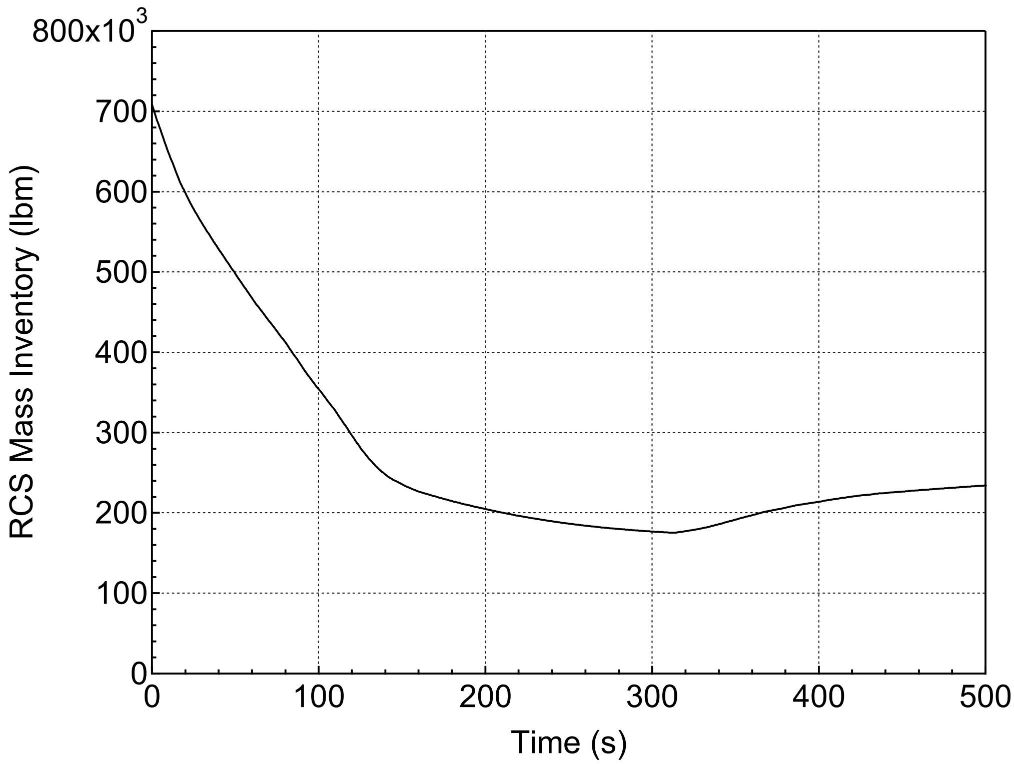

Figure 5.3.1.d-5 RCS Mass Inventory for 7.5-inch Break (Bottom) (Break Orientation Sensitivity Study)

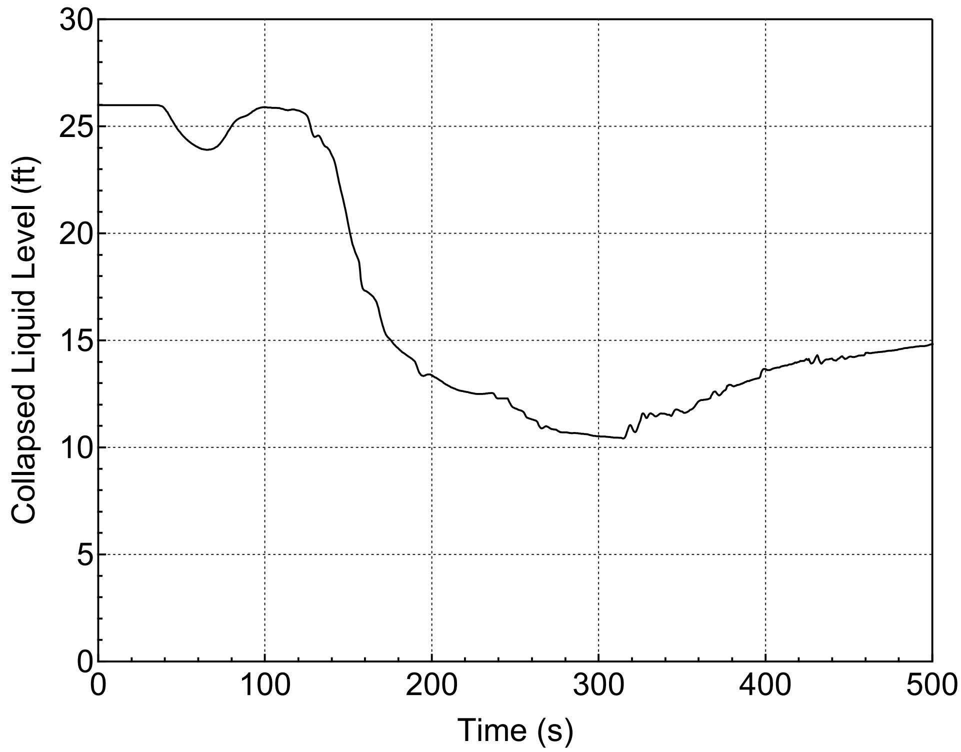

Figure 5.3.1.d-6 Downcomer Collapsed Level for 7.5-inch Break (Bottom) (Break Orientation Sensitivity Study)

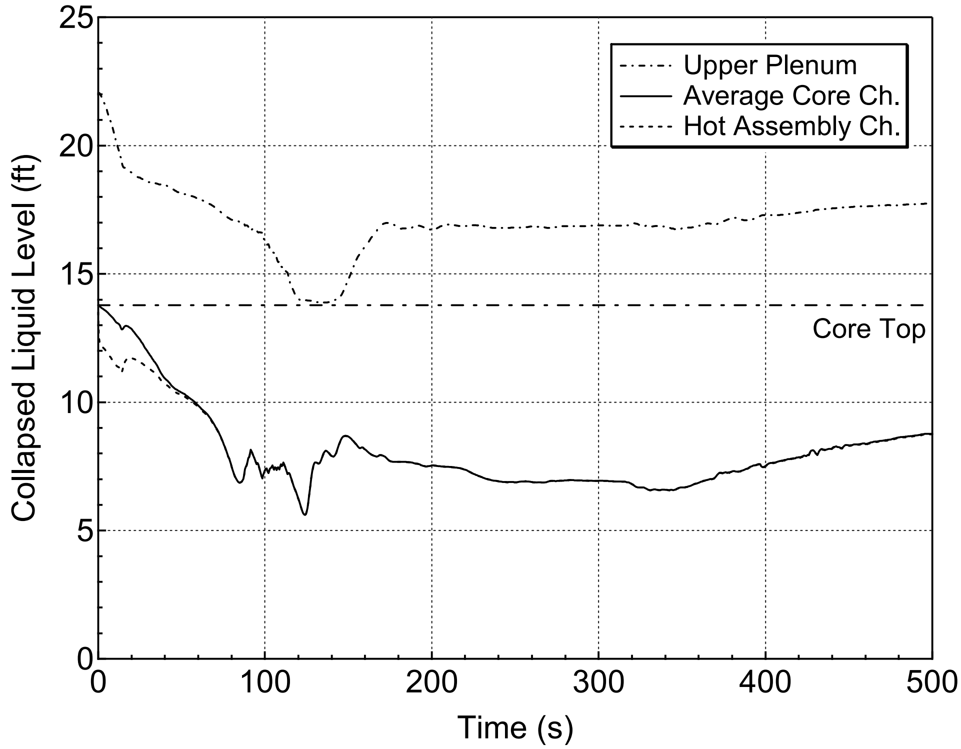

Figure 5.3.1.d-7 Core and Upper Plenum Collapsed Levels for 7.5-inch Break (Bottom) (Break Orientation Sensitivity Study)

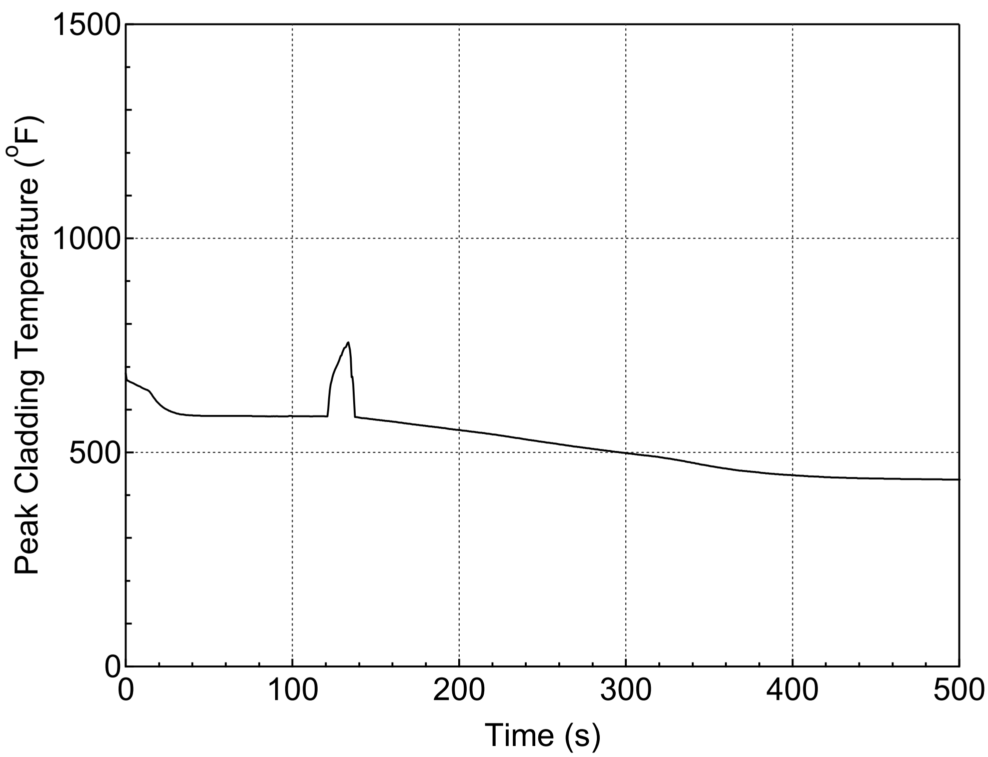

Figure 5.3.1.d-8 PCT at All Elevations for Hot Rod in Hot Assembly for 7.5-inch Break (Bottom) (Break Orientation Sensitivity Study)

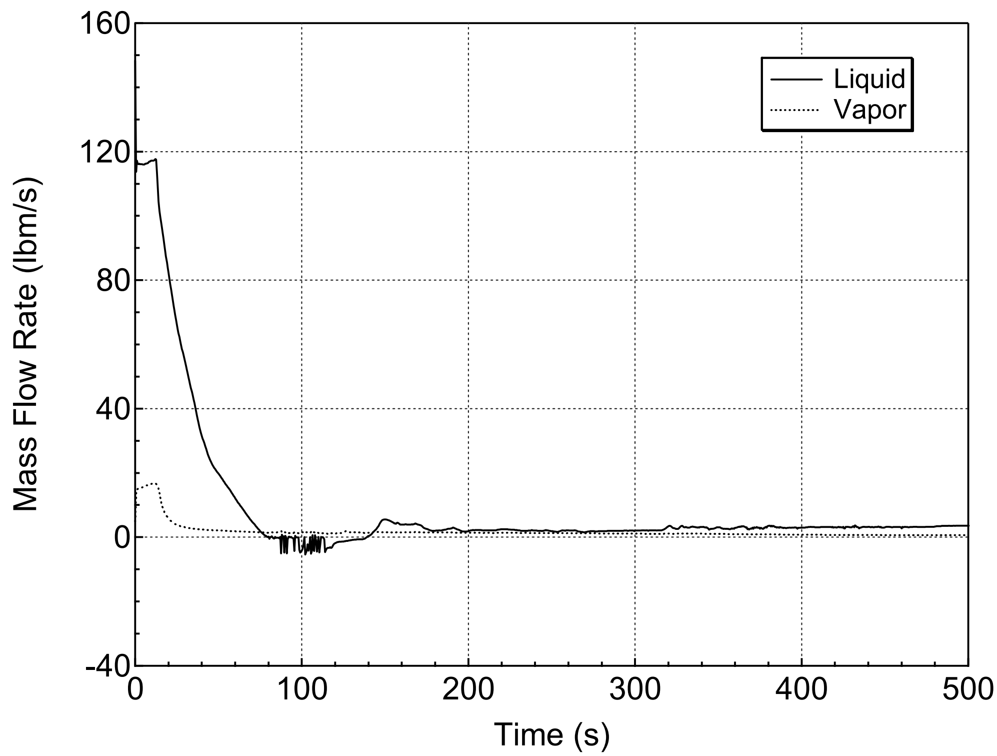

Figure 5.3.1.d-9 Hot Assembly Exit Vapor and Liquid Mass Flowrates for 7.5-inch Break (Bottom) (Break Orientation Sensitivity Study)

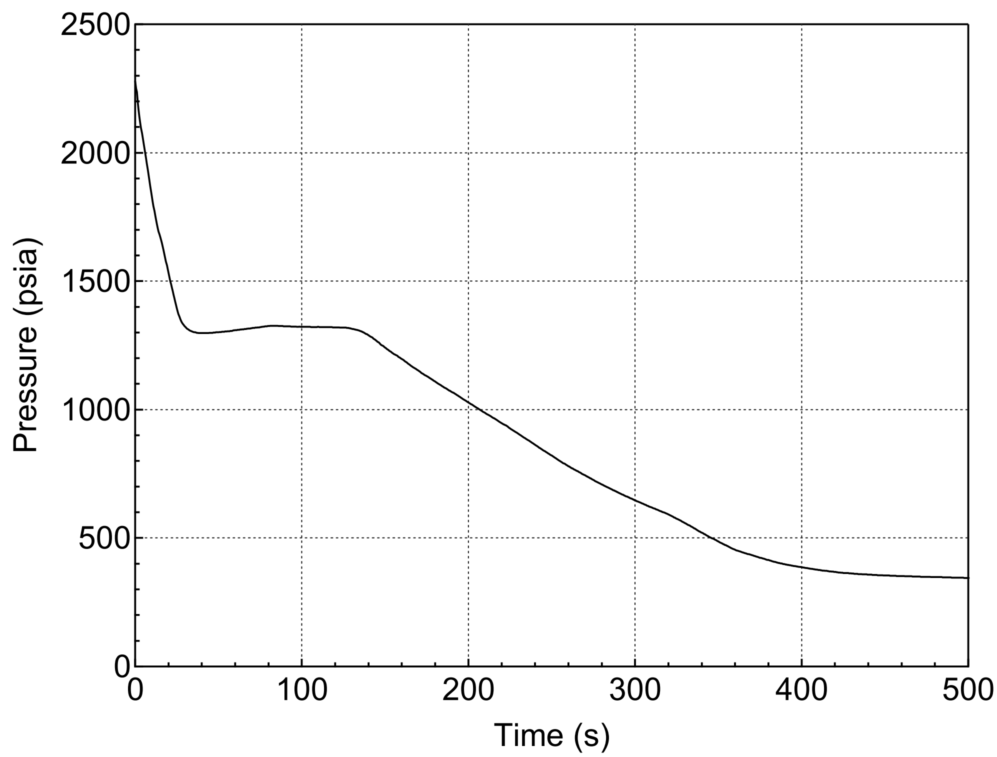

Figure 5.3.1.d-10 RCS (Pressurizer) Pressure Transient for 7.5-inch Break (Top) (Break Orientation Sensitivity Study)

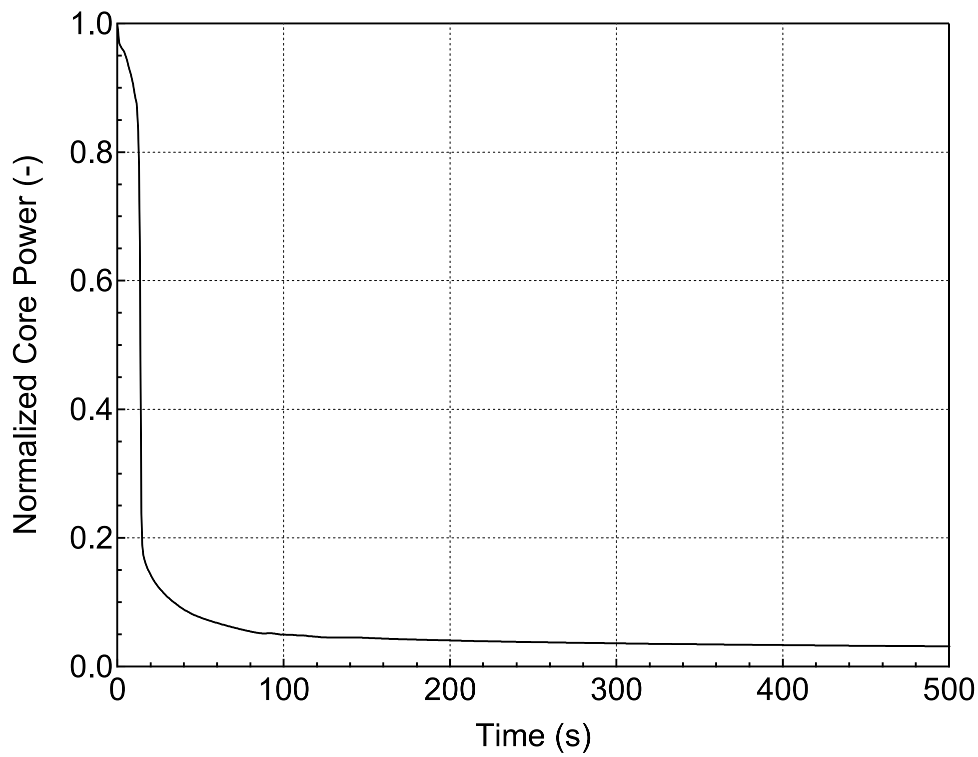

Figure 5.3.1.d-11 Normalized Core Power for 7.5-inch Break (Top) (Break Orientation Sensitivity Study)

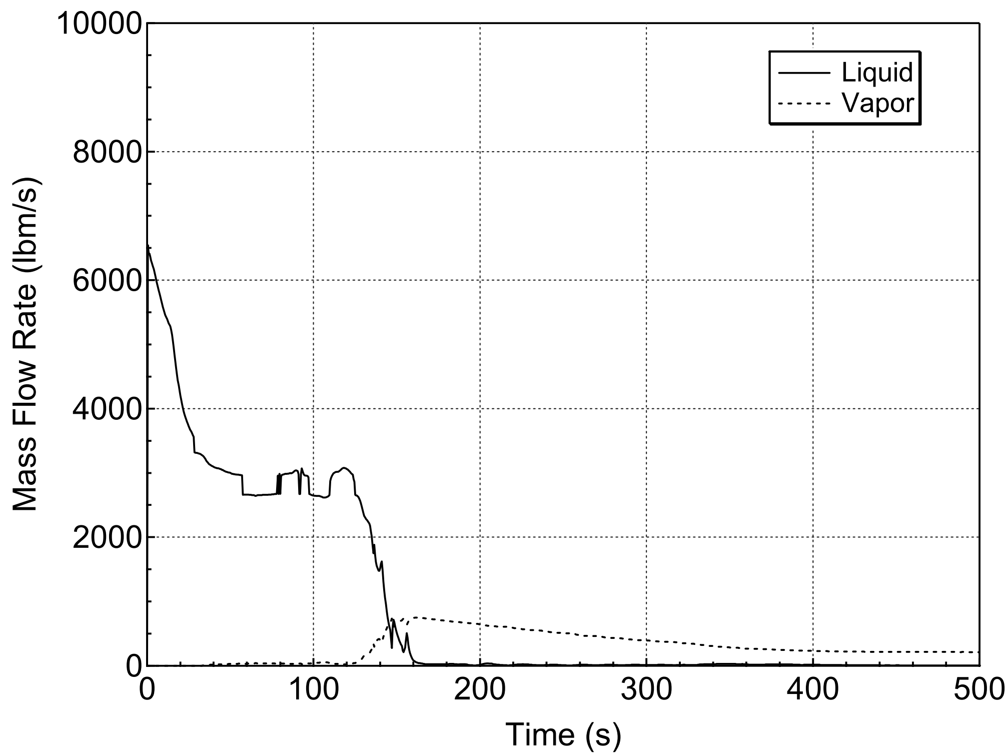

Figure 5.3.1.d-12 Liquid and Vapor Discharges through the Break for 7.5-inch Break (Top) (Break Orientation Sensitivity Study)

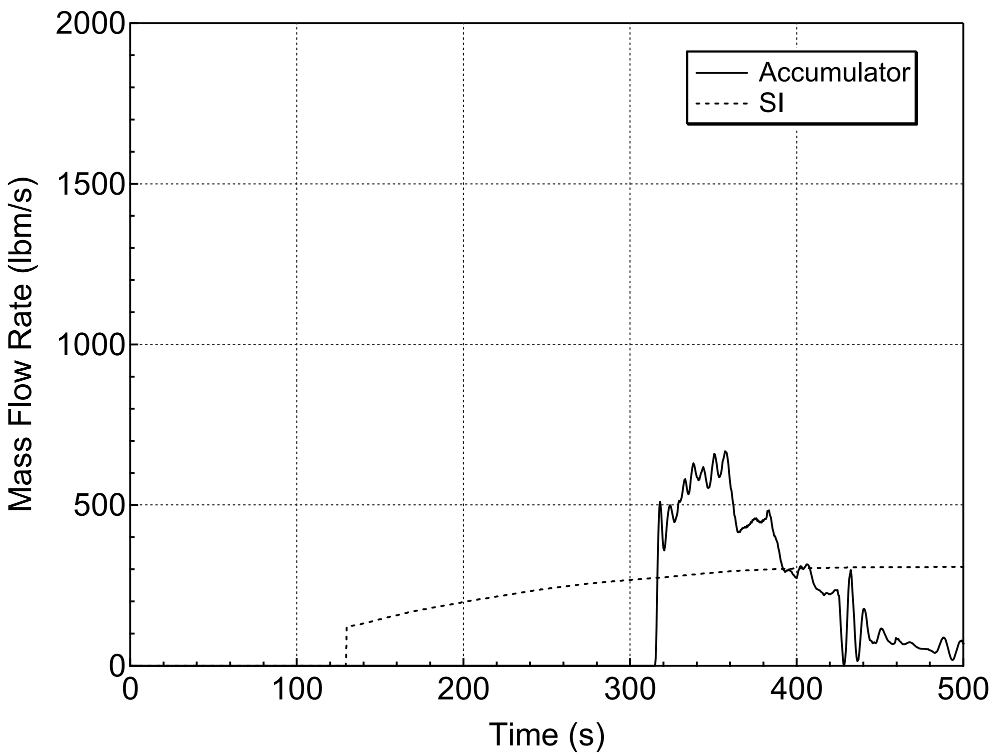

Figure 5.3.1.d-13 Accumulator and Safety Injection Mass Flowrates for 7.5-inch Break (Top) (Break Orientation Sensitivity Study)

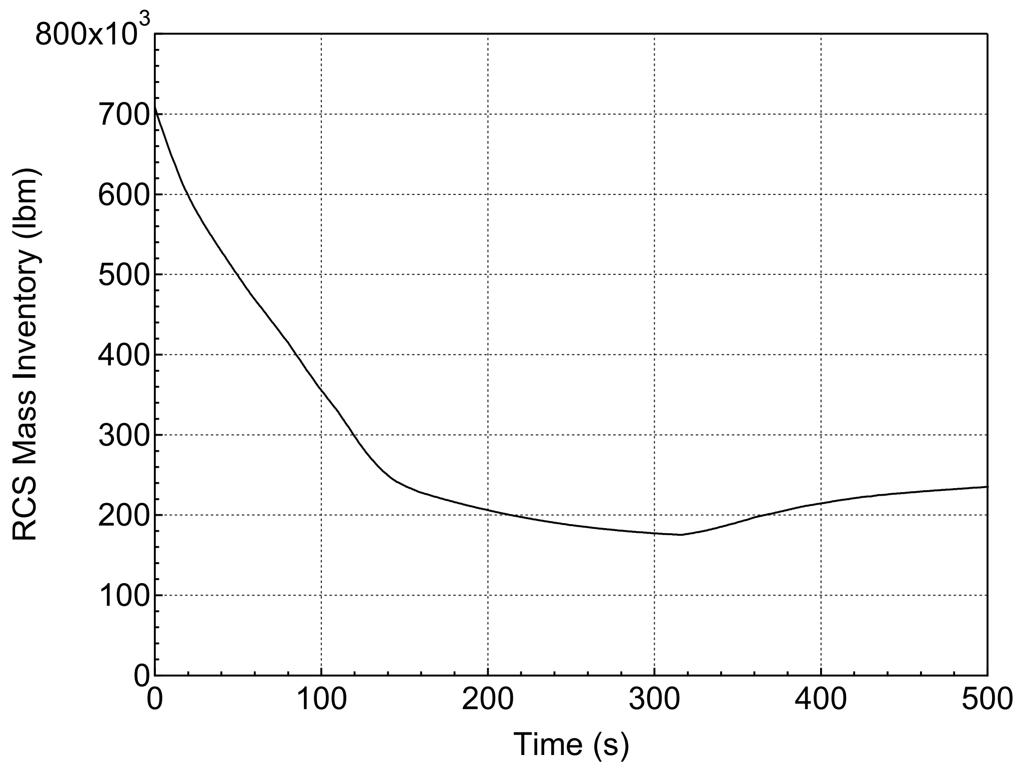

Figure 5.3.1.d-14 RCS Mass Inventory for 7.5-inch Break (Top) (Break Orientation Sensitivity Study)

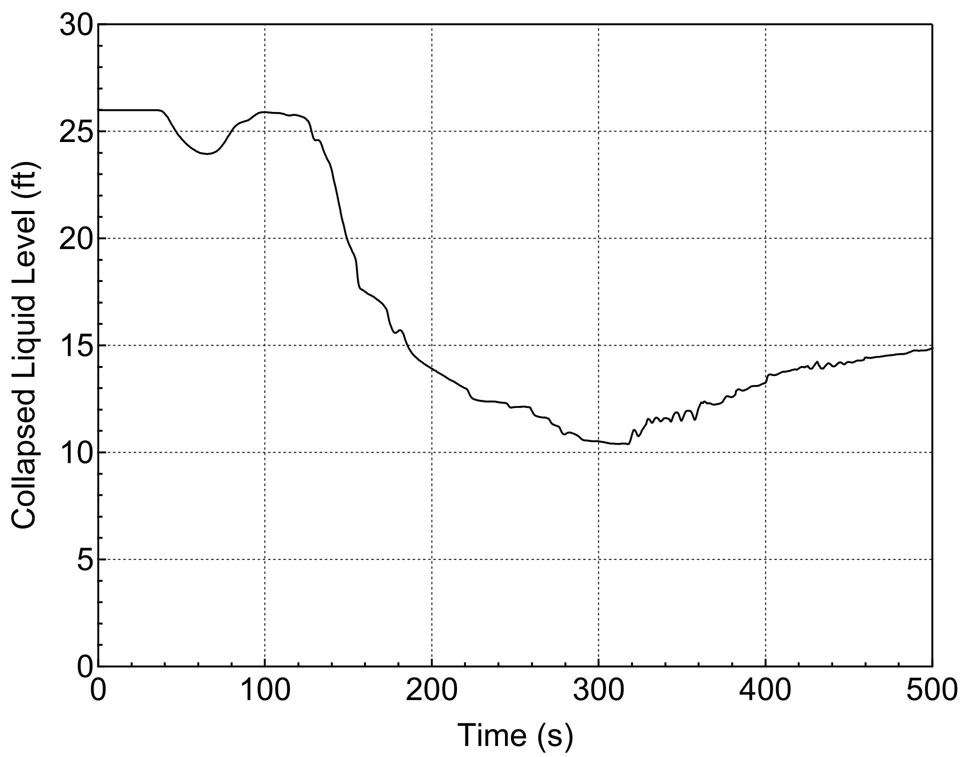

Figure 5.3.1.d-15 Downcomer Collapsed Level for 7.5-inch Break (Top) (Break Orientation Sensitivity Study)

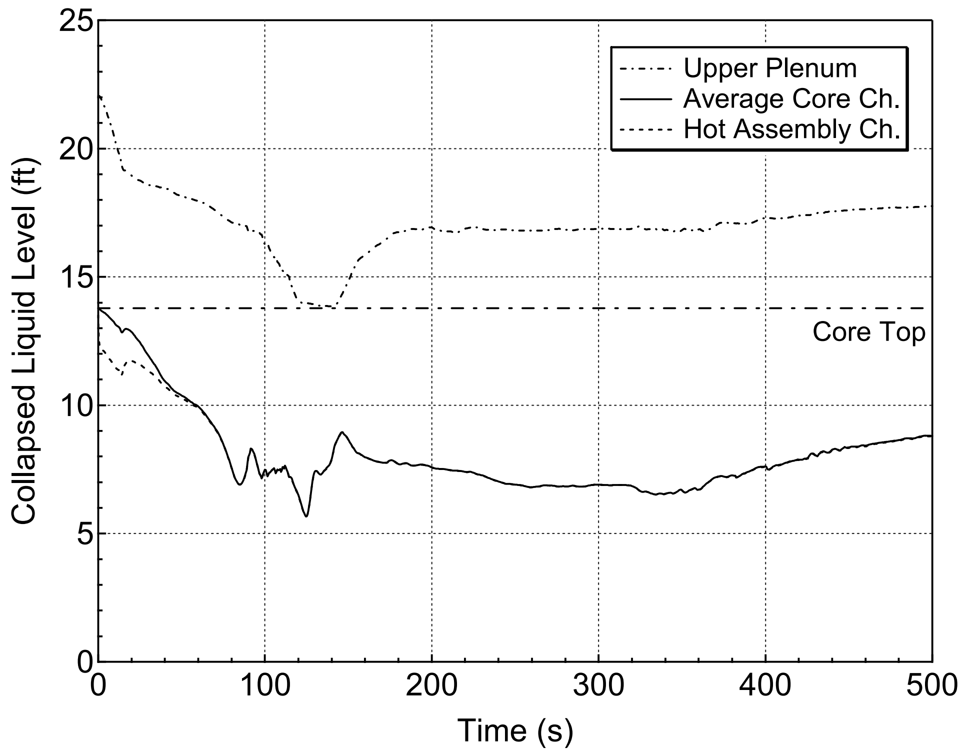

Figure 5.3.1.d-16 Core and Upper Plenum Collapsed Levels for 7.5-inch Break (Top) (Break Orientation Sensitivity Study)

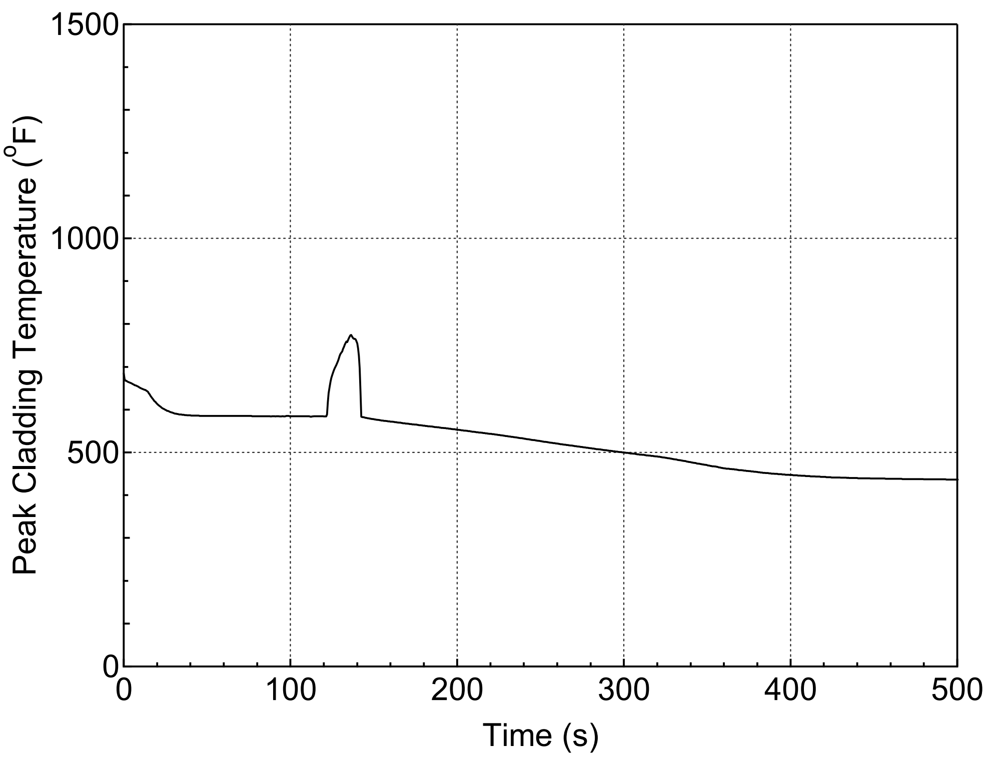

Figure 5.3.1.d-17 PCT at All Elevations for Hot Rod in Hot Assembly for 7.5-inch Break (Top) (Break Orientation Sensitivity Study)

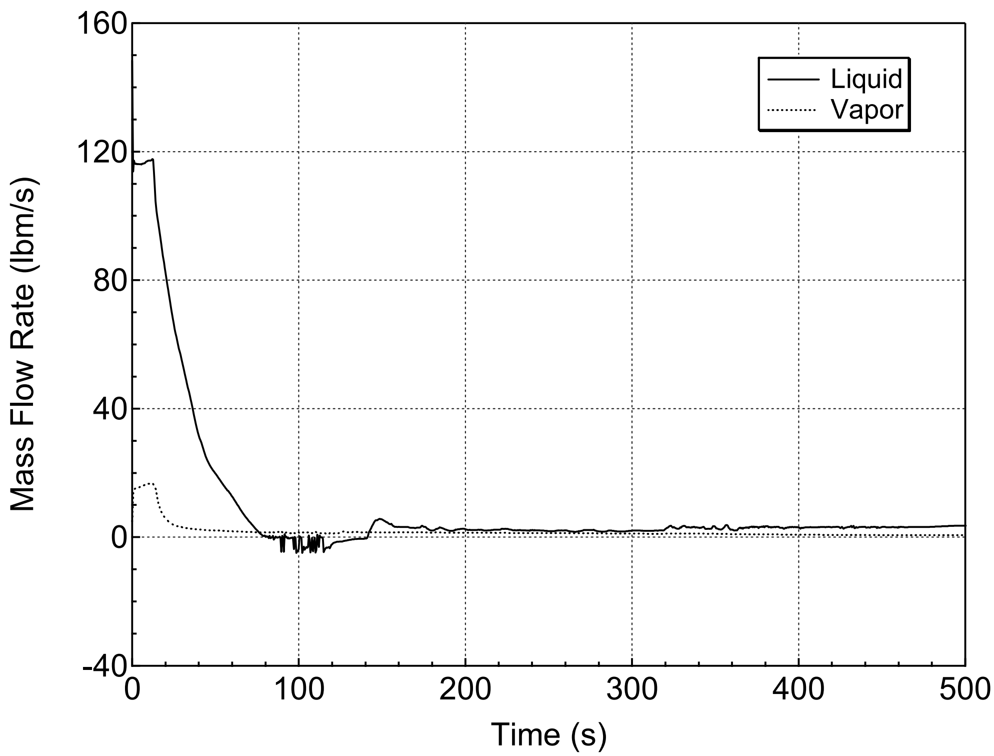

Figure 5.3.1.d-18 Hot Assembly Exit Vapor and Liquid Mass Flowrates for 7.5-inch Break (Top) (Break Orientation Sensitivity Study)

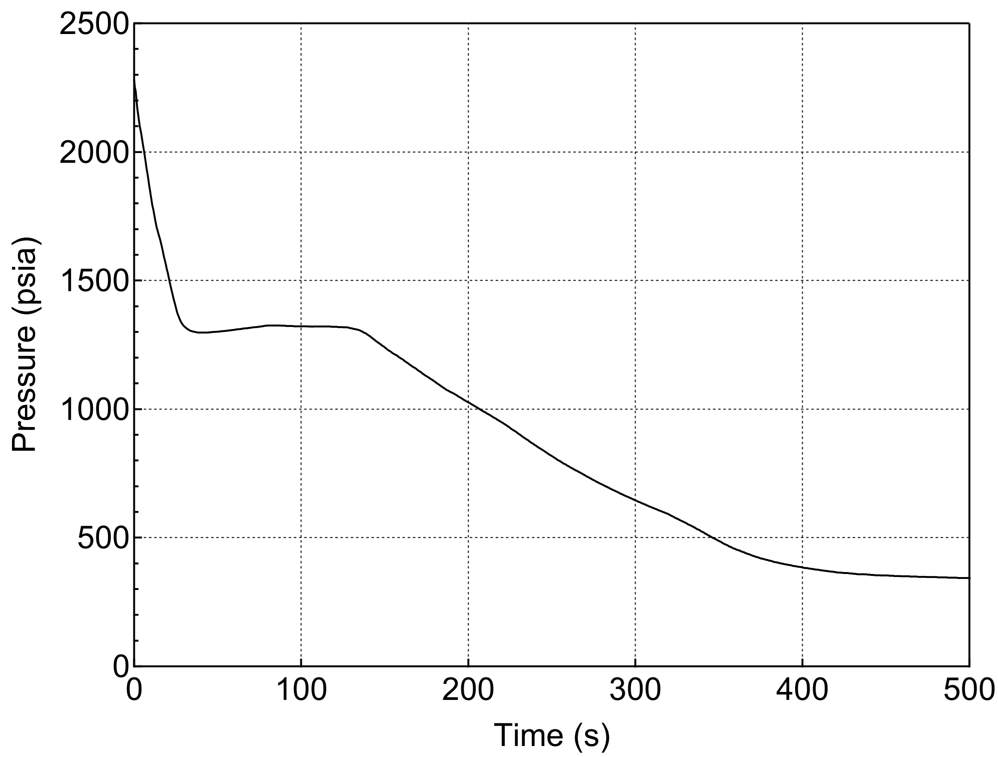

Figure 5.3.1.d-19 RCS (Pressurizer) Pressure Transient for 7.5-inch Break (Side) (Break Orientation Sensitivity Study)

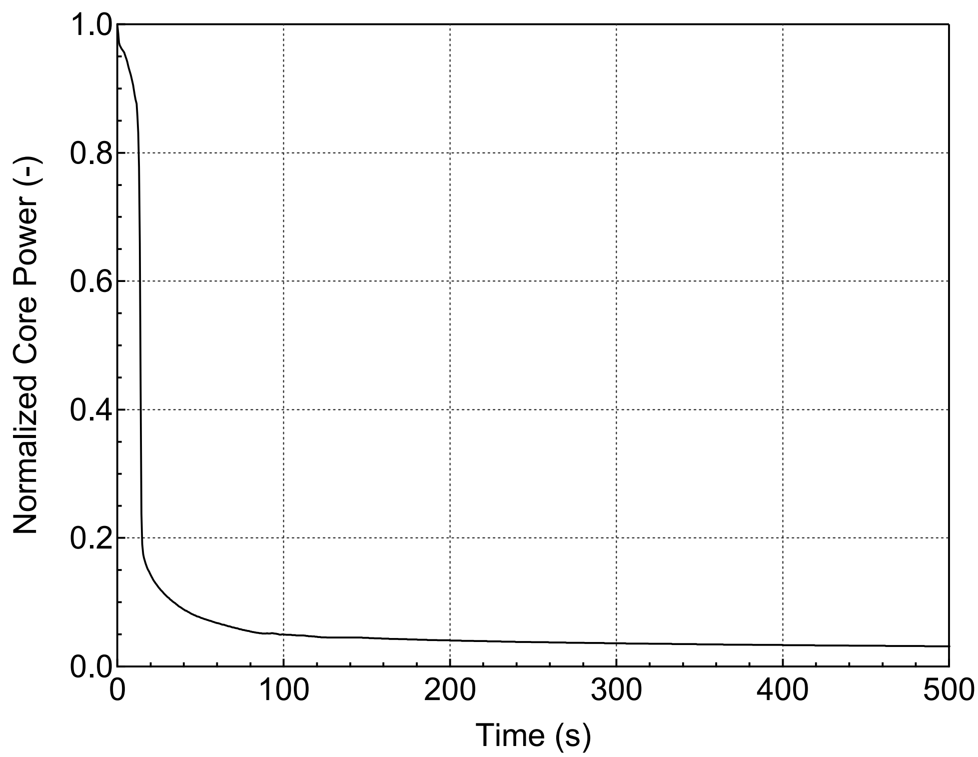

Figure 5.3.1.d-20 Normalized Core Power for 7.5-inch Break (Side) (Break Orientation Sensitivity Study)

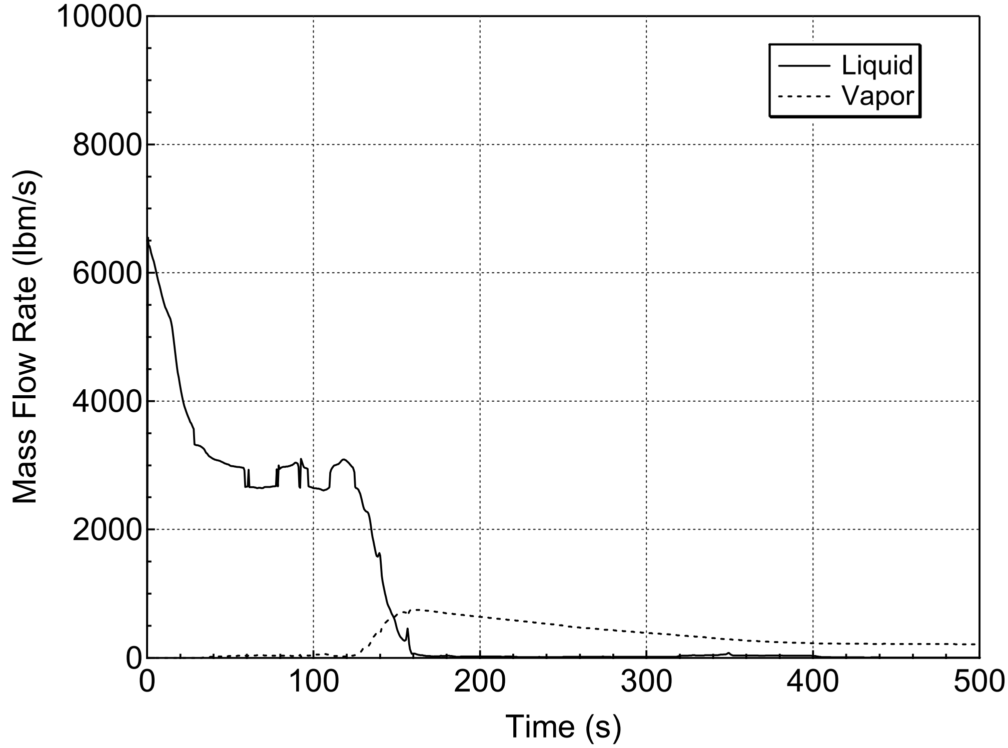

Figure 5.3.1.d-21 Liquid and Vapor Discharges through the Break for 7.5-inch Break (Side) (Break Orientation Sensitivity Study)

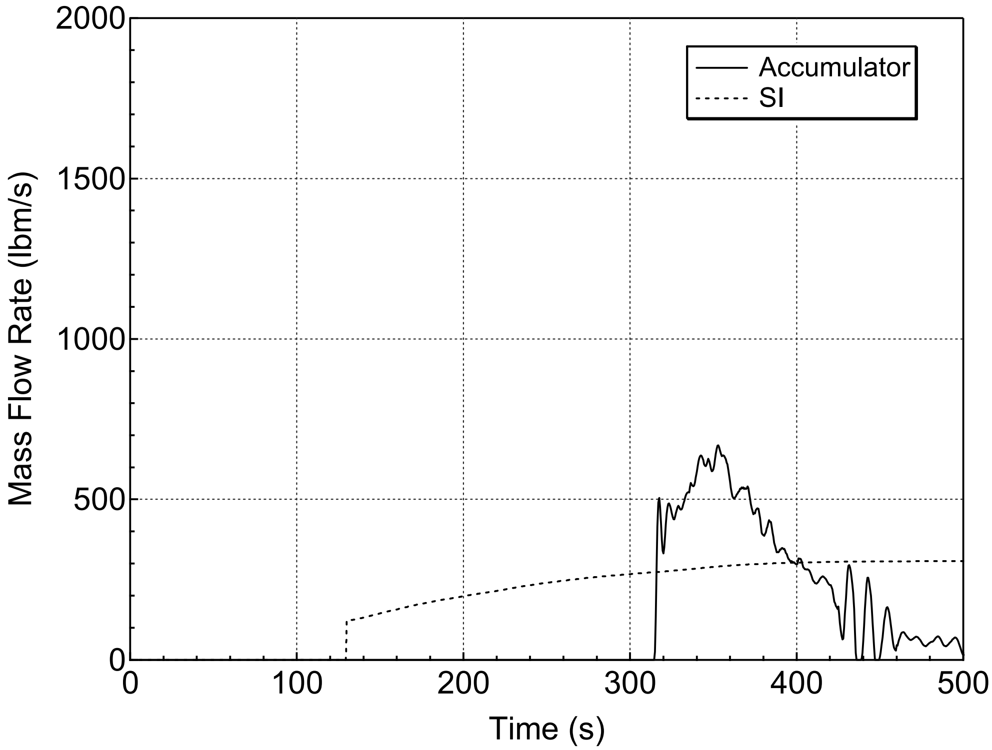

Figure 5.3.1.d-22 Accumulator and Safety Injection Mass Flowrates for 7.5-inch Break (Side) (Break Orientation Sensitivity Study)

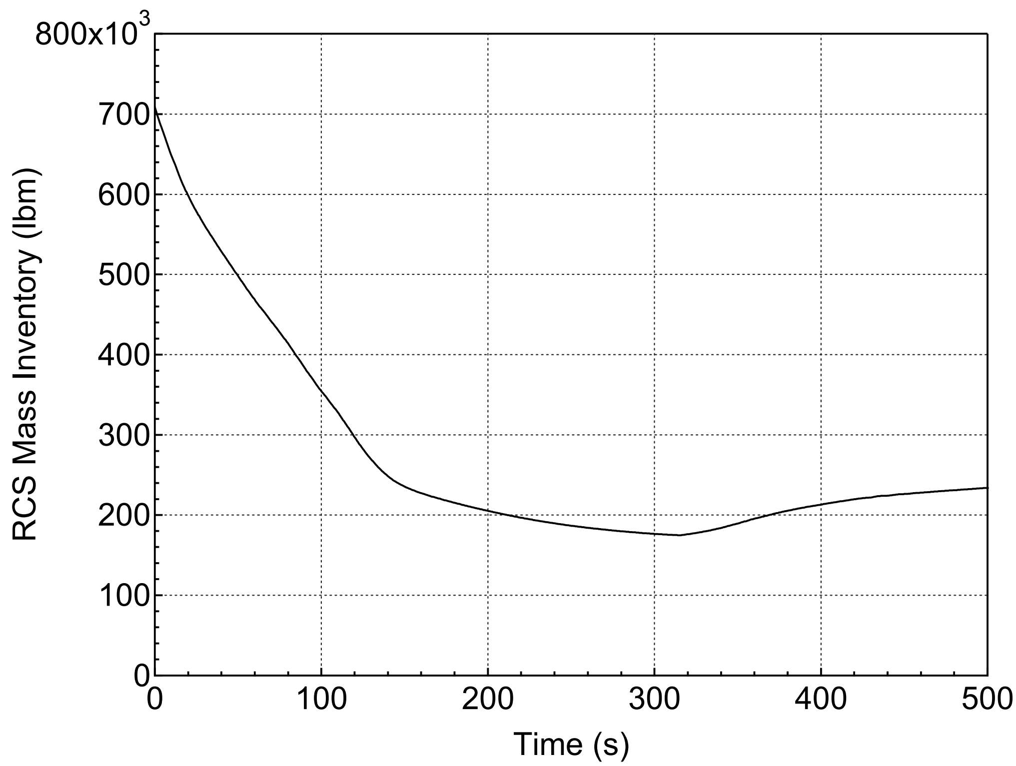

Figure 5.3.1.d-23 RCS Mass Inventory for 7.5-inch Break (Side) (Break Orientation Sensitivity Study)

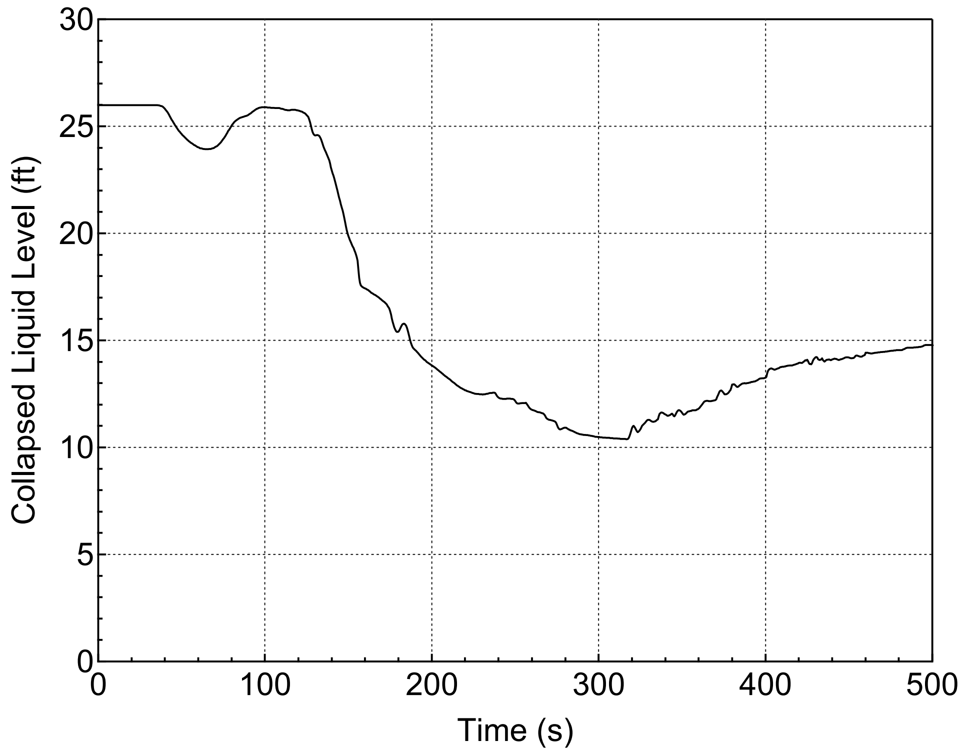

Figure 5.3.1.d-24 Downcomer Collapsed Level for 7.5-inch Break (Side) (Break Orientation Sensitivity Study)

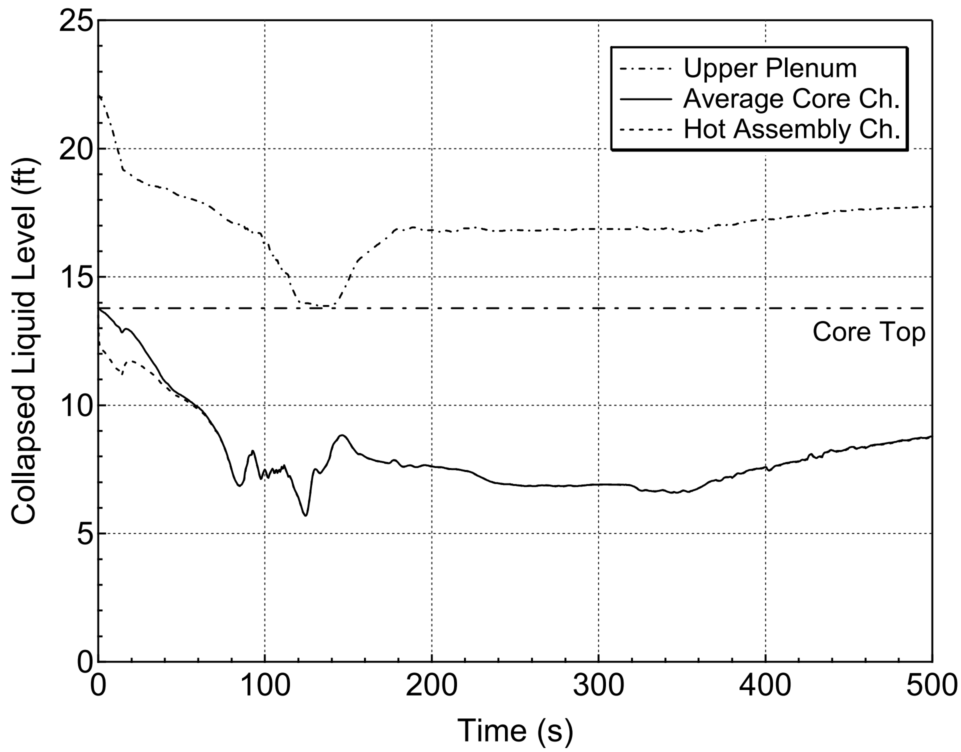

Figure 5.3.1.d-25 Core and Upper Plenum Collapsed Levels for 7.5-inch Break (Side) (Break Orientation Sensitivity Study)

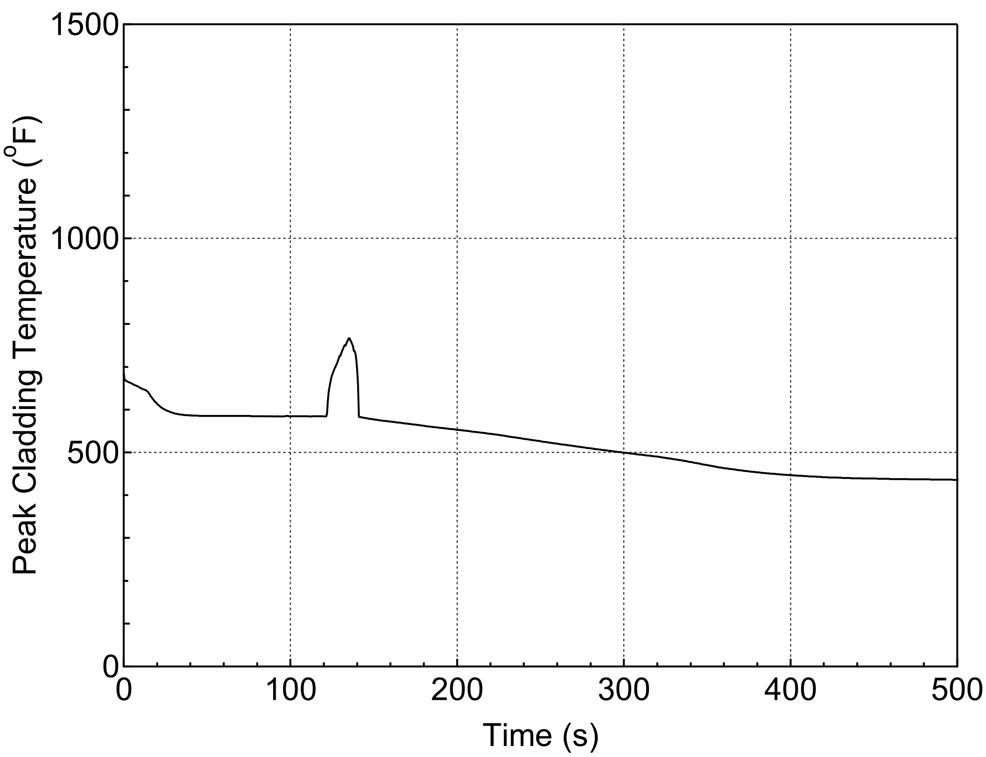

Figure 5.3.1.d-26 PCT at All Elevations for Hot Rod in Hot Assembly for 7.5-inch Break (Side) (Break Orientation Sensitivity Study)

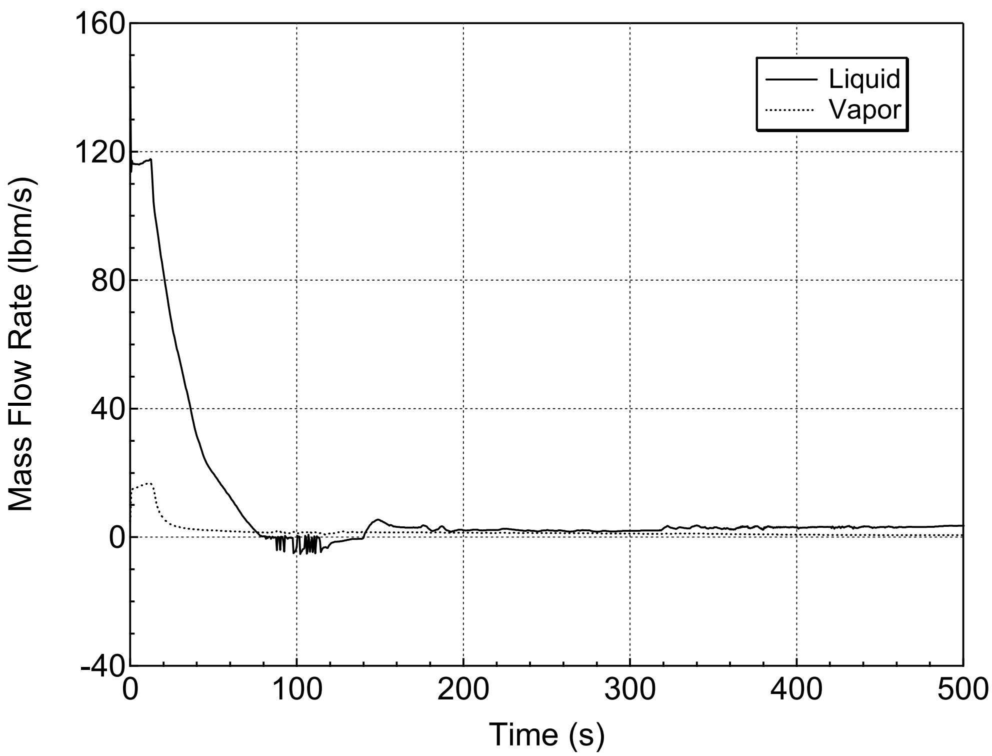

Figure 5.3.1.d-27 Hot Assembly Exit Vapor and Liquid Mass Flowrates for 7.5-inch Break (Side) (Break Orientation Sensitivity Study)

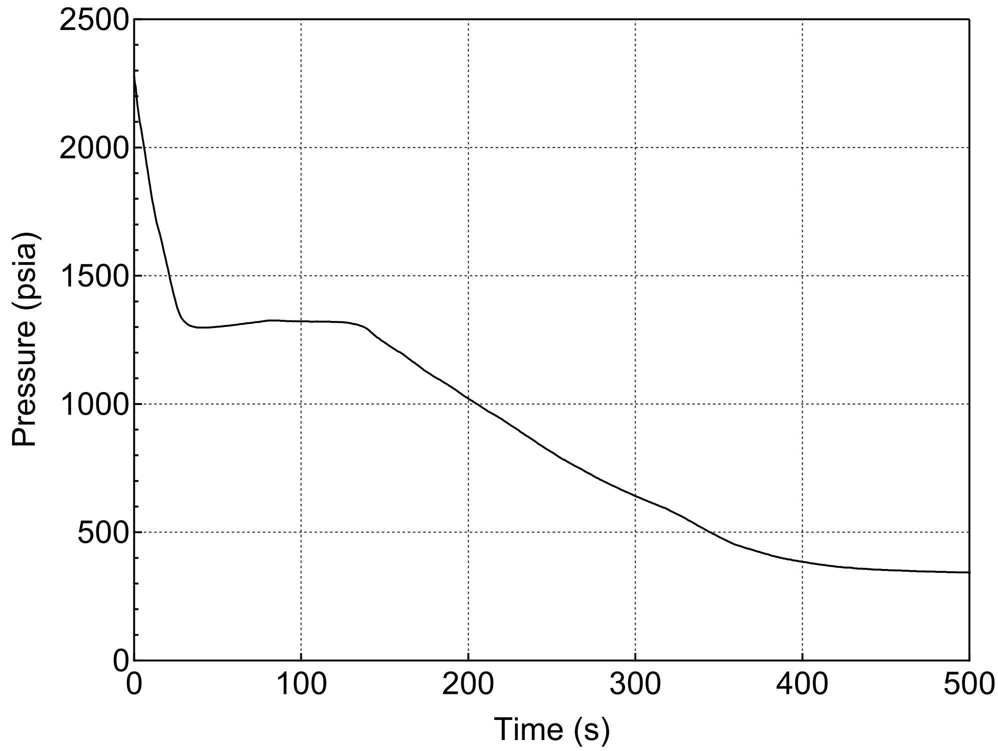

Figure 5.3.1.d-28 RCS (Pressurizer) Pressure Transient for 7.5-inch Break (Homogeneous) (Break Orientation Sensitivity Study)

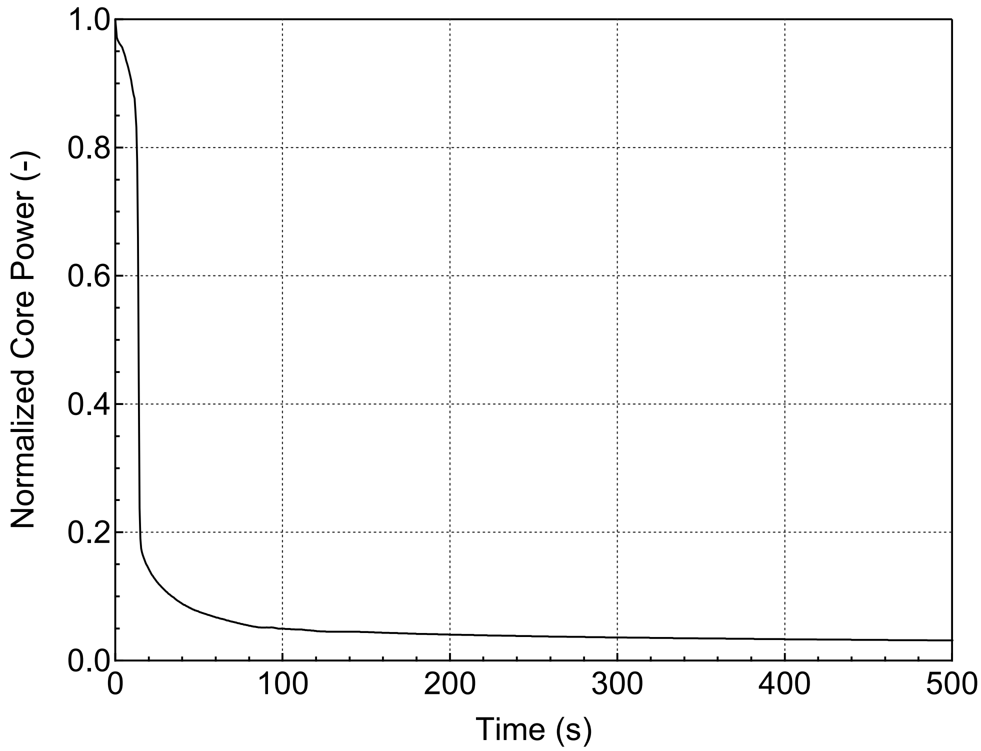

Figure 5.3.1.d-29 Normalized Core Power for 7.5-inch Break (Homogeneous) (Break Orientation Sensitivity Study)

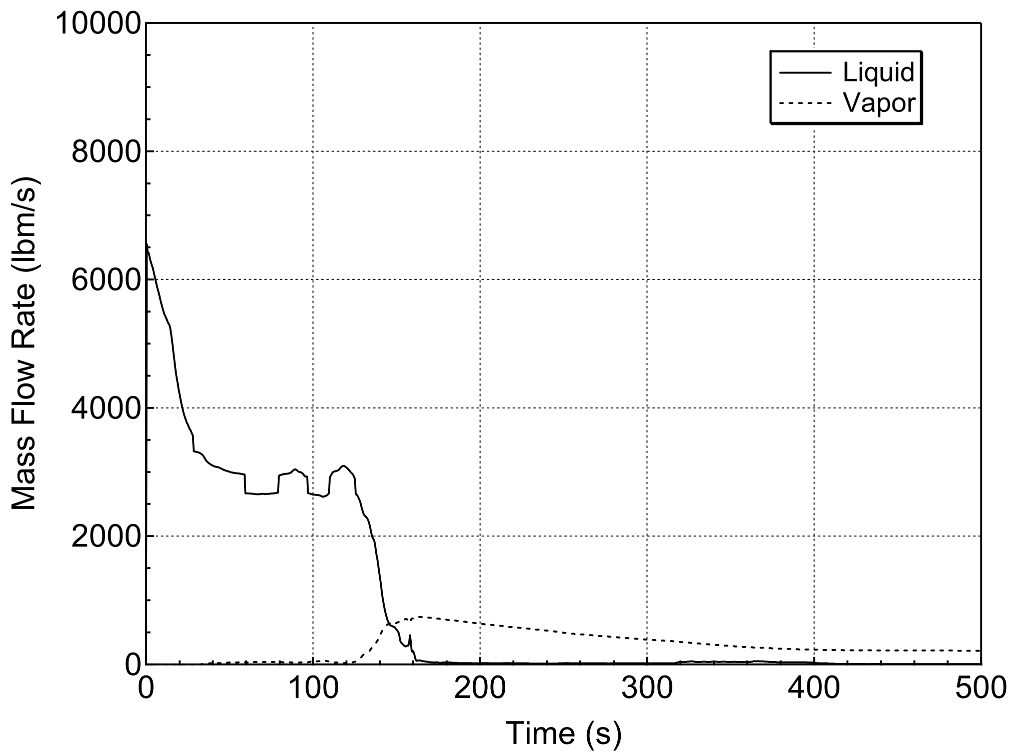

Figure 5.3.1.d-30 Liquid and Vapor Discharges through the Break for 7.5-inch Break (Homogeneous) (Break Orientation Sensitivity Study)

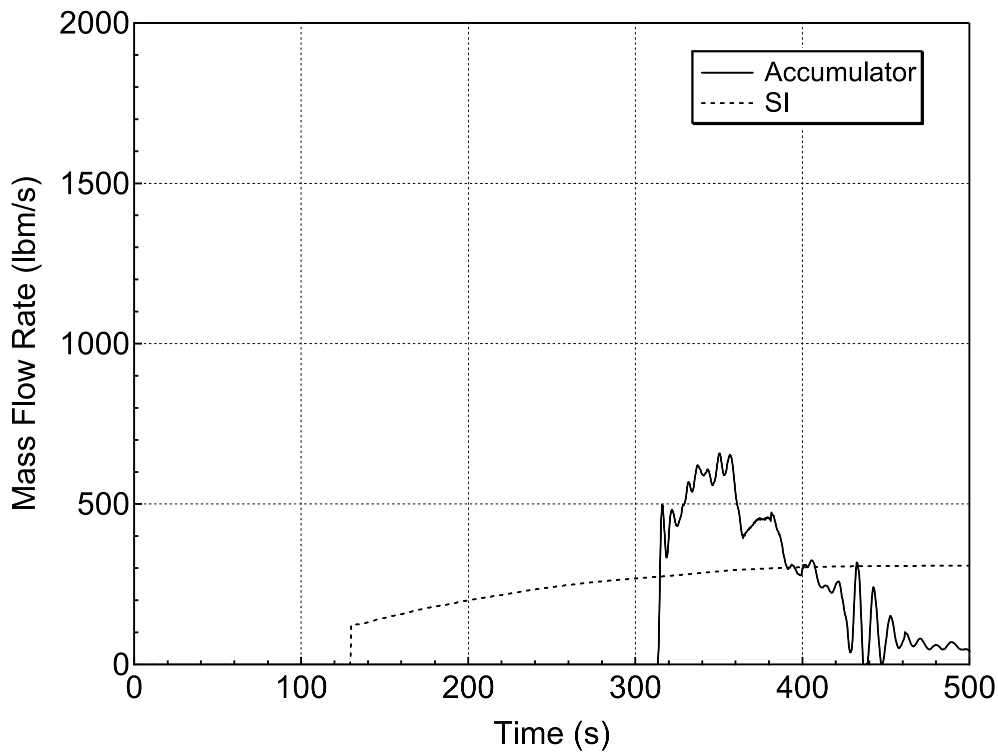

Figure 5.3.1.d-31 Accumulator and Safety Injection Mass Flowrates for 7.5-inch Break (Homogeneous) (Break Orientation Sensitivity Study)

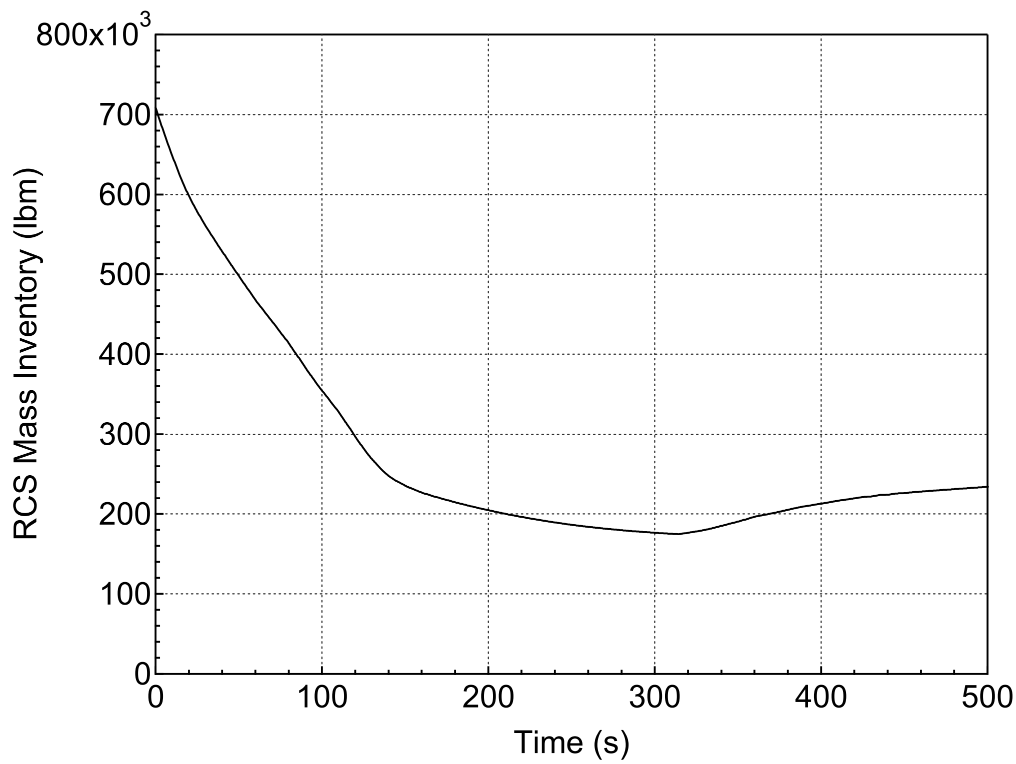

Figure 5.3.1.d-32 RCS Mass Inventory for 7.5-inch Break (Homogeneous) (Break Orientation Sensitivity Study)

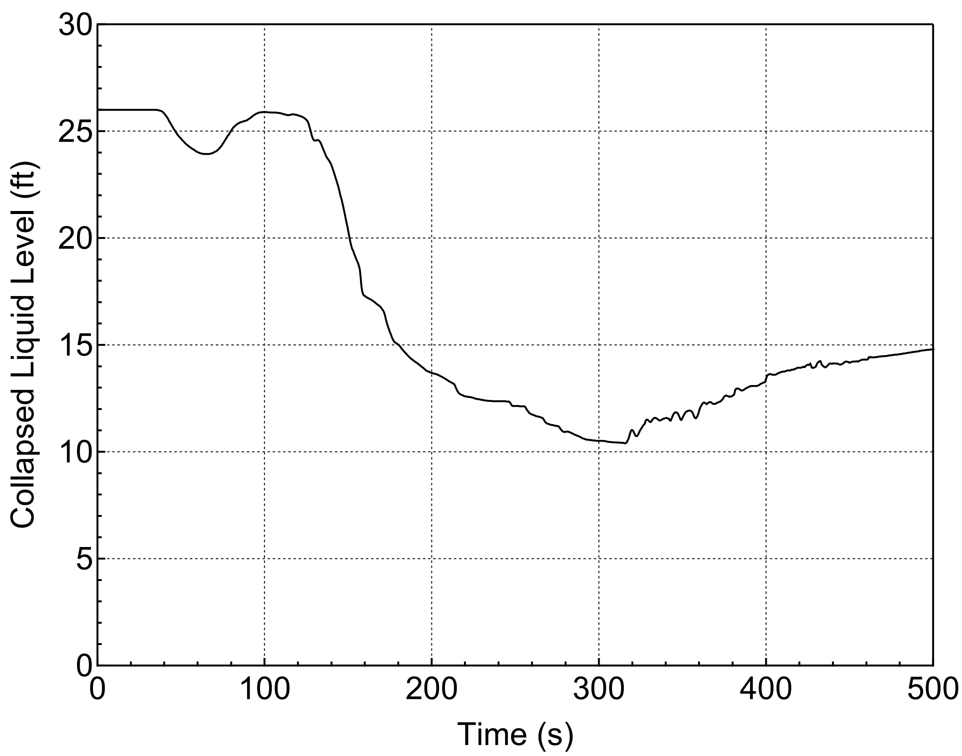

Figure 5.3.1.d-33 Downcomer Collapsed Level for 7.5-inch Break (Homogeneous) (Break Orientation Sensitivity Study)

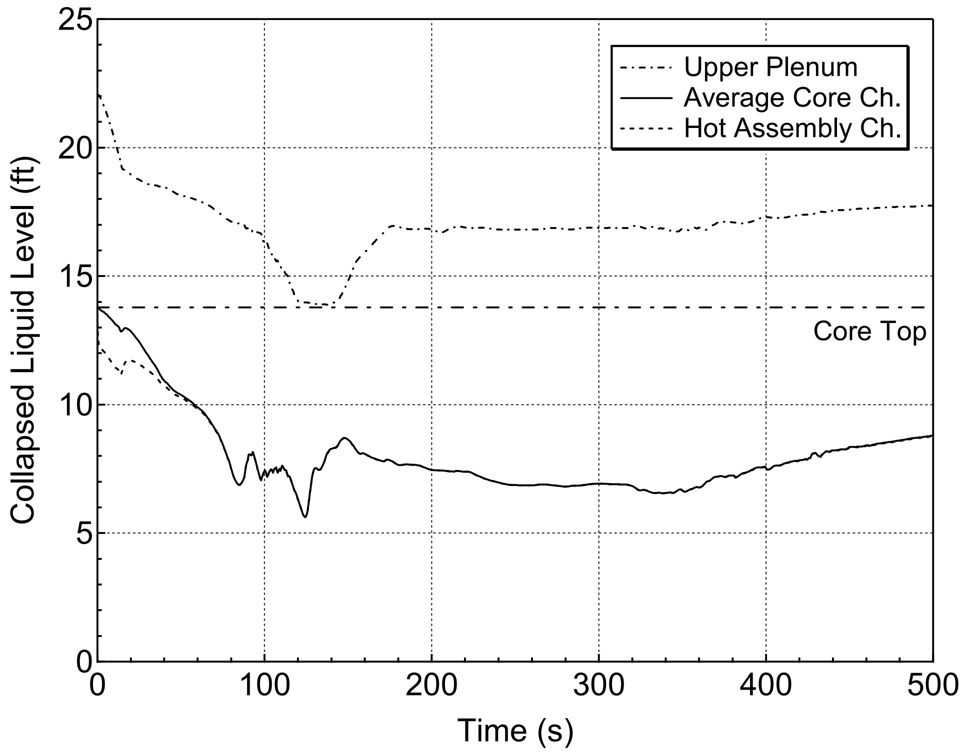

Figure 5.3.1.d-34 Core and Upper Plenum Collapsed Levels for 7.5-inch Break (Homogeneous) (Break Orientation Sensitivity Study)

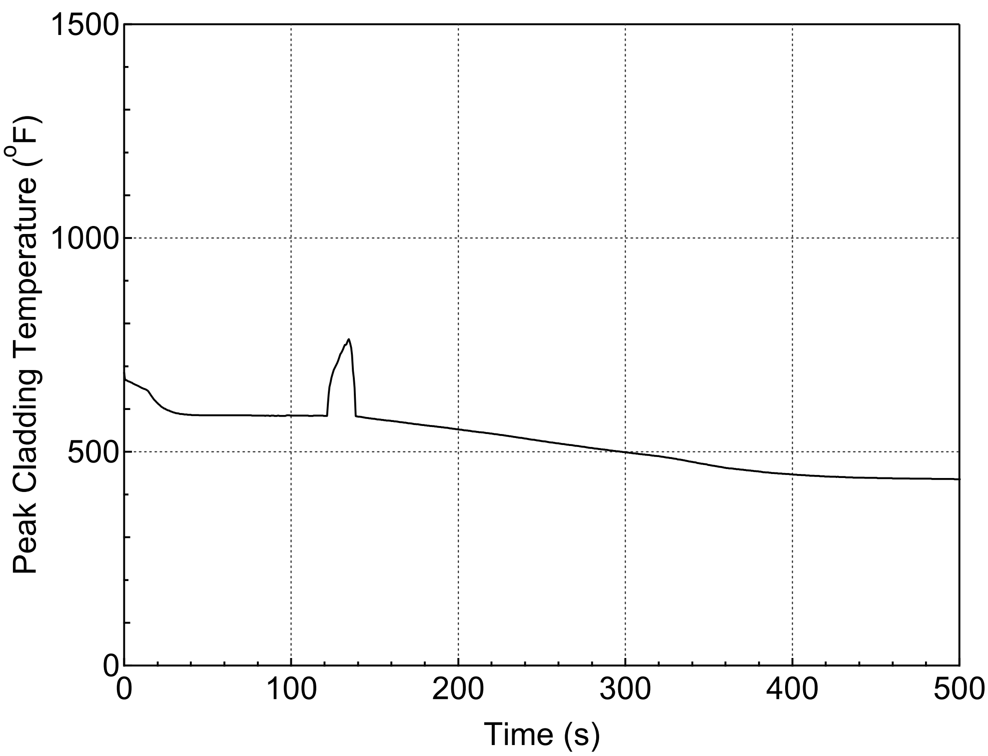

Figure 5.3.1.d-35 PCT at All Elevations for Hot Rod in Hot Assembly for 7.5-inch Break (Homogeneous) (Break Orientation Sensitivity Study)

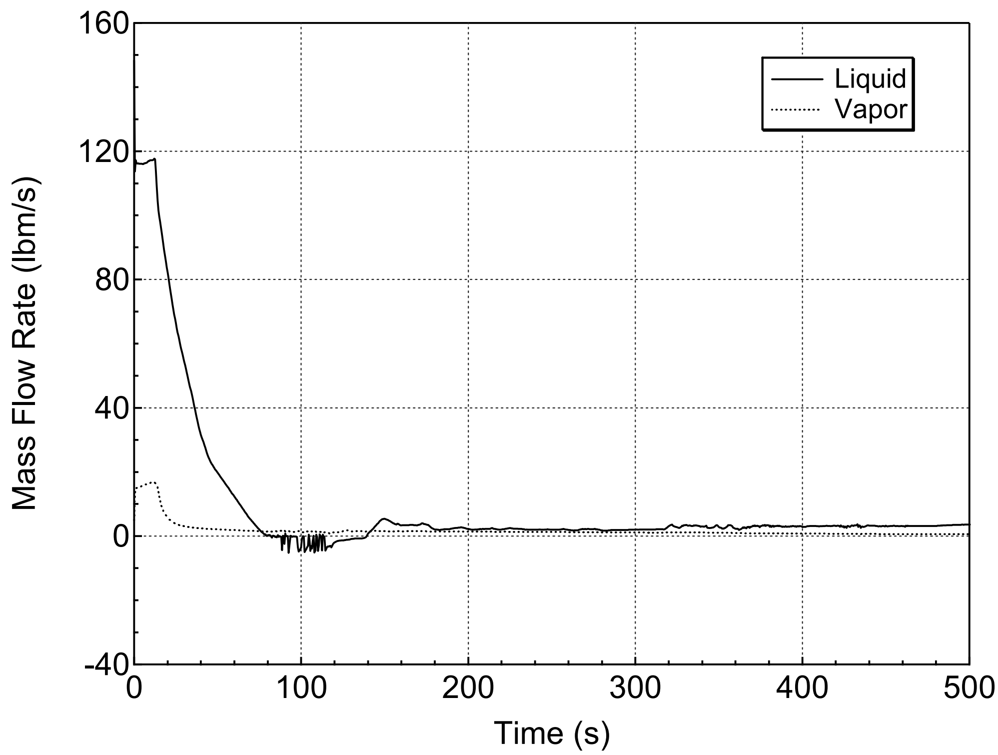

Figure 5.3.1.d-36 Hot Assembly Exit Vapor and Liquid Mass Flowrates for 7.5-inch Break (Homogeneous) (Break Orientation Sensitivity Study)

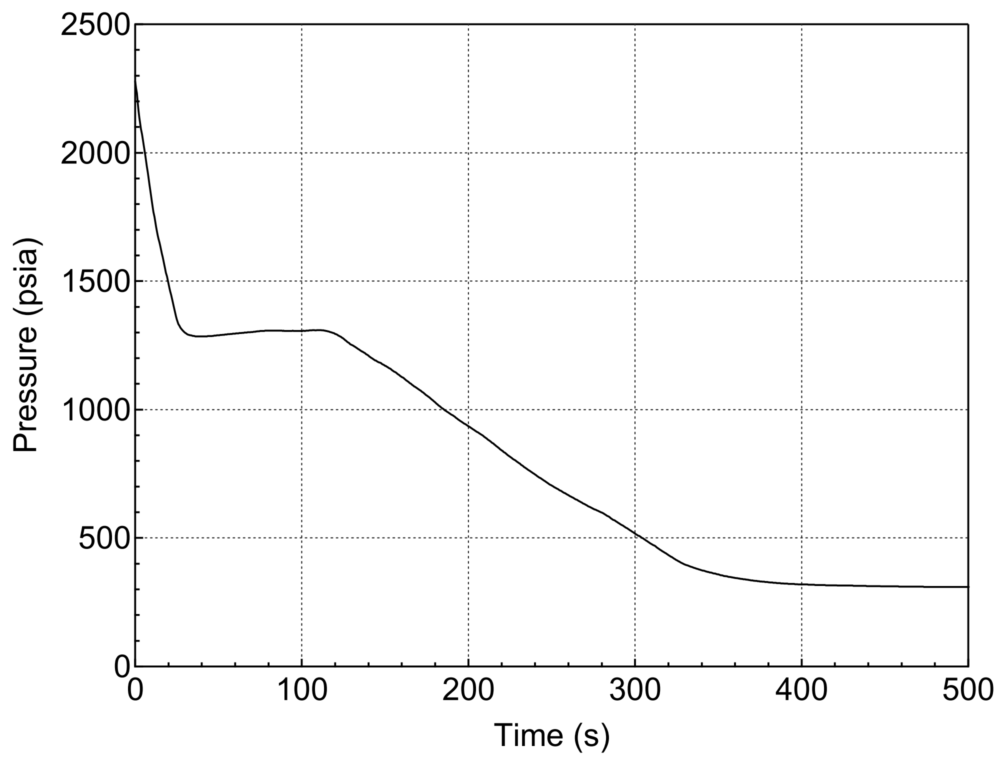

Figure 5.3.1.e-1 RCS (Pressurizer) Pressure Transient for 8-inch Break (Top) (Break Orientation Sensitivity Study)

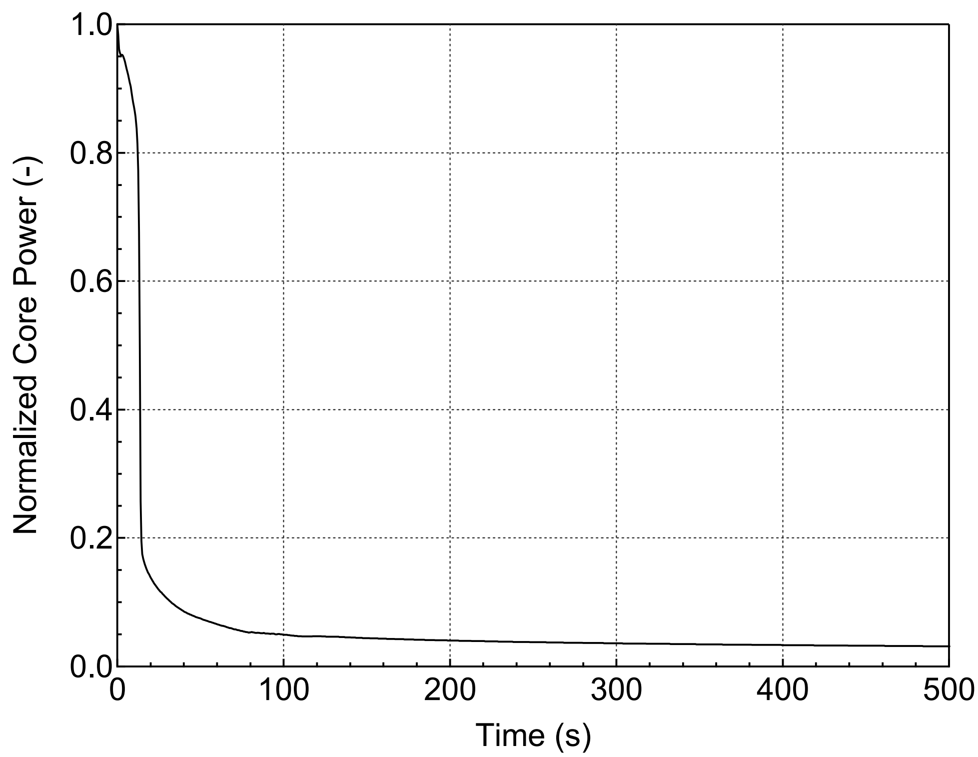

Figure 5.3.1.e-2 Normalized Core Power for 8-inch Break (Top) (Break Orientation Sensitivity Study)

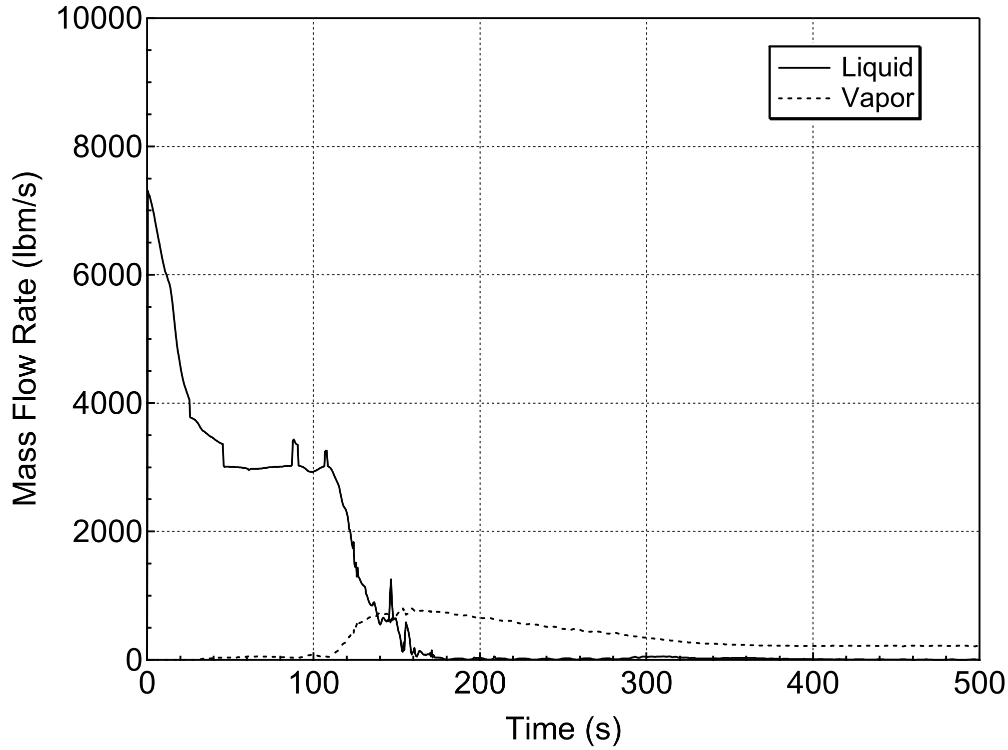

Figure 5.3.1.e-3 Liquid and Vapor Discharges through the Break for 8-inch Break (Top) (Break Orientation Sensitivity Study)

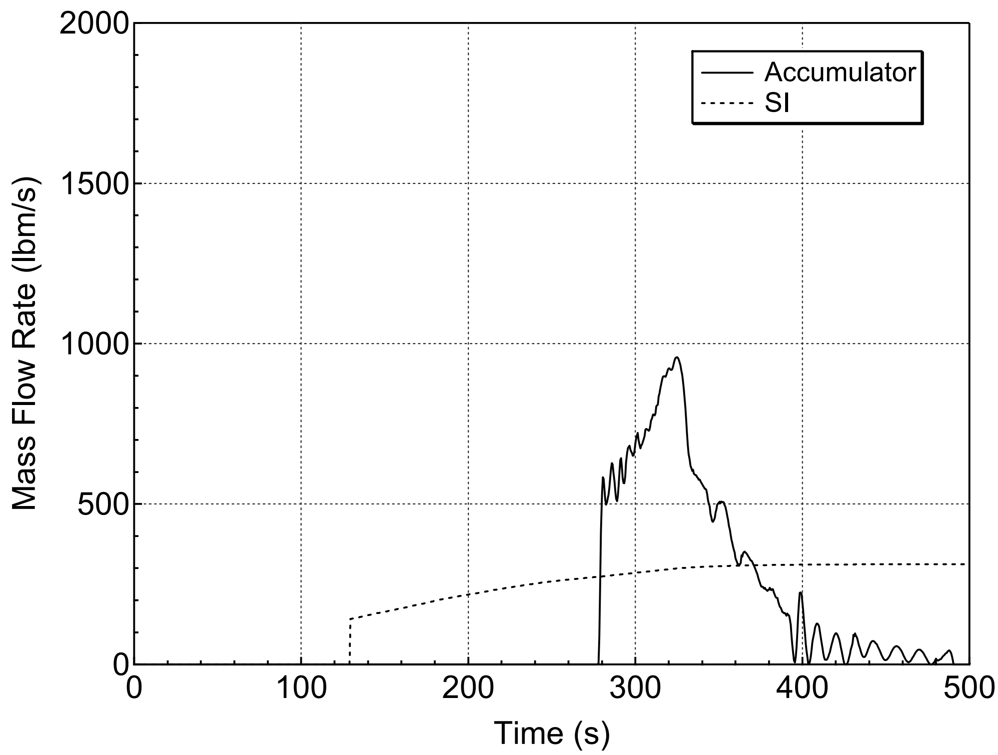

Figure 5.3.1.e-4 Accumulator and Safety Injection Mass Flowrates for 8-inch Break (Top) (Break Orientation Sensitivity Study)

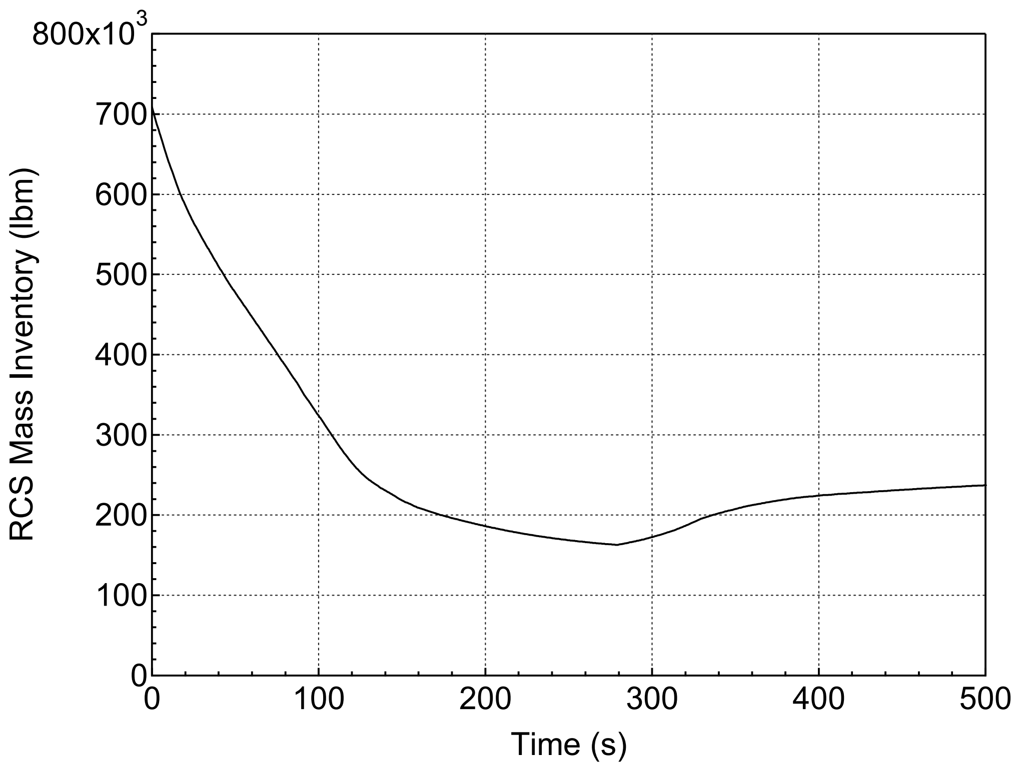

Figure 5.3.1.e-5 RCS Mass Inventory for 8-inch Break (Top)
(Break Orientation Sensitivity Study)

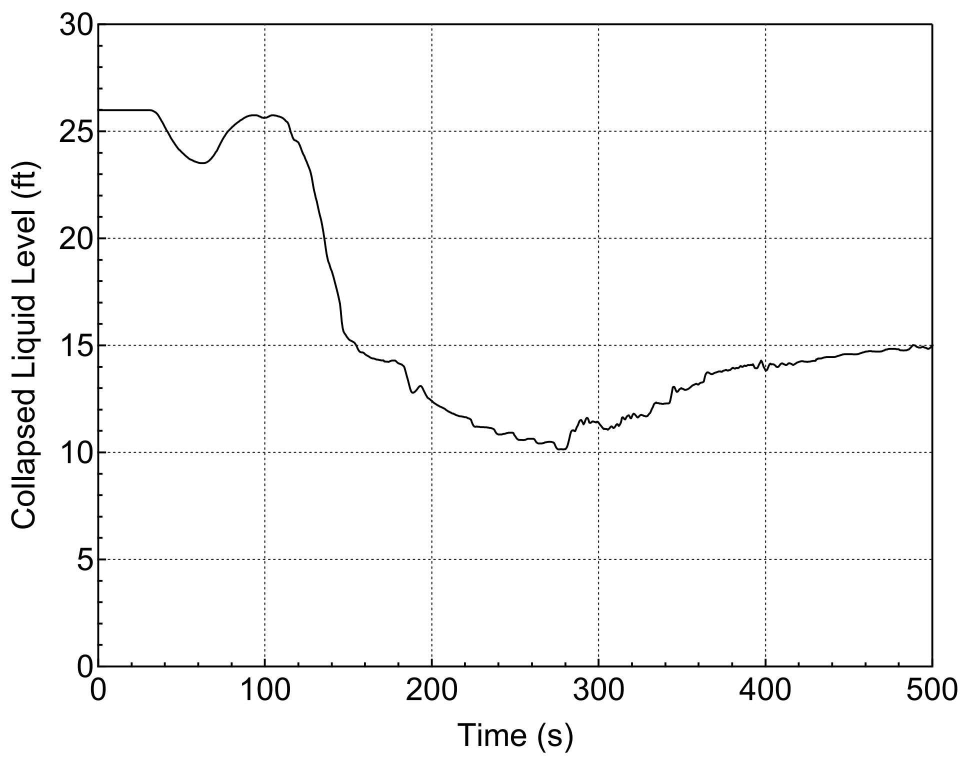

Figure 5.3.1.e-6 Downcomer Collapsed Level for 8-inch Break (Top) (Break Orientation Sensitivity Study)

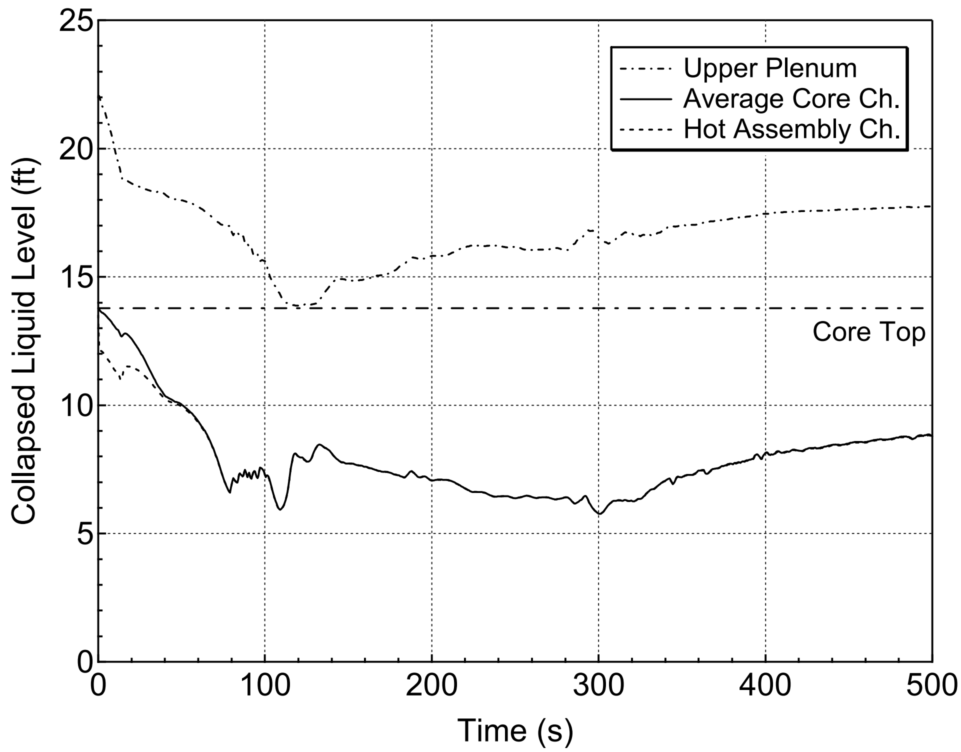

Figure 5.3.1.e-7 Core and Upper Plenum Collapsed Levels for 8-inch Break (Top) (Break Orientation Sensitivity Study)

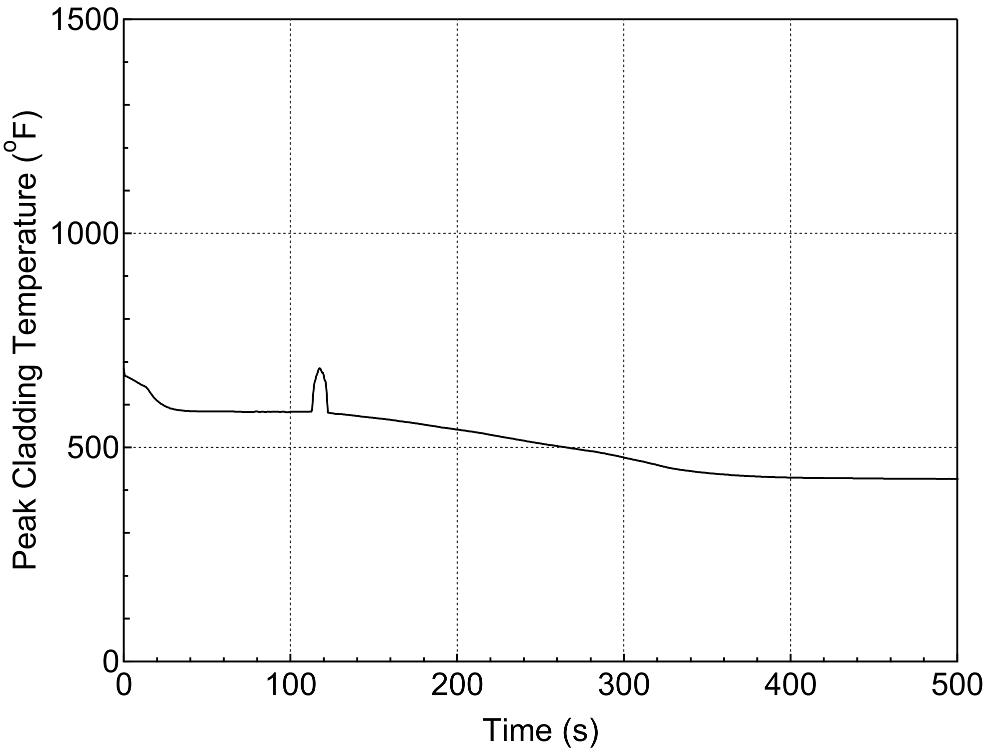

Figure 5.3.1.e-8 PCT at All Elevations for Hot Rod in Hot Assembly for 8-inch Break (Top) (Break Orientation Sensitivity Study)

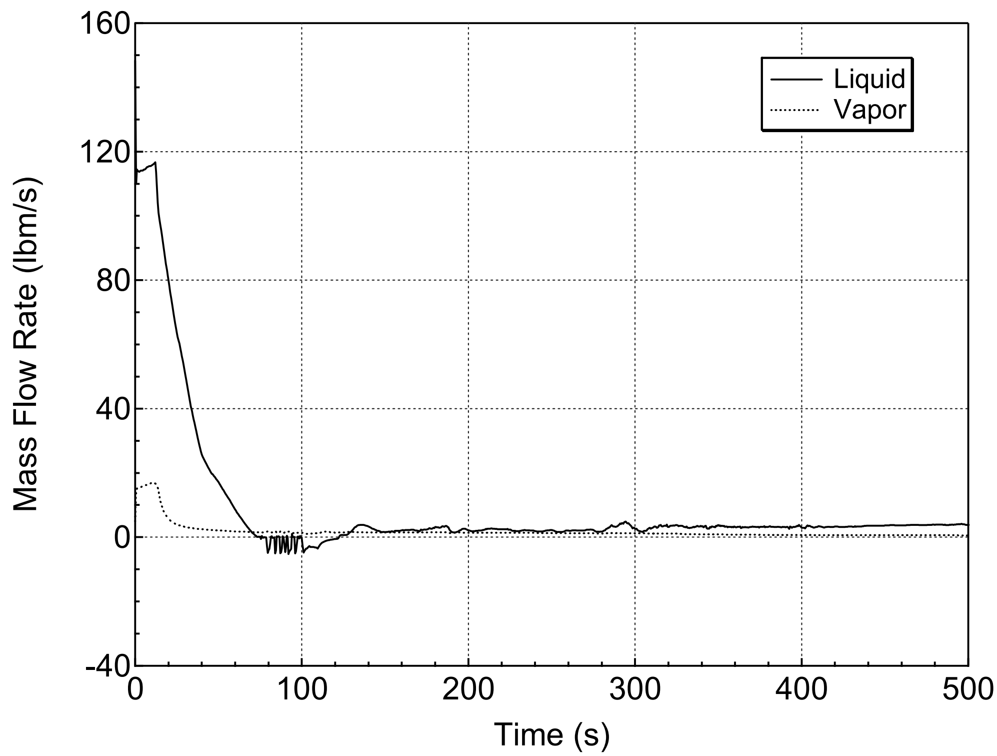

Figure 5.3.1.e-9 Hot Assembly Exit Vapor and Liquid Mass Flowrates for 8-inch Break (Top) (Break Orientation Sensitivity Study)

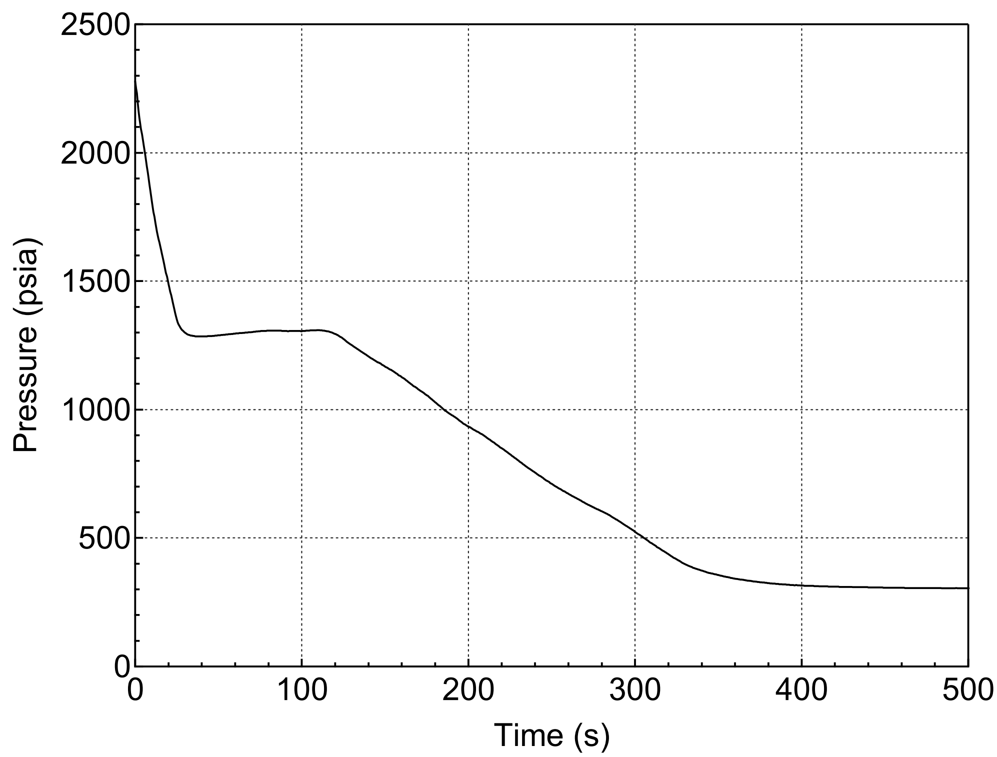

Figure 5.3.1.e-10 RCS (Pressurizer) Pressure Transient for 8-inch Break (Side) (Break Orientation Sensitivity Study)

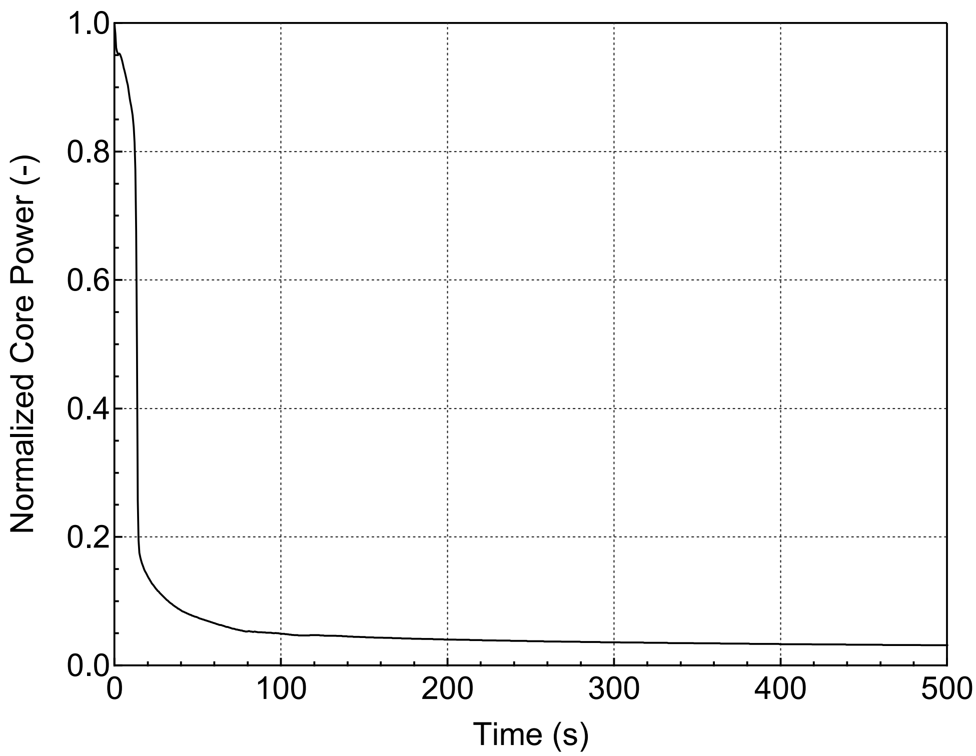

Figure 5.3.1.e-11 Normalized Core Power for 8-inch Break (Side) (Break Orientation Sensitivity Study)

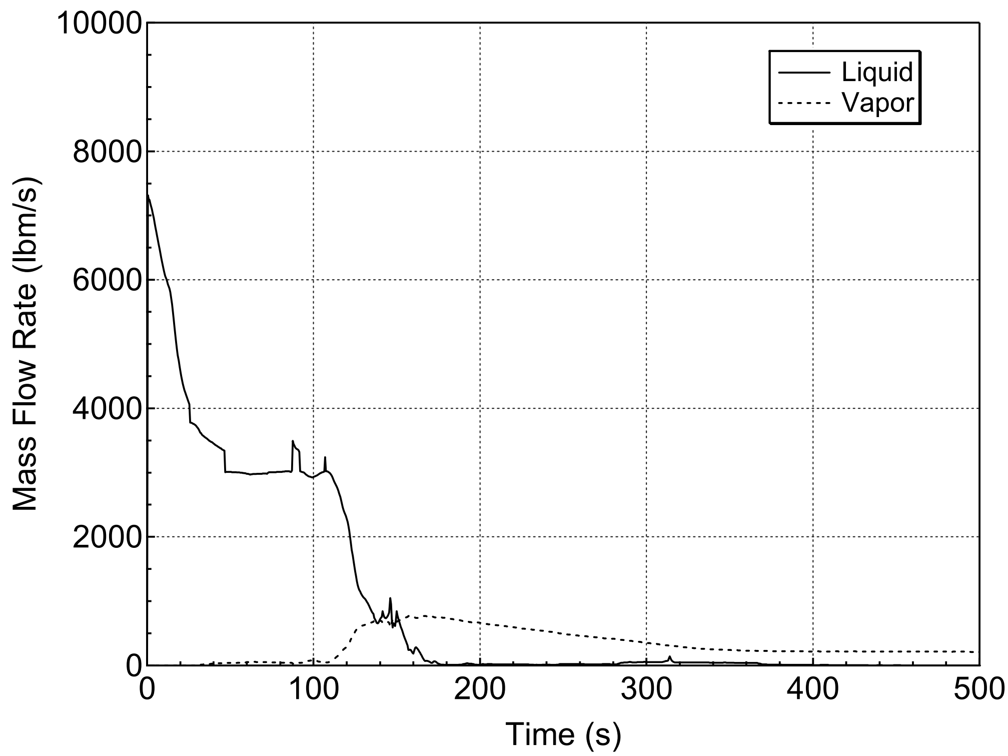

Figure 5.3.1.e-12 Liquid and Vapor Discharges through the Break for 8-inch Break (Side) (Break Orientation Sensitivity Study)

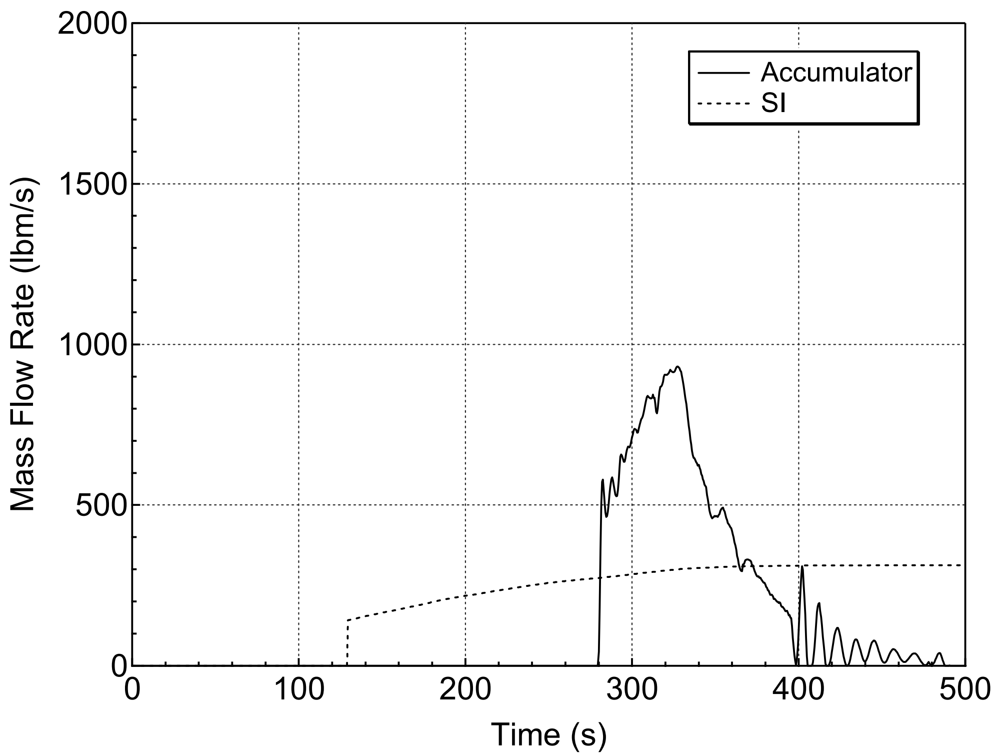

Figure 5.3.1.e-13 Accumulator and Safety Injection Mass Flowrates for 8-inch Break (Side) (Break Orientation Sensitivity Study)

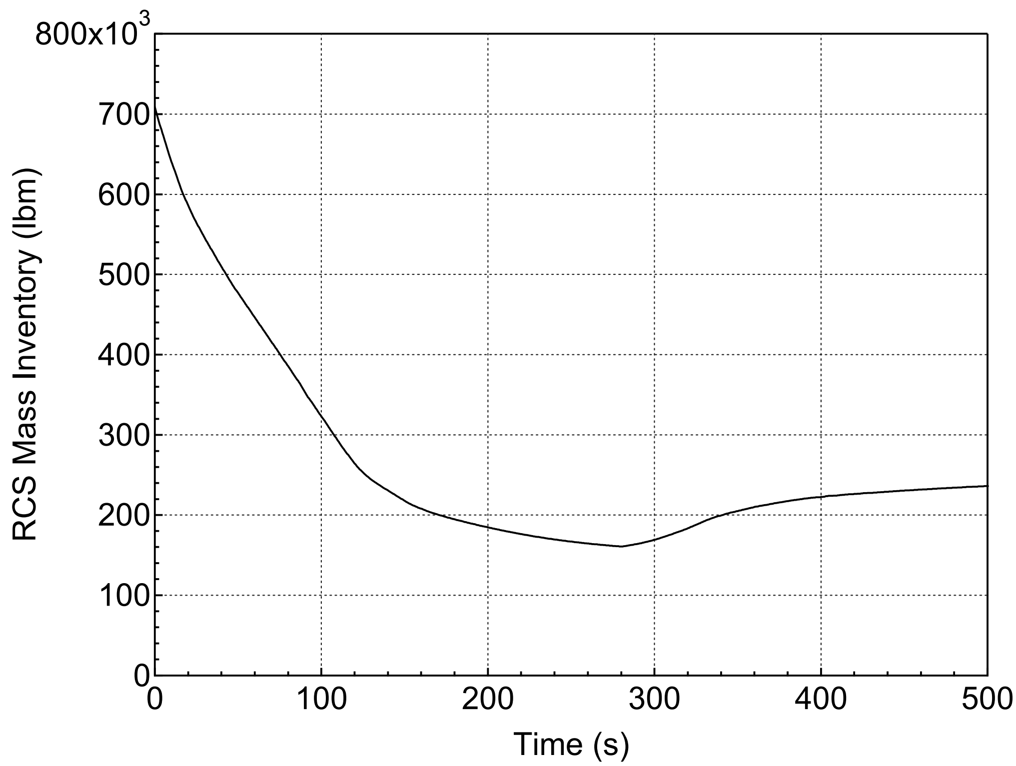

Figure 5.3.1.e-14 RCS Mass Inventory for 8-inch Break (Side)
(Break Orientation Sensitivity Study)

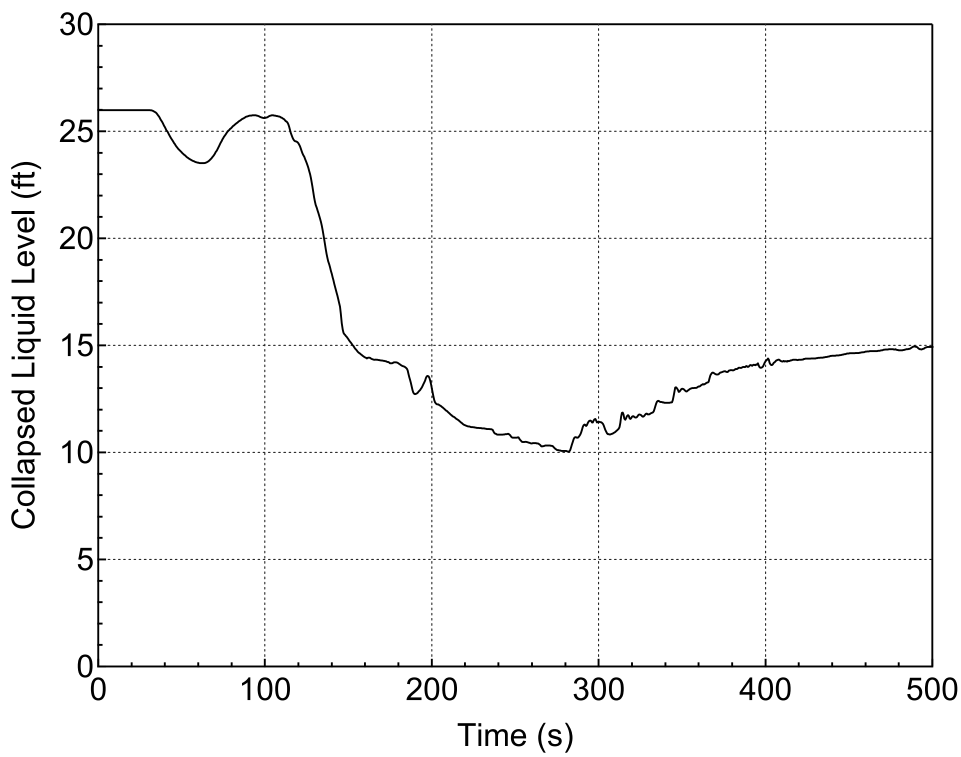

Figure 5.3.1.e-15 Downcomer Collapsed Level for 8-inch Break (Side) (Break Orientation Sensitivity Study)

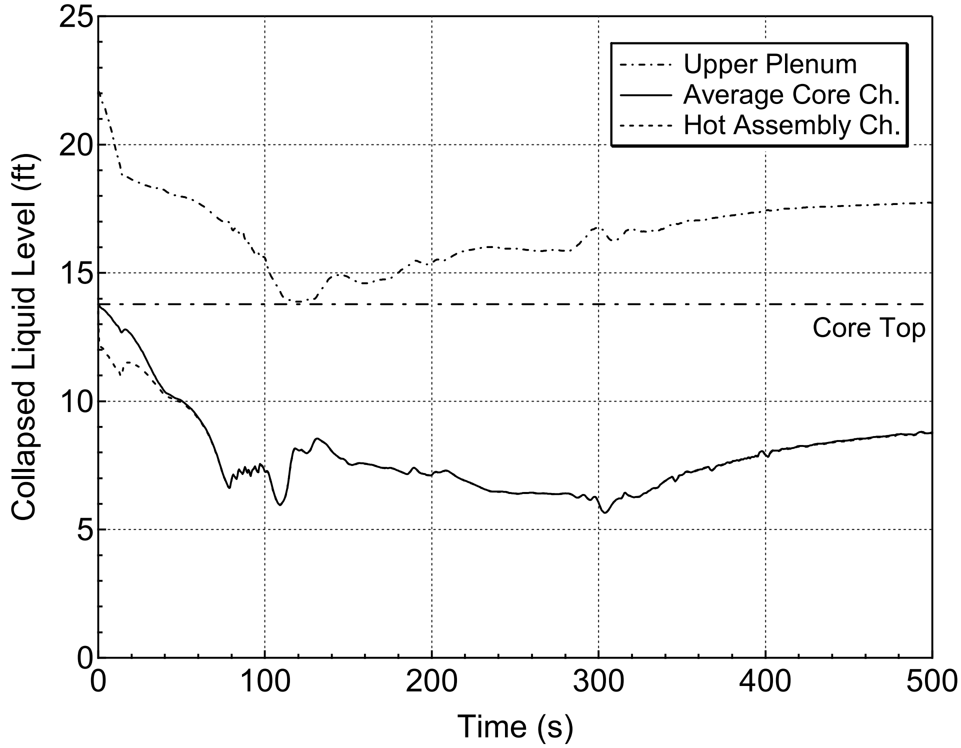

Figure 5.3.1.e-16 Core and Upper Plenum Collapsed Levels for 8-inch Break (Side) (Break Orientation Sensitivity Study)

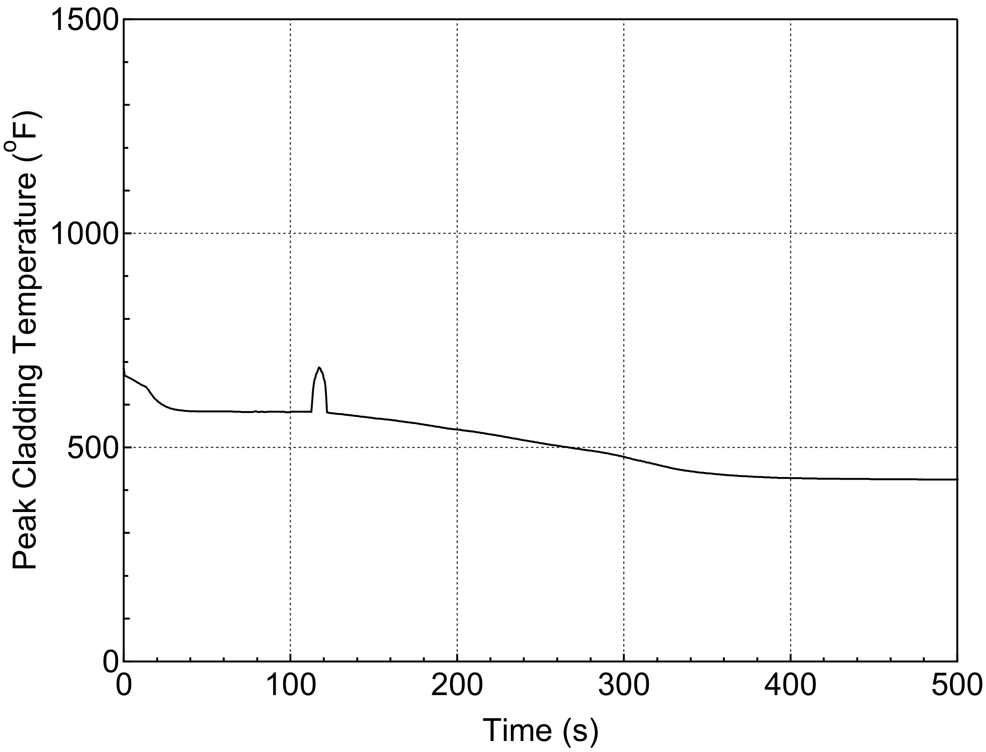

Figure 5.3.1.e-17 PCT at All Elevations for Hot Rod in Hot Assembly for 8-inch Break (Side) (Break Orientation Sensitivity Study)

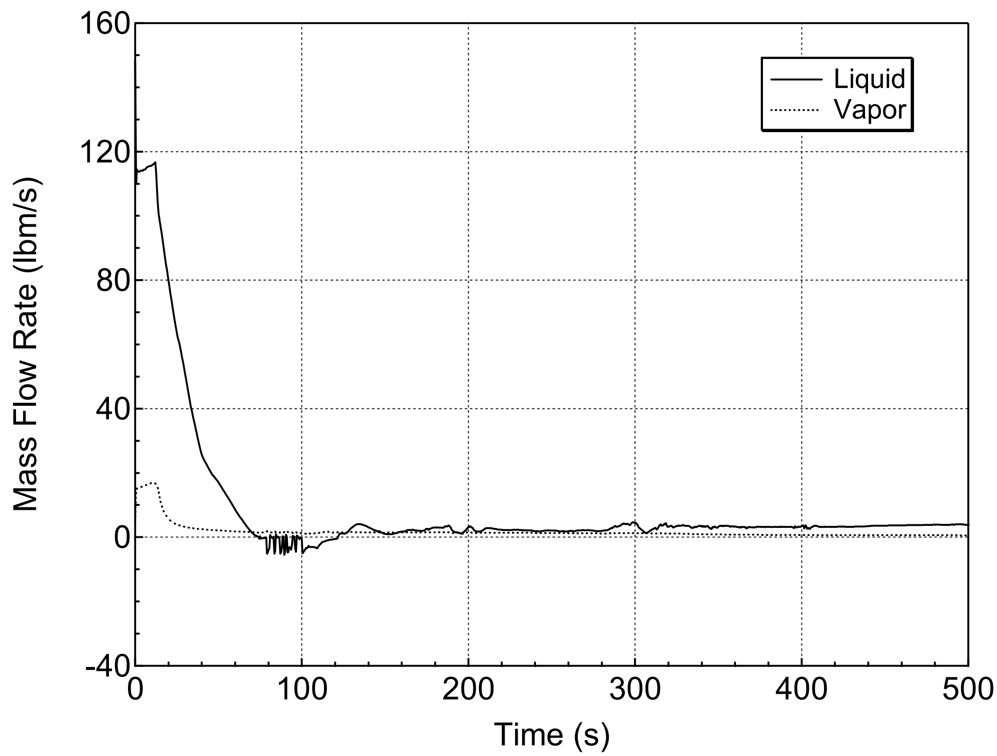

Figure 5.3.1.e-18 Hot Assembly Exit Vapor and Liquid Mass Flowrates for 8-inch Break (Side) (Break Orientation Sensitivity Study)

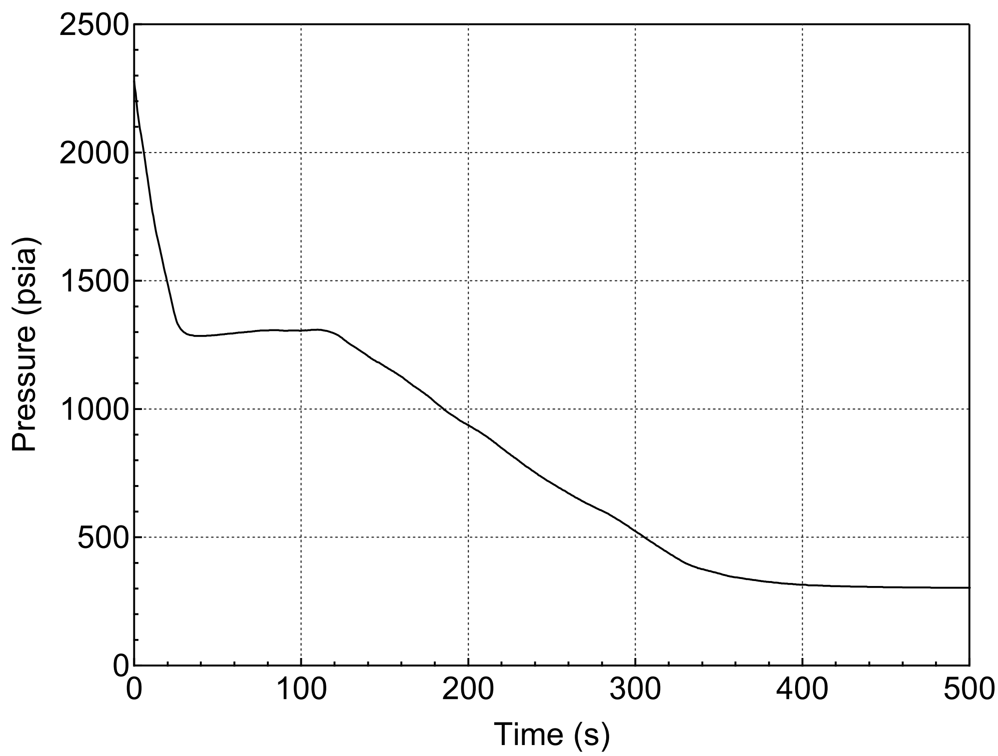

Figure 5.3.1.e-19 RCS (Pressurizer) Pressure Transient for 8-inch Break (Homogeneous) (Break Orientation Sensitivity Study)

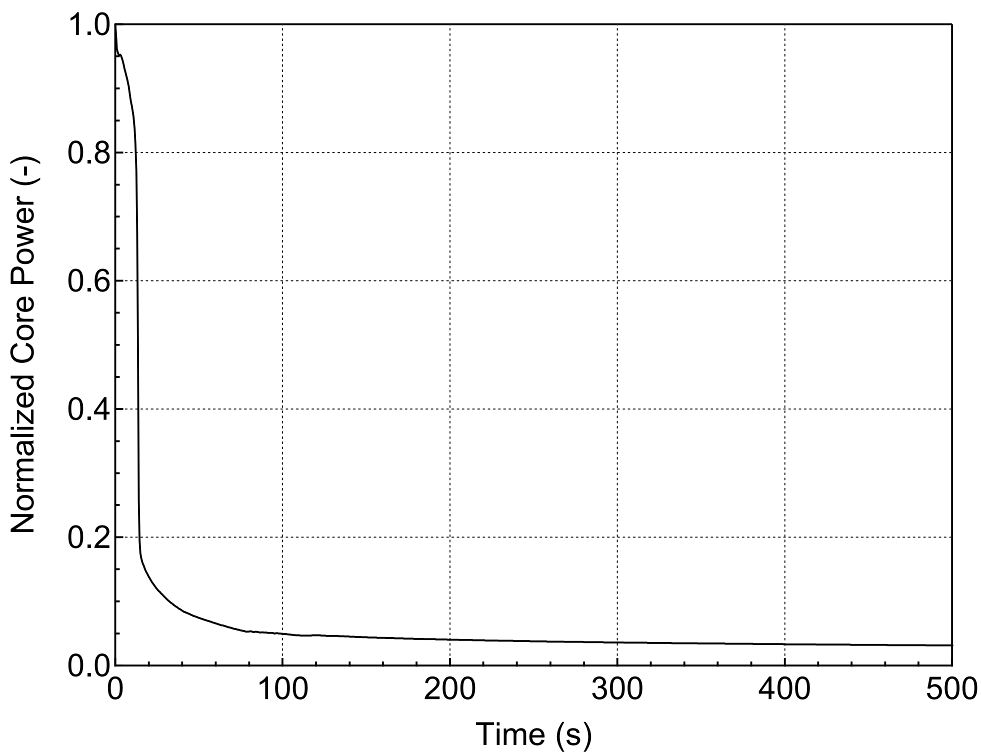

Figure 5.3.1.e-20 Normalized Core Power for 8-inch Break (Homogeneous) (Break Orientation Sensitivity Study)

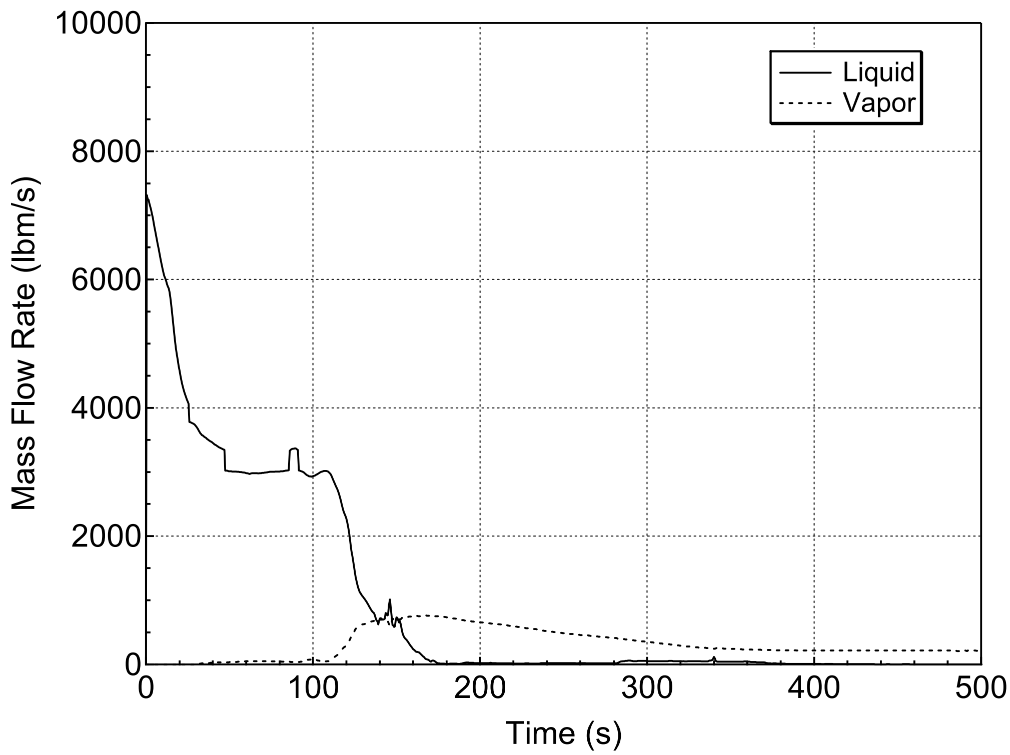

Figure 5.3.1.e-21 Liquid and Vapor Discharges through the Break for 8-inch Break (Homogeneous) (Break Orientation Sensitivity Study)

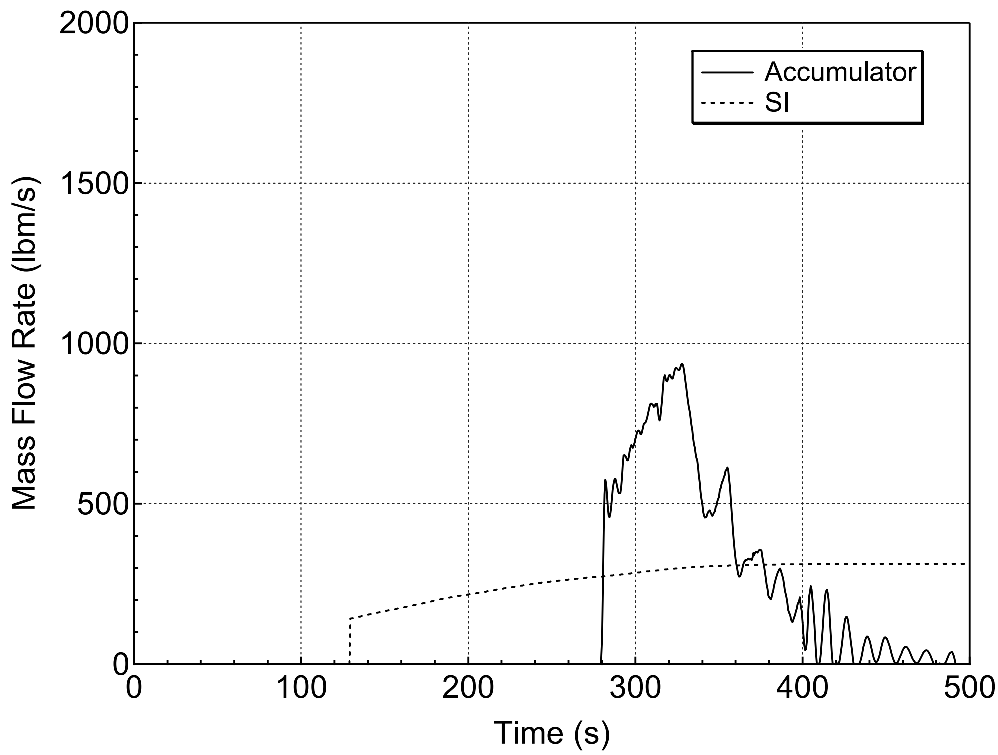

Figure 5.3.1.e-22 Accumulator and Safety Injection Mass Flowrates for 8-inch Break (Homogeneous) (Break Orientation Sensitivity Study)

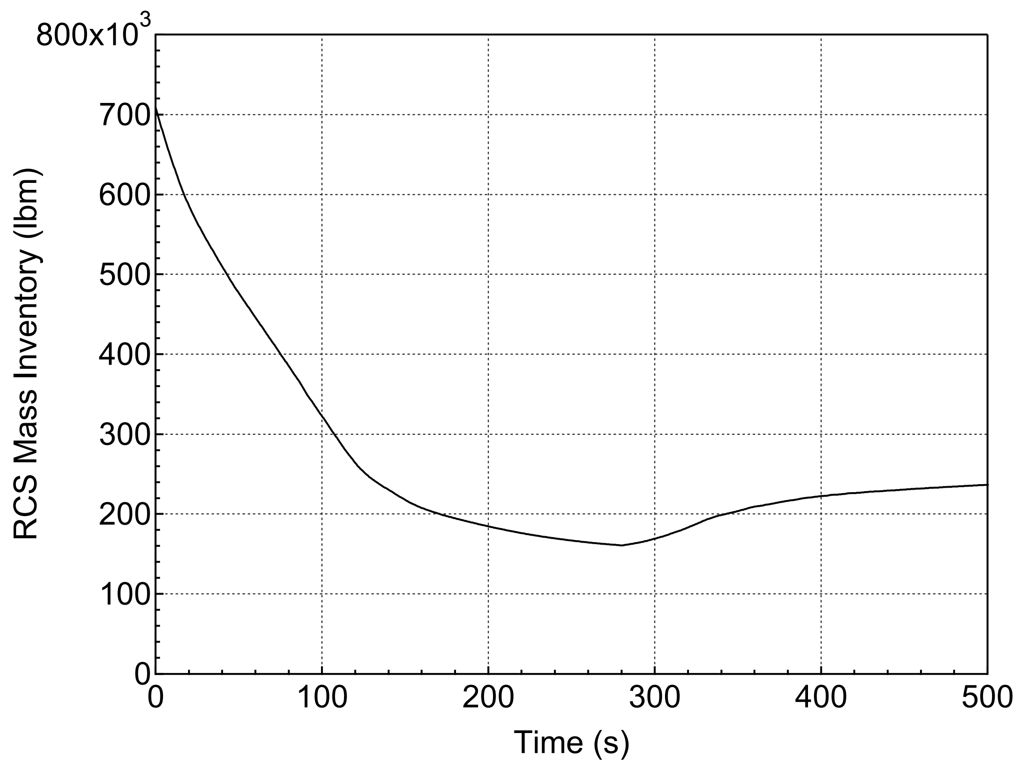

Figure 5.3.1.e-23 RCS Mass Inventory for 8-inch Break (Homogeneous) (Break Orientation Sensitivity Study)

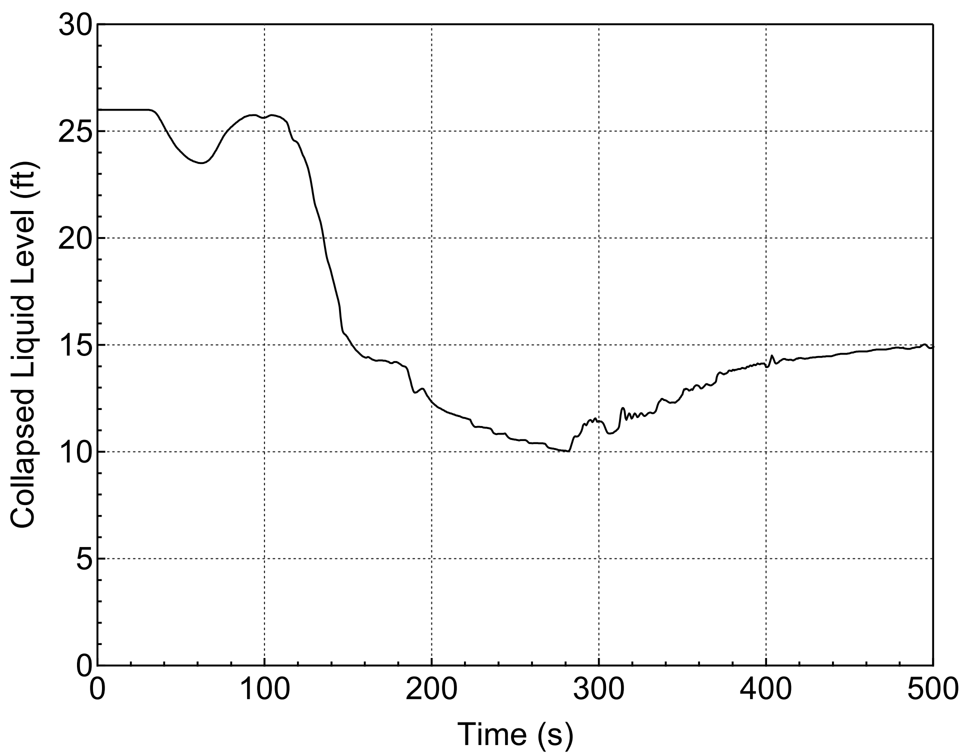

Figure 5.3.1.e-24 Downcomer Collapsed Level for 8-inch Break (Homogeneous) (Break Orientation Sensitivity Study)

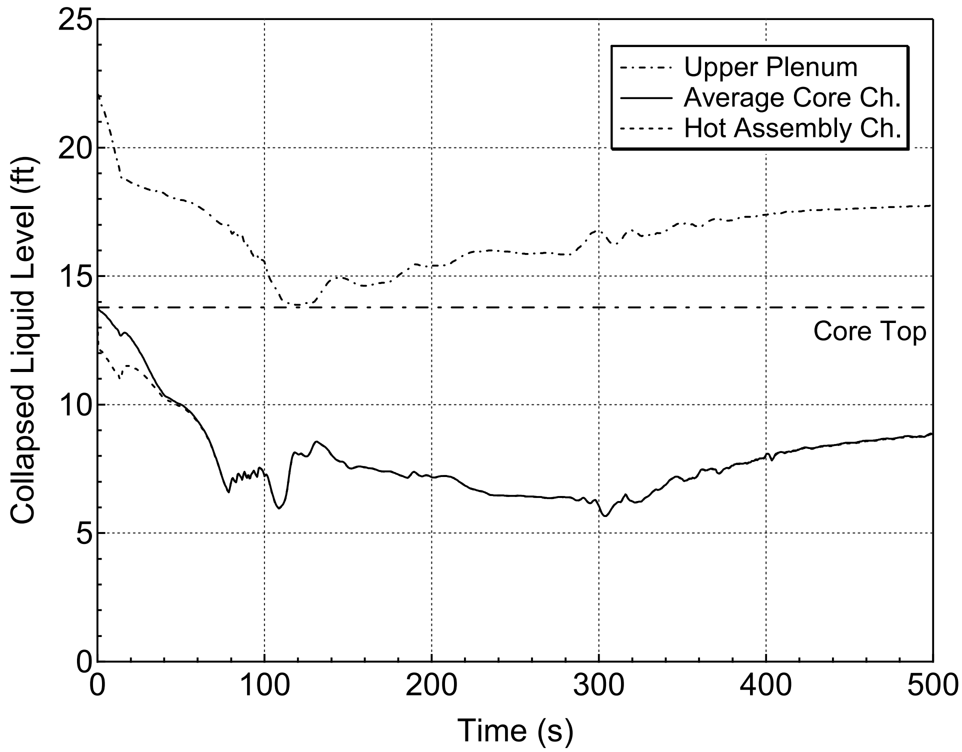

Figure 5.3.1.e-25 Core and Upper Plenum Collapsed Levels for 8-inch Break (Homogeneous) (Break Orientation Sensitivity Study)

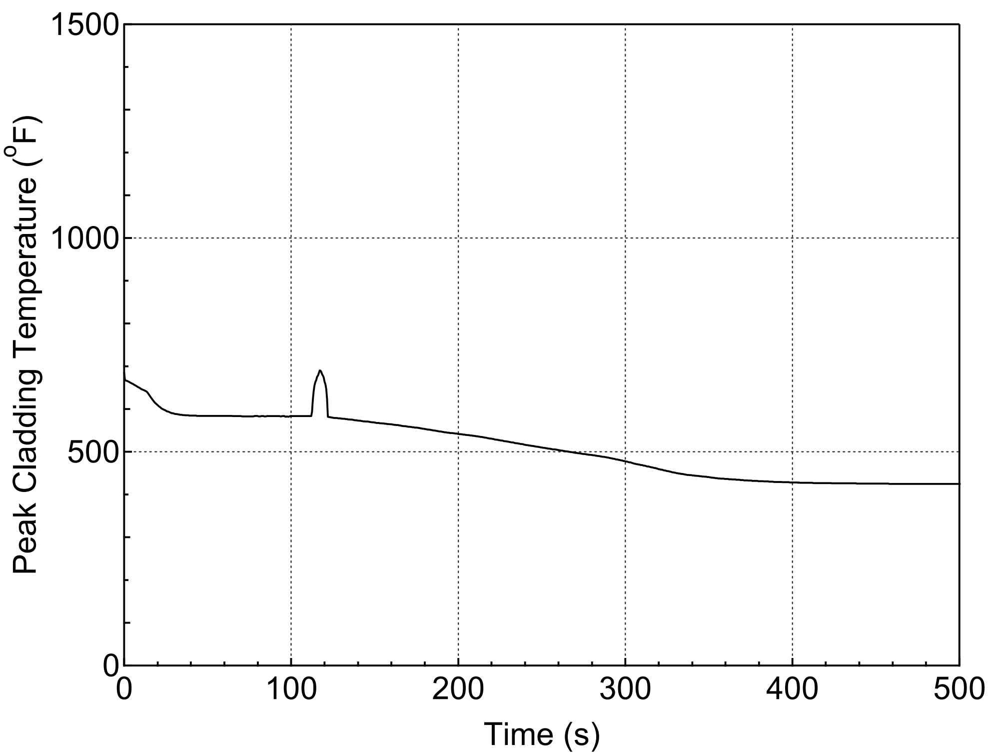

Figure 5.3.1.e-26 PCT at All Elevations for Hot Rod in Hot Assembly for 8-inch Break (Homogeneous) (Break Orientation Sensitivity Study)

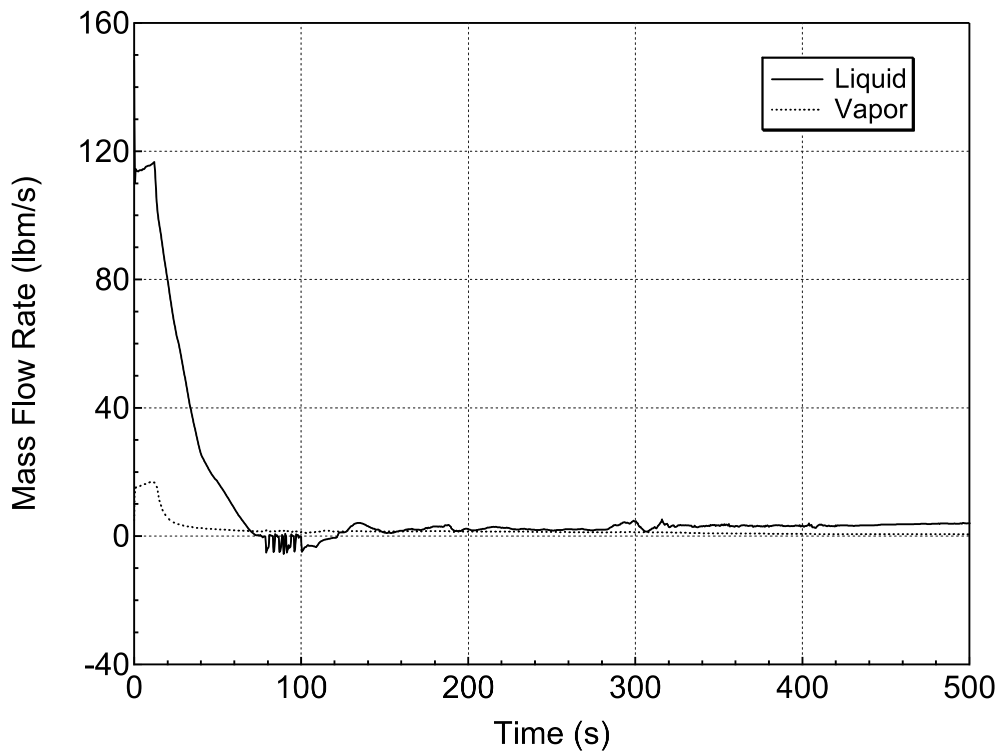

Figure 5.3.1.e-27 Hot Assembly Exit Vapor and Liquid Mass Flowrates for 8-inch Break (Homogeneous) (Break Orientation Sensitivity Study)

5.3.2 Boil-off-PCT

Three break size cases (12 inch, 13 inch, and 1-ft^2 break) were calculated with the break orientations of bottom, top, and side breaks, and homogeneous break flow. Figure 5.3.2.a-1 through 5.3.2.c-18 show the main plots and Table 5.3.2-1 shows the summary of the PCT results for all cases. The highest PCT is 1088°F for 1-ft^2 break of top break. Table 5.3.2-2 shows the sequence of events and Table 5.3.2-3 summarizes the main results for this case and the results of this case are explained below in detail.

Figure 5.3.2.c-1 shows the RCS (pressurizer) pressure transient for the 1-ft^2 cold leg top orientation break. As a result of the break, the RCS rapidly depressurizes from 2280 psia to about 1200 psia within the first 20 seconds, then decreases gradually. A reactor trip signal and ECCS actuation signal are generated when the low pressurizer pressure setpoints of 1860 psia and 1760 psia are reached, consecutively.

Figure 5.3.2.c-2 displays the normalized core power transient following the break. The reactor trips at 7 seconds due to the low pressurizer pressure setpoint. Then, the control rod insertion starts at 8.7 seconds. This figure shows that the core is rapidly shutdown by control rod insertion and void formation in the core. After the reactor trip, the main fraction of the heat generation comes from fission product decay gamma rays.

Figure 5.3.2.c-3 presents the liquid and vapor discharges through the break. The single-phase liquid discharges from the break and rapidly diminishing within 50 seconds. Afterward, flashing occurs as more vapor phase come into the mixture. The liquid flashing decreases as the transient progresses and a low flow rate vapor phase flow out the break.

Figure 5.3.2.c-4 illustrates the sequence of ECCS actuations following the break. The ECCS actuation signal is initiated when the low pressurizer pressure setpoint is attained at 8.3 seconds. First, the accumulators inject the borated water at a large flow rate at 90 seconds. The accumulator injection stops at about 220 seconds, because the RCS pressure reaches constant value of 200 psia. After a 118 seconds time delay in the case of LOOP, the SI pumps supply borated-water from the RWSP into the core at 126 seconds. The SI pumps mass flow rate is constant due to the sufficiently low RCS pressure of about 200 psia.

Figure 5.3.2.c-5 shows the RCS inventory transient. As a result of the break, the coolant inventory of the RCS rapidly decreases within 120 seconds. The actuations of SI pumps and

accumulator injections quickly restore the inventory and prevent further reduction. Then the RCS mass inventory is maintained at about 250,000 lbm.

Figure 5.3.2.c-6 shows the collapsed liquid level in the downcomer. It is observable that the lowest downcomer collapsed level reaches a low value in 120 seconds. Collapsed level in the downcomer decreases corresponding to the decrease in RCS mass inventory displayed in the previous figure. HHIS actuation through DVI lines and accumulator injections into the cold legs prevent further inventory loss. Afterwards, the collapsed level is quickly restored before 200 seconds.

Figure 5.3.2.c-7 depicts that the transient characteristic of collapsed levels in the average core channel, hot assembly channel, as well as in the upper plenum are quite similar, as these parameters fluctuate in the same vertical direction. Borated water injection from the accumulators prevents further reduction of the core collapsed level.

Figure 5.3.2.c-8 shows the PCT at all elevations for the hot rod. The PCT of 1088°F occurs at 169 seconds. This figure demonstrates that the PCT is substantially lower than 2200°F. After the occurrence of boil off PCT, the cladding temperature quickly cools down to 300°F. The injection of borated water by both the accumulators and SI pumps provides for the heat transfer from the core and prevents cladding temperature heatup by keeping sufficient water level in the core.

The hot assembly exit vapor and liquid mass flow rates are shown in Figure 5.3.2.c-9. Mass flow rates of both phases rapidly reduce after the RCP trips due to the LOOP assumption. About 50 seconds after the break, a flow reversal occurs in the core caused by the discharge of subcooled coolant from the break and the performance degradation of the RCPs in the intact loops due to the presence of two-phase mixture.

It is concluded that this case is characterized by the occurrence of the highest PCT caused by boil-off, due to the insufficient upward flow through the core. The accumulators and SI pumps facilitate the heat transfer from the core, thus prevent cladding temperature heatup by maintaining sufficient collapsed level in the core.

Table 5.3.2-1 Spectrum of Peak Cladding Temperature for Boil-off-PCT Cases

Break Orientation / Break Size & Location	Bottom	Top	Side	Homogeneous
12-inch at cold leg	741 (°F)	747 (°F)	825 (°F)	811 (°F)
13-inch at cold leg	971 (°F)	1000 (°F)	946 (°F)	941 (°F)
1-ft^2 at cold leg	1029 (°F)	1088 (°F)	1022 (°F)	995 (°F)

Table 5.3.2-2 Sequence of Events for 1-ft^2 Break (Top) (Break Orientation Sensitivity Study)

Event	Time (sec)
Break occurs; blowdown initiation	0.0
Reactor trip (loss-of-offsite power is assumed)	6.9
ECCS actuation signal	8.3
Control rod insertion starts	8.7
Main steam isolation	8.7
RCP trip	9.9
Main feedwater isolation	14.9
Main steam safety valve open	not actuated
Accumulator injection begins	89
Fuel cladding starts heating up	95
Emergency Power Source initiates	111
High Head Injection System begins	126
Peak Cladding Temperature occurs	151
Emergency feedwater flow begins	141
Fuel cladding rewets	169

Table 5.3.2-3 Core Performance Results for 1-ft^2 Break (Top) (Break Orientation Sensitivity Study)

	Values
Peak Cladding Temperature (°F)	1088
Maximum local cladding oxidation (%)	0.2
Maximum core wide cladding oxidation (%)	less than 0.2

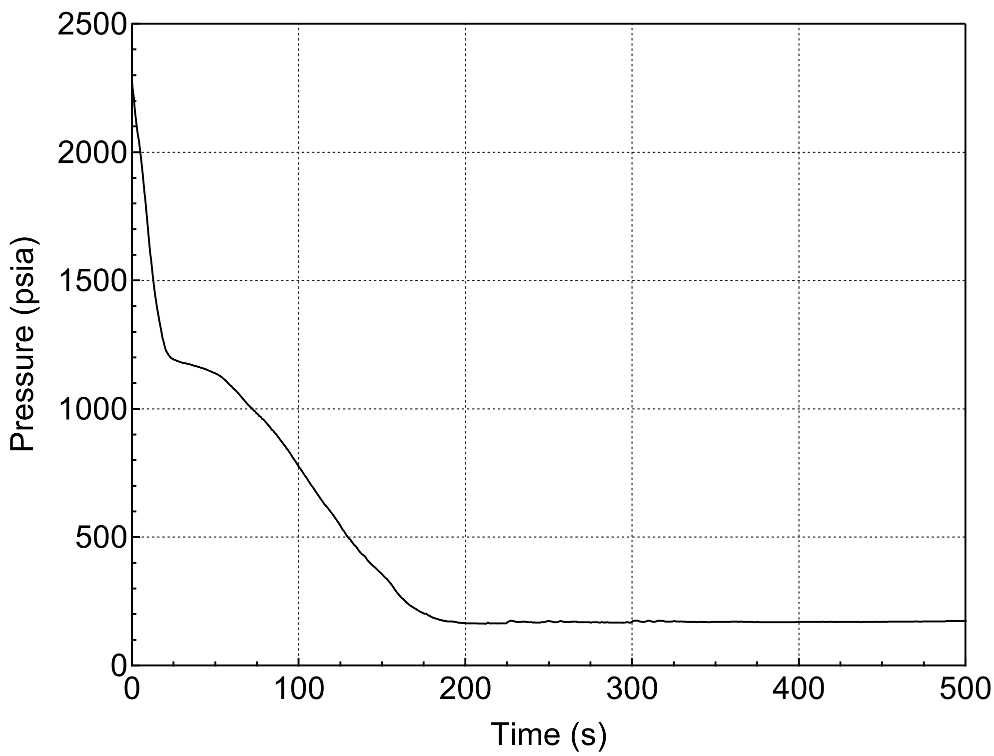

Figure 5.3.2.a-1 RCS (Pressurizer) Pressure Transient for 12-inch Break (Top) (Break Orientation Sensitivity Study)

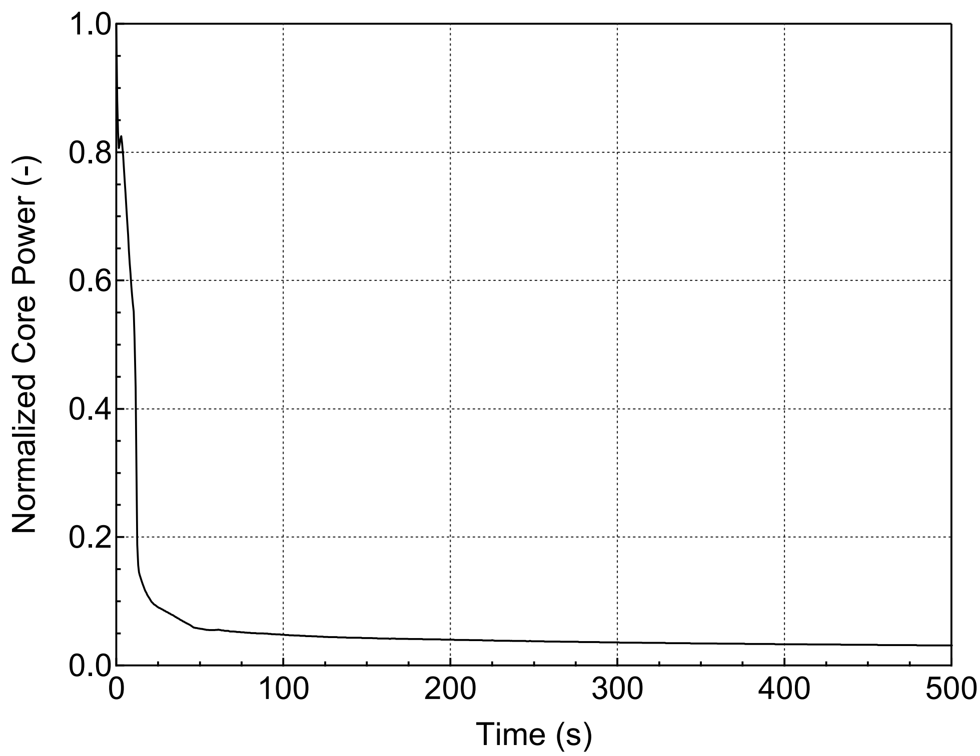

Figure 5.3.2.a-2 Normalized Core Power for 12-inch Break (Top)
(Break Orientation Sensitivity Study)

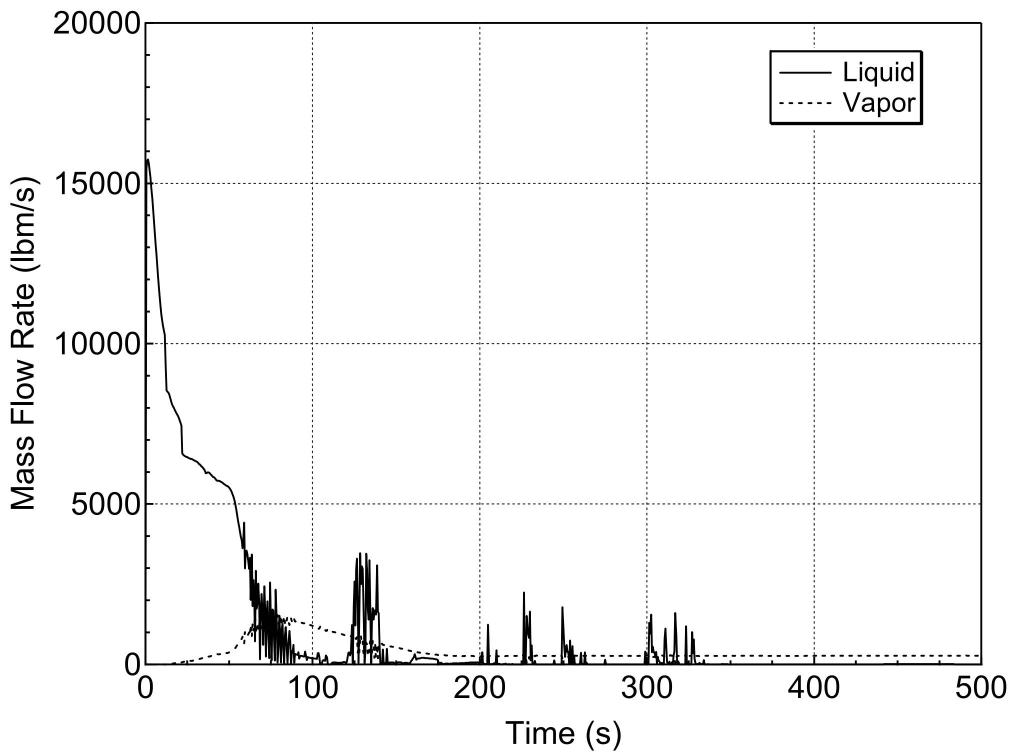

Figure 5.3.2.a-3 Liquid and Vapor Discharges through the Break for 12-inch Break (Top) (Break Orientation Sensitivity Study)

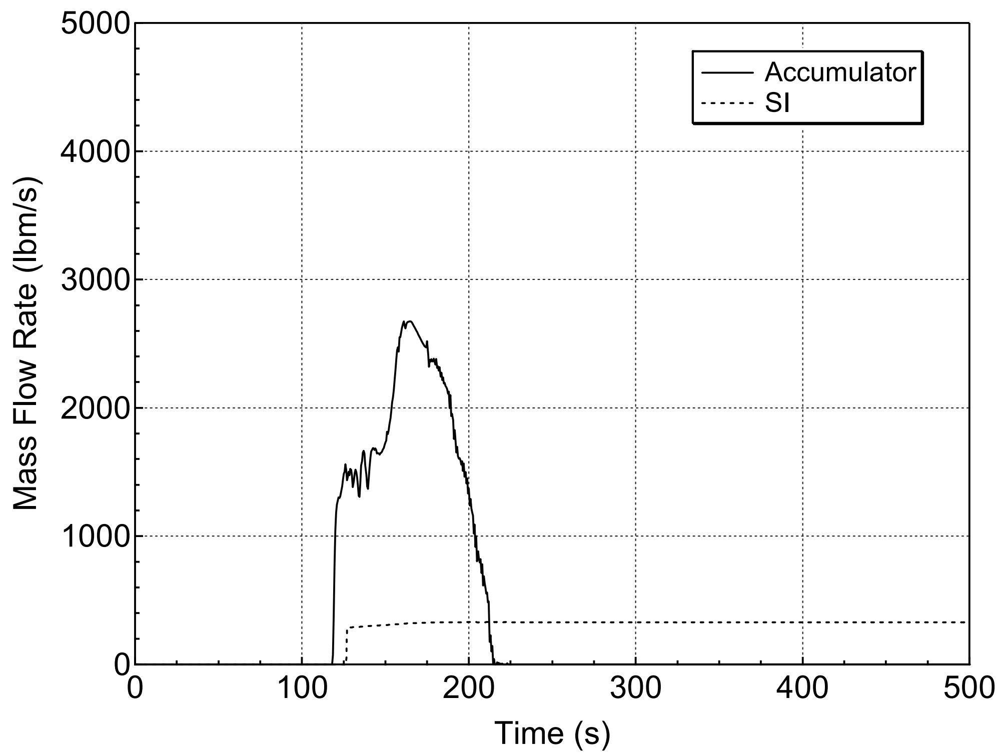

Figure 5.3.2.a-4 Accumulator and Safety Injection Mass Flowrates for 12-inch Break (Top) (Break Orientation Sensitivity Study)

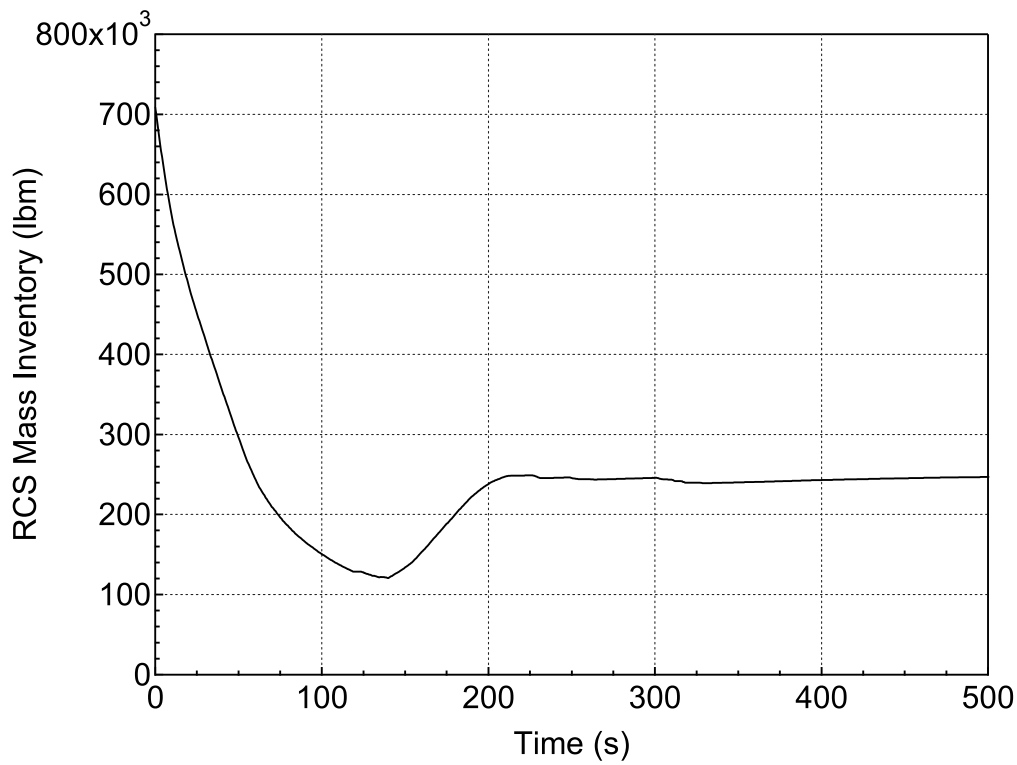

Figure 5.3.2.a-5 RCS Mass Inventory for 12-inch Break (Top)
(Break Orientation Sensitivity Study)

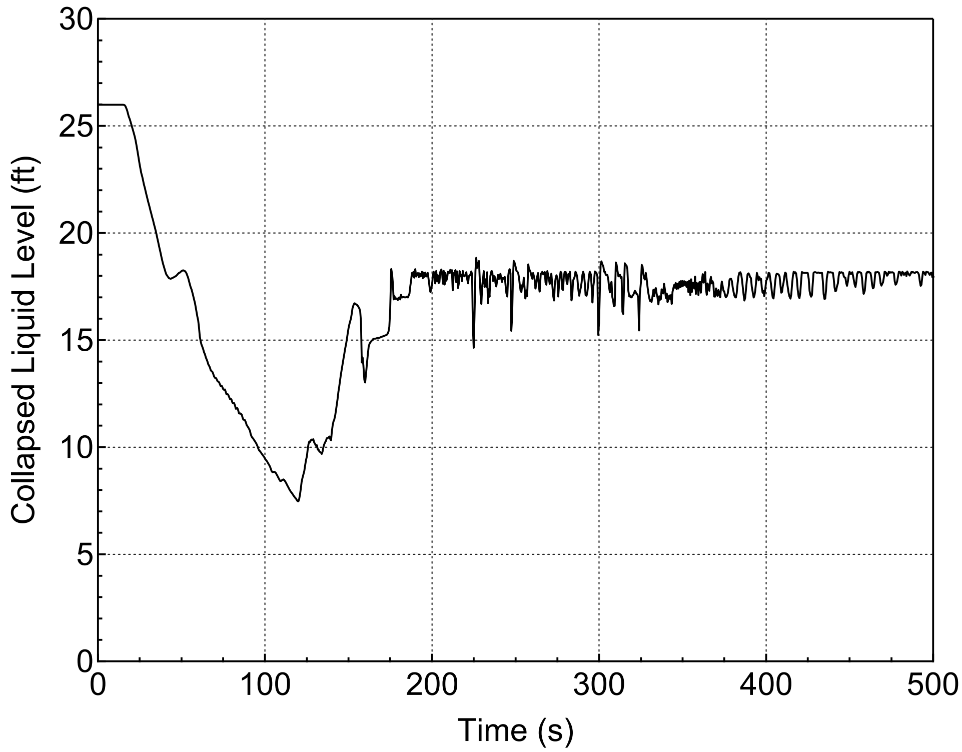

Figure 5.3.2.a-6 Downcomer Collapsed Level for 12-inch Break (Top) (Break Orientation Sensitivity Study)

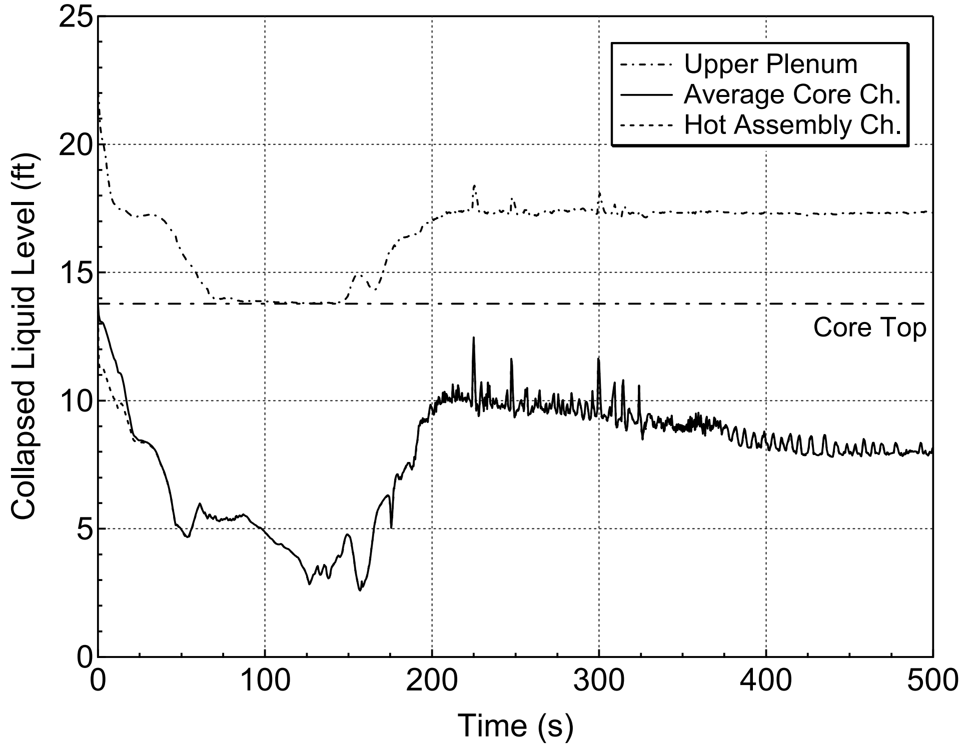

Figure 5.3.2.a-7 Core and Upper Plenum Collapsed Levels for 12-inch Break (Top) (Break Orientation Sensitivity Study)

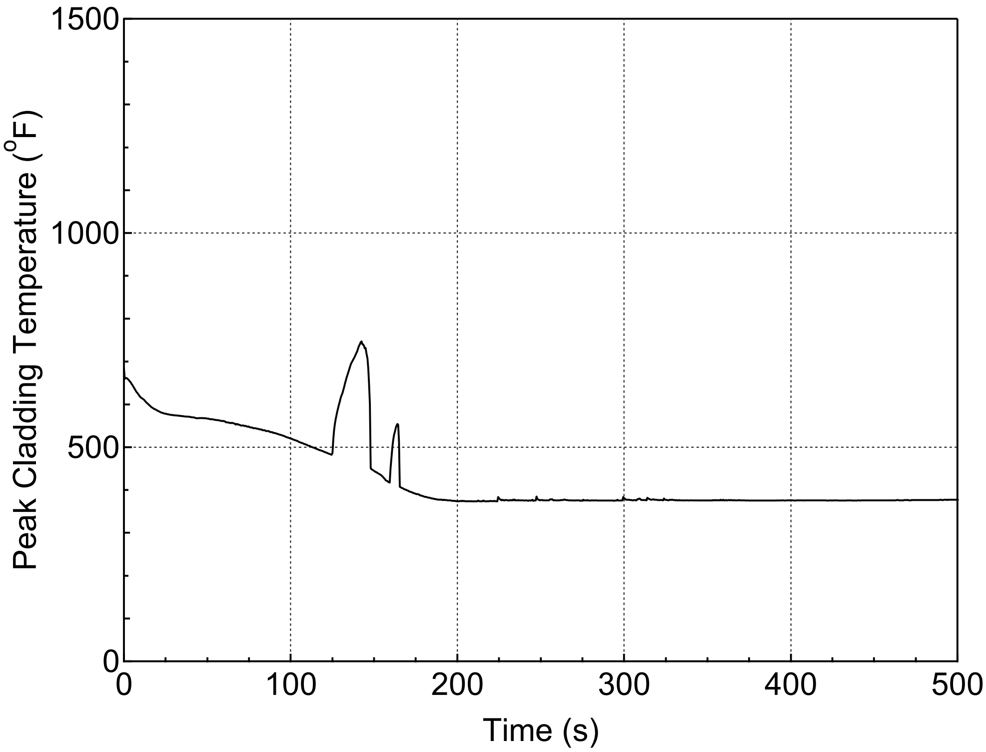

Figure 5.3.2.a-8 PCT at All Elevations for Hot Rod in Hot Assembly for 12-inch Break (Top) (Break Orientation Sensitivity Study)

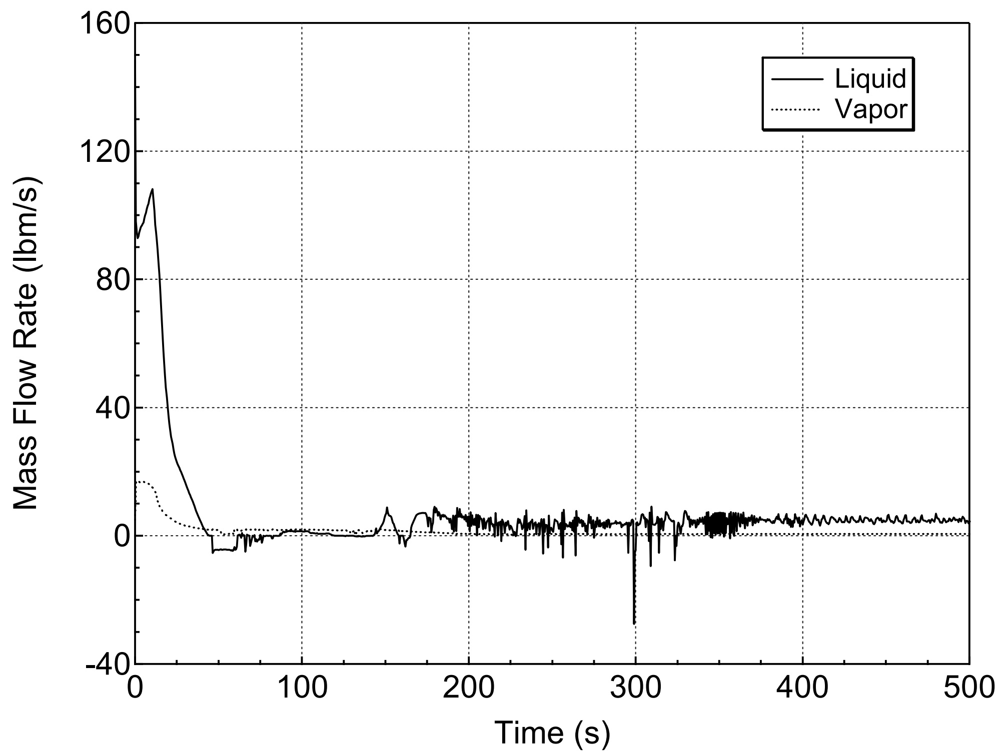

Figure 5.3.2.a-9 Hot Assembly Exit Vapor and Liquid Mass Flowrates for 12-inch Break (Top) (Break Orientation Sensitivity Study)

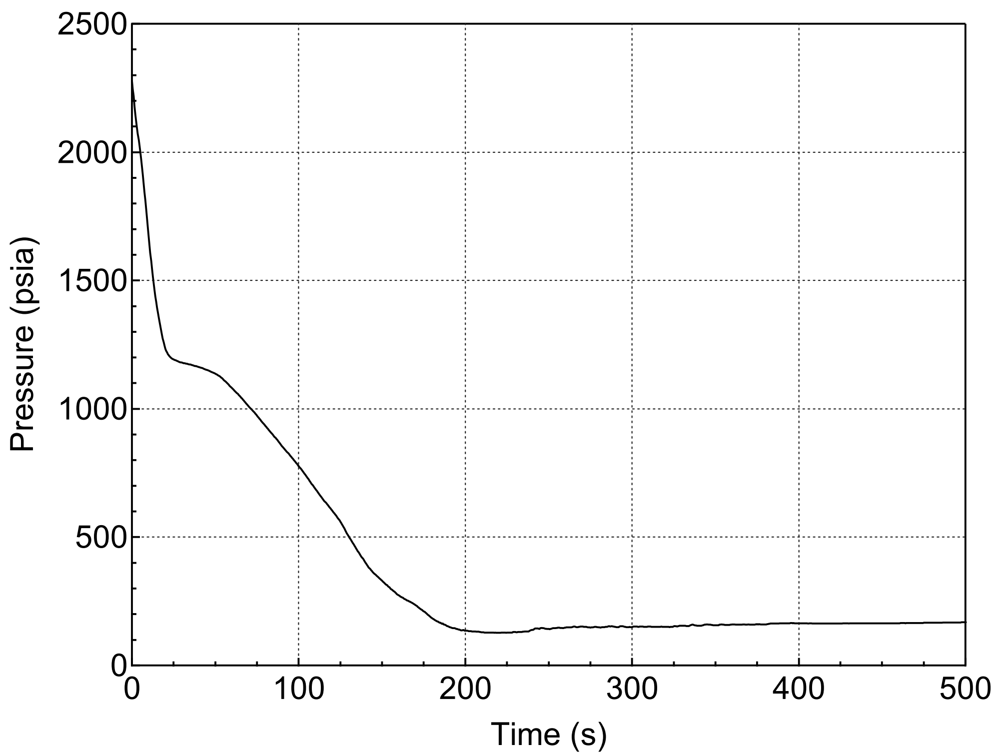

Figure 5.3.2.a-10 RCS (Pressurizer) Pressure Transient for 12-inch Break (Side) (Break Orientation Sensitivity Study)

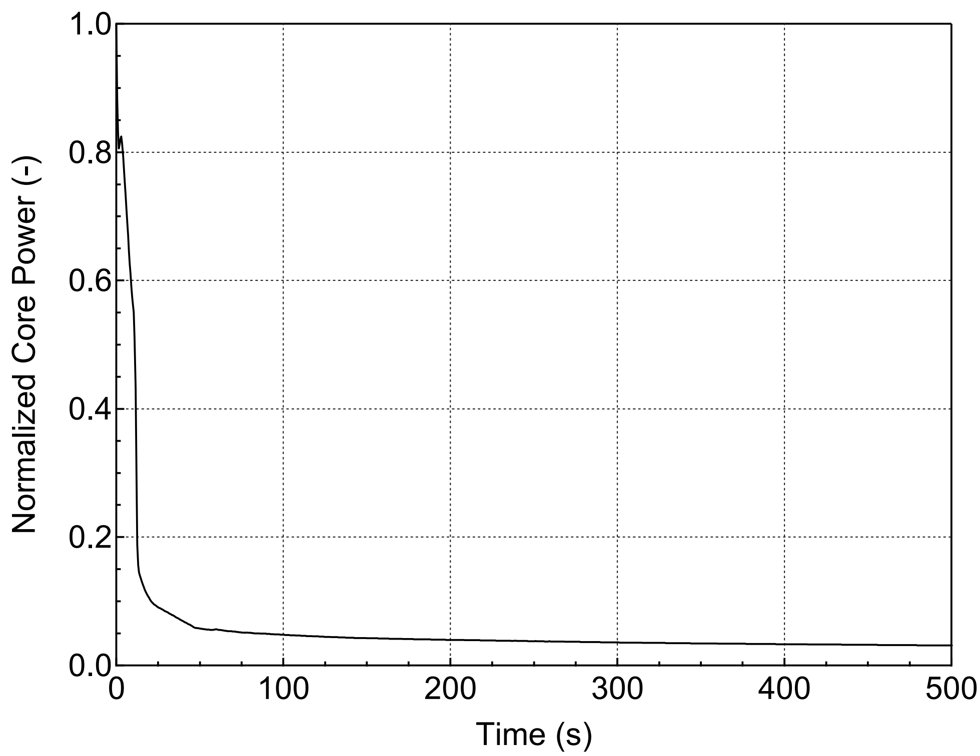

Figure 5.3.2.a-11 Normalized Core Power for 12-inch Break (Side) (Break Orientation Sensitivity Study)

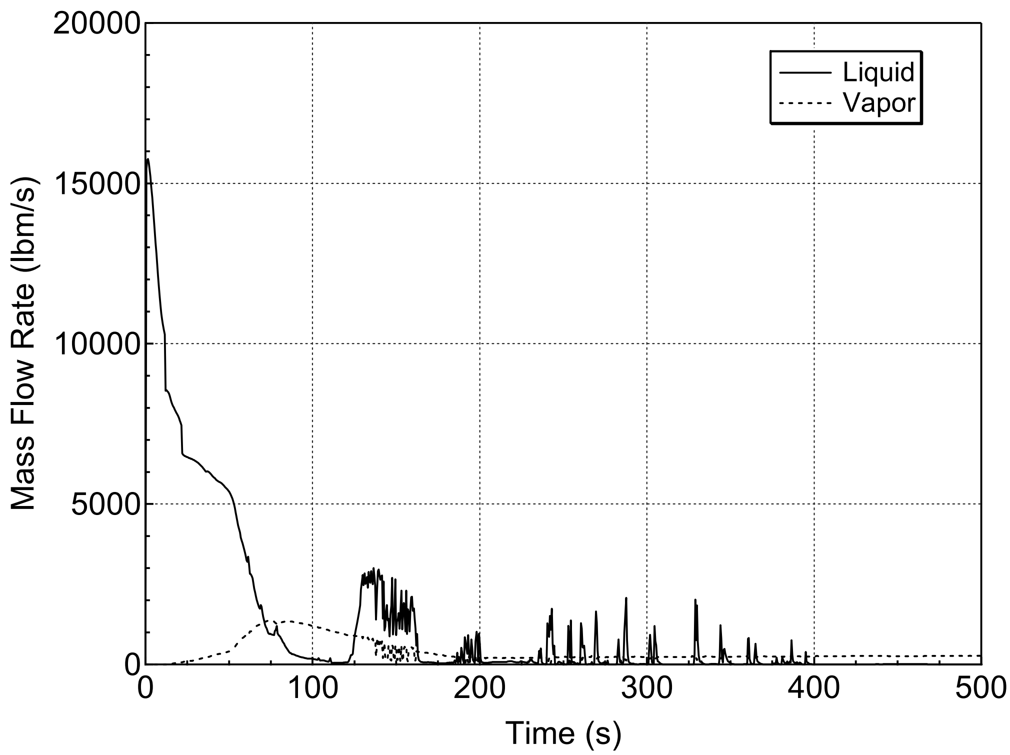

Figure 5.3.2.a-12 Liquid and Vapor Discharges through the Break for 12-inch Break (Side) (Break Orientation Sensitivity Study)

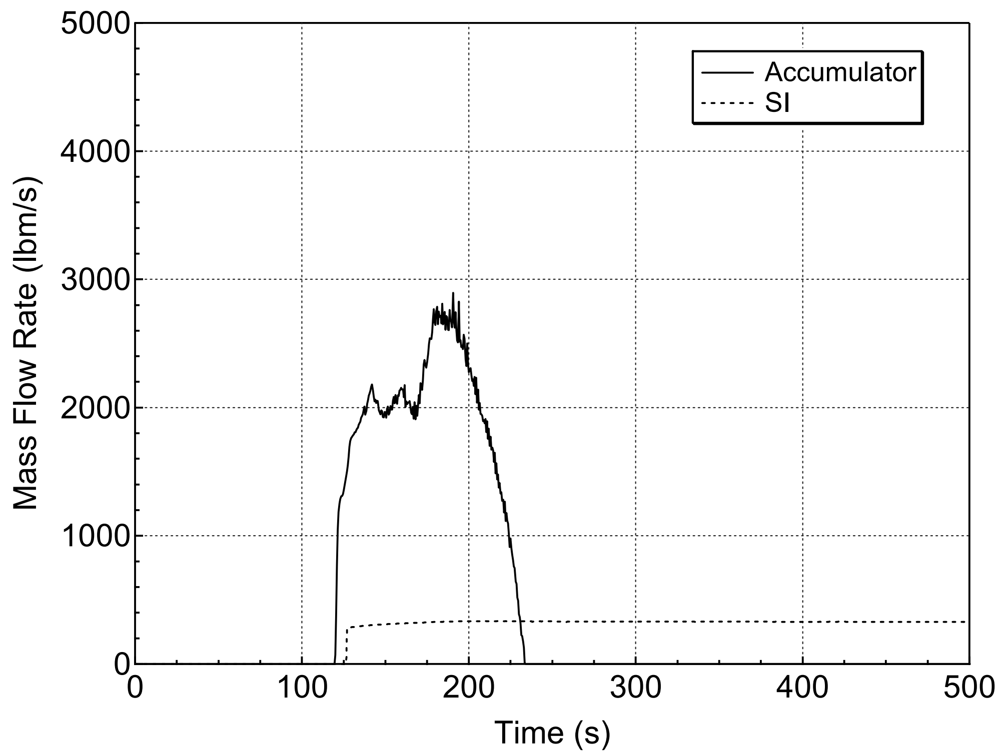

Figure 5.3.2.a-13 Accumulator and Safety Injection Mass Flowrates for 12-inch Break (Side) (Break Orientation Sensitivity Study)

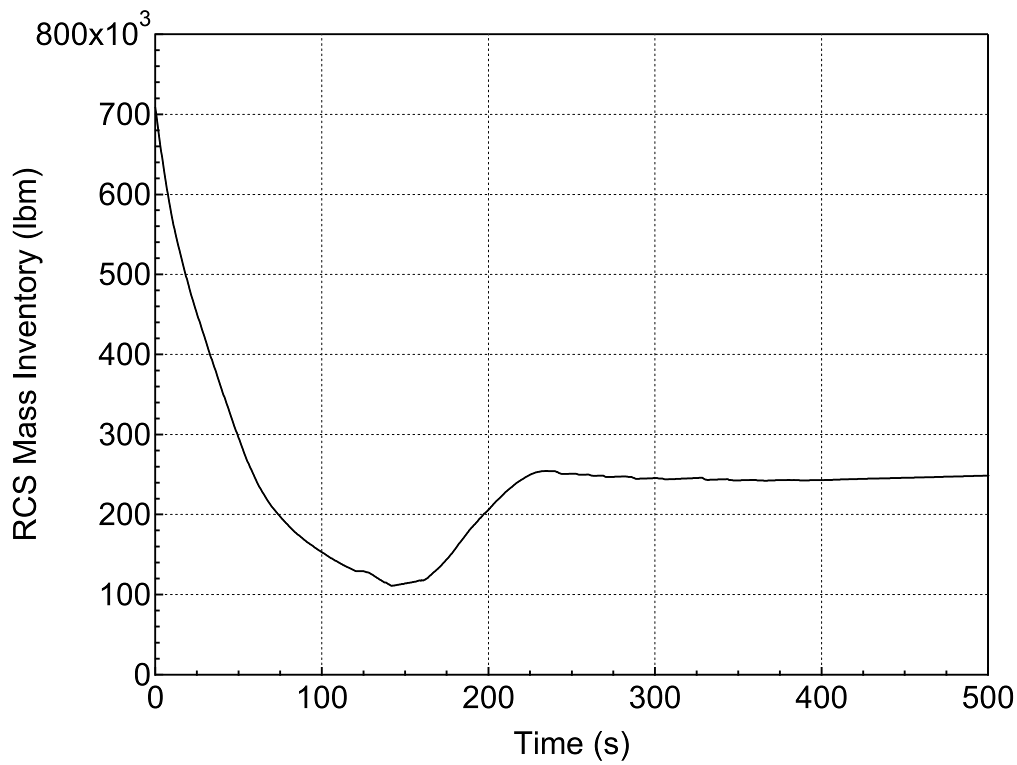

Figure 5.3.2.a-14 RCS Mass Inventory for 12-inch Break (Side) (Break Orientation Sensitivity Study)

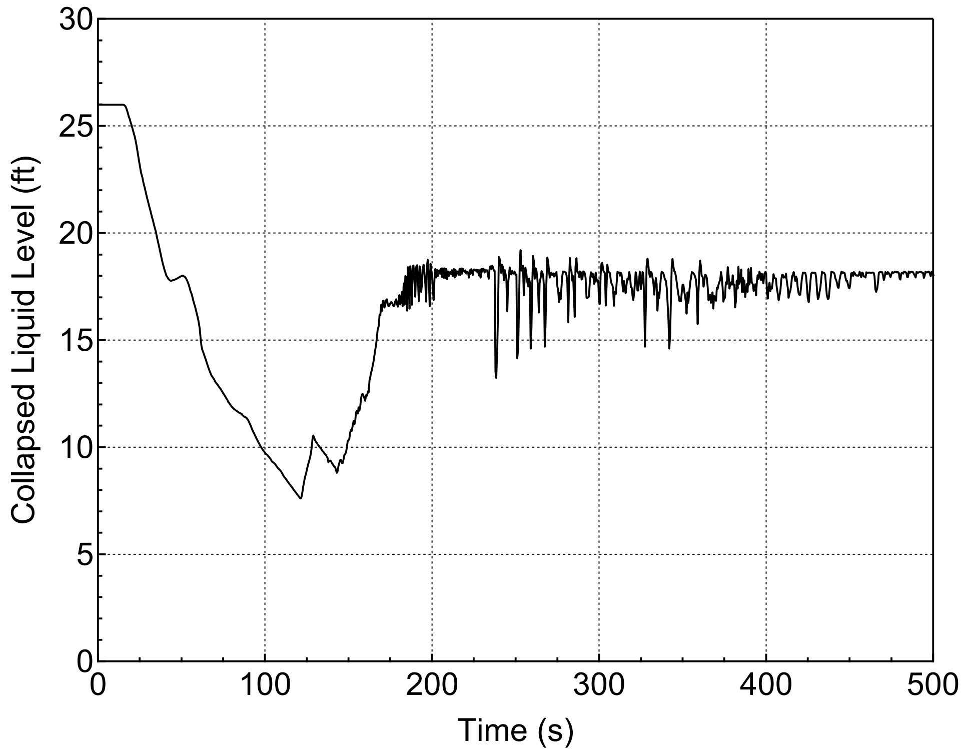

Figure 5.3.2.a-15 Downcomer Collapsed Level for 12-inch Break (Side) (Break Orientation Sensitivity Study)

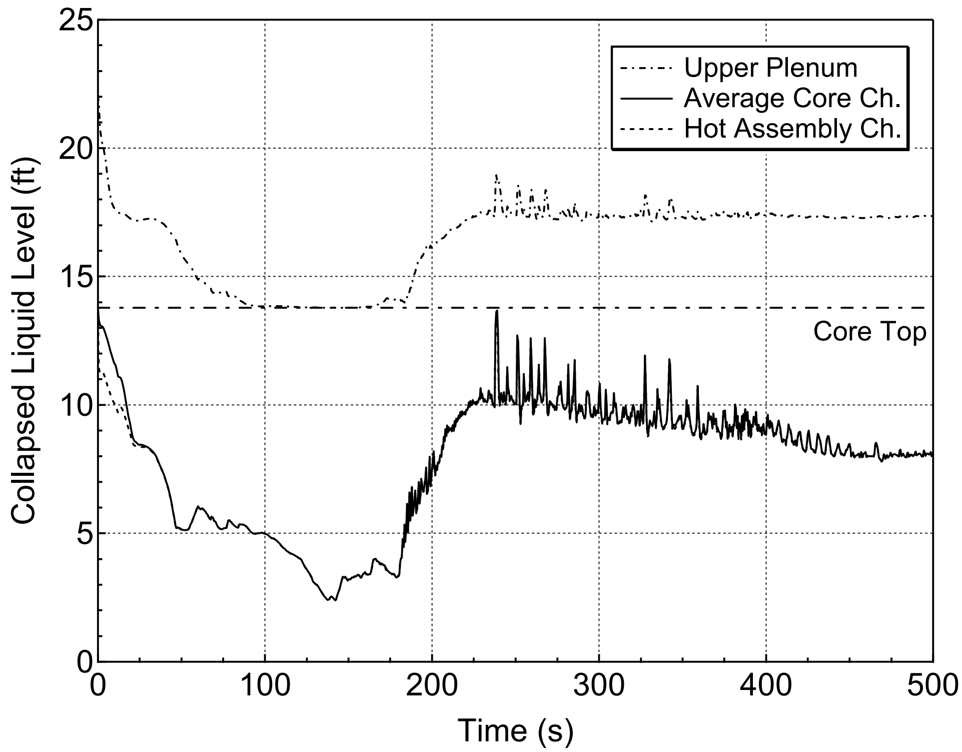

Figure 5.3.2.a-16 Core and Upper Plenum Collapsed Levels for 12-inch Break (Side) (Break Orientation Sensitivity Study)

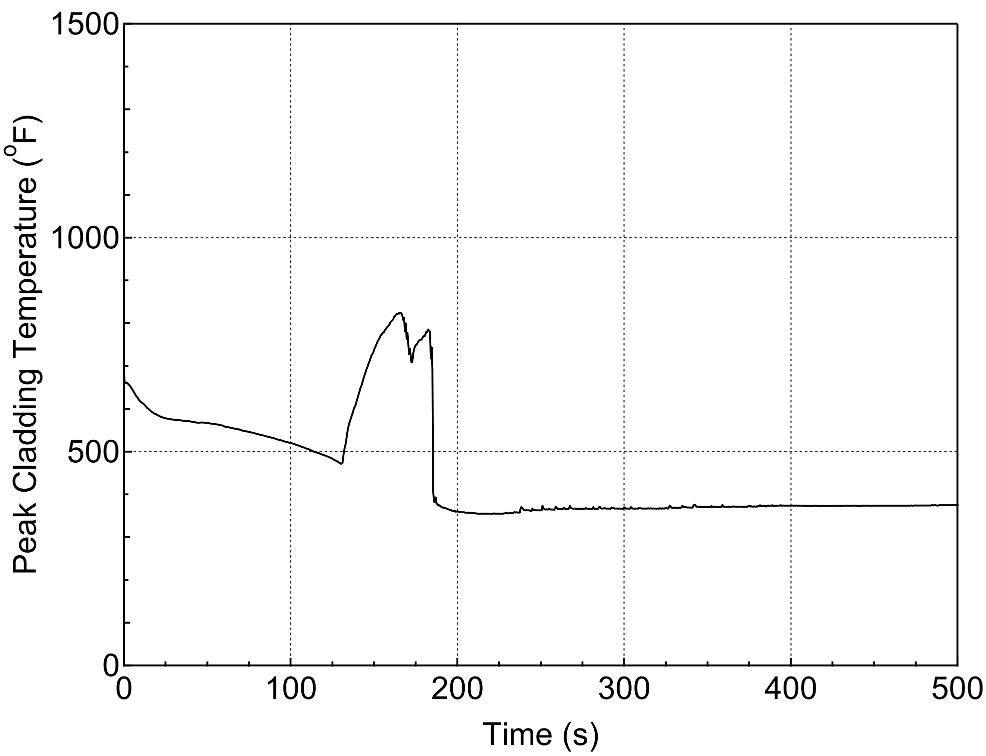

Figure 5.3.2.a-17 PCT at All Elevations for Hot Rod in Hot Assembly for 12-inch Break (Side) (Break Orientation Sensitivity Study)

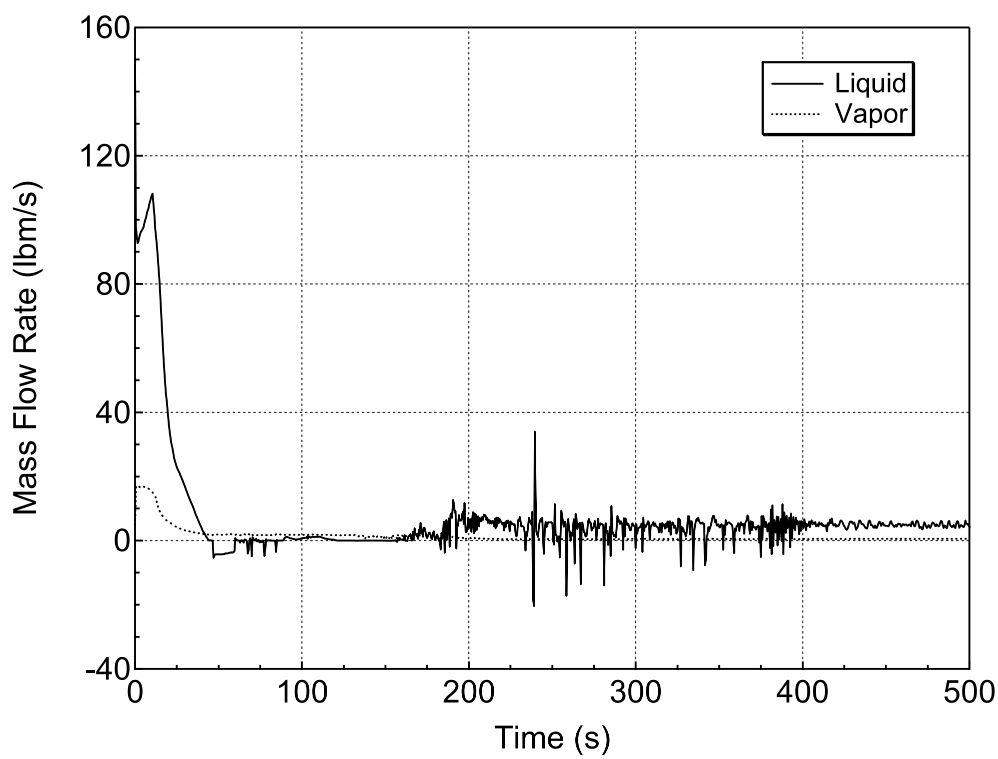

Figure 5.3.2.a-18 Hot Assembly Exit Vapor and Liquid Mass Flowrates for 12-inch Break (Side) (Break Orientation Sensitivity Study)

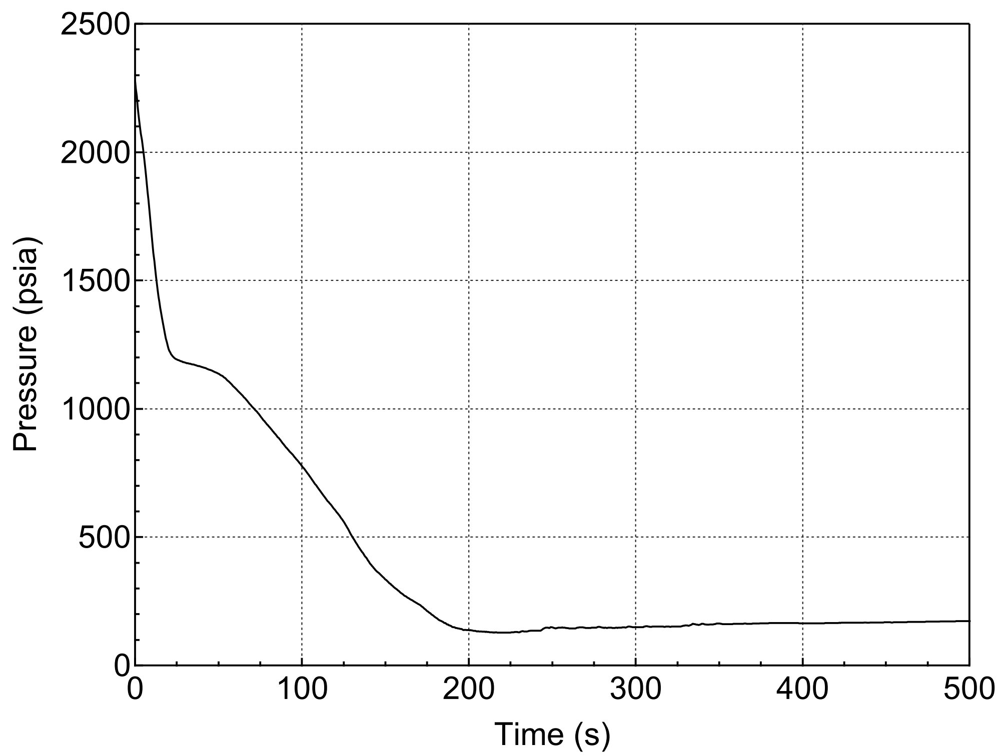

Figure 5.3.2.a-19 RCS (Pressurizer) Pressure Transient for 12-inch Break (Homogeneous) (Break Orientation Sensitivity Study)

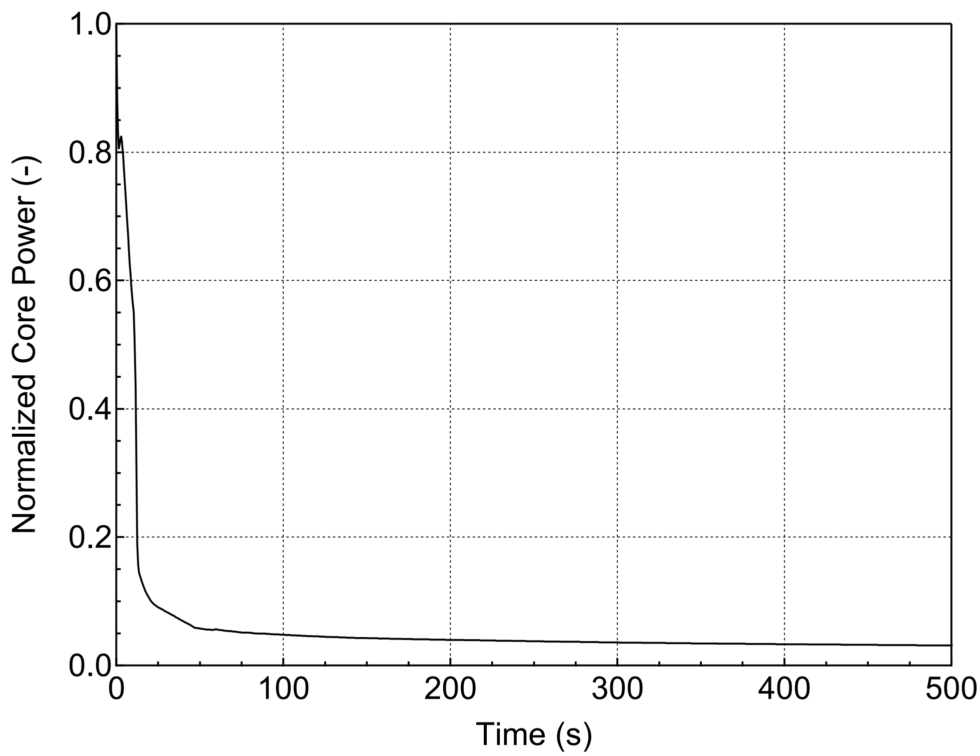

Figure 5.3.2.a-20 Normalized Core Power for 12-inch Break (Homogeneous) (Break Orientation Sensitivity Study)

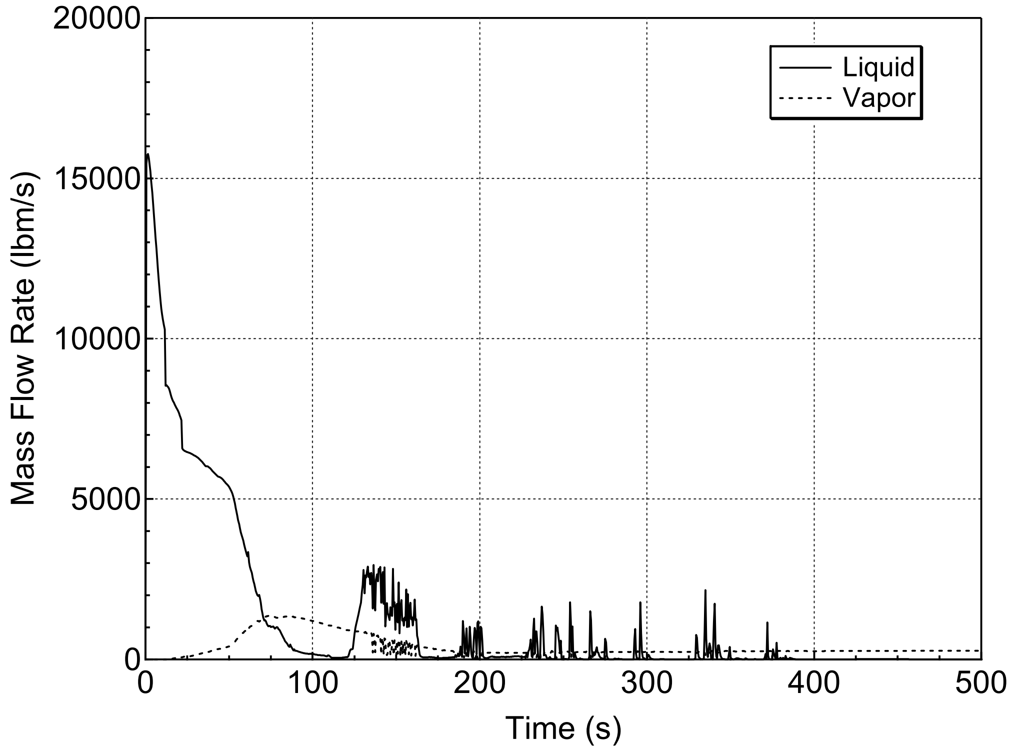

Figure 5.3.2.a-21 Liquid and Vapor Discharges through the Break for 12-inch Break (Homogeneous) (Break Orientation Sensitivity Study)

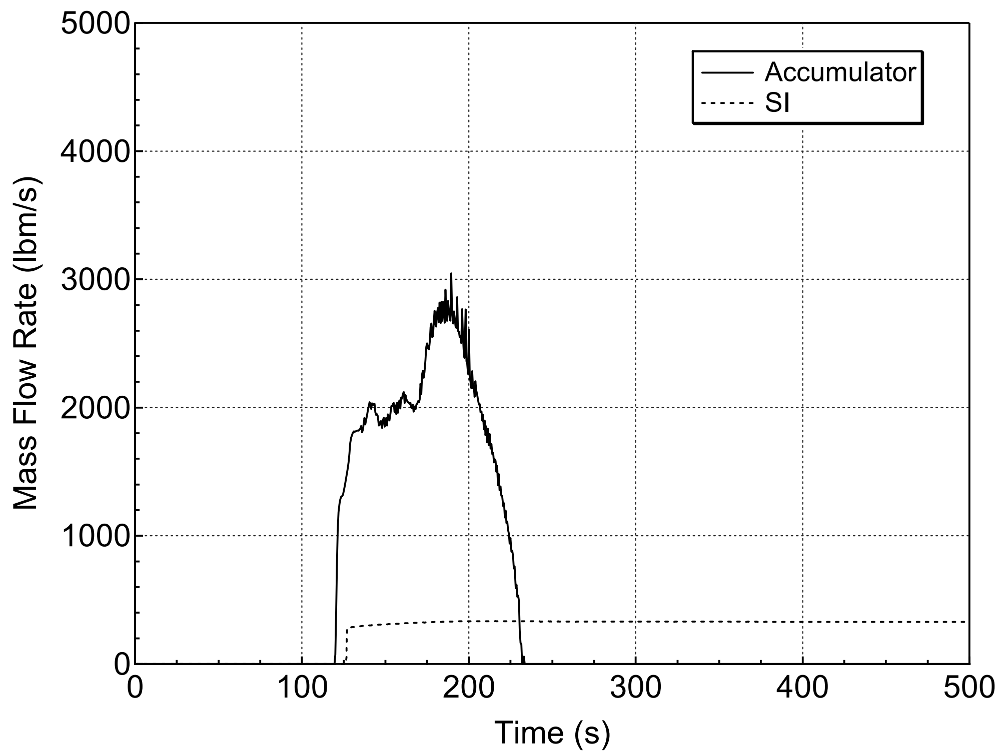

Figure 5.3.2.a-22 Accumulator and Safety Injection Mass Flowrates for 12-inch Break (Homogeneous) (Break Orientation Sensitivity Study)

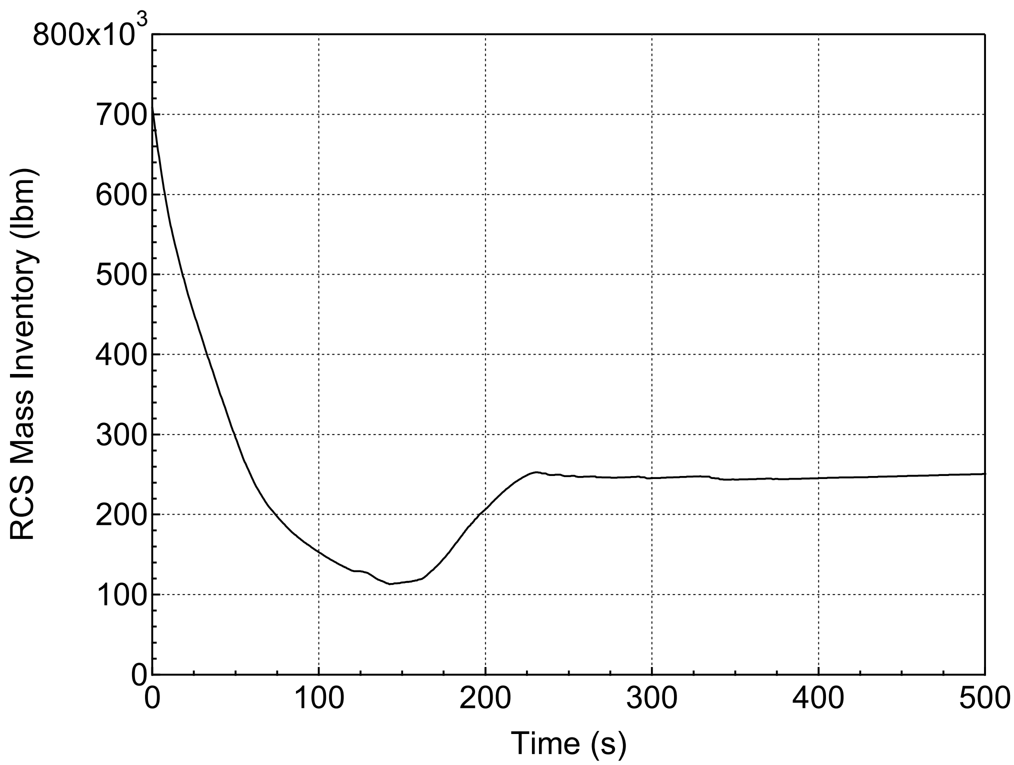

Figure 5.3.2.a-23 RCS Mass Inventory for 12-inch Break (Homogeneous) (Break Orientation Sensitivity Study)

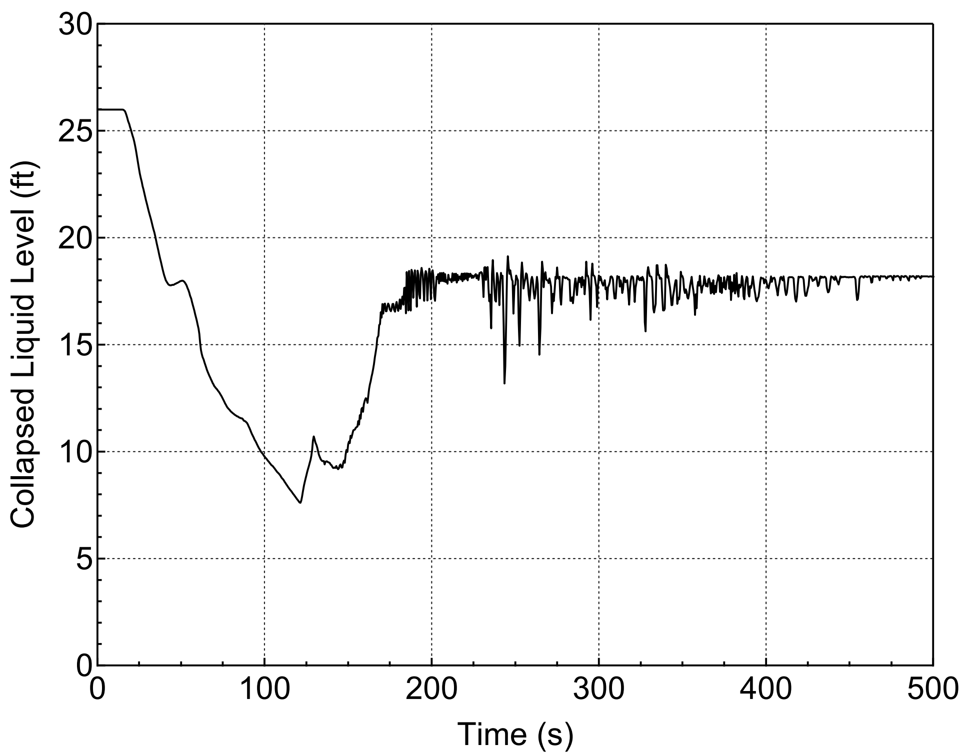

Figure 5.3.2.a-24 Downcomer Collapsed Level for 12-inch Break (Homogeneous) (Break Orientation Sensitivity Study)

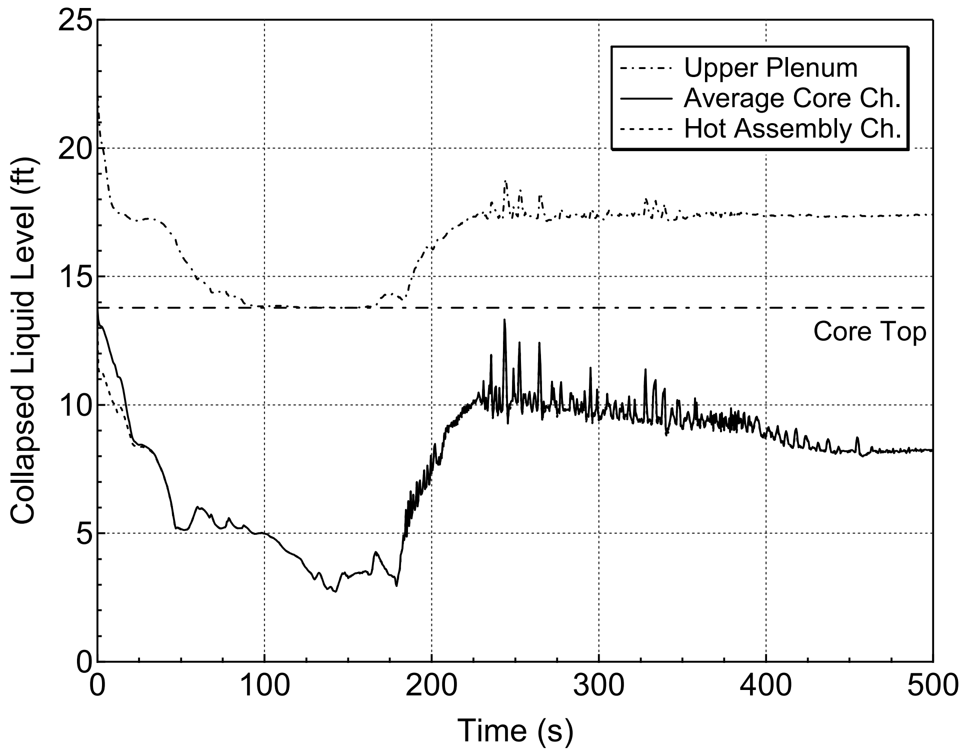

Figure 5.3.2.a-25 Core and Upper Plenum Collapsed Levels for 12-inch Break (Homogeneous) (Break Orientation Sensitivity Study)

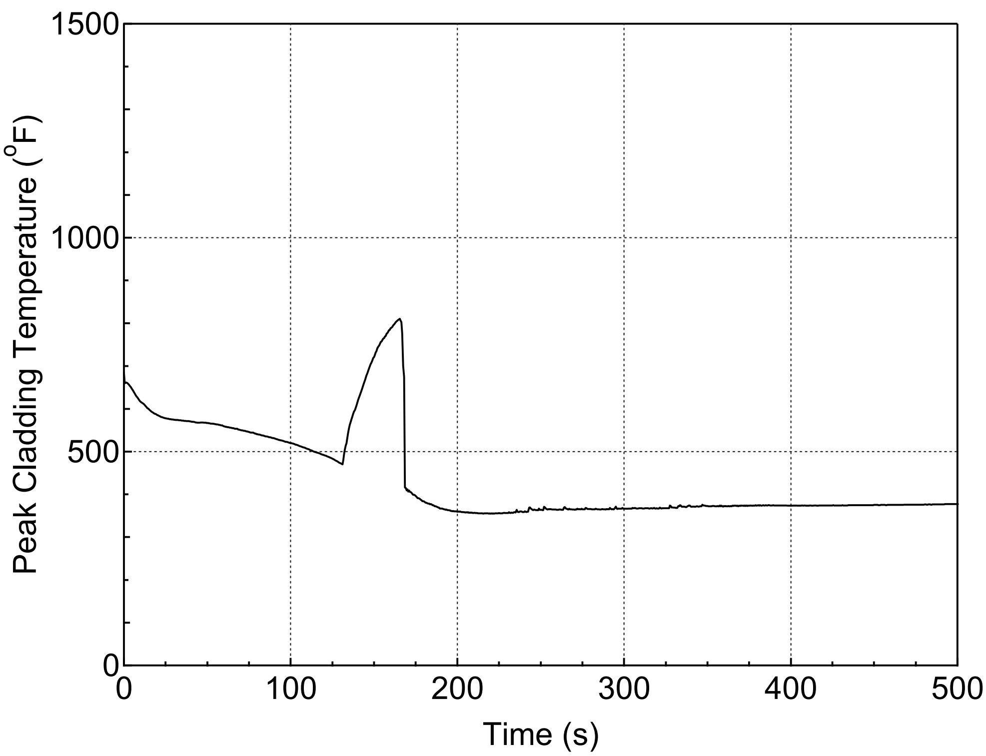

Figure 5.3.2.a-26 PCT at All Elevations for Hot Rod in Hot Assembly for 12-inch Break (Homogeneous) (Break Orientation Sensitivity Study)

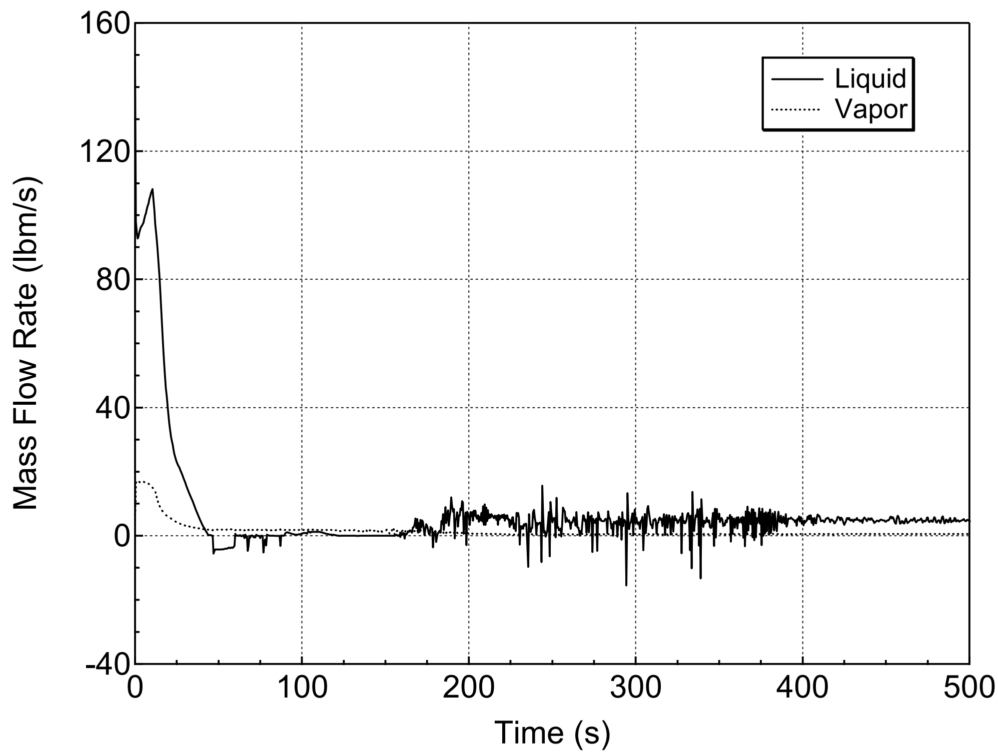

Figure 5.3.2.a-27 Hot Assembly Exit Vapor and Liquid Mass Flowrates for 12-inch Break (Homogeneous) (Break Orientation Sensitivity Study)

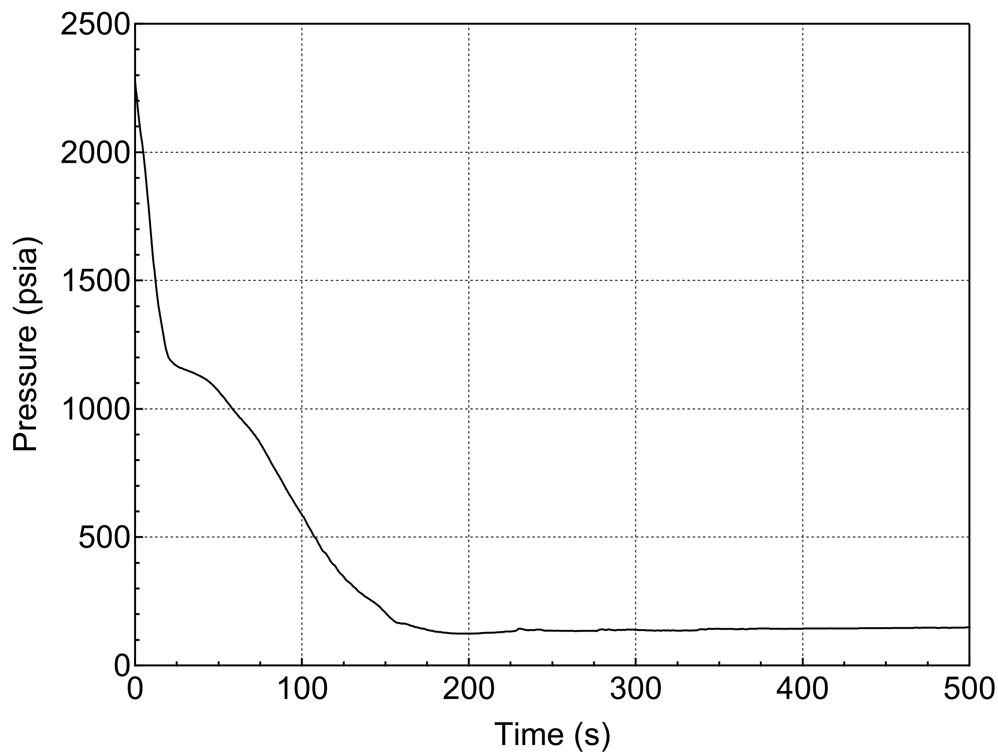

Figure 5.3.2.b-1 RCS (Pressurizer) Pressure Transient for 13-inch Break (Top) (Break Orientation Sensitivity Study)

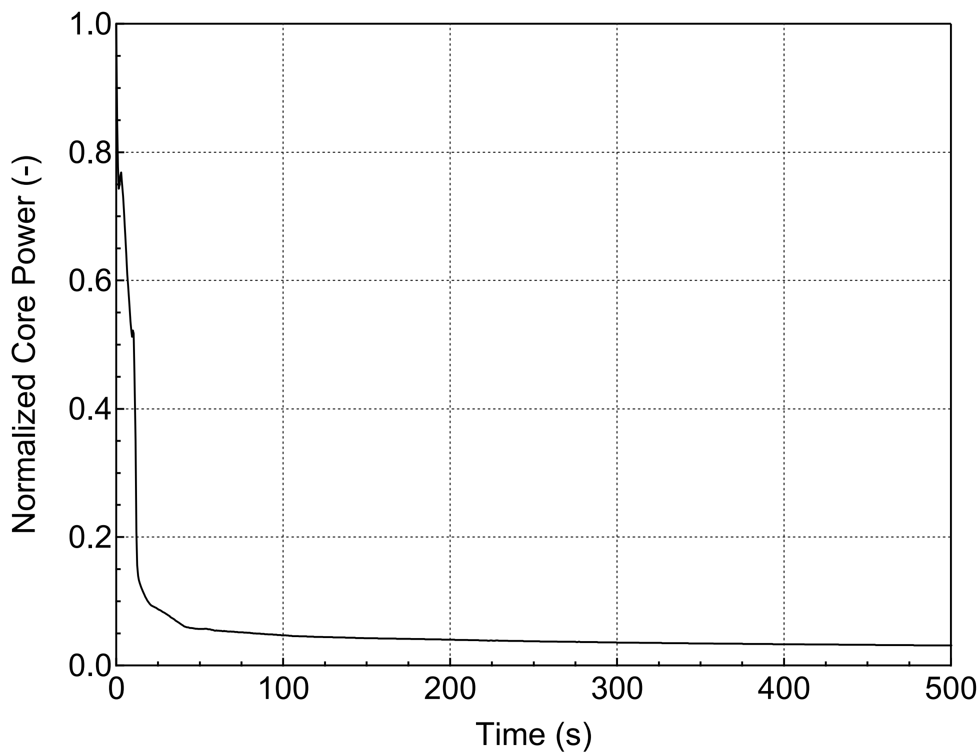

Figure 5.3.2.b-2 Normalized Core Power for 13-inch Break (Top) (Break Orientation Sensitivity Study)

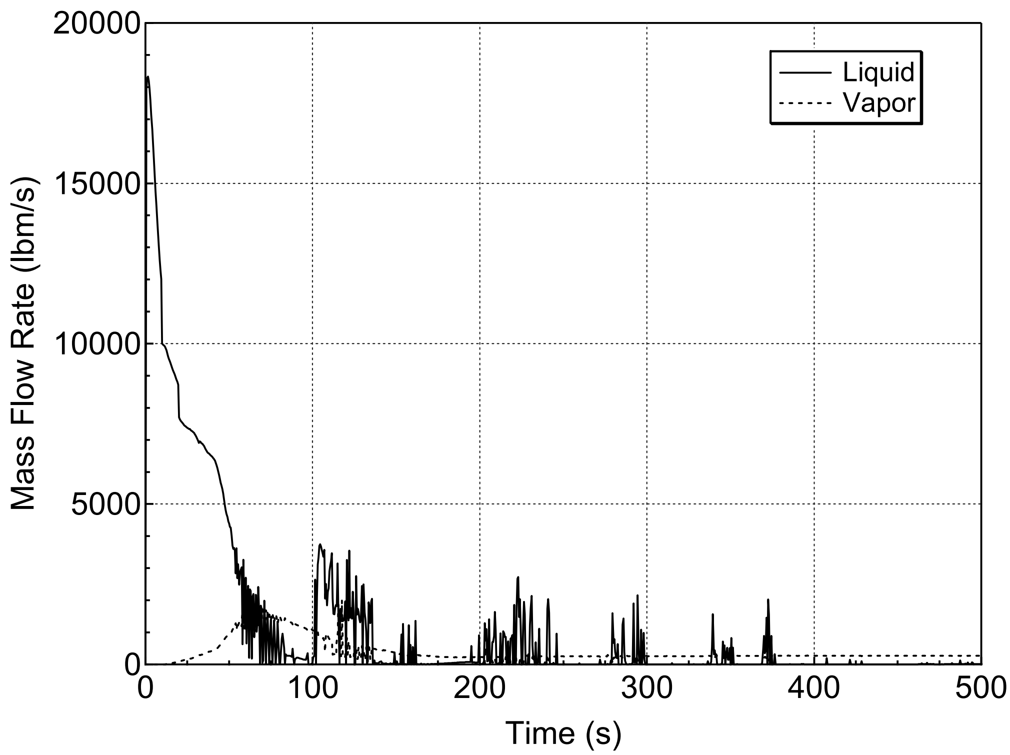

Figure 5.3.2.b-3 Liquid and Vapor Discharges through the Break for 13-inch Break (Top) (Break Orientation Sensitivity Study)

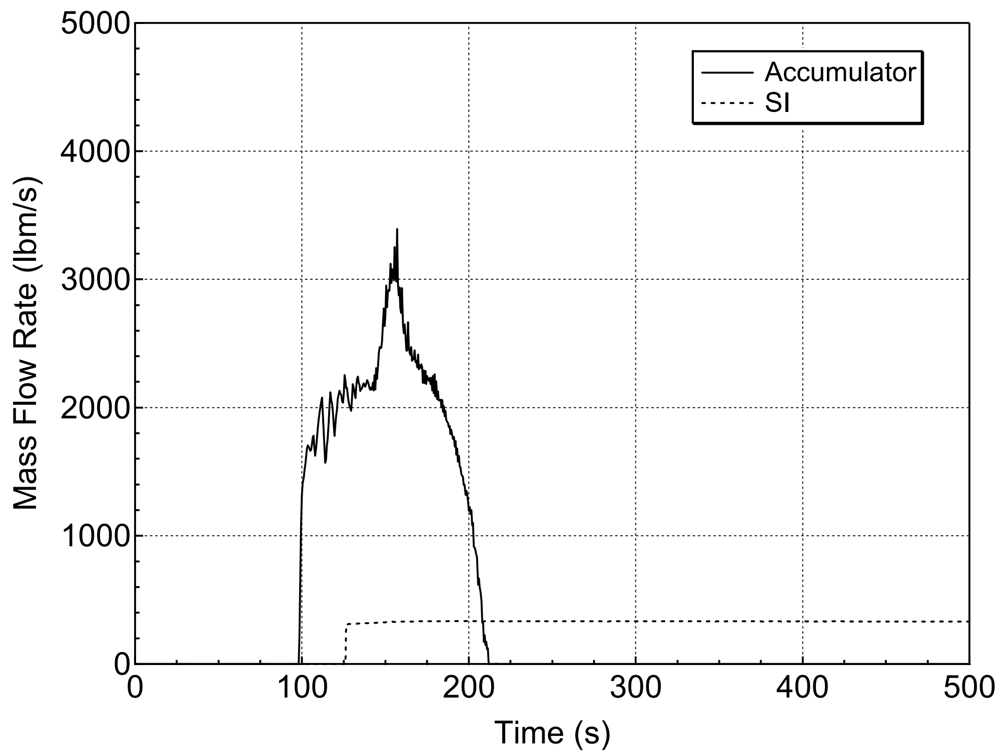

Figure 5.3.2.b-4 Accumulator and Safety Injection Mass Flowrates for 13-inch Break (Top) (Break Orientation Sensitivity Study)

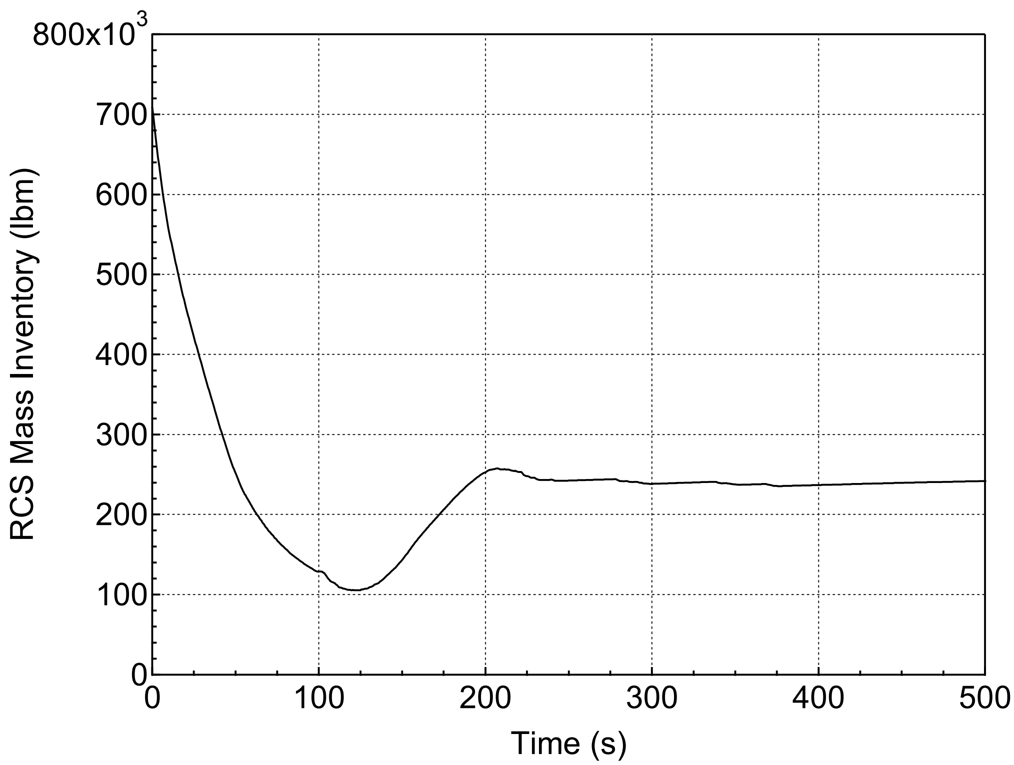

Figure 5.3.2.b-5 RCS Mass Inventory for 13-inch Break (Top)
(Break Orientation Sensitivity Study)

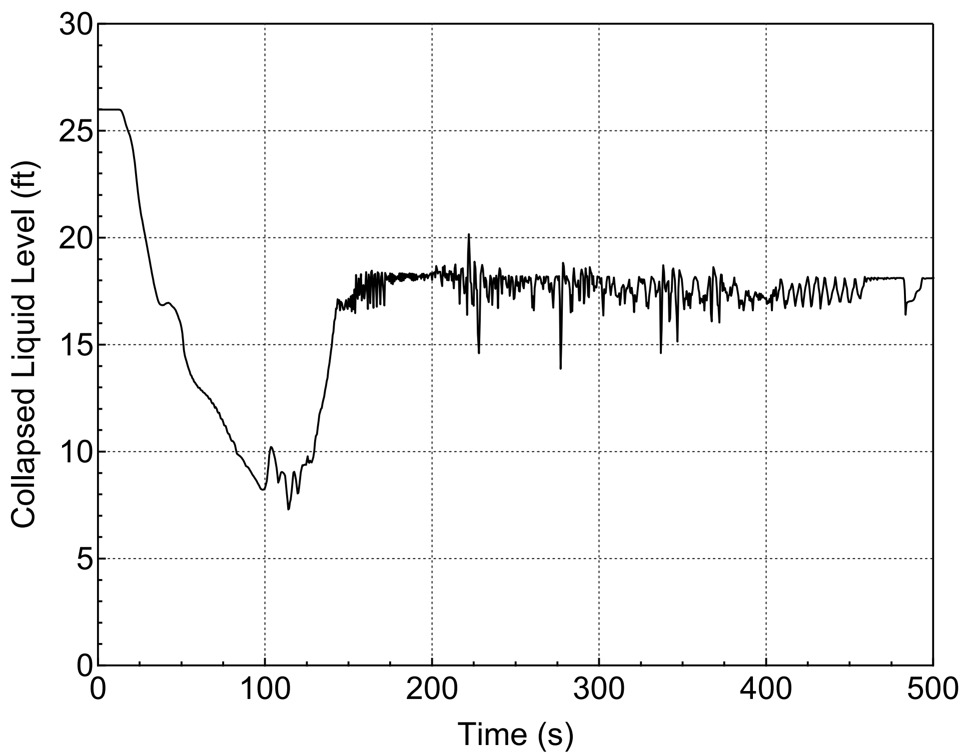

Figure 5.3.2.b-6 Downcomer Collapsed Level for 13-inch Break (Top) (Break Orientation Sensitivity Study)

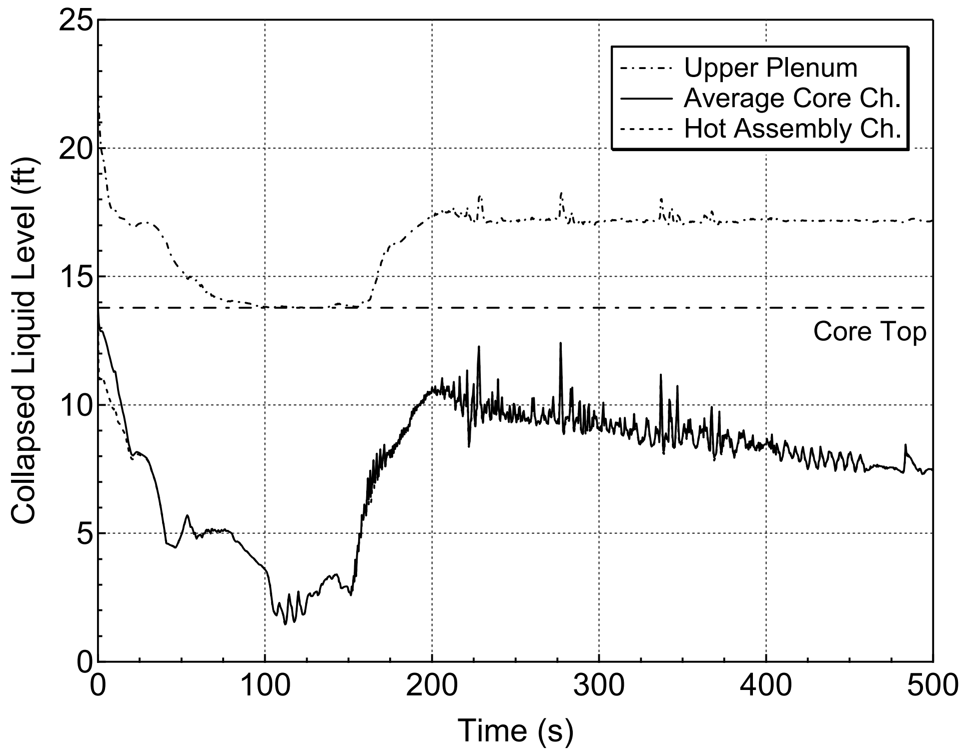

Figure 5.3.2.b-7 Core and Upper Plenum Collapsed Levels for 13-inch Break (Top) (Break Orientation Sensitivity Study)

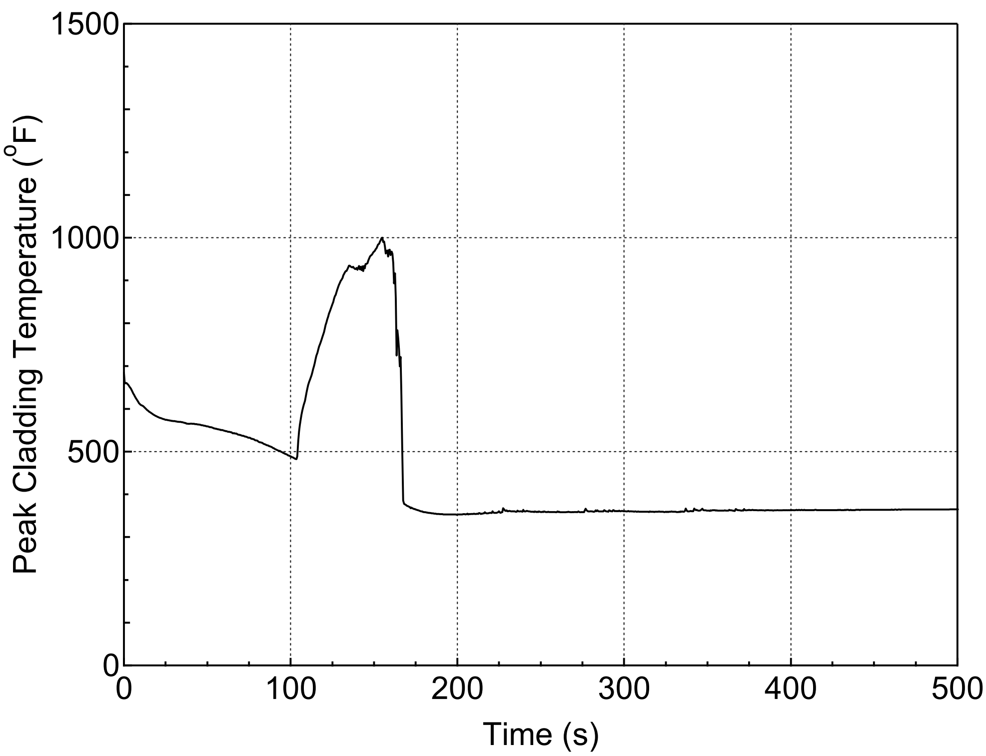

Figure 5.3.2.b-8 PCT at All Elevations for Hot Rod in Hot Assembly for 13-inch Break (Top) (Break Orientation Sensitivity Study)

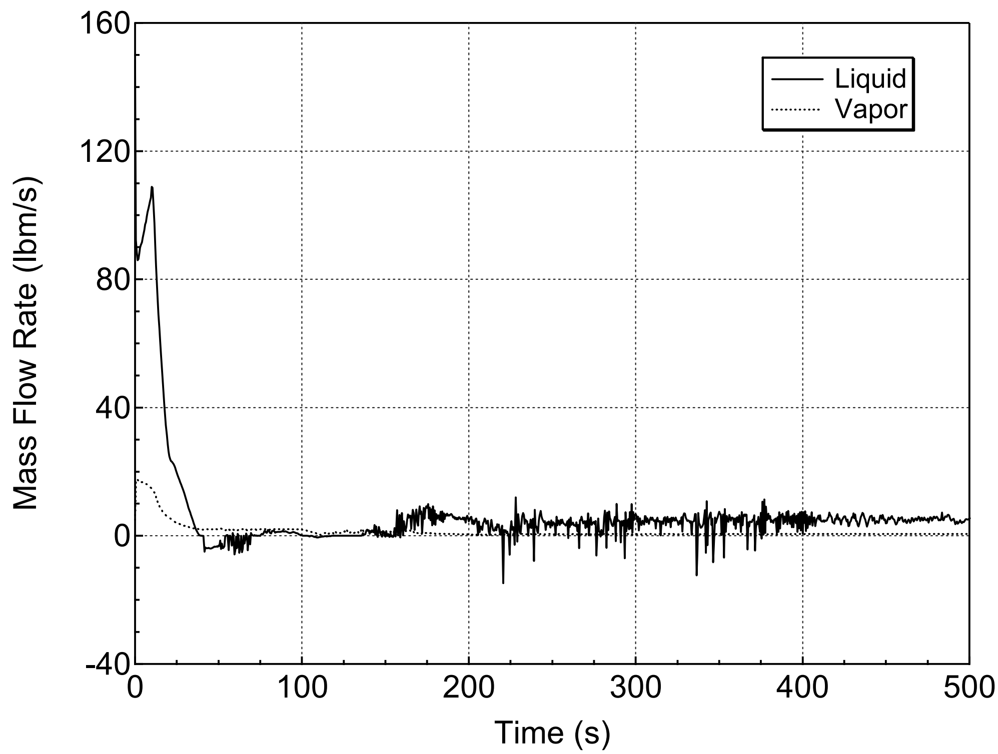

Figure 5.3.2.b-9 Hot Assembly Exit Vapor and Liquid Mass Flowrates for 13-inch Break (Top) (Break Orientation Sensitivity Study)

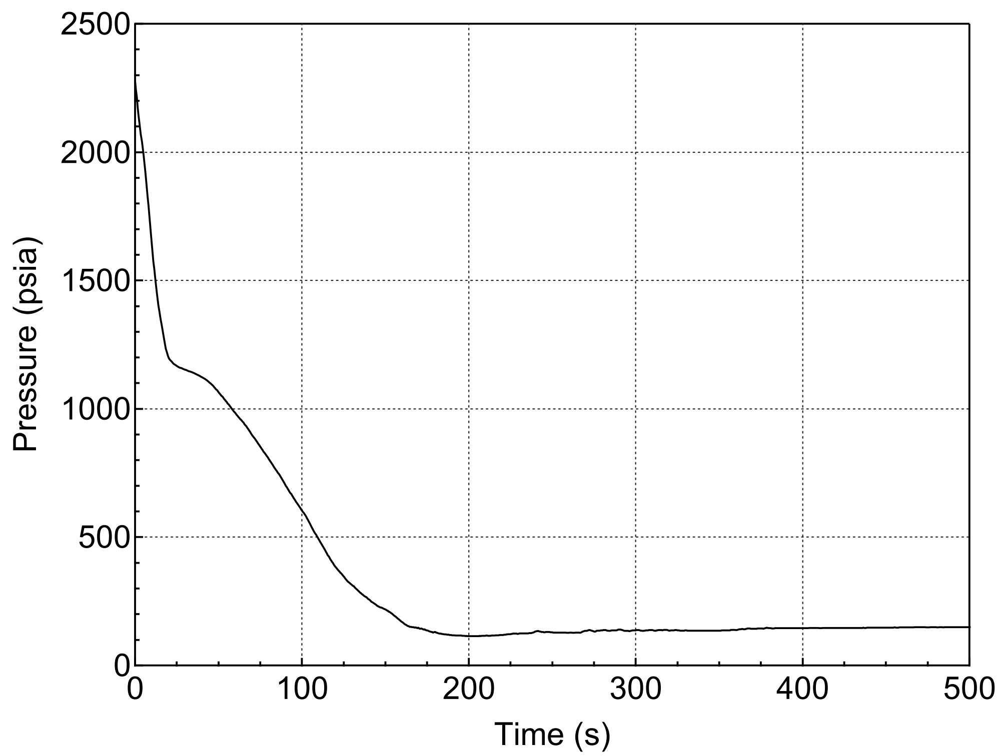

Figure 5.3.2.b-10 RCS (Pressurizer) Pressure Transient for 13-inch Break (Side) (Break Orientation Sensitivity Study)

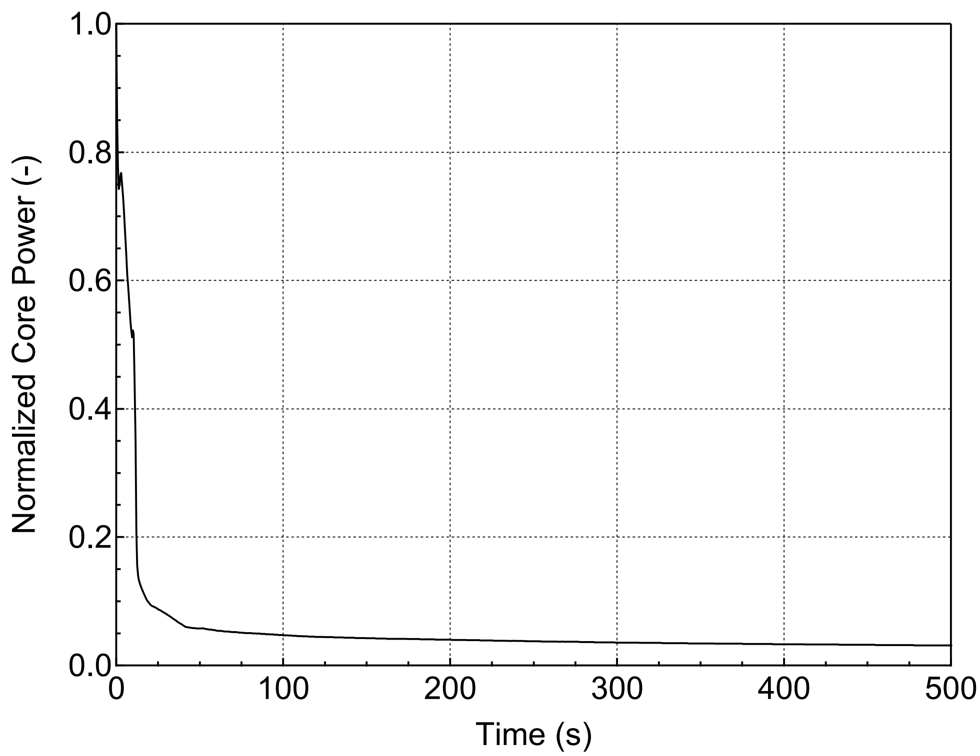

Figure 5.3.2.b-11 Normalized Core Power for 13-inch Break (Side) (Break Orientation Sensitivity Study)

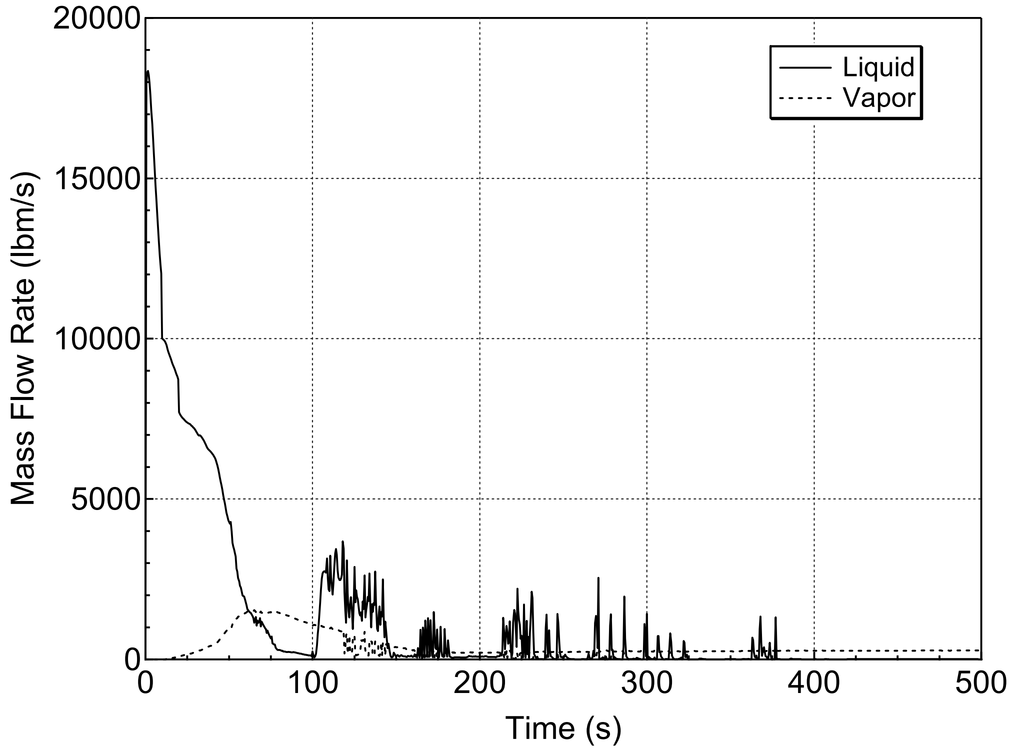

Figure 5.3.2.b-12 Liquid and Vapor Discharges through the Break for 13-inch Break (Side) (Break Orientation Sensitivity Study)

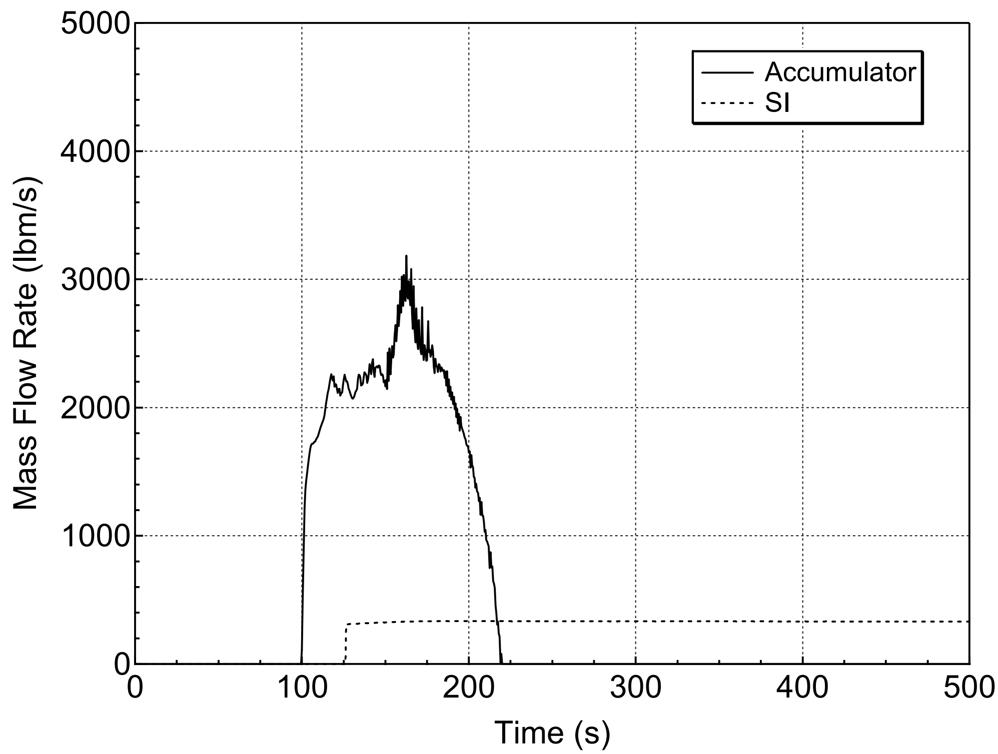

Figure 5.3.2.b-13 Accumulator and Safety Injection Mass Flowrates for 13-inch Break (Side) (Break Orientation Sensitivity Study)

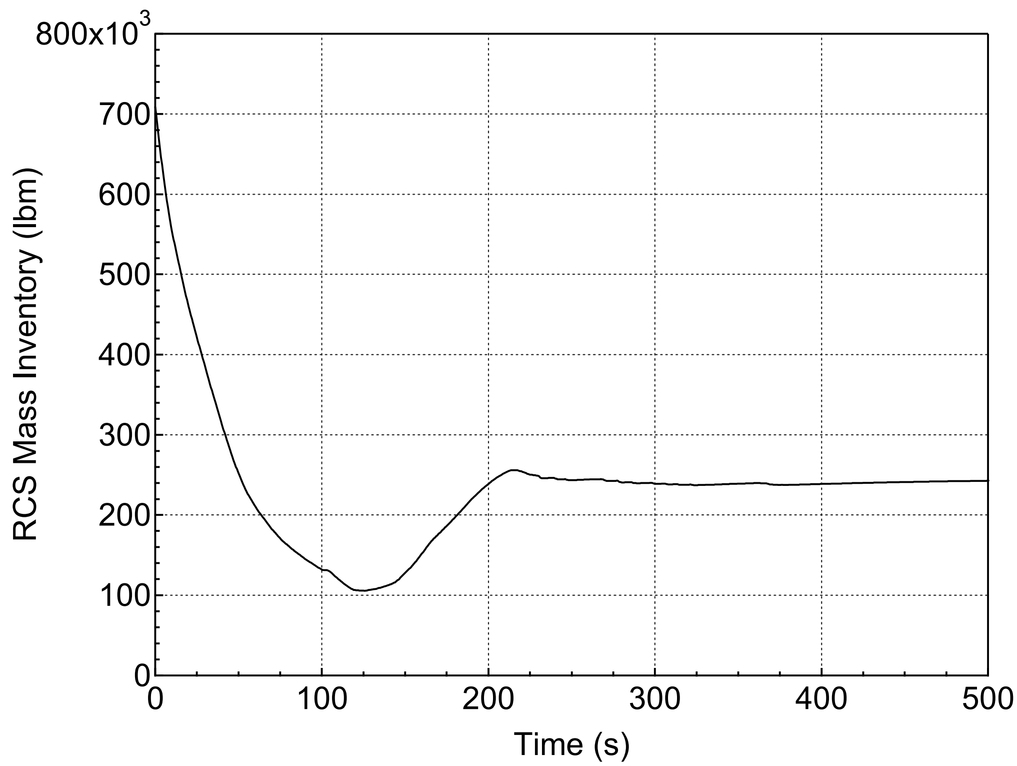

Figure 5.3.2.b-14 RCS Mass Inventory for 13-inch Break (Side) (Break Orientation Sensitivity Study)

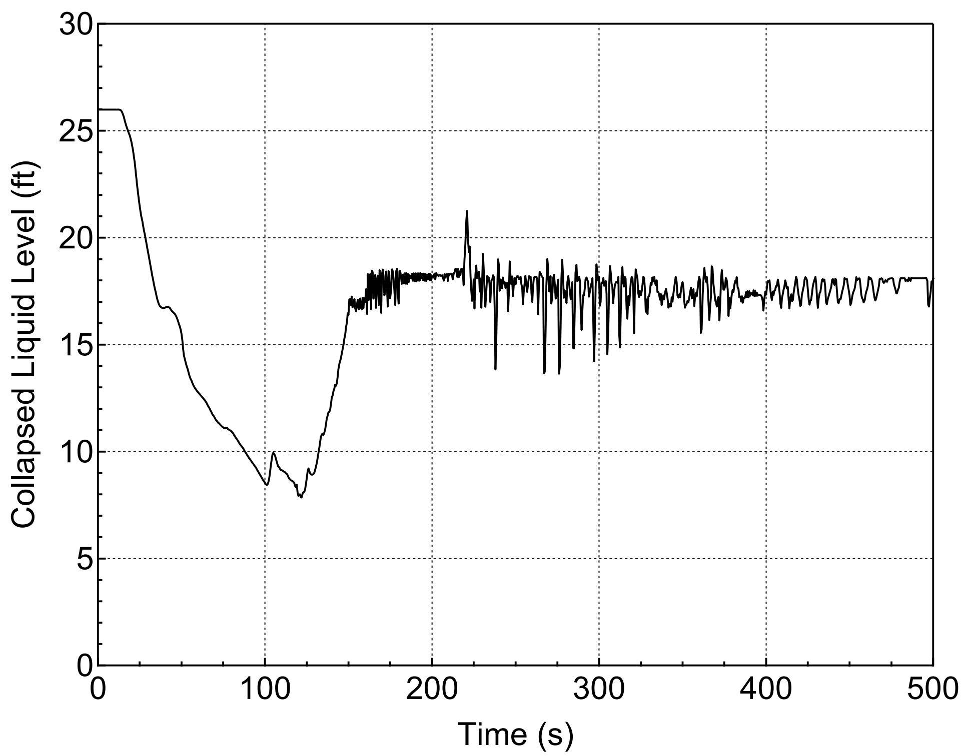

Figure 5.3.2.b-15 Downcomer Collapsed Level for 13-inch Break (Side) (Break Orientation Sensitivity Study)

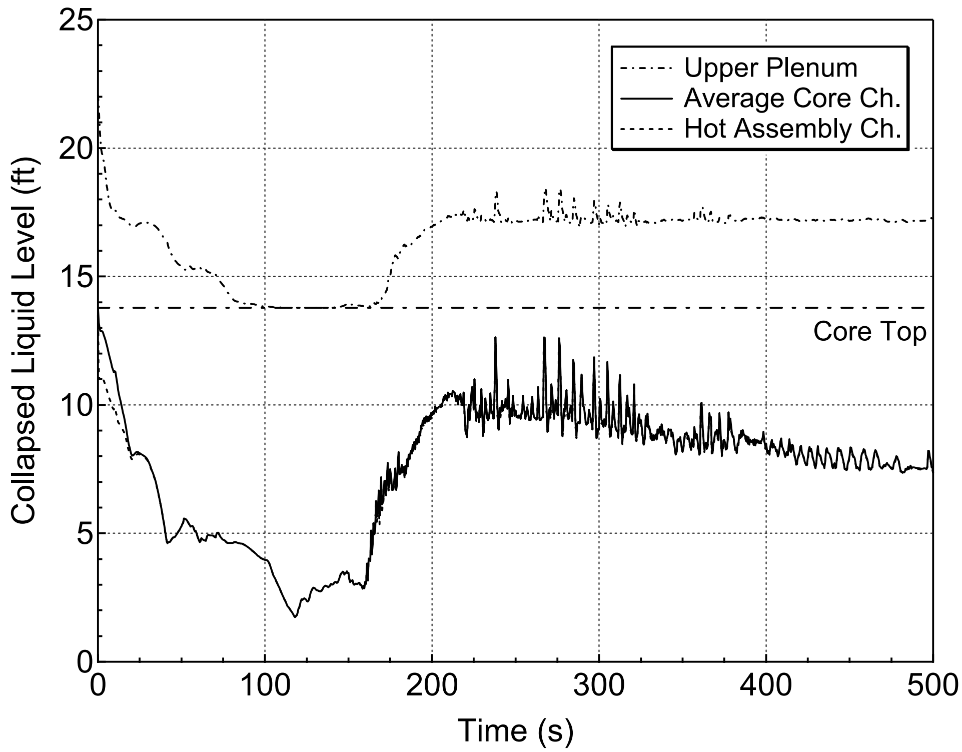

Figure 5.3.2.b-16 Core and Upper Plenum Collapsed Levels for 13-inch Break (Side) (Break Orientation Sensitivity Study)

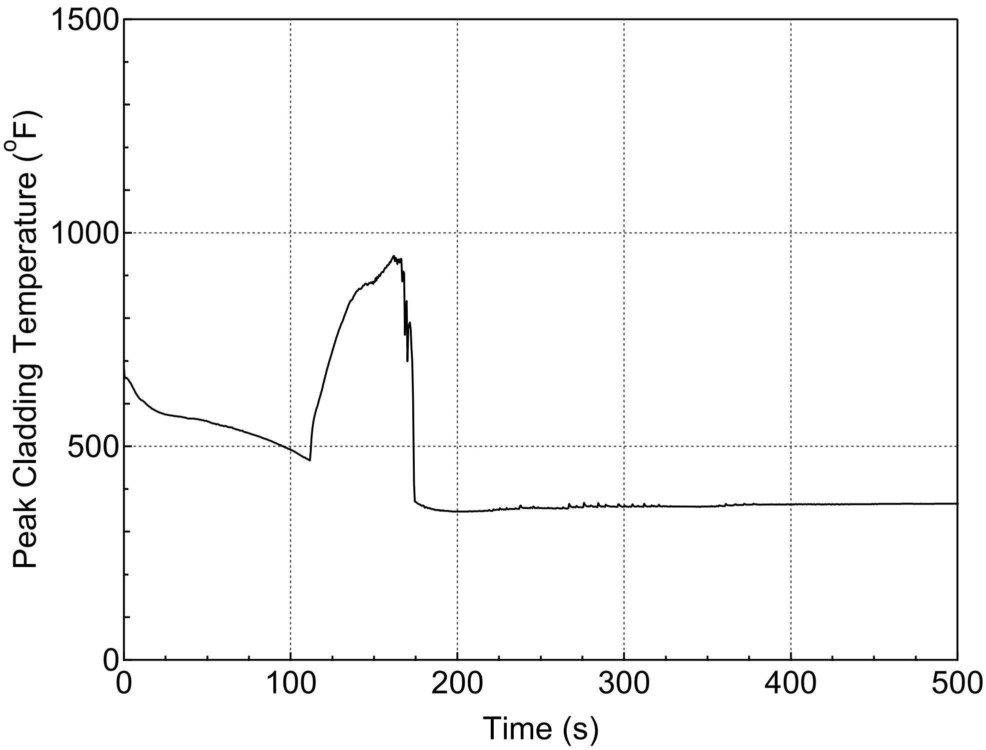

Figure 5.3.2.b-17 PCT at All Elevations for Hot Rod in Hot Assembly for 13-inch Break (Side) (Break Orientation Sensitivity Study)

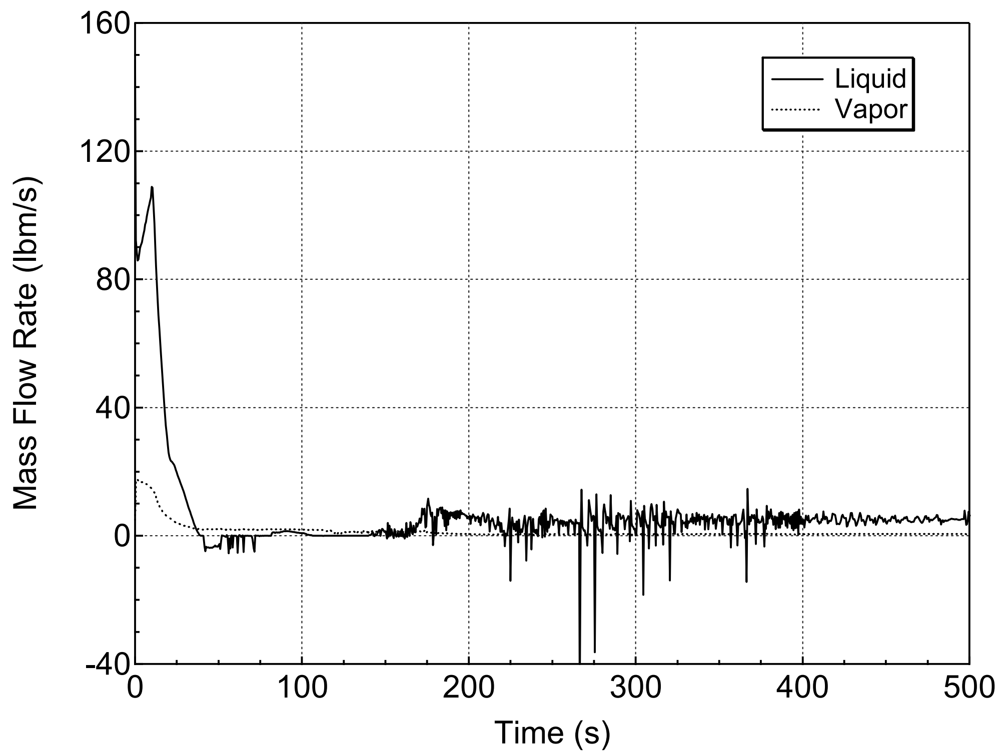

Figure 5.3.2.b-18 Hot Assembly Exit Vapor and Liquid Mass Flowrates for 13-inch Break (Side) (Break Orientation Sensitivity Study)

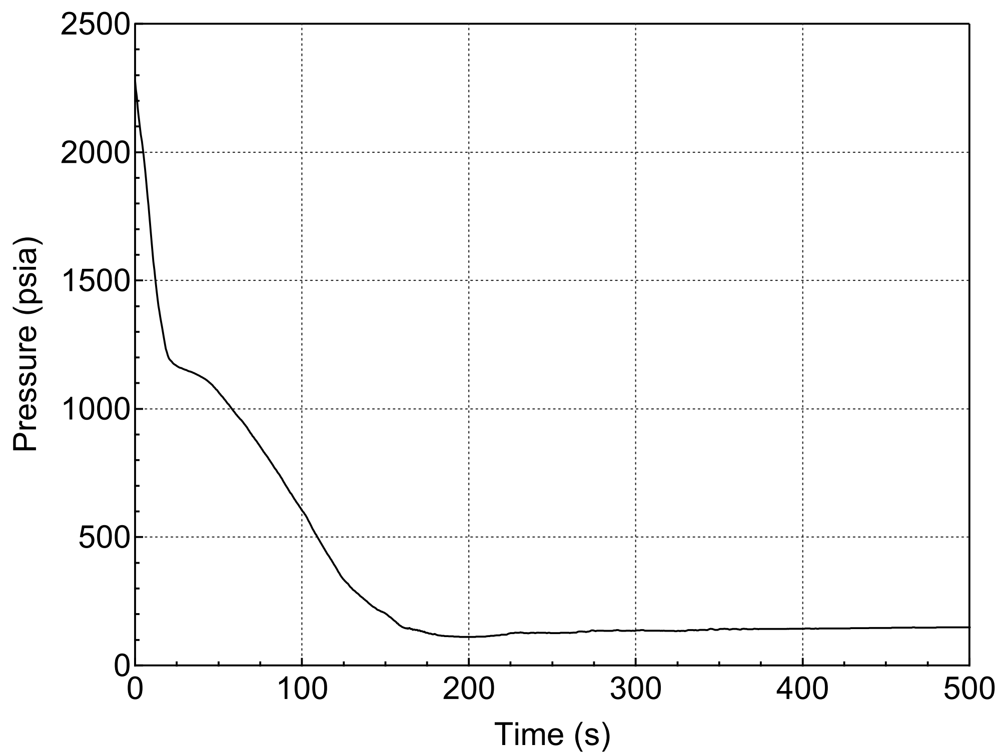

Figure 5.3.2.b-19 RCS (Pressurizer) Pressure Transient for 13-inch Break (Homogeneous) (Break Orientation Sensitivity Study)

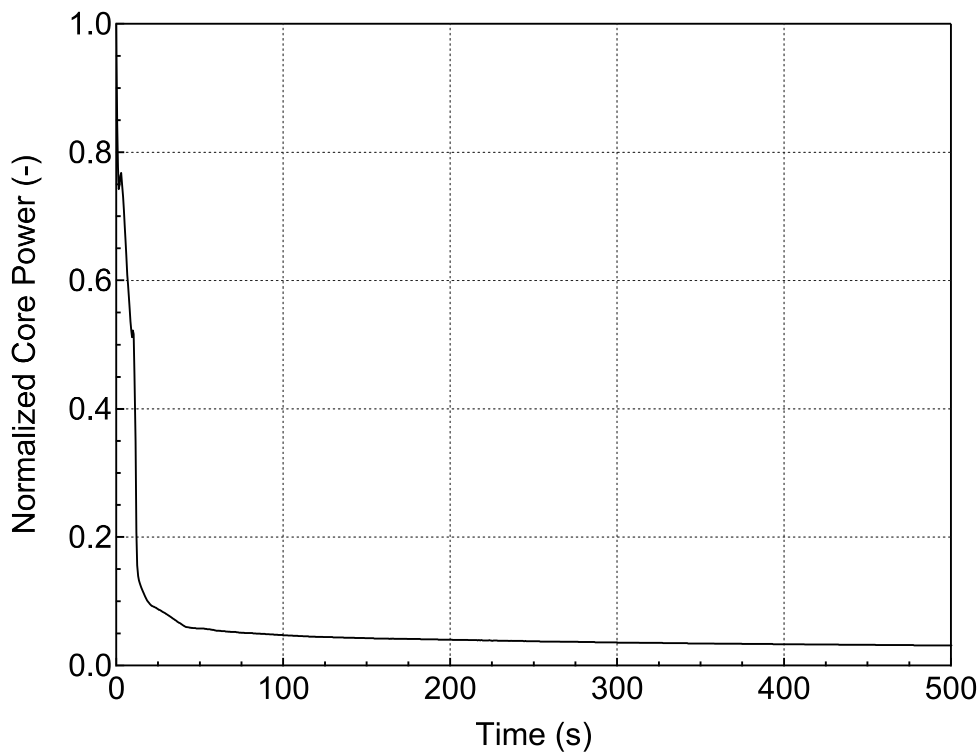

Figure 5.3.2.b-20 Normalized Core Power for 13-inch Break (Homogeneous) (Break Orientation Sensitivity Study)

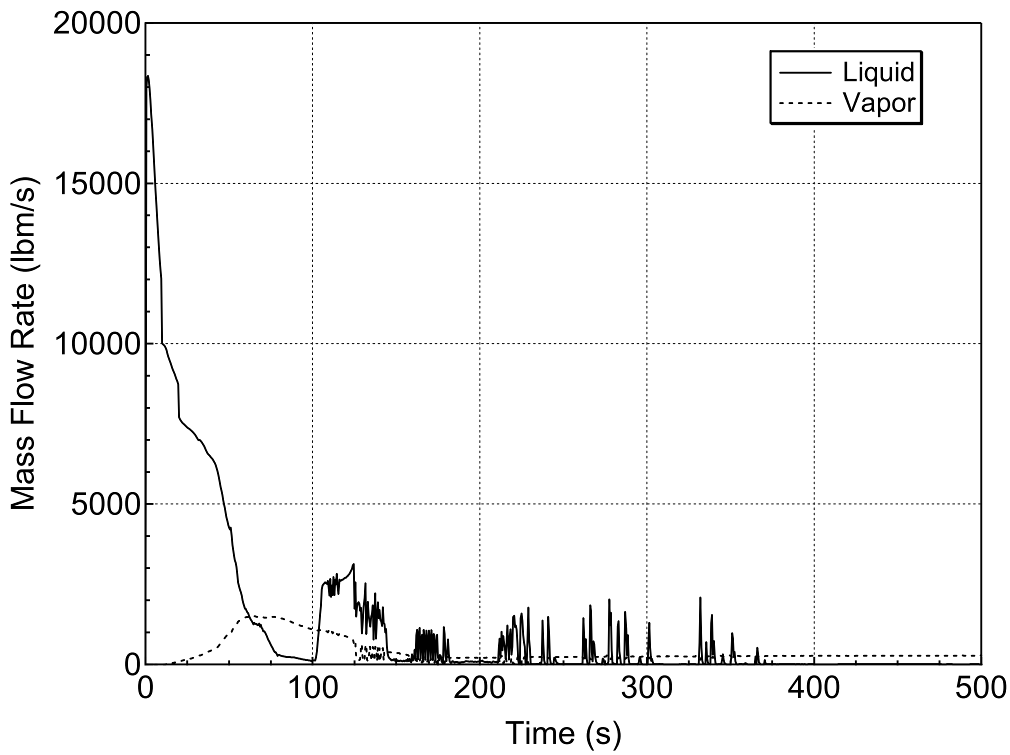

Figure 5.3.2.b-21 Liquid and Vapor Discharges through the Break for 13-inch Break (Homogeneous) (Break Orientation Sensitivity Study)

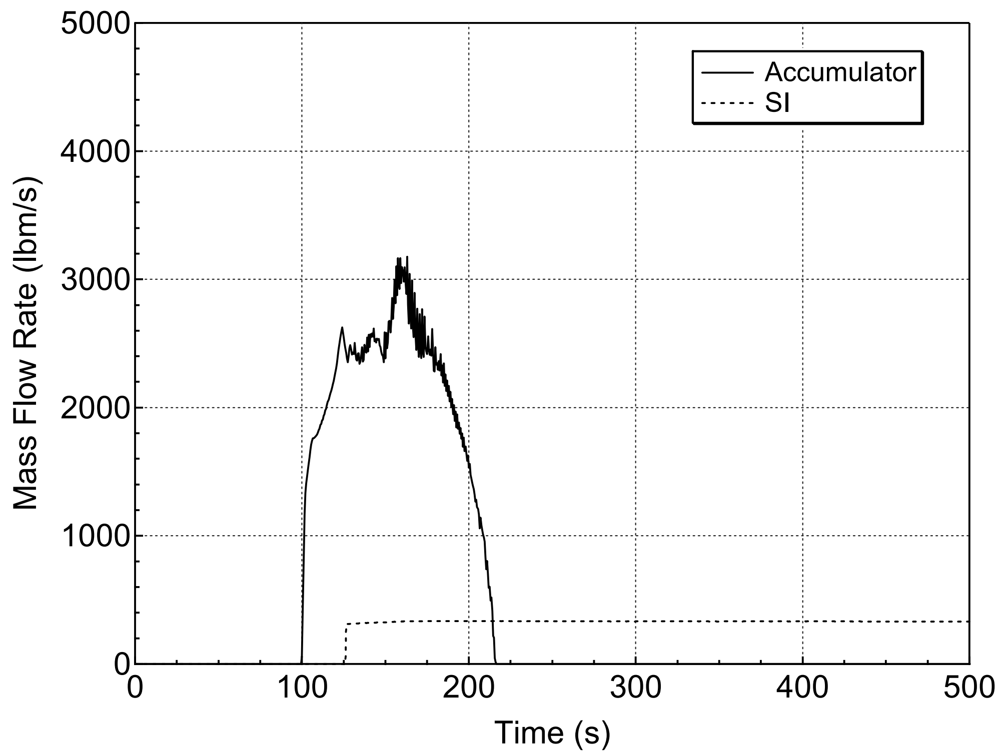

Figure 5.3.2.b-22 Accumulator and Safety Injection Mass Flowrates for 13-inch Break (Homogeneous) (Break Orientation Sensitivity Study)

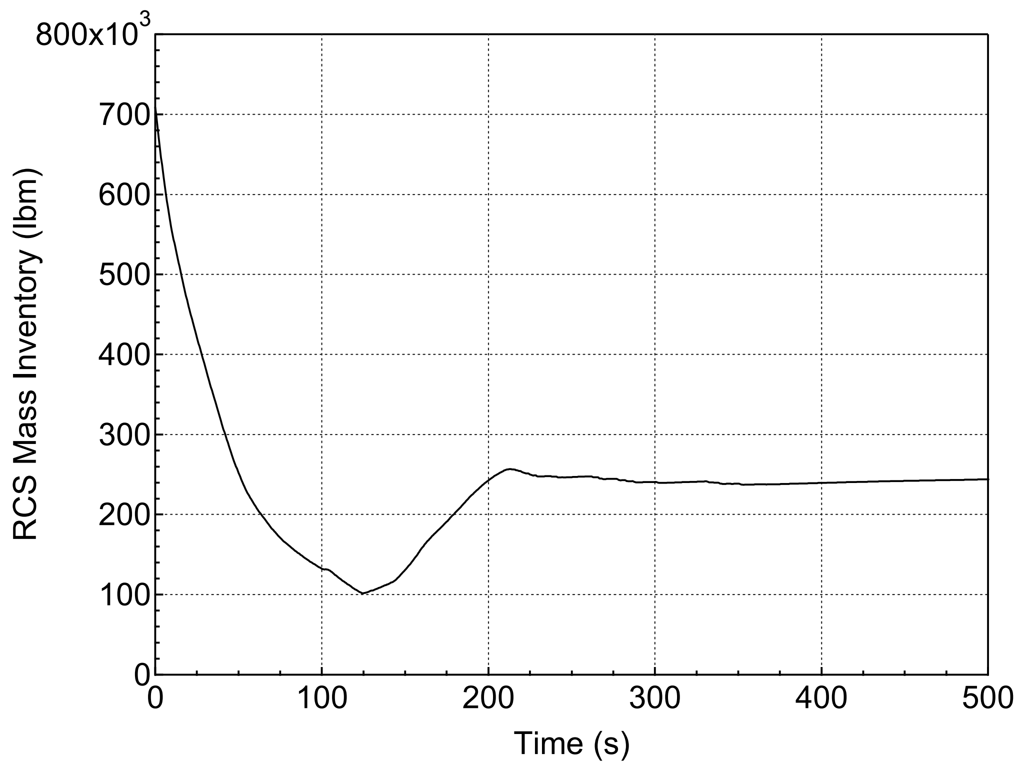

Figure 5.3.2.b-23 RCS Mass Inventory for 13-inch Break (Homogeneous) (Break Orientation Sensitivity Study)

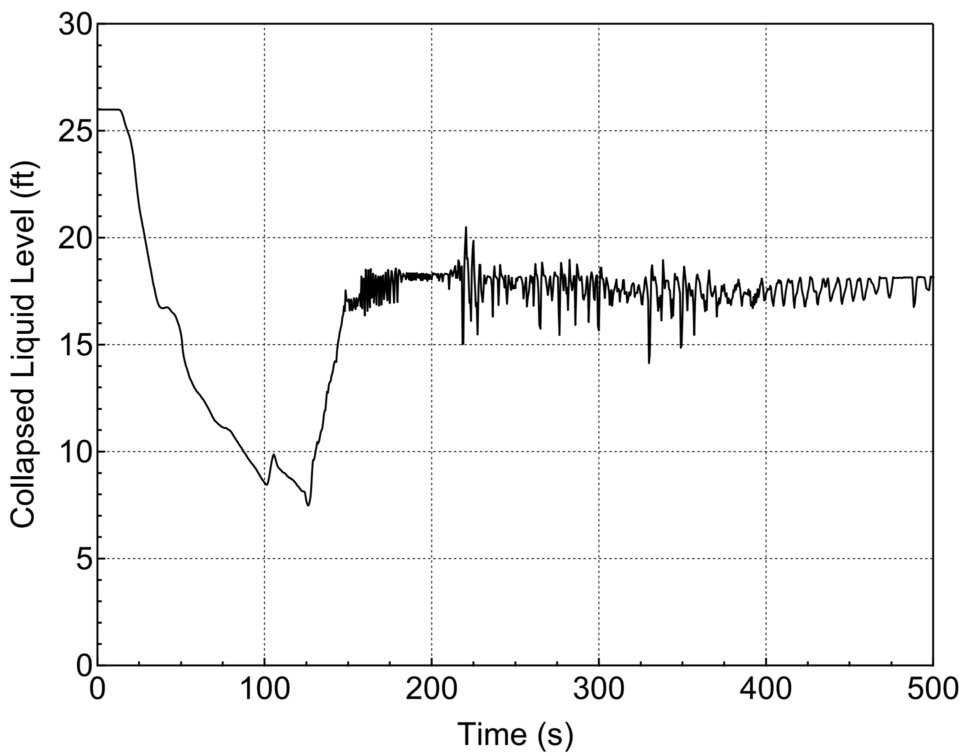

Figure 5.3.2.b-24 Downcomer Collapsed Level for 13-inch Break (Homogeneous) (Break Orientation Sensitivity Study)

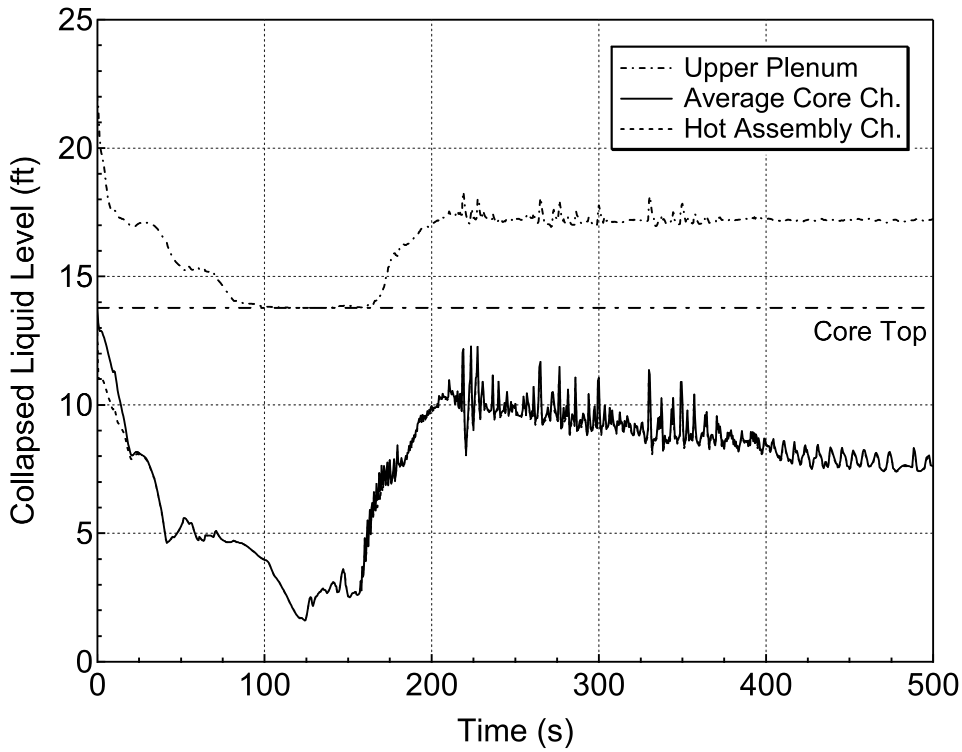

Figure 5.3.2.b-25 Core and Upper Plenum Collapsed Levels for 13-inch Break (Homogeneous) (Break Orientation Sensitivity Study)

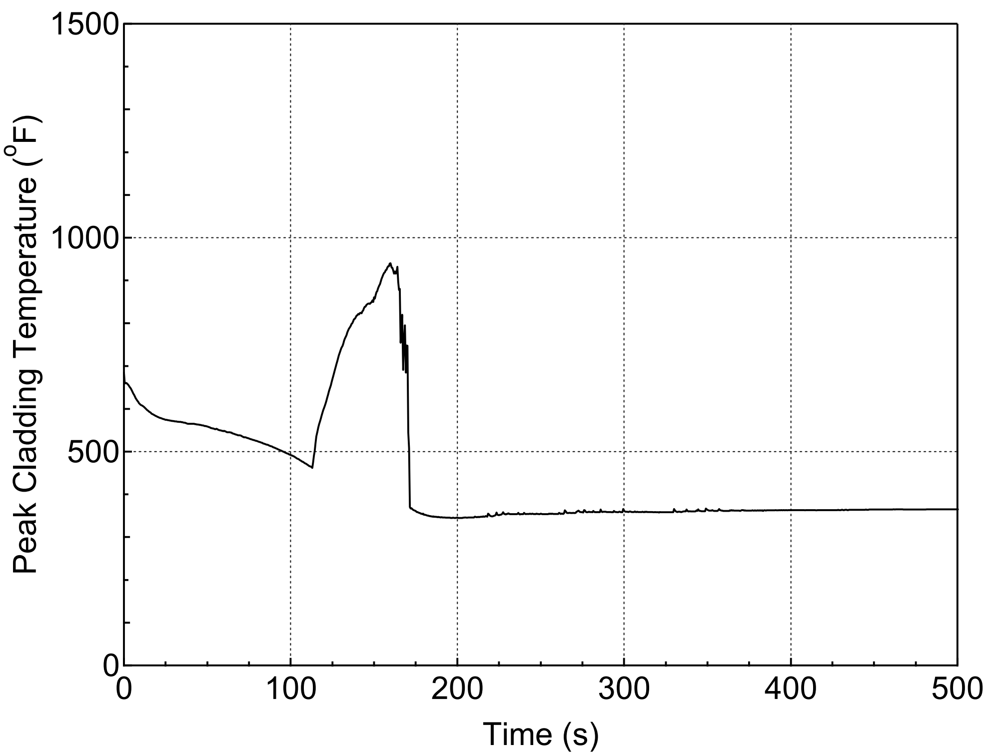

Figure 5.3.2.b-26 PCT at All Elevations for Hot Rod in Hot Assembly for 13-inch Break (Homogeneous) (Break Orientation Sensitivity Study)

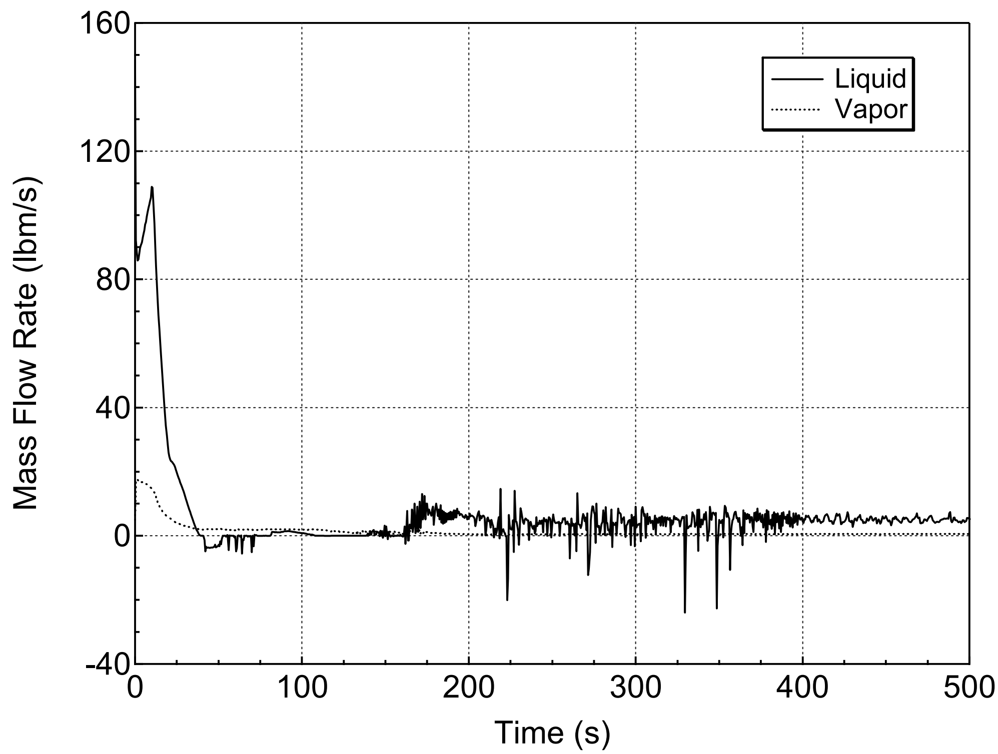

Figure 5.3.2.b-27 Hot Assembly Exit Vapor and Liquid Mass Flowrates for 13-inch Break (Homogeneous) (Break Orientation Sensitivity Study)

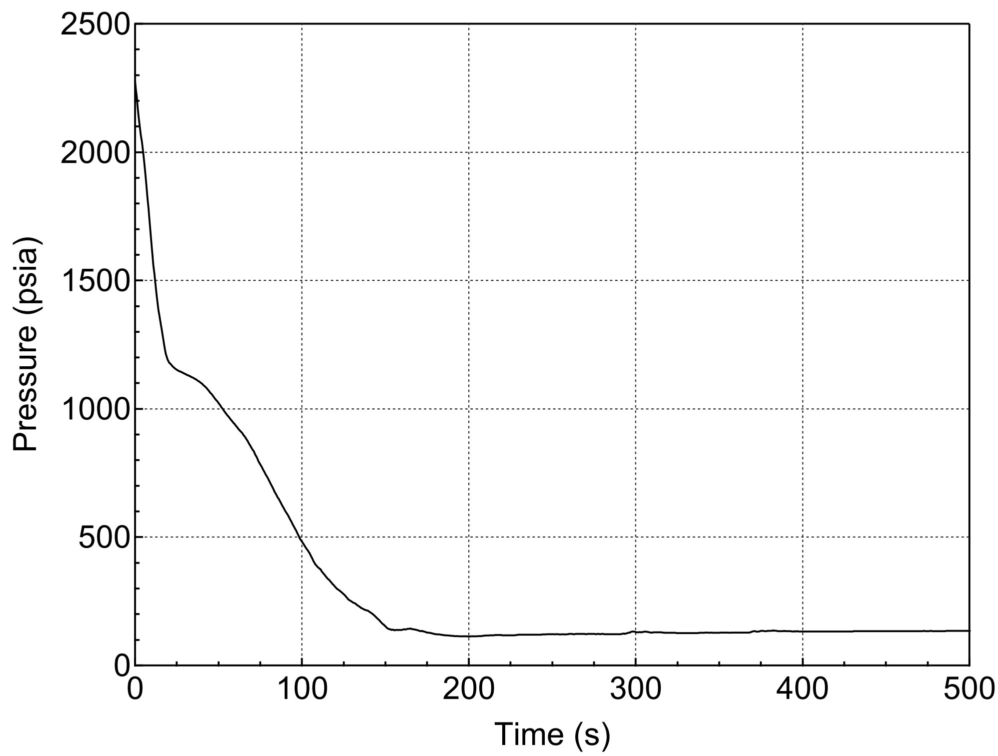

Figure 5.3.2.c-1 RCS (Pressurizer) Pressure Transient for 1-ft^2 Break (Top) (Break Orientation Sensitivity Study)

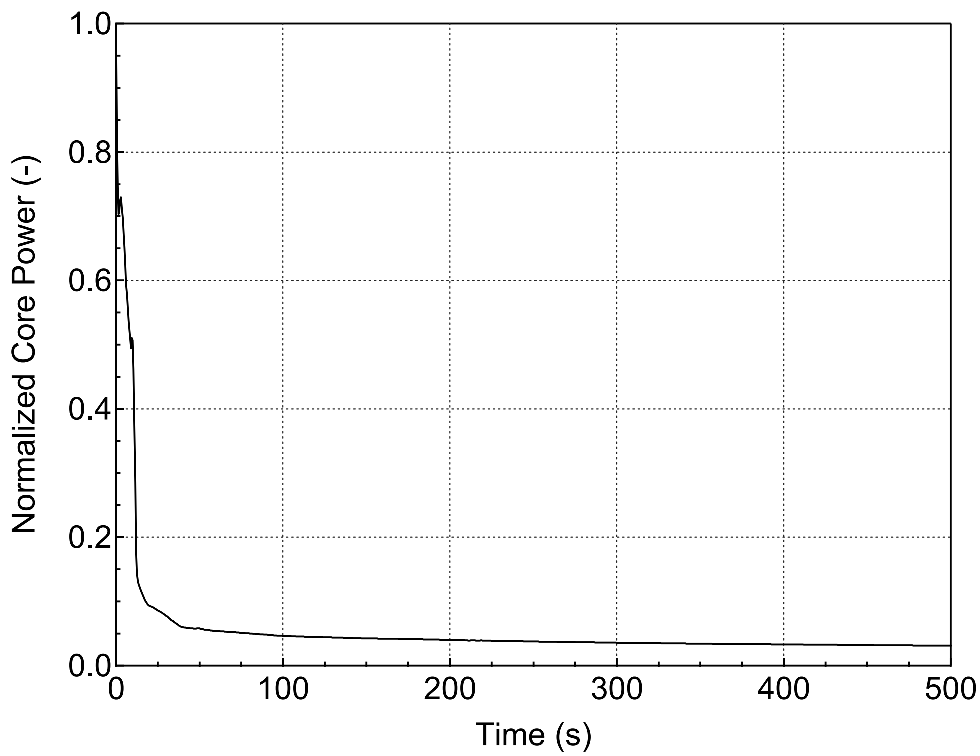

Figure 5.3.2.c-2 Normalized Core Power for 1-ft^2 Break (Top)
(Break Orientation Sensitivity Study)

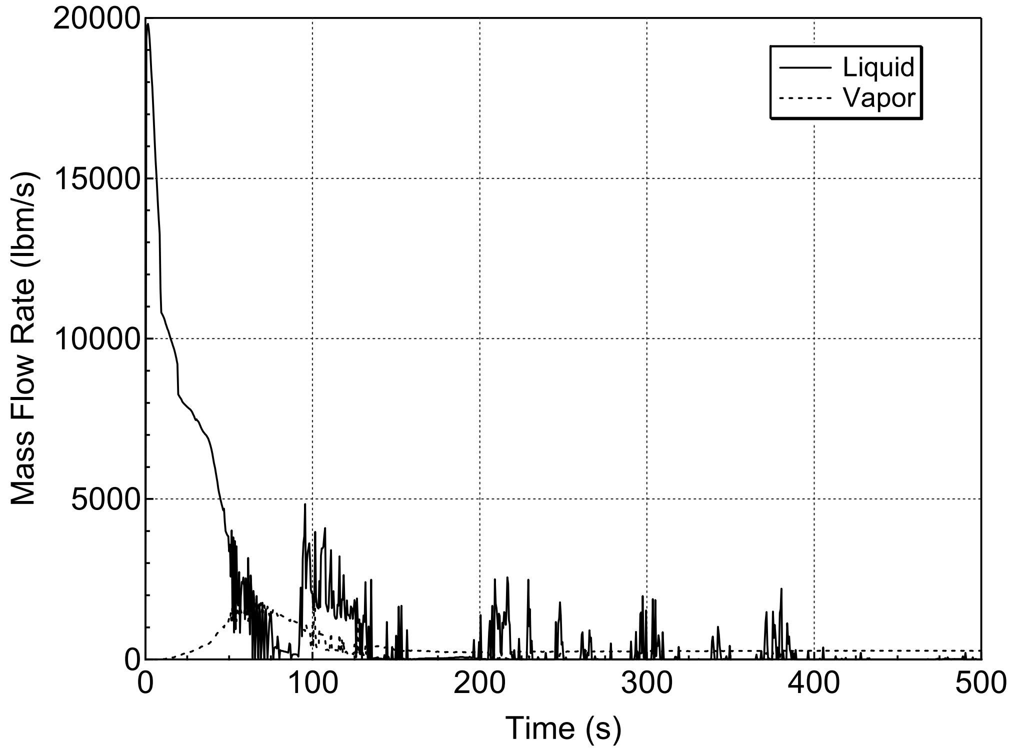

Figure 5.3.2.c-3 Liquid and Vapor Discharges through the Break for 1-ft^2 Break (Top) (Break Orientation Sensitivity Study)

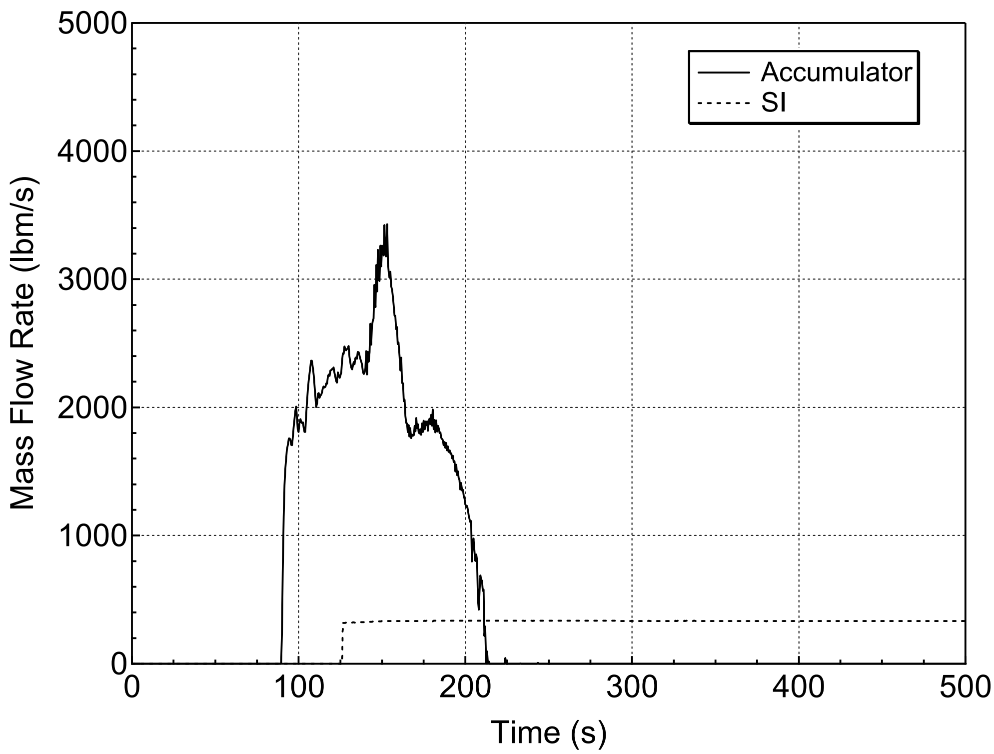

Figure 5.3.2.c-4 Accumulator and Safety Injection Mass Flowrates for 1-ft^2 Break (Top) (Break Orientation Sensitivity Study)

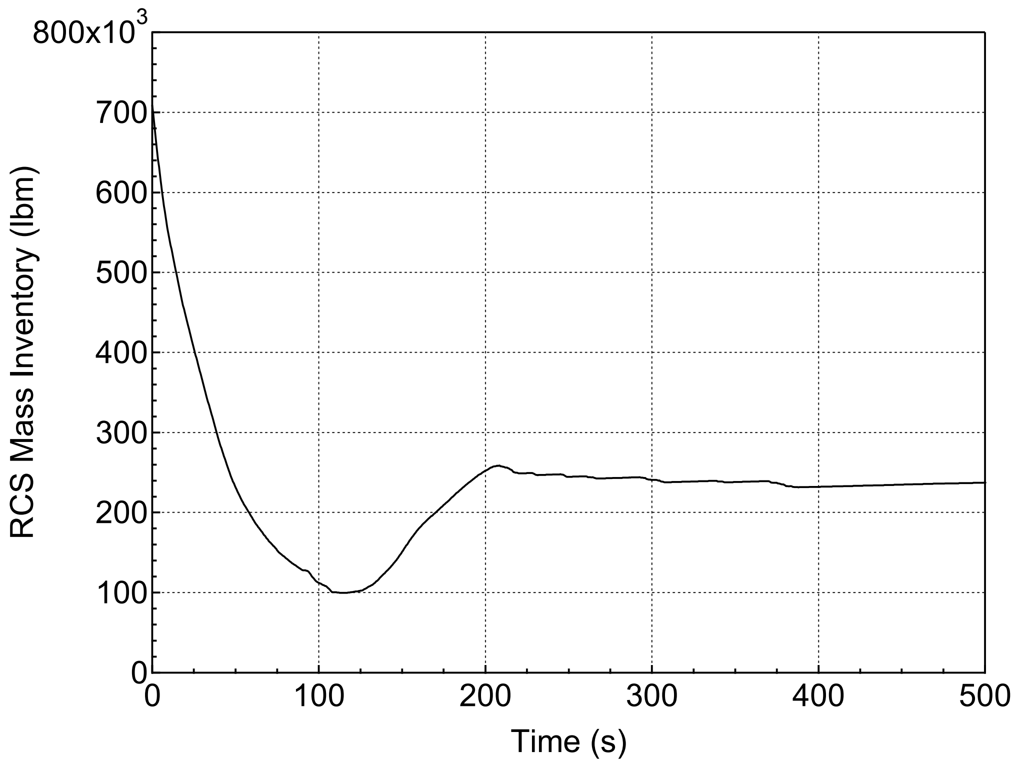

Figure 5.3.2.c-5 RCS Mass Inventory for 1-ft^2 Break (Top) (Break Orientation Sensitivity Study)

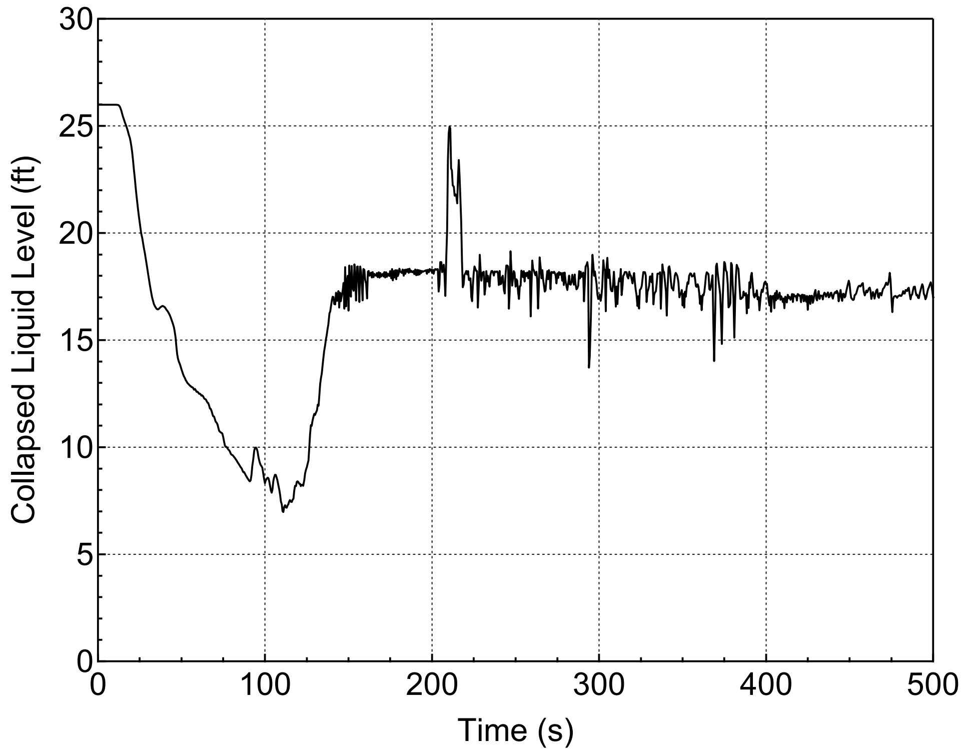

Figure 5.3.2.c-6 Downcomer Collapsed Level for 1-ft^2 Break (Top) (Break Orientation Sensitivity Study)

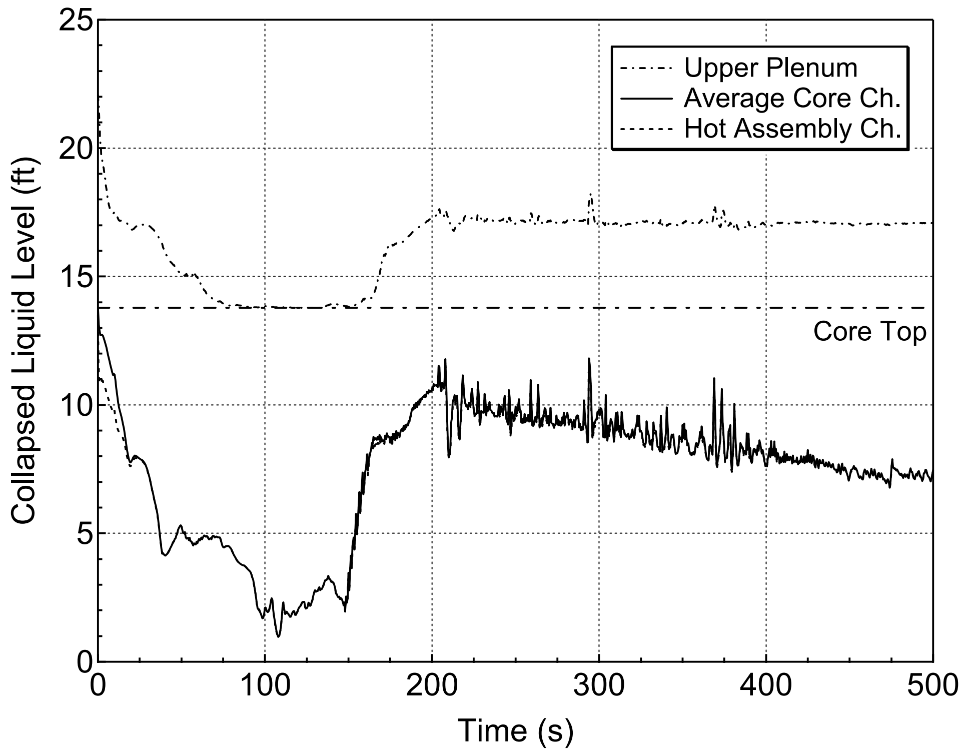

Figure 5.3.2.c-7 Core and Upper Plenum Collapsed Levels for 1-ft^2 Break (Top) (Break Orientation Sensitivity Study)

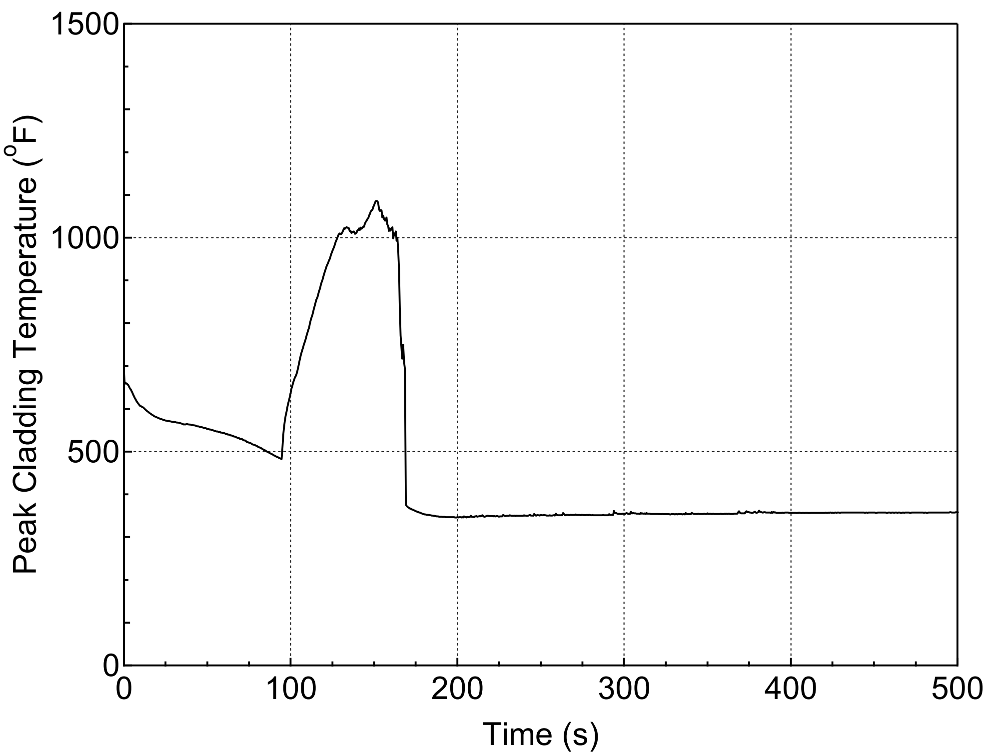

Figure 5.3.2.c-8 PCT at All Elevations for Hot Rod in Hot Assembly for 1-ft^2 Break (Top) (Break Orientation Sensitivity Study)

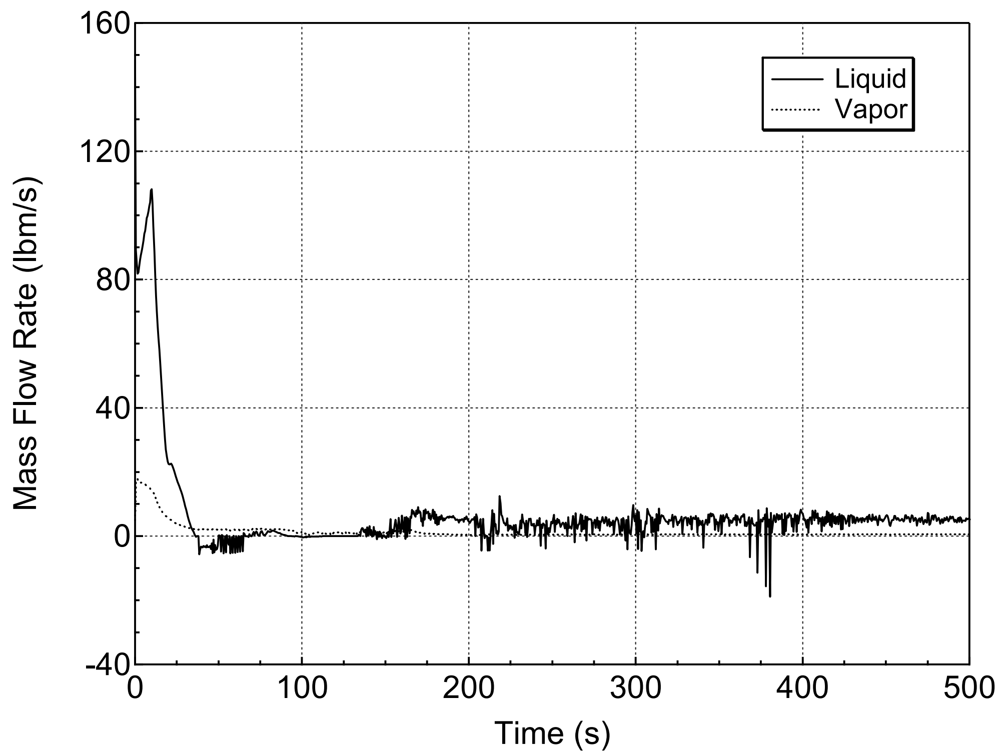

Figure 5.3.2.c-9 Hot Assembly Exit Vapor and Liquid Mass Flowrates for 1-ft^2 Break (Top) (Break Orientation Sensitivity Study)

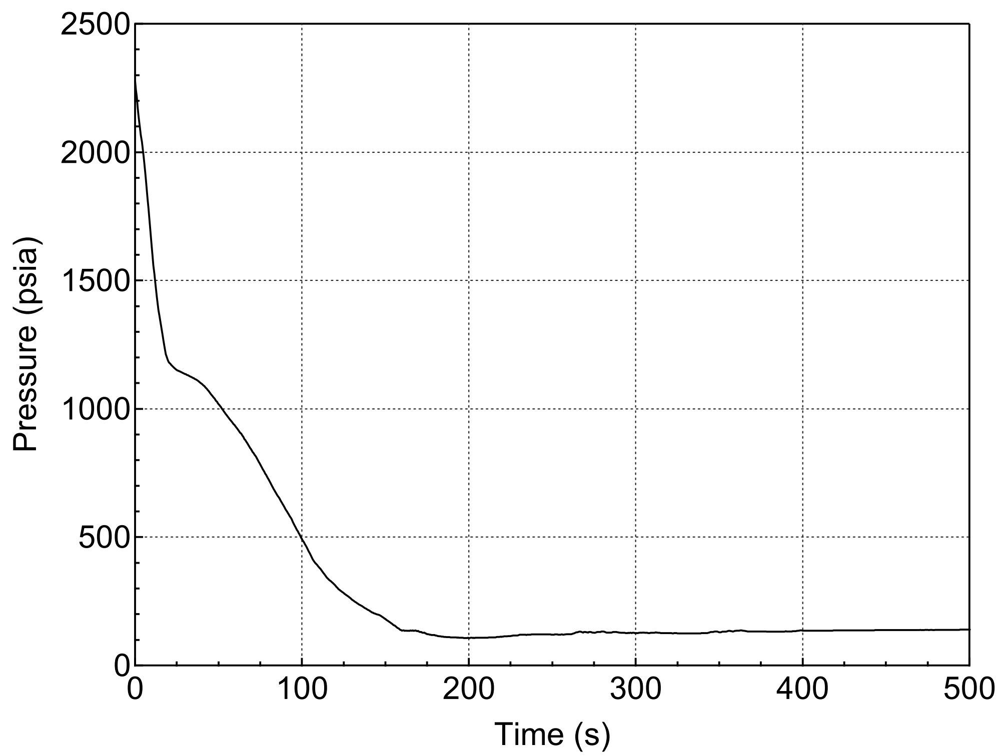

Figure 5.3.2.c-10 RCS (Pressurizer) Pressure Transient for 1-ft^2 Break (Side) (Break Orientation Sensitivity Study)

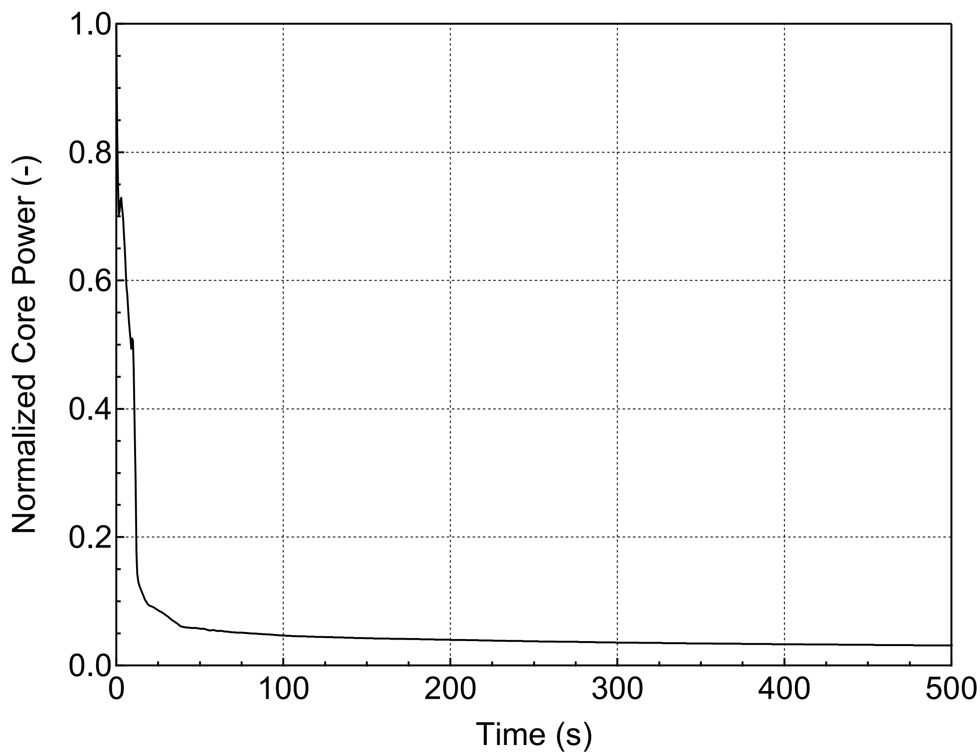

Figure 5.3.2.c-11 Normalized Core Power for 1-ft^2 Break (Side)
(Break Orientation Sensitivity Study)

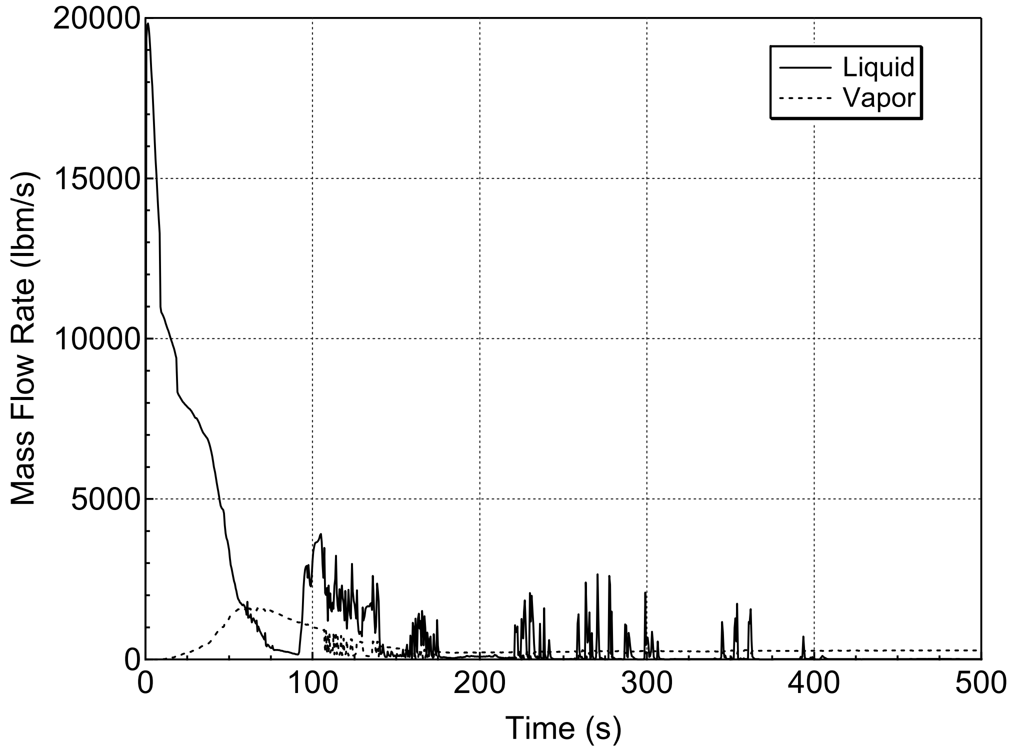

Figure 5.3.2.c-12 Liquid and Vapor Discharges through the Break for 1-ft^2 Break (Side) (Break Orientation Sensitivity Study)

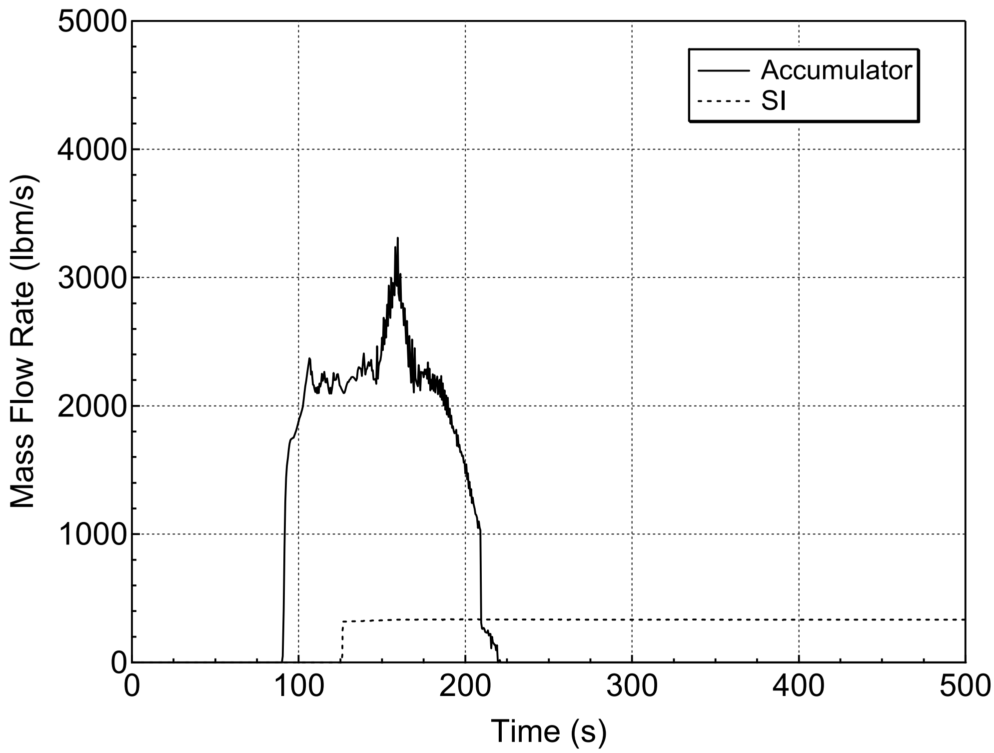

Figure 5.3.2.c-13 Accumulator and Safety Injection Mass Flowrates for 1-ft^2 Break (Side) (Break Orientation Sensitivity Study)

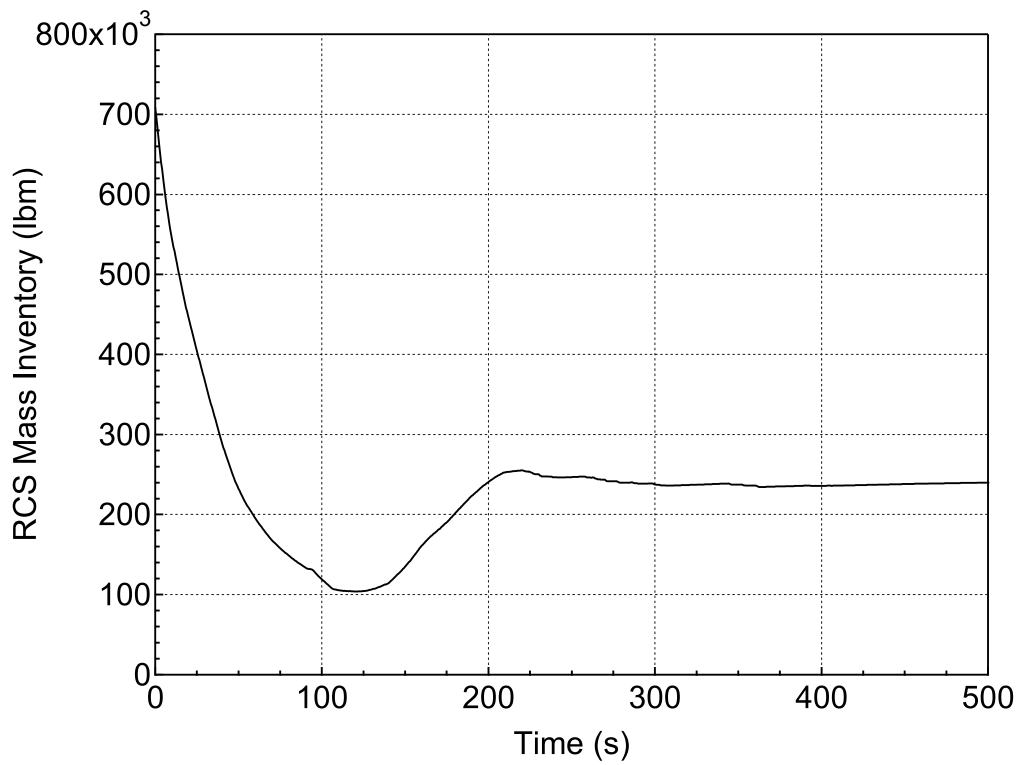

Figure 5.3.2.c-14 RCS Mass Inventory for 1-ft^2 Break (Side)
(Break Orientation Sensitivity Study)

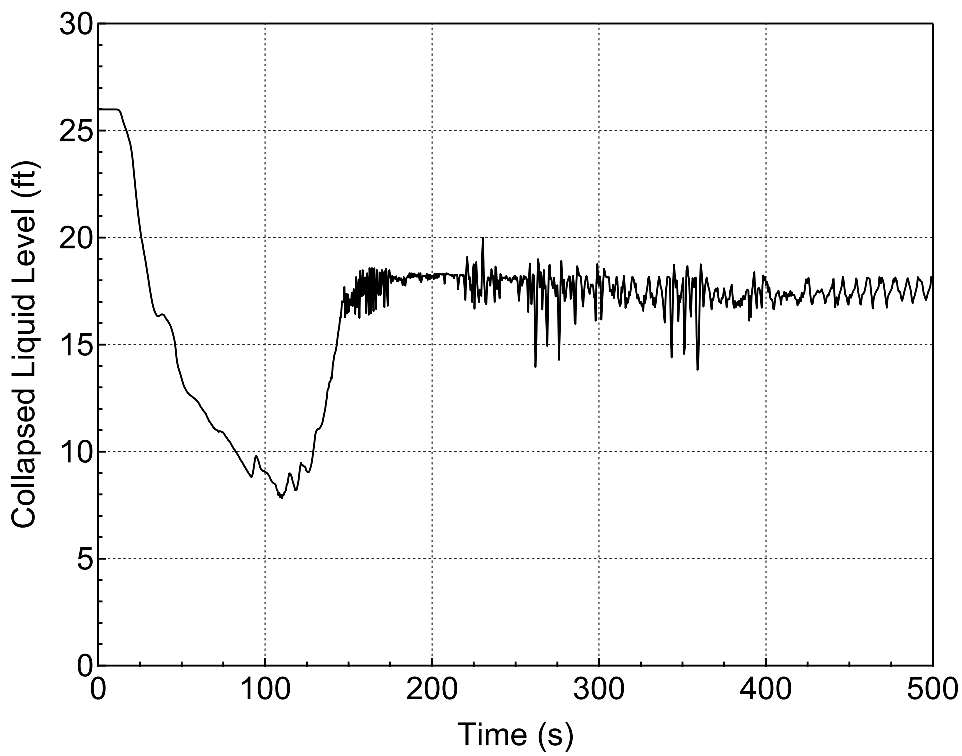

Figure 5.3.2.c-15 Downcomer Collapsed Level for 1-ft^2 Break (Side) (Break Orientation Sensitivity Study)

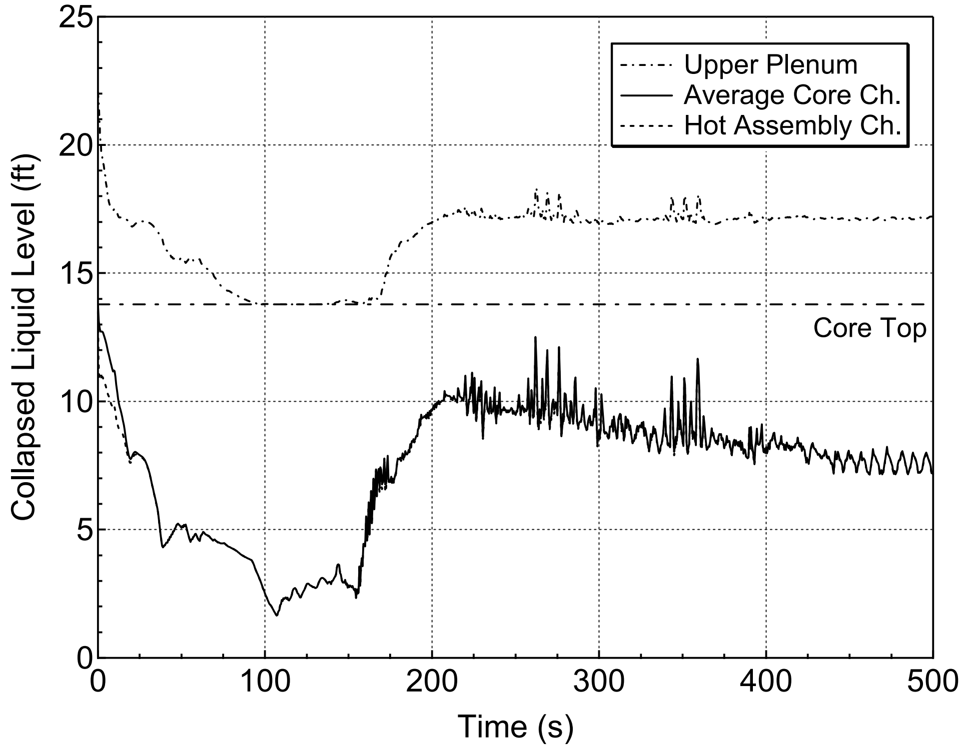

Figure 5.3.2.c-16 Core and Upper Plenum Collapsed Levels for 1-ft^2 Break (Side) (Break Orientation Sensitivity Study)

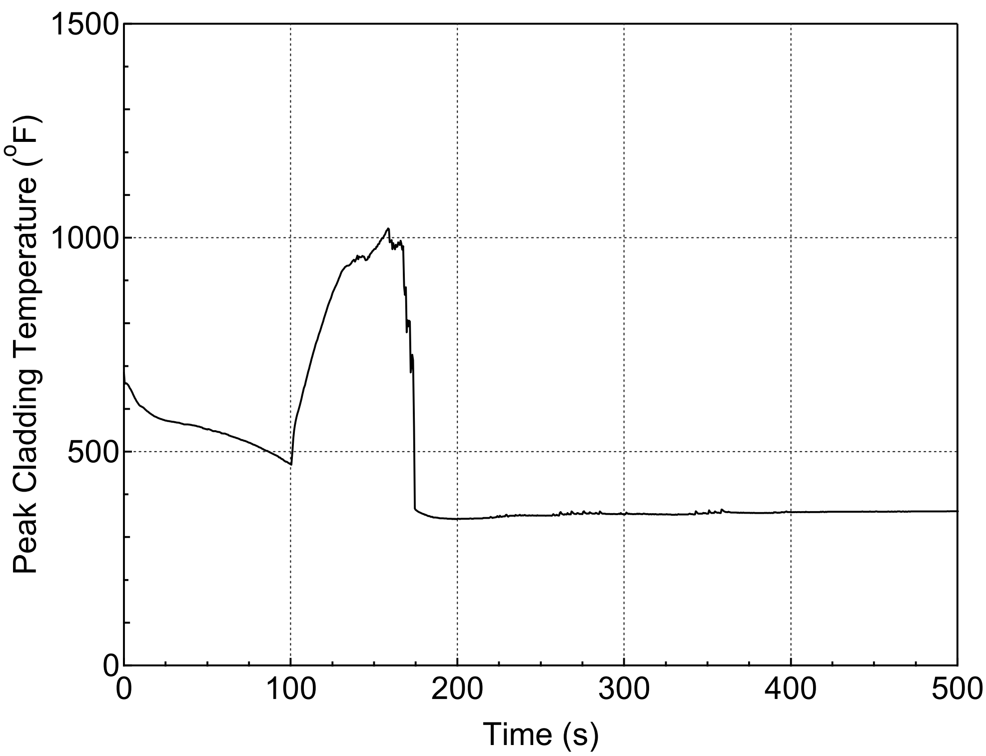

Figure 5.3.2.c-17 PCT at All Elevations for Hot Rod in Hot Assembly for 1-ft² Break (Side) (Break Orientation Sensitivity Study)

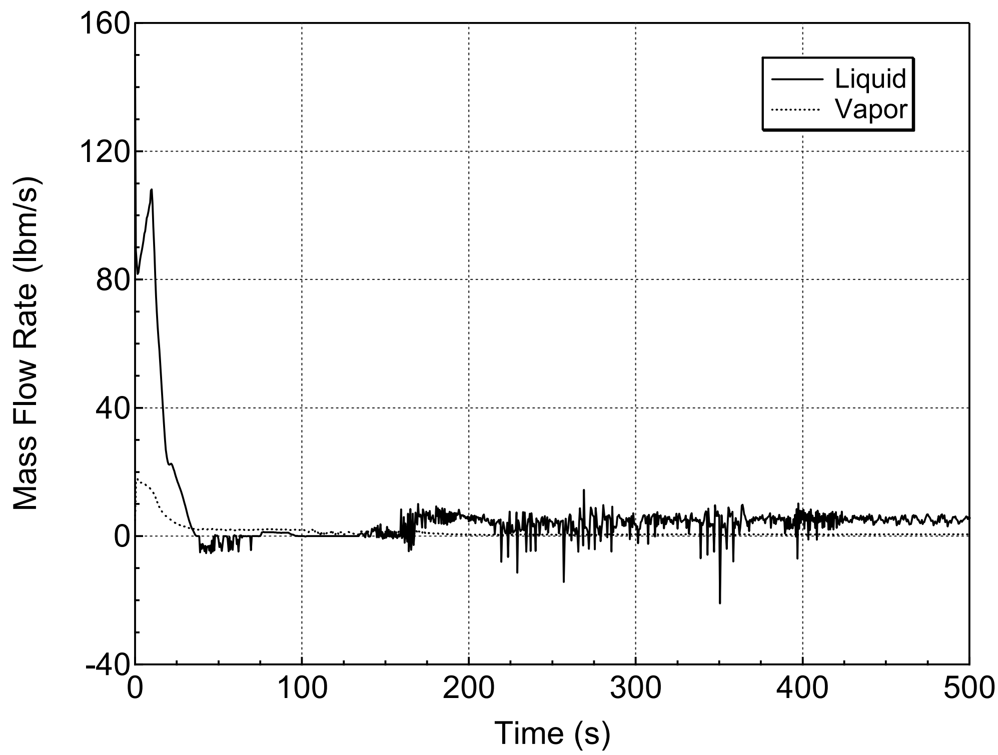

Figure 5.3.2.c-18 Hot Assembly Exit Vapor and Liquid Mass Flowrates for 1-ft^2 Break (Side) (Break Orientation Sensitivity Study)

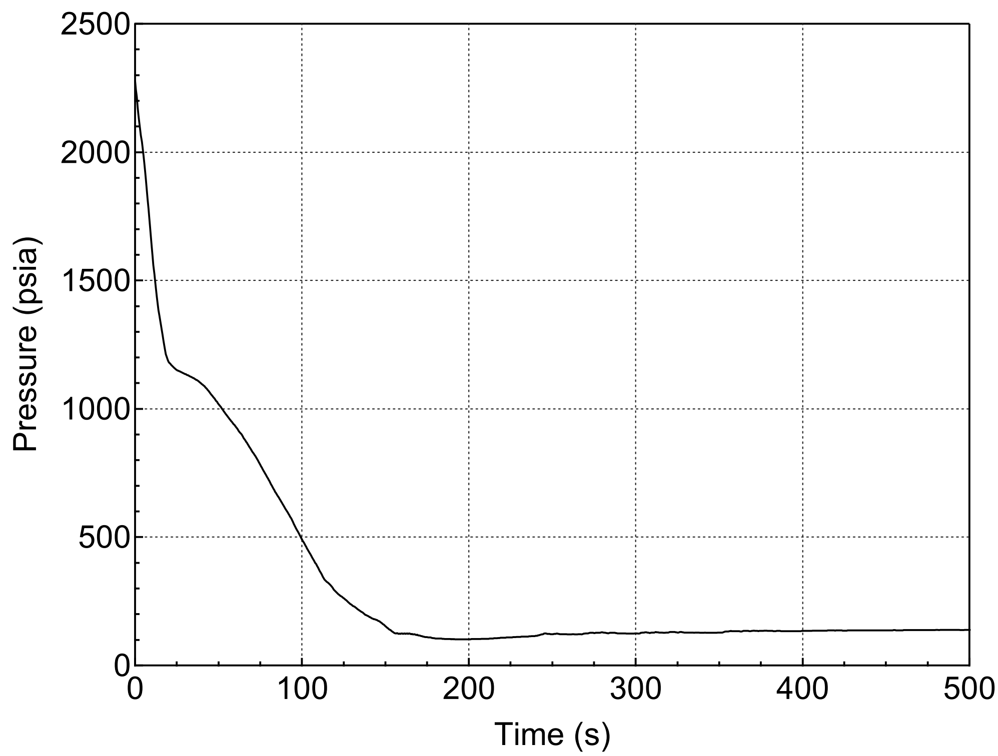

Figure 5.3.2.c-19 RCS (Pressurizer) Pressure Transient for 1-ft^2 Break (Homogeneous) (Break Orientation Sensitivity Study)

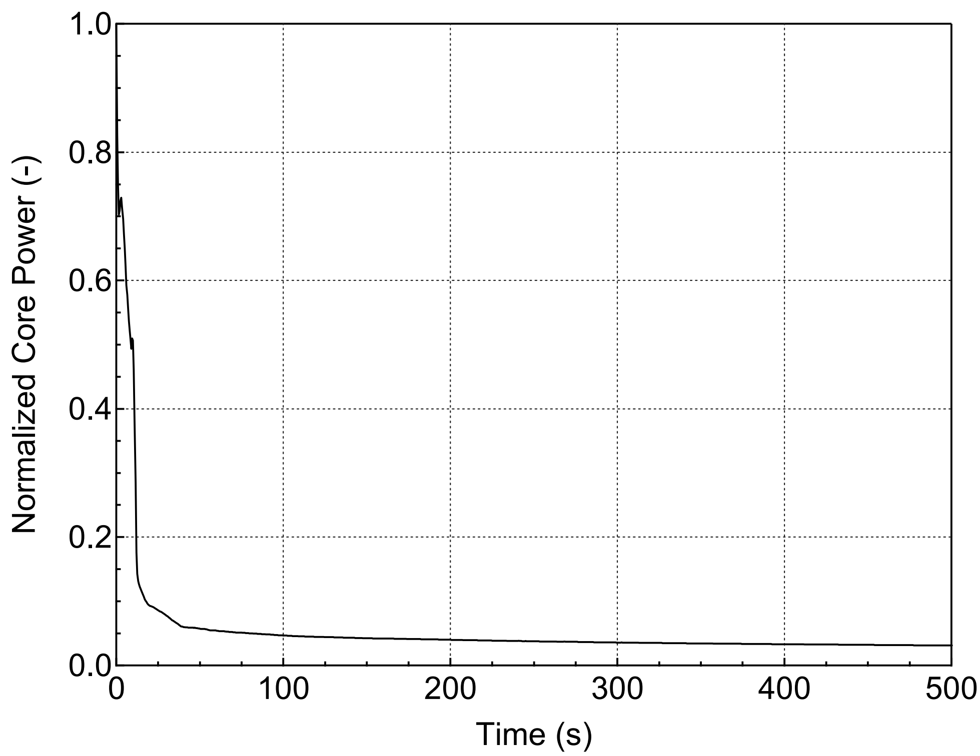

Figure 5.3.2.c-20 Normalized Core Power for 1-ft^2 Break (Homogeneous) (Break Orientation Sensitivity Study)

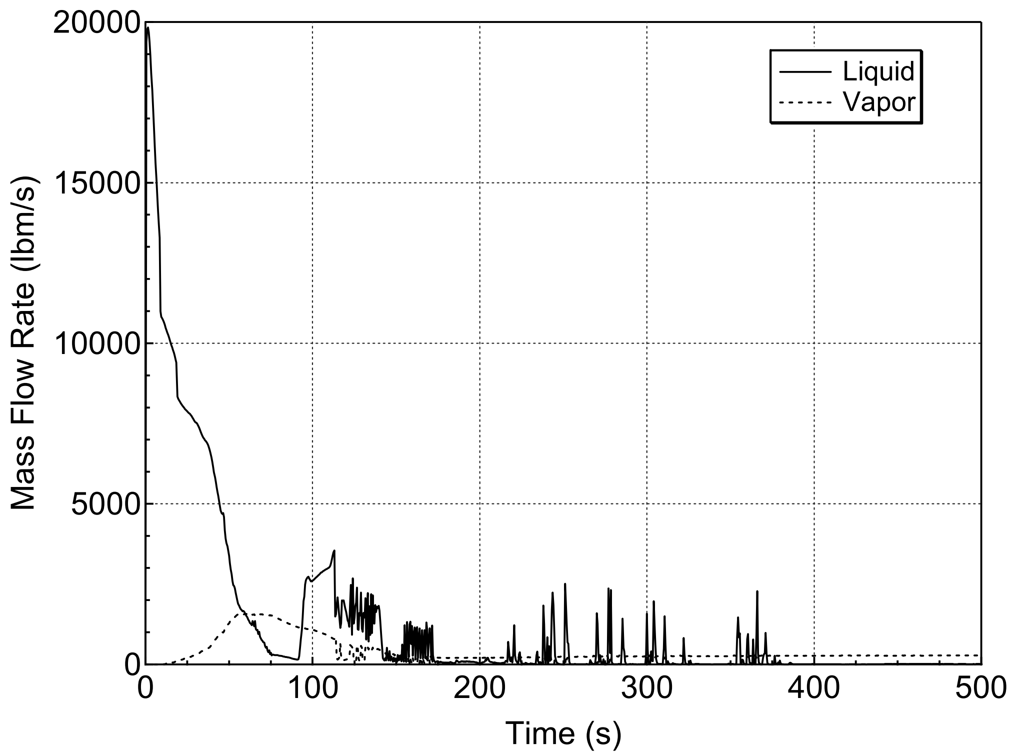

Figure 5.3.2.c-21 Liquid and Vapor Discharges through the Break for 1-ft^2 Break (Homogeneous) (Break Orientation Sensitivity Study)

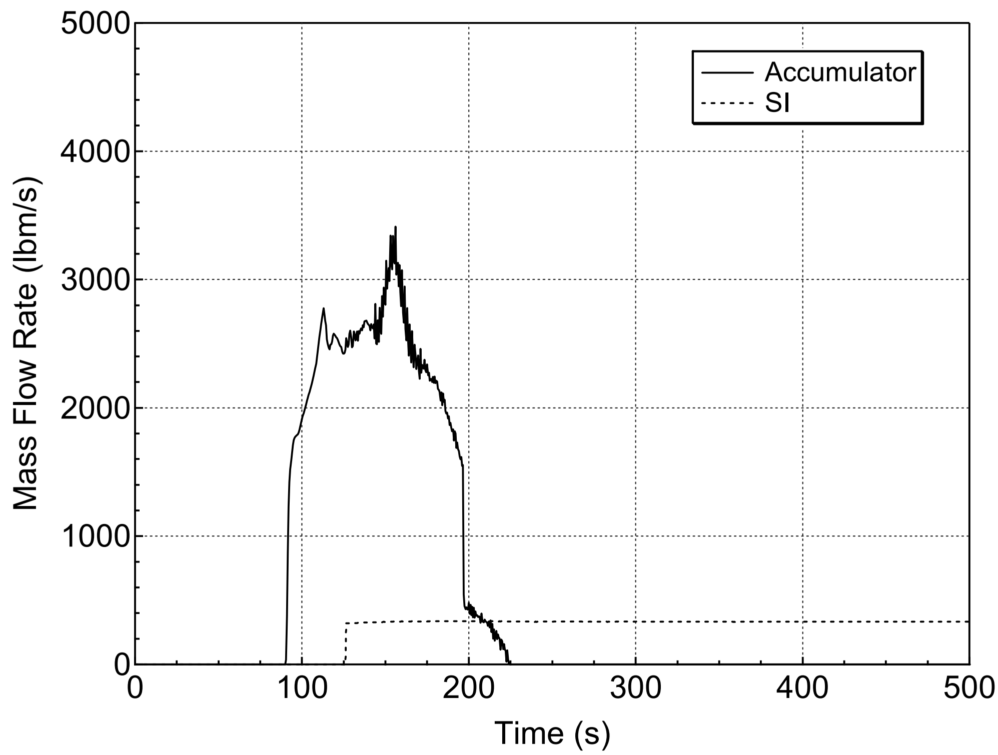

Figure 5.3.2.c-22 Accumulator and Safety Injection Mass Flowrates for 1-ft^2 Break (Homogeneous) (Break Orientation Sensitivity Study)

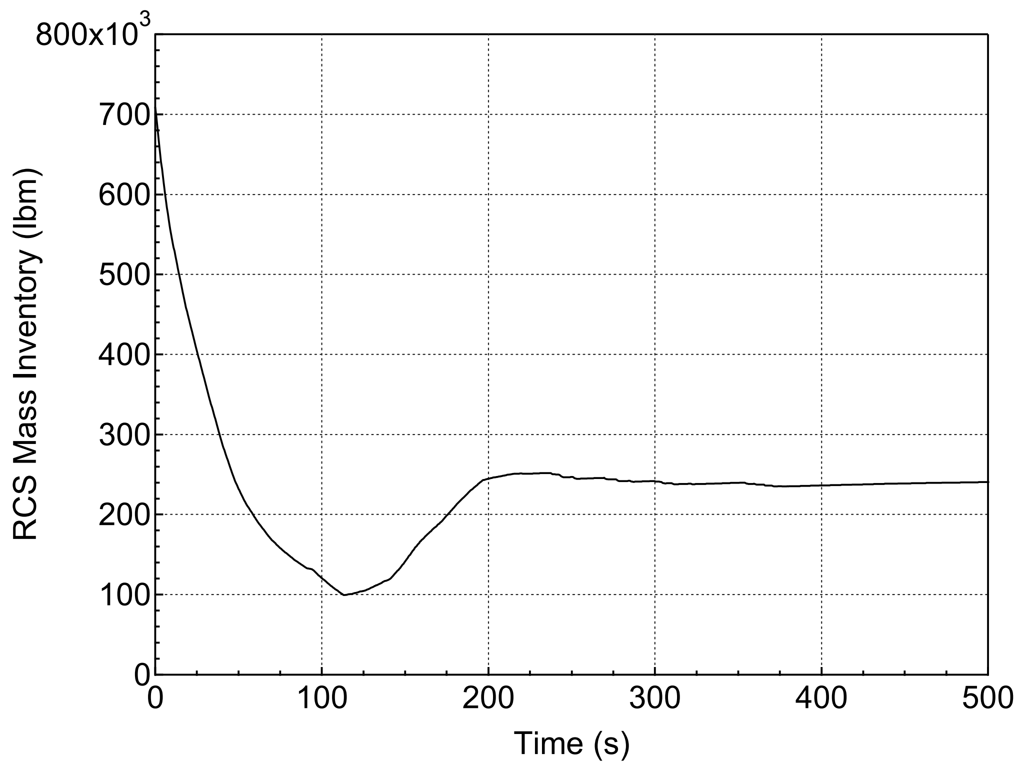

Figure 5.3.2.c-23 RCS Mass Inventory for 1-ft^2 Break (Homogeneous) (Break Orientation Sensitivity Study)

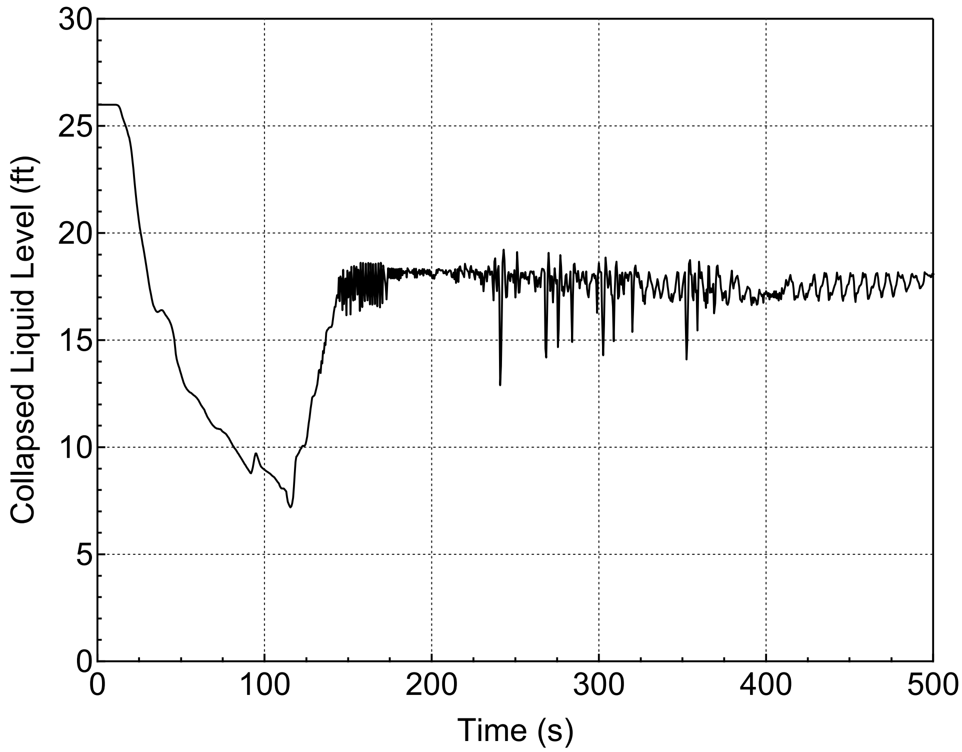

Figure 5.3.2.c-24 Downcomer Collapsed Level for 1-ft^2 Break (Homogeneous) (Break Orientation Sensitivity Study)

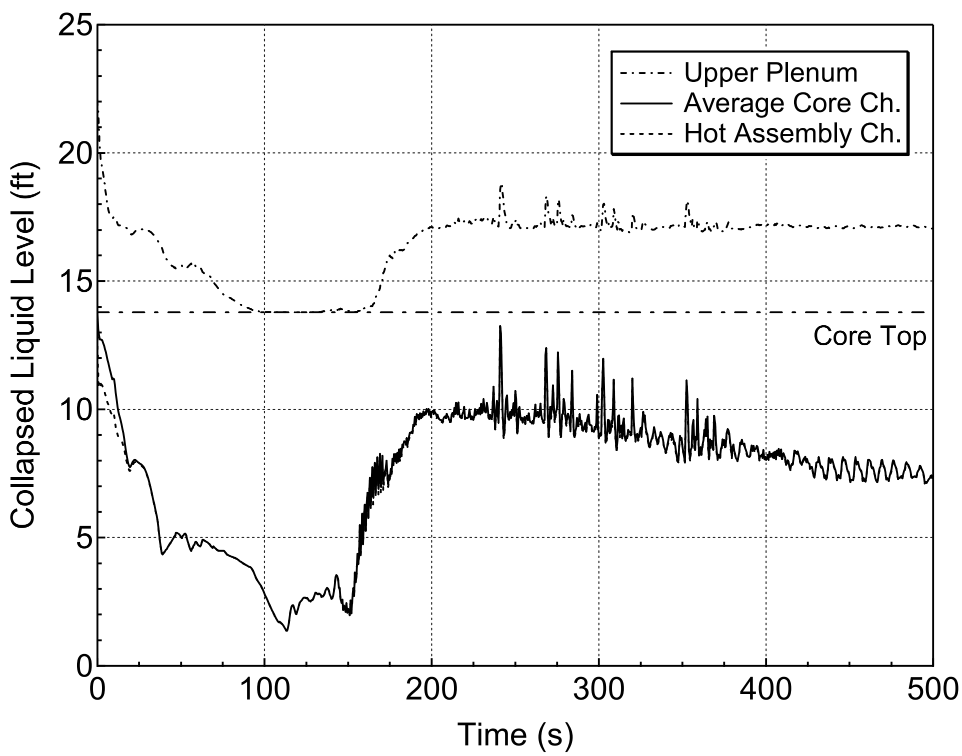

Figure 5.3.2.c-25 Core and Upper Plenum Collapsed Levels for 1-ft^2 Break (Homogeneous) (Break Orientation Sensitivity Study)

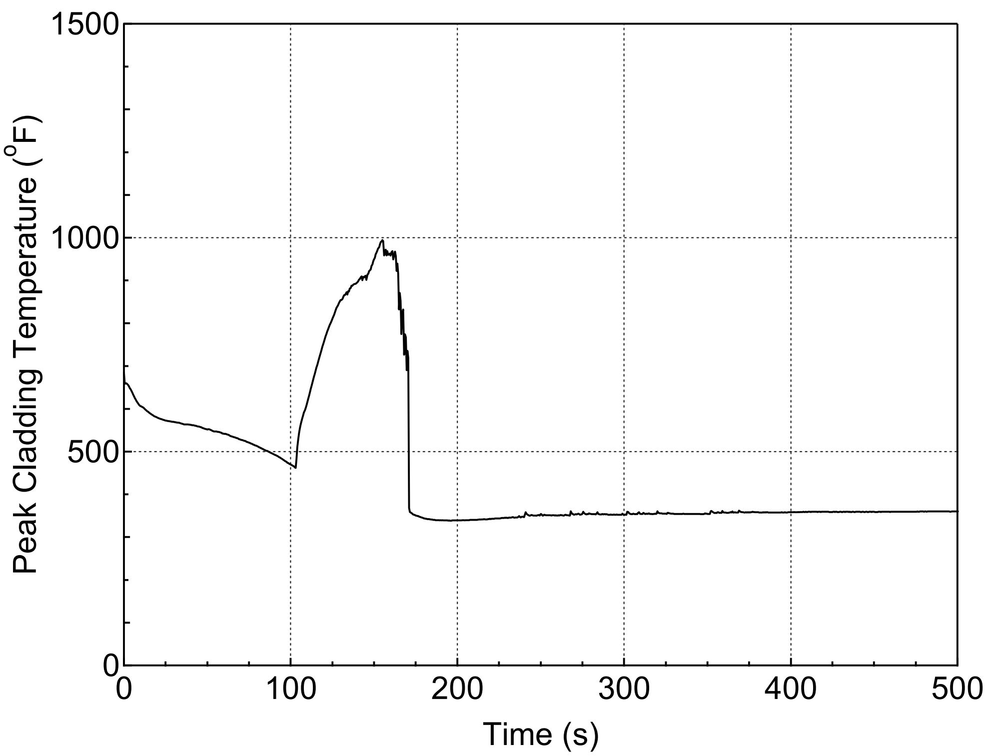

Figure 5.3.2.c-26 PCT at All Elevations for Hot Rod in Hot Assembly for 1-ft^2 Break (Homogeneous) (Break Orientation Sensitivity Study)

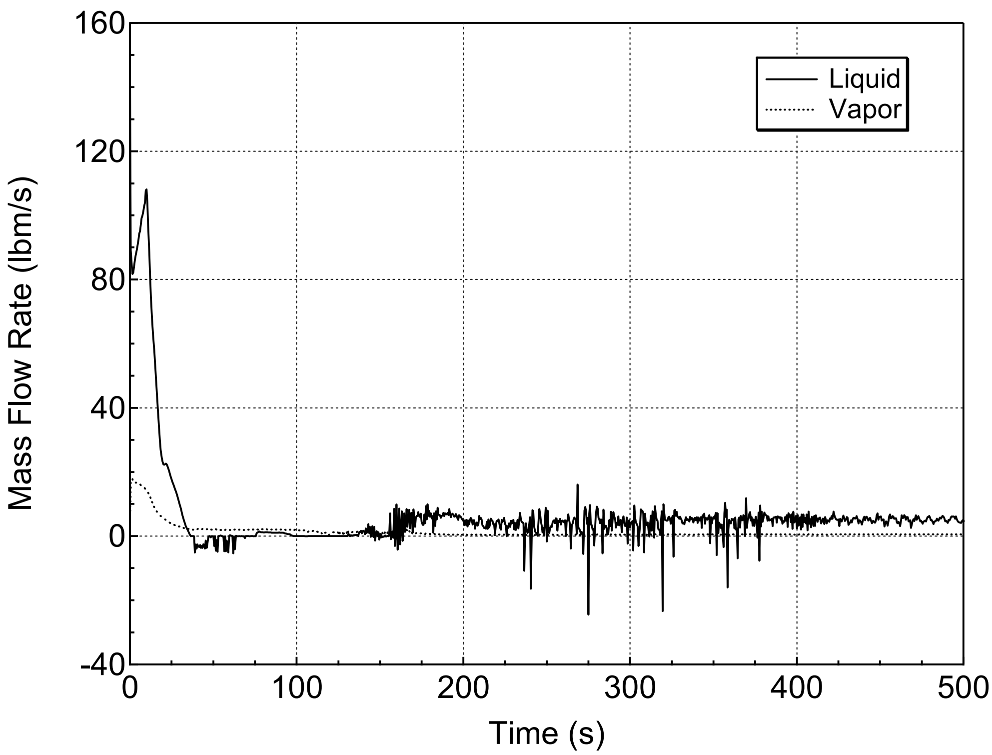

Figure 5.3.2.c-27 Hot Assembly Exit Vapor and Liquid Mass Flowrates for 1-ft^2 Break (Homogeneous) (Break Orientation Sensitivity Study)

5.4 Noding Sensitivity Study

5.4.1 Noding near break sensitivity analysis

Two break cases (7.5-inch and 1-ft^2 cold-leg top orientation breaks) were calculated for noding sensitivity study near break point. As mentioned in Subsection 4.2.3, the number of nodes for cold leg pipe near the break junction is doubled for the sensitivity case.

(1) Results of the 7.5-inch cold leg top orientation break case

Table 5.4.1-1 shows the sequence of events and Table 5.4.1-2 summarizes the main results. These tables show the good agreement between the base case and the sensitivity case. Figures 5.4.1-1 through 5.4.1-13 compare the important transient behaviors between the two cases. It is observed that identical results are obtained.

Figure 5.4.1-1 shows the comparison of base case and sensitivity case on RCS (Pressurizer) pressure transient calculation. It demonstrates that by doubling the number of nodes of cold leg pipe component near the break point, and connecting the break-component to a third volume do not cause any change in the result. The calculation results of base case and sensitivity case are perfectly in agreement.

Figure 5.4.1-2 presents the normalized core power transient. The calculation results prove no sensitivity to the noding change. The results of base case and sensitivity case are perfectly in agreement.

Figure 5.4.1-3 displays the comparison of base case and sensitivity case on the liquid discharge through the break. The results are in good agreement with only very little sensitivity. The vapor discharge through the break is shown in Figure 5.4.1-4. The results are in good agreement with little sensitivity.

Figure 5.4.1-5 shows the comparison of accumulator injection mass flowrate time history. The comparison shows moderate sensitivity in simulating flow oscillation. However, the phenomena and basic transient profiles are well predicted. The calculation results of base case and sensitivity case are similar in terms of transient profile, magnitude and duration.

Figure 5.4.1-6 depicts the time history of safety injection mass flowrate. The calculation results of base case and sensitivity case are perfectly in agreement.

The RCS mass inventory transient is displayed in Figure 5.4.1-7. The calculation results of base case and sensitivity case are also perfectly in agreement.

Figure 5.4.1-8 illustrates the downcomer collapsed level transient. The comparison shows little sensitivity in simulating high frequency non linear amplitudes collapsed level fluctuation. However, the phenomena and basic transient profiles are well predicted.

Figure 5.4.1-9 shows the average core and upper plenum collapsed levels. The comparison shows very little sensitivity and the transient profiles are well predicted.

The hot assembly core and upper plenum collapsed levels are given in Figure 5.4.1-10. The comparison shows very little sensitivity and the transient profiles are well predicted.

The comparison of base case and sensitivity case on PCT at all elevations for hot rod in hot assembly is presented in Figure 5.4.1-11. The results show very small sensitivity in predicting the down slope after the PCT is reached.

Figure 5.4.1-12 presents the hot assembly exit liquid mass flowrate transient calculation comparison between base case and sensitivity case. The results are in good agreement, the oscillating high frequency low amplitude flow reversal are well predicted by both cases.

Figure 5.4.1-13 presents the hot assembly exit vapor mass flowrate. The calculation results of base case and sensitivity case are also perfectly in agreement.

Therefore it is concluded that the noding of the broken-loop cold leg is adequate to simulate upstream conditions of the break flow in case that the loop-seal phenomena dominate PCT.

(2) Results of the 1-ft^2 cold leg top orientation break case

Table 5.4.1-3 shows the sequence of events and Table 5.4.1-4 shows the main results. These tables indicate that the base case gives more conservative results than the sensitivity case which uses finer noding. These results are discussed below in detail focusing on the duration related to the PCT, which is between 100 seconds and 200 seconds.

Figures 5.4.1-14 through 5.4.1-26 compare the important transient behaviors between the two cases.

The RCS (Pressurizer) pressure transient given in Figure 5.4.1-14 shows that the base case calculation slightly underpredicts the RCS pressure until hitting the lowest value after accumulator injection. This lower pressure causes larger SI and accumulator flows as shown in Figures 5.4.1-18 and 5.4.1-19. Nevertheless, the RCS inventory of the base case is smaller than that of the sensitivity case before it bottoms out as shown in Figure 5.4.1-20.

This implies that the coarse noding tends to overpredict the break mass and energy flow rates, which results in the lower RCS pressure and smaller inventory, that in turn causing a higher PCT. Meanwhile, the lower pressure accelerates ECCS injection causing an early turn around of the cladding temperature.

Normalized core power reduction is presented in Figure 5.4.1-15. The calculation results of base case and sensitivity case are perfectly in agreement.

Liquid discharge characteristic through the break is shown in Figure 5.4.1-16. The calculation results show moderate sensitivity in predicting the flashing two-phase flow from the break.

Figure 5.4.1-17 shows the vapor discharge characteristic through the break. The calculation results of base case and sensitivity case are perfectly in agreement.

The accumulator injection mass flowrate is displayed in Figure 5.4.1-18. The calculation results show little sensitivity when calculating the steep up-slope and down-slope of the accumulator injection mass flow rates. The sensitivity case with finer noding yields a small delay caused by a slower response to pressure drop.

Figure 5.4.1-19 illustrates the safety injection mass flowrate. The calculation results of base case and sensitivity case are in good agreement.

Figure 5.4.1-20 shows the RCS mass inventory transient. The calculation shows minor sensitivity. The base case slightly undershoots the decreasing slope but slightly overshoots the increasing slope.

Figure 5.4.1-21 presents the downcomer collapsed level. The calculation results show moderate sensitivity.

Figure 5.4.1-22 shows the average core and upper plenum collapsed levels. The results show only moderate sensitivity in calculating collapsed level transient.

The transient of collapsed levels in the hot assembly core and upper plenum are explained in Figure 5.4.1-23. The results also only show moderate sensitivity in calculating collapsed level transient.

Figure 5.4.1-24 demonstrates the PCT at all elevations for hot rod in the hot assembly. A moderate sensitivity is shown on the comparison results. The results of PCT values and their timing are slightly different. The sensitivity case with finer noding predicts slightly lower PCT by 52°F and the PCT time comes a little delay by 4 seconds. The finer noding shows little sensitivity.

Figure 5.4.1-25 presents the hot assembly exit liquid mass flowrate. The results are in good agreement, the oscillating high frequency low amplitude flow reversal are well predicted in both cases.

Figure 5.4.1-26 displays the hot assembly exit vapor mass flowrate. The calculation results of base case and sensitivity case are perfectly in agreement.

The results show that the noding of the cold leg in the broken loop is adequate to predict the upstream conditions of the break flow when the PCT occurs during the boil-off phase for the 1-ft^2 top orientation cold-leg break.

5.4.2 Plant Noding sensitivity analysis

For sensitivity study for SG U-tube and crossover-leg noding, 7.5-inch break with top break was calculated for the effect for Loop-seal PCT. Figure 5.4.2-1 shows the RCS (Pressurizer) pressure transient. It demonstrates that by doubling the SG tubes noding, and doubling the crossover leg noding show only little sensitivity. The minor sensitivity occurs in predicting pressure transient in lower pressure range.

Figure 5.4.2-2 presents the normalized core power transient. The results of base case and sensitivity case are perfectly in agreement.

Figure 5.4.2-3 displays the liquid discharge through the break. The results of base case and sensitivity case are in good agreement when predicting mass flow rate transient in higher pressure, but very small sensitivity occurs in predicting lower flow rate transient at low pressure range.

The vapor discharge through the break is shown in Figure 5.4.2-4. The results of base case and sensitivity case are in good agreement. Loop seal clearance is identified by the increase in vapor flowrate after about 120 seconds.

Figure 5.4.2-5 shows the time history of accumulator injection mass flowrate. The calculation results show little sensitivity when calculating the oscillation amplitude of the accumulator injection mass flow rates.

Figure 5.4.2-6 depicts the time history of safety injection mass flowrate. The results of base case and sensitivity case are in good agreement.

The RCS mass inventory transient is displayed in Figure 5.4.2-7. The results of base case and sensitivity case are also in good agreement.

Figure 5.4.2-8 illustrates the downcomer collapsed level. The results of base case and sensitivity case show little sensitivity in the beginning of transient, and moderate sensitivity in the later part of transient.

Figure 5.4.2-9 shows the average core and upper plenum collapsed levels. The results show moderate sensitivity in calculating collapsed level transient. Sensitivity case predicts early loop seal clearance time.

The hot assembly core and upper plenum collapsed levels are given in Figure 5.4.2-10. The results also only show moderate sensitivity in calculating collapsed level transient. The loop seal clearance occurs early in the sensitivity case.

The PCT at all elevations for hot rod in hot assembly is presented in Figure 5.4.2-11. The results of PCT values and their timing are slightly different. The base case with coarser noding predicts a PCT of 775°F at 136 seconds. However, the sensitivity case does not generate any heatup after the break due to the shorter loop-seal period.

Figure 5.4.2-12 presents the hot assembly exit liquid mass flowrate. The calculation result shows small sensitivity caused by the difference in loop seal clearance time.

Figure 5.4.2-13 presents the hot assembly exit vapor mass flowrate. The results of base case and sensitivity case are also in perfect agreement.

It is concluded that the effect of varying the plant noding induces small sensitivity to the results, in general. A moderate sensitivity is shown on the PCT comparison results. The finer noding does not generate any heatup after the break, because the loop seal period is shorter.

5.4.3 Noding near the DVI injection point sensitivity analysis

Two break cases (7.5-inch and 1-ft^2 cold-leg top orientation breaks) were calculated for noding sensitivity study near the DVI injection point. **[**

]

(1) Results of the 7.5-inch cold leg top orientation case

Table 5.4.3-1 shows the sequence of events and Table 5.4.3-2 summarizes the main results. These tables show the good agreement between the base case and the sensitivity case. Figures 5.4.3-1 through 5.4.3-13 compare important transient behaviors between the two cases. It is observed that identical results are obtained.

Figure 5.4.3-1 shows the comparison of base case and sensitivity case on RCS (Pressurizer) pressure transient calculation. The calculation result of the sensitivity case agrees with the base case.

Figure 5.4.3-2 presents the normalized core power transient. The calculation result proves no sensitivity to the noding change. The results of base case and sensitivity case are perfectly in agreement.

Figure 5.4.3-3 displays the comparison of base case and sensitivity case on the liquid discharge through the break. The results are in good agreement. The vapor discharge through the break is shown in Figure 5.4.3-4. The results are in good agreement with little sensitivity.

Figure 5.4.3-5 shows the comparison of accumulator injection mass flowrate time history. The results are in good agreement with little sensitivity.

Figure 5.4.3-6 depicts the time history of safety injection mass flowrate. The calculation results of base case and sensitivity case are in good agreement with only little sensitivity.

The RCS mass inventory transient is displayed in Figure 5.4.3-7. The calculation results of base case and sensitivity case are in good agreement.

Figure 5.4.3-8 illustrates the downcomer collapsed level transient. The sensitivity case has lower downcomer level. However, the phenomena and basic transient profiles are well predicted.

Figure 5.4.3-9 shows the average core and upper plenum collapsed levels. The results are in good agreement with little sensitivity.

The hot assembly core and upper plenum collapsed levels are given in Figure 5.4.3-10. The results are in good agreement with little sensitivity.

The comparison of base case and sensitivity case on PCT at all elevations for hot rod in hot assembly is presented in Figure 5.4.3-11. The results show very small sensitivity in predicting the down slope after the PCT is reached.

Figure 5.4.3-12 presents the hot assembly exit liquid mass flowrate transient calculation comparison between base case and sensitivity case. The results are in good agreement, the oscillating high frequency low amplitude flow reversal are well predicted by both cases.

Figure 5.4.3-13 presents the hot assembly exit vapor mass flowrate. The calculation results of base case and sensitivity case are also perfectly in agreement.

Therefore it is concluded that the noding near the DVI injection point is adequate to simulate the loop-seal phenomena dominates PCT.

(2) Results of the 1-ft^2 cold leg top orientation break case

Table 5.4.3-3 shows the sequence of events and Table 5.4.3-4 shows the main results. These tables indicate that the base case gives more conservative results than the sensitivity case which uses finer noding. These results are discussed below in detail focusing on the duration related to the PCT, which is between 100 seconds and 200 seconds.

Figures 5.4.3-14 through 5.4.3-26 compare the important transient behaviors between the two cases.

The RCS (Pressurizer) pressure transient given in Figure 5.4.3-14 shows that the calculation results of the sensitivity case agrees with the base case.

Normalized core power reduction is presented in Figure 5.4.3-15. The calculation results of base case and sensitivity case are perfectly in agreement.

Liquid discharge characteristic through the break is shown in Figure 5.4.3-16. The calculation results show little sensitivity.

Figure 5.4.3-17 shows the vapor discharge characteristic through the break. The calculation results of base case and sensitivity case are perfectly in agreement.

The accumulator injection mass flowrate is displayed in Figure 5.4.3-18. The calculation results show little sensitivity when calculating the steep down-slope of the accumulator injection mass flow rates.

Figure 5.4.3-19 illustrates the safety injection mass flowrate. The calculation results of base case and sensitivity case are in good agreement.

Figure 5.4.3-20 shows the RCS mass inventory transient. The calculation shows minor sensitivity. The sensitivity case is smaller in the increasing slope.

Figure 5.4.3-21 presents the downcomer collapsed level. The calculation shows minor sensitivity.

Figure 5.4.3-22 shows the average core and upper plenum collapsed levels. The results show only moderate sensitivity in calculating collapsed level transient.

The transient of collapsed levels in the hot assembly core and upper plenum are explained in Figure 5.4.3-23. The results also only show moderate sensitivity in calculating collapsed level transient.

Figure 5.4.3-24 demonstrates the PCT at all elevations for hot rod in the hot assembly. A moderate sensitivity is shown on the comparison results. The results of PCT values and their timing are slightly different. The sensitivity case with finer noding predicts slightly lower PCT by 20°F and the PCT time delay is about 5 seconds.

Figure 5.4.3-25 presents the hot assembly exit liquid mass flowrate. The results are in good agreement, the oscillating high frequency low amplitude flow reversal are well predicted in both cases.

Figure 5.4.3-26 displays the hot assembly exit vapor mass flowrate. The calculation results of base case and sensitivity case are perfectly in agreement.

It is concluded that the effect of varying the DVI injection point noding induces small sensitivity to the results, in general. A moderate sensitivity is shown on the PCT comparison results. The noding used in the licensing analysis gives conservative result in comparison with the finer noding.

Table 5.4.1-1 Sequence of Events for 7.5-inch Break (Top)
(Noding near Break Point Sensitivity Study)

Event	Time (sec)	
	Base case	Sensitivity case
Break occurs; blowdown initiation	0.0	0.0
Reactor trip (loss-of-offsite power is assumed)	9.3	9.3
Control rod insertion starts	11.1	11.1
Main steam isolation	11.1	11.1
ECCS actuation signal	11.9	11.9
RCP trip	12.3	12.3
Main feedwater isolation	17.3	17.3
Main steam safety valve open	81	81
Emergency Power Source initiates	115	115
Fuel cladding starts heating up	122	122
High Head Injection System begins	130	130
Peak Cladding Temperature occurs	136	135
Fuel cladding rewets	143	139
Emergency feedwater flow begins	145	145
Accumulator injection begins	315	314

Table 5.4.1-2 Core Performance Results for 7.5-inch Break (Top)
(Noding near Break Point Sensitivity Study)

	Values	
	Base case	Sensitivity case
Peak Cladding Temperature (°F)	775	763
Maximum local cladding oxidation (%)	0.2	0.2
Maximum core wide cladding oxidation (%)	less than 0.2	less than 0.2

Table 5.4.1-3 Sequence of Events for 1-ft^2 Break (Top)
(Noding near Break Point Sensitivity Study)

Event	Time (sec)	
	Base case	Sensitivity case
Break occurs; blowdown initiation	0.0	0.0
Reactor trip (loss-of-offsite power is assumed)	6.9	6.9
ECCS actuation signal	8.3	8.3
Control rod insertion starts	8.7	8.7
Main steam isolation	8.7	8.7
RCP trip	9.9	9.9
Main feedwater isolation	14.9	14.9
Main steam safety valve open	not actuated	not actuated
Accumulator injection begins	89	90
Fuel cladding starts heating up	95	96
Emergency Power Source initiates	111	111
High Head Injection System begins	126	126
Emergency feedwater flow begins	141	141
Peak Cladding Temperature occurs	151	155
Fuel cladding rewets	169	170

Table 5.4.1-4 Core Performance Results for 1-ft^2 Break (Top)
(Noding near Break Point Sensitivity Study)

	Values	
	Base case	Sensitivity case
Peak Cladding Temperature (°F)	1088	1036
Maximum local cladding oxidation (%)	0.2	0.2
Maximum core wide cladding oxidation (%)	less than 0.2	less than 0.2

Table 5.4.2-1 Sequence of Events for 7.5-inch Break (Top)
(Loop Noding Sensitivity Study)

Event	Time (sec)	
	Base case	Sensitivity case
Break occurs; blowdown initiation	0.0	0.0
Reactor trip (loss-of-offsite power is assumed)	9.3	9.4
Control rod insertion starts	11.1	11.2
Main steam isolation	11.1	11.2
ECCS actuation signal	11.9	12.0
RCP trip	12.3	12.4
Main feedwater isolation	17.3	17.4
Main steam safety valve open	81	72
Emergency Power Source initiates	115	115
Fuel cladding starts heating up	122	126
High Head Injection System begins	130	130
Peak Cladding Temperature occurs	136	lower than the initial temperature
Fuel cladding rewets	143	131
Emergency feedwater flow begins	145	145
Accumulator injection begins	315	309

Table 5.4.2-2 Core Performance Results for 7.5-inch Break (Top)
(Loop Noding Sensitivity Study)

	Values	
	Base case	Sensitivity case
Peak Cladding Temperature (°F)	775	lower than the initial temperature
Maximum local cladding oxidation (%)	0.2	0.2
Maximum core wide cladding oxidation (%)	less than 0.2	less than 0.2

Table 5.4.3-1 Sequence of Events for 7.5-inch Break (Top)
(Noding near the DVI Injection Point Sensitivity Study)

Event	Time (sec)	
	Base case	Sensitivity case
Break occurs; blowdown initiation	0.0	0.0
Reactor trip (loss-of-offsite power is assumed)	9.3	9.3
Control rod insertion starts	11.1	11.1
Main steam isolation	11.1	11.1
ECCS actuation signal	11.9	11.9
RCP trip	12.3	12.3
Main feedwater isolation	17.3	17.3
Main steam safety valve open	81	81
Emergency Power Source initiates	115	115
Fuel cladding starts heating up	122	123
High Head Injection System begins	130	130
Peak Cladding Temperature occurs	136	134
Fuel cladding rewets	143	138
Emergency feedwater flow begins	145	145
Accumulator injection begins	315	314

Table 5.4.3-2 Core Performance Results for 7.5-inch Break (Top)
(Noding near the DVI Injection Point Sensitivity Study)

	Values	
	Base case	Sensitivity case
Peak Cladding Temperature (°F)	775	759
Maximum local cladding oxidation (%)	0.2	0.2
Maximum core wide cladding oxidation (%)	less than 0.2	less than 0.2

Table 5.4.3-3 Sequence of Events for 1-ft^2 Break (Top)
(Noding near the DVI Injection Point Sensitivity Study)

Event	Time (sec)	
	Base case	Sensitivity case
Break occurs; blowdown initiation	0.0	0.0
Reactor trip (loss-of-offsite power is assumed)	6.9	6.9
ECCS actuation signal	8.3	8.3
Control rod insertion starts	8.7	8.7
Main steam isolation	8.7	8.7
RCP trip	9.9	9.9
Main feedwater isolation	14.9	14.9
Main steam safety valve open	not actuated	not actuated
Accumulator injection begins	89	89
Fuel cladding starts heating up	95	95
Emergency Power Source initiates	111	111
High Head Injection System begins	126	126
Peak Cladding Temperature occurs	151	156
Emergency feedwater flow begins	141	141
Fuel cladding rewets	169	174

Table 5.4.3-4 Core Performance Results for 1-ft^2 Break (Top)
(Noding near the DVI Injection Point Sensitivity Study)

	Values	
	Base case	Sensitivity case
Peak Cladding Temperature (°F)	1088	1068
Maximum local cladding oxidation (%)	0.2	0.2
Maximum core wide cladding oxidation (%)	less than 0.2	less than 0.2

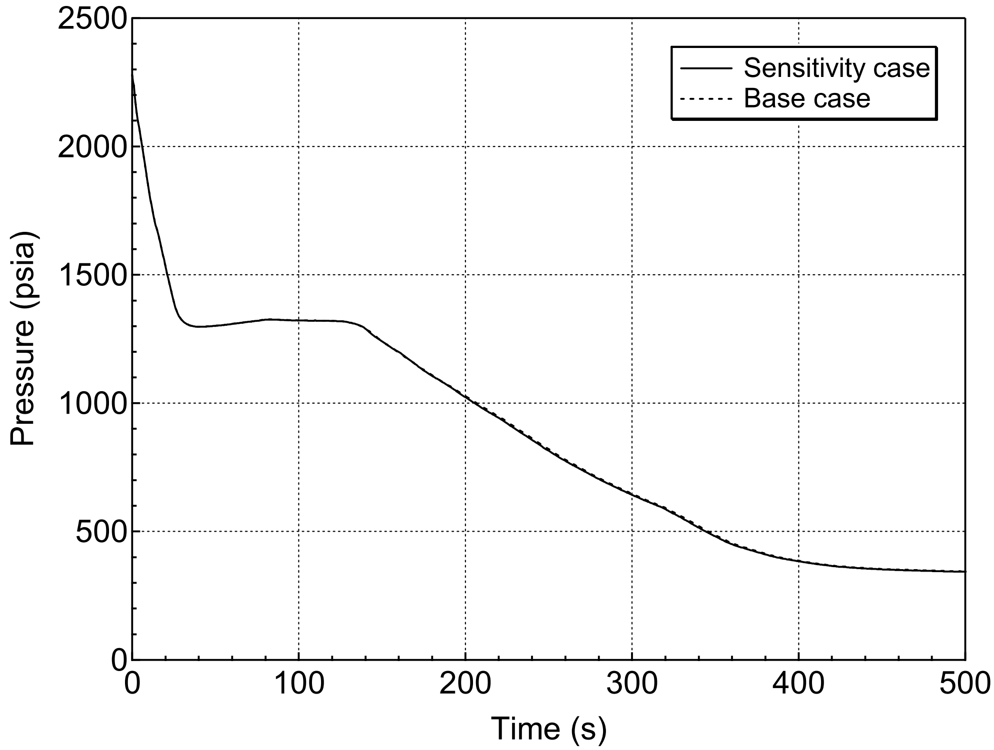

Figure 5.4.1-1 RCS (Pressurizer) Pressure Transient for 7.5-inch Break (Top) (Noding near Break Point Sensitivity Study)

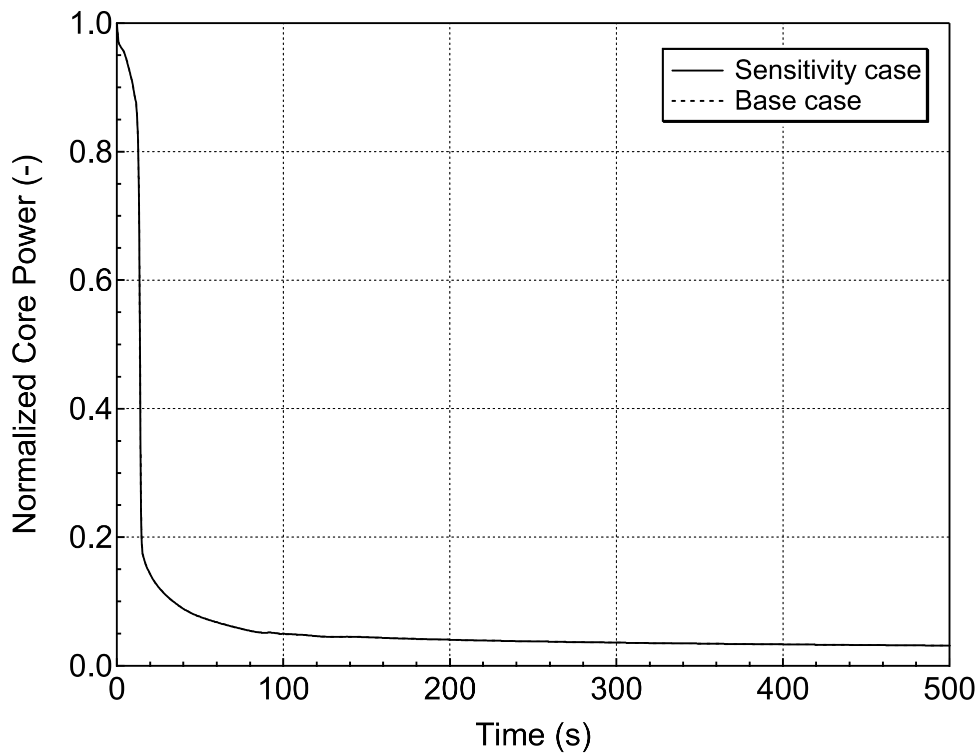

Figure 5.4.1-2 Normalized Core Power for 7.5-inch Break (Top)
(Noding near Break Point Sensitivity Study)

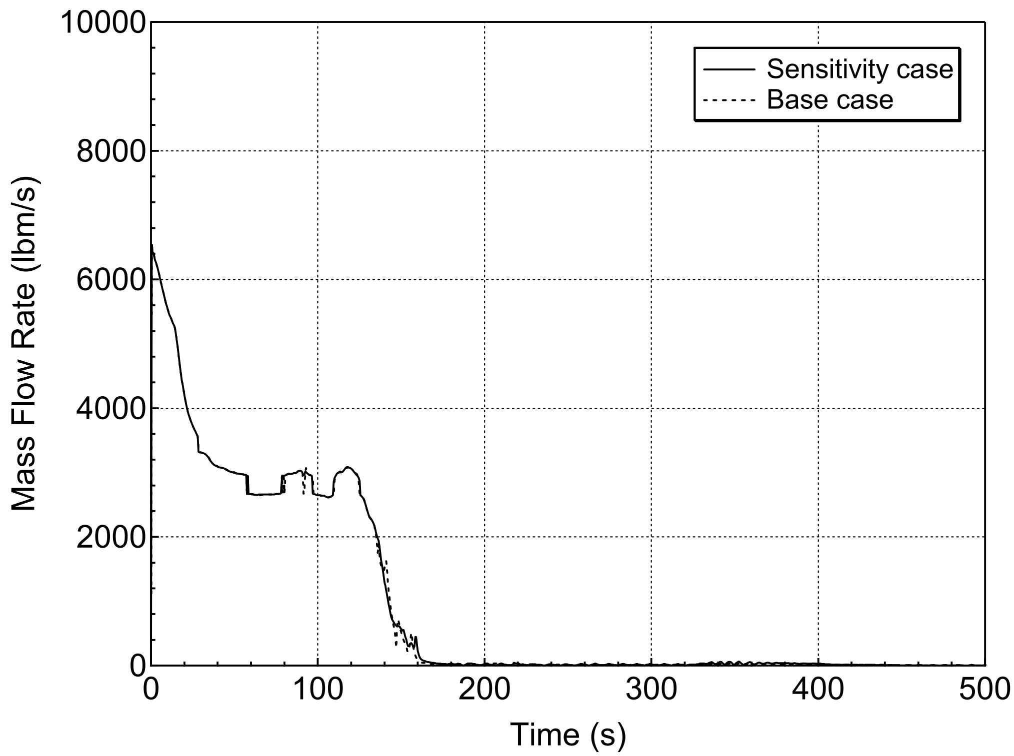

Figure 5.4.1-3 Liquid Discharge through the Break for 7.5-inch Break (Top) (Noding near Break Point Sensitivity Study)

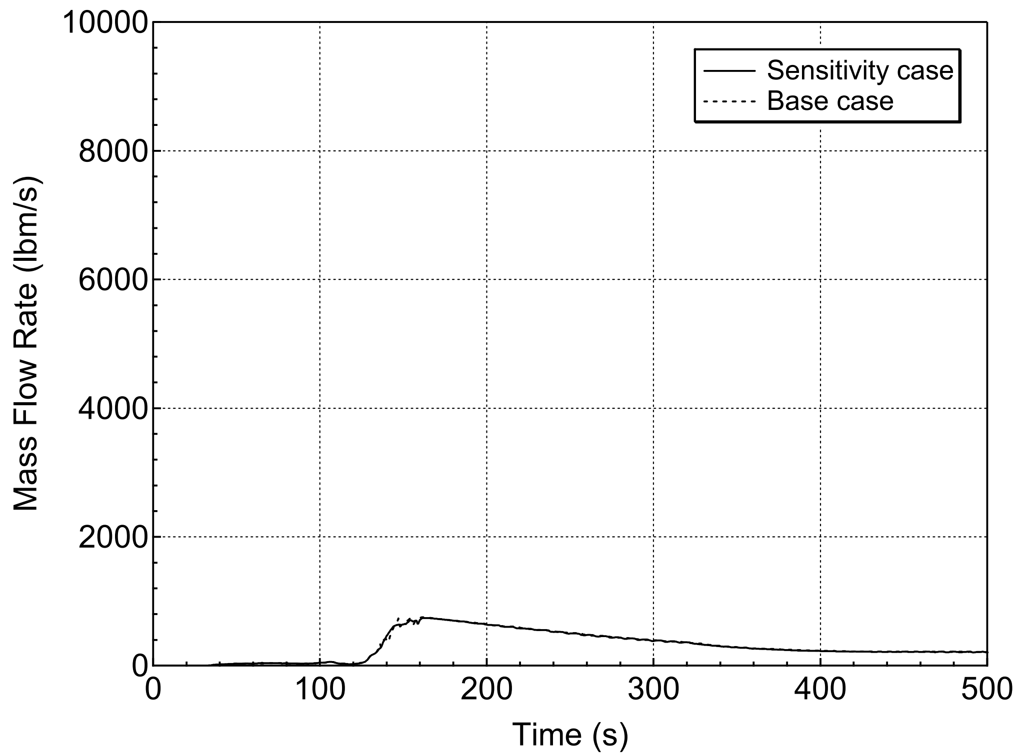

Figure 5.4.1-4 Vapor Discharge through the Break for 7.5-inch Break (Top) (Noding near Break Point Sensitivity Study)

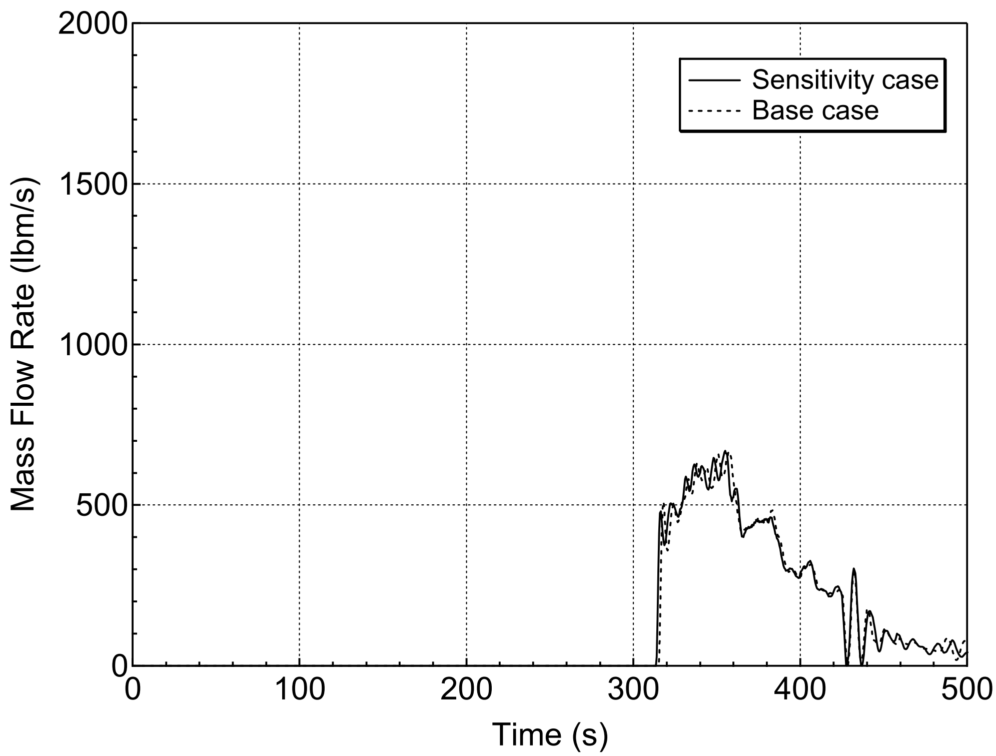

Figure 5.4.1-5 Accumulator Injection Mass Flowrate for 7.5-inch Break (Top) (Noding near Break Point Sensitivity Study)

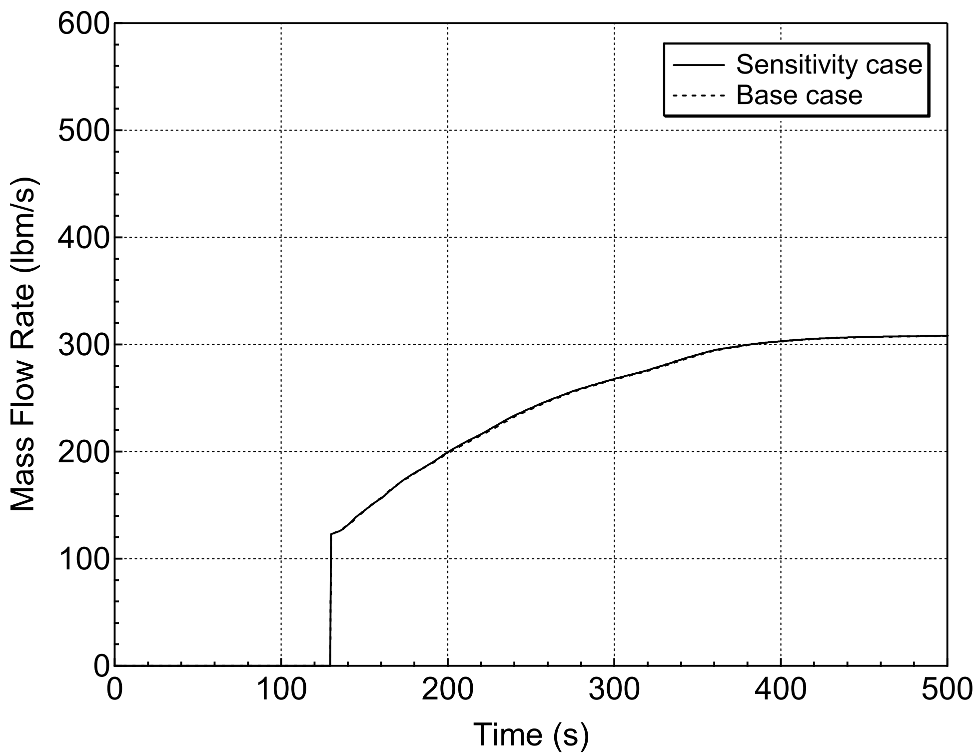

Figure 5.4.1-6 Safety Injection Mass Flowrate for 7.5-inch Break (Top) (Noding near Break Point Sensitivity Study)

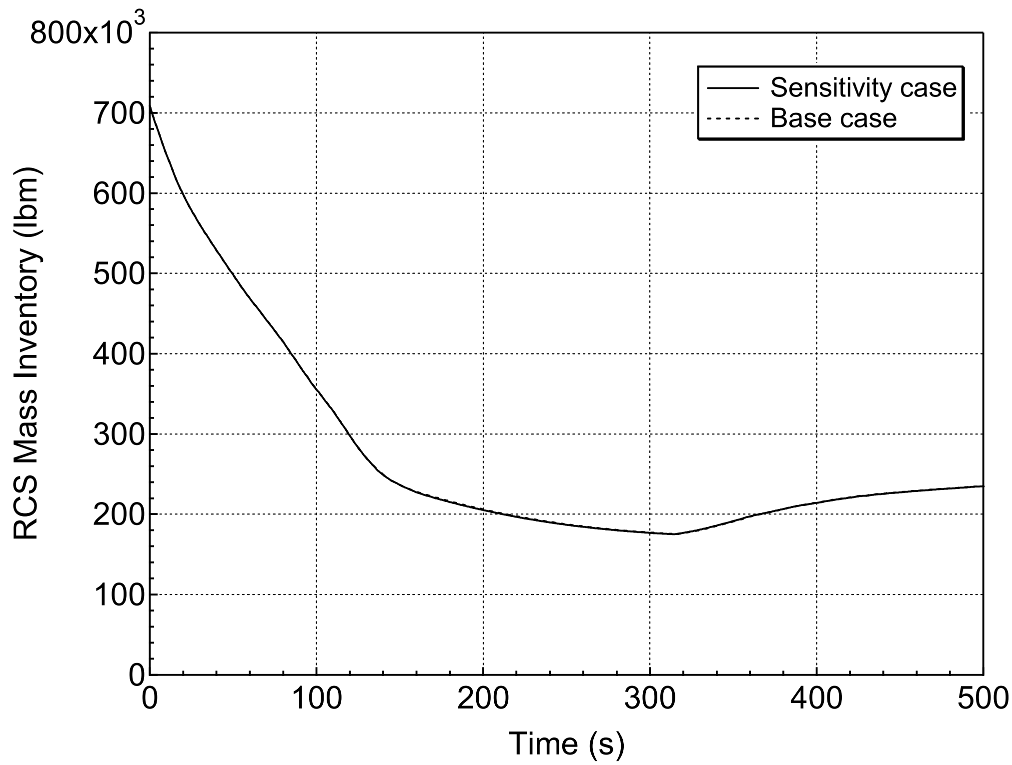

Figure 5.4.1-7 RCS Mass Inventory for 7.5-inch Break (Top)
(Noding near Break Point Sensitivity Study)

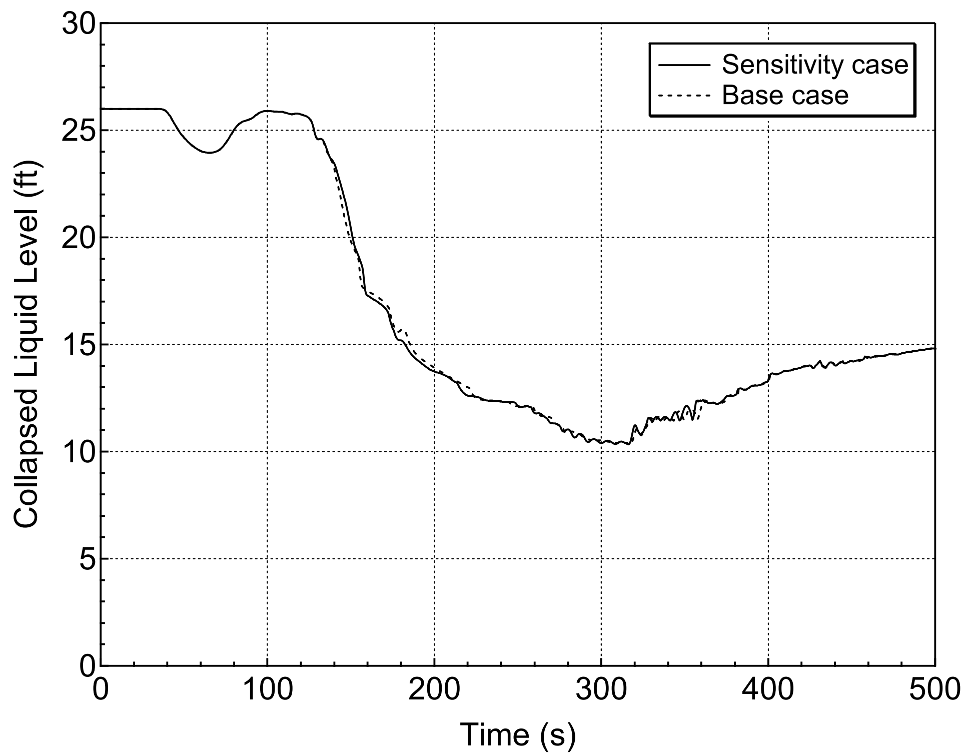

Figure 5.4.1-8 Downcomer Collapsed Level for 7.5-inch Break (Top) (Noding near Break Point Sensitivity Study)

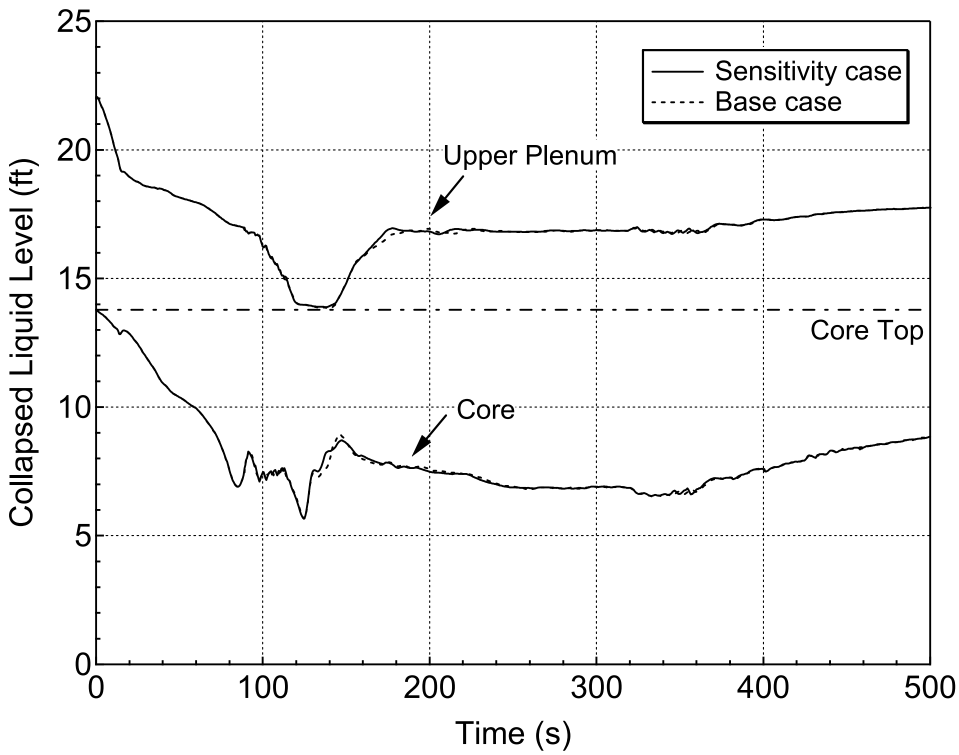

Figure 5.4.1-9 Average Core and Upper Plenum Collapsed Levels for 7.5-inch Break (Top) (Noding near Break Point Sensitivity Study)

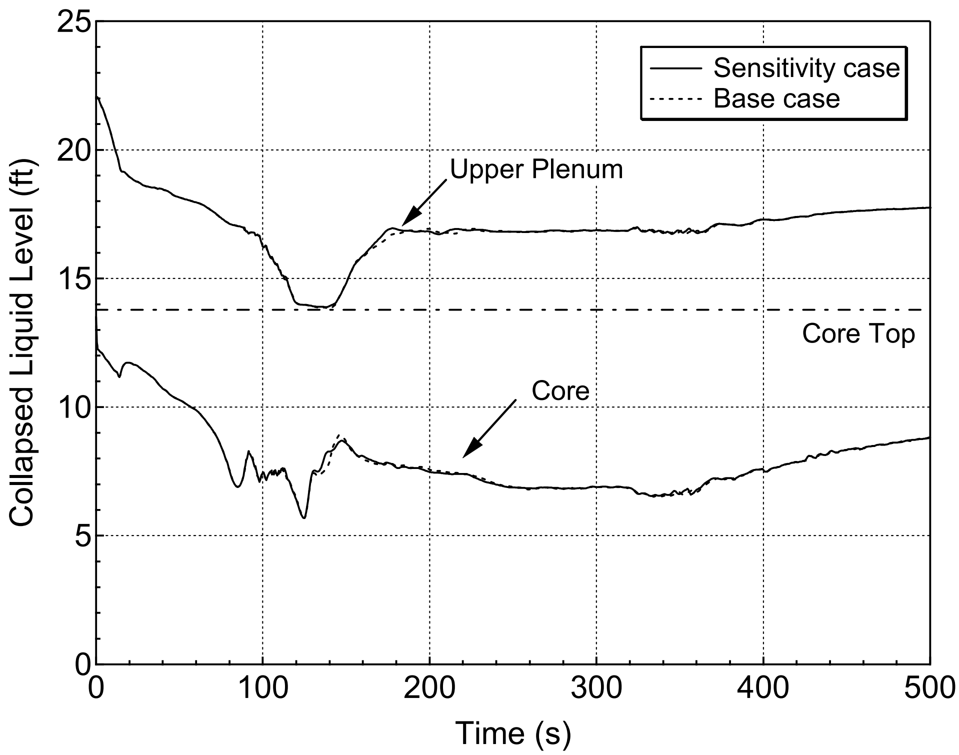

Figure 5.4.1-10 Hot Assembly Core and Upper Plenum Collapsed Levels for 7.5-inch Break (Top) (Noding near Break Point Sensitivity Study)

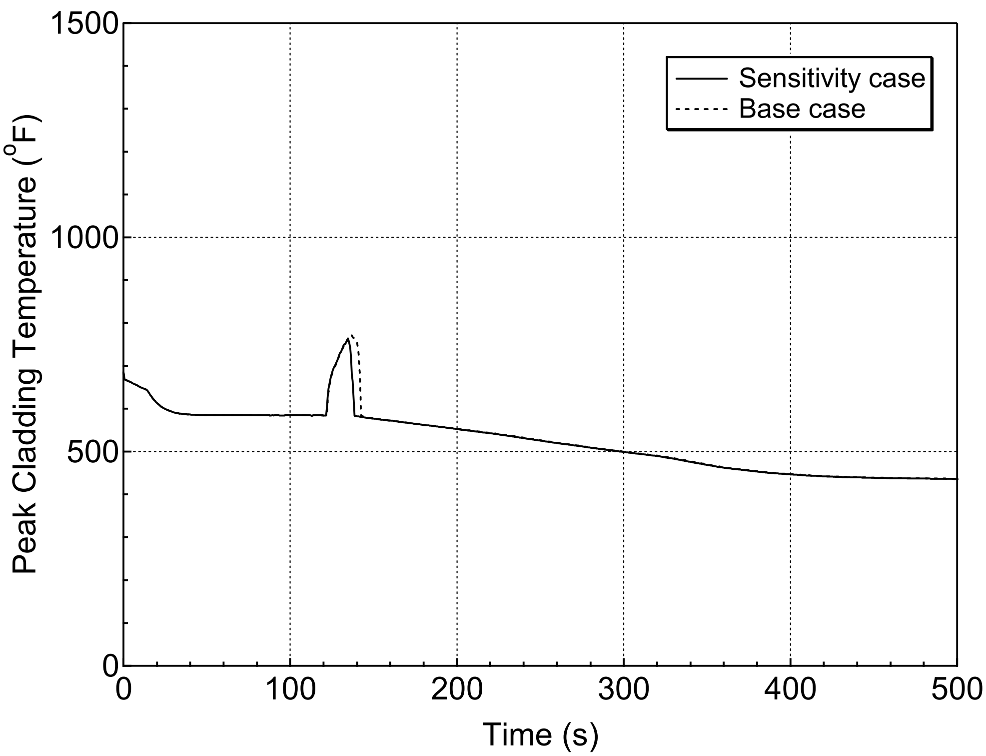

Figure 5.4.1-11 PCT at All Elevations for Hot Rod in Hot Assembly for 7.5-inch Break (Top) (Noding near Break Point Sensitivity Study)

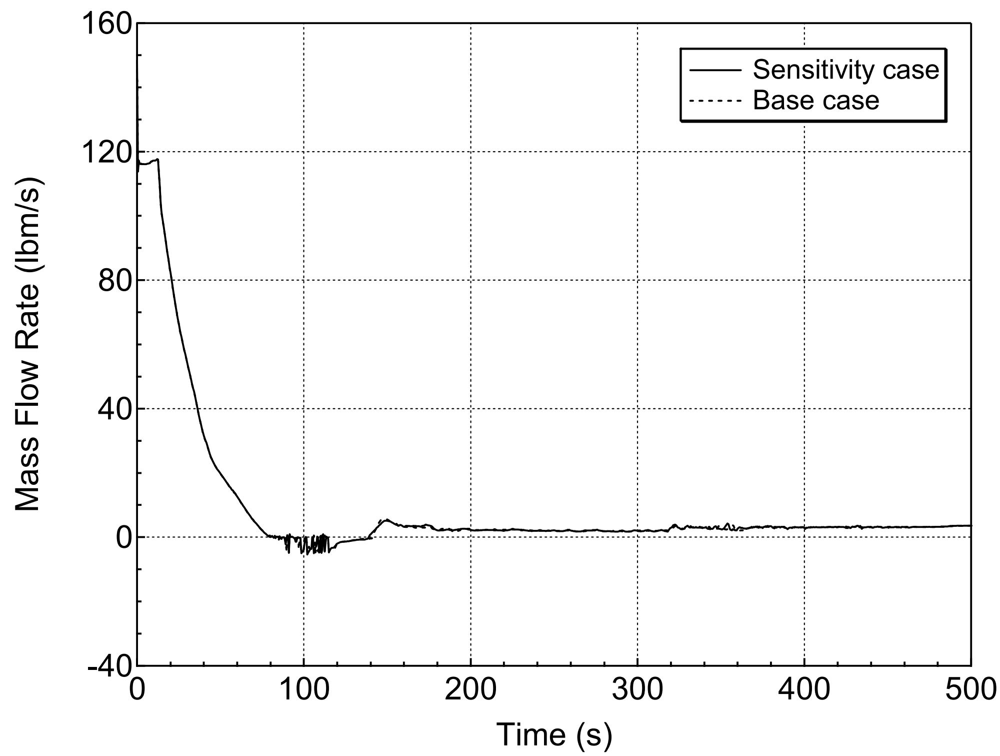

Figure 5.4.1-12 Hot Assembly Exit Liquid Mass Flowrate for 7.5-inch Break (Top) (Noding near Break Point Sensitivity Study)

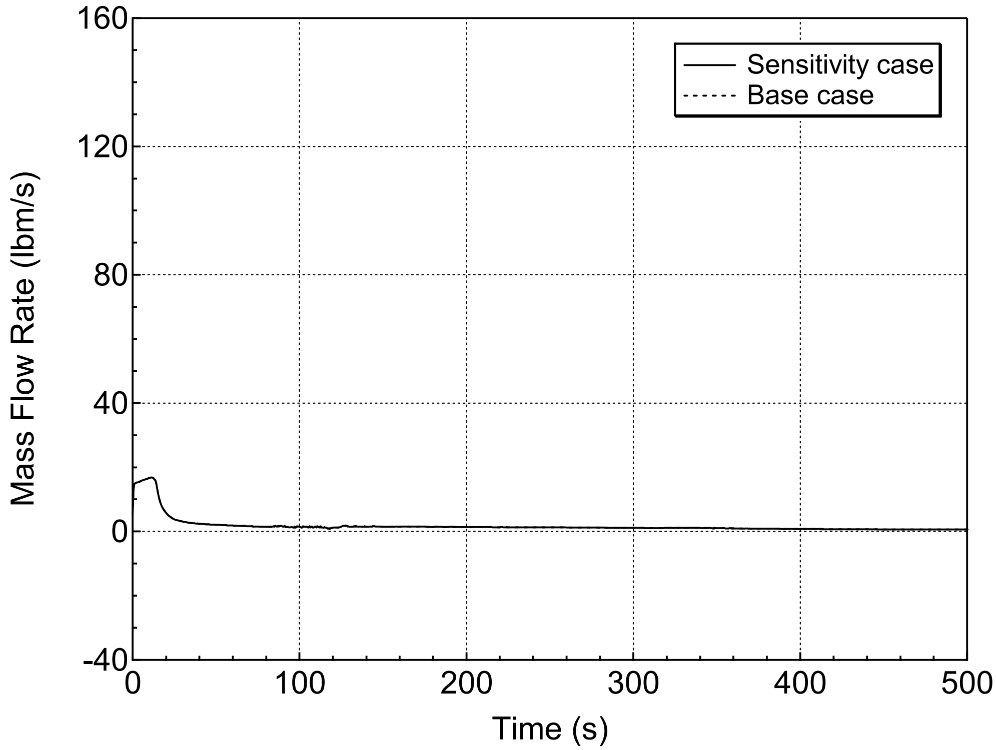

Figure 5.4.1-13 Hot Assembly Exit Vapor Mass Flowrate for 7.5-inch Break (Top) (Noding near Break Point Sensitivity Study)

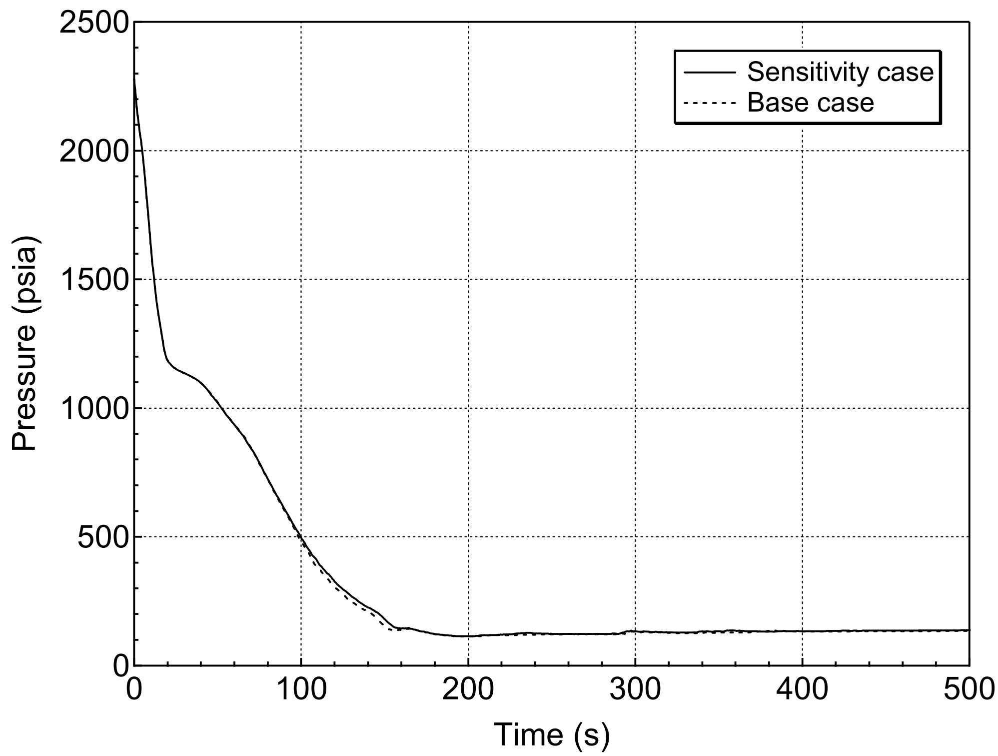

Figure 5.4.1-14 RCS (Pressurizer) Pressure Transient for 1-ft^2 Break (Top) (Noding near Break Point Sensitivity Study)

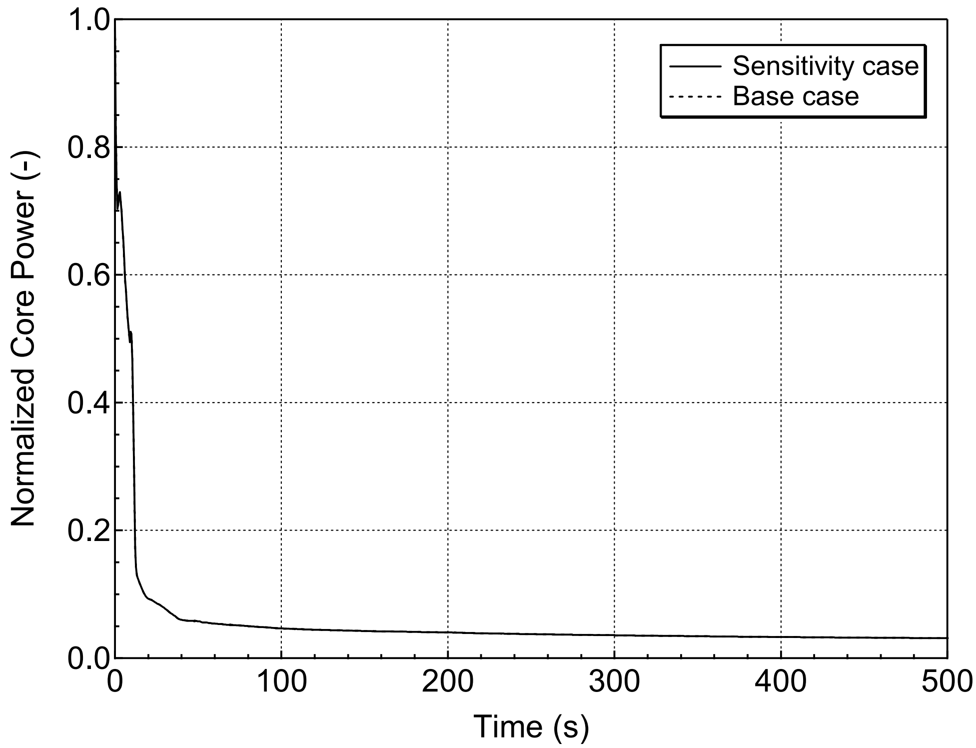

Figure 5.4.1-15 Normalized Core Power for 1-ft^2 Break (Top)
(Noding near Break Point Sensitivity Study)

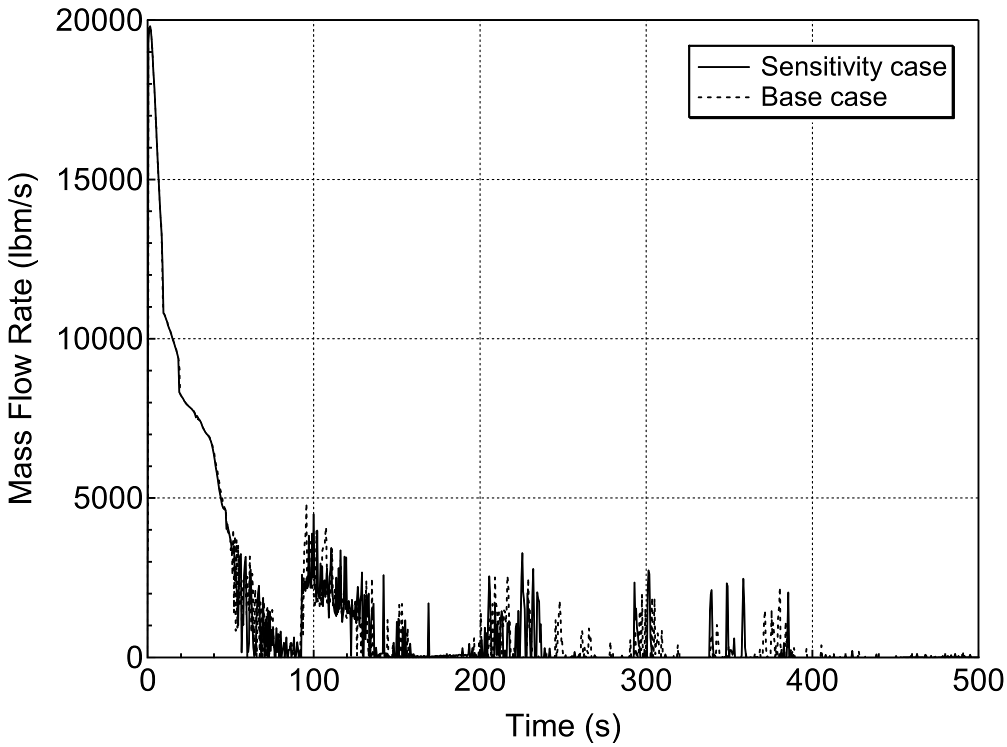

Figure 5.4.1-16 Liquid Discharge through the Break for 1-ft^2 Break (Top) (Noding near Break Point Sensitivity Study)

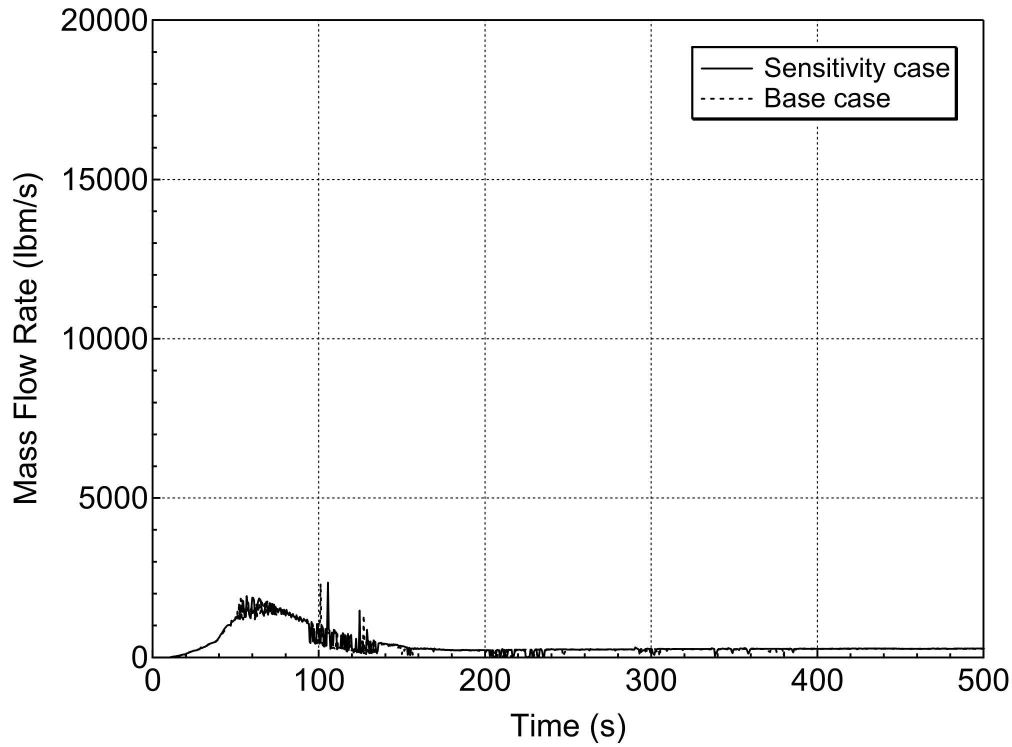

Figure 5.4.1-17 Vapor Discharge through the Break for 1-ft^2 Break (Top) (Noding near Break Point Sensitivity Study)

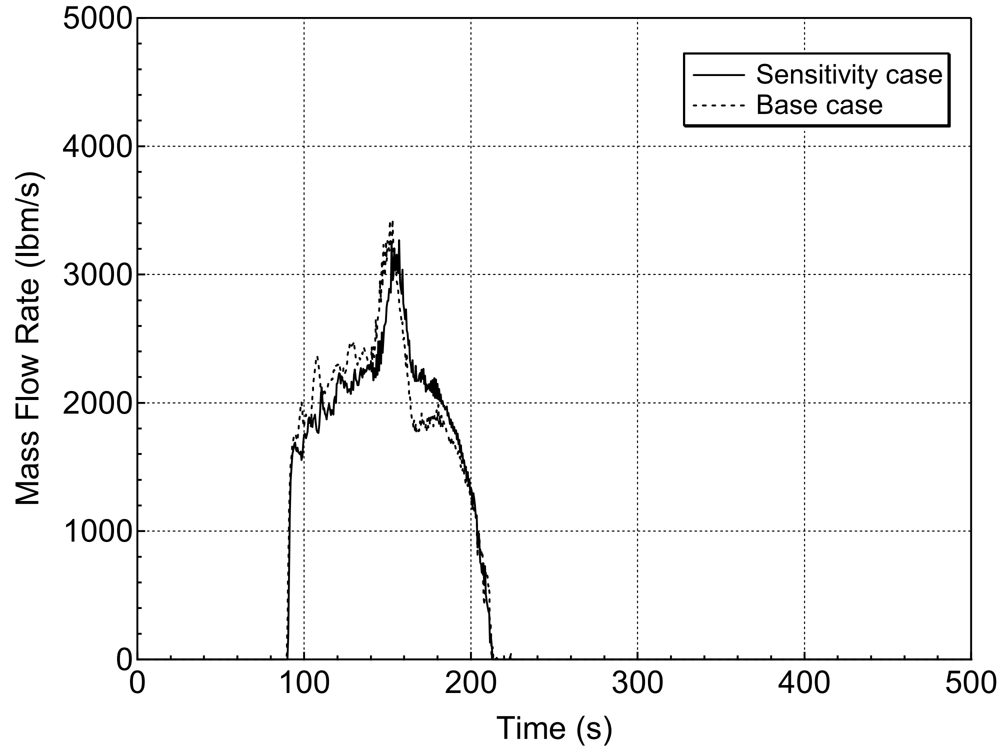

Figure 5.4.1-18 Accumulator Injection Mass Flowrate for 1-ft^2 Break (Top) (Noding near Break Point Sensitivity Study)

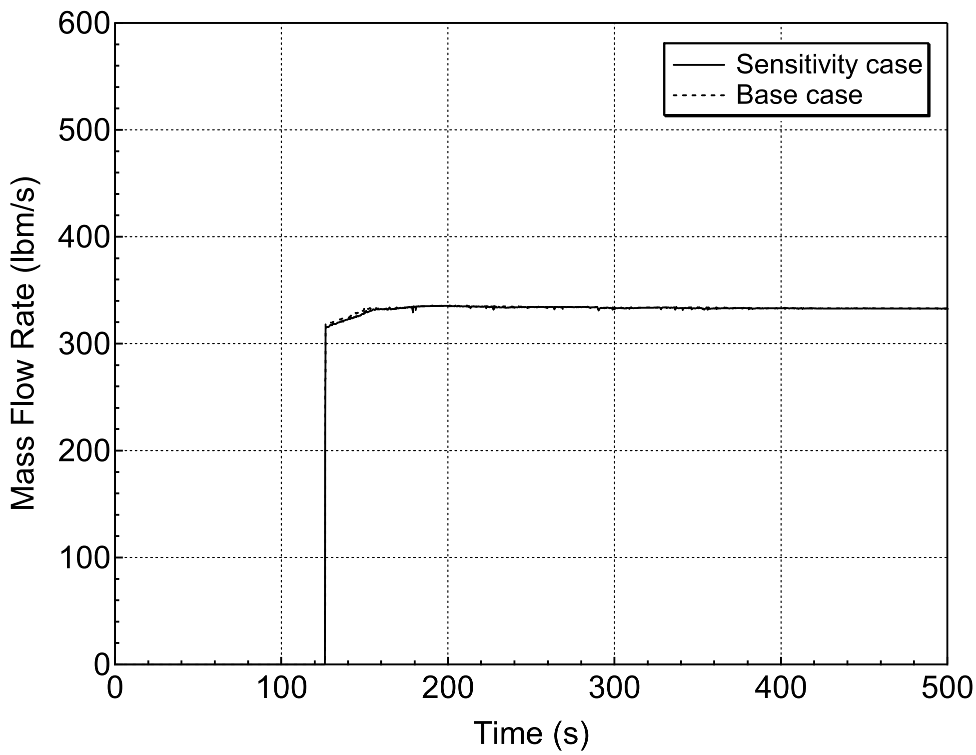

Figure 5.4.1-19 Safety Injection Mass Flowrate for 1-ft^2 Break (Top) (Noding near Break Point Sensitivity Study)

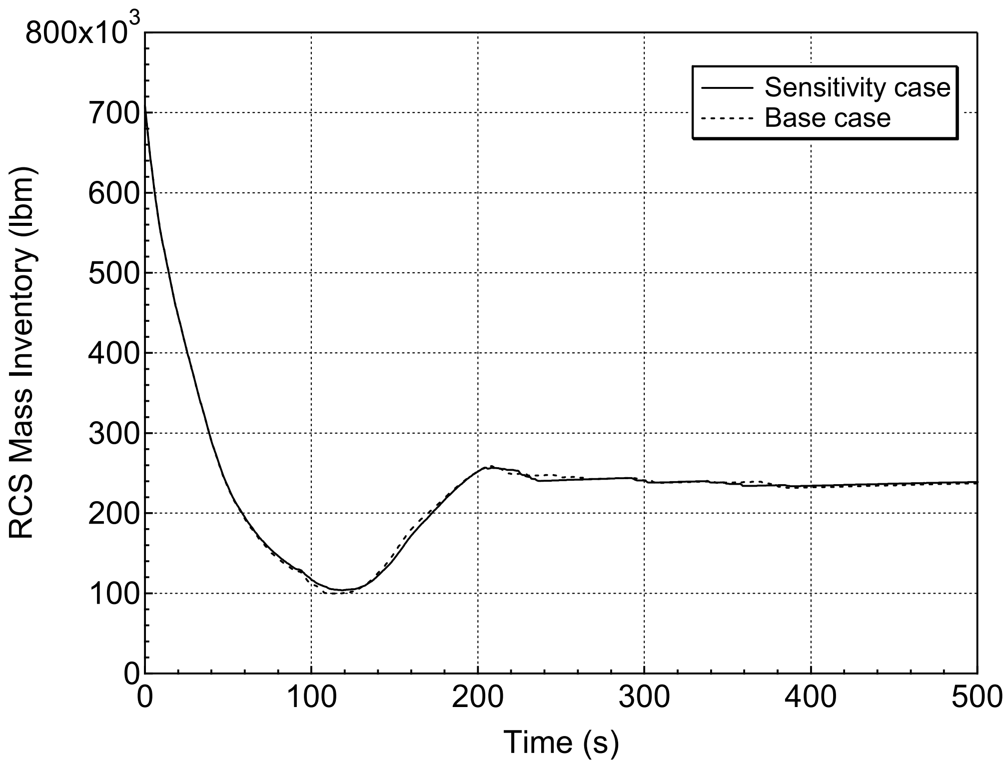

Figure 5.4.1-20 RCS Mass Inventory for 1-ft^2 Break (Top)
(Noding near Break Point Sensitivity Study)

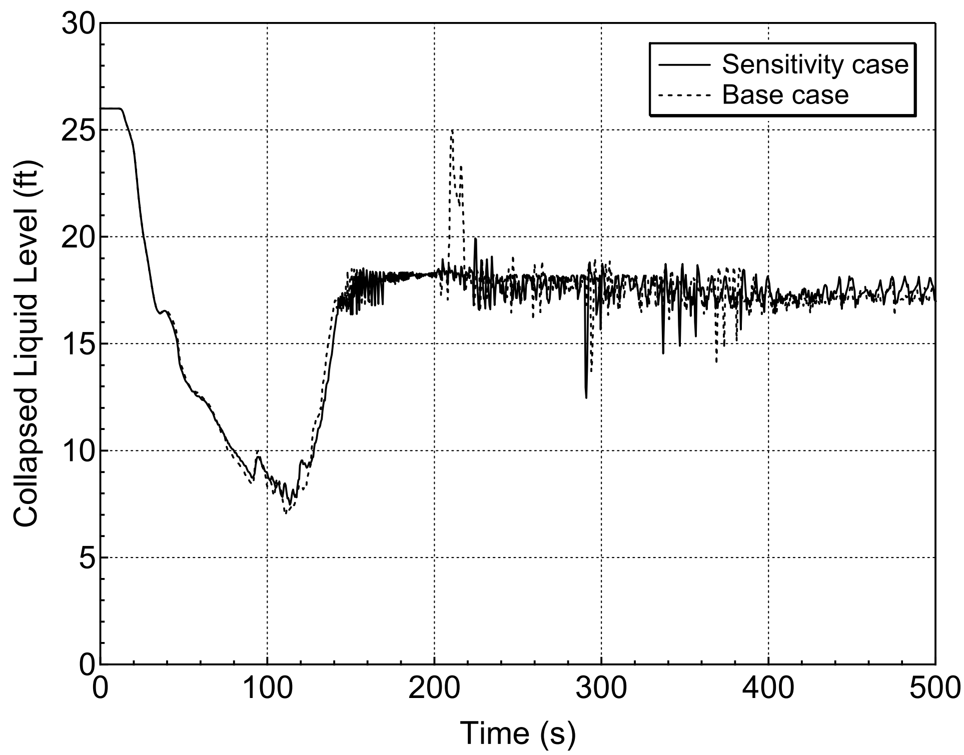

Figure 5.4.1-21 Downcomer Collapsed Level for 1-ft^2 Break (Top) (Noding near Break Point Sensitivity Study)

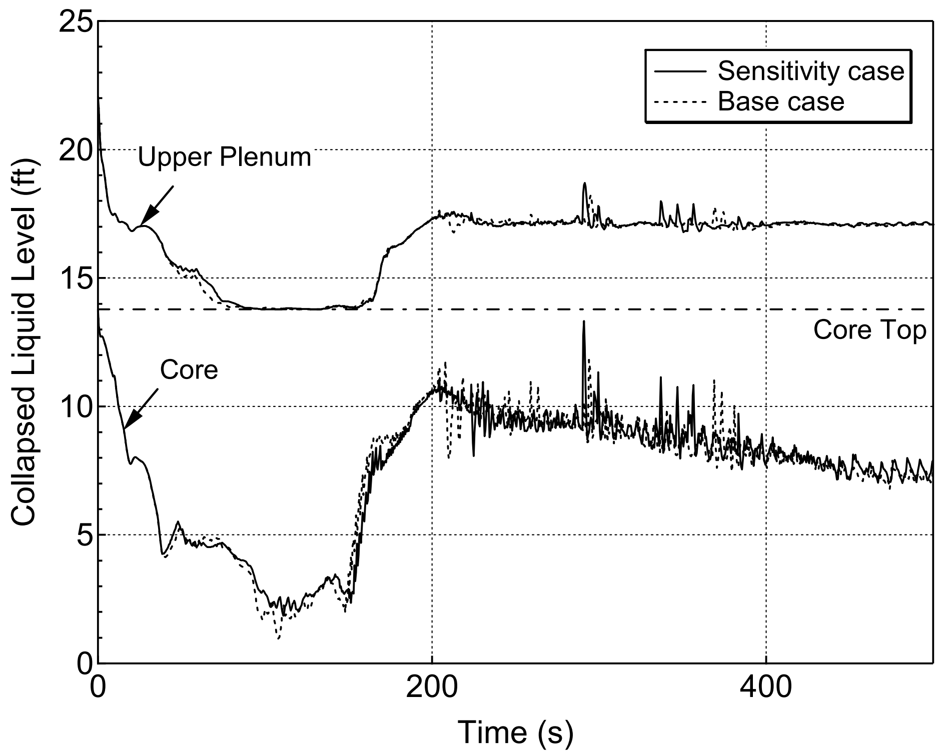

Figure 5.4.1-22 Average Core and Upper Plenum Collapsed Levels for 1-ft^2 Break (Top) (Noding near Break Point Sensitivity Study)

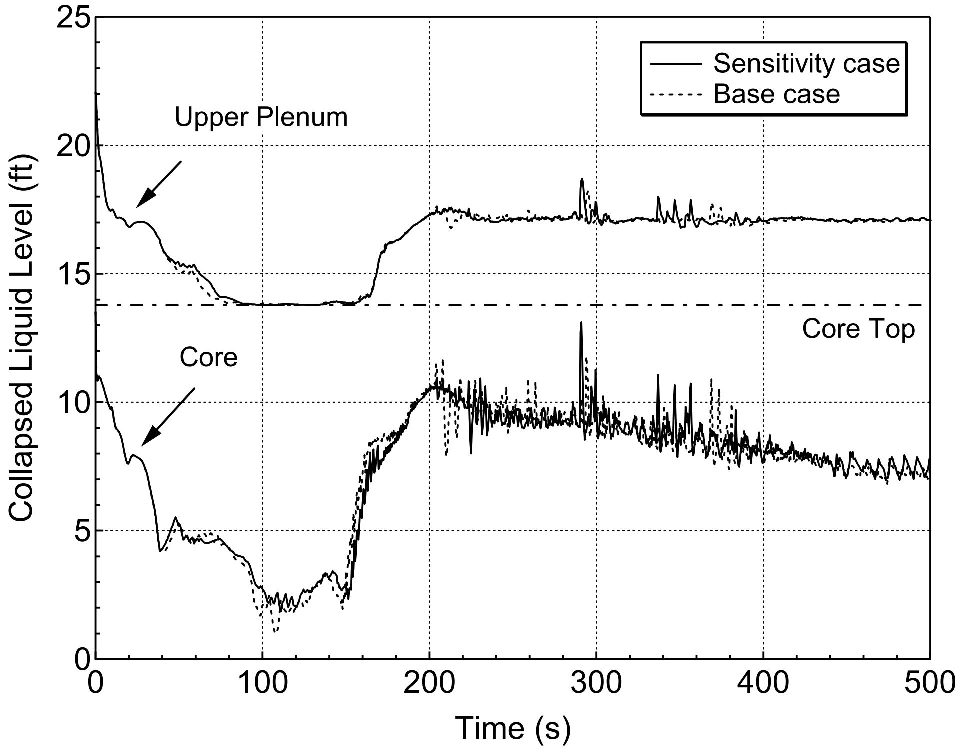

Figure 5.4.1-23 Hot Assembly Core and Upper Plenum Collapsed Levels for 1-ft^2 Break (Top) (Noding near Break Point Sensitivity Study)

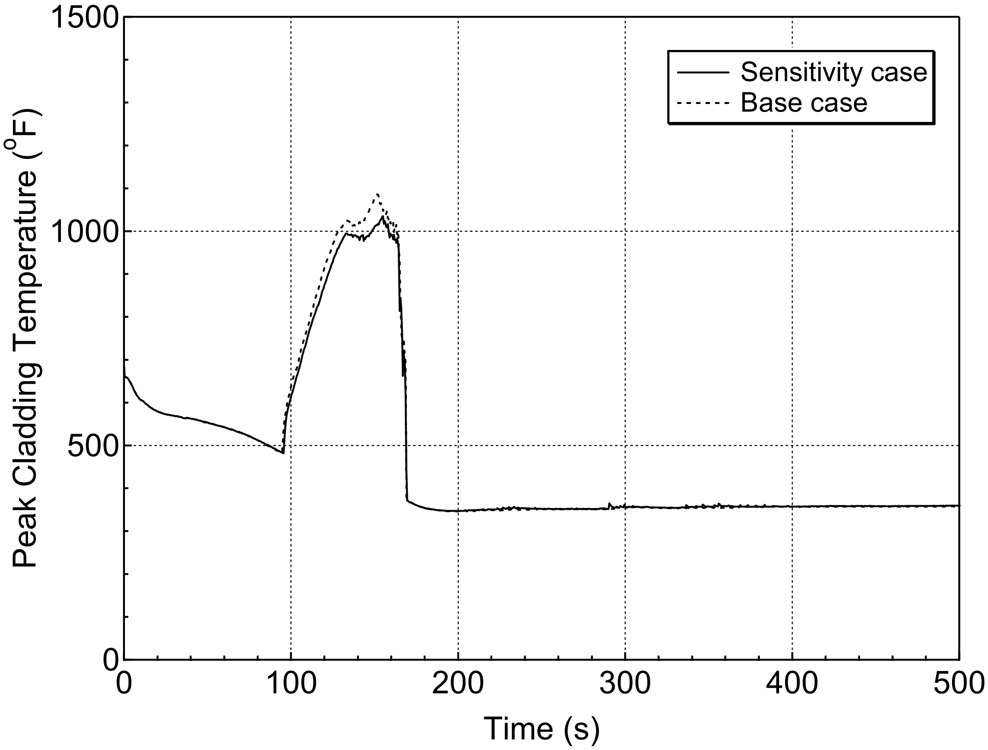

Figure 5.4.1-24 PCT at All Elevations for Hot Rod in Hot Assembly for 1-ft^2 Break (Top) (Noding near Break Point Sensitivity Study)

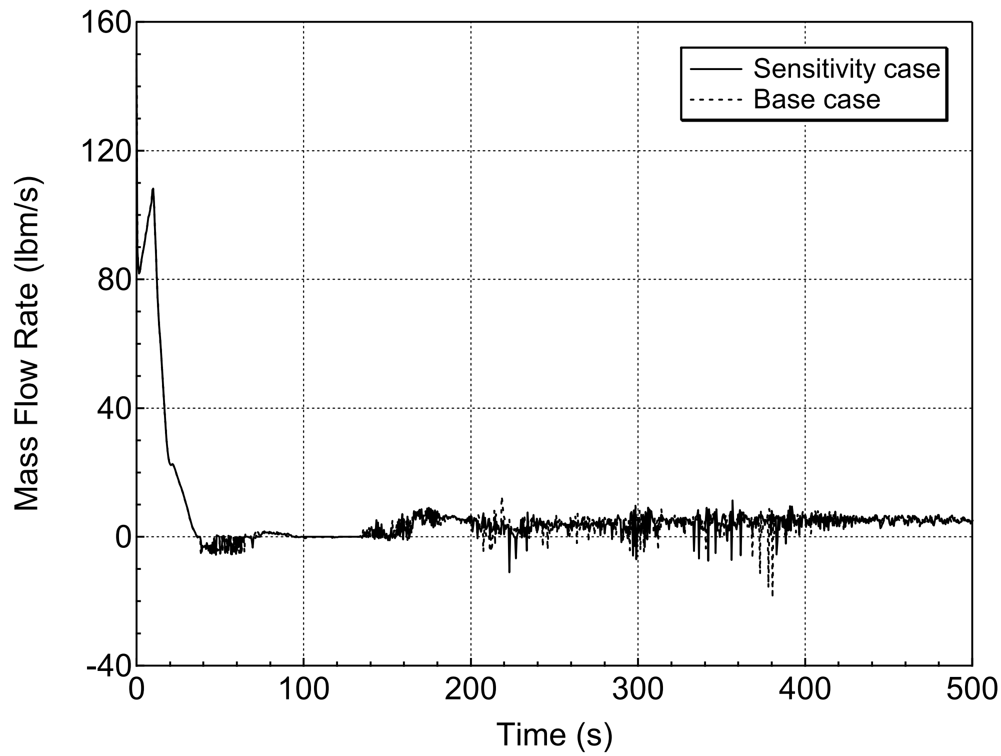

Figure 5.4.1-25 Hot Assembly Exit Liquid Mass Flowrate for 1-ft^2 Break (Top) (Noding near Break Point Sensitivity Study)

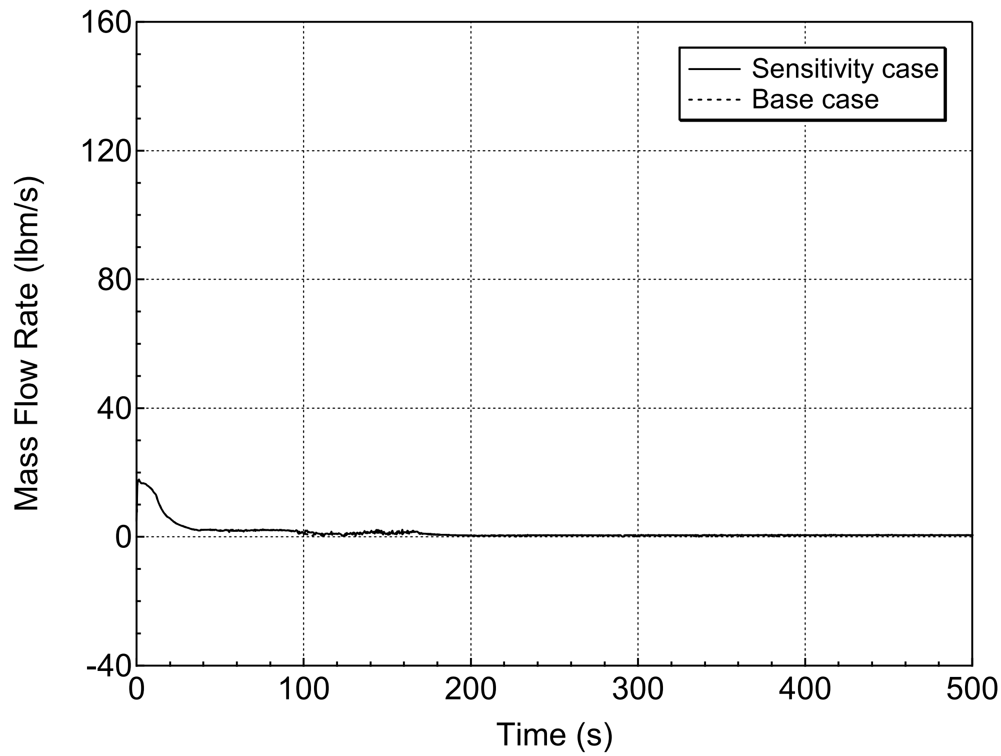

Figure 5.4.1-26 Hot Assembly Exit Vapor Mass Flowrate for 1-ft^2 Break (Top) (Noding near Break Point Sensitivity Study)

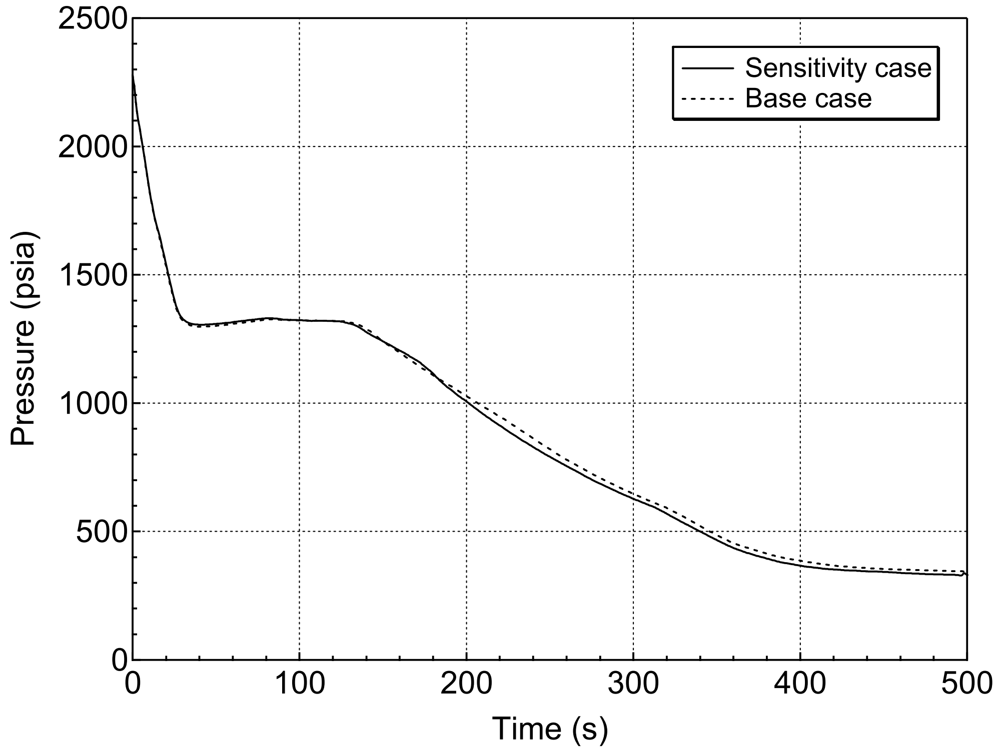

Figure 5.4.2-1 RCS (Pressurizer) Pressure Transient for 7.5-inch Break (Top) (Loop Noding Sensitivity Study)

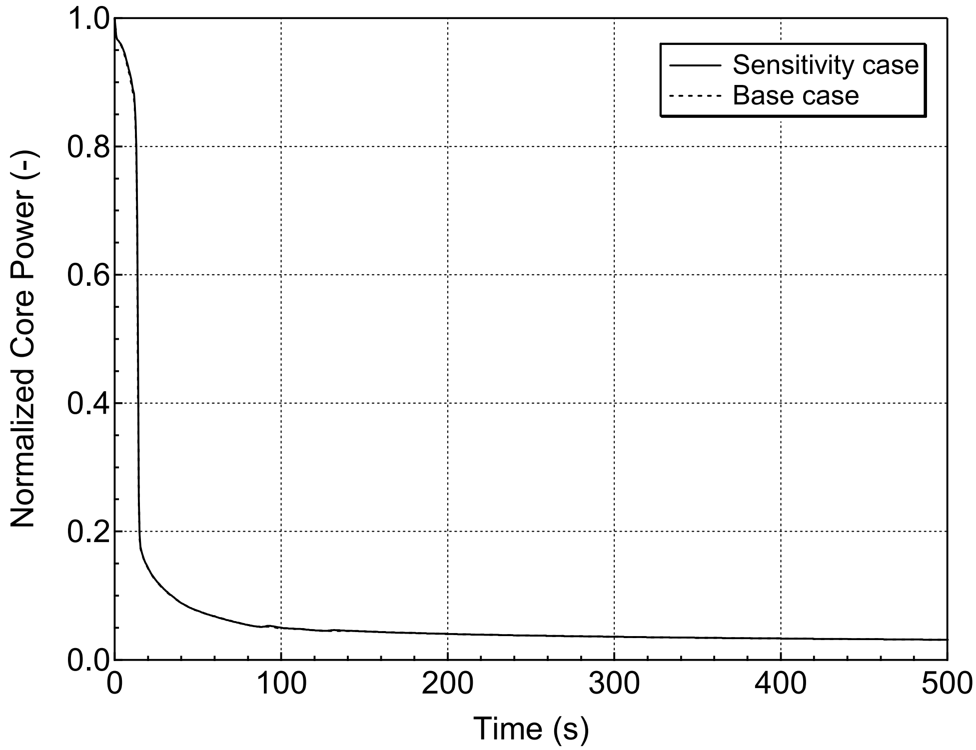

Figure 5.4.2-2 Normalized Core Power for 7.5-inch Break (Top) (Loop Noding Sensitivity Study)

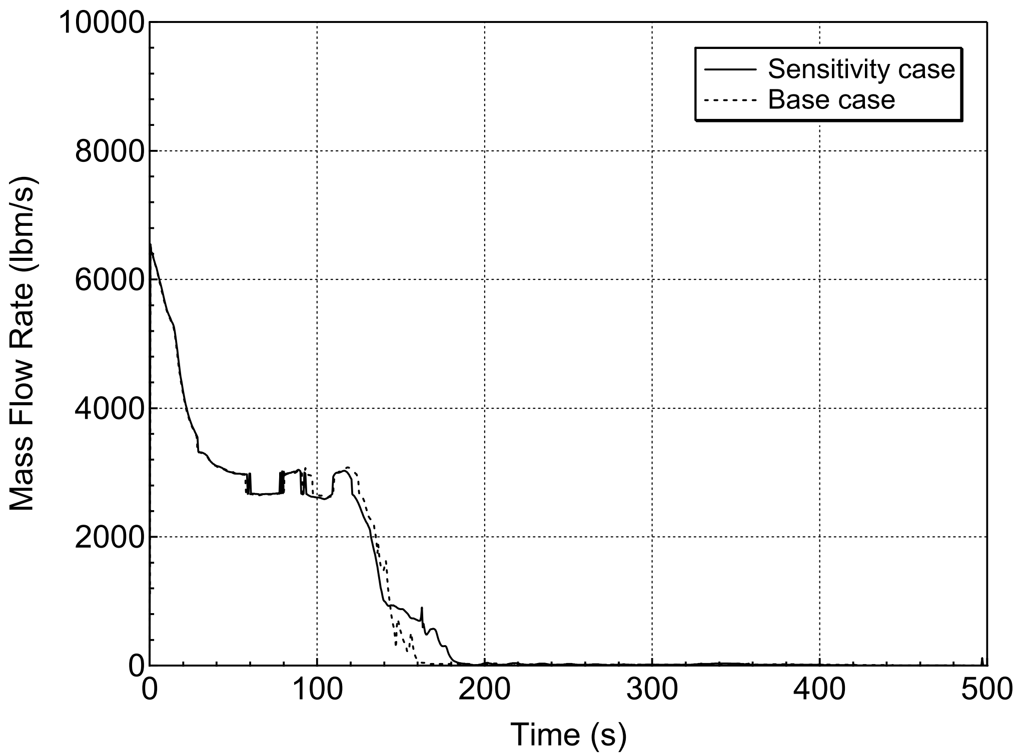

Figure 5.4.2-3 Liquid Discharge through the Break for 7.5-inch Break (Top) (Loop Noding Sensitivity Study)

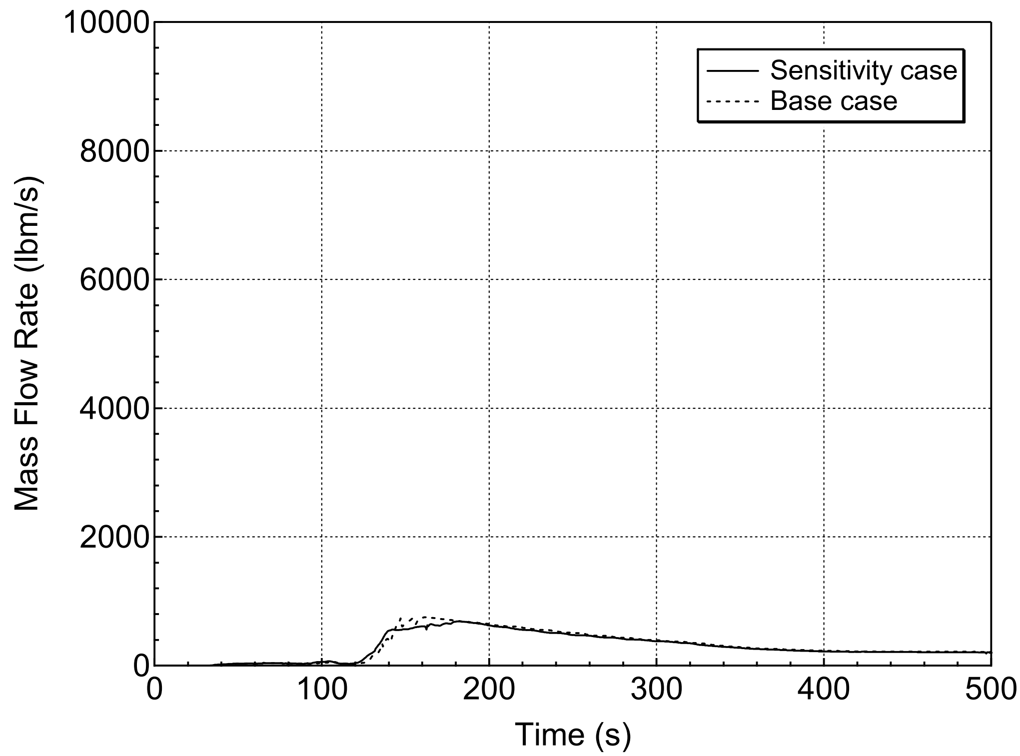

Figure 5.4.2-4 Vapor Discharge through the Break for 7.5-inch Break (Top) (Loop Noding Sensitivity Study)

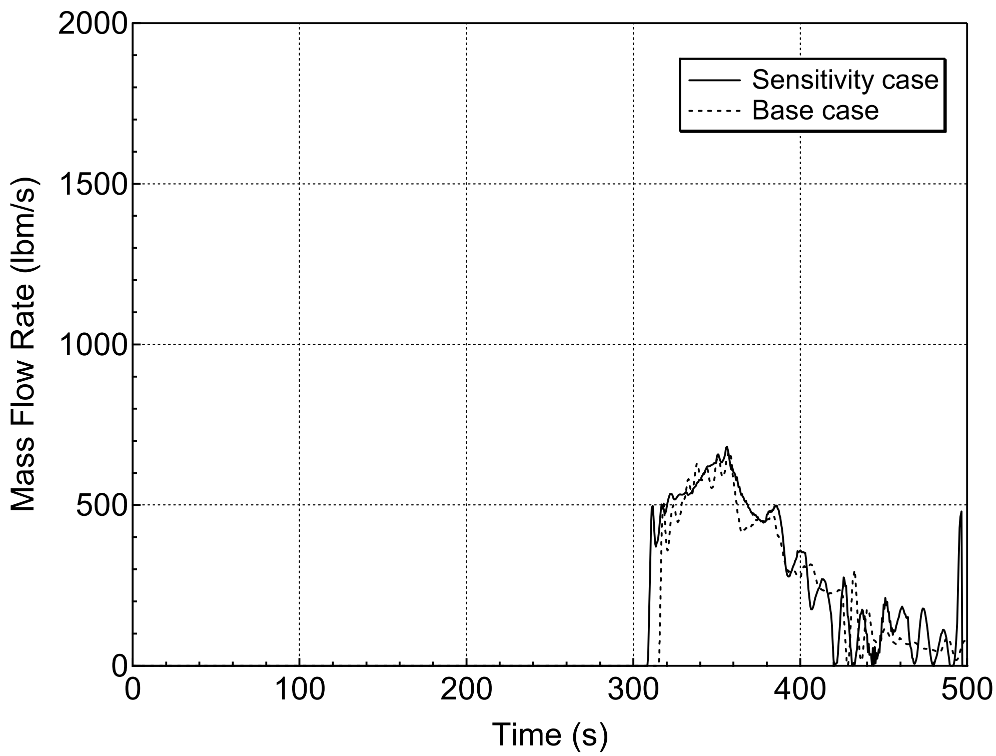

Figure 5.4.2-5 Accumulator Injection Mass Flowrate for 7.5-inch Break (Top) (Loop Noding Sensitivity Study)

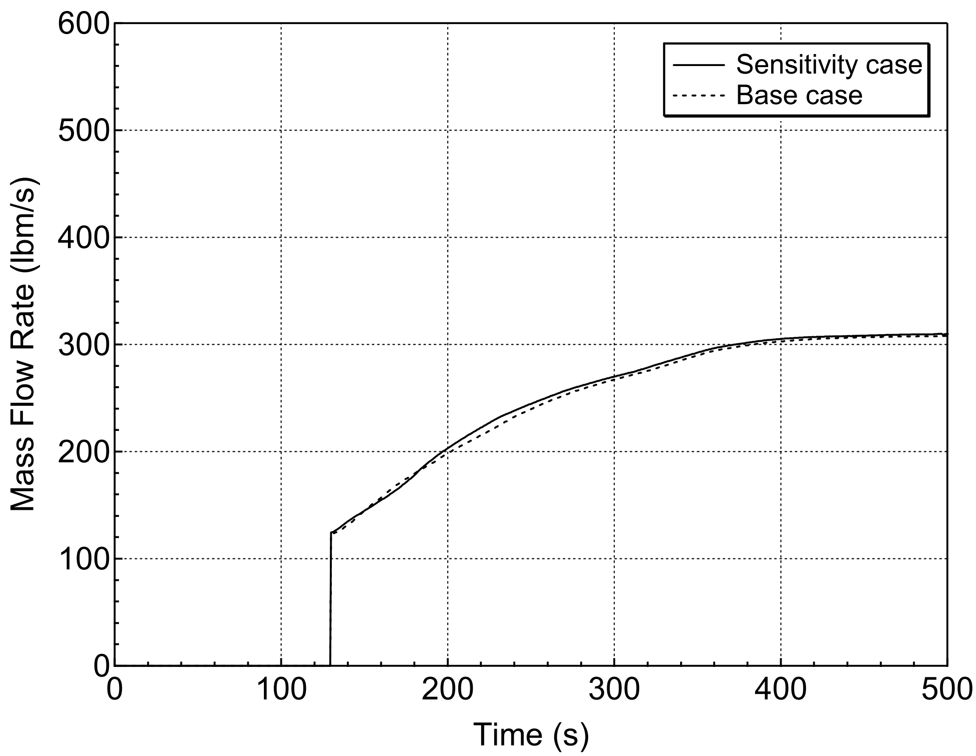

Figure 5.4.2-6 Safety Injection Mass Flowrate for 7.5-inch Break (Top) (Loop Noding Sensitivity Study)

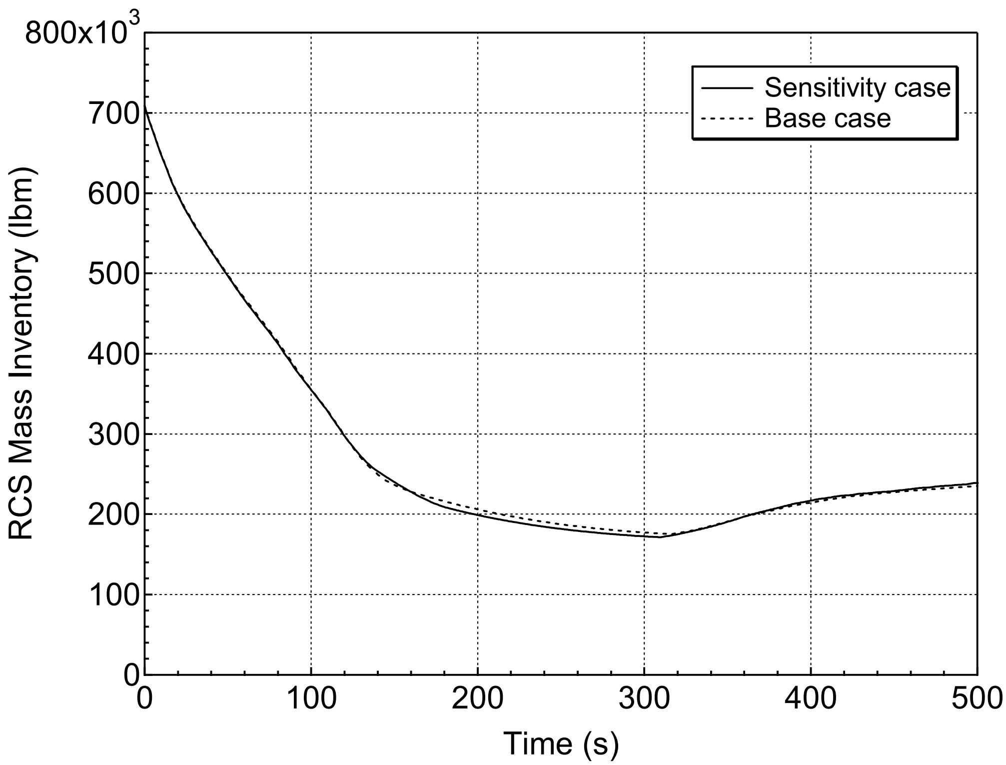

Figure 5.4.2-7 RCS Mass Inventory for 7.5-inch Break (Top)
(Loop Noding Sensitivity Study)

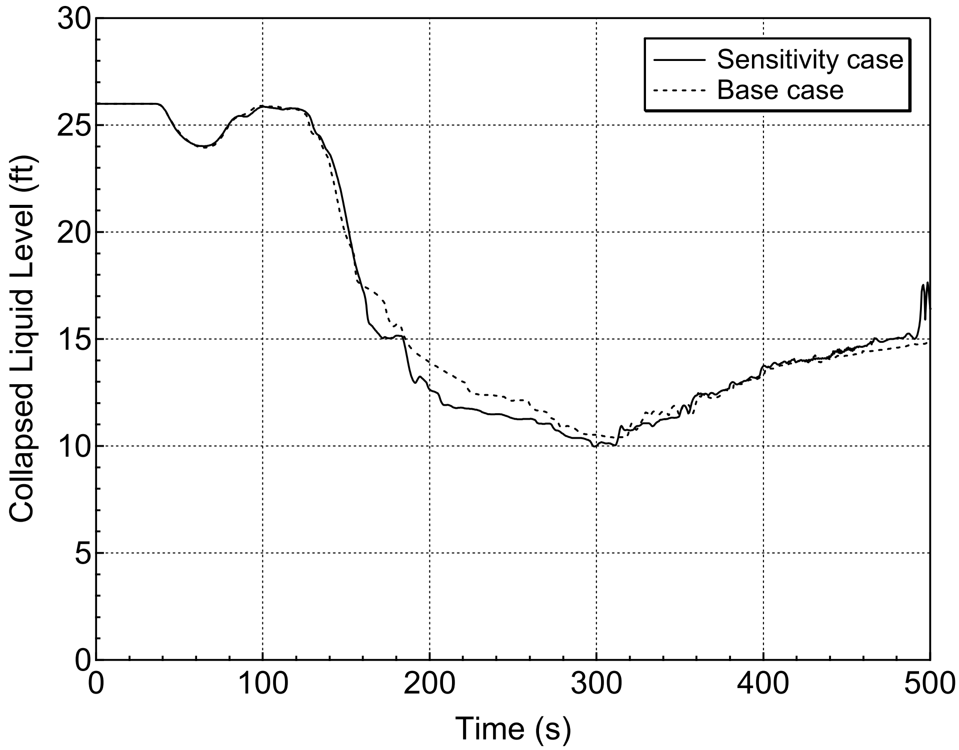

Figure 5.4.2-8 Downcomer Collapsed Level for 7.5-inch Break (Top) (Loop Noding Sensitivity Study)

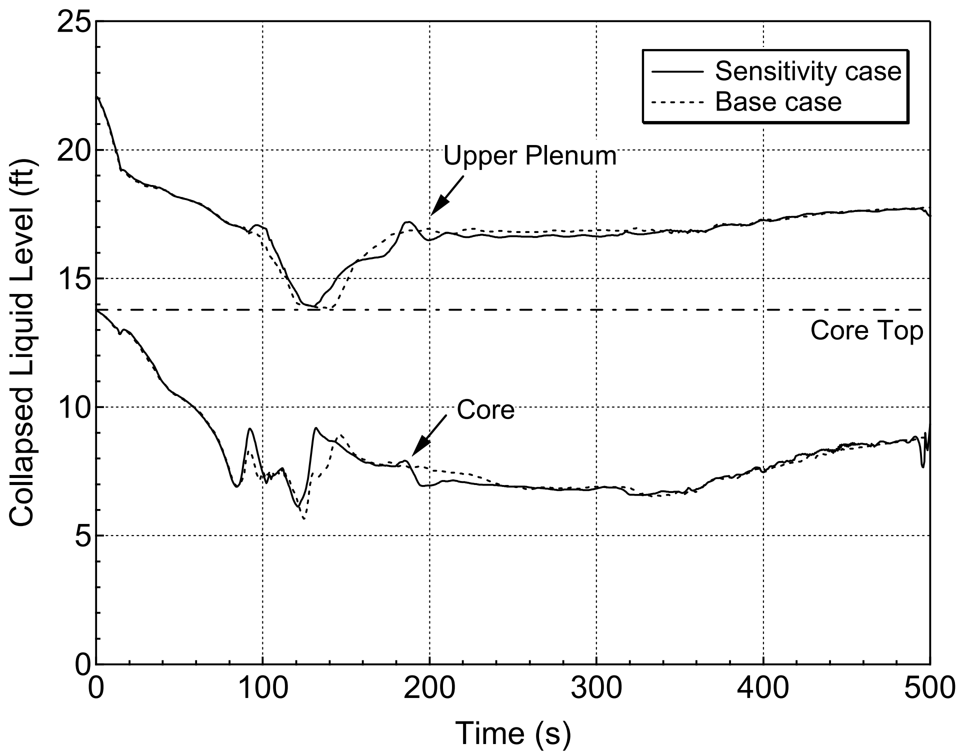

Figure 5.4.2-9 Average Core and Upper Plenum Collapsed Levels for 7.5-inch Break (Top) (Loop Noding Sensitivity Study)

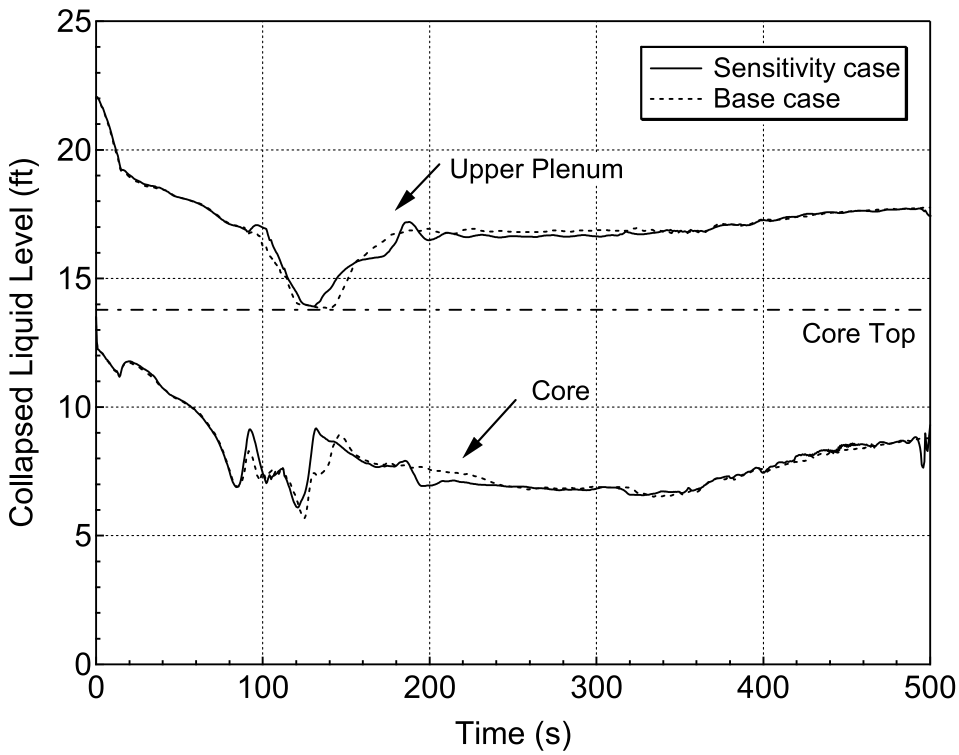

Figure 5.4.2-10 Hot Assembly Core and Upper Plenum Collapsed Levels for 7.5-inch Break (Top) (Loop Noding Sensitivity Study)

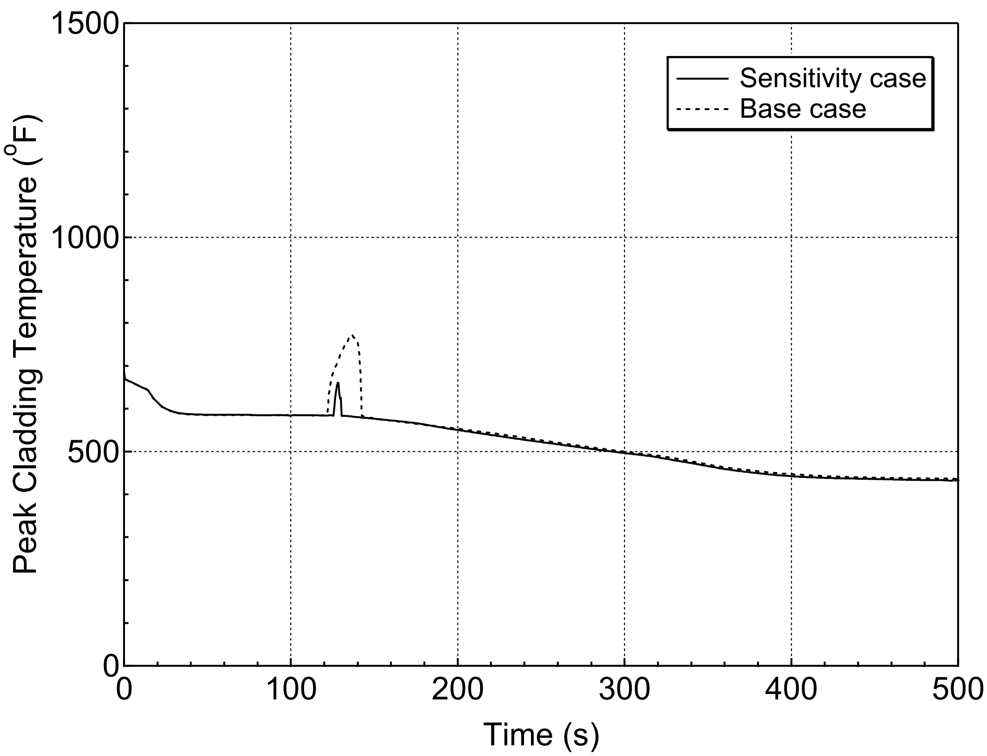

Figure 5.4.2-11 PCT at All Elevations for Hot Rod in Hot Assembly for 7.5-inch Break (Top) (Loop Noding Sensitivity Study)

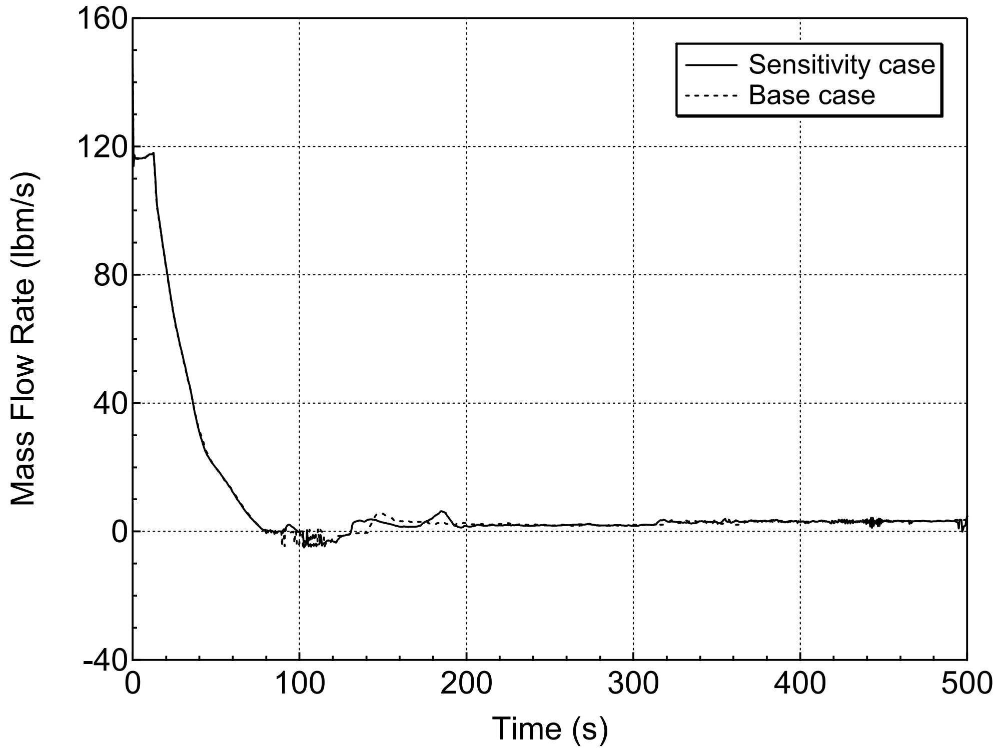

Figure 5.4.2-12 Hot Assembly Exit Liquid Mass Flowrate for 7.5-inch Break (Top) (Loop Noding Sensitivity Study)

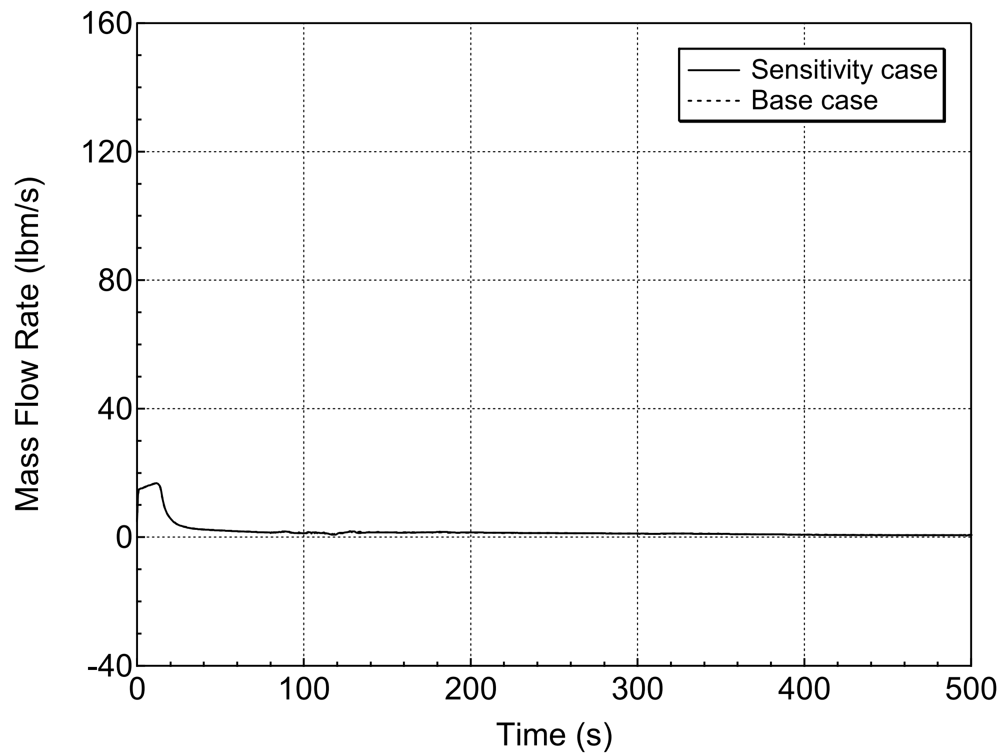

Figure 5.4.2-13 Hot Assembly Exit Vapor Mass Flowrate for 7.5-inch Break (Top) (Loop Noding Sensitivity Study)

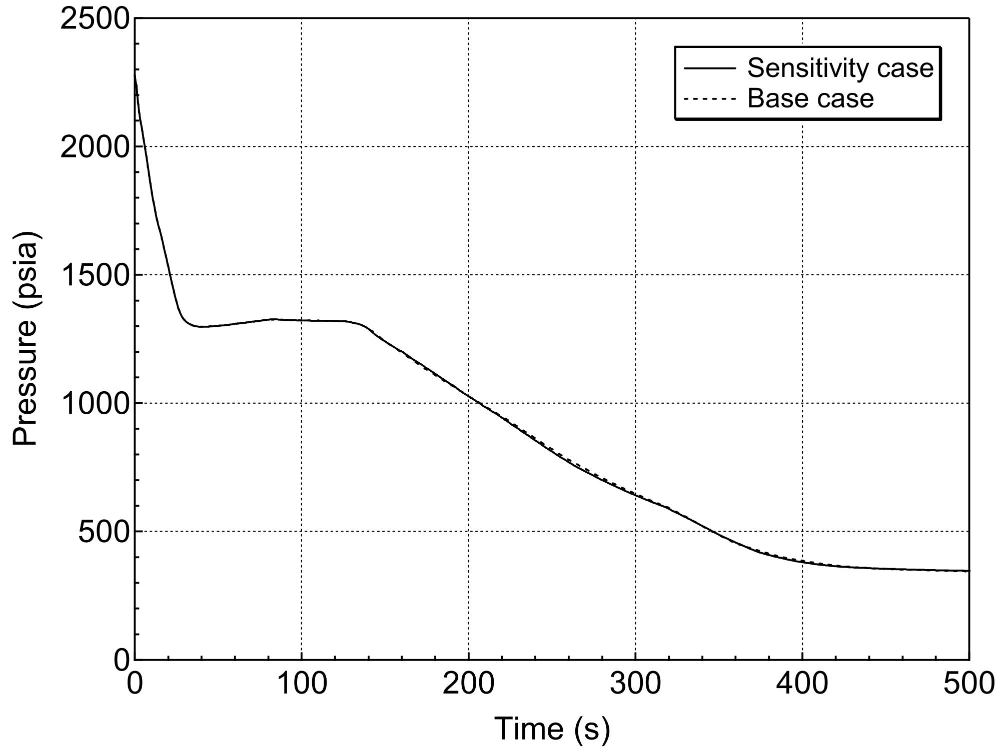

Figure 5.4.3-1 RCS (Pressurizer) Pressure Transient for 7.5-inch Break (Top) (Noding near the DVI Injection Point Sensitivity Study)

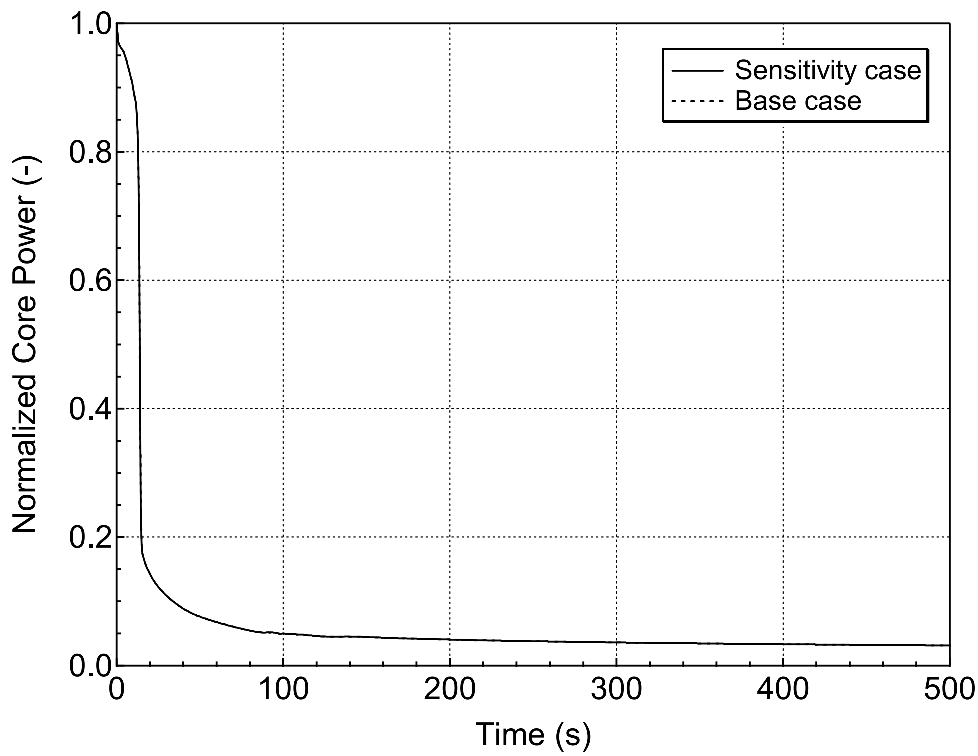

Figure 5.4.3-2 Normalized Core Power for 7.5-inch Break (Top)
(Noding near the DVI Injection Point Sensitivity Study)

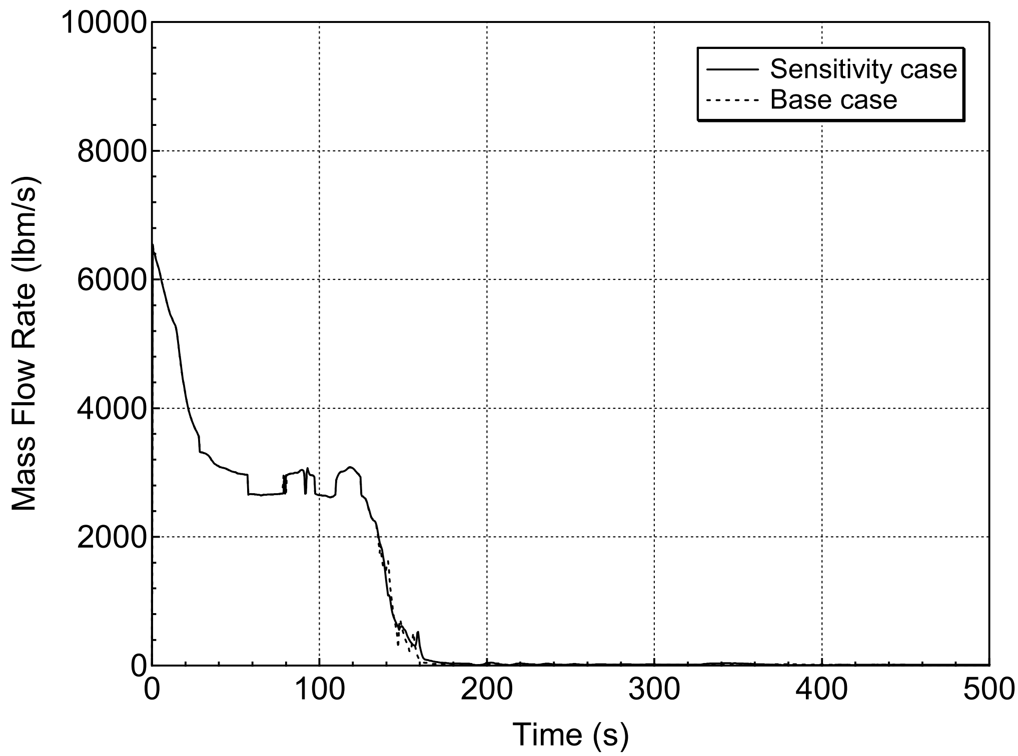

Figure 5.4.3-3 Liquid Discharge through the Break for 7.5-inch Break (Top) (Noding near the DVI Injection Point Sensitivity Study)

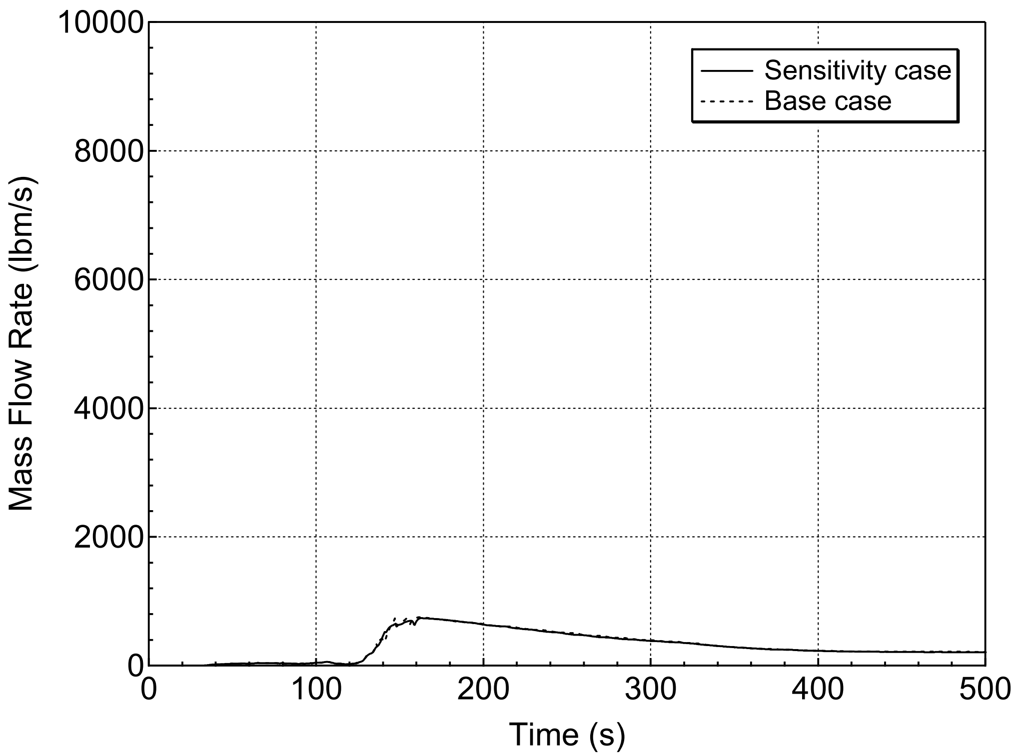

Figure 5.4.3-4 Vapor Discharge through the Break for 7.5-inch Break (Top) (Noding near the DVI Injection Point Sensitivity Study)

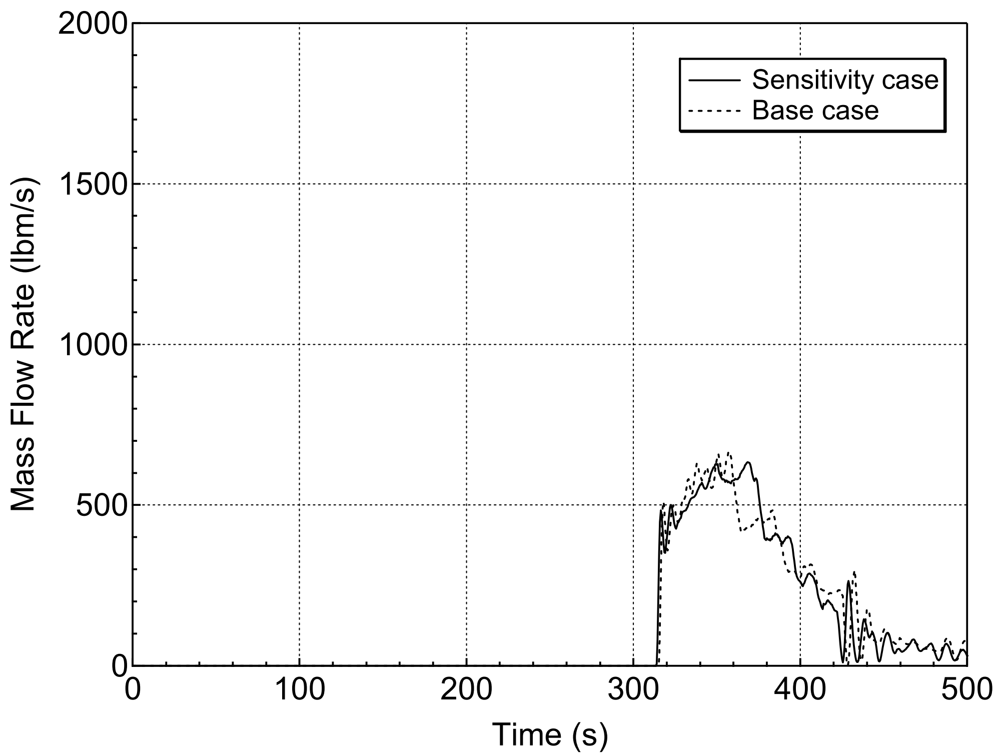

Figure 5.4.3-5 Accumulator Injection Mass Flowrate for 7.5-inch Break (Top) (Noding near the DVI Injection Point Sensitivity Study)

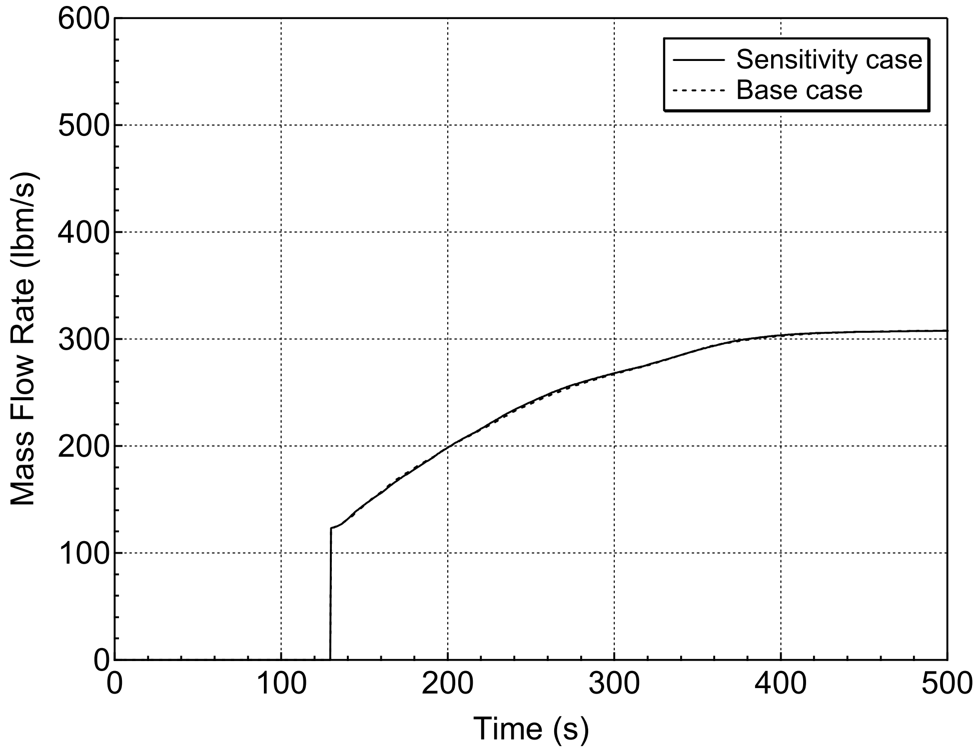

Figure 5.4.3-6 Safety Injection Mass Flowrate for 7.5-inch Break (Top) (Noding near the DVI Injection Point Sensitivity Study)

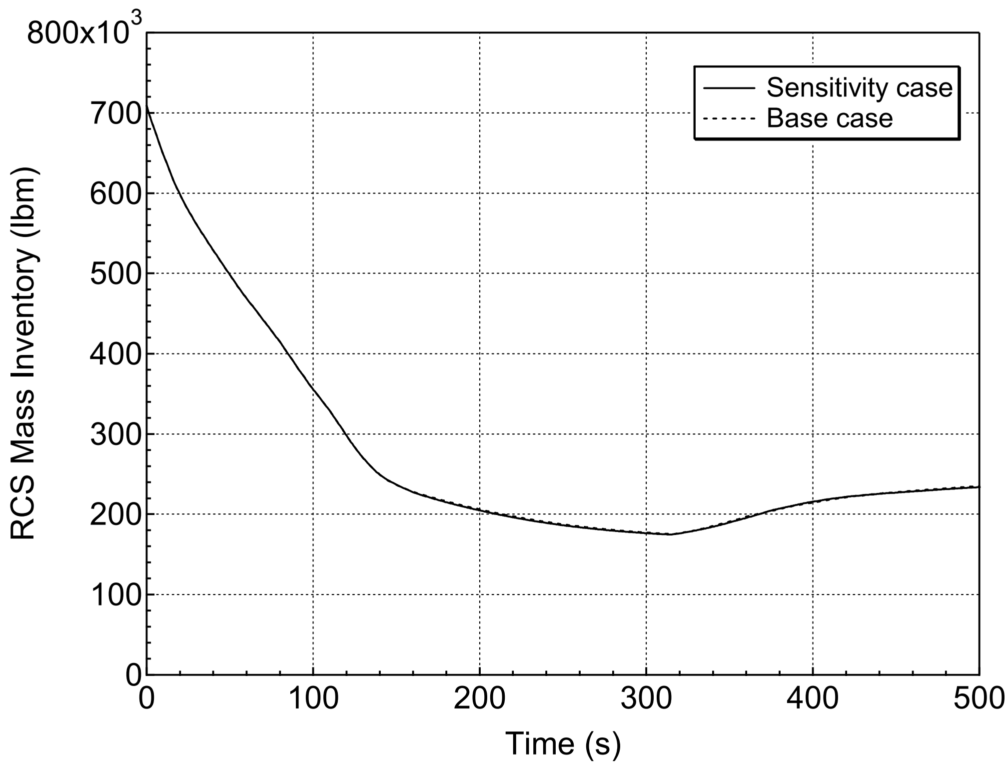

Figure 5.4.3-7 RCS Mass Inventory for 7.5-inch Break (Top)
(Noding near the DVI Injection Point Sensitivity Study)

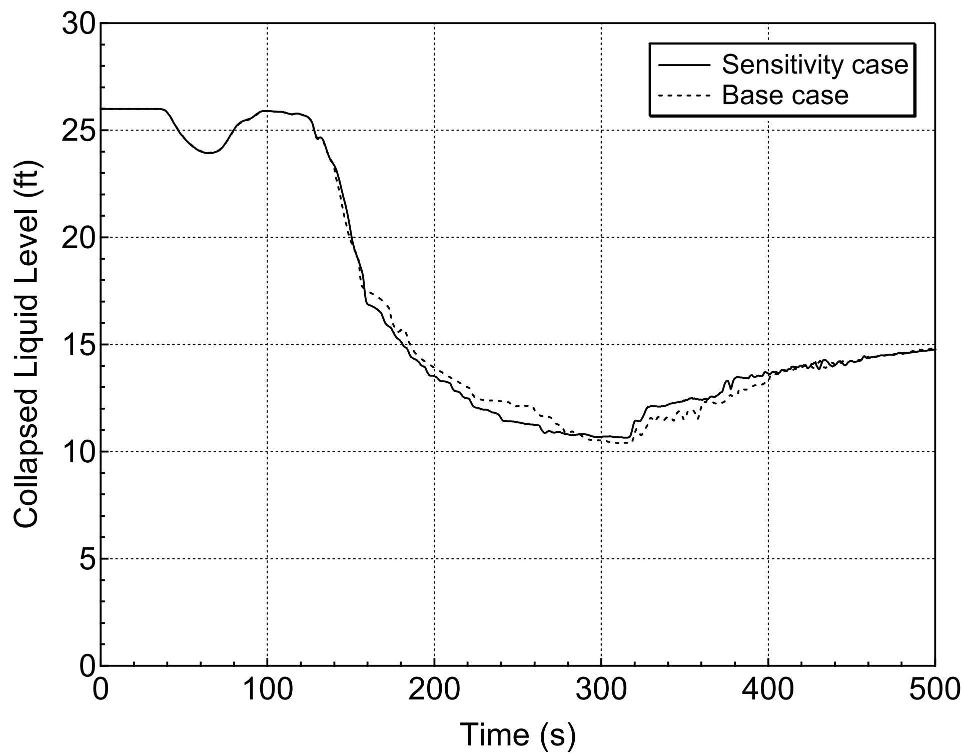

Figure 5.4.3-8 Downcomer Collapsed Level for 7.5-inch Break (Top) (Noding near the DVI Injection Point Sensitivity Study)

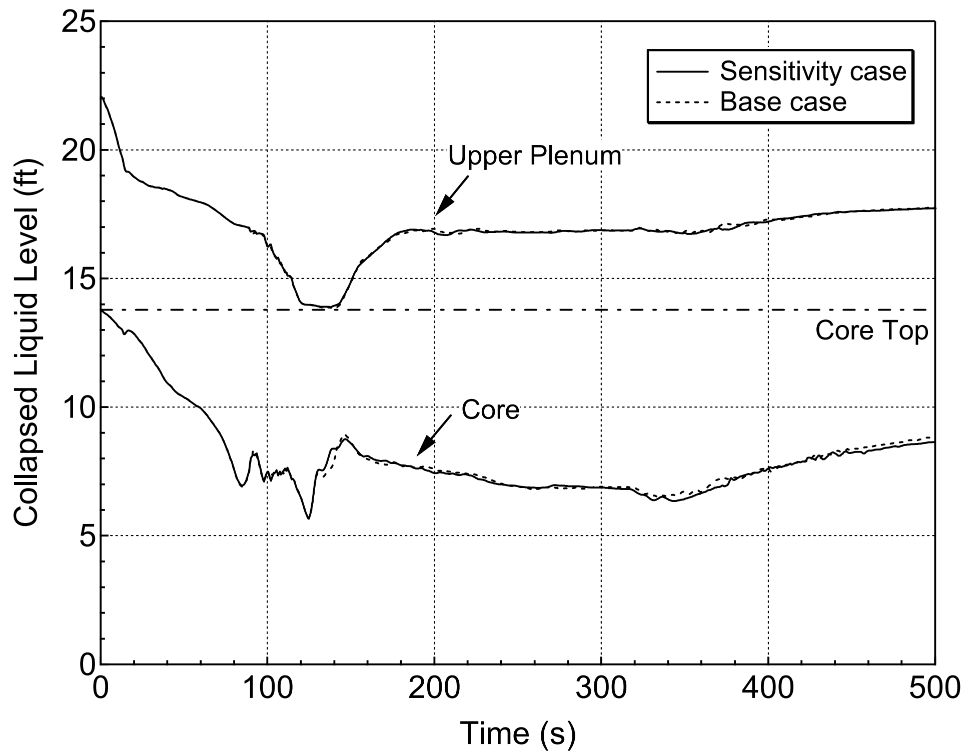

Figure 5.4.3-9 Average Core and Upper Plenum Collapsed Levels for 7.5-inch Break (Top) (Noding near the DVI Injection Point Sensitivity Study)

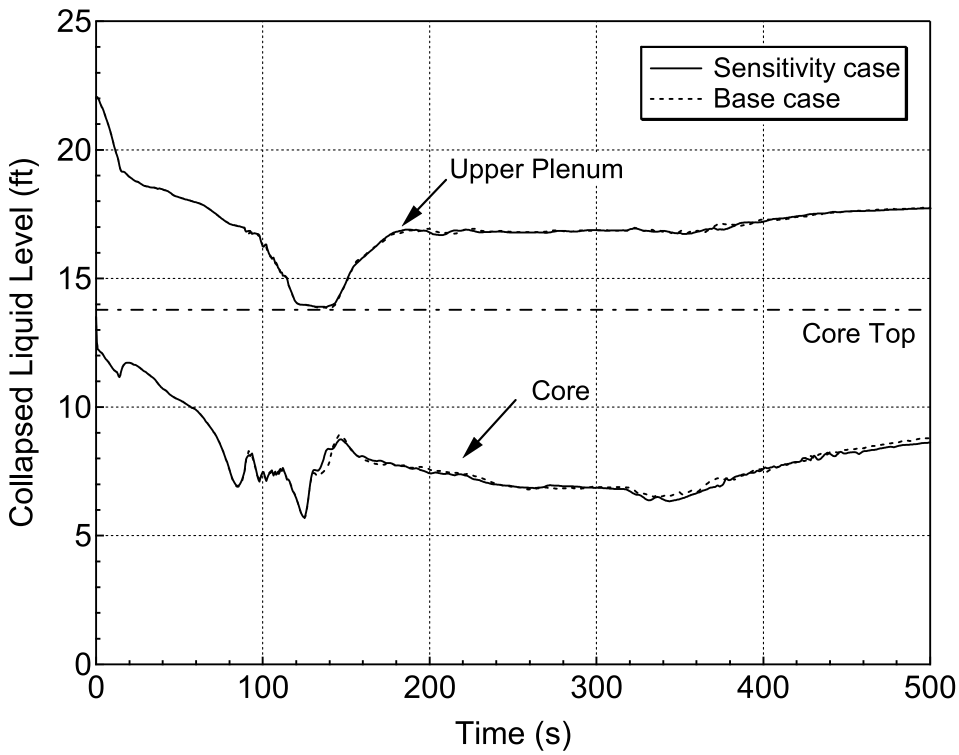

Figure 5.4.3-10 Hot Assembly Core and Upper Plenum Collapsed Levels for 7.5-inch Break (Top) (Noding near the DVI Injection Point Sensitivity Study)

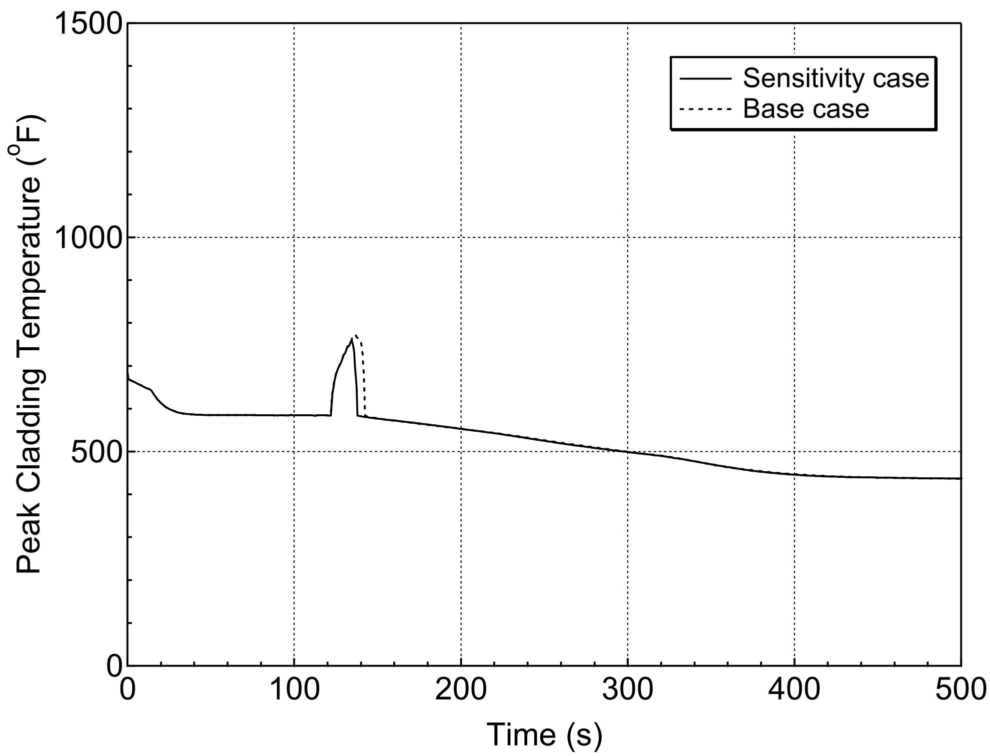

Figure 5.4.3-11 PCT at All Elevations for Hot Rod in Hot Assembly for 7.5-inch Break (Top) (Noding near the DVI Injection Point Sensitivity Study)

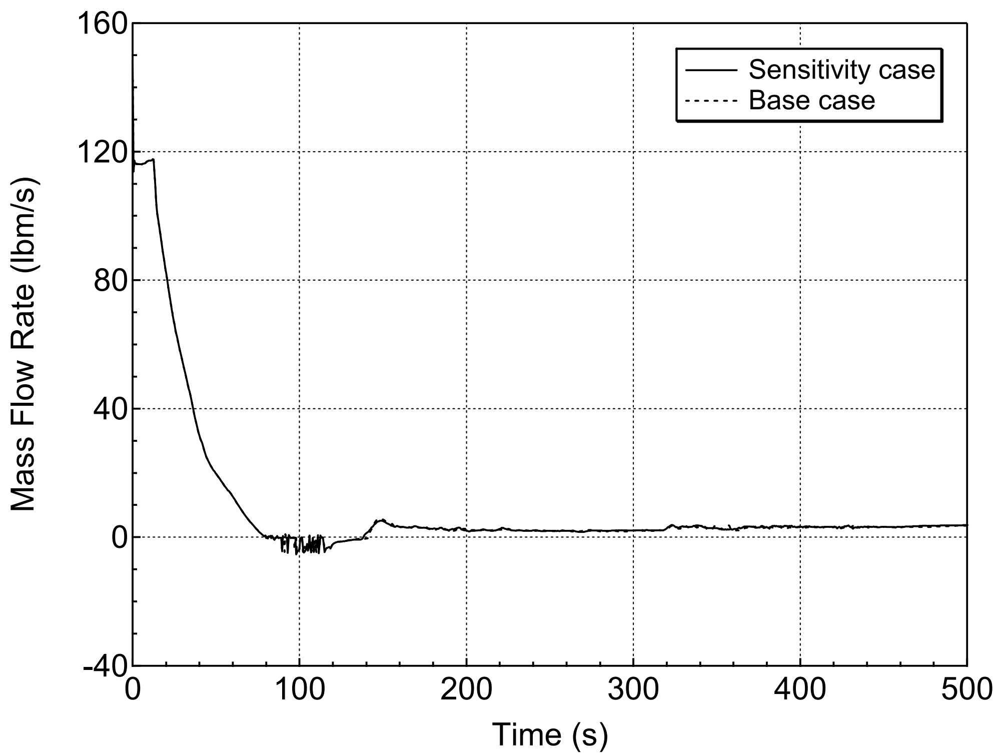

Figure 5.4.3-12 Hot Assembly Exit Liquid Mass Flowrate for 7.5-inch Break (Top) (Noding near the DVI Injection Point Sensitivity Study)

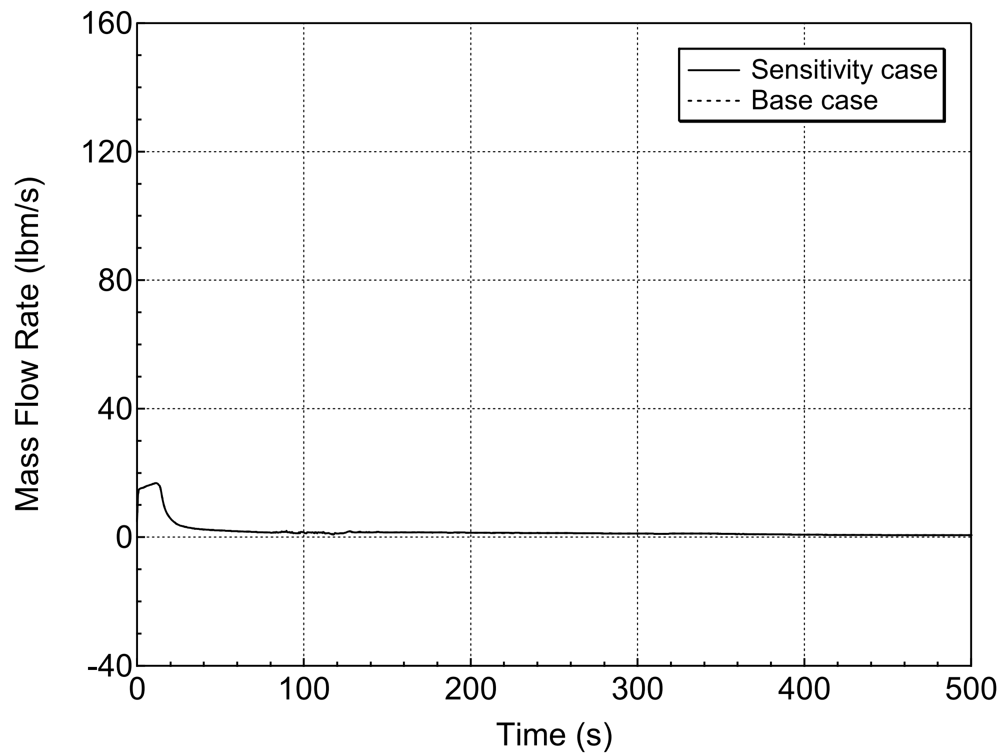

Figure 5.4.3-13 Hot Assembly Exit Vapor Mass Flowrate for 7.5-inch Break (Top) (Noding near the DVI Injection Point Sensitivity Study)

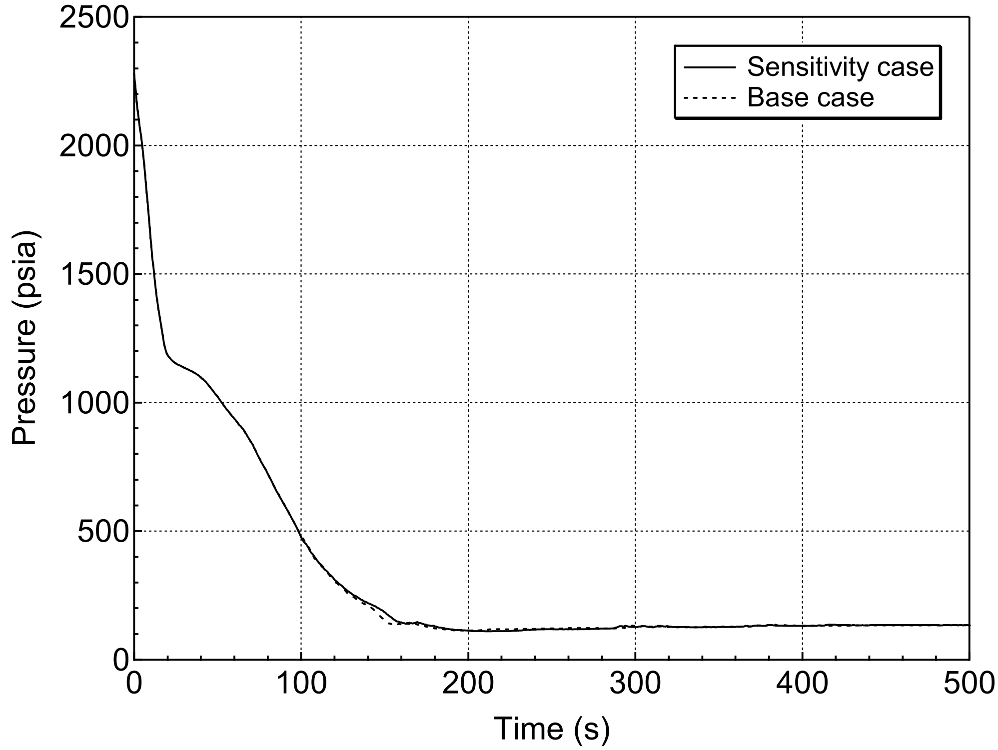

Figure 5.4.3-14 RCS (Pressurizer) Pressure Transient for 1-ft^2 Break (Top) (Noding near the DVI Injection Point Sensitivity Study)

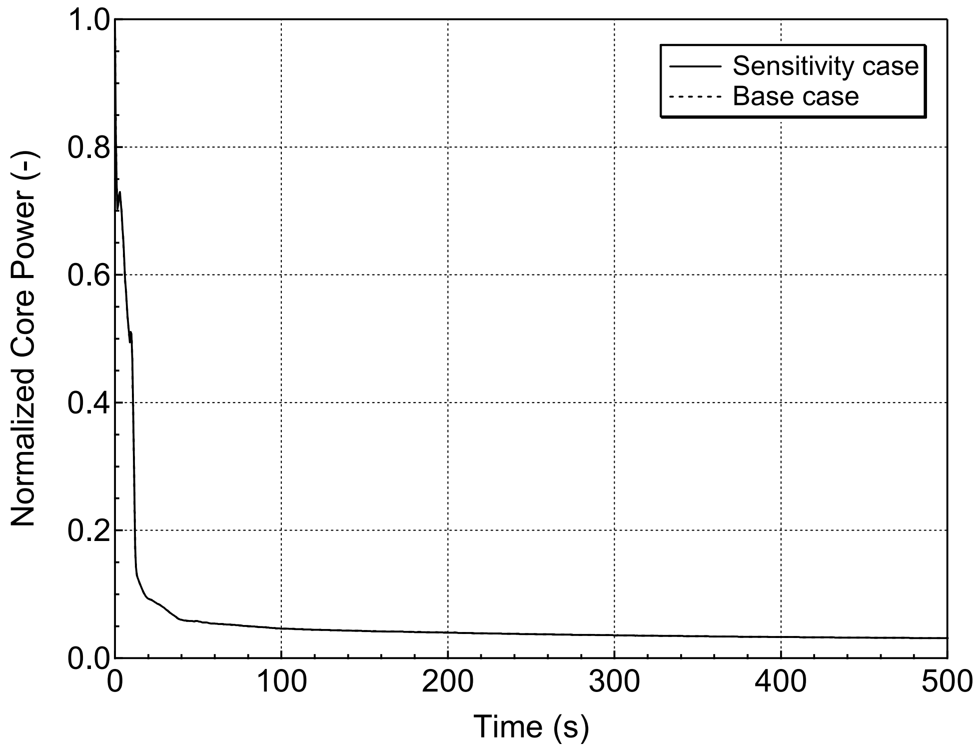

Figure 5.4.3-15 Normalized Core Power for 1-ft^2 Break (Top)
(Noding near the DVI Injection Point Sensitivity Study)

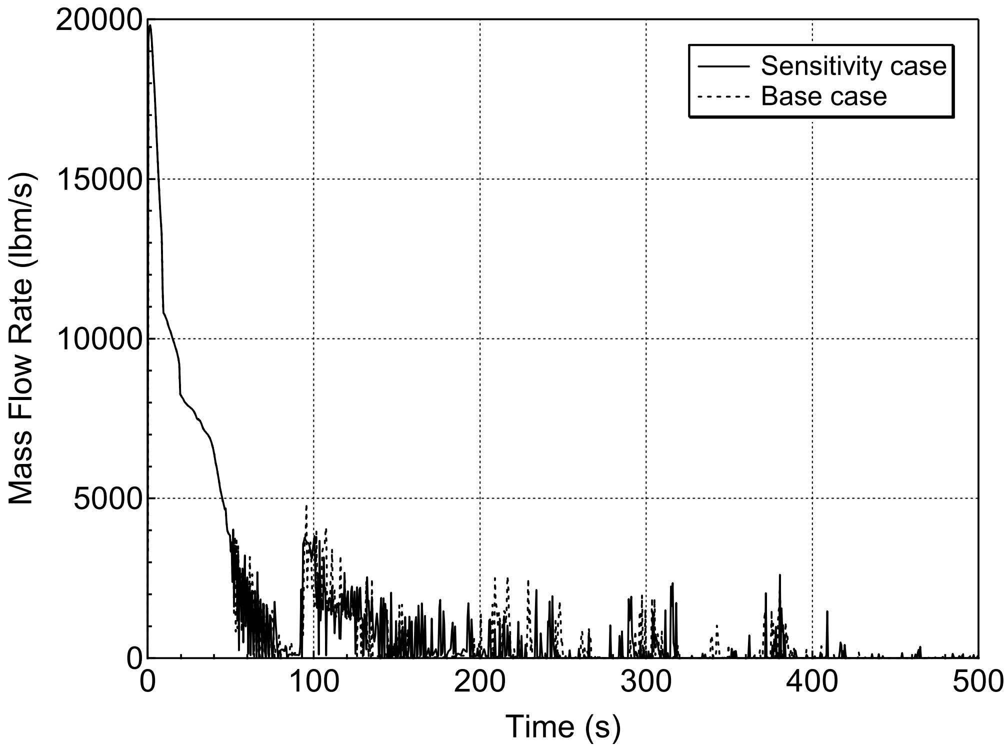

Figure 5.4.3-16 Liquid Discharge through the Break for 1-ft^2 Break (Top) (Noding near the DVI Injection Point Sensitivity Study)

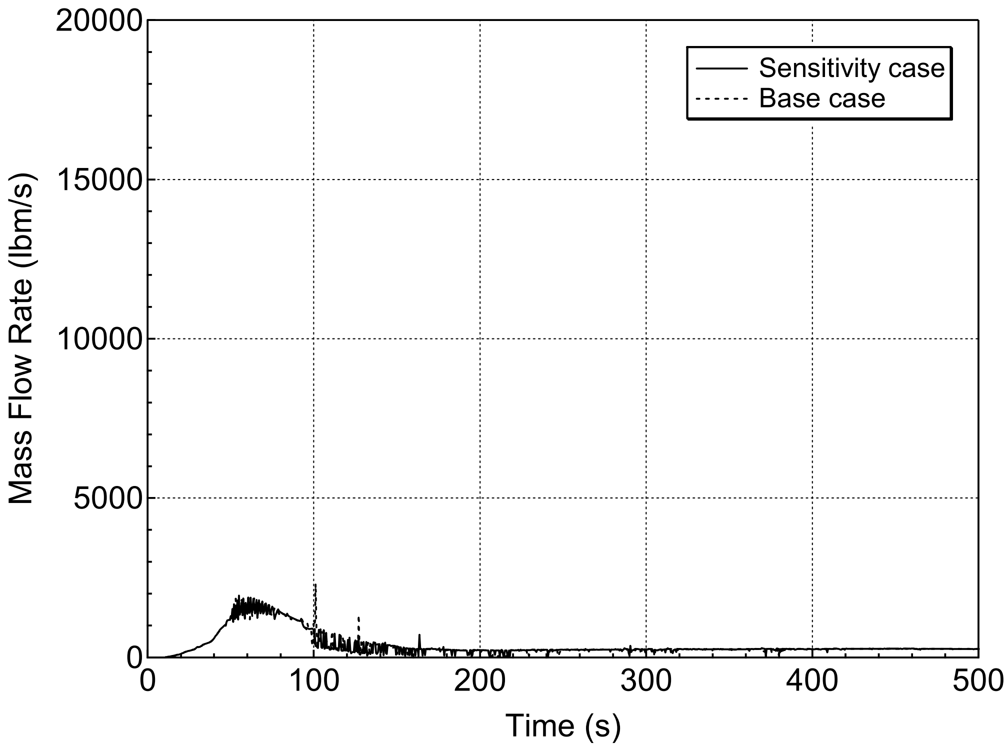

Figure 5.4.3-17 Vapor Discharge through the Break for 1-ft^2 Break (Top) (Noding near the DVI Injection Point Sensitivity Study)

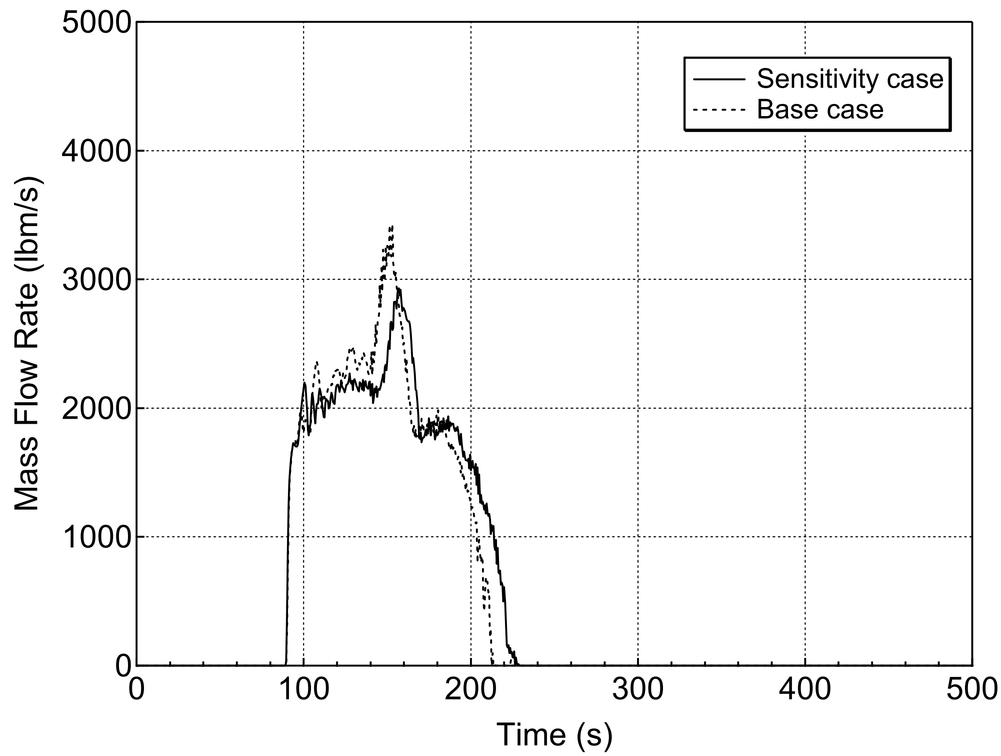

Figure 5.4.3-18 Accumulator Injection Mass Flowrate for 1-ft^2 Break (Top) (Noding near the DVI Injection Point Sensitivity Study)

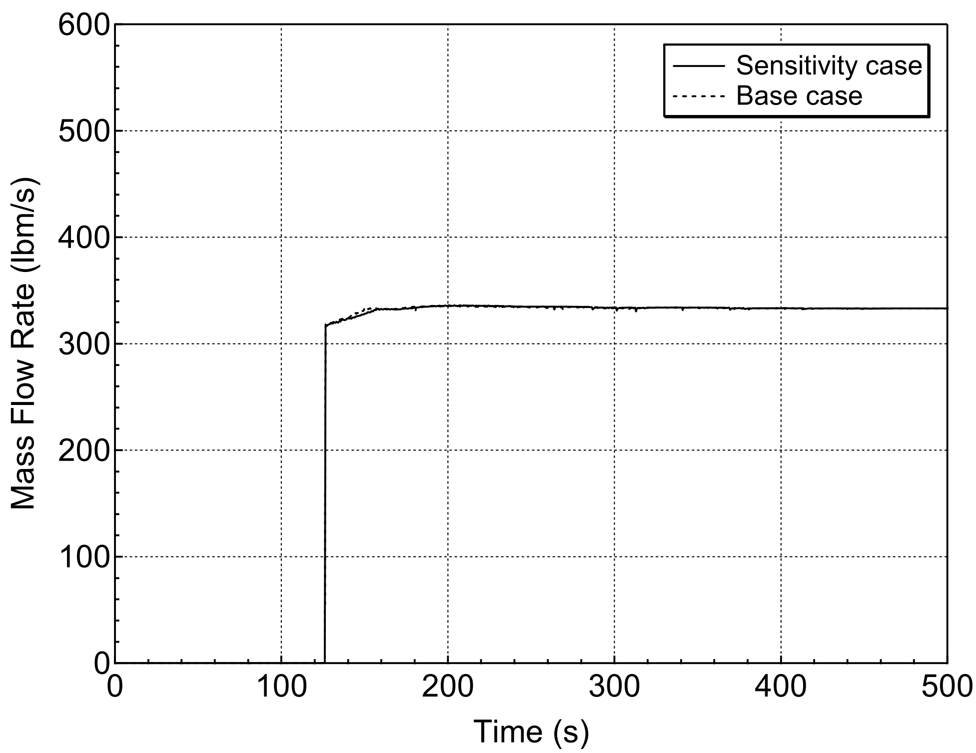

Figure 5.4.3-19 Safety Injection Mass Flowrate for 1-ft^2 Break (Top) (Noding near the DVI Injection Point Sensitivity Study)

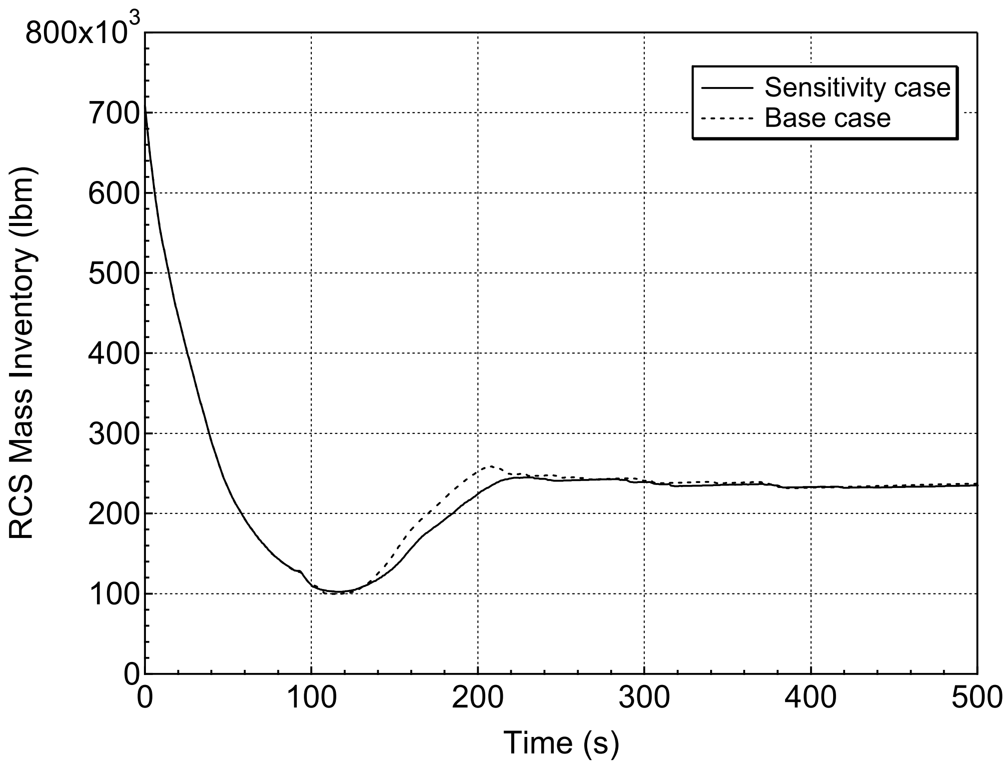

Figure 5.4.3-20 RCS Mass Inventory for 1-ft^2 Break (Top)
(Noding near the DVI Injection Point Sensitivity Study)

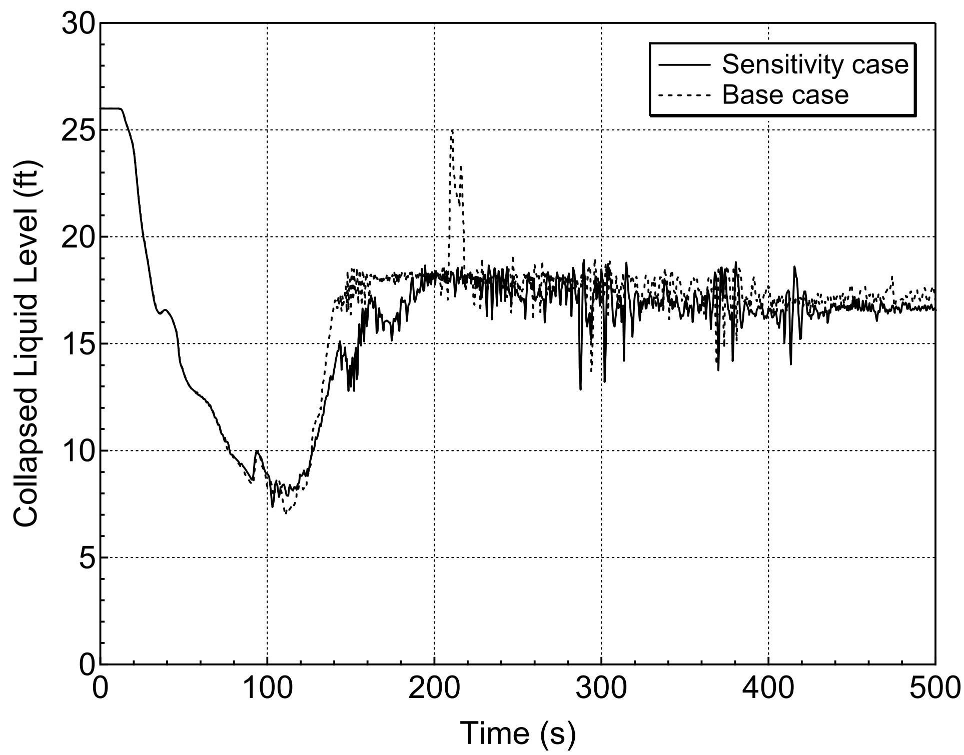

Figure 5.4.3-21 Downcomer Collapsed Level for 1-ft^2 Break (Top) (Noding near the DVI Injection Point Sensitivity Study)

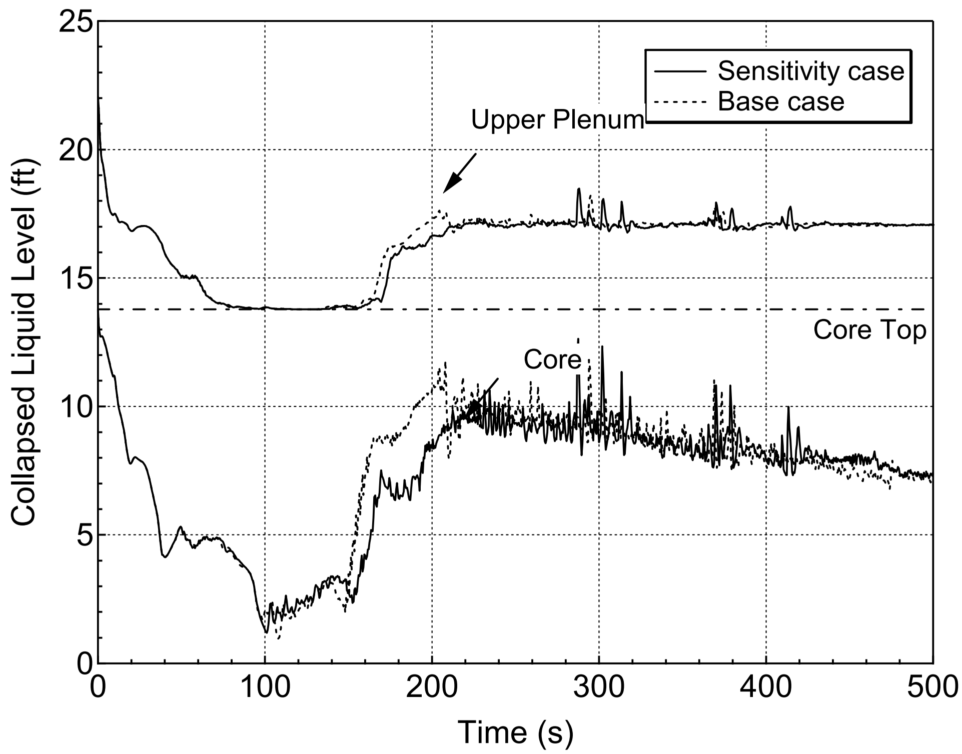

Figure 5.4.3-22 Average Core and Upper Plenum Collapsed Levels for 1-ft^2 Break (Top) (Noding near the DVI Injection Point Sensitivity Study)

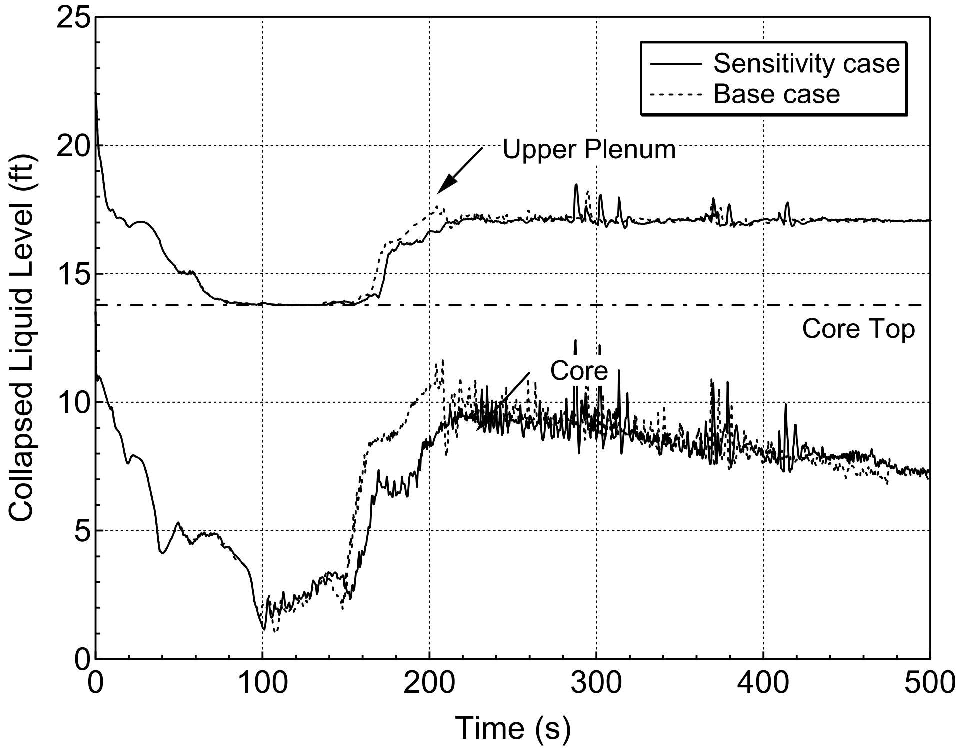

Figure 5.4.3-23 Hot Assembly Core and Upper Plenum Collapsed Levels for 1-ft^2 Break (Top) (Noding near the DVI Injection Point Sensitivity Study)

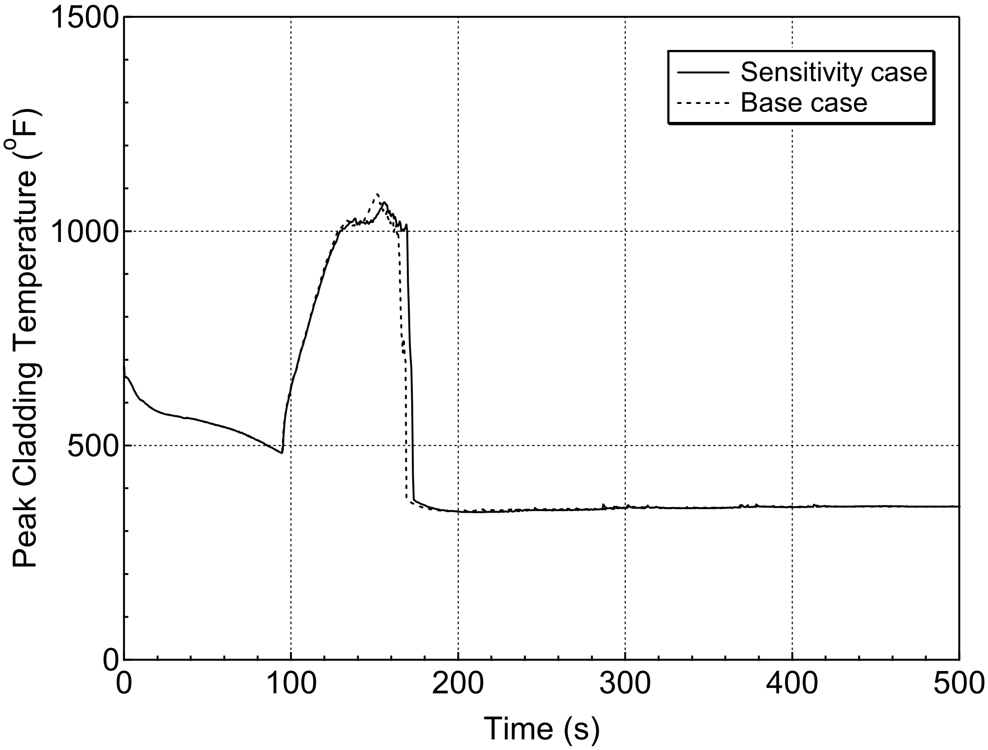

Figure 5.4.3-24 PCT at All Elevations for Hot Rod in Hot Assembly for 1-ft^2 Break (Top) (Noding near the DVI Injection Point Sensitivity Study)

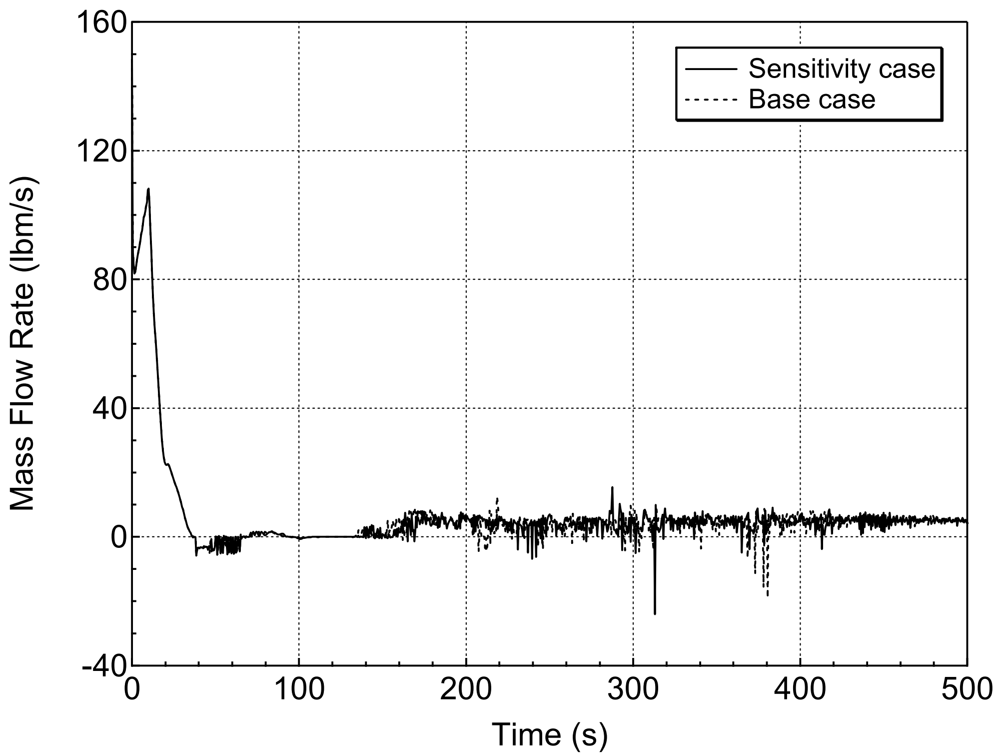

Figure 5.4.3-25 Hot Assembly Exit Liquid Mass Flowrate for 1-ft^2 Break (Top) (Noding near the DVI Injection Point Sensitivity Study)

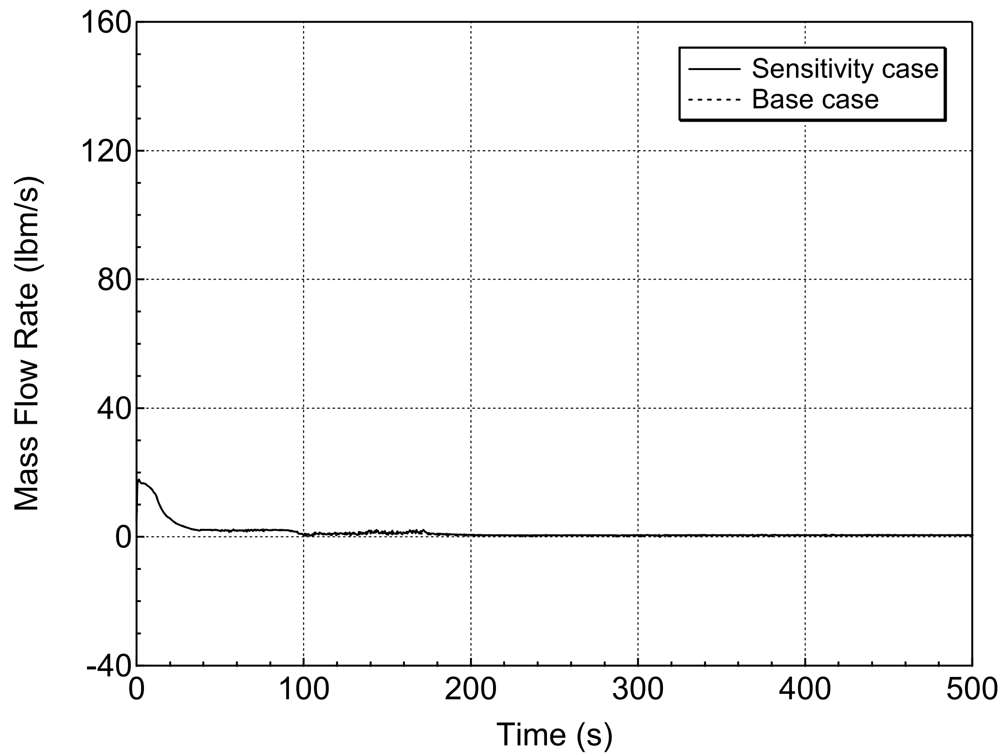

Figure 5.4.3-26 Hot Assembly Exit Vapor Mass Flowrate for 1-ft^2 Break (Top) (Noding near the DVI Injection Point Sensitivity Study)

5.5 Time Step Size Sensitivity Study

Time step size sensitivity calculations were performed for the following cases:

- 7.5-inch top break (limiting case for Loop-seal-PCT)
- 1-ft^2 top break (limiting case for Boil-off -PCT)
- DVI line break, 3.4-inch break

(1) Results of the 7.5-inch cold leg top orientation break case

Figure 5.5.a-1 shows the comparison of base case and sensitivity case on RCS (Pressurizer) pressure transient calculation. For the 7.5-inch loop seal PCT limiting break case, it reveals that by reducing the maximum time step to half does not cause any change in the result. The calculation results of base case and sensitivity case are perfectly in agreement.

Figure 5.5.a-2 presents the normalized core power transient. The results of base case and sensitivity case are perfectly in agreement.

Figure 5.5.a-3 displays the comparison of base case and sensitivity case on the liquid discharge through the break. The results of base case and sensitivity case are perfectly in agreement.

The vapor discharge through the break is shown in Figure 5.5.a-4. The results of base case and sensitivity case are perfectly in agreement.

Figure 5.5.a-5 shows the comparison of accumulator injection mass flowrate time history. The comparison shows little sensitivity.

Figure 5.5.a-6 depicts the time history of safety injection mass flowrate. The calculation results of base case and sensitivity case are perfectly in agreement.

The RCS mass inventory transient is displayed in Figure 5.5.a-7. The calculation results of base case and sensitivity case are also perfectly in agreement.

Figure 5.5.a-8 illustrates the downcomer collapsed level transient. The comparison shows very good agreement from the beginning of the transient.

Figure 5.5.a-9 shows the average core and upper plenum collapsed levels. The comparison is

in good agreement and the transient profiles are well calculated.

The hot assembly core and upper plenum collapsed levels are given in Figure 5.5.a-10. The comparison is in good agreement and the transient profiles are well calculated.

The comparison of base case and sensitivity case on PCT at all elevations for hot rod in hot assembly is presented in Figure 5.5.a-11. The results of PCT calculations are in good agreement for both time steps.

Figure 5.5.a-12 presents the hot assembly exit liquid mass flowrate transient calculation comparison between base case and sensitivity case. The results are in good agreement, the oscillating high frequency low amplitude flow reversal are well calculated by both cases.

Figure 5.5.a-13 presents the hot assembly exit vapor mass flowrate. The calculation results of base case and sensitivity case are also perfectly in agreement.

(2) Results of the 1-ft^2 cold-leg top orientation break case

Figure 5.5.b-1 shows the comparison of base case and sensitivity case on RCS (Pressurizer) pressure transient calculation. For the 1-ft^2 boil-off PCT limiting break case, it reveals that by reducing the time step does not cause any change in the result. The calculation results of base case and sensitivity case are in good agreement with very small sensitivity.

Figure 5.5.b-2 presents the normalized core power transient. The results of base case and sensitivity case are perfectly in agreement.

Figure 5.5.b-3 displays the comparison of base case and sensitivity case on the liquid discharge through the break. The results of base case and sensitivity case are in general agreement.

The vapor discharge through the break is shown in Figure 5.5.b-4. The results of base case and sensitivity case are in good agreement.

Figure 5.5.b-5 shows the comparison of accumulator injection mass flowrate time history. The phenomena and basic transient profiles are well calculated.

Figure 5.5.b-6 depicts the time history of safety injection mass flowrate. The calculation results

of base case and sensitivity case are perfectly in agreement.

The RCS mass inventory transient is displayed in Figure 5.5.b-7. The calculation results of base case and sensitivity case show little sensitivity.

Figure 5.5.b-8 illustrates the downcomer collapsed level transient. The calculation results of base case and sensitivity case are perfectly in agreement.

Figure 5.5.b-9 shows the average core and upper plenum collapsed levels. The comparison is in good agreement and the transient profiles are well calculated.

The hot assembly core and upper plenum collapsed levels are given in Figure 5.5.b-10. The comparison is in good agreement and the transient profiles are well calculated.

The comparison of base case and sensitivity case on PCT at all elevations for hot rod in hot assembly is presented in Figure 5.5.b-11. The results of PCT calculations are in good agreement for both time steps.

Figure 5.5.b-12 presents the hot assembly exit liquid mass flowrate transient calculation comparison between base case and sensitivity case. The results are in good agreement, the oscillating high frequency low amplitude flow reversal are well calculated in both cases.

Figure 5.5.b-13 presents the hot assembly exit vapor mass flowrate. The calculation results of base case and sensitivity case are also perfectly in agreement.

(3) Results of the DVI-line break case

The results of time step sensitivity study for the DVI-line break are shown in Figure 5.5.c-1 through 5.5.c-13. It is clearly observable that the results are in good agreement. It implies that for the DVI line break, the calculation with reduced time step does not show any sensitivity. In this case, PCT does not occur because there is no core uncovery.

It is concluded that reducing the maximum time step by half does not cause any significant sensitivity in the result. The results of PCT calculations are in good agreement for both time steps.

Table 5.5.a-1 Sequence of Events for 7.5-inch Break (Top)
(Time Step Size Sensitivity Study)

Event	Time (sec)	
	Base case	Sensitivity case
Break occurs; blowdown initiation	0.0	0.0
Reactor trip (loss-of-offsite power is assumed)	9.3	9.3
Control rod insertion starts	11.1	11.1
Main steam isolation	11.1	11.1
ECCS actuation signal	11.9	11.9
RCP trip	12.3	12.3
Main feedwater isolation	17.3	17.3
Main steam safety valve open	81	81
Emergency Power Source initiates	115	115
Fuel cladding starts heating up	122	122
High Head Injection System begins	130	130
Peak Cladding Temperature occurs	136	136
Fuel cladding rewets	143	141
Emergency feedwater flow begins	145	145
Accumulator injection begins	315	314

Table 5.5.a-2 Core Performance Results for 7.5-inch Break (Top)
(Time Step Size Sensitivity Study)

	Values	
	Base case	Sensitivity case
Peak Cladding Temperature (°F)	775	770
Maximum local cladding oxidation (%)	0.2	0.2
Maximum core wide cladding oxidation (%)	less than 0.2	less than 0.2

Table 5.5.b-1 Sequence of Events for 1-ft^2 Break (Top) (Time Step Size Sensitivity Study)

Event	Time (sec)	
	Base case	Sensitivity case
Break occurs; blowdown initiation	0.0	0.0
Reactor trip (loss-of-offsite power is assumed)	6.9	6.9
ECCS actuation signal	8.3	8.3
Control rod insertion starts	8.7	8.7
Main steam isolation	8.7	8.7
RCP trip	9.9	9.9
Main feedwater isolation	14.9	14.9
Main steam safety valve open	not actuated	not actuated
Accumulator injection begins	89	90
Fuel cladding starts heating up	95	95
Emergency Power Source initiates	111	111
High Head Injection System begins	126	126
Emergency feedwater flow begins	141	141
Peak Cladding Temperature occurs	151	150
Fuel cladding rewets	169	168

Table 5.5.b-2 Core Performance Results for 1-ft^2 Break (Top) (Time Step Size Sensitivity Study)

	Values	
	Base case	Sensitivity case
Peak Cladding Temperature (°F)	1088	1099
Maximum local cladding oxidation (%)	0.2	0.2
Maximum core wide cladding oxidation (%)	less than 0.2	less than 0.2

Table 5.5.c-1 Sequence of Events for DVI-line Break (Time Step Size Sensitivity Study)

Event	Time (sec)	
	Base case	Sensitivity case
Break occurs; blowdown initiation	0.0	0.0
Reactor trip (loss-of-offsite power is assumed)	25.8	25.8
Control rod insertion starts	27.6	27.6
Main steam isolation	27.6	27.6
RCP trip	28.8	28.8
Main feedwater isolation	33.8	33.8
ECCS actuation signal	35.4	35.4
Main steam safety valve open	57	57
Emergency Power Source initiates	138	138
High Head Injection System begins	153	153
Emergency feedwater flow begins	168	168
Accumulator injection begins	3020	not actuated
Fuel cladding starts heating up	not occur	not occur
Peak Cladding Temperature occurs	lower than the initial temperature	lower than the initial temperature
Fuel cladding rewets	N/A	N/A

Table 5.5.c-2 Core Performance Results for DVI-line Break (Time Step Size Sensitivity Study)

	Values	
	Base case	Sensitivity case
Peak Cladding Temperature (°F)	lower than the initial temperature	lower than the initial temperature
Maximum local cladding oxidation (%)	0.2	0.2
Maximum core wide cladding oxidation (%)	less than 0.2	less than 0.2

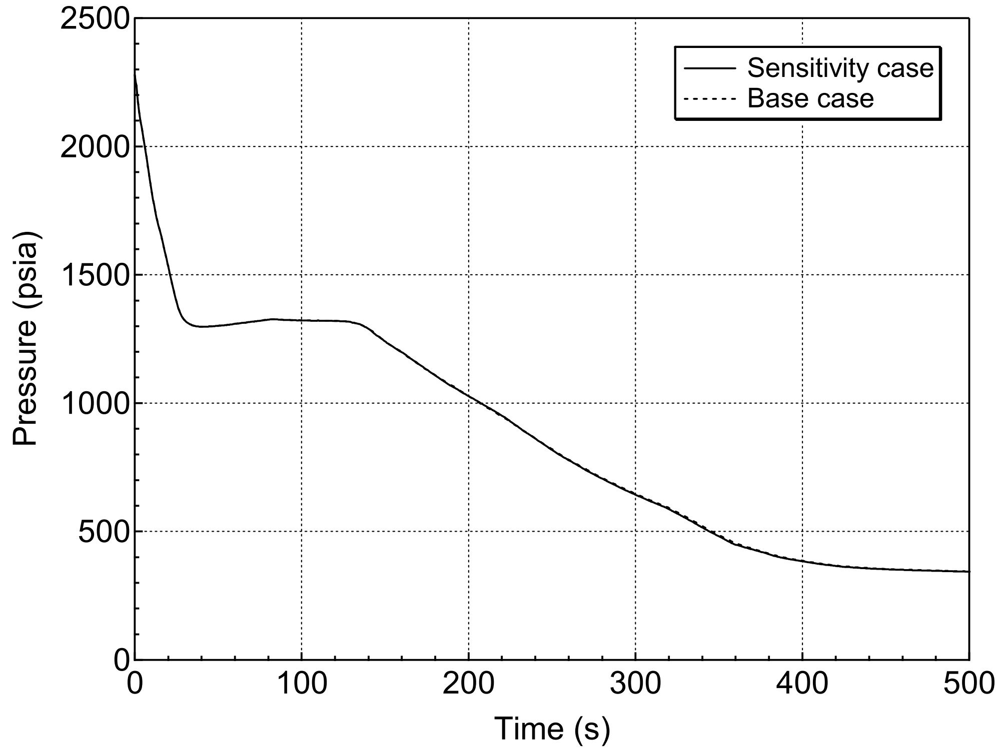

Figure 5.5.a-1 RCS (Pressurizer) Pressure Transient for 7.5-inch Break (Top) (Time Step Size Sensitivity Study)

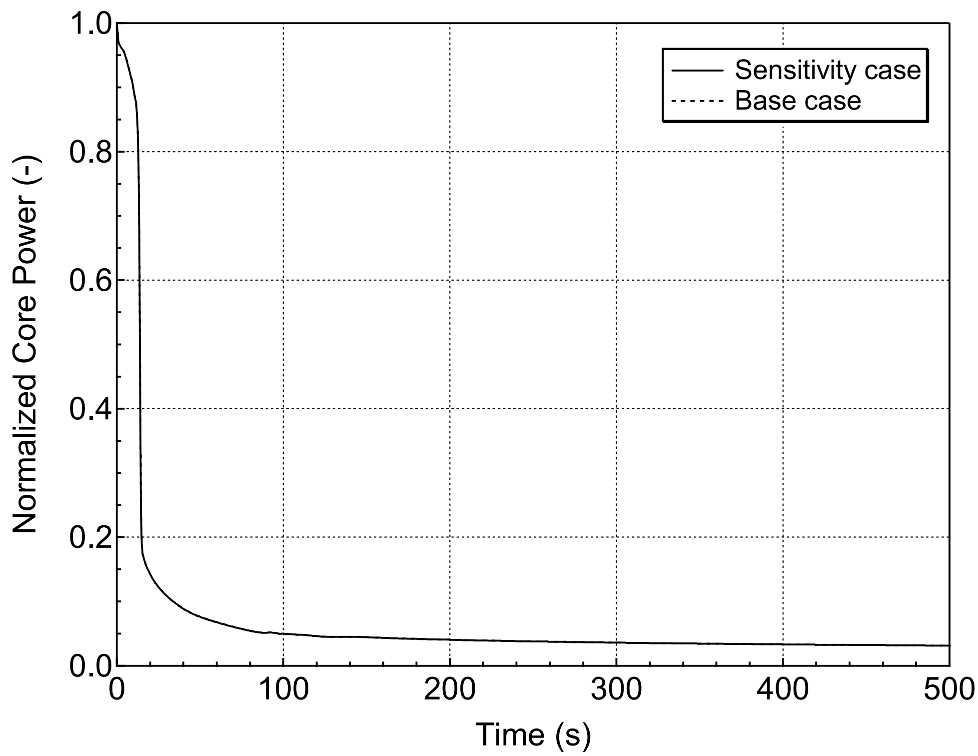

Figure 5.5.a-2 Normalized Core Power for 7.5-inch Break (Top)
(Time Step Size Sensitivity Study)

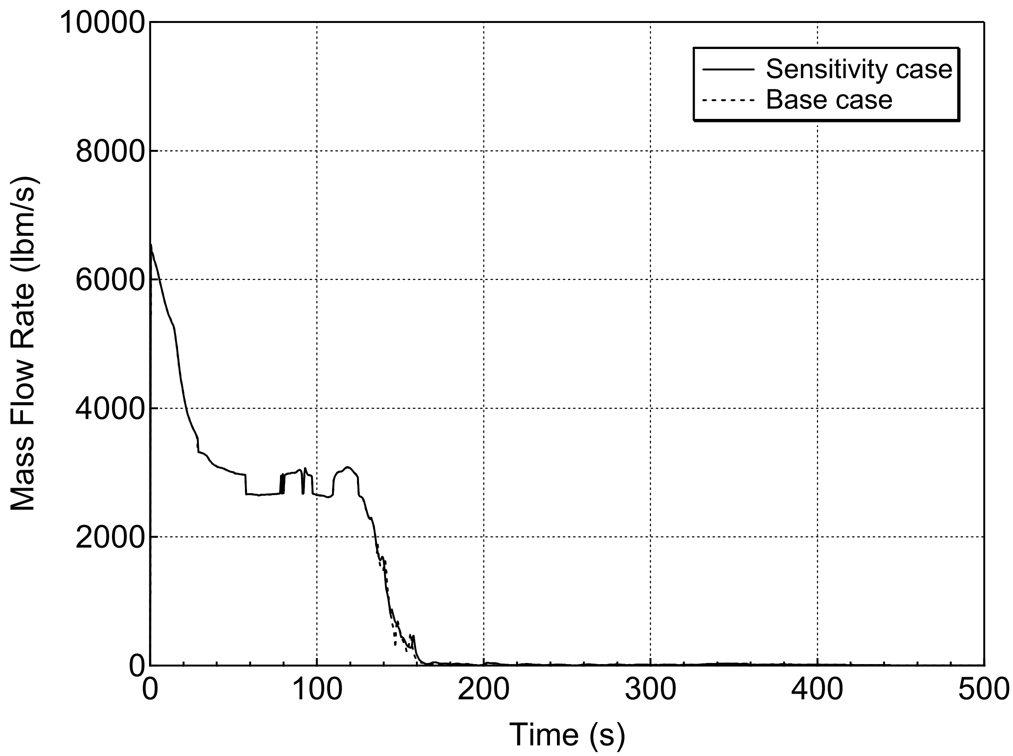

Figure 5.5.a-3 Liquid Discharge through the Break for 7.5-inch Break (Top) (Time Step Size Sensitivity Study)

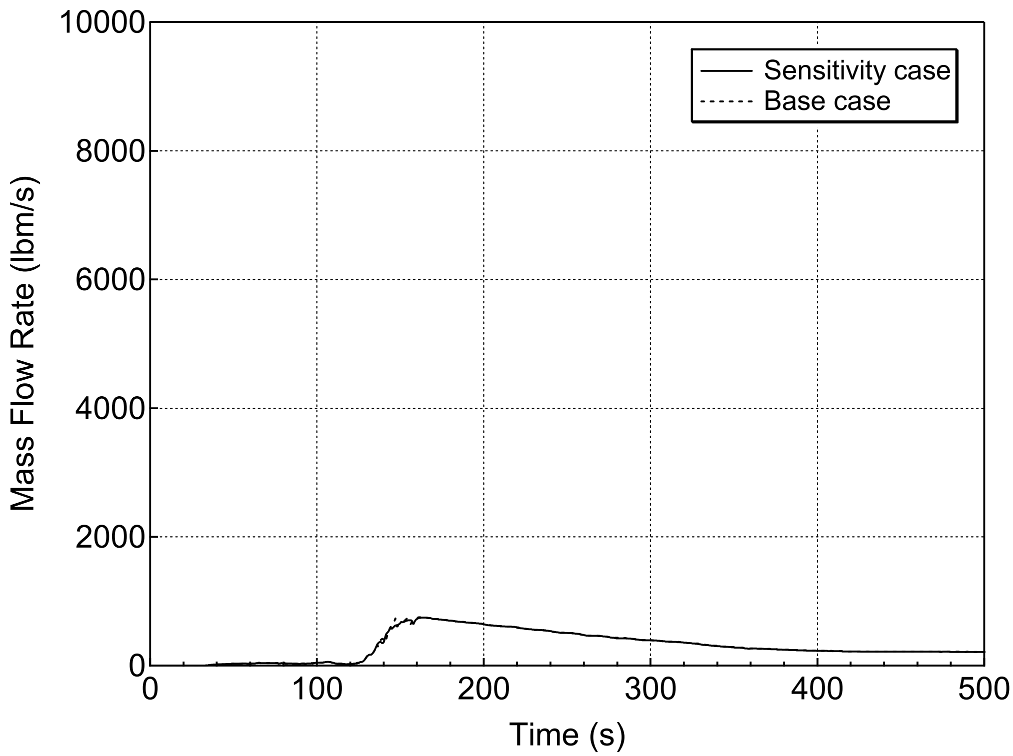

Figure 5.5.a-4 Vapor Discharge through the Break for 7.5-inch Break (Top) (Time Step Size Sensitivity Study)

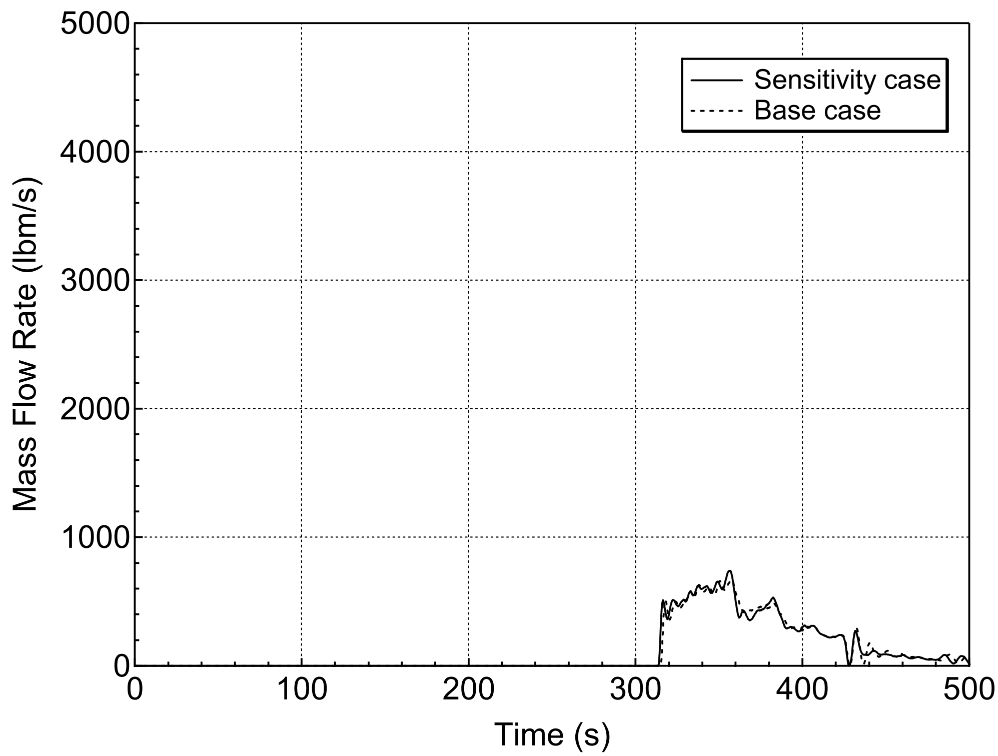

Figure 5.5.a-5 Accumulator Injection Mass Flowrate for 7.5-inch Break (Top) (Time Step Size Sensitivity Study)

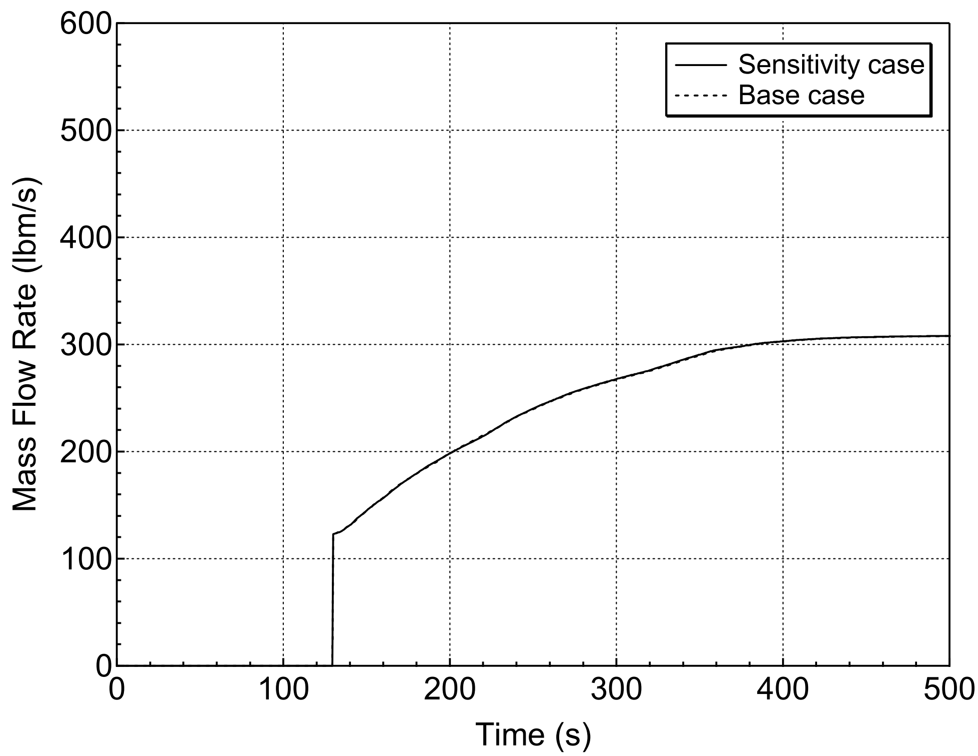

Figure 5.5.a-6 Safety Injection Mass Flowrate for 7.5-inch Break (Top) (Time Step Size Sensitivity Study)

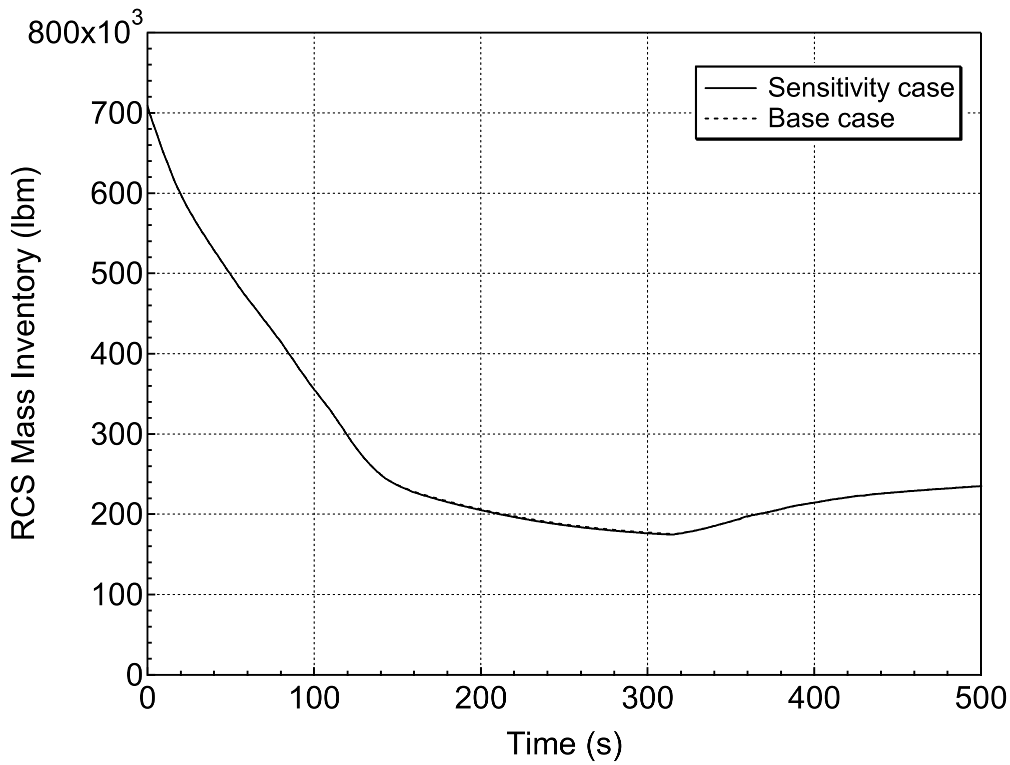

Figure 5.5.a-7 RCS Mass Inventory for 7.5-inch Break (Top) (Time Step Size Sensitivity Study)

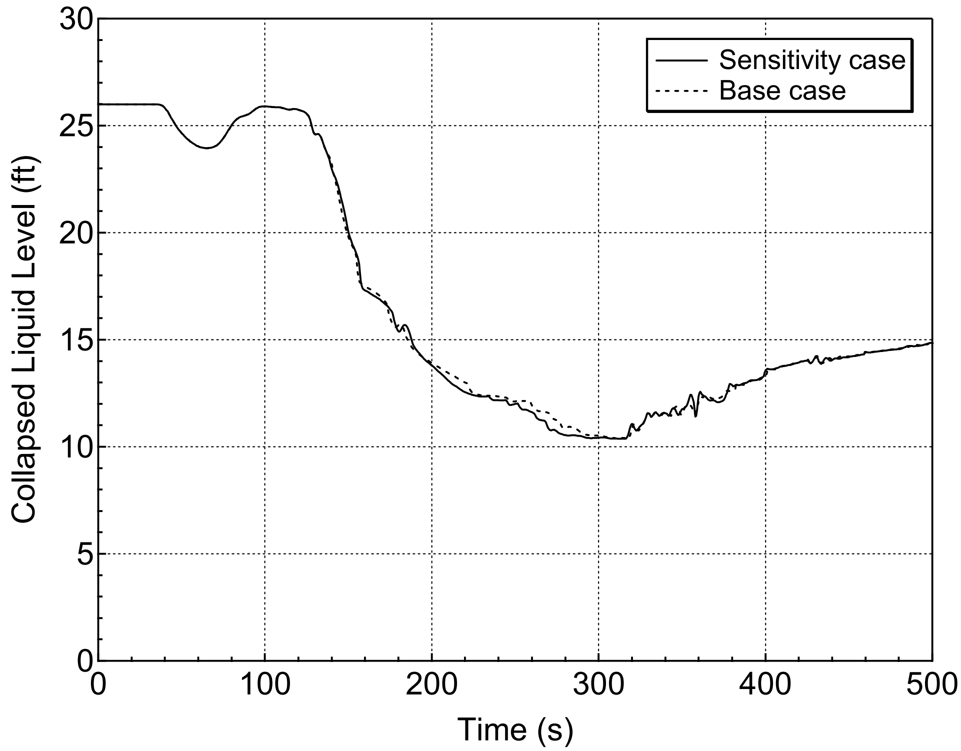

Figure 5.5.a-8 Downcomer Collapsed Level for 7.5-inch Break (Top)
(Time Step Size Sensitivity Study)

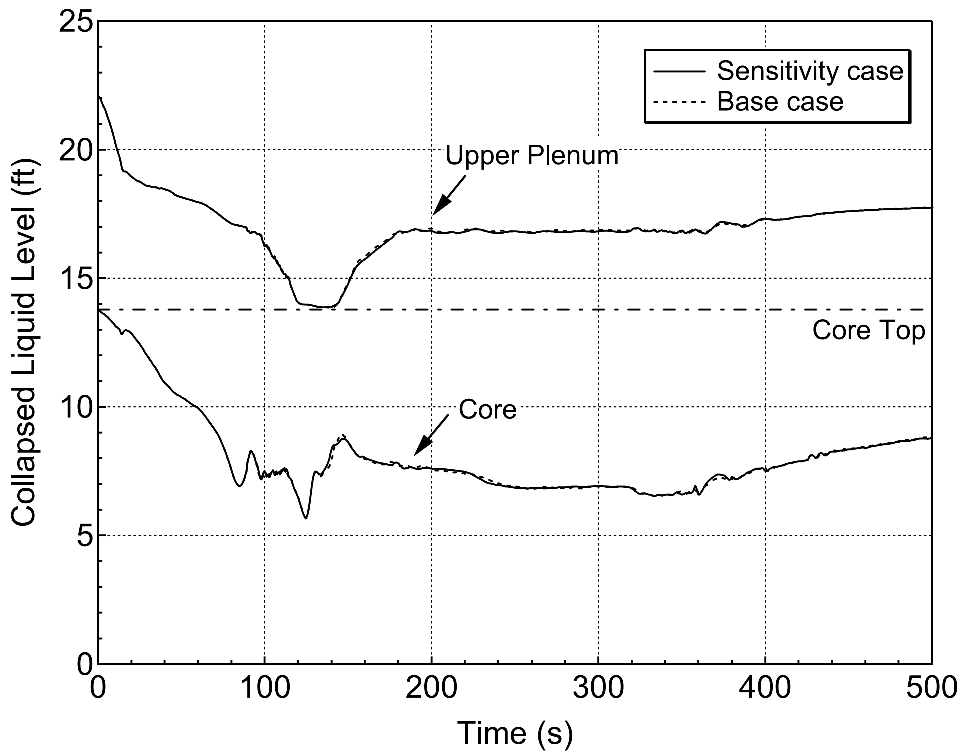

Figure 5.5.a-9 Average Core and Upper Plenum Collapsed Levels for 7.5-inch Break (Top) (Time Step Size Sensitivity Study)

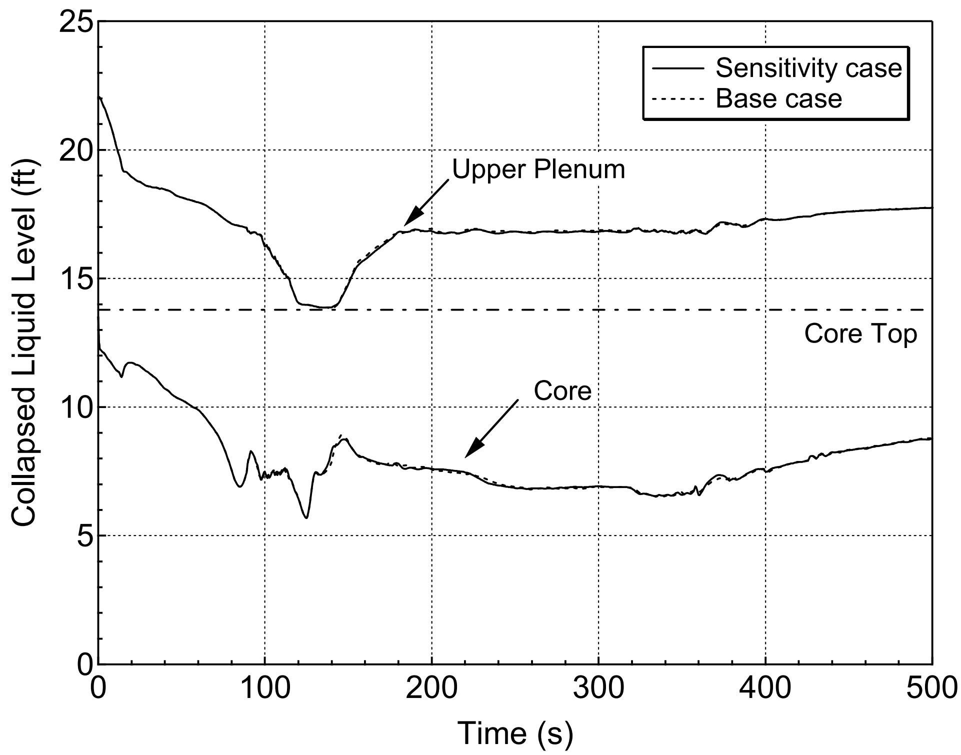

Figure 5.5.a-10 Hot Assembly Core and Upper Plenum Collapsed Levels for 7.5-inch Break (Top) (Time Step Size Sensitivity Study)

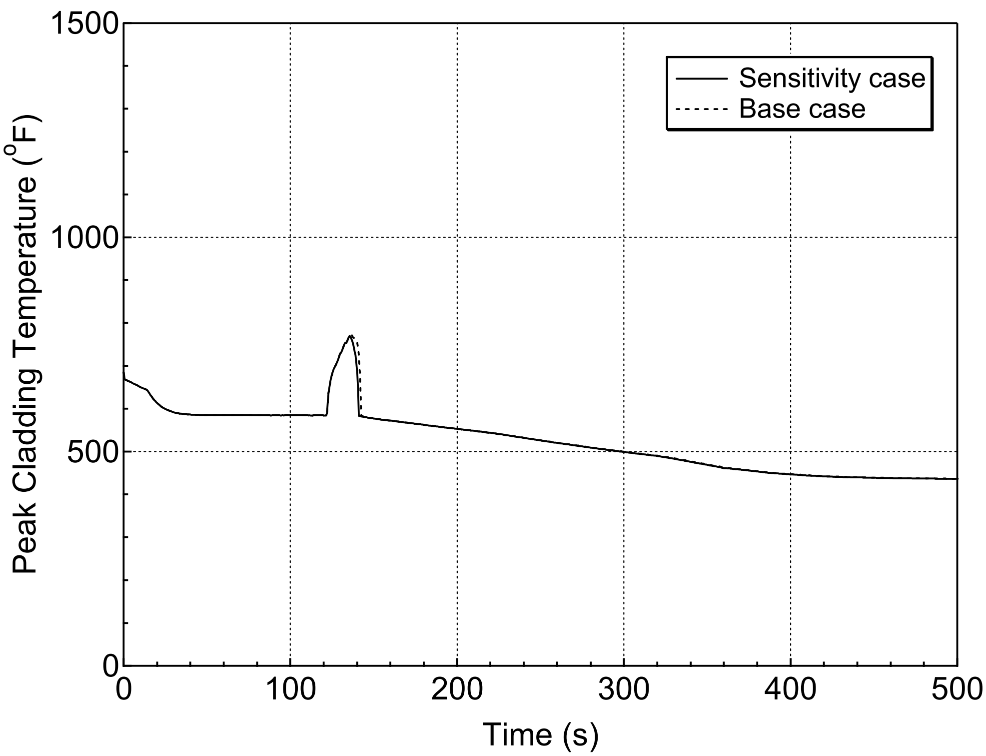

Figure 5.5.a-11 PCT at All Elevations for Hot Rod in Hot Assembly for 7.5-inch Break (Top) (Time Step Size Sensitivity Study)

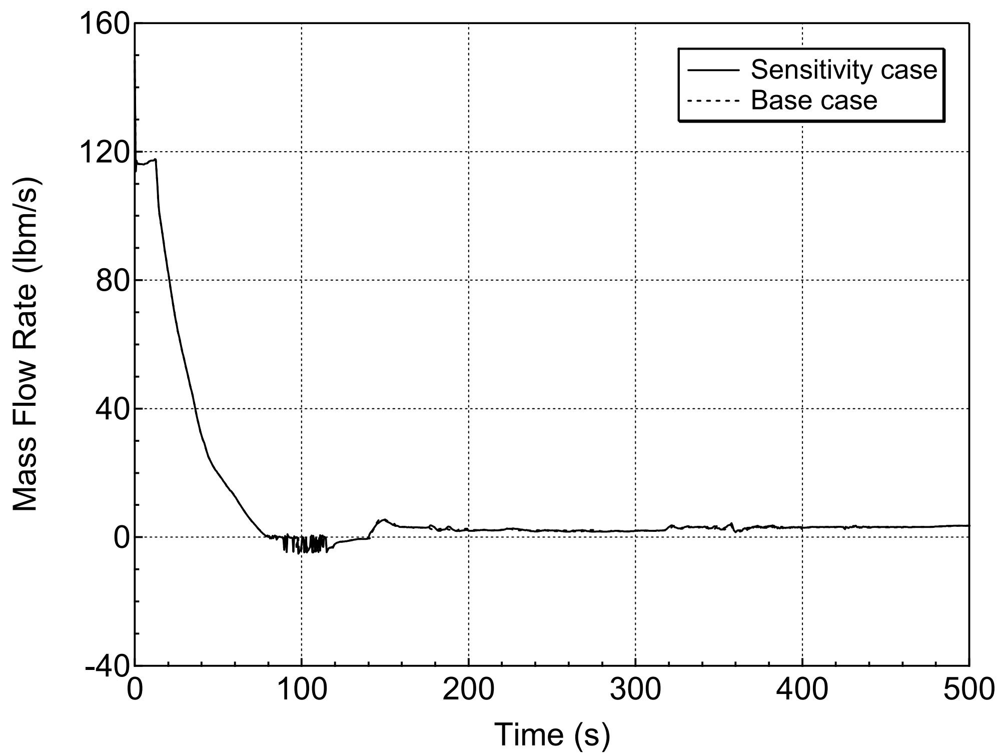

Figure 5.5.a-12 Hot Assembly Exit Liquid Mass Flowrate for 7.5-inch Break (Top) (Time Step Size Sensitivity Study)

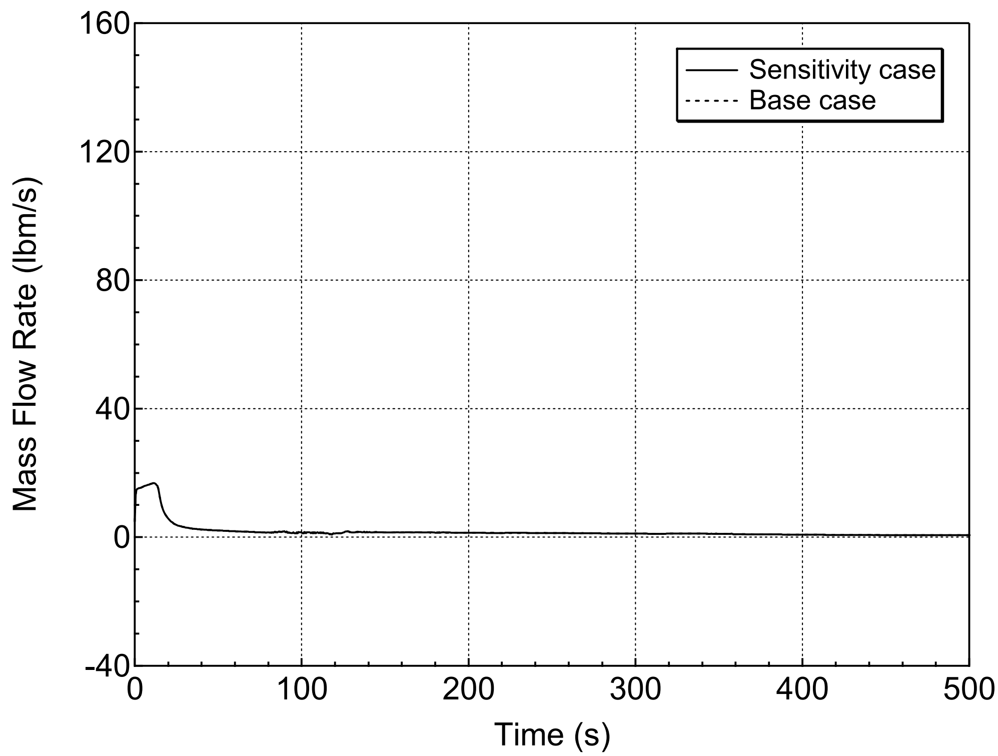

Figure 5.5.a-13 Hot Assembly Exit Vapor Mass Flowrate for 7.5-inch Break (Top) (Time Step Size Sensitivity Study)

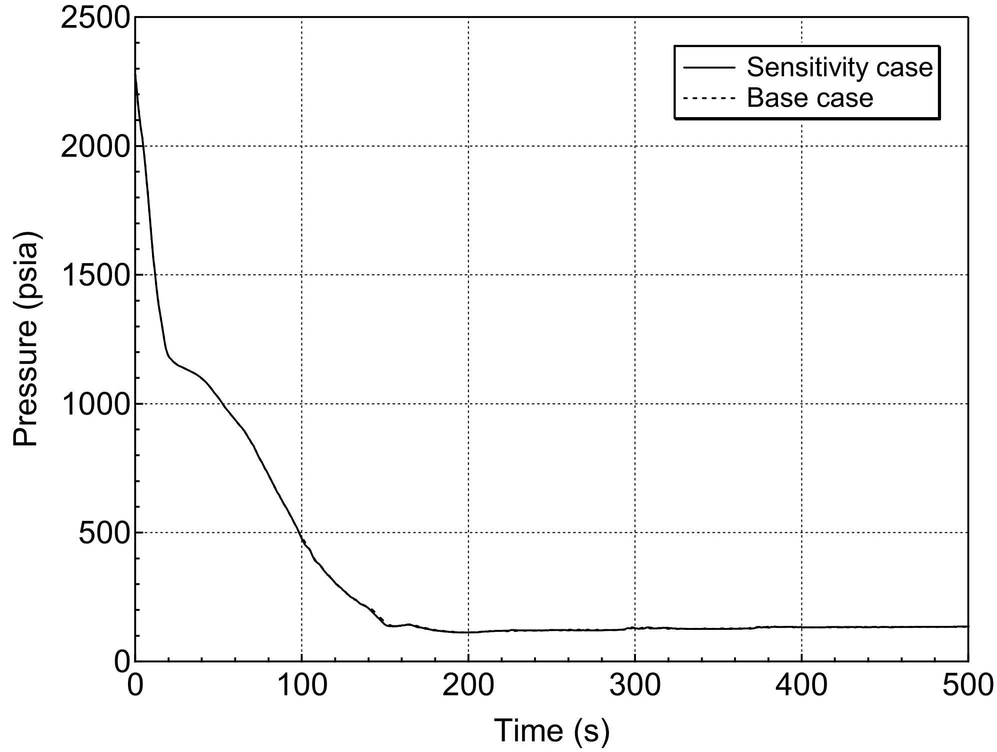

Figure 5.5.b-1 RCS (Pressurizer) Pressure Transient for 1-ft^2 Break (Top) (Time Step Size Sensitivity Study)

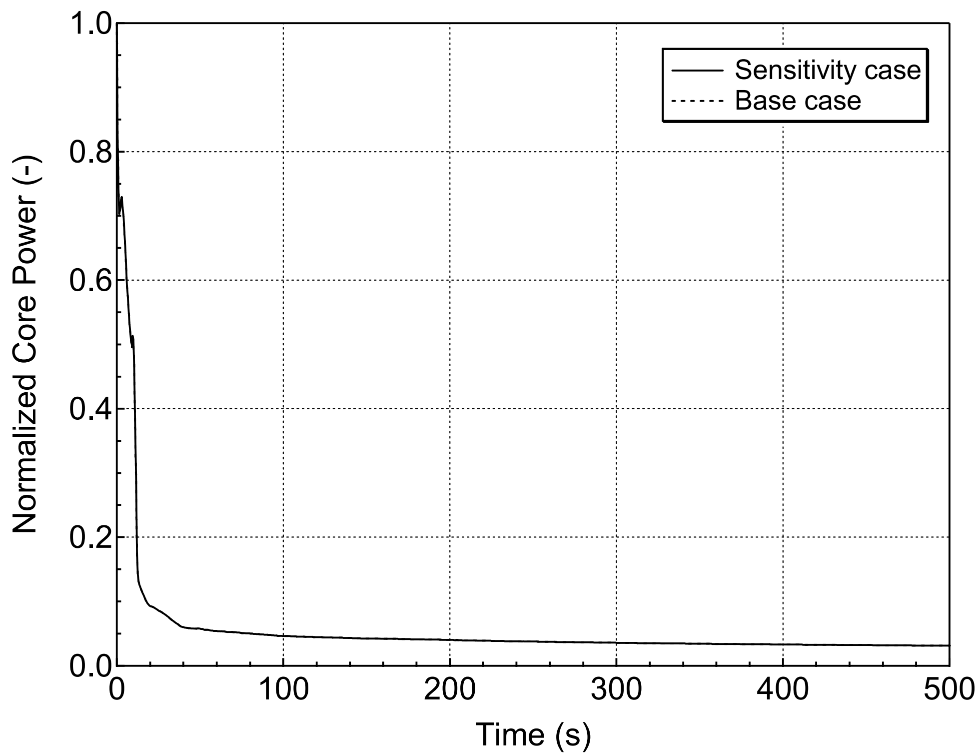

Figure 5.5.b-2 Normalized Core Power for 1-ft² Break (Top)
(Time Step Size Sensitivity Study)

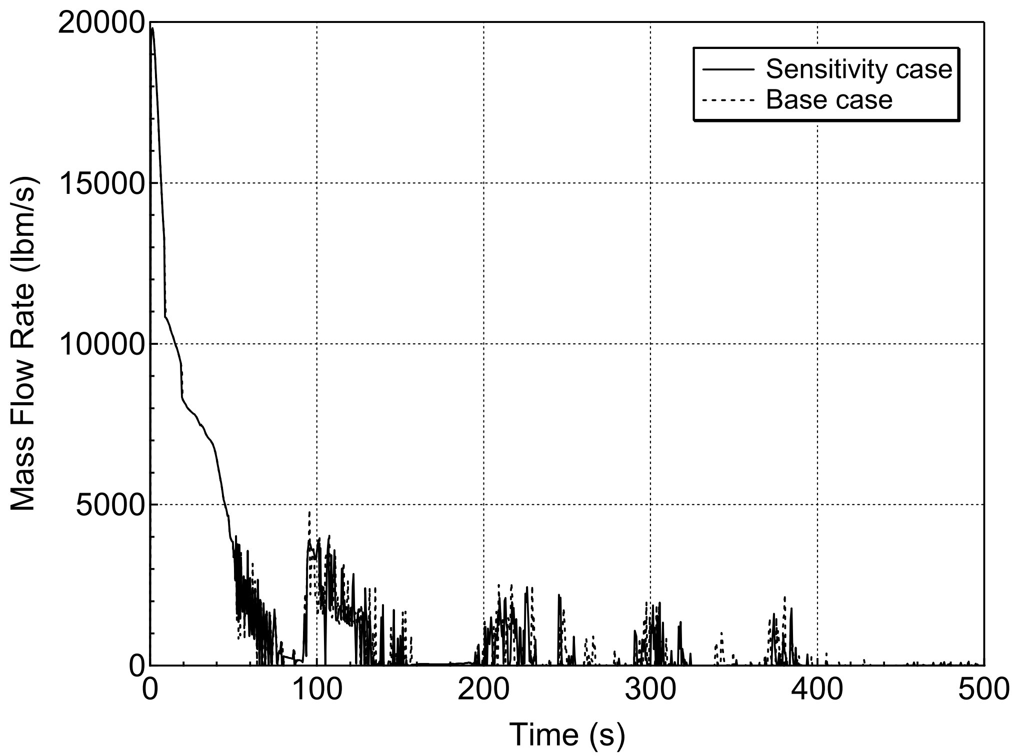

Figure 5.5.b-3 Liquid Discharge through the Break for 1-ft^2 Break (Top)
(Time Step Size Sensitivity Study)

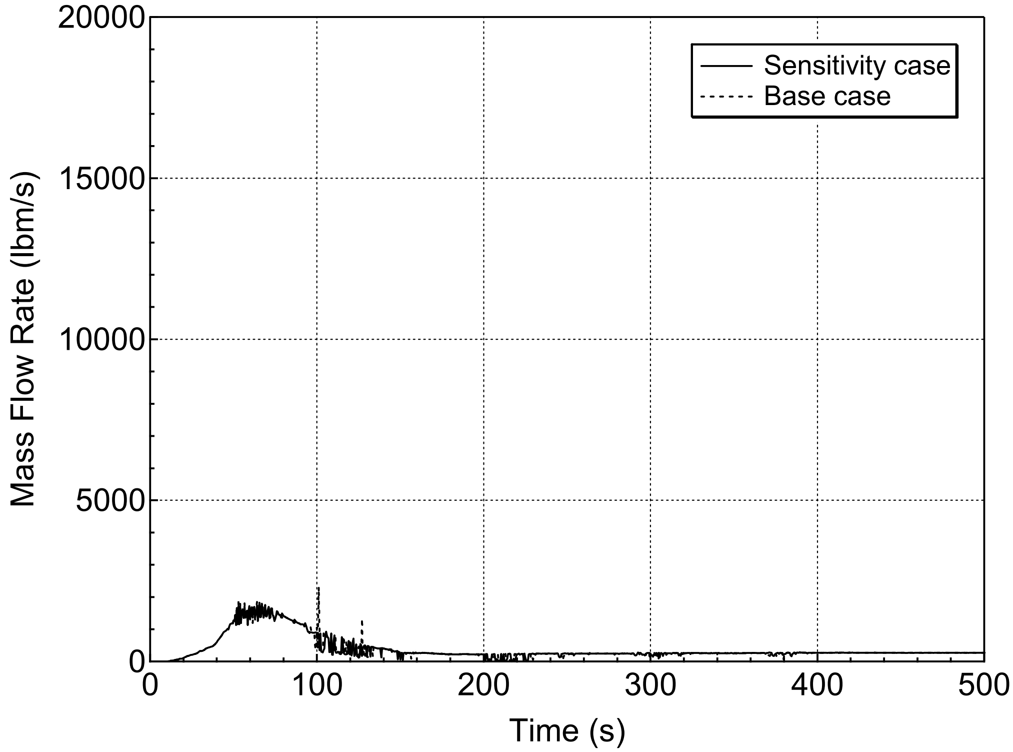

Figure 5.5.b-4 Vapor Discharge through the Break for 1-ft^2 Break (Top) (Time Step Size Sensitivity Study)

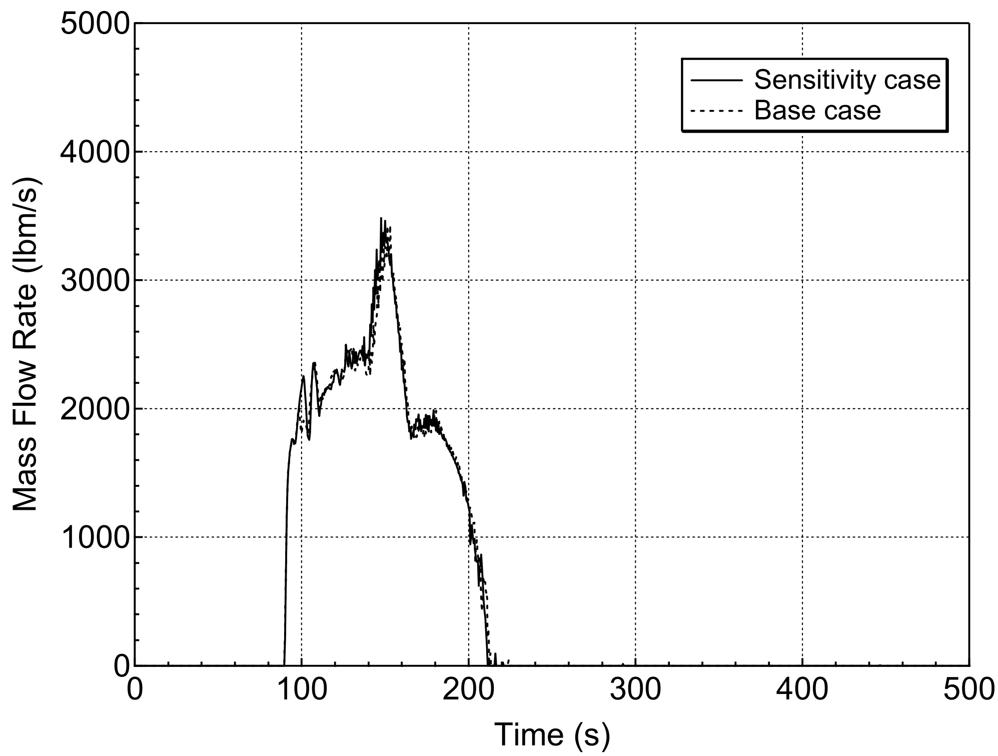

Figure 5.5.b-5 Accumulator Injection Mass Flowrate for 1-ft^2 Break (Top) (Time Step Size Sensitivity Study)

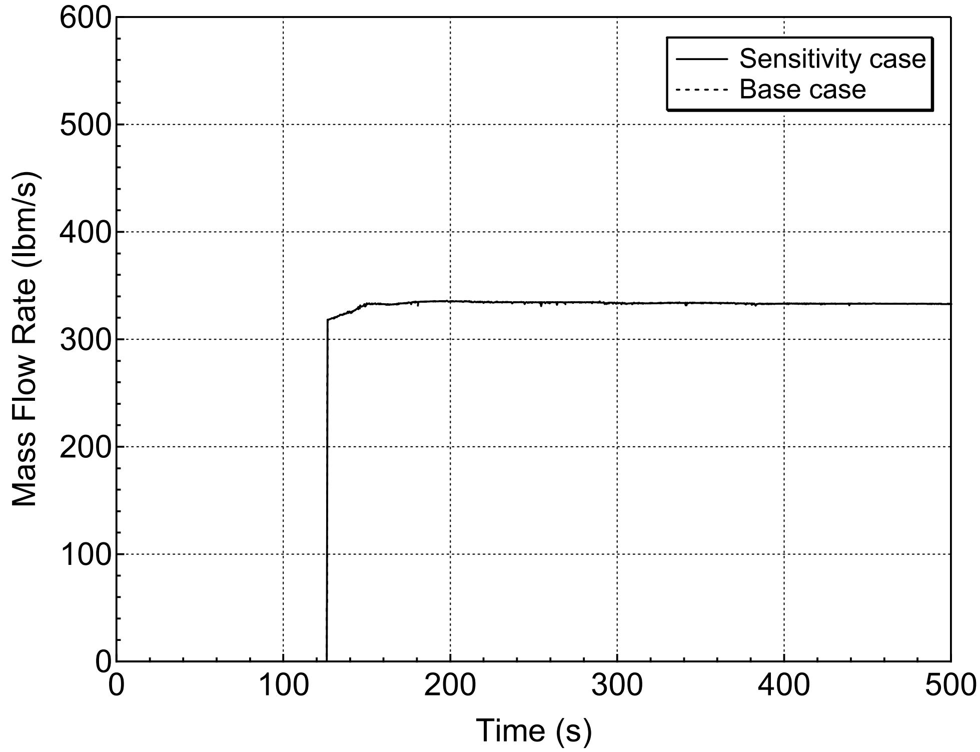

Figure 5.5.b-6 Safety Injection Mass Flowrate for 1-ft^2 Break (Top) (Time Step Size Sensitivity Study)

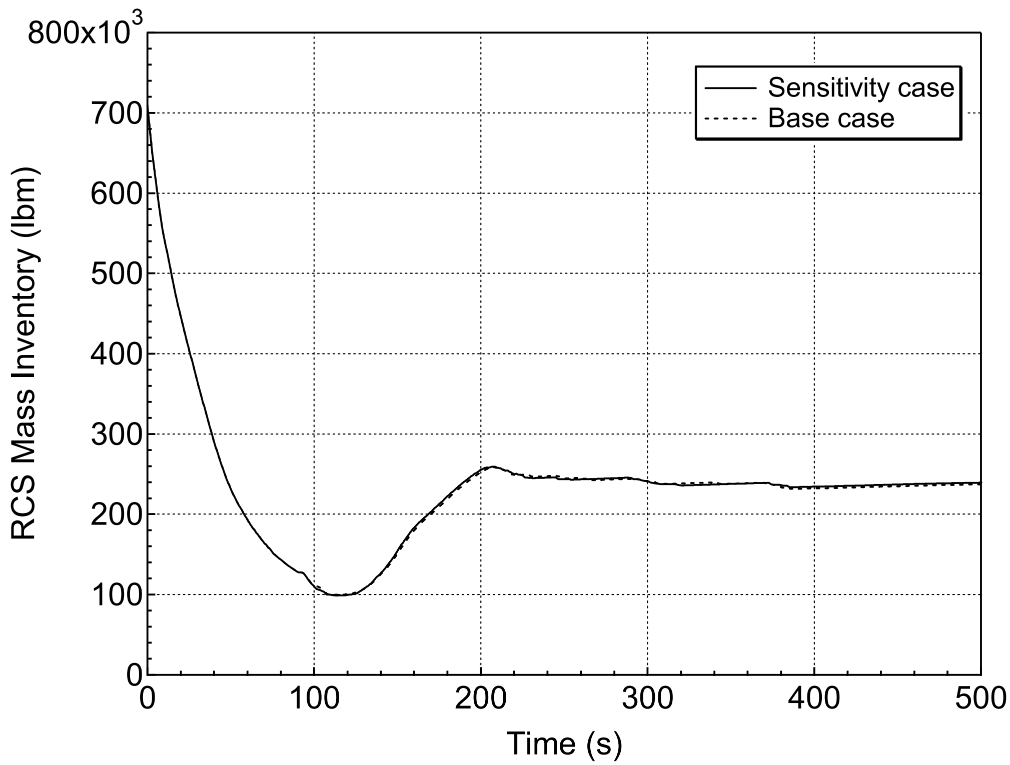

Figure 5.5.b-7 RCS Mass Inventory for 1-ft^2 Break (Top)
(Time Step Size Sensitivity Study)

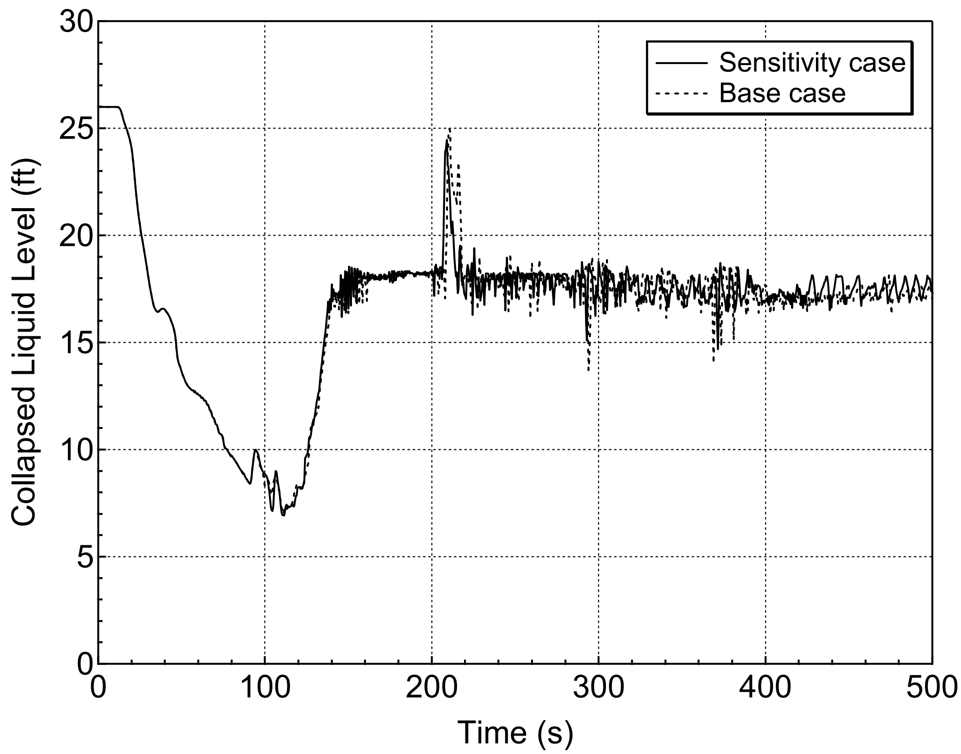

Figure 5.5.b-8 Downcomer Collapsed Level for 1-ft^2 Break (Top)
(Time Step Size Sensitivity Study)

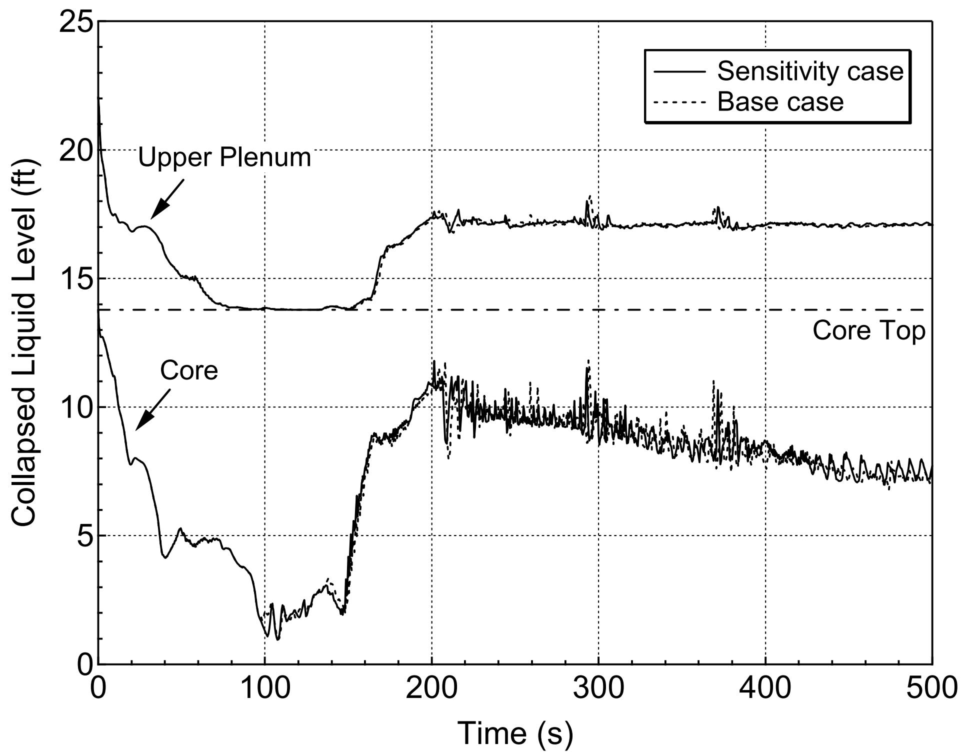

Figure 5.5.b-9 Average Core and Upper Plenum Collapsed Levels for 1-ft^2 Break (Top) (Time Step Size Sensitivity Study)

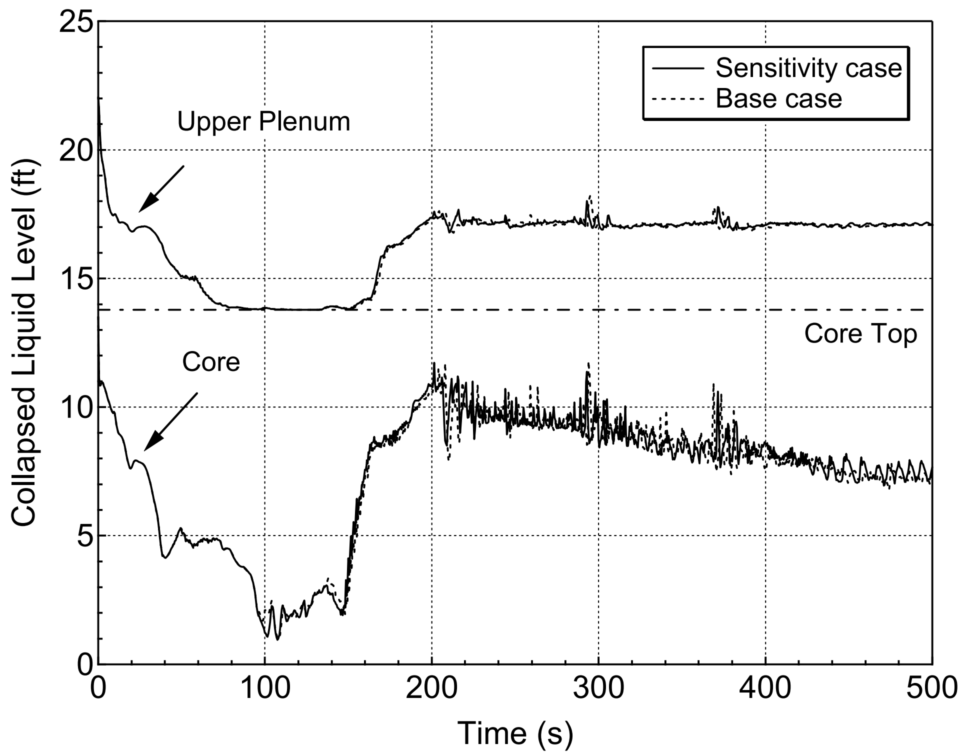

Figure 5.5.b-10 Hot Assembly Core and Upper Plenum Collapsed Levels for 1-ft^2 Break (Top) (Time Step Size Sensitivity Study)

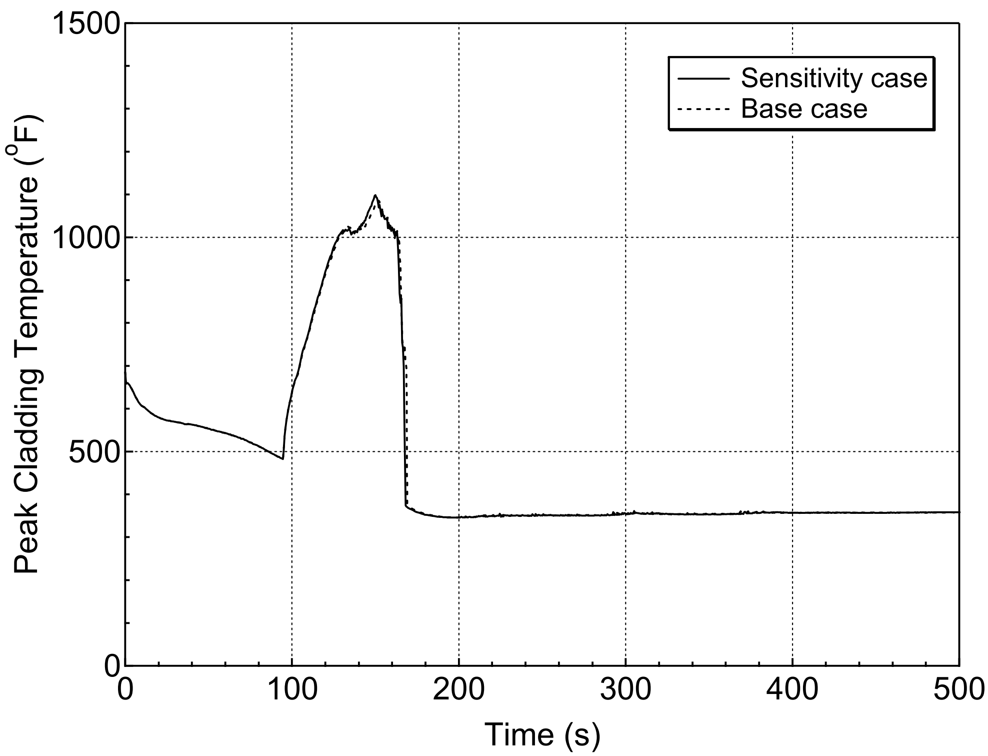

Figure 5.5.b-11 PCT at All Elevations for Hot Rod in Hot Assembly for 1-ft^2 Break (Top) (Time Step Size Sensitivity Study)

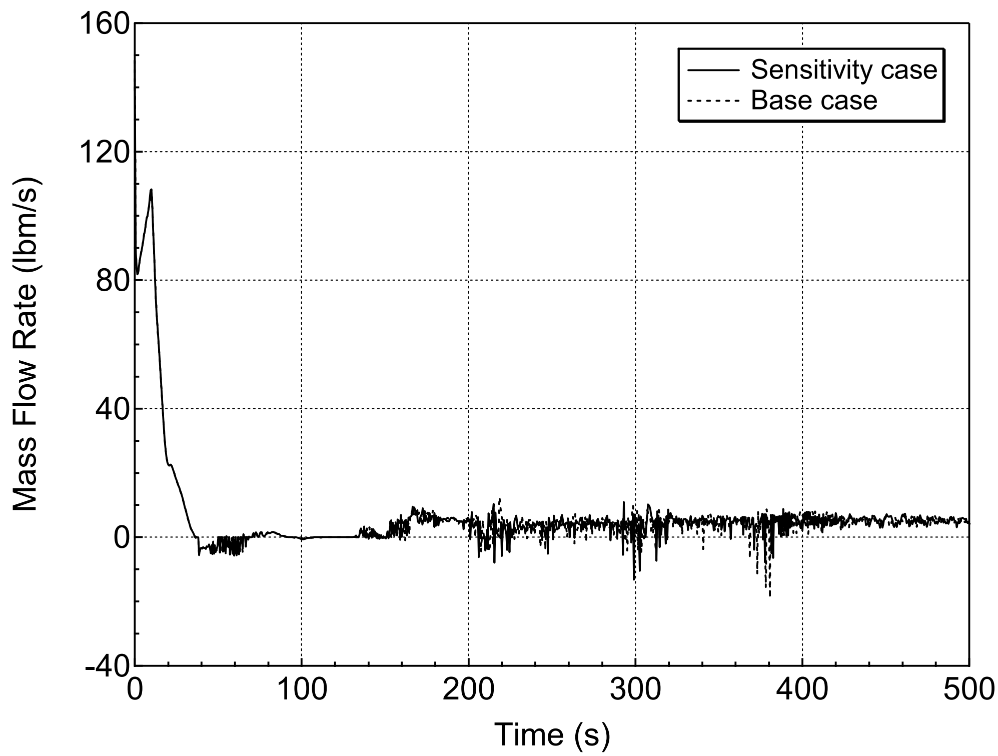

Figure 5.5.b-12 Hot Assembly Exit Liquid Mass Flowrate for 1-ft^2 Break (Top) (Time Step Size Sensitivity Study)

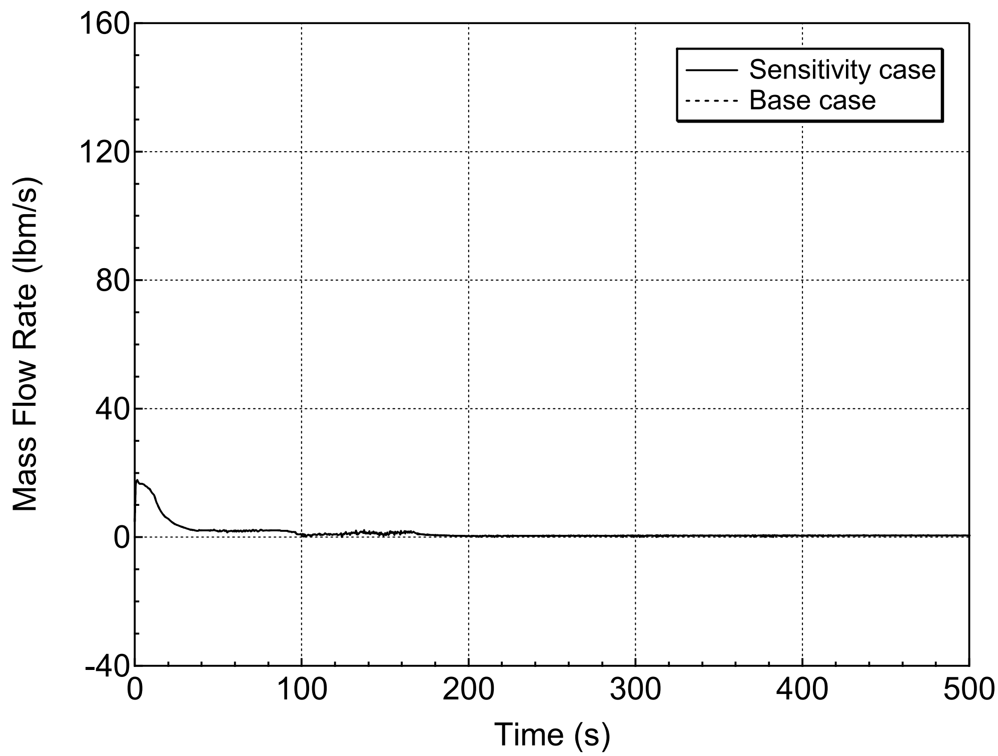

Figure 5.5.b-13 Hot Assembly Exit Vapor Mass Flowrate for 1-ft^2 Break (Top) (Time Step Size Sensitivity Study)

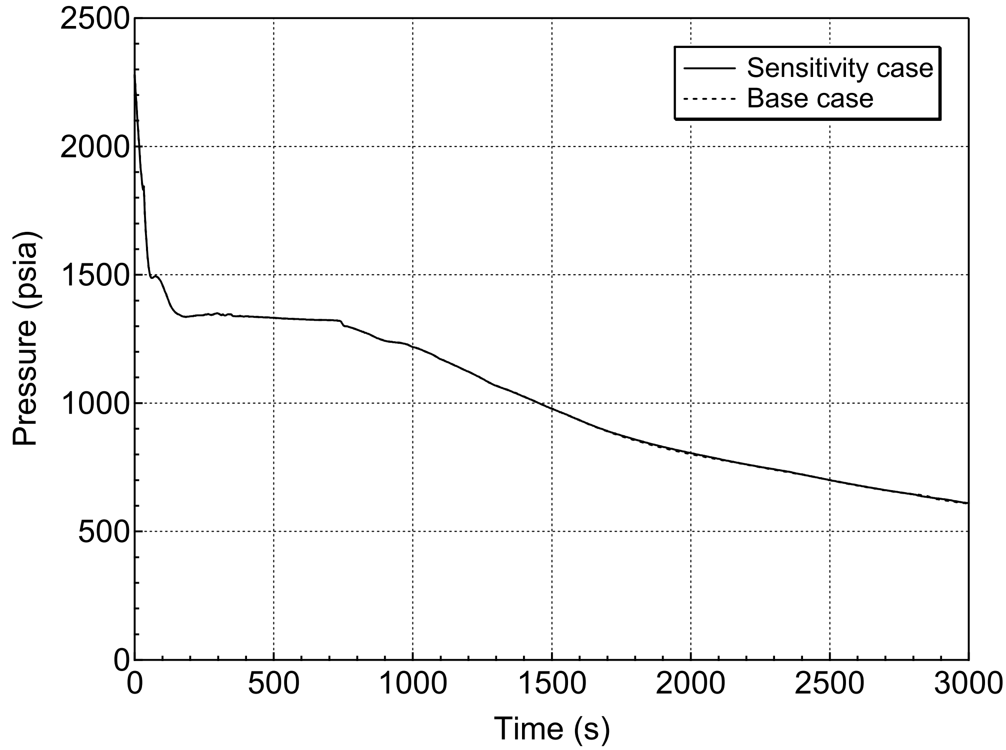

Figure 5.5.c-1 RCS (Pressurizer) Pressure Transient for DVI-line Break (Time Step Size Sensitivity Study)

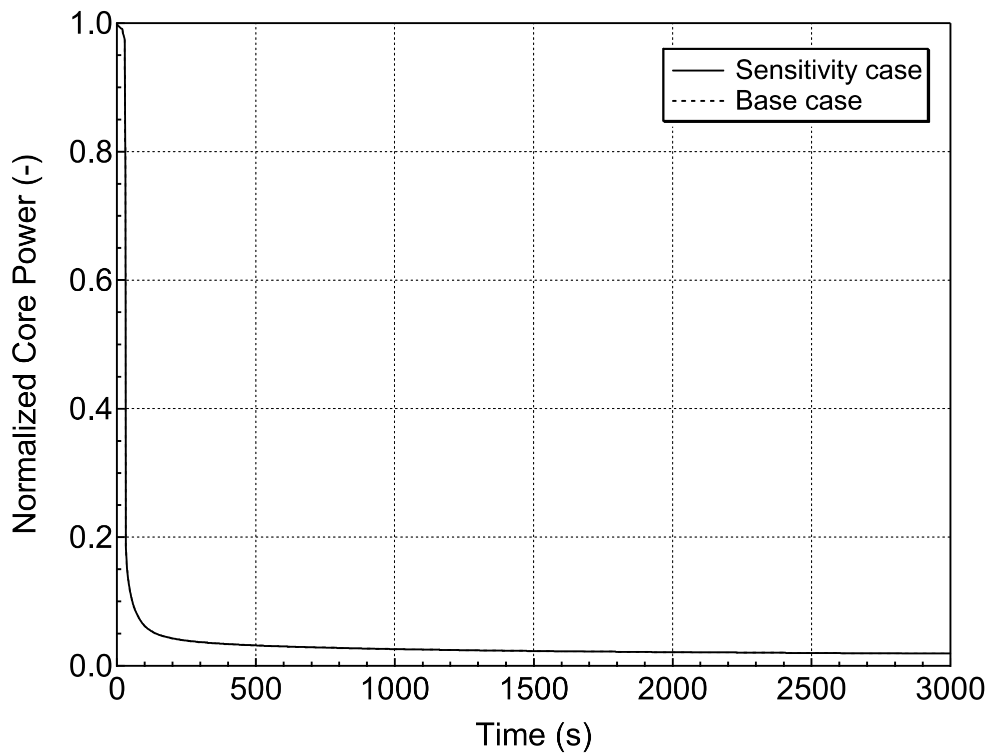

Figure 5.5.c-2 Normalized Core Power for DVI-line Break (Time Step Size Sensitivity Study)

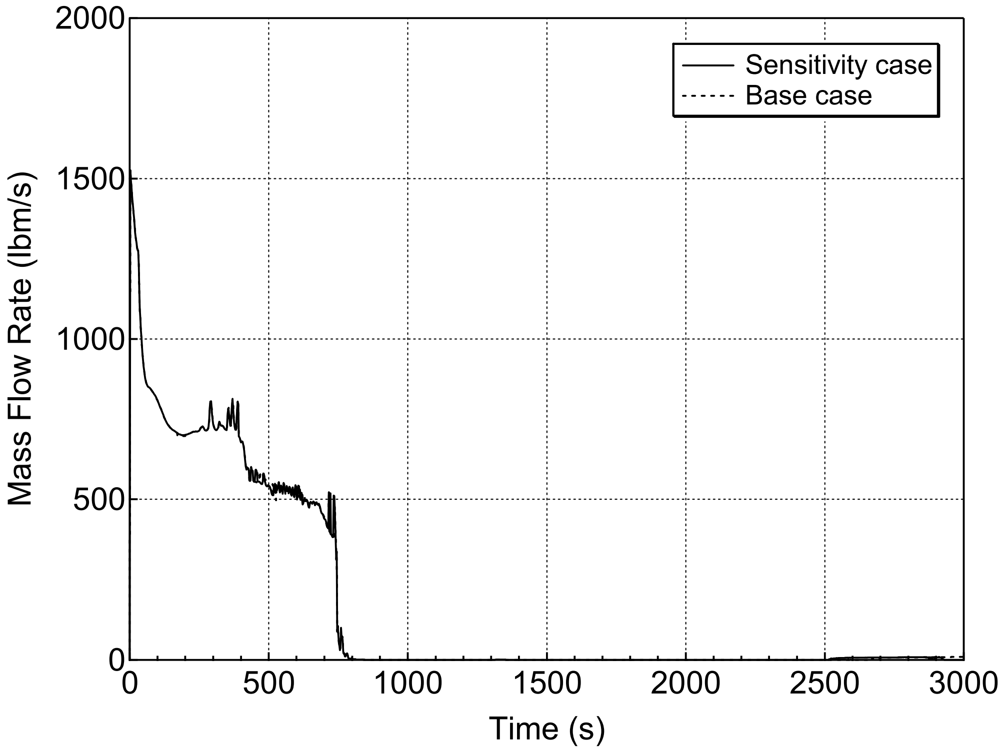

Figure 5.5.c-3 Liquid Discharge through the Break for DVI-line Break (Time Step Size Sensitivity Study)

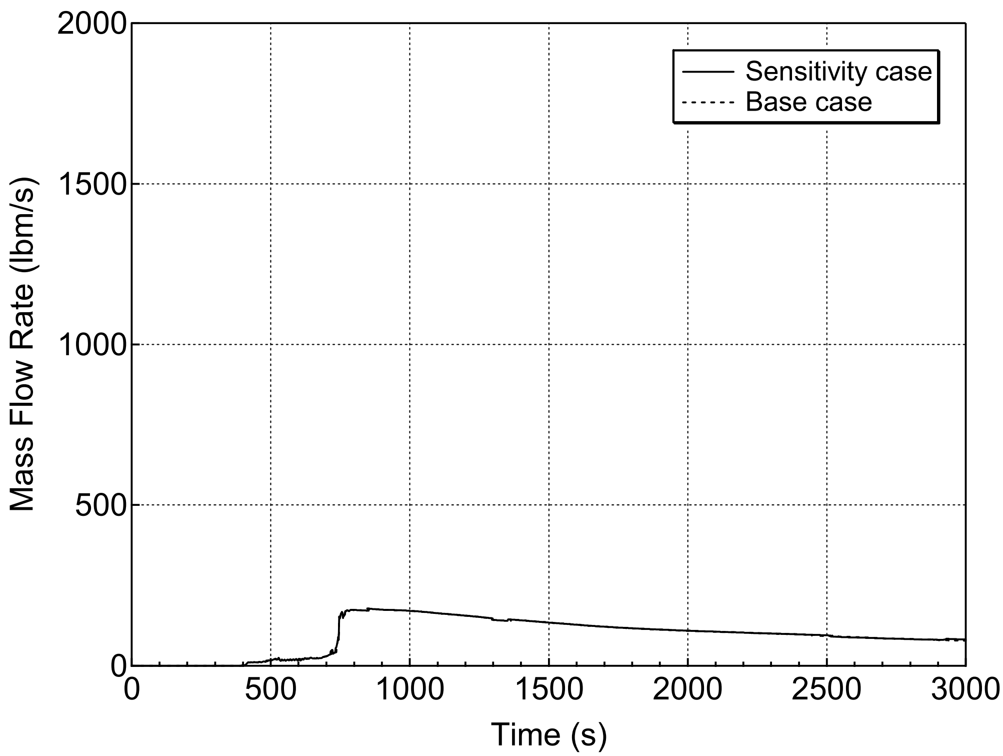

Figure 5.5.c-4 Vapor Discharge through the Break for DVI-line Break (Time Step Size Sensitivity Study)

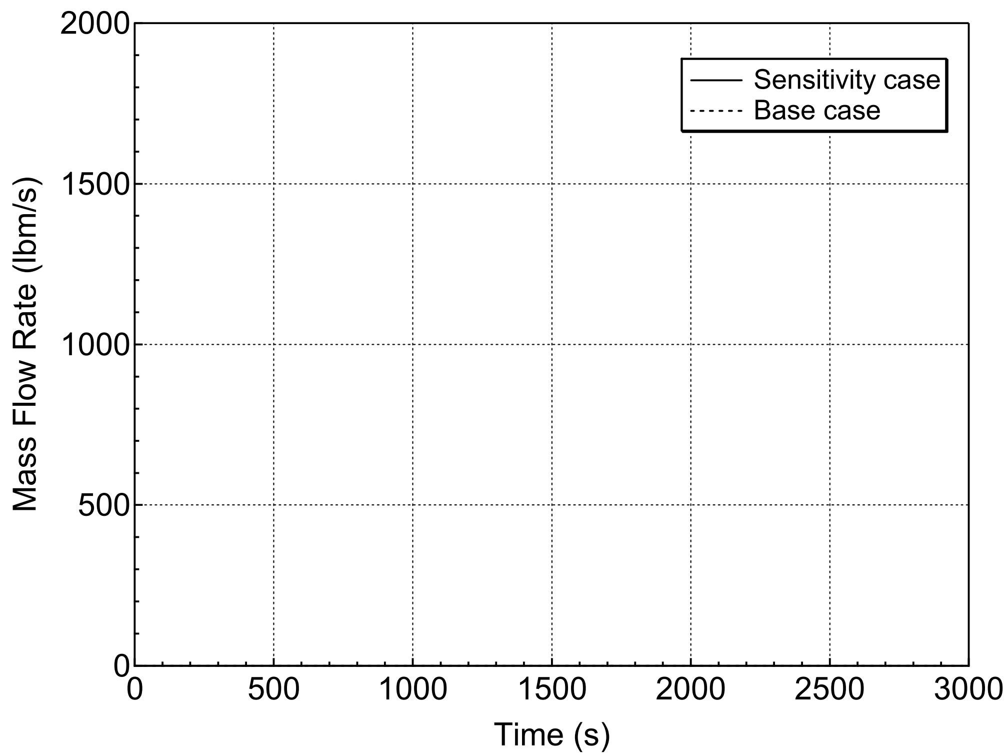

Figure 5.5.c-5 Accumulator Injection Mass Flowrate for DVI-line Break (Time Step Size Sensitivity Study)

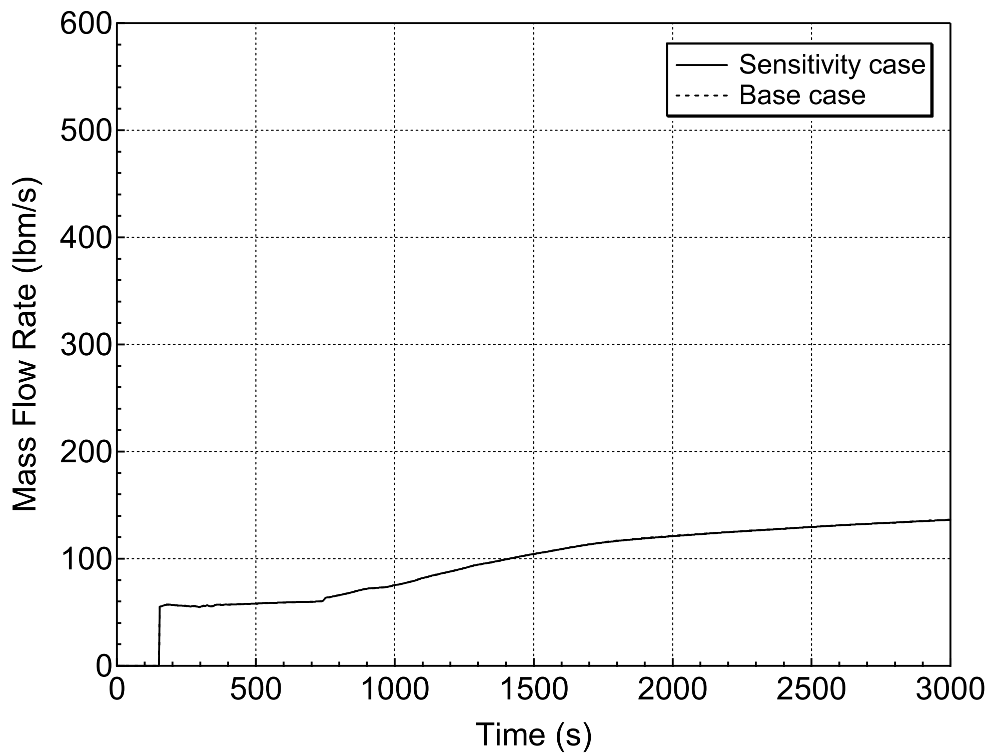

Figure 5.5.c-6 Safety Injection Mass Flowrate for DVI-line Break (Time Step Size Sensitivity Study)

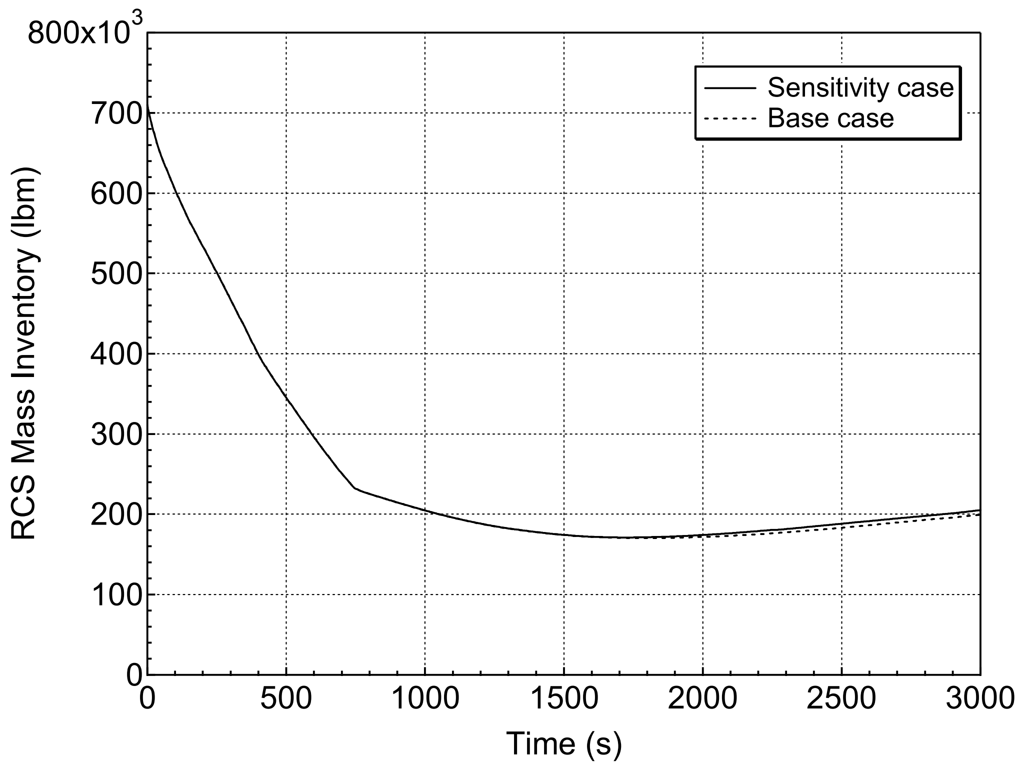

Figure 5.5.c-7 RCS Mass Inventory for DVI-line Break (Time Step Size Sensitivity Study)

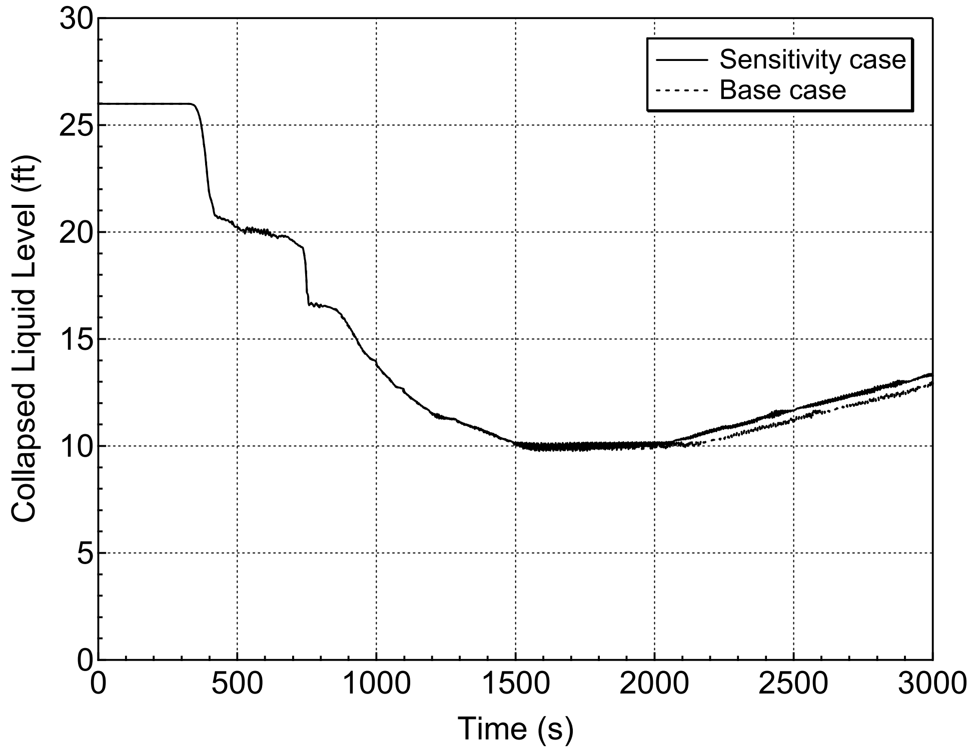

Figure 5.5.c-8 Downcomer Collapsed Level for DVI-line Break (Time Step Size Sensitivity Study)

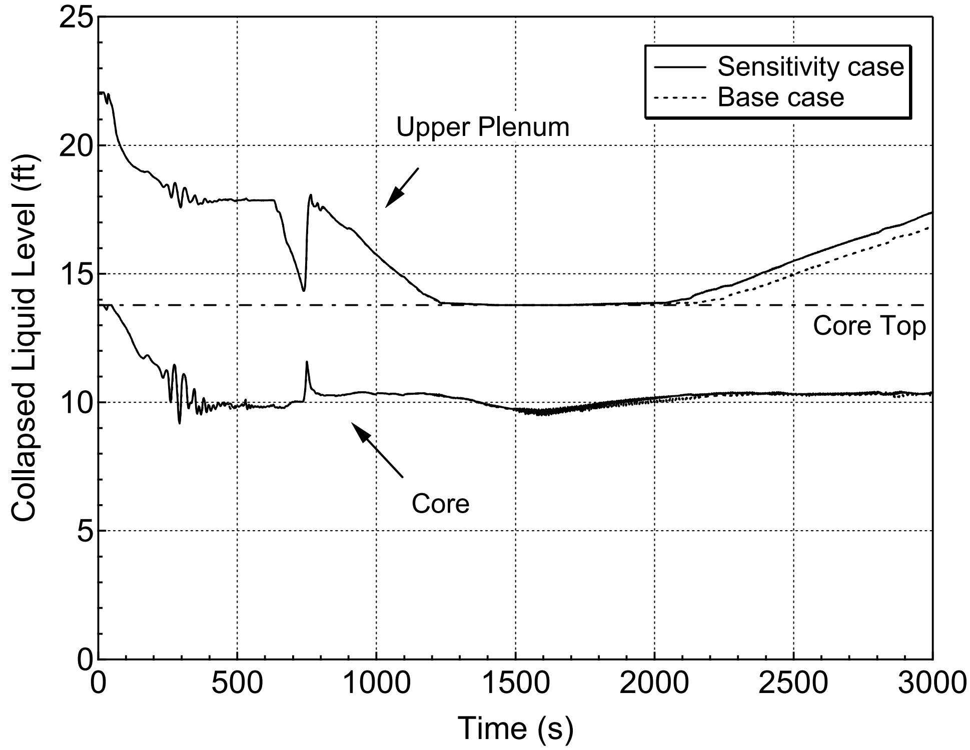

Figure 5.5.c-9 Average Core and Upper Plenum Collapsed Levels for DVI-line Break (Time Step Size Sensitivity Study)

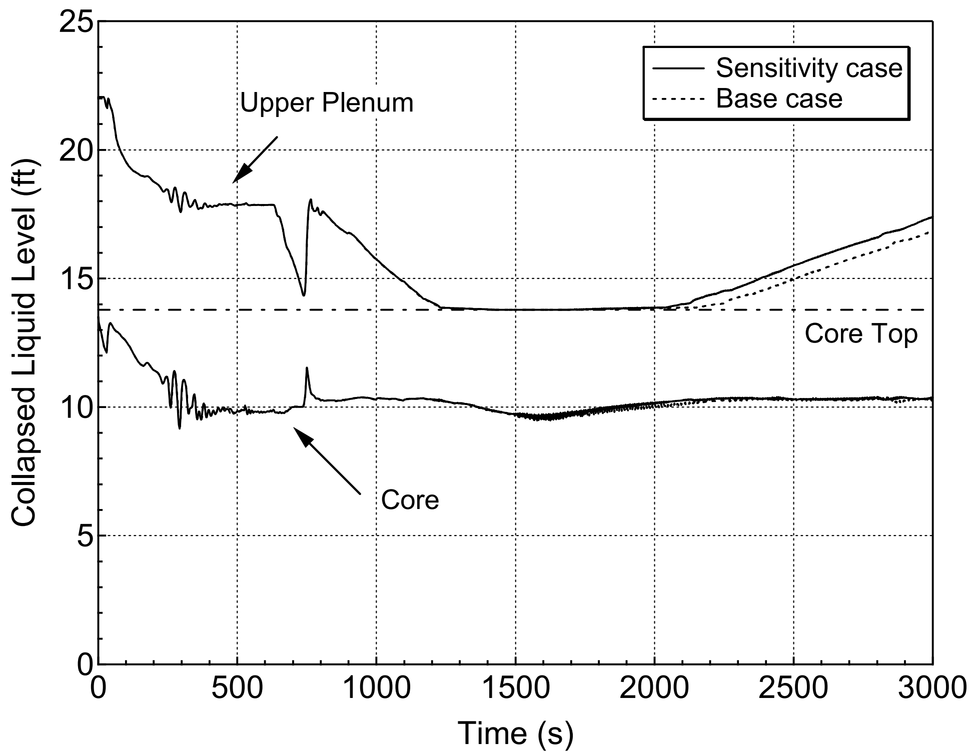

Figure 5.5.c-10 Hot Assembly Core and Upper Plenum Collapsed Levels for DVI-line Break (Time Step Size Sensitivity Study)

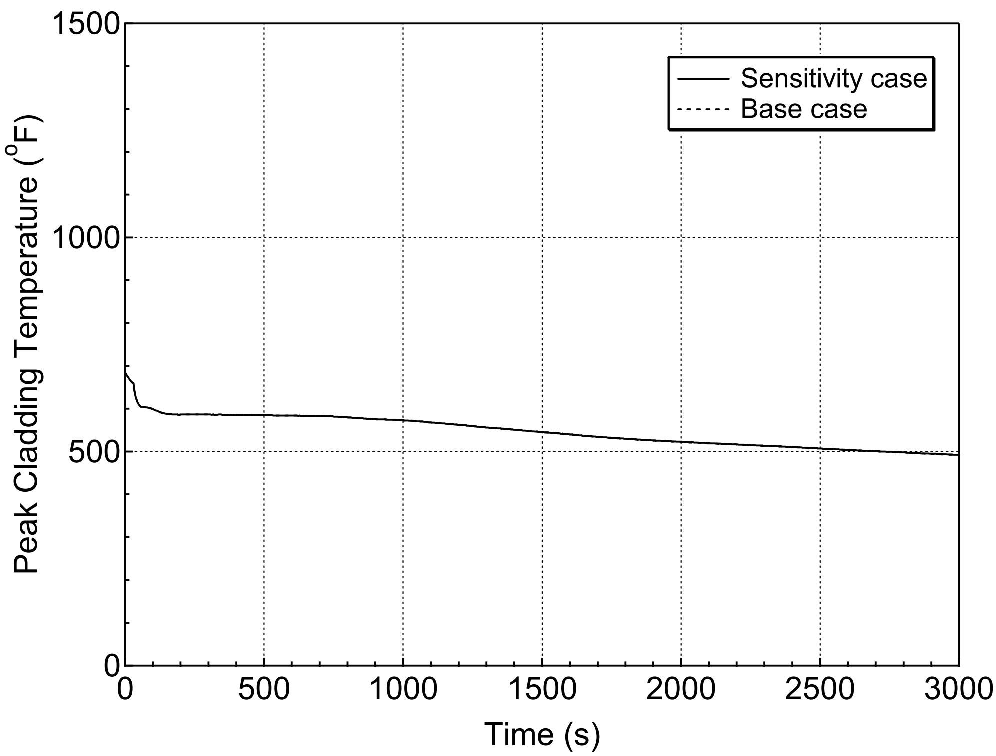

Figure 5.5.c-11 PCT at All Elevations for Hot Rod in Hot Assembly for DVI-line Break (Time Step Size Sensitivity Study)

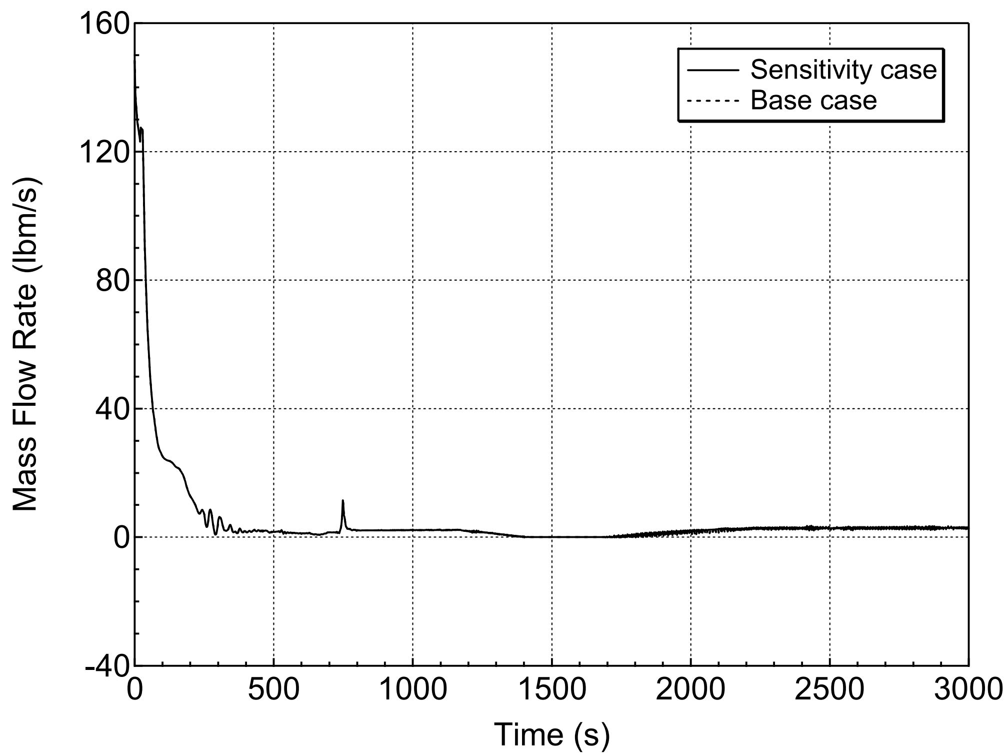

Figure 5.5.c-12 Hot Assembly Exit Liquid Mass Flowrate for DVI-line Break (Time Step Size Sensitivity Study)

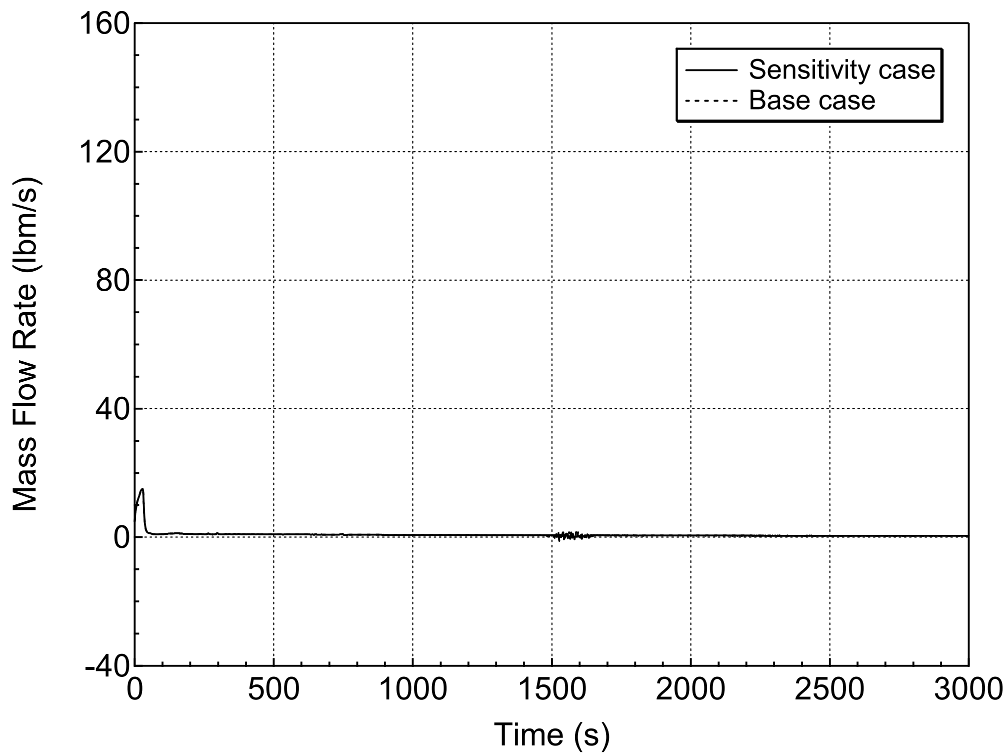

Figure 5.5.c-13 Hot Assembly Exit Vapor Mass Flowrate for DVI-line Break (Time Step Size Sensitivity Study)

5.6 Additional Sensitivity Study

Appendix A to 10 CFR Part 50 (Ref. 5-1) requires that a single failure shall be considered when analyzing ECCS performance, and that the analysis considers the effect of using only onsite power and only offsite power. Therefore, the additional sensitivity analyses were carried out to investigate the influence of adopting the single failure criteria and loss-of-offsite power assumption into the evaluation of ECCS performance in mitigating the limiting cases of SBLOCA scenarios.

5.6.1 Single Failure Criteria Sensitivity Analysis

The US-APWR adopts the four-train safety system. The assumed limiting single failure in the SBLOCA analysis is the loss of one ECCS train, with one additional train out-of-service for maintenance. In this case, only two SI pumps are available. In addition, two EFWS trains are also lost. However, all the four steam generators are still receiving EFW flow, supplied through the tie-lines from the available two EFW pumps.

On the contrary, when the single failure criteria are not adopted, three SI pumps are available because one train is still assumed out-of-service for maintenance. Three EFW pumps are available for cases without single failure criteria.

In this sensitivity analysis, the calculation with single failure criteria is compared with that without single failure criteria. Two limiting small break LOCA cases (7.5-inch and 1-ft^2 cold leg top orientation break) were selected for the analysis.

(1) Results of the 7.5-inch cold leg top orientation break case

Table 5.6.1-1 shows the sequence of events, and Table 5.6.1-2 summarizes the main results. Figure 5.6.1-1 shows the comparison of base-case and sensitivity-case on RCS (pressurizer) pressure transient calculation. The adoption of the criteria does not yield any influence in the first 150 seconds, then a slight change occurs as the base-case with the assumed single failure criteria calculates lower pressure values at the end of transient.

Figure 5.6.1-2 presents the normalized core power transient. The calculation results prove no influence caused by the single failure criteria.

Figure 5.6.1-3 displays the comparison of base-case and sensitivity-case on the liquid discharge through the break. The results are in agreement with very little difference.

The vapor discharge through the break is shown in Figure 5.6.1-4. It shows that the single failure criteria do not cause significant influence.

Figure 5.6.1-5 shows the comparison of accumulator injection mass flowrate time history. The comparison shows that a moderate impact occurs when simulating flow oscillation. The phenomena and basic transient profiles are similar.

Figure 5.6.1-6 depicts the time history of safety injection mass flowrate. The calculation results show that the sensitivity-case with three SI pumps available is capable to supply significantly higher mass flowrate into the core compared to the single failure case.

The RCS mass inventory transient is displayed in Figure 5.6.1-7. The calculation results of base-case and sensitivity-case are in agreement in the beginning of the transient. Then, the sensitivity-case calculates a higher gain in mass inventory from 150 seconds through the end of transient.

Figure 5.6.1-8 illustrates the downcomer collapsed level transient. The calculation results are in agreement in the beginning of the transient. Then the sensitivity-case calculates a higher gain in collapsed level from 250 seconds through the end of transient

Figure 5.6.1-9 shows the average core and upper plenum collapsed levels. The comparison shows moderate influence of adopting the single failure criteria, but the transient profiles are similar.

The hot assembly core and upper plenum collapsed levels are given in Figure 5.6.1-10. The comparison shows moderate influence of the single failure criteria, but again the transient profiles are similar. The sensitivity-case with three SI pumps available is capable to regain the collapsed level compared to the base-case.

The comparison of base-case and sensitivity-case on PCT at all elevations for hot rod in hot assembly is presented in Figure 5.6.1-11. The results show small influence of the single failure criteria in calculating the down slope after the PCT and also towards the end of the transient.

Figure 5.6.1-12 presents the hot assembly exit liquid mass flowrate transient calculation comparison between base-case and sensitivity-case. In both cases, the oscillating high frequency low amplitude flow reversals are similar.

Figure 5.6.1-13 presents the hot assembly exit vapor mass flowrate. The calculation results of base-case and sensitivity-case are also in agreement.

(2) Results of the 1-ft^2 cold leg top orientation break case

Table 5.6.1-3 shows the sequence of events and Table 5.6.1-4 summarizes the main results. Figure 5.6.1-14 shows the comparison of base-case and sensitivity-case on RCS (pressurizer) pressure transient calculation. The calculation results are in good agreement in the first 150 seconds, then a slight difference occurs as the sensitivity-case with three SI pumps available calculates initially higher pressure in the middle of transient.

Figure 5.6.1-15 presents the normalized core power transient. The calculation results prove no influence caused by the adoption of single failure criteria. The results of base-case and sensitivity-case are in agreement.

Figure 5.6.1-16 displays the comparison of base-case and sensitivity-case on the liquid discharge through the break. The results are in agreement with moderate difference in calculating the flashing phenomena of flow discharge from the break.

The vapor discharge through the break is shown in Figure 5.6.1-17. The results are in agreement.

Figure 5.6.1-18 shows the comparison of accumulator injection mass flowrate time history. The comparison shows a good agreement.

Figure 5.6.1-19 depicts the time history of safety injection mass flowrate. The sensitivity-case with three SI pumps available is capable to supply significantly higher mass flowrate from the SI pumps into the core compared to the single failure case.

The RCS mass inventory transient is displayed in Figure 5.6.1-20. The calculation results of base-case and sensitivity-case are in agreement from the beginning of the transient to the end of transient.

Figure 5.6.1-21 illustrates the downcomer collapsed level transient. The calculation results of base-case and sensitivity-case are in agreement in the beginning of the transient, then the sensitivity-case calculates higher gain in collapsed level due to the availability of three SI pumps.

Figure 5.6.1-22 shows the average core and upper plenum collapsed levels. The comparison shows moderate influence of single failure criteria but the transient profiles are similar.

The hot assembly core and upper plenum collapsed levels are given in Figure 5.6.1-23. The comparison shows moderate influence but again the transient profiles are similar. The sensitivity-case with three SI pumps available is capable to regain the collapsed level compared with the base case.

The comparison of base case and sensitivity case on PCT at all elevations for hot rod in hot assembly is presented in Figure 5.6.1-24. The results show a small influence when calculating the down slope after the PCT, and also at the end of the transient. The base-case shows a slight delay in upper core recovery due to the single failure assumption.

Figure 5.6.1-25 presents the hot assembly exit liquid mass flowrate transient calculation comparison between base-case and sensitivity-case. In both cases, the oscillating high frequency low amplitude flow reversals are similar.

Figure 5.6.1-26 presents the hot assembly exit vapor mass flowrate. The calculation results of base-case and sensitivity-case are also perfectly in agreement.

It is concluded that the effect of single failure assumption is that it results in a slightly higher calculated PCT.

5.6.2 Offsite Power Availability Sensitivity Analysis

In this sensitivity analysis, the calculation with the loss-of-offsite power (LOOP) assumption (base-case) is compared against that with offsite power available (sensitivity-case). Two limiting small break LOCA cases (7.5-inch and 1-ft^2 cold leg top orientation break) are selected for the analysis.

(1) Results of the 7.5-inch cold leg top orientation break case

Figure 5.6.2-1 shows the comparison of base-case and sensitivity-case on RCS (pressurizer) pressure transient calculation. The calculation results show moderate influence of the offsite power availability as the sensitivity-case predicts slightly higher pressure transient compared with the base case with the assumed LOOP.

Figure 5.6.2-2 presents the normalized core power transient. The results of base-case and sensitivity-case are in agreement.

Figure 5.6.2-3 displays the comparison of base-case and sensitivity-case on the liquid discharge through the break. The results are in agreement and show only a slight influence of the offsite power availability.

The vapor discharge through the break is shown in Figure 5.6.2-4. The results are in agreement with only a slight difference

Figure 5.6.2-5 shows the comparison of accumulator injection mass flowrate time history. The comparison shows a moderate influence when simulating the flow oscillation. The base-case (LOOP) calculates early injection of accumulator at 315 seconds where for the sensitivity-case with offsite power available shows that the accumulator injection occurs about 25 seconds later. However, the phenomena and basic transient profiles are similar.

Figure 5.6.2-6 depicts the time history of safety injection mass flowrate. The calculation results of sensitivity-case actuate the SI pumps at 30 seconds, which is 100 seconds earlier than the LOOP base-case. However, it calculates lower SI pumps mass flow rate.

The RCS mass inventory transient is displayed in Figure 5.6.2-7. The calculation results of base-case and sensitivity-case are in agreement in the beginning of the transient. Then the sensitivity-case calculates higher gain in mass inventory from 30 seconds through the middle of transient.

Figure 5.6.2-8 illustrates the downcomer collapsed level transient. The calculation results of base-case and sensitivity-case show a moderate influence of offsite power availability, in which the base-case calculates substantially higher collapsed level gain.

Figure 5.6.2-9 shows the average core and upper plenum collapsed levels. The comparison shows a moderate impact of LOOP. For the core collapsed level, the sensitivity case calculates higher level gain in the beginning through the middle of transient. A similar explanation also applies for the upper plenum collapsed level transient.

The hot assembly core and upper plenum collapsed levels are given in Figure 5.6.2-10. The same explanation as above applies to this figure.

The comparison of base-case and sensitivity-case on PCT at all elevations for hot rod in hot assembly is presented in Figure 5.6.2-11. The results show a significant influence of offsite power availability in the PCT. For the base-case (LOOP), the PCT of 775°F occurs at 136 seconds. In contrast, for the offsite power available case, no heatup occurs after the break.

Figure 5.6.2-12 presents the hot assembly exit liquid mass flowrate transient calculation comparison between base-case and sensitivity-case. The results show some differences. The sensitivity-case calculates a slight delay in the reduction of mass flow rate, because the RCP trip is delayed.

Figure 5.6.2-13 presents the hot assembly exit vapor mass flowrate. The calculation results of base case and sensitivity case are in good agreement.

(2) Results of the 1-ft^2 cold leg top orientation break case

Similar explanation applies for the 1-ft^2 small-break case. From the comparison results between the base-case with LOOP assumption and the sensitivity-case with the offsite power available, there occurs small to moderate differences when calculating the main parameters of interest. For the PCT calculation, substantial difference occurs, which is understandable for the offsite power sensitivity study. The base-case calculates the PCT of 1088°F that occurs at 169 seconds, while the sensitivity-case yields 773°F which is 315°F lower than the base-case, 17 seconds earlier. The difference is comprehensible, because the high head injection system (HHIS) and the EFW pumps are operated much earlier when the offsite power is available. Hence, the sensitivity-case generates lower PCT that occurs at a later time, because the RCPs run longer and the SI pumps start earlier.

It is concluded that the effect of LOOP assumption is that it results in a higher calculated PCT.

Table 5.6.1-1 Sequence of Events for 7.5-inch Break (Top)
(No Single Failure Sensitivity Study)

Event	Time (sec)	
	Base case	Sensitivity case
Break occurs; blowdown initiation	0.0	0.0
Reactor trip (loss-of-offsite power is assumed)	9.3	9.3
Control rod insertion starts	11.1	11.1
Main steam isolation	11.1	11.1
ECCS actuation signal	11.9	11.9
RCP trip	12.3	12.3
Main feedwater isolation	17.3	17.3
Main steam safety valve open	81	81
Emergency Power Source initiates	115	115
Fuel cladding starts heating up	122	122
High Head Injection System begins	130	130
Peak Cladding Temperature occurs	136	136
Fuel cladding rewets	143	142
Emergency feedwater flow begins	145	145
Accumulator injection begins	315	312

Table 5.6.1-2 Core Performance Results for 7.5-inch Break (Top)
(No Single Failure Sensitivity Study)

	Values	
	Base case	Sensitivity case
Peak Cladding Temperature (°F)	775	772
Maximum local cladding oxidation (%)	0.2	0.2
Maximum core wide cladding oxidation (%)	less than 0.2	less than 0.2

Table 5.6.1-3 Sequence of Events for 1-ft^2 Break (Top)
(No Single Failure Sensitivity Study)

Event	Time (sec)	
	Base case	Sensitivity case
Break occurs; blowdown initiation	0.0	0.0
Reactor trip (loss-of-offsite power is assumed)	6.9	6.9
ECCS actuation signal	8.3	8.3
Control rod insertion starts	8.7	8.7
Main steam isolation	8.7	8.7
RCP trip	9.9	9.9
Main feedwater isolation	14.9	14.9
Main steam safety valve open	not actuated	not actuated
Accumulator injection begins	89	89
Fuel cladding starts heating up	95	95
Emergency Power Source initiates	111	111
High Head Injection System begins	126	126
Emergency feedwater flow begins	141	141
Peak Cladding Temperature occurs	151	151
Fuel cladding rewets	169	167

Table 5.6.1-4 Core Performance Results for 1-ft^2 Break (Top)
(No Single Failure Sensitivity Study)

	Values	
	Base case	Sensitivity case
Peak Cladding Temperature (°F)	1088	1086
Maximum local cladding oxidation (%)	0.2	0.2
Maximum core wide cladding oxidation (%)	less than 0.2	less than 0.2

Table 5.6.2-1 Sequence of Events for 7.5-inch Break (Top) (Offsite Power Available Sensitivity Study)

Event	Time (sec)	
	Base case	Sensitivity case
Break occurs; blowdown initiation	0.0	0.0
Reactor trip	9.3	9.3
Control rod insertion starts	11.1	11.1
Main steam isolation	11.1	11.1
ECCS actuation signal	11.9	11.9
RCP trip	12.3	29.9
Main feedwater isolation	17.3	17.3
Main steam safety valve open	81	113
Emergency Power Source initiates	115	N/A (Offsite power available)
Fuel cladding starts heating up	122	not occur
High Head Injection System begins	130	29.9
Peak Cladding Temperature occurs	136	lower than the initial temperature
Fuel cladding rewets	143	N/A
Emergency feedwater flow begins	145	72
Accumulator injection begins	315	339

Table 5.6.2-2 Core Performance Results for 7.5-inch Break (Top) (Offsite Power Available Sensitivity Study)

	Values	
	Base case	Sensitivity case
Peak Cladding Temperature (°F)	775	lower than the initial temperature
Maximum local cladding oxidation (%)	0.2	0.2
Maximum core wide cladding oxidation (%)	less than 0.2	less than 0.2

Table 5.6.2-3 Sequence of Events for 1-ft^2 Break (Top)
(Offsite Power Available Sensitivity Study)

Event	Time (sec)	
	Base case	Sensitivity case
Break occurs; blowdown initiation	0.0	0.0
Reactor trip	6.9	6.9
ECCS actuation signal	8.3	8.3
Control rod insertion starts	8.7	8.7
Main steam isolation	8.7	8.7
RCP trip	9.9	26.3
Main feedwater isolation	14.9	14.9
Main steam safety valve open	not actuated	not actuated
Accumulator injection begins	89	94
Fuel cladding starts heating up	95	100
Emergency Power Source initiates	111	N/A (Offsite power available)
High Head Injection System begins	126	26.3
Emergency feedwater flow begins	141	68
Peak Cladding Temperature occurs	151	129
Fuel cladding rewets	169	154

Table 5.6.2-4 Core Performance Results for 1-ft^2 Break (Top)
(Offsite Power Available Sensitivity Study)

	Values	
	Base case	Sensitivity case
Peak Cladding Temperature (°F)	1088	773
Maximum local cladding oxidation (%)	0.2	0.2
Maximum core wide cladding oxidation (%)	less than 0.2	less than 0.2

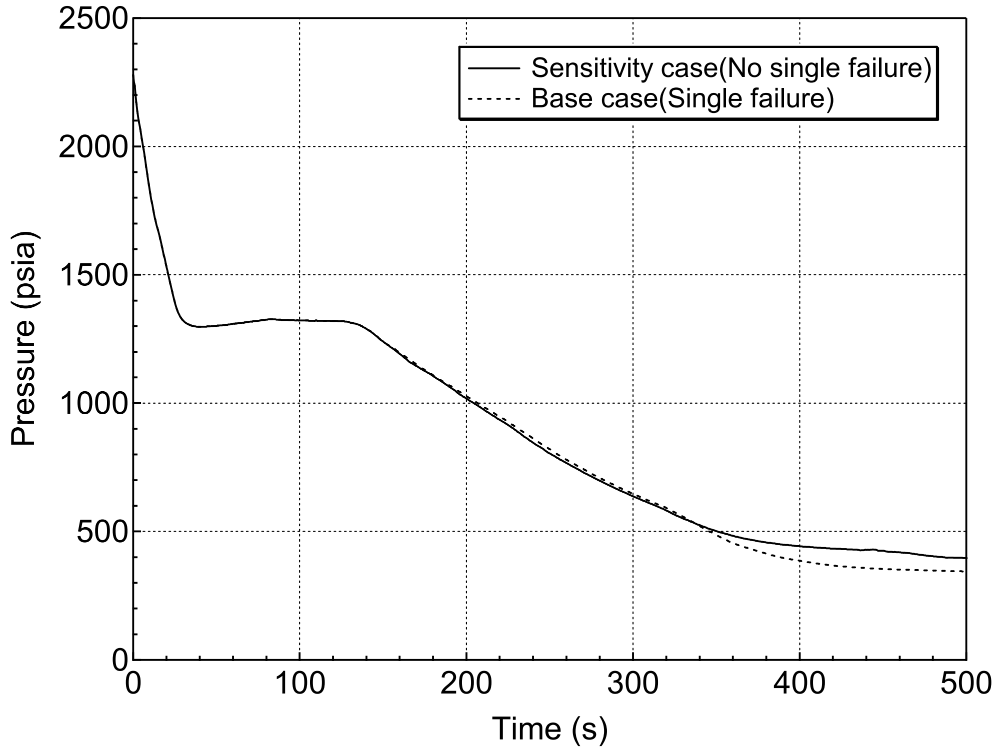

Figure 5.6.1-1 RCS (Pressurizer) Pressure Transient for 7.5-inch Break (Top) (No Single Failure Sensitivity Study)

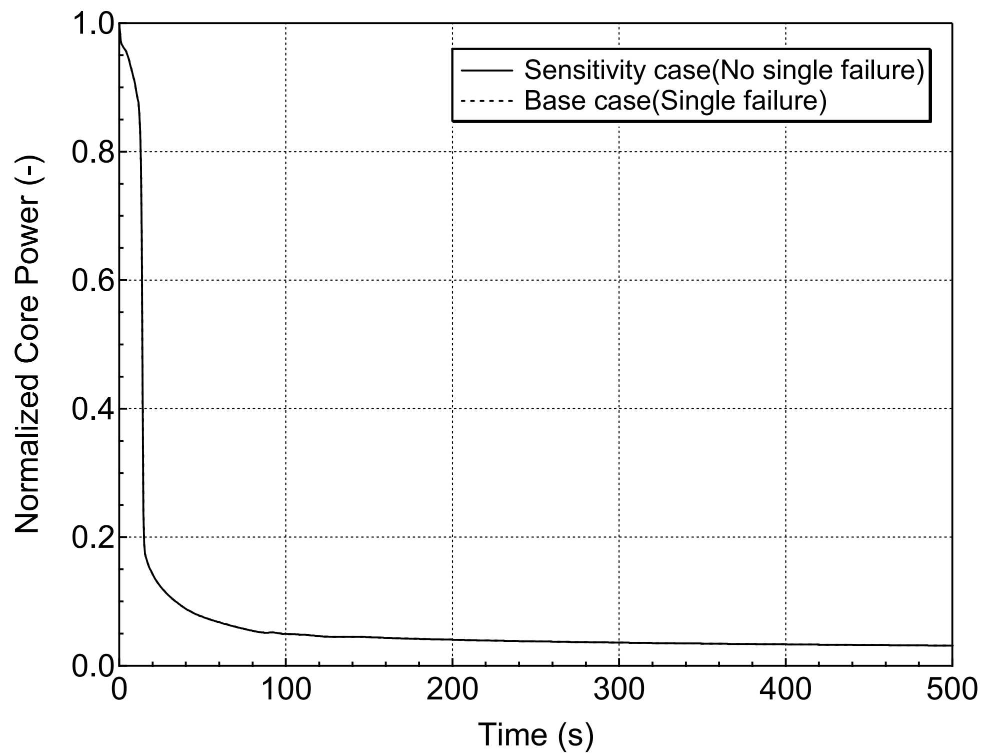

Figure 5.6.1-2 Normalized Core Power for 7.5-inch Break (Top)
(No Single Failure Sensitivity Study)

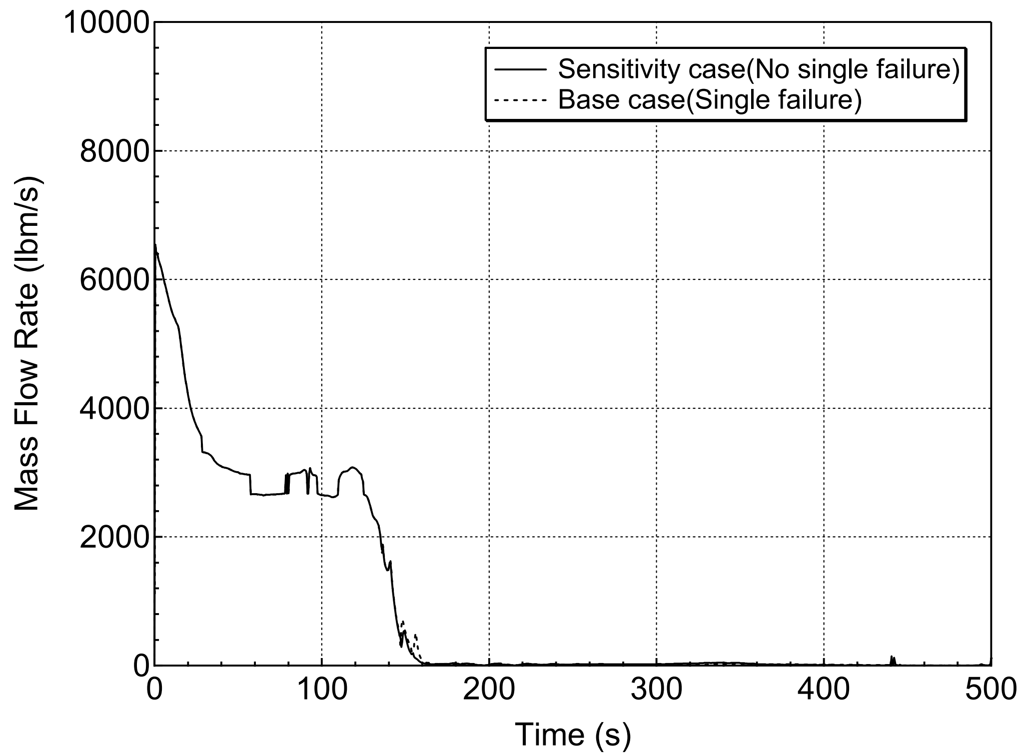

Figure 5.6.1-3 Liquid Discharge through the Break for 7.5-inch Break (Top) (No Single Failure Sensitivity Study)

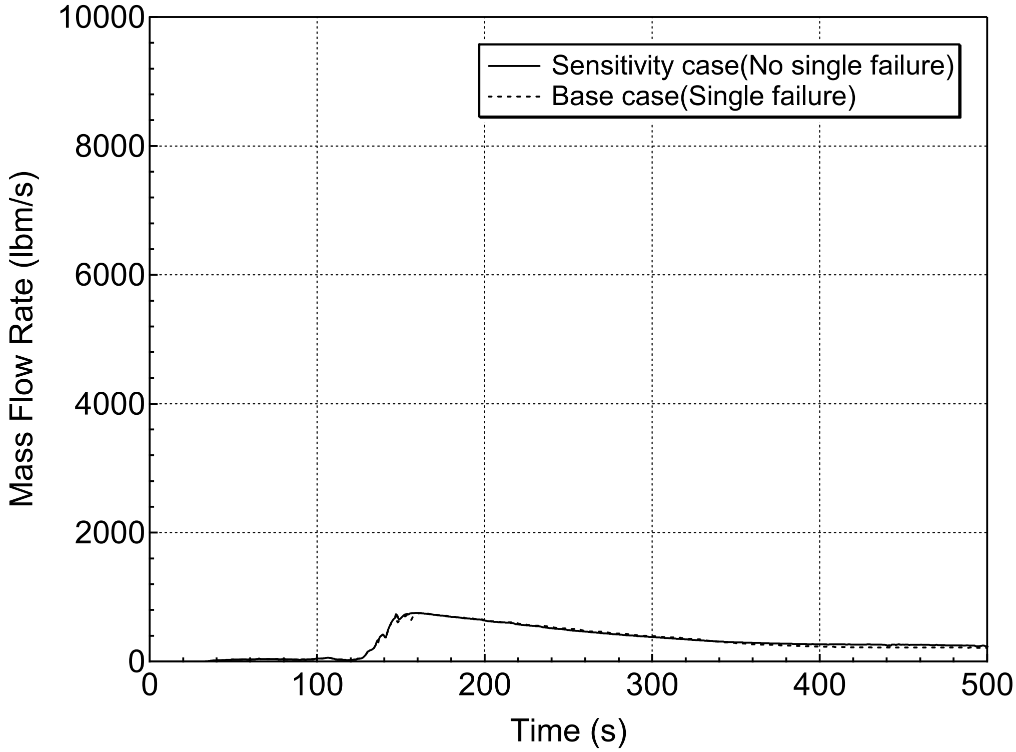

Figure 5.6.1-4 Vapor Discharge through the Break for 7.5-inch Break (Top) (No Single Failure Sensitivity Study)

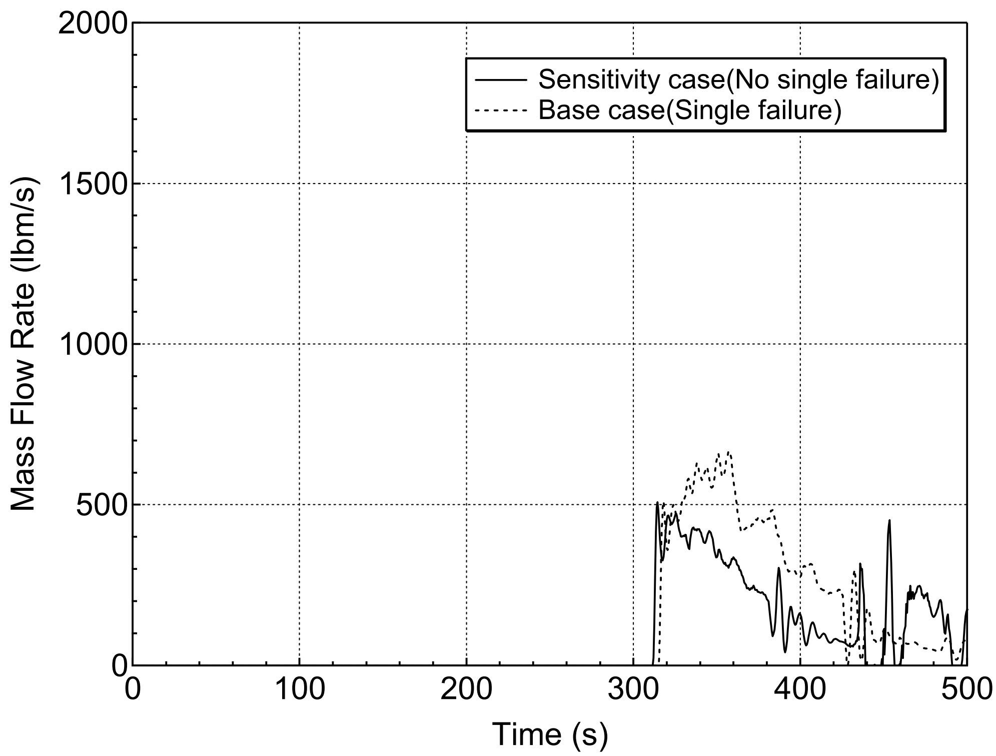

Figure 5.6.1-5 Accumulator Mass Flowrate for 7.5-inch Break (Top)
(No Single Failure Sensitivity Study)

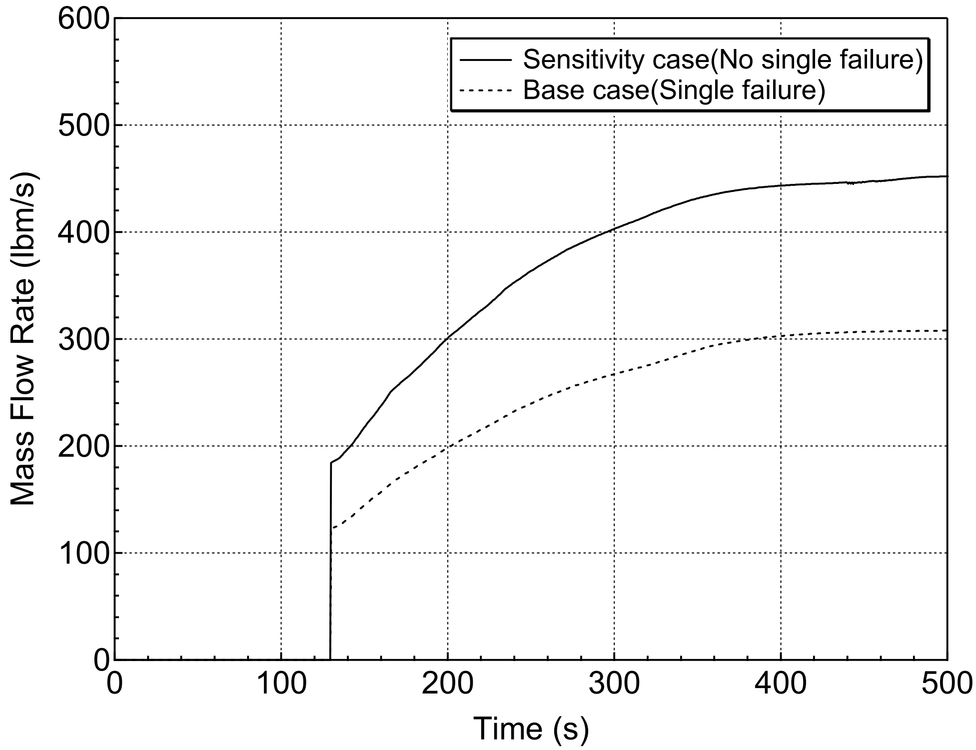

Figure 5.6.1-6 Safety Injection Mass Flowrate for 7.5-inch Break (Top)
(No Single Failure Sensitivity Study)

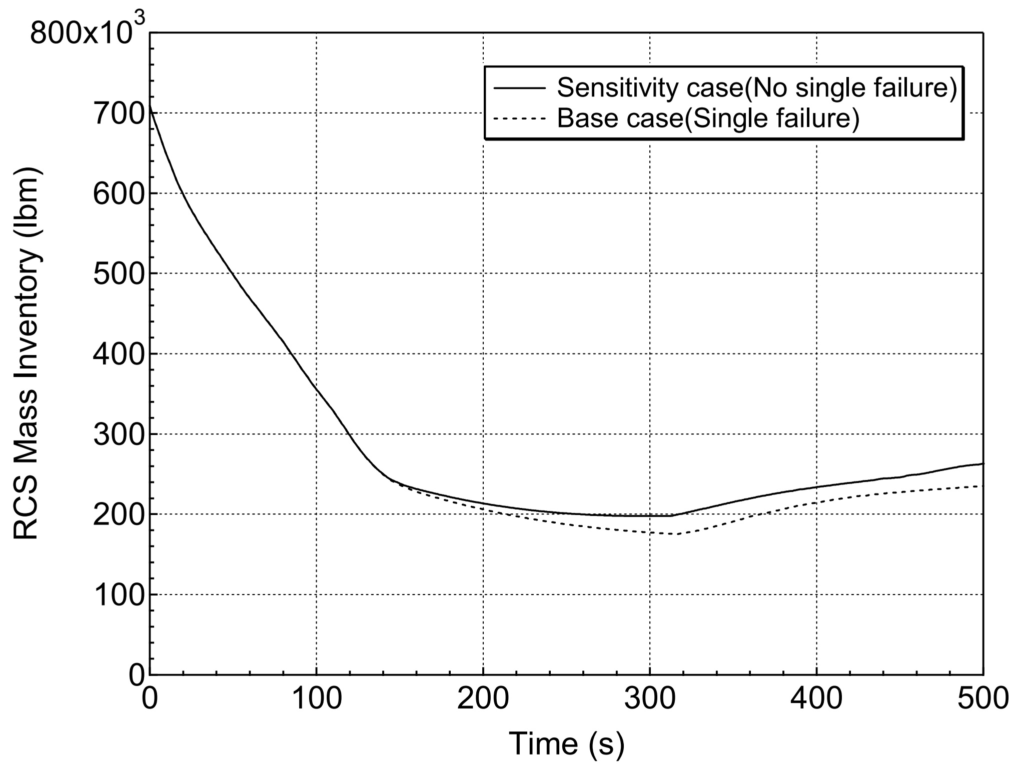

Figure 5.6.1-7 RCS Mass Inventory for 7.5-inch Break (Top)
(No Single Failure Sensitivity Study)

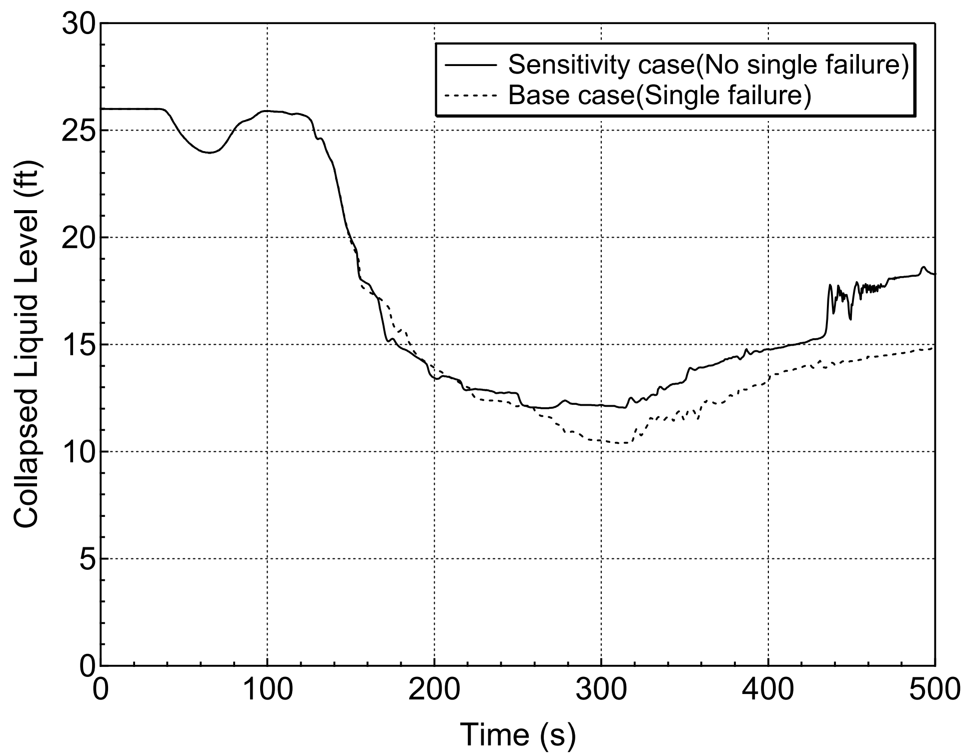

Figure 5.6.1-8 Downcomer Collapsed Level for 7.5-inch Break (Top)
(No Single Failure Sensitivity Study)

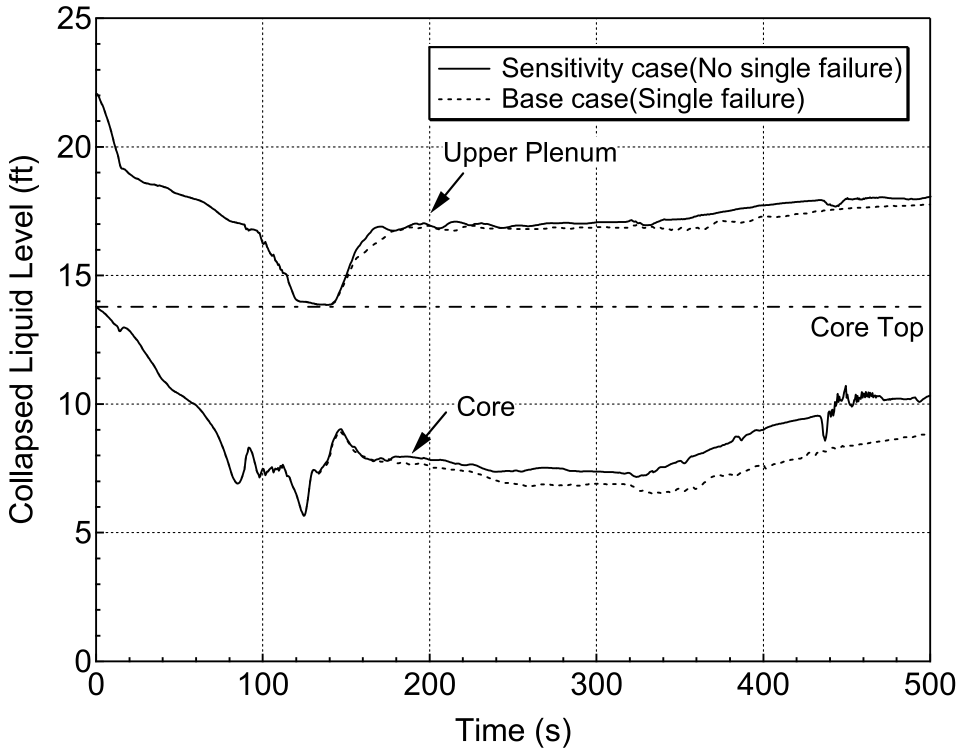

Figure 5.6.1-9 Average Core and Upper Plenum Collapsed Levels for 7.5-inch Break (Top) (No Single Failure Sensitivity Study)

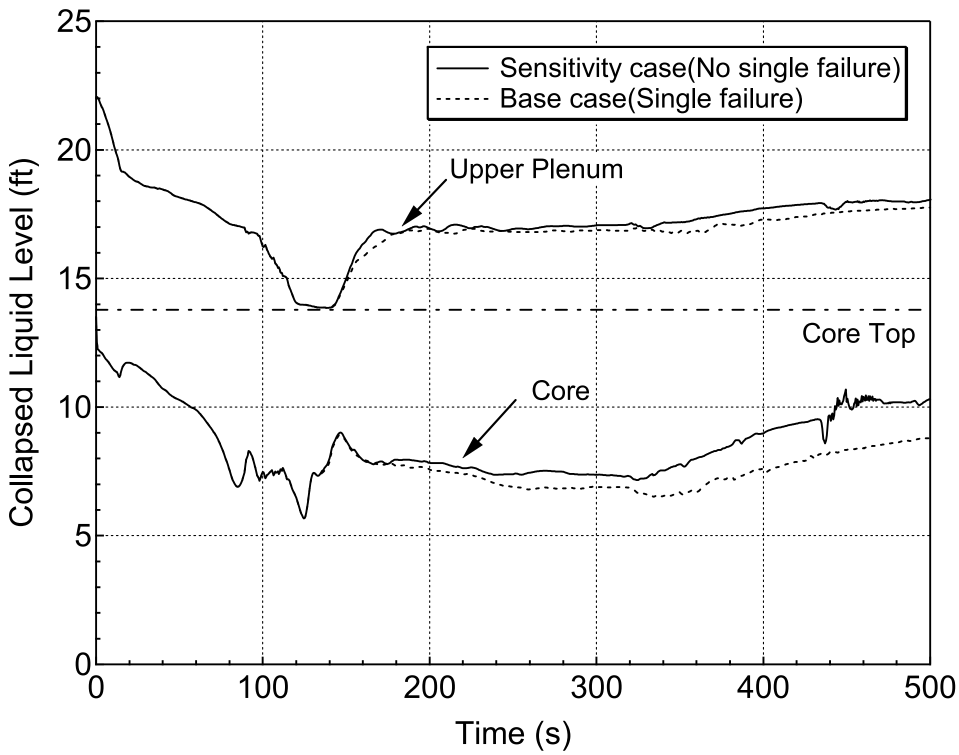

Figure 5.6.1-10 Hot Assembly Core and Upper Plenum Collapsed Levels for 7.5-inch Break (Top) (No Single Failure Sensitivity Study)

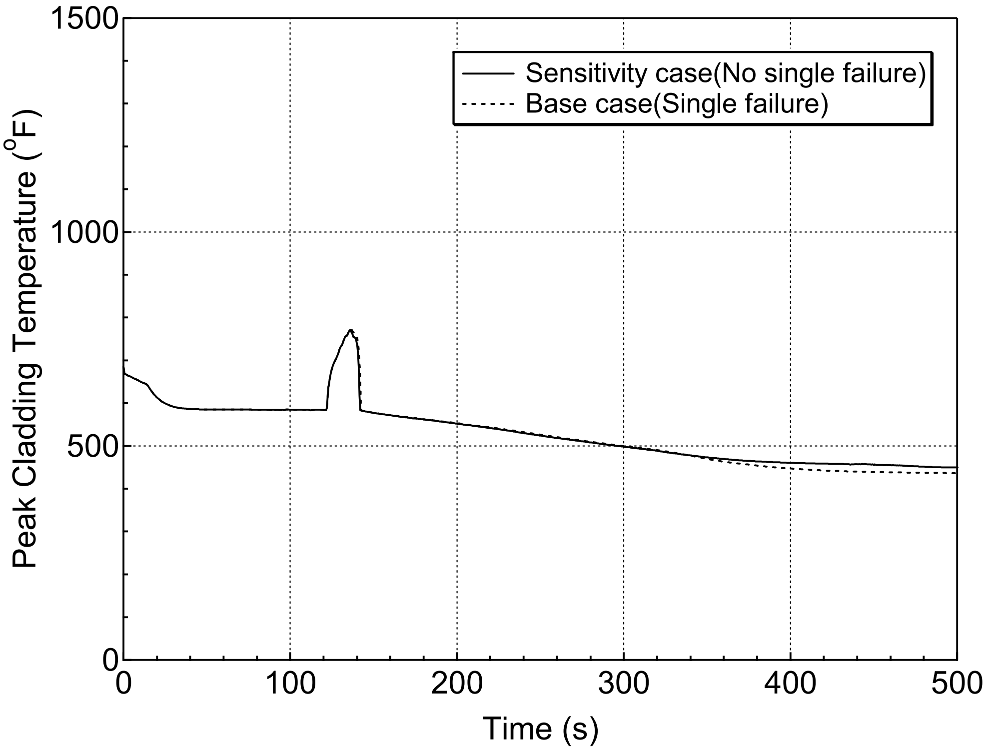

Figure 5.6.1-11 PCT at All Elevations for Hot Rod in Hot Assembly for 7.5-inch Break (Top)

(No Single Failure Sensitivity Study)

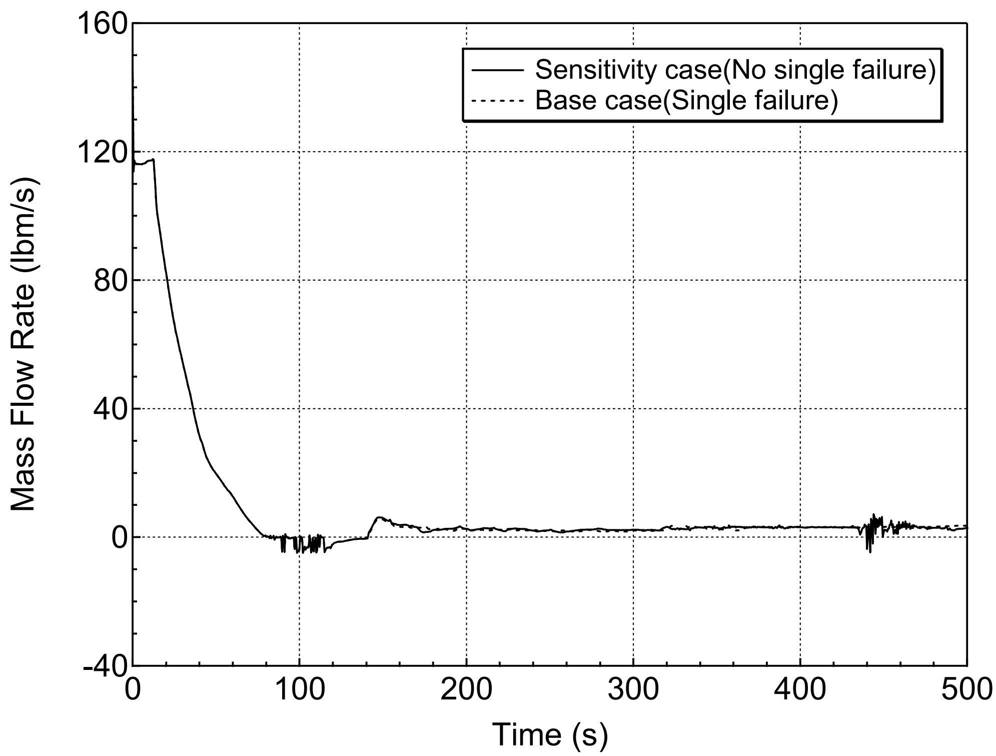

Figure 5.6.1-12 Hot Assembly Exit Liquid Mass Flowrate for 7.5-inch Break (Top) (No Single Failure Sensitivity Study)

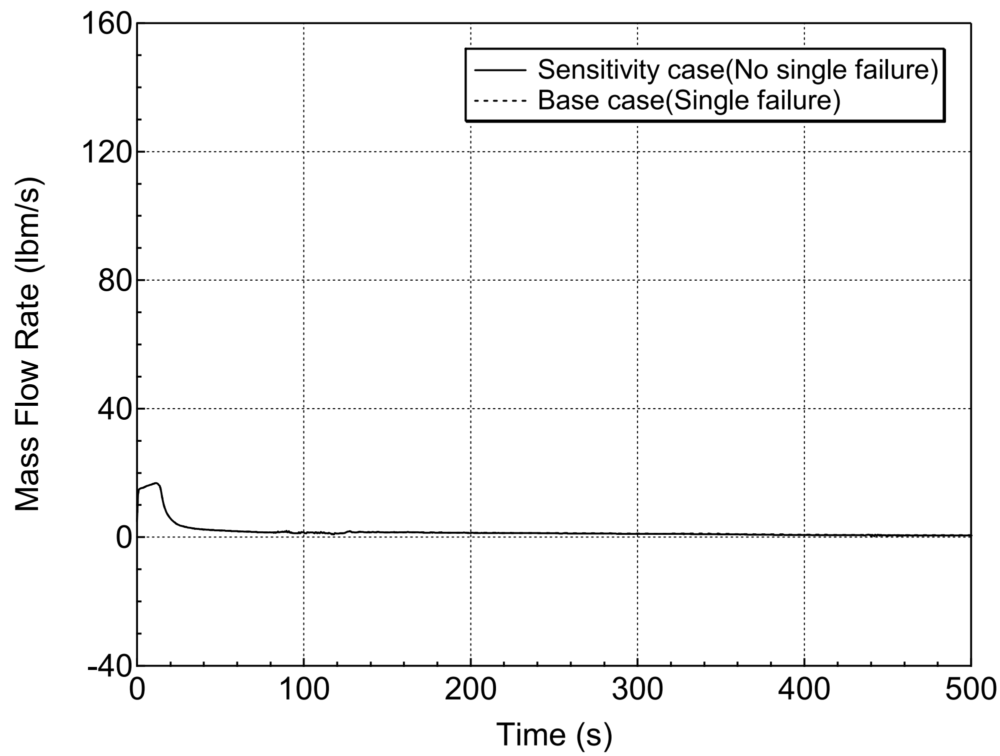

Figure 5.6.1-13 Hot Assembly Exit Vapor Mass Flowrate for 7.5-inch Break (Top) (No Single Failure Sensitivity Study)

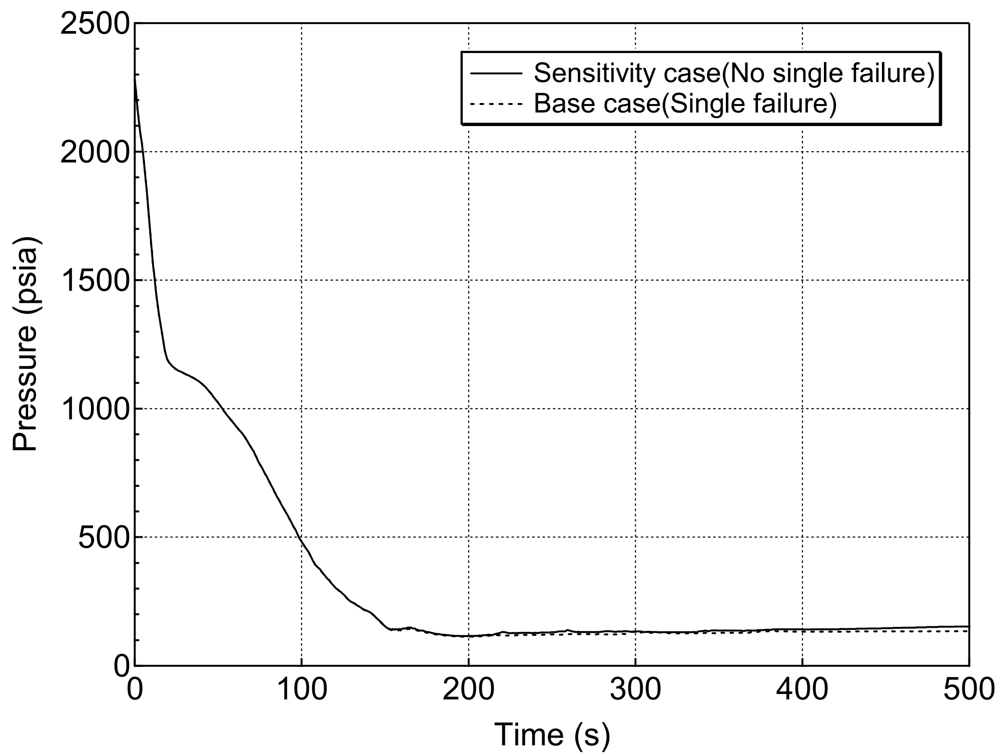

Figure 5.6.1-14 RCS (Pressurizer) Pressure Transient for 1-ft^2 Break (Top) (No Single Failure Sensitivity Study)

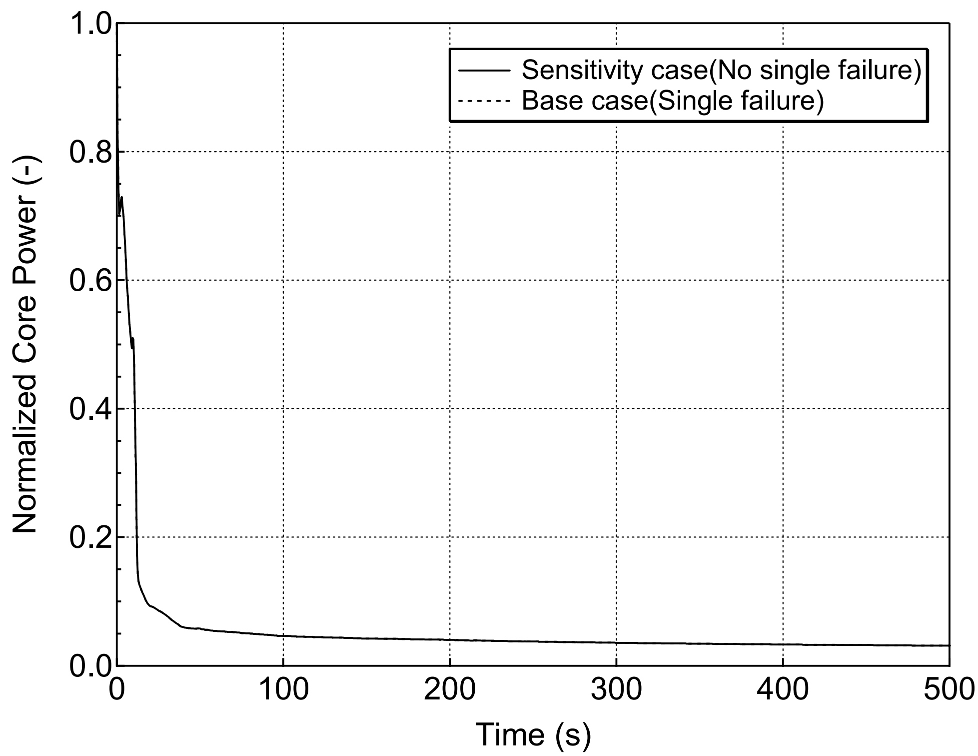

Figure 5.6.1-15 Normalized Core Power for 1-ft^2 Break (Top)
(No Single Failure Sensitivity Study)

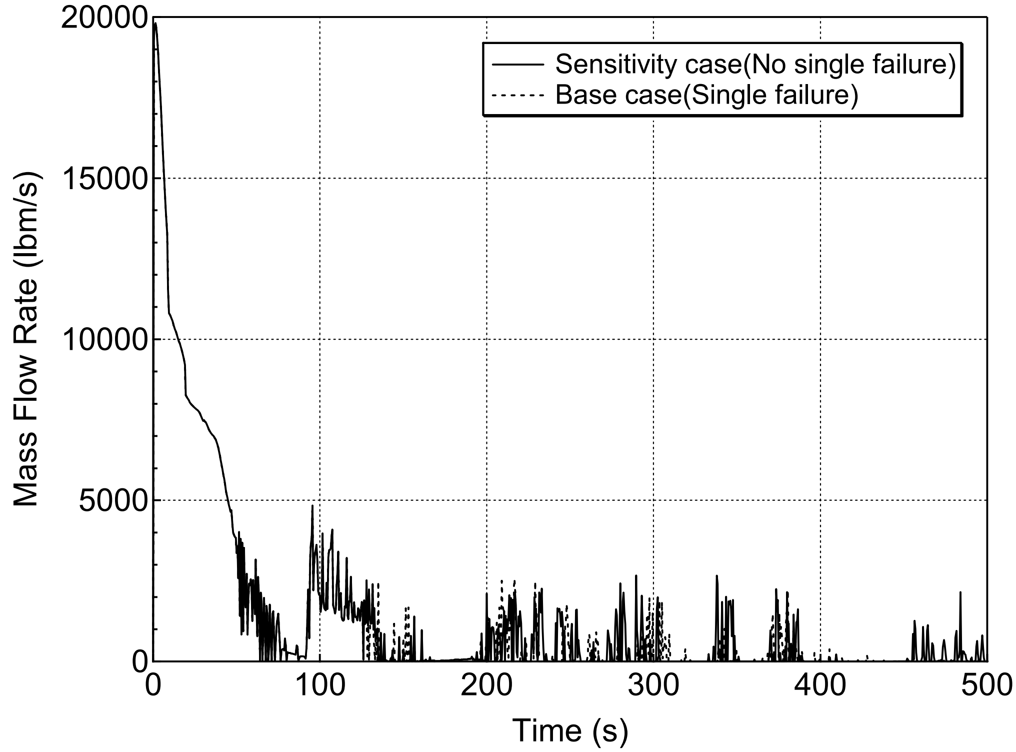

Figure 5.6.1-16 Liquid Discharge through the Break for 1-ft^2 Break (Top) (No Single Failure Sensitivity Study)

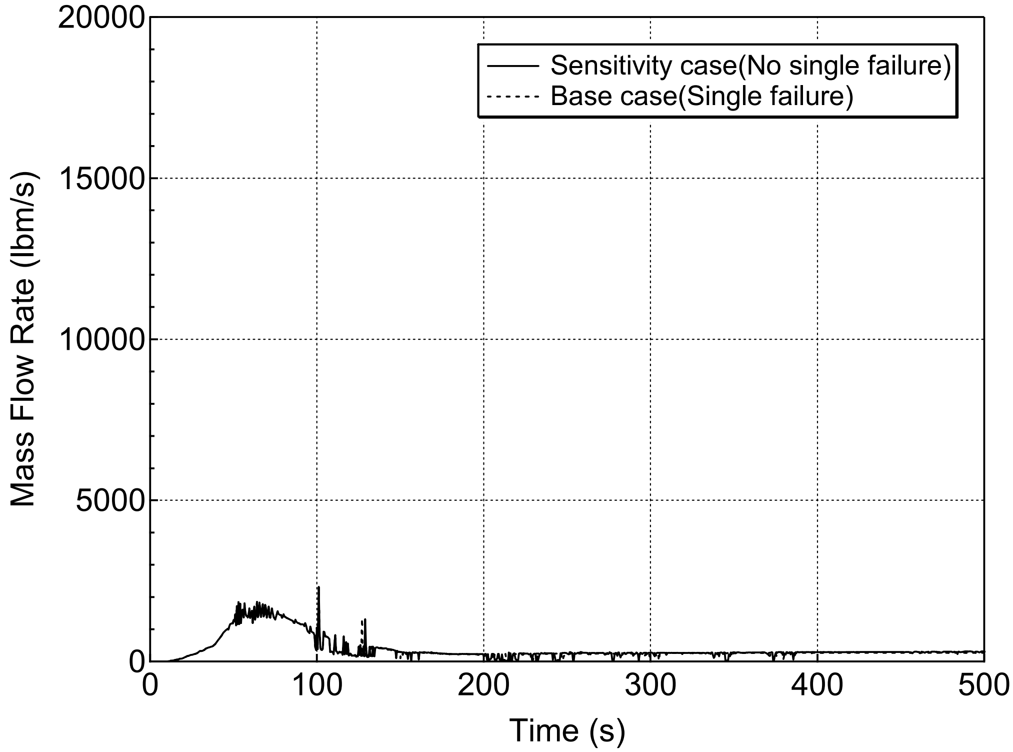

Figure 5.6.1-17 Vapor Discharge through the Break for 1-ft^2 Break (Top)
(No Single Failure Sensitivity Study)

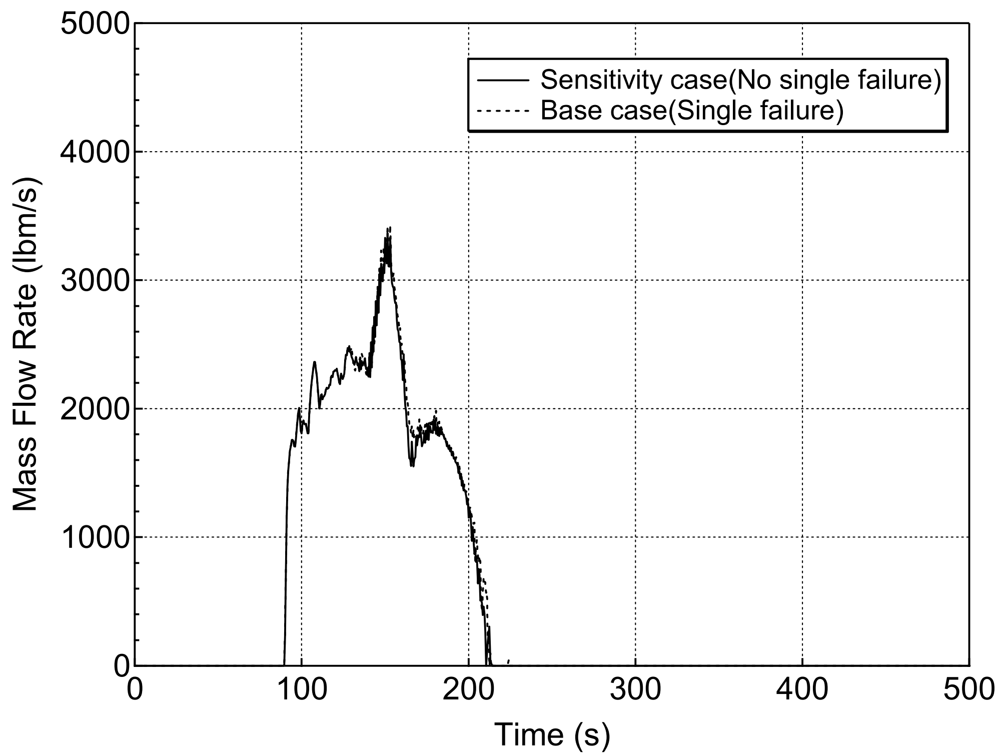

Figure 5.6.1-18 Accumulator Mass Flowrate for 1-ft^2 Break (Top)
(No Single Failure Sensitivity Study)

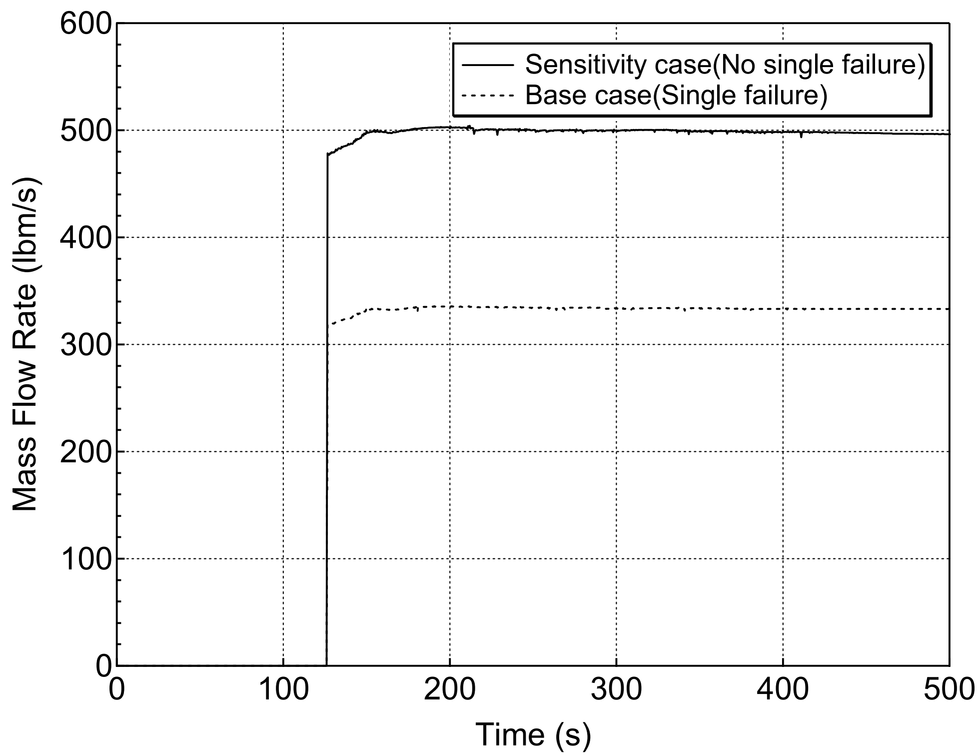

Figure 5.6.1-19 Safety Injection Mass Flowrate for 1-ft^2 Break (Top)
(No Single Failure Sensitivity Study)

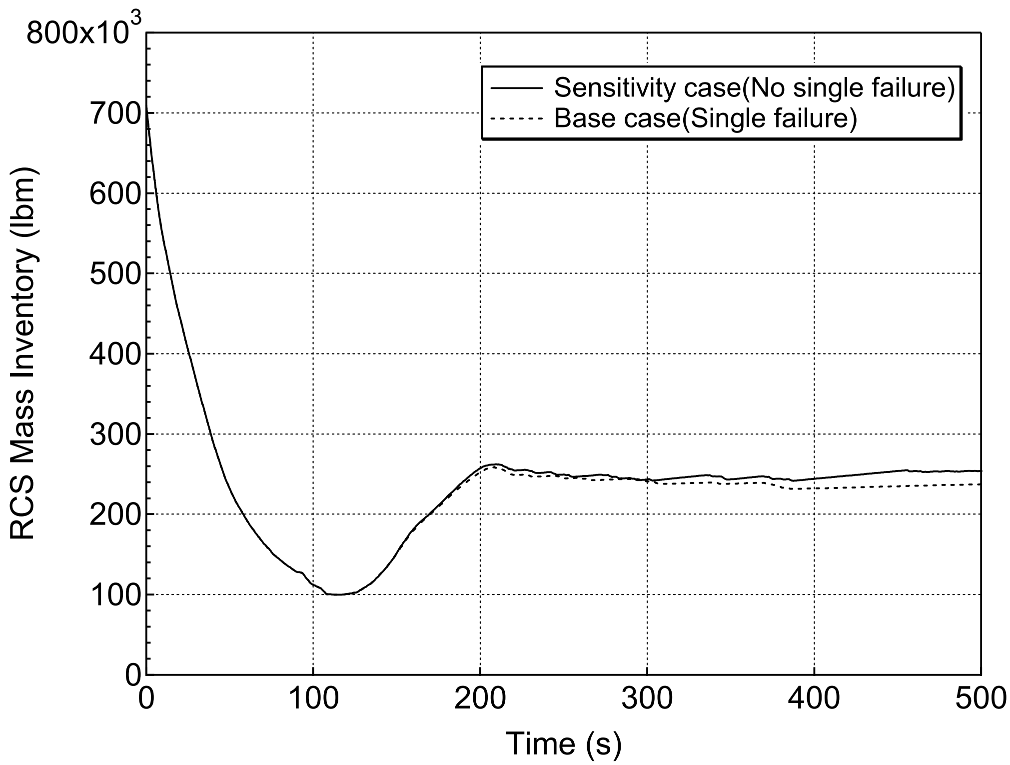

Figure 5.6.1-20 RCS Mass Inventory for 1-ft^2 Break (Top)
(No Single Failure Sensitivity Study)

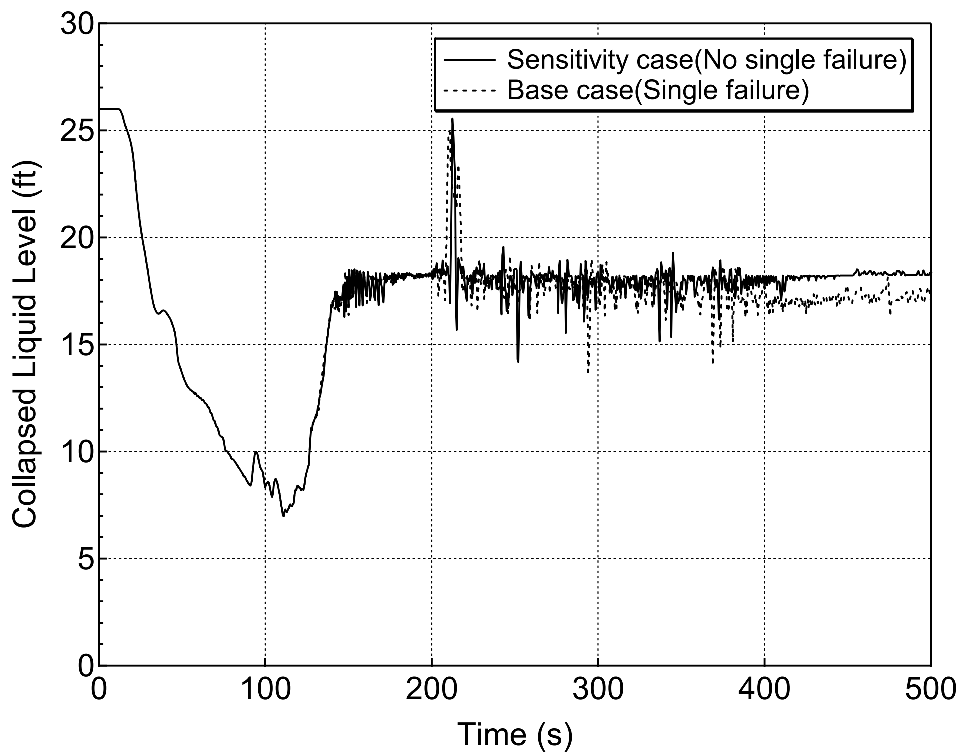

Figure 5.6.1-21 Downcomer Collapsed Level for 1-ft^2 Break (Top)
(No Single Failure Sensitivity Study)

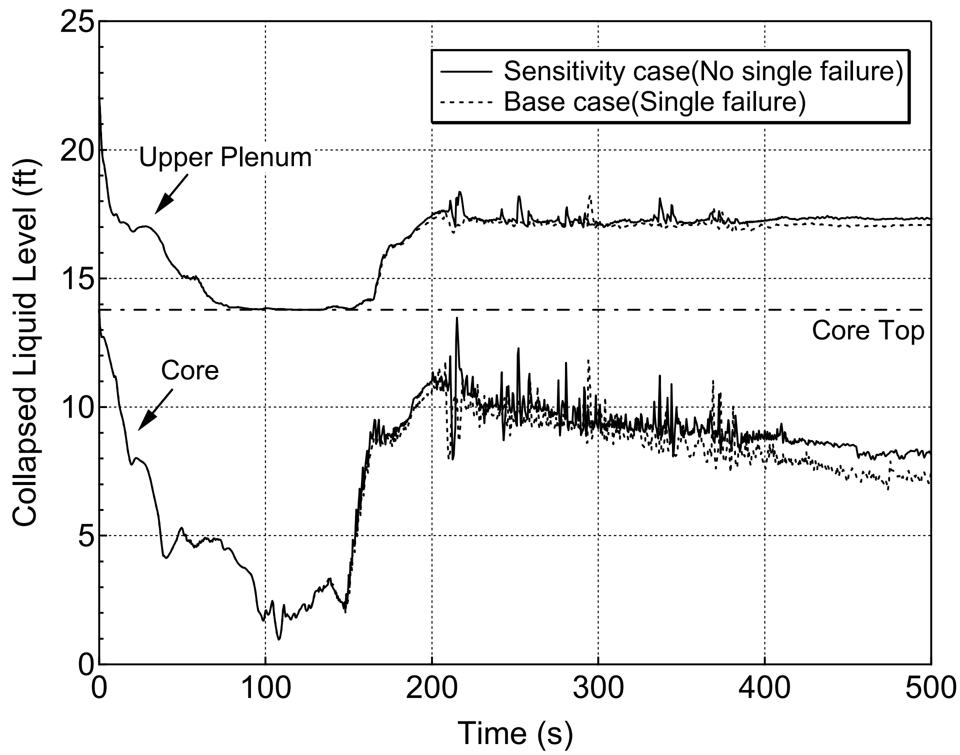

Figure 5.6.1-22 Average Core and Upper Plenum Collapsed Levels for 1-ft^2 Break (Top) (No Single Failure Sensitivity Study)

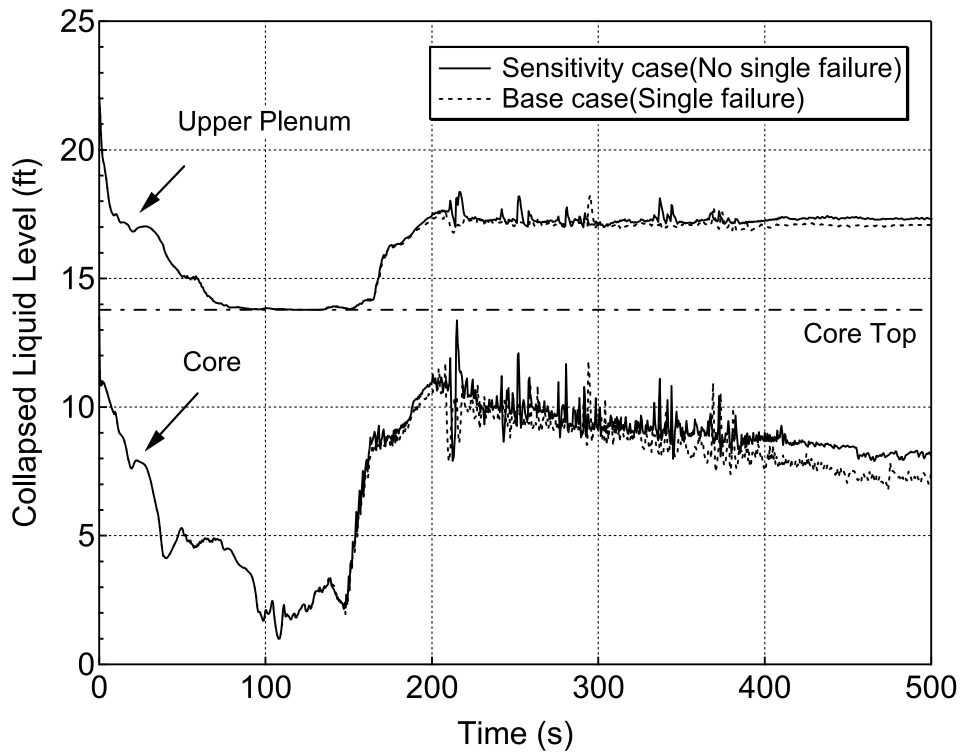

Figure 5.6.1-23 Hot Assembly Core and Upper Plenum Collapsed Levels for 1-ft^2 Break (Top) (No Single Failure Sensitivity Study)

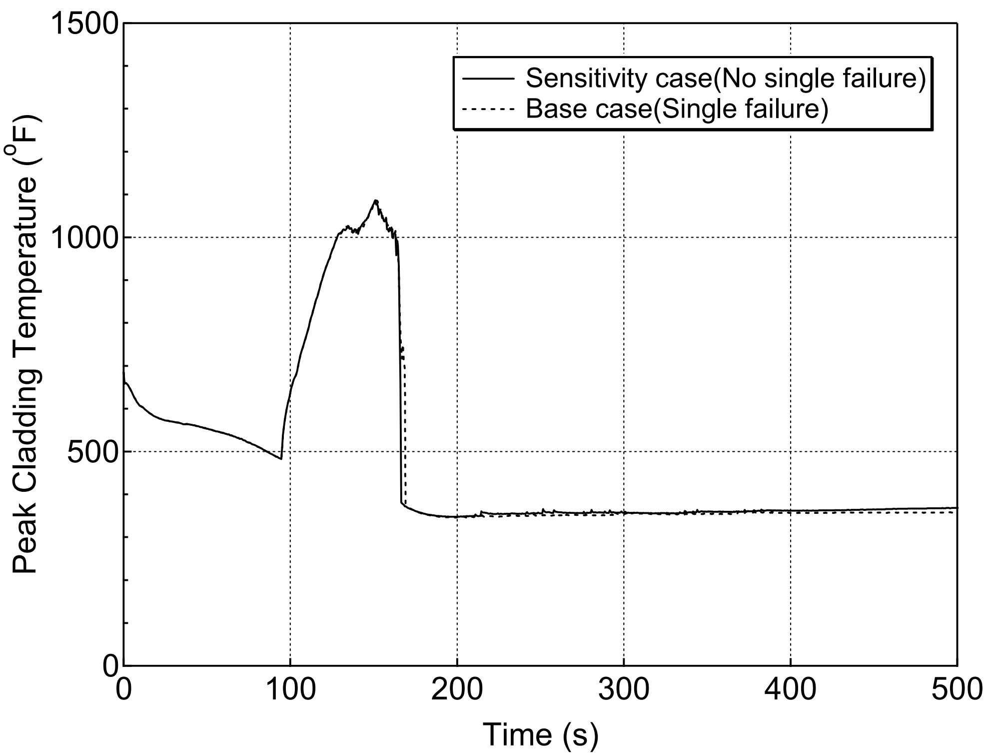

Figure 5.6.1-24 PCT at All Elevations for Hot Rod in Hot Assembly for 1-ft^2 Break (Top) (No Single Failure Sensitivity Study)

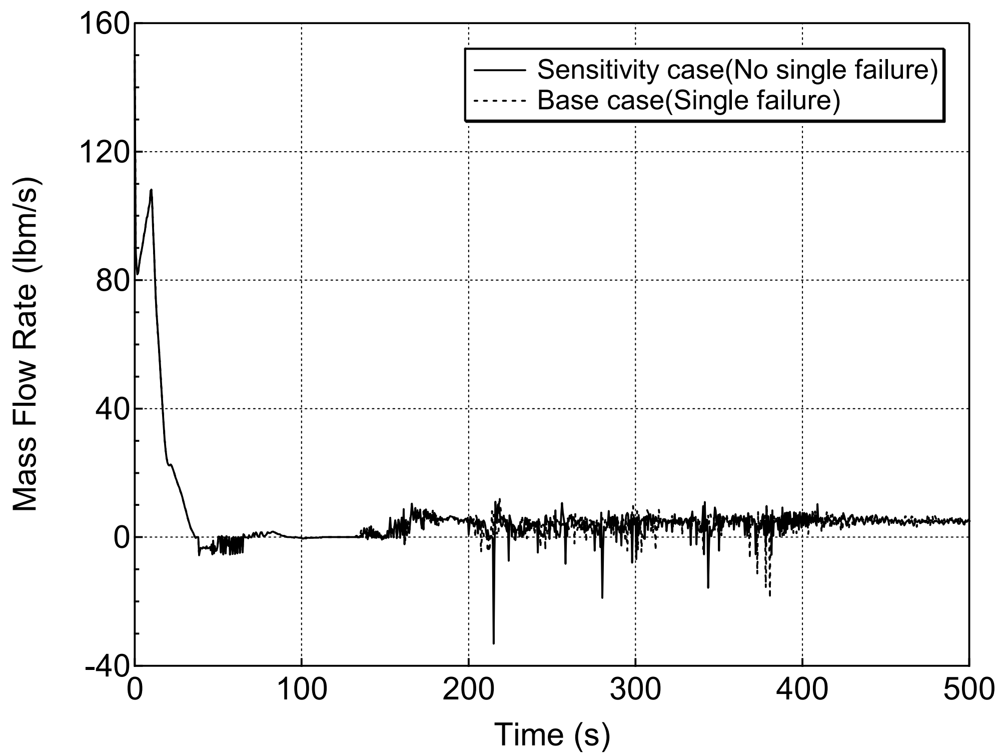

Figure 5.6.1-25 Hot Assembly Exit Liquid Mass Flowrate for 1-ft^2 Break (Top) (No Single Failure Sensitivity Study)

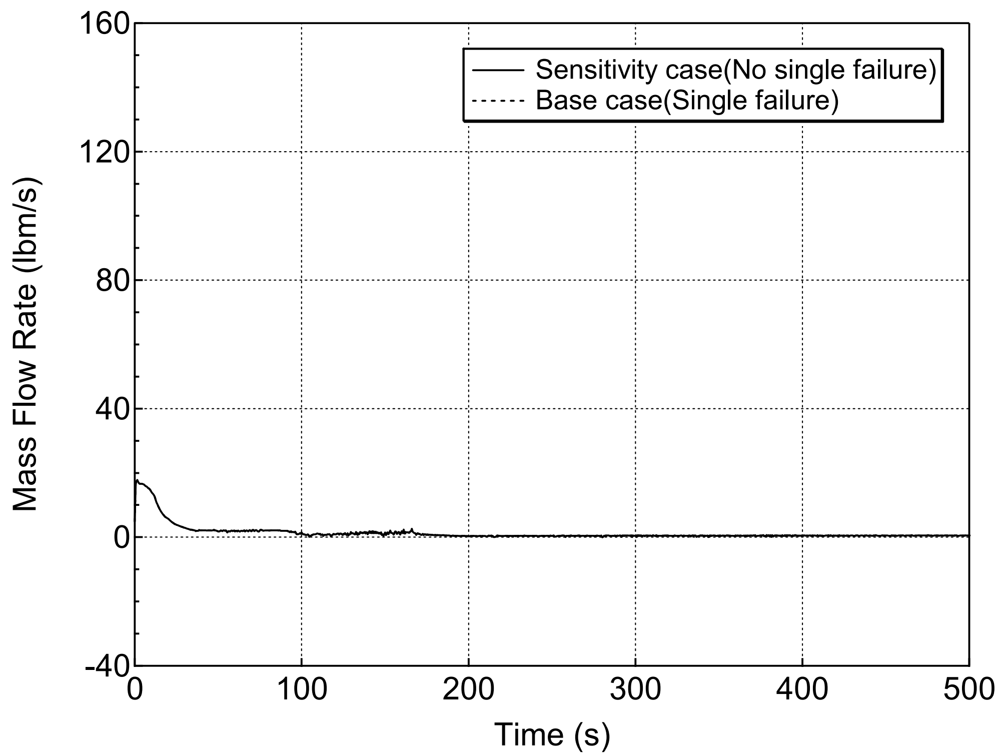

Figure 5.6.1-26 Hot Assembly Exit Vapor Mass Flowrate for 1-ft^2 Break (Top) (No Single Failure Sensitivity Study)

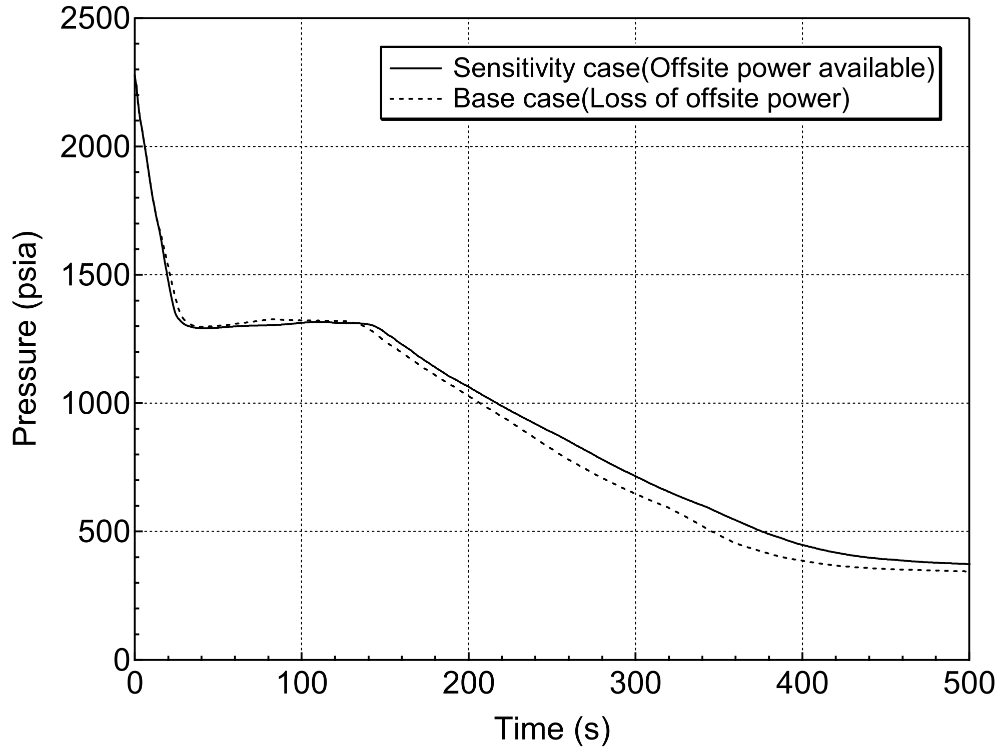

Figure 5.6.2-1 RCS (Pressurizer) Pressure Transient for 7.5-inch Break (Top) (Offsite Power Available Sensitivity Study)

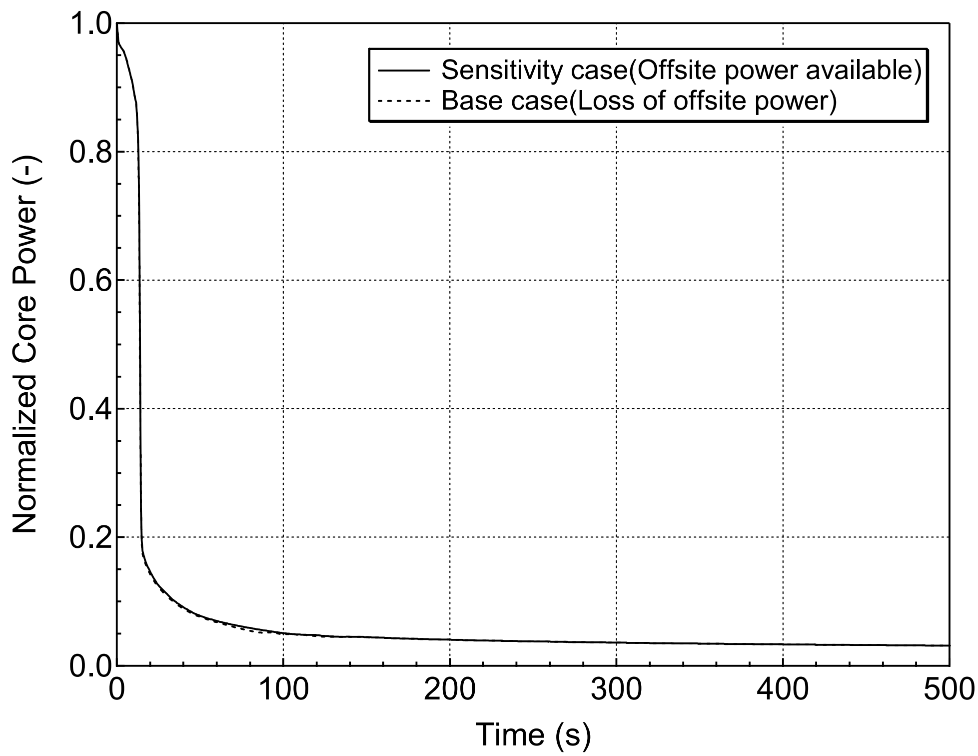

Figure 5.6.2-2 Normalized Core Power for 7.5-inch Break (Top) (Offsite Power Available Sensitivity Study)

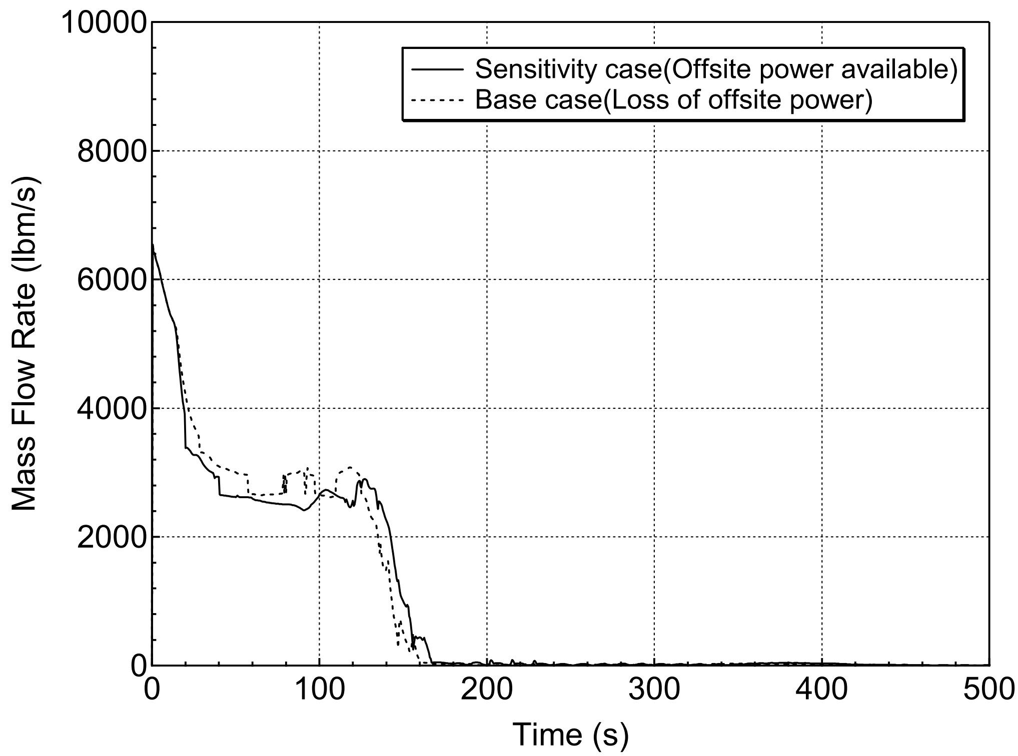

Figure 5.6.2-3 Liquid Discharge through the Break for 7.5-inch Break (Top) (Offsite Power Available Sensitivity Study)

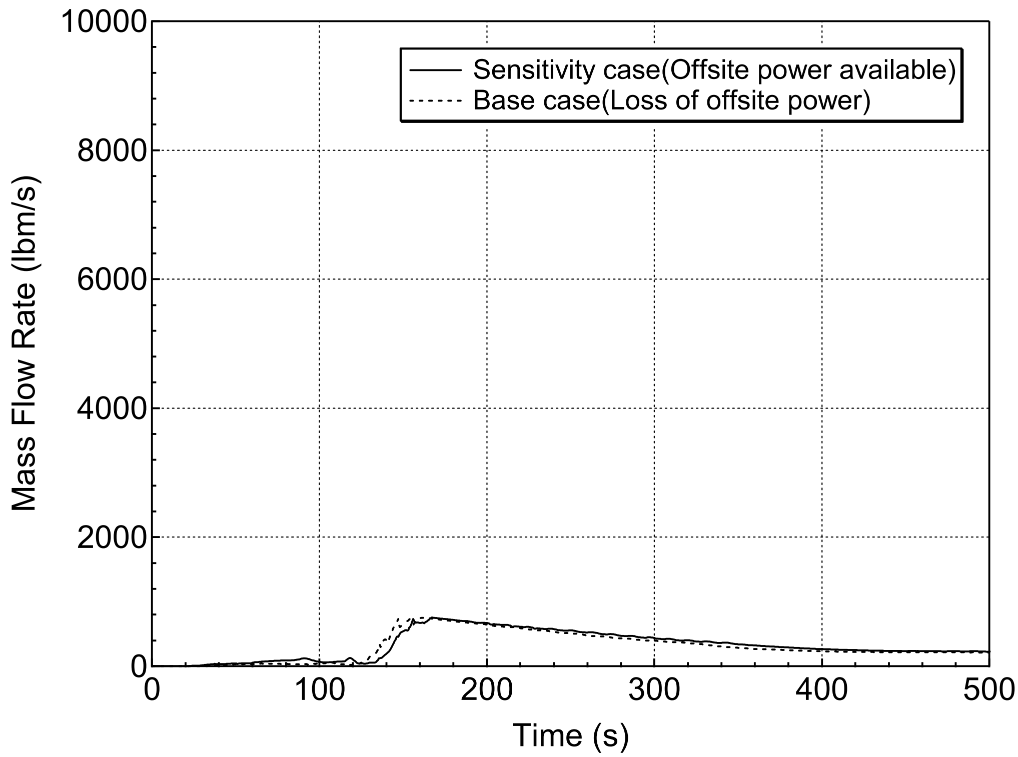

Figure 5.6.2-4 Vapor Discharge through the Break for 7.5-inch Break (Top) (Offsite Power Available Sensitivity Study)

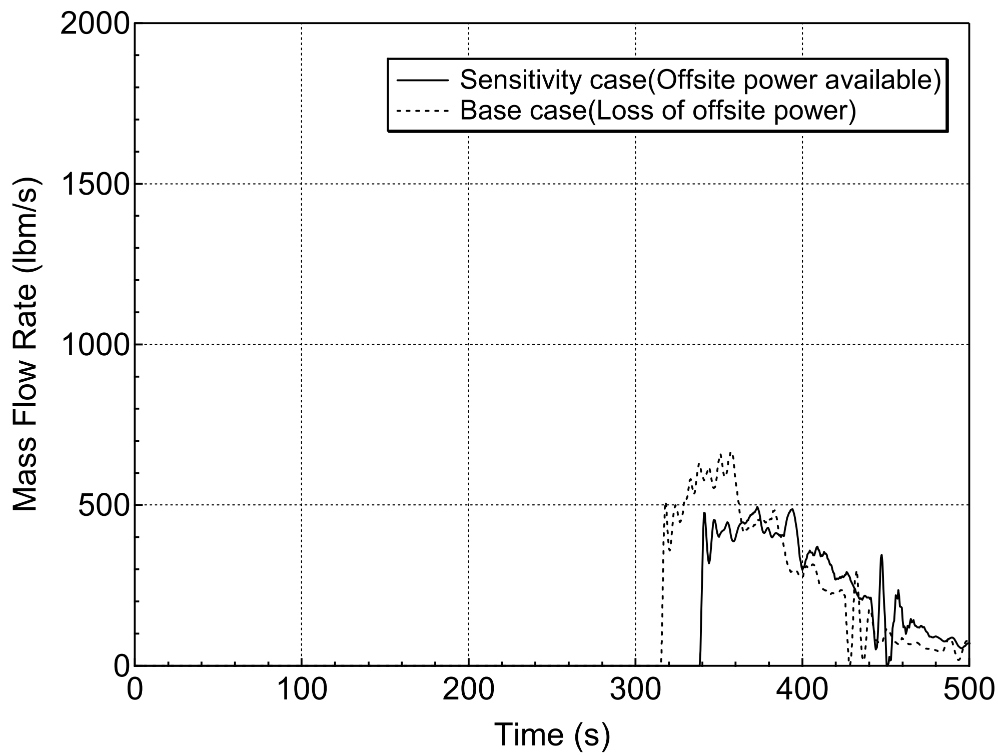

Figure 5.6.2-5 Accumulator Mass Flowrate for 7.5-inch Break (Top)
(Offsite Power Available Sensitivity Study)

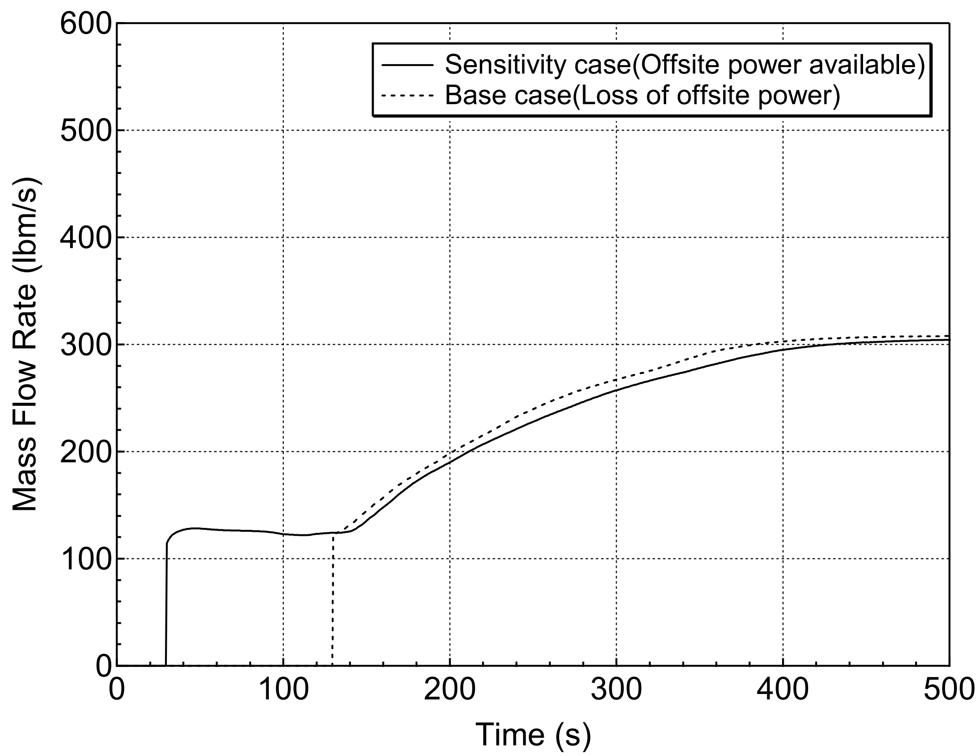

Figure 5.6.2-6 Safety Injection Mass Flowrate for 7.5-inch Break (Top) (Offsite Power Available Sensitivity Study)

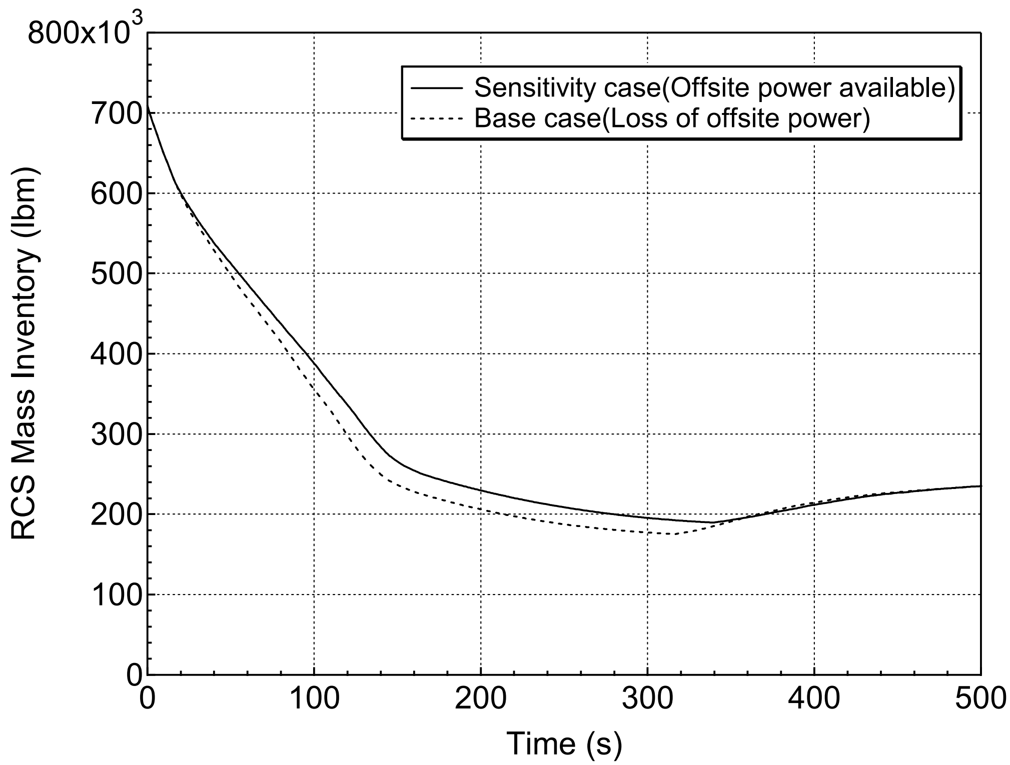

Figure 5.6.2-7 RCS Mass Inventory for 7.5-inch Break (Top)
(Offsite Power Available Sensitivity Study)

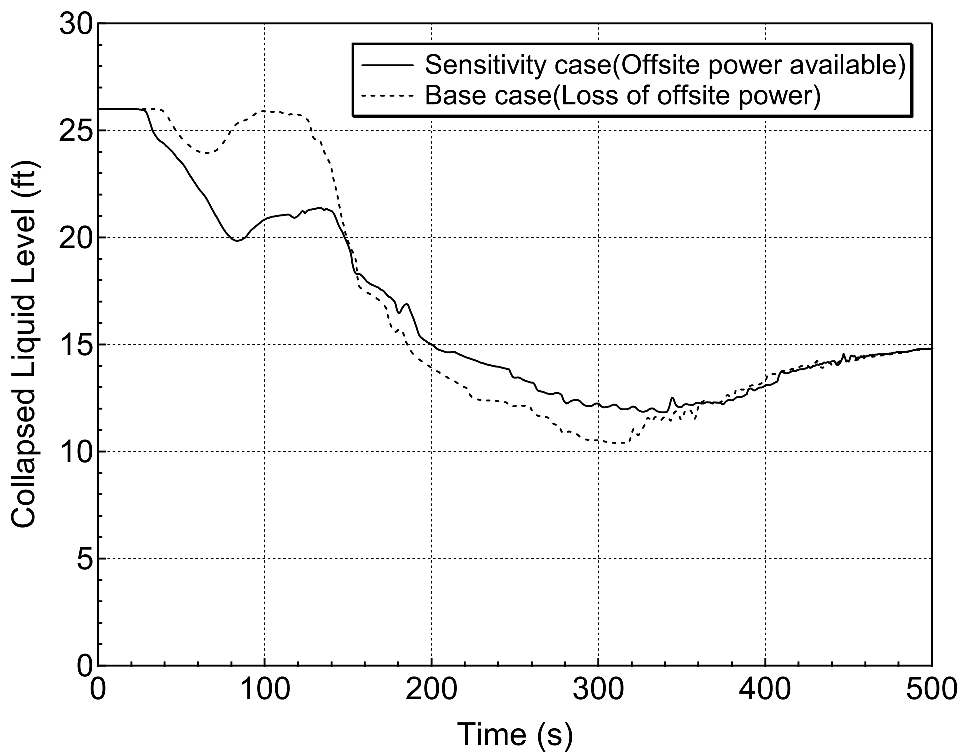

Figure 5.6.2-8 Downcomer Collapsed Level for 7.5-inch Break (Top) (Offsite Power Available Sensitivity Study)

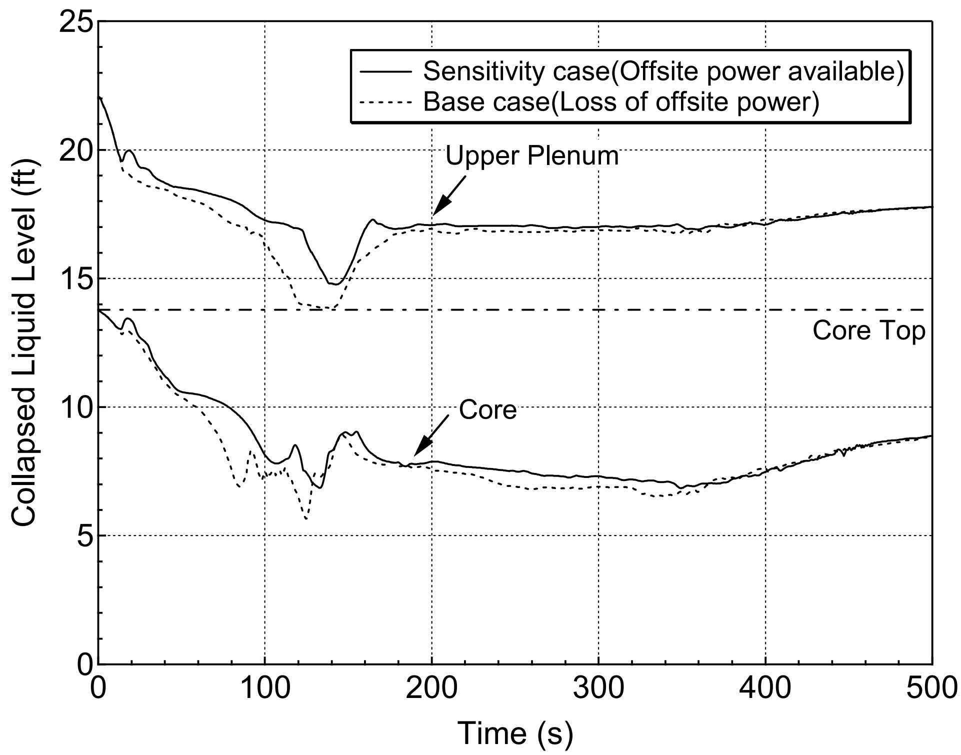

Figure 5.6.2-9 Average Core and Upper Plenum Collapsed Levels for 7.5-inch Break (Top) (Offsite Power Available Sensitivity Study)

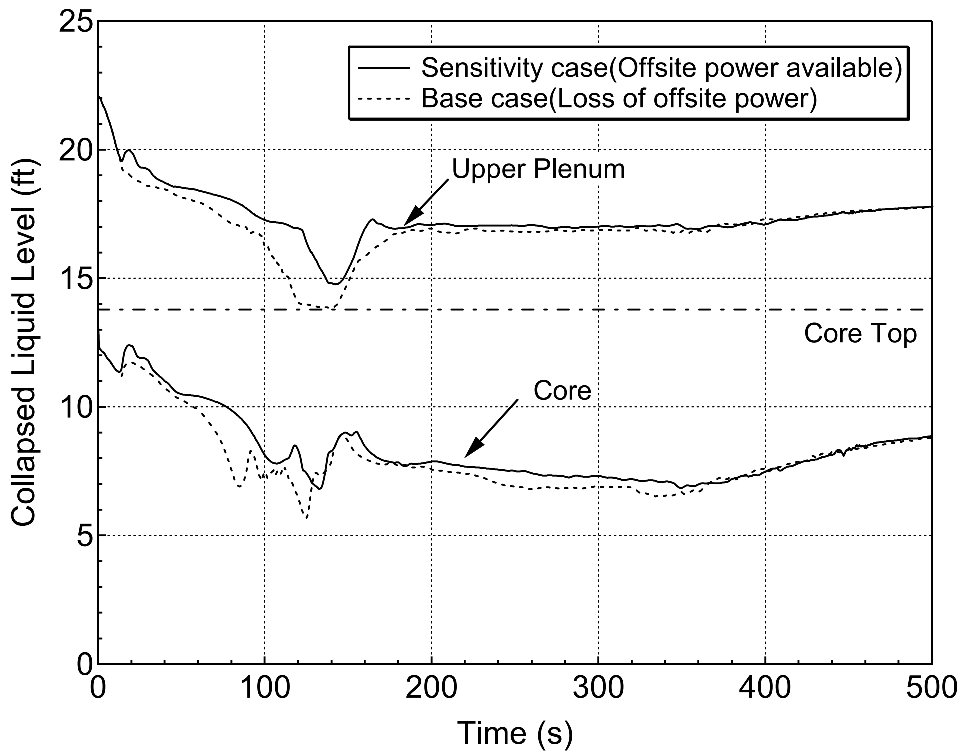

Figure 5.6.2-10 Hot Assembly Core and Upper Plenum Collapsed Levels for 7.5-inch Break (Top) (Offsite Power Available Sensitivity Study)

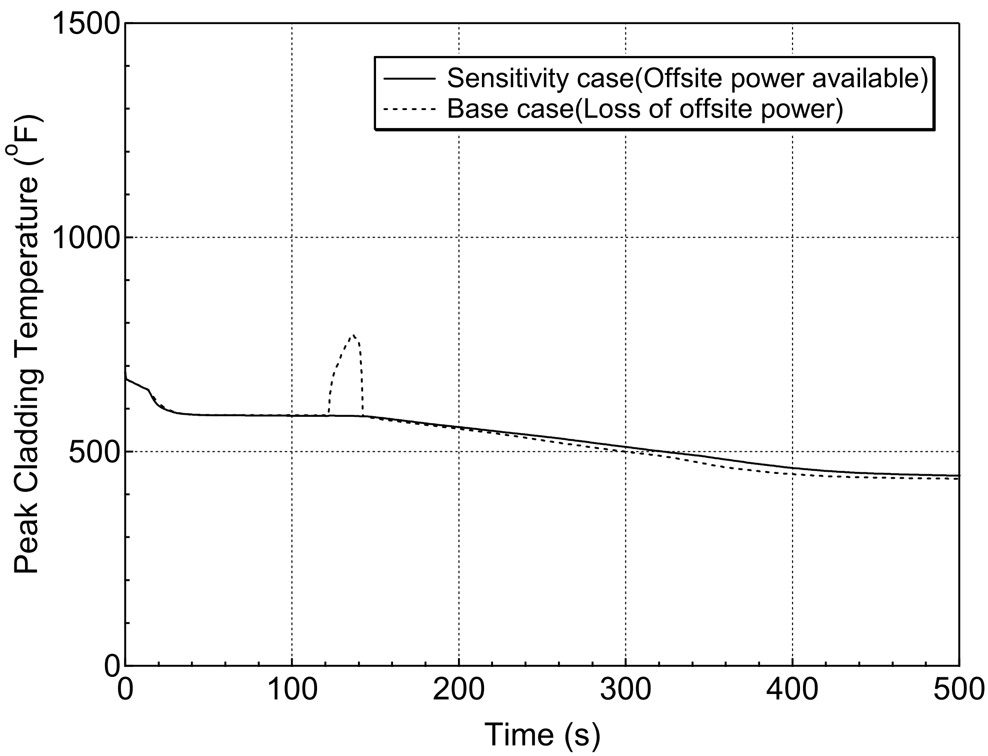

Figure 5.6.2-11 PCT at All Elevations for Hot Rod in Hot Assembly for 7.5-inch Break (Top) (Offsite Power Available Sensitivity Study)

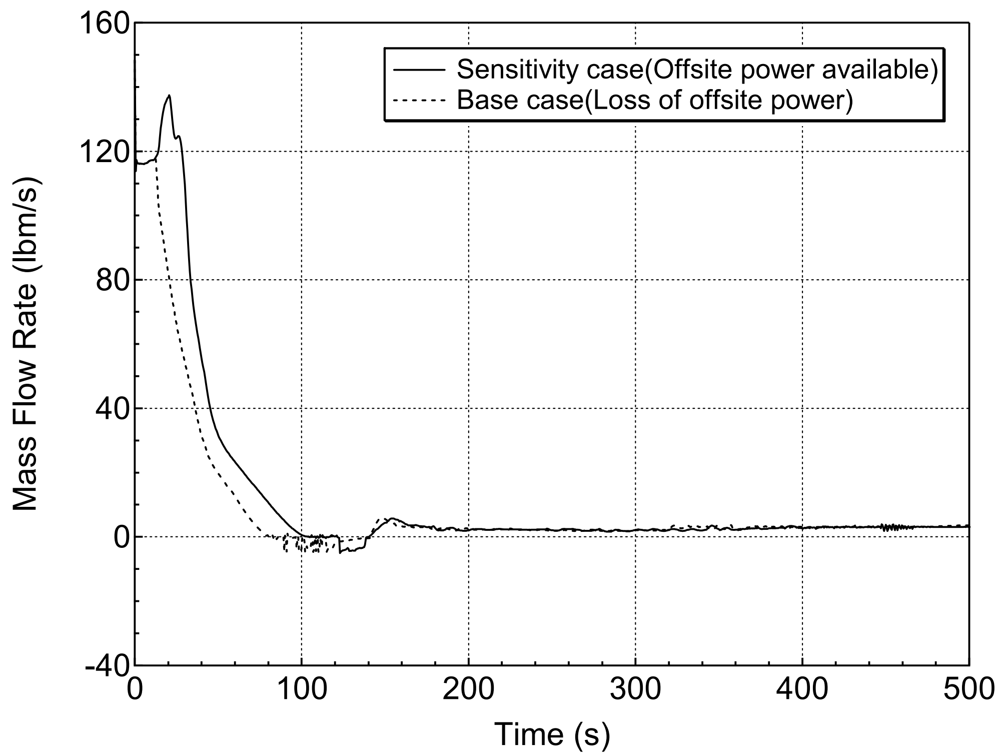

Figure 5.6.2-12 Hot Assembly Exit Liquid Mass Flowrate for 7.5-inch Break (Top) (Offsite Power Available Sensitivity Study)

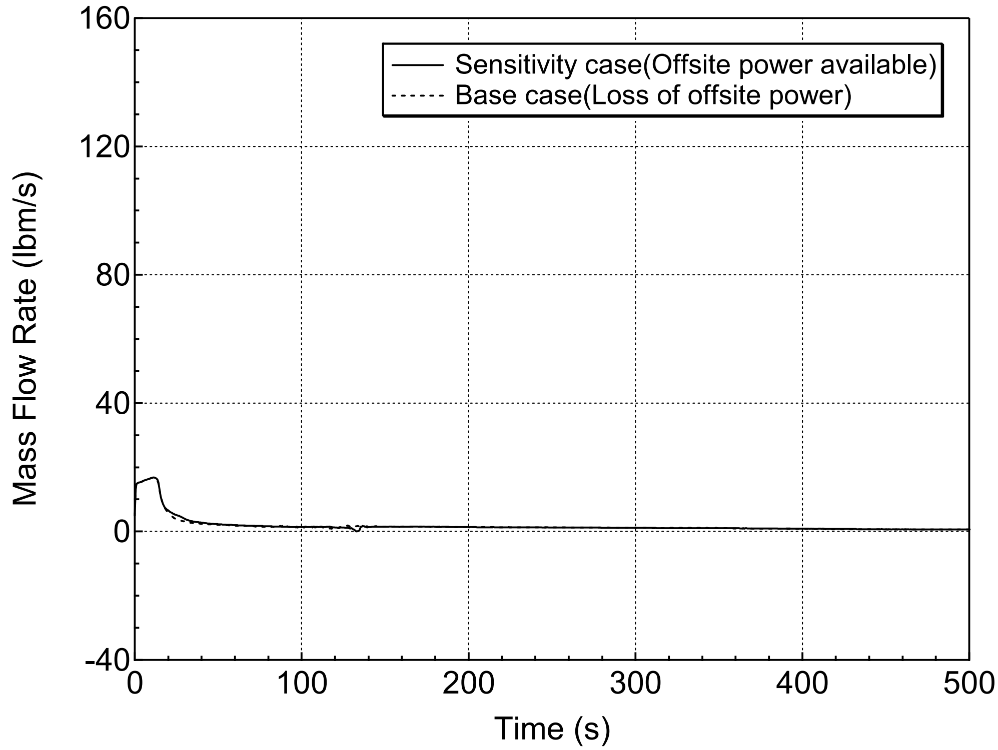

Figure 5.6.2-13 Hot Assembly Exit Vapor Mass Flowrate for 7.5-inch Break (Top) (Offsite Power Available Sensitivity Study)

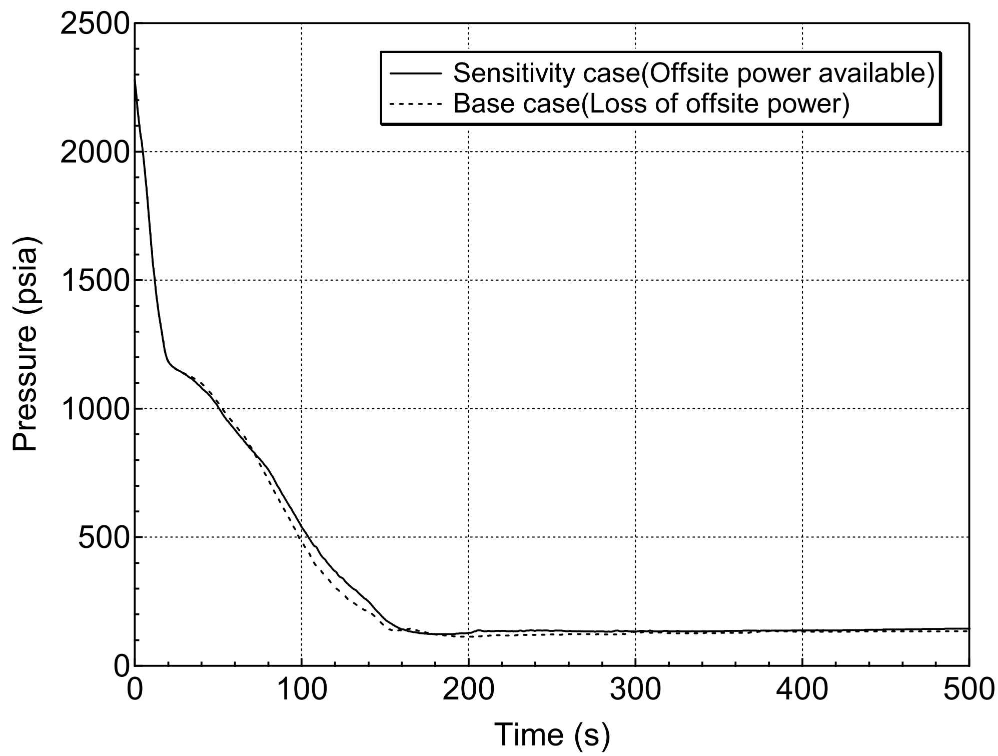

Figure 5.6.2-14 RCS (Pressurizer) Pressure Transient for 1-ft^2 Break (Top) (Offsite Power Available Sensitivity Study)

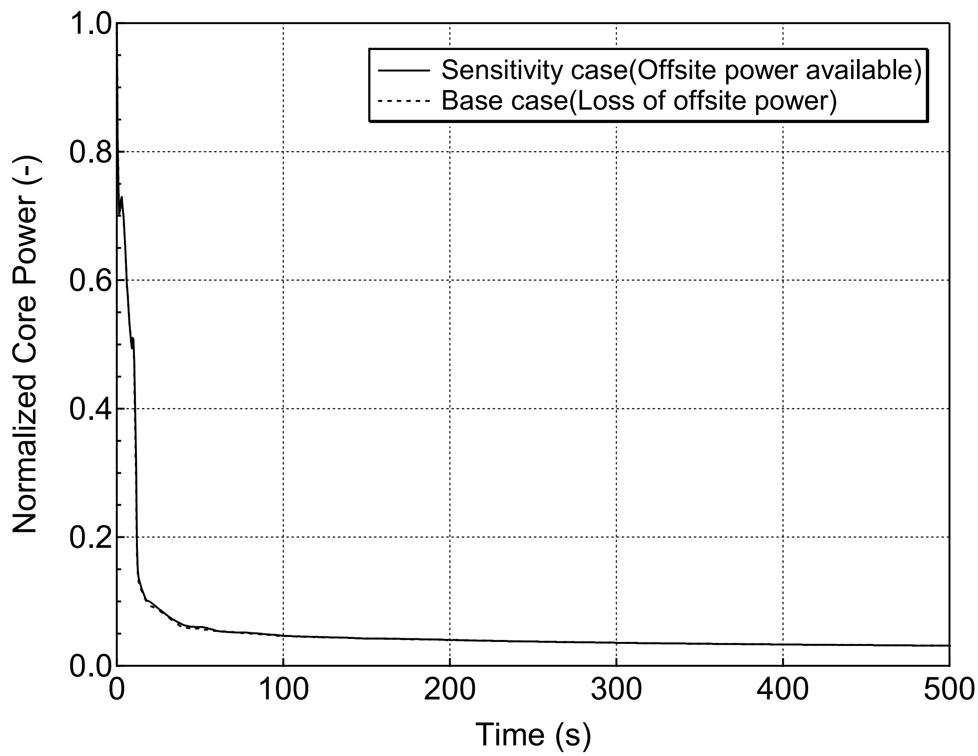

Figure 5.6.2-15 Normalized Core Power for 1-ft^2 Break (Top) (Offsite Power Available Sensitivity Study)

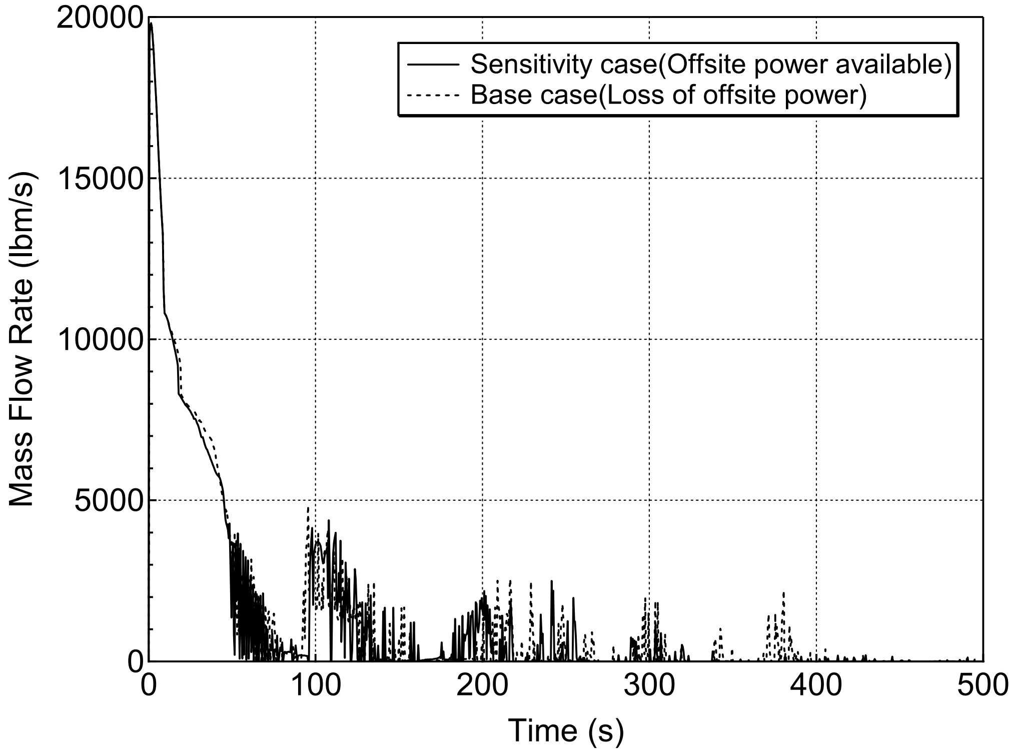

Figure 5.6.2-16 Liquid Discharge through the Break for 1-ft^2 Break (Top) (Offsite Power Available Sensitivity Study)

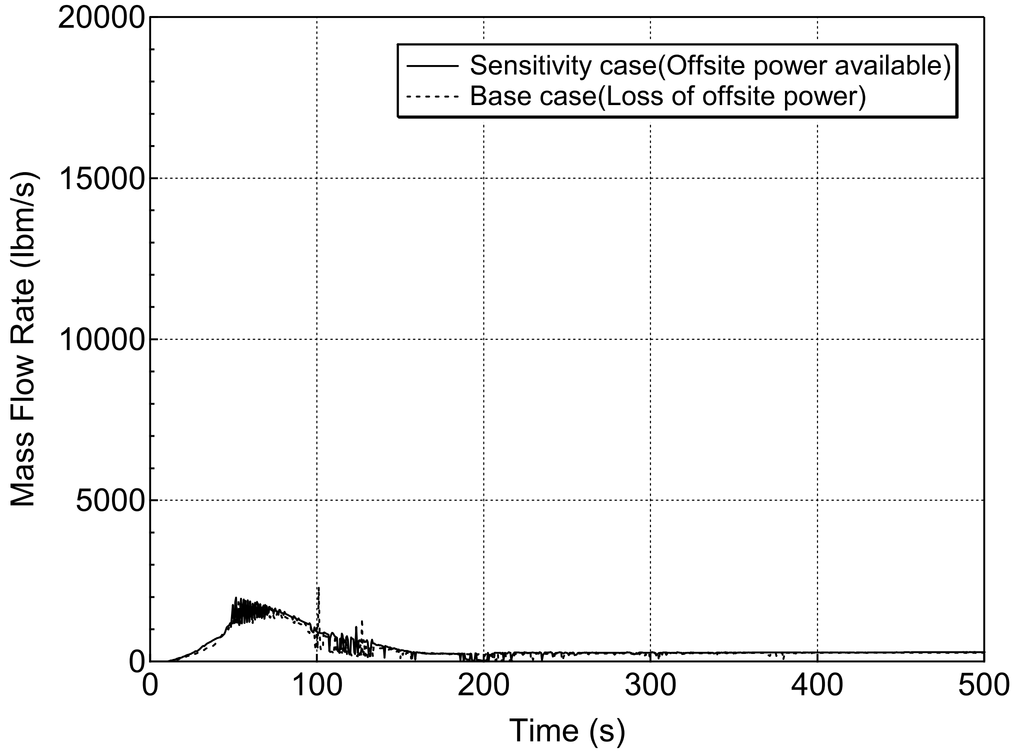

Figure 5.6.2-17 Vapor Discharge through the Break for 1-ft^2 Break (Top) (Offsite Power Available Sensitivity Study)

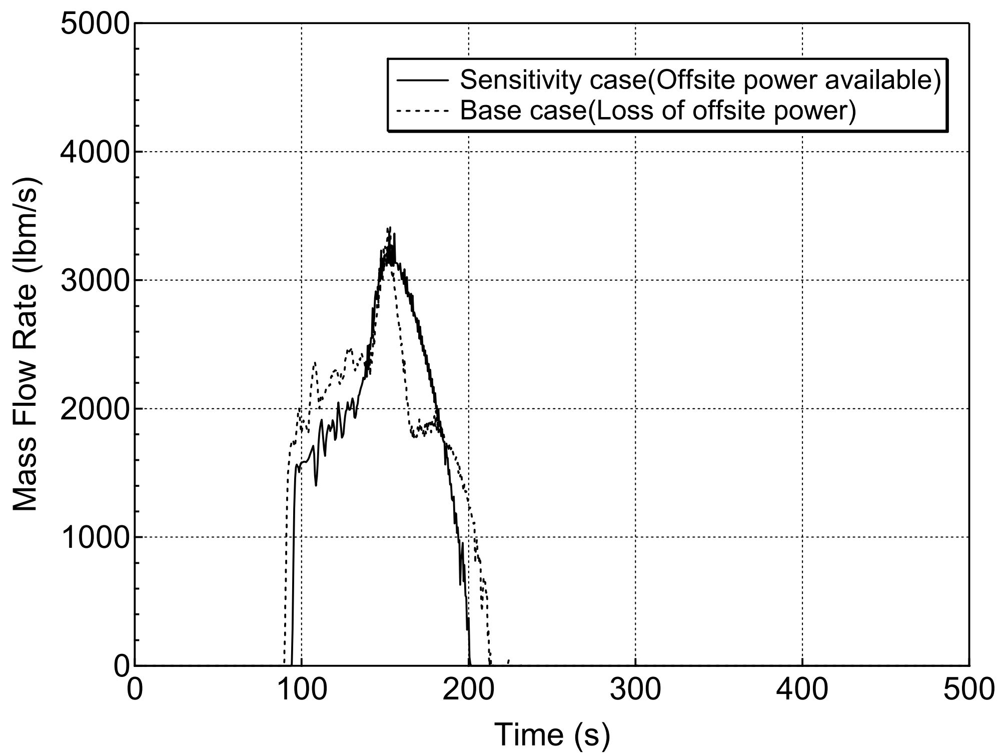

Figure 5.6.2-18 Accumulator Mass Flowrate for 1-ft^2 Break (Top) (Offsite Power Available Sensitivity Study)

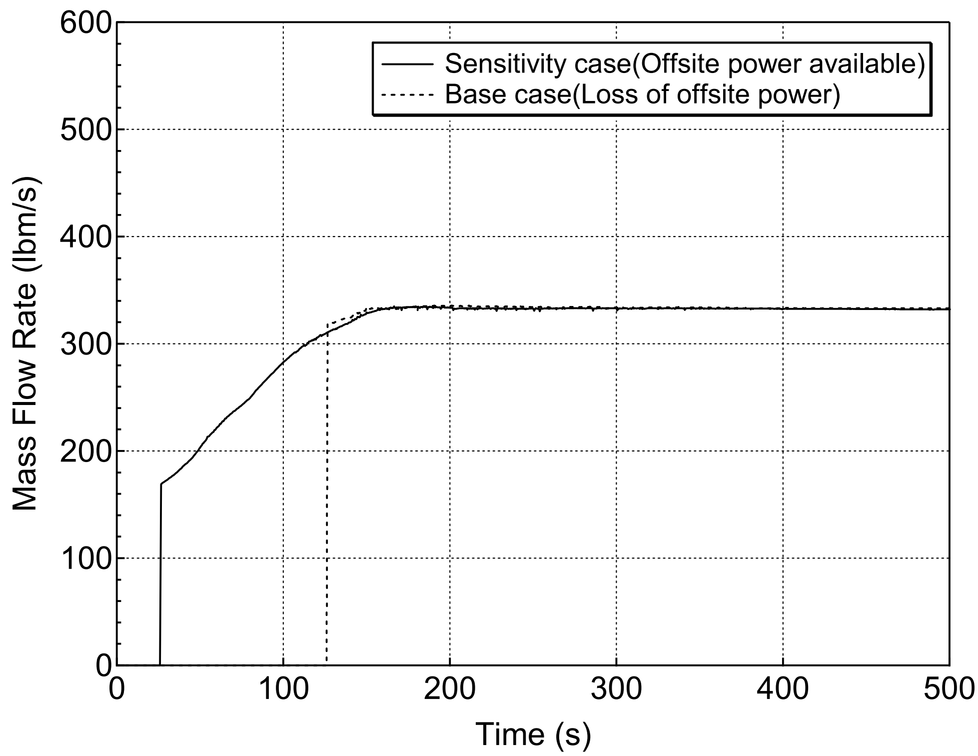

Figure 5.6.2-19 Safety Injection Mass Flowrate for 1-ft^2 Break (Top)
(Offsite Power Available Sensitivity Study)

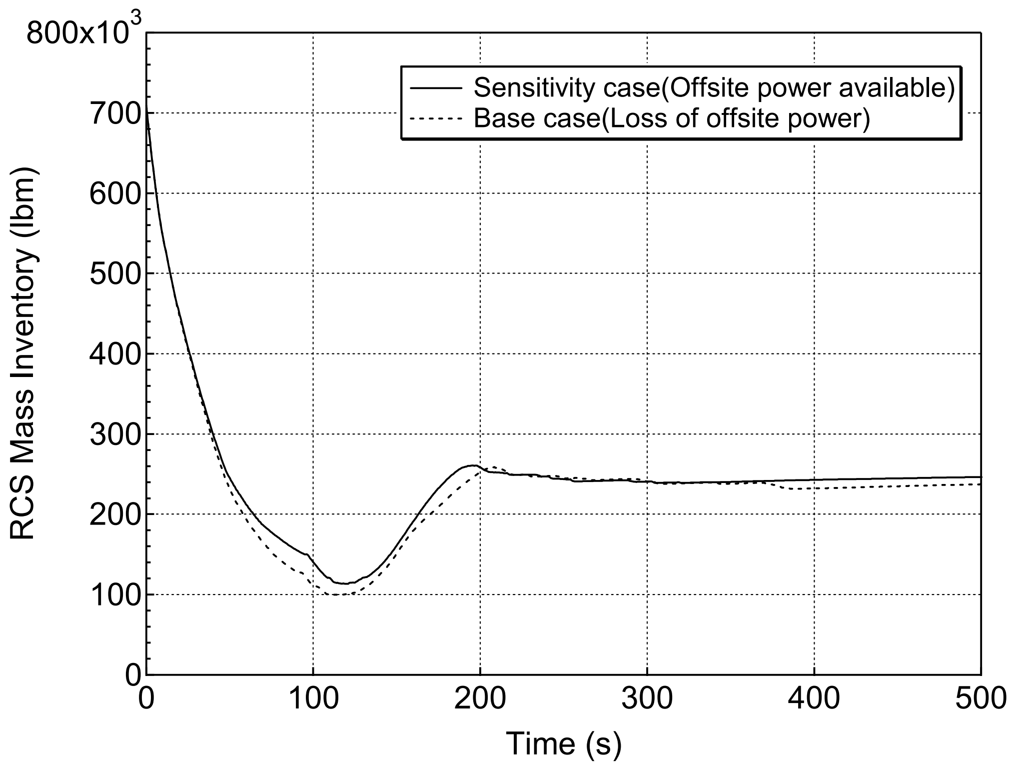

Figure 5.6.2-20 RCS Mass Inventory for 1-ft^2 Break (Top)
(Offsite Power Available Sensitivity Study)

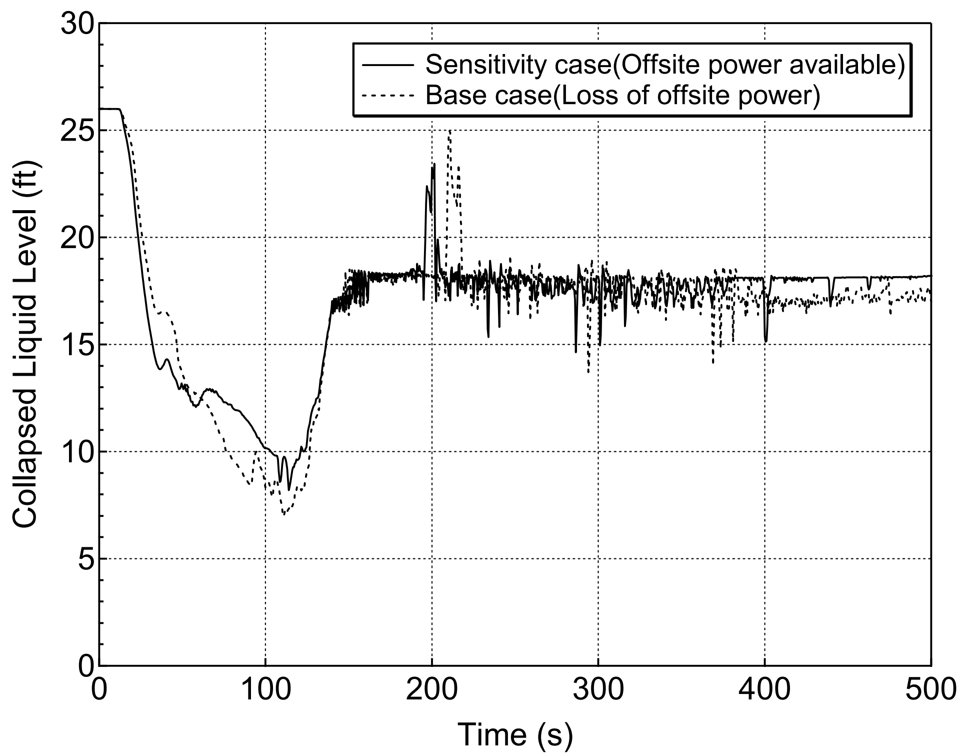

Figure 5.6.2-21 Downcomer Collapsed Level for 1-ft^2 Break (Top) (Offsite Power Available Sensitivity Study)

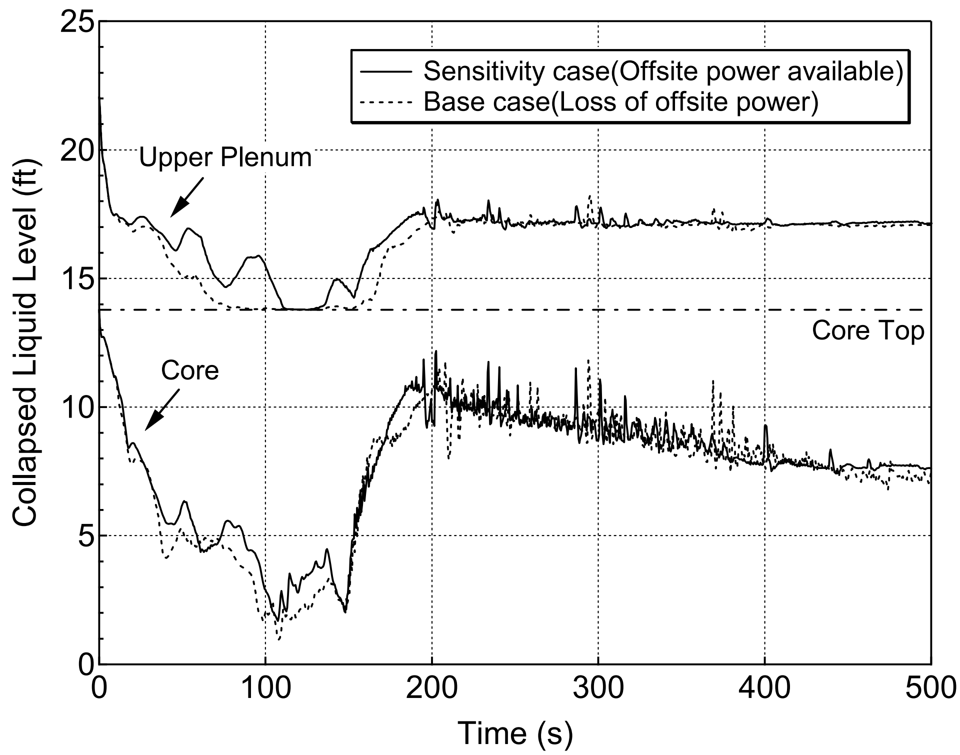

Figure 5.6.2-22 Average Core and Upper Plenum Collapsed Levels for 1-ft^2 Break (Top) (Offsite Power Available Sensitivity Study)

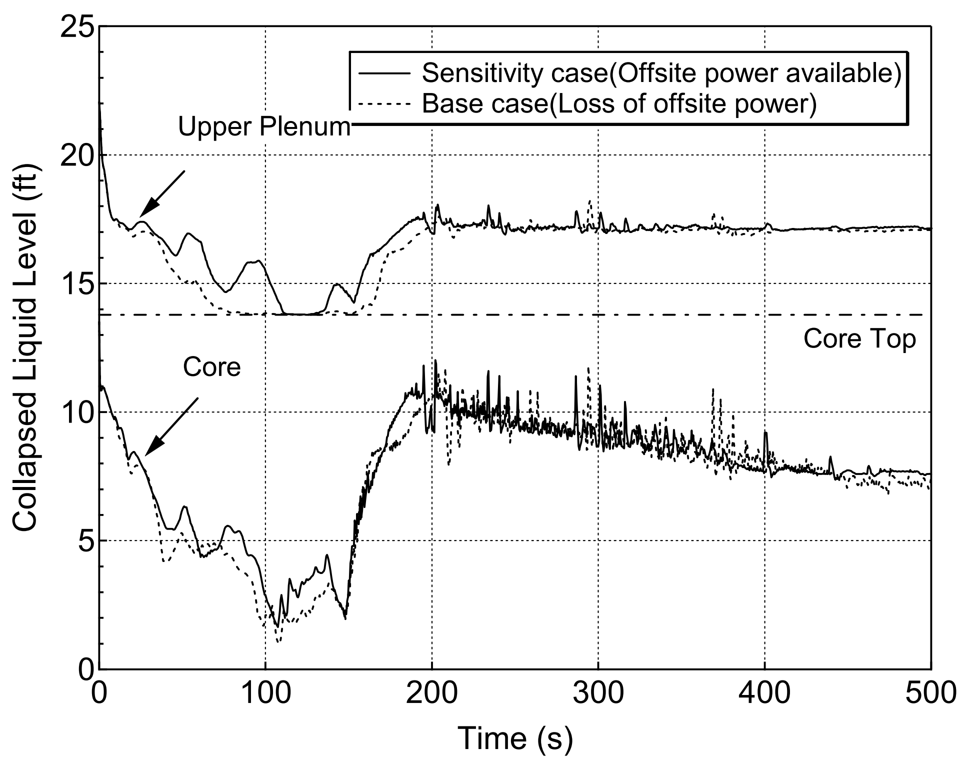

Figure 5.6.2-23 Hot Assembly Core and Upper Plenum Collapsed Levels for 1-ft^2 Break (Top) (Offsite Power Available Sensitivity Study)

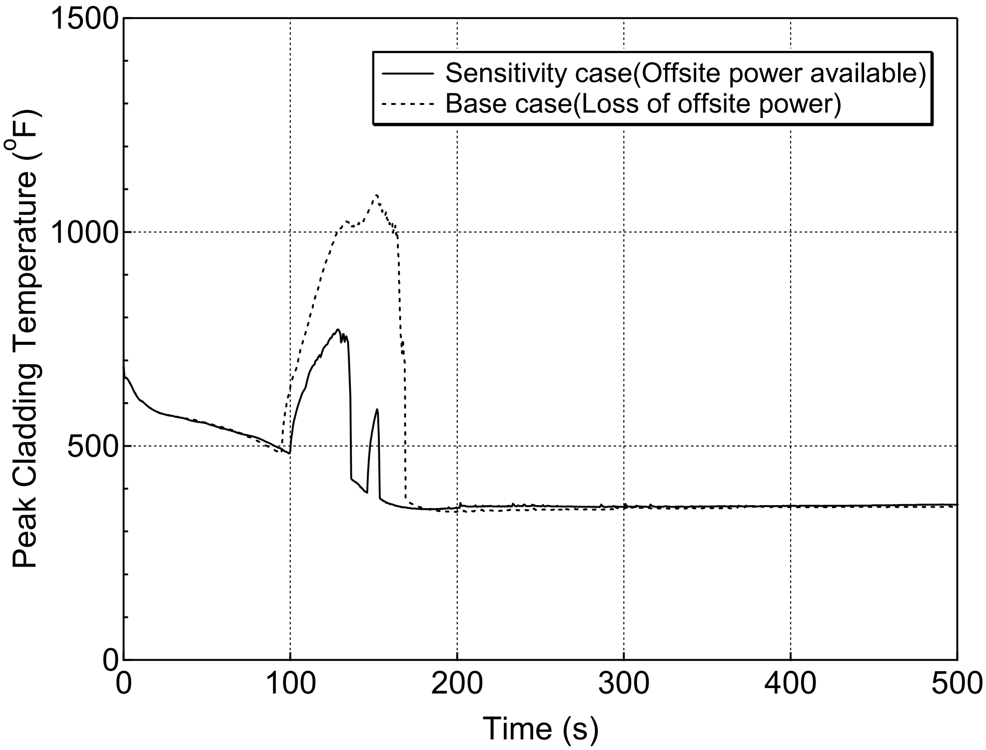

Figure 5.6.2-24 PCT at All Elevations for Hot Rod in Hot Assembly for 1-ft^2 Break (Top) (Offsite Power Available Sensitivity Study)

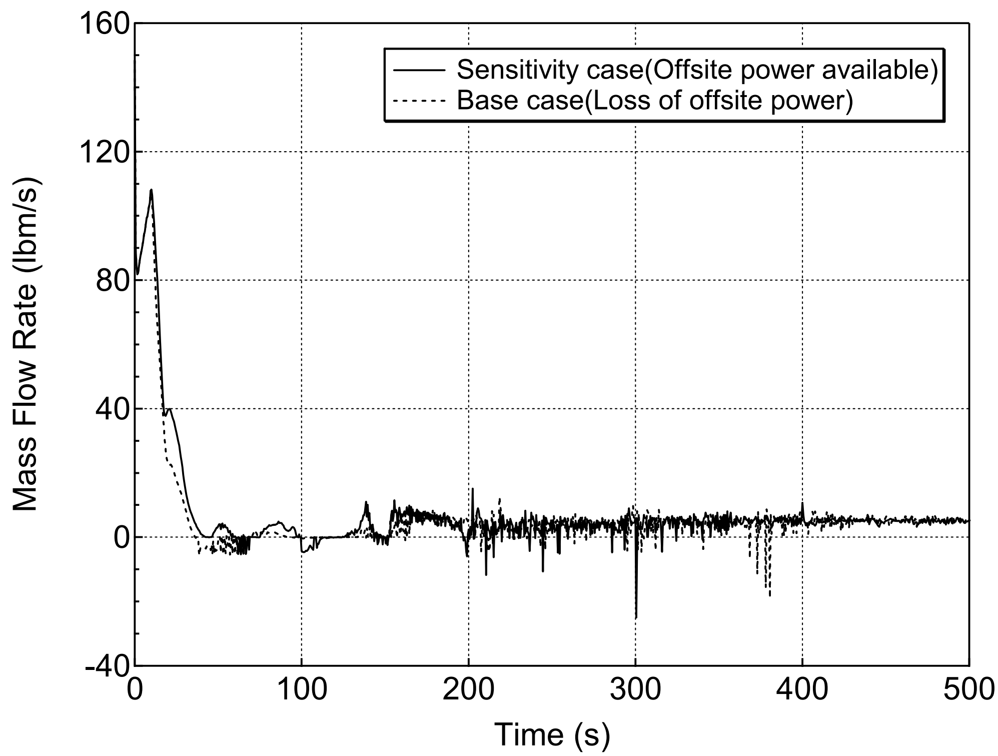

Figure 5.6.2-25 Hot Assembly Exit Liquid Mass Flowrate for 1-ft^2 Break (Top) (Offsite Power Available Sensitivity Study)

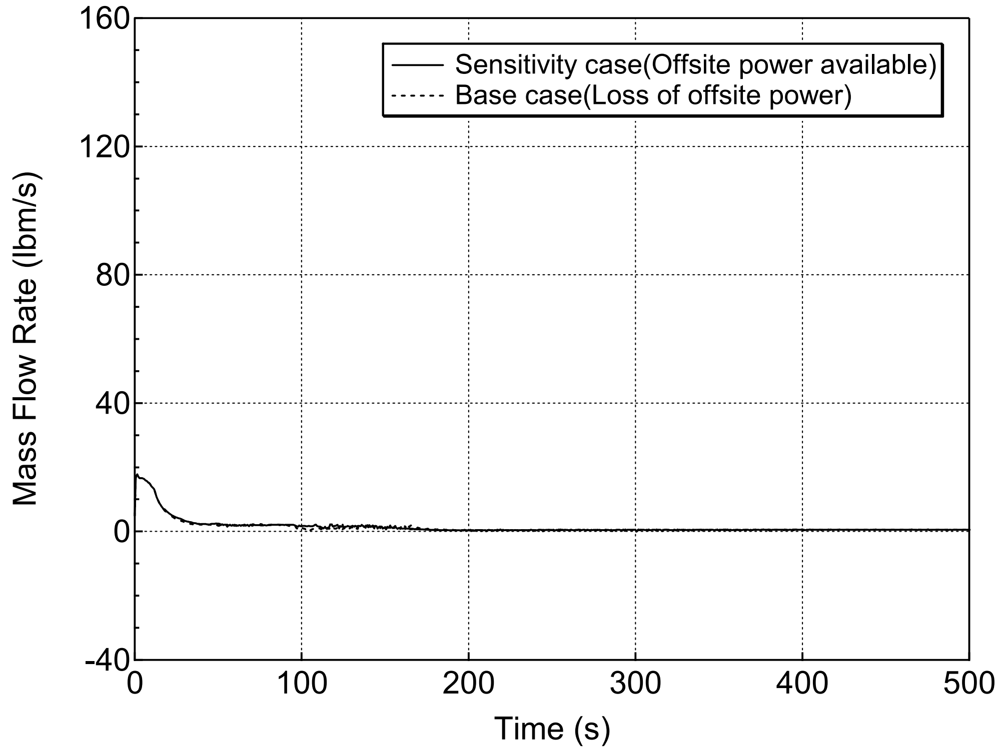

Figure 5.6.2-26 Hot Assembly Exit Vapor Mass Flowrate for 1-ft^2 Break (Top) (Offsite Power Available Sensitivity Study)

6.0 CONCLUSIONS

For the US-APWR SBLOCA analysis, MHI has specifically selected the RELAP5-3D computer code and modified it as M-RELAP5 in order to meet the requirements in 10CFR Part 50 Appendix K ,"ECCS Evaluation Models". In the M-RELAP5, some Appendix K requirements are achieved through the implementation of new models or modifications. The capability of the M-RELAP5 to analyze the SBLOCA transients is confirmed by performing validation analyses involving a series of integral effect tests and separate effect tests focusing on the models related to the important phenomena occurring in the US-APWR during SBLOCA.

In support of the US-APWR Design Certification application, this Technical Report describes the sensitivity analyses on SBLOCA conducted using M-RELAP5. The necessary sensitivity study cases are selected based on the requirements of the Appendix-K and SRP 15.6.5.

The results of the break spectrum sensitivity calculations specified the limiting break conditions including break location, break size, and break orientation for loop-seal PCT and boil-off PCT case. The sensitivity calculations also show the noding near break point and the noding of loop part are appropriate for SBLOCA of US-APWR because a moderate sensitivity is shown on the PCT comparison. The time step size is sufficiently small for code solution convergence because the reducing the maximum time step to half causes little change in the PCT results. The analyses results also show that assumptions of single failure and loss of offsite power are adequately selected to calculate the higher PCT.

The results of the SBLOCA sensitivity analyses in this report show that the calculation by M-RELAP5 meet the requirements of Appendix-K. It is confirmed by the sensitivity analyses that the ECCS of the US-APWR satisfies the required safety performance to mitigate a wide spectrum of postulated SBLOCAs.

7.0 REFERENCES

1-1 10 CFR Part 50, Appendix K, “ECCS Evaluation Models.”

1-2 “Small Break LOCA methodology for US-APWR,” MUAP-07013-P(R1) (Proprietary), May 2010

1-3 NUREG-0800 : STANDARD REVIEW PLAN “15.6.5 LOSS-OF-COOLANT ACCIDNETS RESUTLING FROM SPECTRUM OF POSTULATED PIPING BREAKS WITHIN THE REACTOR COOLANT PRESSURE BOUNDARY.” Revision 3, March 2007

2-1 “Small Break LOCA methodology for US-APWR, “ MUAP-07013-P(R1) (Proprietary), May 2010

3-1 “Small Break LOCA Methodology for US-APWR,” MUAP-07013-P(R1) (Proprietary), May 2010

4-1 “SATAN VI PRGRAM: Comprehensive Space-Time Dependent Analysis of Loss-of-Coolant,” WCAP-8302 (Proprietary), July 1974

4-2 NUREG-0800 : STANDARD REVIEW PLAN “9.2.5 ULTIMATE HEAT SINK.” Revision 3, March 2007

4-3 “Large Break LOCA Applicability Report for US-APWR,” MUAP-07011-P(R0) (Proprietary), July 2007

4-4 “Small Break LOCA Methodology for US-APWR,” MUAP-07013-P(R1) (Proprietary), May 2010

5-1 10 CFR Part 50, Appendix A, “General Design Criteria for Nuclear Power Plants”